# ENTRAINMENT OF BIOLOGICAL RHYTHMS

EDITED BY: Rodolfo Costa and Charalambos P. Kyriacou
PUBLISHED IN: Frontiers in Physiology

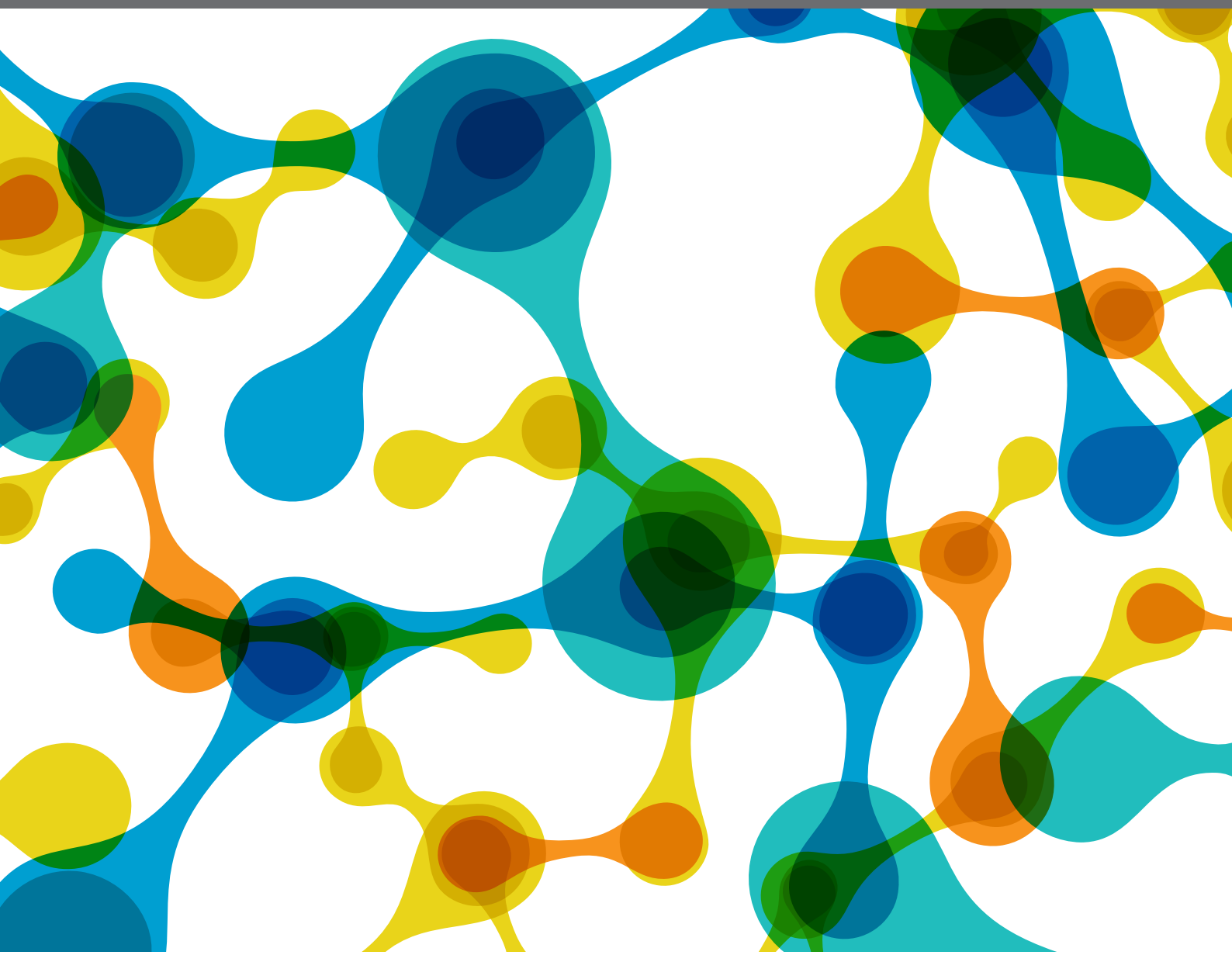

frontiers Research Topics

# frontiers



ISSN 1664-8714
ISBN 978-2-88971-566-4
DOI 10.3389/978-2-88971-566-4

## About Frontiers

Frontiers is more than just an open-access publisher of scholarly articles: it is a pioneering approach to the world of academia, radically improving the way scholarly research is managed. The grand vision of Frontiers is a world where all people have an equal opportunity to seek, share and generate knowledge. Frontiers provides immediate and permanent online open access to all its publications, but this alone is not enough to realize our grand goals.

## Frontiers Journal Series

The Frontiers Journal Series is a multi-tier and interdisciplinary set of open-access, online journals, promising a paradigm shift from the current review, selection and dissemination processes in academic publishing. All Frontiers journals are driven by researchers for researchers; therefore, they constitute a service to the scholarly community. At the same time, the Frontiers Journal Series operates on a revolutionary invention, the tiered publishing system, initially addressing specific communities of scholars, and gradually climbing up to broader public understanding, thus serving the interests of the lay society, too.

## Dedication to Quality

Each Frontiers article is a landmark of the highest quality, thanks to genuinely collaborative interactions between authors and review editors, who include some of the world's best academicians. Research must be certified by peers before entering a stream of knowledge that may eventually reach the public - and shape society; therefore, Frontiers only applies the most rigorous and unbiased reviews.
Frontiers revolutionizes research publishing by freely delivering the most outstanding research, evaluated with no bias from both the academic and social point of view. By applying the most advanced information technologies, Frontiers is catapulting scholarly publishing into a new generation.

## What are Frontiers Research Topics?

Frontiers Research Topics are very popular trademarks of the Frontiers Journals Series: they are collections of at least ten articles, all centered on a particular subject. With their unique mix of varied contributions from Original Research to Review Articles, Frontiers Research Topics unify the most influential researchers, the latest key findings and historical advances in a hot research area! Find out more on how to host your own Frontiers Research Topic or contribute to one as an author by contacting the Frontiers Editorial Office: frontiersin.org/about/contact

# ENTRAINMENT OF BIOLOGICAL RHYTHMS

Topic Editors:
**Rodolfo Costa,** University of Padua, Italy
**Charalambos P. Kyriacou,** University of Leicester, United Kingdom

**Citation:** Costa, R., Kyriacou, C. P., eds. (2021). Entrainment of Biological Rhythms. Lausanne: Frontiers Media SA. doi: 10.3389/978-2-88971-566-4

# Table of Contents

frontiers in Physiology

EDITORIAL
published: 13 September 2021
doi: 10.3389/fphys.2021.757000

# Editorial: Entrainment of Biological Rhythms

*Rodolfo Costa*[1,2]* *and Charalambos Kyriacou*[3]*

[1] Department of Biology, University of Padua, Padua, Italy, [2] Neuroscience Institute of the Italian National Research Council (CNR), Padua, Italy, [3] Department of Genetics and Genome Biology, University of Leicester, Leicester, United Kingdom

**Keywords: circadian rhythms, entrainment, environmental "zeitgebers", biological rhythms, biological clocks**

## Editorial on the Research Topic

## Entrainment of Biological Rhythms

Circadian rhythms are ubiquitous and are observed in nearly all organisms that have been studied which inhabit our planet. These include animals, plants, fungi as well as some bacteria. These endogenous clocks will tick along nicely with an approximately 24 h period in constant conditions because they are generated by the so-called "transcriptional-translation-feedback-loops" (TTFLs) that were first described in Drosophila. The pioneers of this fly research, Jeff Hall, Michael Rosbash, and Mike Young were awarded the 2017 Nobel Prize in Medicine or Physiology reflecting the importance of their contribution to understanding a fundamental feature of life, namely, rhythmicity. These TTFLs appear to be bolted on and interconnected to a more primitive metabolic oscillator, which, under certain conditions, can be observed in the absence of the TTFL in a number of model species (Edgar et al., 2012).

While these oscillators are endogenous, their major role is presumed to be in anticipating the regular fluctuations in the environment that are associated with the Earth spinning on its axis every 24 h and preparing the organism for its daily chores. For animals this might mean foraging, finding a mate, outwitting predators and avoiding extreme daily heat or cold. In addition there are other geophysical cycles to which organisms are sensitive, for example the seasonal changes caused by the Earth's tilt around its axis as it circles the Sun. There is also the gravitational pull of the Moon on the oceans which generates 12.4 h cycles in the ebb and flow of the tides to which shoreline algae, animals and plants have responded by evolving circatidal cycles of behaviour and physiology. Other lunar-related cycles include semi-lunar (∼15 days) and lunar cycles (29.5 days) which have important implications for the reproductive cycles of many organisms. All of these cycles, circadian and non-circadian entrain to environmental "Zeitgebers" (time-givers) the most important of which is the light cycle, but temperature cycles, social stimuli, seasonal photoperiodic changes, vibration or water pressure changes can be equally effective in "entraining" a biological clock to its optimal phase. It is entrainment that determines the time of day or chronotype, yet this property of circadian clocks is less well understood than free running rhythm.

This special edition of *Frontiers* is dedicated to "entrainment" in all its various forms. There are two extensive Drosophila reviews, one by George and Stanewsky, who focus on temperature entrainment of the fly clock and how the peripheral sense organs send temperature information to the brain and the other by Mazzotta et al. who review the neurogenetic basis for the effects of light on sleep in the fly. Light and temperature entrainment is developed further by Kaniewska et al. in the linden bug *(Pyrrhocoris apterus)*, a relatively new model for seasonal biology in which environmental inputs to the circadian clock have yet to be explored.

In flies, the original M and E hierarchical oscillator neurogenetic model has dedicated M (morning) clock neurons that are important for the morning burst of locomotor activity at dawn and the E (evening) neurons determine the late afternoon activity before lights off. By expressing the



***Edited and reviewed by:***
*Martha Merrow, Ludwig Maximilian University of Munich, Germany*

***Correspondence:**
*Rodolfo Costa*
*rodolfo.costa@unipd.it*
*Charalambos Kyriacou*
*cpk@le.ac.uk*

***Specialty section:***
*This article was submitted to Chronobiology, a section of the journal Frontiers in Physiology*

***Received:*** *11 August 2021*
***Accepted:*** *19 August 2021*
***Published:*** *13 September 2021*

***Citation:***
*Costa R and Kyriacou C (2021) Editorial: Entrainment of Biological Rhythms. Front. Physiol. 12:757000. doi: 10.3389/fphys.2021.757000*

canonical clock protein PER in only M or E neurons, Menegazzi et al. show that under changing photoperiods the flies had difficulty in regulating their M or E activity at the appropriate times. This adds to the growing body of evidence that the M and E clock neurons are required to act as interacting network to generate normal locomotor activity, particularly under the more natural photoperiodic conditions found in temperate regions. The clock network is further studied by Van De Maas de Azevedo et al. who show that glutamate signalling from dorsal neurons in the clock network is required to generate the normal response to constant light, which is arrhythmicity. This also has implications because under natural conditions Drosophila species in the extreme northern hemisphere are not (nor need to be) strongly rhythmic under very long daylengths (Bertolini et al., 2019).

This theme of extreme environmental conditions such as constant light or long or short photoperiods that are prevalent in polar regions is the focus of the contribution by Appenroth et al. who study the High Arctic Svalbard ptarmigan (*Lagopus muta hyperborea*) and by Carmona et al. who study the effects of photoperiodic chronodisruption on pregnant female rats and the lingering effects this has on gene expression in their male progeny. In the former study, by investigating core body temperature and locomotor activity cycles, the authors reveal that the ptarmigan shows very weak rhythms, if at all, in both phenotypes under both constant light (LL) and constant darkness (DD) but are rhythmic under both long and short photoperiods under light-dark (LD) cycles. As shown in studies of reindeer, polar animals need not stay rhythmic under arrhythmic environmental conditions (Lu et al., 2010). In Carmona's et al. paper, pregnant female rats exposed to repeated abrupt reversals of the LD cycle gave birth to males, who at 90 days of age showed not only altered liver clock gene expression compared to animals who had gestated in an unchanging LD cycle, but also in genes that are risk factors for cardiovascular disease. There are clear medical implications for chronodisruption during pregnancy.

In zebrafish, unlike mammals, it has been long established that peripheral tissues have light sensitive clocks (Whitmore et al., 2000). Zebrafish encode a bewildering array of opsin genes (>30), and Steindal and Whitmore reveal that one third of these are expressed in cell lines from early larvae and about half of these are clock-controlled. Canonical clock genes such as *Per1* can also be induced and their circadian cycle of expression phase shifted in these cells by a broad range of light wavelengths reflecting multi-opsin gene expression. Because the clock controls the cycles of opsin expression that feed light information into the clock, the clock in effect determines the input to the pacemaker, a concept termed the "Zeitnehmer" ("time-taker") that has been described in Neurospora (Merrow et al., 2003). The Zeitnehmer idea is followed up in the paper by Philippou et al. who use a chemical approach to disturb nuclear oscillations in Arabidopsis. Various chemical interventions implicate the electron transport chain in chloroplasts as being important for clock function. In particular, salicylic acid (SA) appears to be a signalling molecule that is gated by light in the first 3 h of the day and which can drive nuclear oscillations, thereby the light-mediated SA input to the clock modifies the gate by which SA influences the oscillation, i.e., input is output and *vice versa.*

Mathematical modelling of the clock and its environmental inputs is also represented by three papers. Ananthasubramaniam and Meijer use a probabilistic Markov model to study the rest-wake cycle of mice under both light dark (LD) and constant dark conditions (DD). They observe how light and the phase of the clock predict the animal's behaviour in the next time interval. Tokuda et al. use relatively simple amplitude-phase models in an attempt to reproduce the findings of vertebrate entrainment, jet-lag and seasonality experiments. One interesting finding from the model that is intuitively appealing is that the effects of jet-lag can be reduced when the amplitude of the rhythm is small, so resetting the clock phase is easier. The free-running endogenous period of any organism is not exactly set to the natural light cycle of 24 h. Schmal et al. incorporate a clock algorithm with a geophysical model of naturally varying seasonal light intensities and durations at different latitudes. Given an endogenous period and amplitude, the model predicts systematic seasonal and latitudinal changes in the phase on entrainment and the geographical distribution of chronotypes.

Switching to humans, Formentin et al. report a small-scale study from a hospital in Padova (Italy) where patients were fitted with glasses to give them bright light treatment in the morning and with lenses that filtered out blue light in the evening. They then assessed their sleep quality and mood which were generally improved in the treatment vs. control group. Finally, Roenneberg et al. argue the case for and against using Daylight Savings Time (DST), a complex political and social "hot potato." They suggest that any decision needs to be based on biology and include social time, biological time and sun time. They favour an approach that dispenses with DST but realigns countries with their sun clock/body clock time. They also advocate a flexible approach in the workplace whereby subjects adjust their working time to that which best suits their body clock.

We would therefore like to thank all the authors for putting together such an interesting and varied collection of articles as well as the referees who helped improve the manuscripts. It was a pleasure to read and edit them, and we both learned a lot during the process.

## AUTHOR CONTRIBUTIONS

Both authors listed have made a substantial, direct and intellectual contribution to the work, and approved it for publication.

## REFERENCES

Bertolini, E., Schubert, F. K., Zanini, D., Sehadova, H., Helfrich-Forster, C., and Menegazzi, P. (2019). Life at high latitudes does not require circadian behavioral rhythmicity under constant darkness. *Curr. Biol.* 22, 3928–3936.e3. doi: 10.1016/j.cub.2019.09.032

Edgar, R. S., Green, E. W., Zhao, Y., van Ooijen, G., Olmedo, M., Qin, X., et al. (2012). Peroxiredoxins are conserved markers of circadian rhythms. *Nature* 7399, 459–464. doi: 10.1038/nature11088

Lu, W., Meng, Q. J., Tyler, N. J., Stokkan, K. A., and Loudon, A. S. (2010). A circadian clock is not required in an arctic mammal. *Curr. Biol.* 6, 533–537. doi: 10.1016/j.cub.2010.01.042

Merrow, M., Dragovic, Z., Tan, Y., Meyer, G., Sveric, K., Mason, M., et al. (2003). Combining theoretical and experimental approaches to understand the circadian clock. *Chronobiol. Int.* 4, 559–575. doi: 10.1081/cbi-120023678

Whitmore, D., Foulkes, N. S., Strahle, U., and Sassone-Corsi, P. (2000). Light acts directly on organs and cells in culture to set the vertebrate circadian clock. *Nature* 6773, 87–91. doi: 10.1038/3703

**Conflict of Interest:** The authors declare that the research was conducted in the absence of any commercial or financial relationships that could be construed as a potential conflict of interest.

frontiers in Physiology

REVIEW
published: 07 August 2019
doi: 10.3389/fphys.2019.00944

# Daylight Saving Time and Artificial Time Zones – A Battle Between Biological and Social Times

*Till Roenneberg[1]*, Eva C. Winnebeck[1] and Elizabeth B. Klerman[2]*

*[1] Institute of Medical Psychology, Ludwig Maximilian University of Munich, Munich, Germany, [2] Division of Sleep and Circadian Disorders, Brigham and Women's Hospital, Harvard Medical School, Boston, MA, United States*

Many regions and countries are reconsidering their use of Daylight Saving Time (DST) but their approaches differ. Some, like Japan, that have not used DST over the past decades are thinking about introducing this twice-a-year change in clock time, while others want to abolish the switch between DST and Standard Time, but don't agree which to use: California has proposed keeping *perennial* DST (i.e., all year round), and the EU debates between *perennial* Standard Time and *perennial* DST. Related to the discussion about DST is the discussion to which time zone a country, state or region should belong: the state of Massachusetts in the United States is considering switching to Atlantic Standard Time, i.e., moving the timing of its *social clock* (local time) 1 h further east (which is equivalent to perennial DST), and Spain is considering leaving the Central European Time to join Greenwich Mean Time (GMT), i.e., moving its social timing 1 h further west. A wave of DST discussions seems to periodically sweep across the world. Although DST has always been a political issue, we need to discuss the biology associated with these decisions because the circadian clock plays a crucial role in how the outcome of these discussions potentially impacts our health and performance. Here, we give the necessary background to understand how the *circadian clock*, *the social clock*, *the sun clock*, time zones, and DST interact. We address numerous fallacies that are propagated by lay people, politicians, and scientists, and we make suggestions of how problems associated with DST and time-zones can be solved based on circadian biology.

**Keywords: circadian, social jetlag, circadian misalignment, time zones, entrainment (light)**

OPEN ACCESS

***Edited by:***
*Sara Montagnese, University of Padova, Italy*

***Reviewed by:***
*Alireza Mani, University College London, United Kingdom*
*Horacio De La Iglesia, University of Washington Tacoma, United States*

****Correspondence:***
*Till Roenneberg*
*roenneberg@lmu.de*

***Specialty section:***
*This article was submitted to Chronobiology, a section of the journal Frontiers in Physiology*

***Received:*** *07 May 2019*
***Accepted:*** *09 July 2019*
***Published:*** *07 August 2019*

***Citation:***
*Roenneberg T, Winnebeck EC and Klerman EB (2019) Daylight Saving Time and Artificial Time Zones – A Battle Between Biological and Social Times. Front. Physiol. 10:944. doi: 10.3389/fphys.2019.00944*

## INTRODUCTION

The issue of Daylight Saving Time (DST) is an indirect consequence of dividing the surface of Earth into time zones. After decades of measurements, this action was taken at a conference in Washington DC in 1884 to facilitate communication and travel between places with different sun times [as exquisitely recounted in Kehlmann (2009)]. Our Earth takes (at present) 24 h for one rotation. Notably, Earth's day was not always 24 h. When the first biological clocks developed to organize physiology on a daily level (i.e., circadian clocks),

probably something like 3 billion years ago in ancestors of today's cyanobacteria (Dvornyk et al., 2003), days on Earth were 22 h or even shorter (Williams, 2000); days have lengthened by approximately 2 ms every century since. The current 24-h-day translates to an angular velocity of 4 min per longitudinal degree, so the Earth rotates by 15° every hour.

Since 1884, the world's reference clock ticks on Observatory Hill in Greenwich east of London – it defines the zero meridian. Meridians are imaginary lines that run between the North and the South Pole and cut the earth into 360 even "apple slices." Theoretically, time zones (for the social local clock time) are centered around every 15th meridian, stretching half a sun hour (7.5 longitudinal degrees) to the east and half a sun hour to the west. Prague for example, is one sun-hour to the east of Greenwich, St. Petersburg is 2 h and Bagdad is three. The opposite side of Earth from Greenwich forms the date line and conveniently consists almost exclusively of Pacific Ocean water.

We will repeatedly refer to three different clocks or time frames here. (i) The *sun clock* shows the local time of the apparent progression of the sun; noon being when the sun is highest and midnight being exactly half way between dusk and dawn. (ii) The *social clock* shows the local time determined by policy in form of devices on walls, on wrists or in phones; it is a social construct referring to the sun time at the meridian that was chosen for that time zone (see below). (iii) The *body clock* determines the organism's internal time as defined by the circadian clock. Almost all physiological functions from reading certain genes and activating certain proteins to cognitive capabilities and the time when an individual sleeps best are determined by the *body clock* (Borbély et al., 2016). *Body clocks* are predominantly set by light and darkness (Roenneberg et al., 2003a) and can adopt a highly individual relationship to the *sun clock* (e.g., to dawn). The light from the *sun clock* is a stronger stimulus than artificial (e.g., electric) light; we will discuss this more later. We will return to how these clocks synchronize to the solar day below.

If you live directly on an hour-meridian, the *social clocks* at these locations report *sun time*. At all times in any other location, *social clocks* only report the social constructs referring to the sun time at the meridian that was chosen for that time zone. Although time zones were meant to span one sun-hour, it should be noted that time zones are often much wider than 15° longitude. For example, when Galicians in north-western Spain look at their *social clock* in winter and it says noon, it is only 10:30 a.m. by the *sun clock*, since Spain has decided to be part of the Central European Time (CET) zone with its meridian running approximately through Prague. China is even more extreme since all *social clocks* are set according to Beijing's *sun clock* at the country's eastern edge despite its western edge being almost five sun-hours away. An understanding of time zones is essential for appreciating the effects of DST because **switching to DST is nothing else but assigning the respective location to one time zone further east.** This switch increases the discrepancy between the *sun clock* and the *social clock* by 1 h. This means that for Galicia during summer, it is only 9:30 am by the *sun clock* when *social clock* claims noon, since they now have to live according to the hour-meridian that runs roughly through St. Petersburg.

## DST AND THE BODY CLOCK

The association between health and the *body clock* depends on the degree of misalignment between *body clock* and *social clock*. To appreciate this association and its changes over time, one has to understand the mechanisms of entrainment that are at the heart of the *body clock* staying in synch with the 24-h environment.

The "master" *body clock* in the *nucleus suprachiasmaticus* of the hypothalamus receives light via the retina and the optic nerves. The neurons of this master clock actively synchronize (or *entrain*) to the environment's light–dark signals (*zeitgeber*) and in turn provide entraining signals for the circadian clocks in the rest of the body, i.e., the rest of the nervous system as well as peripheral organs and tissues (Saini et al., 2015). This process involves many components, most of which are proteins controlled by genes. The entraining process shows individual variations in the relationship between the *body clock* and the light–dark cycle (e.g., earlier or later) – the colloquial "larks" and "owls," or *chronotypes* in general. The number of people in a population that belong to different *chronotypes* shows a statistically close-to-normal distribution, usually with a surplus on the late chronotype ("*owls*") end of the curve (Fischer et al., 2017). The term chronotype has some times been associated with a relatively stable personality trait or with so-called daily preferences (Horne and Ostberg, 1976), whereas we use it here as the *actual* phase (i.e., time) of entrainment. Phase of entrainment can be assessed in different ways both subjectively and objectively. An example for the former is the Munich ChronoType Questionnaire (MCTQ) that uses subjectively assessed sleep and wake times, specifically the midpoint between sleep onset and offset (Roenneberg et al., 2003b) and an example for the latter are dim-light melatonin onset (DLMO) times (Benloucif et al., 2008).

Historically in humans and other seasonally reproducing animals, the *body clock* responded to the number of hours of daylight that corresponded internally to the number of hours the internal circadian signal melatonin is secreted (Bittman et al., 1985; Wehr et al., 2001; Stothard et al., 2017). The nocturnal duration of melatonin expanded in winter and was compressed in summer. With the invention of artificial light, this zeitgeber has been drastically weakened since we now predominantly spend most of our days in buildings, thereby rarely getting full sunlight, and we switch on artificial light after sunset, thereby only being exposed to darkness (but not necessarily total darkness) when we sleep. One consequence of this weakening zeitgeber strength – on the annual level – is that seasonal rhythms like human reproduction have become weaker and possibly only socially driven (Roenneberg, 2004). Another consequence – on a daily level – is that most individuals' *body clock* entrains to a later time in relationship to the light–dark cycle, except for the very early larks, who may actually become even earlier under weak zeitgebers. This zeitgeber-strength-dependent change in entrainment can be

predicted from circadian formalisms (Roenneberg et al., 2003b) and has been shown for both birds (Dominoni et al., 2013) and humans (Wright et al., 2013). As a consequence, the distribution of chronotypes has become later and much wider than in pre-industrialized conditions (Roenneberg et al., 2007a): while the body clock of extreme larks and owls is somewhere between 2 and 5 h apart in the absence of electrical light (Samson et al., 2017a), they are up to 12 h apart in urbanized regions of the industrialized world (Roenneberg et al., 2007a). When the *social clock* does not follow the large delays of the *body clock*, significant discrepancies between these two clocks arise; this so-called *circadian misalignment* can be assessed for some situations by calculating social jetlag (SJL), which is the difference between sleep-timing on work and work-free days (Wittmann et al., 2006). We discuss the importance of SJL later in this paper.

## VIRTUAL TIME ZONES

An individual's chronotype is usually reported in local time (i.e., by the *social clock*). However, since chronotype is inherently linked with an individual's light–dark cycle (see above), chronotype is more tightly coupled to the *sun clock* (Roenneberg et al., 2007b). Different chronotypes can therefore be translated to or conceived (in a thought experiment) as living in different longitudinal locations. According to this translation, every chronotype virtually lives in its own chronobiological time zone that – unfortunately in many cases – is different from where the individual actually lives. While all people from Chicago physically live in Chicago [yellow arrows in **Figure 1**, which was first presented at the Sapporo Symposium 2018 (Roenneberg et al., 2019)], their *body clocks* virtually "live" east or west of Chicago, depending on their chronotype. The discrepancy between the physical time zone and the chronobiological time zone was small when we lived without artificial light as shown in **Figure 1A**. Corresponding to this virtual time-zone metaphor, the larks "lived" slightly east of the city, the owls slightly west and the intermediate chronotypes (which we will refer to as the "doves") "lived" near the city center. The average midpoint of sleep (a marker for chronotype) in industrialized/urban areas is around 4 a.m., in pre-industrialized eras it was much closer to midnight (Wright et al., 2013; Samson et al., 2017b; Pilz et al., 2018b).

Under conditions of a weakened zeitgeber and more phase-delaying light exposure in the evening, most people's *body clocks* have delayed although the earliest larks have advanced, thereby pulling apart the time-zone chronobiology, so that the distribution of *body clocks* that belong to people who live and work in Chicago would look like shown in **Figure 1B**. We can use the chronotype distribution of the United States population represented in the MCTQ database ($N$ = 25,339; the MCTQ database is curated by TR) to translate chronotypes into the equivalent location east-west of Chicago. If we align the median of this distribution ($\approx$ 3:30 a.m.) to the center of Chicago, about 36% of Chicago's population live both physically and chronobiologically within $\pm$30 min of Chicago's *sun time*, about 24% would "live" further east, about 18% would live "west," (matching the longitude of United States state of Nebraska), 12% would "live" even further west between Denver and San Francisco, while another 10% would "live" somewhere in the Pacific between San Francisco and Tokyo. Note that the owners of these *body clocks* have to work in Chicago.

This situation becomes even worse when *social clocks* are switched to DST, which means that the people of Chicago now have to work according to the *sun clock* in Nova Scotia, Canada which is 1 h earlier (pink, illustrated in **Figure 1C**).

The general delay of the industrialized population's *body clocks* must be considered when we make decisions about work and school start times. In the pre-industrial era, humans slept mostly between 8 p.m. and 6 a.m. and could easily be at work around 8 a.m. According to the MCTQ database, only 23% United States Americans would – judged by their sleep and wake times on their free-days – wake up before 7 a.m.; the rest would sleep too late

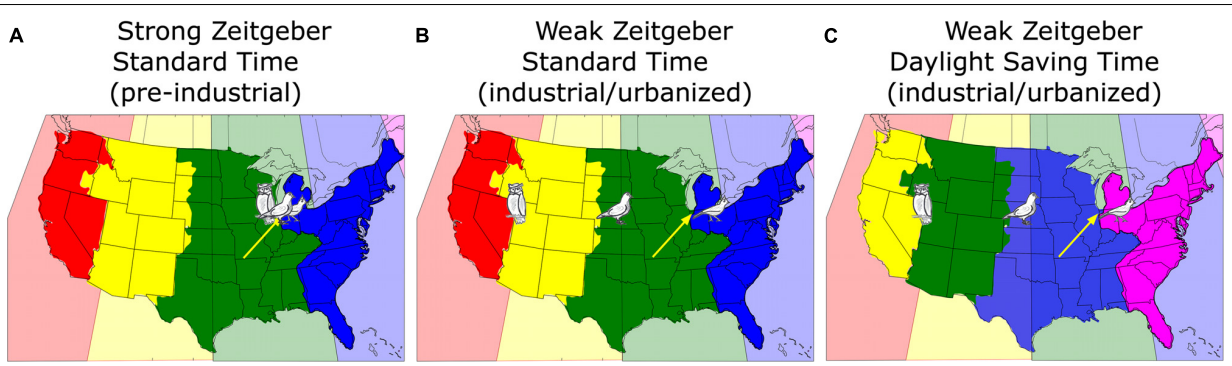


**FIGURE 1 |** A map of the continental United States showing the actual time zones color-coded in the background, i.e., every 15th longitude to the west of Greenwich ± 7.5° (pink: –4 h; blue: –5 h; green: –6 h; yellow: –7 h; red: –8 h). The political time zones adopted by some areas and states of the United States differ from the physical time zones. The bird drawings reflect the virtual position of three different chronotypes (lark = early; owl = late; dove = intermediate; see text for details) living in Chicago (yellow arrows) under different conditions. **(A)** Pre-industrial without electric light (blue: Eastern; green: Central; yellow: Mountain; red: Pacific); **(B)** in post-industrial times with electric light but under Standard Time; **(C)** as **(B)**, but under Daylight Saving Time, which amounts to a reassignment of the political time zones [note the color change compared to **(A)** and **(B)**].

relative to needing to be at work at 9 a.m. Not surprisingly, 78% of the working United States population represented in the MCTQ database indicates that they use an alarm clock in winter and 72% in summer; as noted above, *body clocks* are later in winter than in summer, probably because zeitgeber strength is stronger in summer as people spend more time outside (Kantermann et al., 2007; Hadlow et al., 2014, 2018; Hashizaki et al., 2018) and therefore more people would be expected to need alarm clocks in the winter. As one can see in **Figure 1A**, DST adds an hour to the discrepancy between the *social* and the *body clock* thereby fueling the battle between biological and social time and increasing SJL.

## MYTH-UNDERSTANDINGS AND CONFUSIONS SURROUNDING DST

In summer 2018, the EU asked its citizens to give their opinion about DST in an online poll. 84% of the (predominantly German) participants voted to abolish the twice yearly switch between different clock times; of these a slight majority favored establishing DST all year (European Commission, 2018). Unfortunately, opinions expressed in poll answers and potential decisions based on such opinions may not be based on scientific evidence. In addition, both the lay public and scientists use language in relationship with DST that invites prejudice. For example, in many countries, DST is referred to as "summer time" and Standard Time as "winter time"; the EU poll specifically asked people whether they prefer perennial "summer time" to perennial "winter time." It is not surprising that more people would chose "summer time" over "winter time." Other misleading terms are: *we change the time*; *days become longer*; *the sun sets later*; or: *it's only one hour and we cross many more time zones when we travel* (**Table 1**). However, with DST, we do not change time, we only change *social clocks*; the *sun clock* with its midday and midnight remains the same and dawn and dusk continue their gradual seasonal photoperiodical/day-length changes. Importantly, days are not becoming additionally longer and the sun does not set additionally later because of DST, we simply come home earlier (in reference to the *sun clock*) because we start work or school earlier (in reference to the *sun clock*). DST changes are not comparable with time changes after transmeridian flight (known as jet lag) because we stay where we are instead of exposing our *body clocks* to the new light–dark cycles of our travel destination.

People often belittle the effects of DST by stressing that "it's *only one hour*." Note that this 1 h can actually translate into throwing our body clock's relationship to social clock back weeks in the seasonal changes between sunrise and work start time (Kantermann et al., 2007): in mid-winter (before we switch to DST), most people at higher latitudes (e.g., further from the equator) get up on workdays before sunrise; weeks later in spring (during Standard Time, still before the DST switch), they start getting up with the sun and then in the following weeks, the sun gets up before them. However, when the switch to DST occurs, they are getting up before the sun again, throwing the relationship between sunrise and get-up back by three weeks or more (depending on latitude) in their seasonal trajectory. The question is, however, what happens if this mismatch of 1 h is maintained throughout the DST period (see below)?

In September 2018, two sleep researchers from the University of Salzburg claimed in an interview that there is no hard scientific evidence against perennial DST and that the risks would be negligible (Press Release University of Salzburg, 2018). This press release contained several statements that echo widespread incorrect beliefs and is therefore an excellent substrate for clarifying fallacies (**Table 1**).

Their first fallacy refers to reported acute effects of DST: "*Sleep problems, performance deficits, and even increased risks for cardiac infarction are reported, effects that are however equalized in autumn.*" This refers to a paper published in the New England Journal of Medicine (Janszky and Ljung, 2008) showing a relative increase of myocardial infarction after the spring DST change and a relative decrease after its release in autumn, and the many studies reporting increased myocardial risk just after the switch to DST in the spring have recently been reviewed (Manfredini et al., 2018). The above statement by the Salzburg researchers is misleading in two ways. First, the spring and the autumn effect do not balance each other out on the *individual* level and the higher risk in spring is avoidable by abolishing DST. Second, the paper by Janszky and Ljung show a decrease in risk on the days immediately following the autumn release from DST. If physiology had fully adapted to DST and if the decreased cardiac risk was not only from the extra hour of sleep the night DST ends, this decrease should not occur. Thus, the results of this paper suggest that the risk for myocardial infarction was elevated throughout DST.

The second fallacy concerns entrainment: "*The endogenous clock is predominantly but not exclusively set by sunlight, artificial light and environmental temperature play also a role.*" It is true both that light is the major zeitgeber for the circadian clock, and that there is no reason to separate sunlight from other light sources: as long one can define the light's intensity and spectral composition one can make predictions about its strength to entrain (Lucas et al., 2014). In contrast, entrainment by external temperature changes is most likely not relevant in mammals (Buhr et al., 2010). A paper investigating sleep in pre-industrial societies (Yetish et al., 2015) claims that the tribes they studied are awoken by cold morning temperatures. But cold morning temperatures *per se* do not <u>*entrain*</u> the human clock and are thus more comparable to an alarm clock than to a zeitgeber.

The press release adds that "*. . . many people extensively use smart phones or laptops shortly before they go to bed. The strong blue components . . . are the true robbers of sleep. . . . the potential effects of summer time can be neglected in comparison.*" Indeed, several studies have shown that the usage of artificial light in the evening, and specifically that of electronic screens, does "*rob*" sleep and delays the circadian clock (Cajochen et al., 2011; Chang et al., 2015; Chinoy et al., 2018). The second half of the statement, however, is missing the point: the combination of nighttime light exposure and DST is far worse than nighttime night exposure alone. The nighttime light exposures delay the *body clock* in relation to the *sun clock* (Roenneberg et al., 2003a), which translates to living further

**TABLE 1 |** Short summary of Myth-Understandings surrounding DST, providing short explanations and references.

| Myth-Understandings | Explanation | References |
|---|---|---|
| Summer Time | The colloquial term is used for DST in many countries, but it is misleading since it implies that DST may be responsible for positive attributes of summer (sunny days, warm temperatures, long days) producing falsely positive connotations. Although DST is mostly during summer months, DST is simply an advance of the social clock (we agree to do everything 1 h earlier) and does not "make it summer" | See text for details |
| Winter Time | This term used for Standard Time is a consequence of calling DST "Summer Time." It is just as misleading, because Standard Time refers to the social time defined by the time zone and has nothing to do with winter: it does not "make it winter" nor cause short days, cold temperatures or snow | See text for details |
| Time Change | This term is misleading because DST does not change time but only the local clock, which is used as reference for local (social) time | See text for details |
| Under DST, "days are longer" or "the sun sets later" | DST does not change day length or the time of sunset; day length changes with *season* in most parts of the world. During DST, people go to work an hour earlier (relative to sunrise) and come home an hour earlier (relative to sunset) | See text for details |
| DST is like traveling to the next time zone | It is correct that people can readily adapt to traveling one time zone west or east, but they adapt because their circadian clocks are exposed to the new natural light–dark cycle. DST, however, does NOT change the natural light–dark cycle. DST changes are therefore NOT comparable to traveling to different time zones | See text for details |
| It is only 1 h | It is true that DST clock-changes are usually 1 h, but the relationship between sunrise and when we start work can change by many weeks. Also, a mismatch of 1 h/day is enough for adverse effects, especially if it lasts chronically for 7 months | See text for details |
| Negative DST effects in spring are compensated for in autumn | Although the two opposite effects are true epidemiologically, the autumn "relief" cannot rescue the spring victim on an individual level. The spring victims can be only rescued by abolishing the clock advance (DST) Also, the autumn relief indicates the existence of a stressor prior to the clock change, even if that stressor is "merely" chronic sleep deficiency | Manfredini et al., 2018 See text for details |
| Sun time plays only a minor role for the body clock since it is mainly set by artificial light in modern humans. Environmental temperatures play also a role | The human circadian clock can be set by both sunlight and artificial light, but sunlight is usually up to 1,000-fold more intense and has been shown to affect the clock's synchronization even in mostly indoor-living people. There is no evidence for clock synchronization by environmental temperature in humans (although sleep times may be affected) | Lucas et al., 2014; Roenneberg et al., 2007b; Buhr et al., 2010; Hadlow et al., 2018 |
| The effects of DST can be neglected compared to those elicited by the use of smart phones | Use of smart phones in the evening can delay the body clock. However, this effect does not compete with the light effects of DST, on the contrary, the two act additively in the same direction, thereby worsening social jetlag (SJL)<br>Evening light delays the clock and morning light advances the clock. Thus, DST decreases circadian clock advances and increases circadian clock delays | Cajochen et al., 2011; Chang et al., 2015; Chinoy et al., 2018; Roenneberg et al., 2003a |
| Perennial DST does not significantly increase SJL | The reverse is true: the number of people NOT suffering from SJL doubles when switching away from perennial DST to Standard Time (e.g., time zone time) and the number of people suffering from higher levels of SJL are significantly and greatly reduced<br>There have been multiple attempts to implement perennial DST over the past 100 years (e.g., in Russia, the United Kingdom and the United States). In each of these cases, the "experiment" was abandoned after few years | Borisenkov et al., 2017; Ripley, 1974; Uk Time Zone History, 2019; Gray and Jenkins, 2018 |

west is a time zone, while DST advances the *social clock* in relation to the *sun clock*, which translates into moving the time zone further east. Thus, in DST, the two effects additively (i.e., both delaying the *body clock* and advancing the *social clock* in relation to the *sun clock*) increase SJL since both effects increase the difference between the mid-sleep on work-free days (closer to the individual circadian mid-point of sleep) and mid-sleep on workdays.

The last fallacy concerns the interpretation of data in a paper published by Russian researchers analyzing the three different *social clock* constructs in Russia's recent history (Borisenkov et al., 2017): the traditional DST pattern of usage in only some months of the year, the extension of DST to the entire year (which was abandoned after 4 years) and the subsequent permanent Standard Time (which the government finally adopted after going through these different nation-wide "experiments"). The

researchers showed that SJL gradually increased from perennial Standard Time to traditional DST/Standard Time switching to perennial DST. In reference to the 2017 Borisenkov paper, the Salzburg sleep researchers said: "*At first glance, the study seems to support . . . that permanent summer time fosters social jetlag. If you look at the results carefully, the reported effects are very small.*" When analyzing the results of a population-based study, it is always beneficial to look at the actual distributions of results rather than changes only in average results of the population. When we do this, we see that permanent DST would increase the average SJL by more than half an hour which may be statistically small but is biologically large. The distributions published by Borisenkov and colleagues show that the transition from perennial DST to perennial Standard Time led to doubling of people who do not suffer from SJL, those who suffer from only 1 h SJL increased by about 30% and those who suffer from higher SJL are reduced by 25%. Therefore, Standard Time reduced SJL.

Russia was not the only country to try and then abandon permanent DST. The United States has tried it twice (one after WWII and one in the 1970s) and the United Kingdom tried it in the 1970s. Expected energy savings were not observed in the United States or elsewhere, and in both the United States and the United Kingdom, permanent DST was highly unpopular (Ripley, 1974; Uk Time Zone History, 2019). The US Congress even ended the 1970s DST plan early because of its unpopularity. A revealing review of the political considerations within the United States of the DST laws is available in Gray and Jenkins (2018); farmers, parents of children who waited for school buses in the dark, and people in higher latitudes were especially vocal against permanent DST. In the United States, minimal or no energy savings were observed (as noted above), and there were some increases in traffic accidents in the morning. Two interesting additional political facts from this Gray and Jenkins reference include: (i) one group lobbying for more months of DST were candy manufacturers and "concerned" parents who wanted Halloween Trick-or-Treating to happen during sunlight hours; and (ii) members of Congress living on the western portion of each time zone were less likely to vote for DST, as would be expected from the biology we have been describing.

## TIME ZONES AND HEALTH

There are good sides to DST, such as coming home "earlier" (by the *sun clock* but not by the s*ocial clock*) from school or work and therefore having more hours of daylight during the free time after work. These positive effects may go beyond subjective feelings. A study has shown for example that activity increases with longer evening daylight (Goodman et al., 2014) – albeit with small biological effect sizes (≈6% difference in the daily activity between the Standard Time of the year and DST, adjusted for photoperiod). Interestingly these results of the above study were culture-specific: a significant increase was mainly observed in Europe and to some extent in Australia, while no significant effects or even slightly negative effects were seen in the United States and Brazil.

It is important to note that DST transitions can elicit short and/or long-term effects, which we will refer to as *acute* and *chronic* effects, respectively. The first days after the DST change in spring show *acute* effects: sleep is shortened (Barnes and Wagner, 2009), adolescents are sleepier during the day (Schneider and Randler, 2009), general accidents and visits to the emergency room increase (Ferrazzi et al., 2018), so do myocardial infarctions (Janszky and Ljung, 2008; Manfredini et al., 2018), ischemic stroke (Sipilä et al., 2016), the risk of *in vitro* fertilized mothers losing their babies (Liu et al., 2017), and suffering from negative mood changes (Monk and Folkard, 1976; Monk and Aplin, 1980). In these last two papers, the authors suggest that the effects of DST are similar to those of shift-work, which has known multiple adverse effects on health and safety due to the mismatch between the *body clock* and the *social/work clock* (Scott, 2000; Knutsson, 2003). On the Monday after the DST transition, the known stock market weekend effect (i.e., a predictable negative influence on stock-trading each Monday morning), is augmented by 200–500% in several international markets, implying a $31 billion one-day loss in the United States markets alone (Kamstra et al., 2000). Reports have been contradictory on the *acute* effects of DST on traffic accidents (Carey and Sarma, 2017). Some find an increase after transitions to and from DST (Hicks et al., 1983), others find an increase in spring (to DST) and a decrease in fall (from DST) (Coren, 1996a,b), some find no change (Huang and Levinson, 2010; Lahti et al., 2010) or even the reverse effect (Ferguson et al., 1995) though this last paper used as their reference the light patterns for one city in the center of the United States rather than those where the accident occurred. Similarly contradictory are reports on hospital admissions. While a Finish study finds no effects (Lahti et al., 2008), an Italian study (Ferrazzi et al., 2018) finds a significant increase in spring and a decrease in autumn. One possible explanation for the different results is that the effects may be latitude-dependent and/or depend on the exact time point of the DST change in relationship to photoperiod, since *acute* DST effects will be different whether the switch is before, at, or, after the spring equinox (note, the date of DST switch changes from year to year and can differ by weeks between different countries).

There are very few reports on the *chronic* effects of DST. These are difficult to study as comparison between periods with DST and Standard Time are usually inherently confounded by seasonal effects. The *chronic* effects may be small on an individual level, but they accumulate over time in individuals and both across time and space in populations resulting in big effects, the costs of which can be assessed similarly to those of insufficient sleep (Hafner et al., 2017). From a chronobiological perspective, *chronic* effects are very likely because, throughout the months of DST, *body* and *social clocks* are likely set to different time zones in most people, as we explained above. Due to the fact that mostly only the transitions to and from DST in spring and autumn have been studied rather than the steady state effects in summer and winter it is still unclear whether and how much people actually adjust to DST through artificial light exposure. When daily sleep timing as well as activity profiles are recorded for several weeks before and after the transitions, one can see that sleep times adapt relative quickly to the new

social time regime – especially on workdays (Kantermann et al., 2007) – while activity profiles on work-free days seem to be relatively insensitive to the DST change hinting at no or very slow adjustment of daily activity rhythms to DST (Roenneberg et al., 2013). An *increased* mismatch between *body clock* and *social clock* time during DST is supported by the only two published steady-state studies that we know of. In the first study performed in Australia, cortisol rhythms were found to be advanced by only 2 min during DST (not the 1 h corresponding to full adjustment) when comparing 3,000 summer samples taken during a 3-year-DST-test phase versus 9,000 summer samples during Australian non-DST summers (Hadlow et al., 2014). This finding suggests no change in *body clocks* despite the change in *social clock* during DST. This lack of change in the *body clocks*' timing during DST compared to during Standard Time demonstrates that our *body clocks* do not heed *social clocks* because *body clocks* are based on *sun clocks* and not political laws; political laws cannot determine health – they can only influence it for the better or worse. In the second study, the analysis of the three different states of DST in Russia (i.e., traditional switching, perennial DST and perennial Standard Time) found an increase in SJL during perennial DST (see above) (Borisenkov et al., 2017). The same study also found a small decrease in winter depression symptoms during perennial Standard Time (Borisenkov et al., 2017). As mentioned above, any study showing long-term positive effects with the cessation of DST in autumn suggests that *chronic* negative effects have likely been acting throughout the months of DST. Even if the positive effects are due to sleep extension on the one night of the DST-to-Standard Time transition, they would indicate a prior sleep debt during DST (Klerman and Dijk, 2005).

In addition to these few studies that address chronic DST effects directly, there are four indirect ways of estimating *chronic* DST effects: (i) relative position in a time zone (i.e., distance from the eastern border of the time zone as indicated in **Figure 1**; (ii) SJL; (iii) being a late chronotype; and (iv) sleep-loss.

(i) *Relative position in time zones.* Several studies have investigated the prevalence of different cancer types as well as general and cancer-specific mortality as a function of distance from the eastern border of the time zone: (Borisenkov, 2011; Gu et al., 2017; VoPham et al., 2018). All three studies conclude that risks increase and longevity decreases from the eastern to the western border of time zones. The most recent example of studies that examine east-west gradients in time zones (Giuntella and Mazzonna, 2019) finds that "an extra hour of natural light in the evening reduces sleep duration by an average of 19 min" with significant effects on health (e.g., obesity, diabetes, cardiovascular diseases, and breast cancer) and on economic performance (per capita income).

These results suggest that the discrepancy between the *social clock* and the *sun clock* even within a time zone can have a significant effect on health; on the western edge of a time zone, *social clock* time is later than *sun clock* time (as is the case during DST) and at the eastern edge it is earlier. Similar findings are reported for the incidence of winter depression, which also gradually increases within time zones, i.e., the later the sun rises in reference to the social clock (White et al., 2006). This is in contrast to Olders (2003), who finds that later sunrise times, i.e., more western positions in the time zone, are associated with a lower depression prevalence in urban populations. The author argues that sleeping late increases REM sleep, and thus may increase depression risk and suggests that later sunrise times mean earlier rising times in relation to sunrise and therefore proposes to switch to perennial DST. If one would simply extrapolate the results shown in their Figure 1, an increase in average sunrise time of about 1 h would decrease depression prevalence by 50%. This would be a huge effect and has not been documented and would also predict that depression prevalence in winter should be >50% lower than in summer (which is the opposite of what is reported). It is also contrary to the well-documented, beneficial effects of early morning light in mood disorders (Wirz-Justice and Benedetti, 2019). Also, in their Figure 1, which is based on 1-year averages, demonstrates only an association that does not allow causal inference. Furthermore, there are many confounding variables that can affect the prevalence of depression (such as age, sex, socioeconomic status, etc.) that were not adjusted for in the analysis, which may have led to this unexpected finding of an association between lower depression prevalence and later sunrise times. Later sunset times are also associated with fewer hours of sleep, poorer academic performance, and lower wages among adults in a study of people in India, Indonesia, and China (Jagnani, 2018).

The health effects that depend on the east-west position within a time zone described above have not yet been investigated in the CET zone. Of interest, results from the MCTQ database from the CET zone indicate that the expected negative effects may be countered by compensatory behavior. The further west people live within the CET zone, the later they organize their lives in reference to *social* time. Anecdotal evidence suggests that Germans dine later than Hungarians, the French eat later than Germans and Spaniards go to dinner later than the French. Note that France and Spain strictly speaking should not be in the CET since their longitude is further west (see **Figure 2**); if their time zones were matched to their longitudes, they would not be eating "late" by *social clock* time [because 9 p.m. CET is at the same time as 8 p.m. Greenwich Mean Time (GMT)]. More quantifiable questionnaire results from the MCTQ support this anecdotal evidence and also show that work-start times become progressively later in Europe from its eastern to its western border (**Figure 3**; Roenneberg et al., 2019). These behavioral changes mean that people eat and work closer to their *body clock* time (rather than the *social clock* time). If the negative east-west health effects shown for Russia, China and the United States turn out to be smaller in Central Europe, it could be due to this compensatory behavior and the east-west slope would be greater if the SJL was not reduced by compensatory behavior.

(ii) *Social jetlag (SJL).* That human *body clocks* entrain to light–dark cycles as circadian clocks do in all other animals and plants is still true for industrialized societies (Roenneberg et al., 2007b). DST increases the discrepancy between the *sun clock* and the *social clock* and will

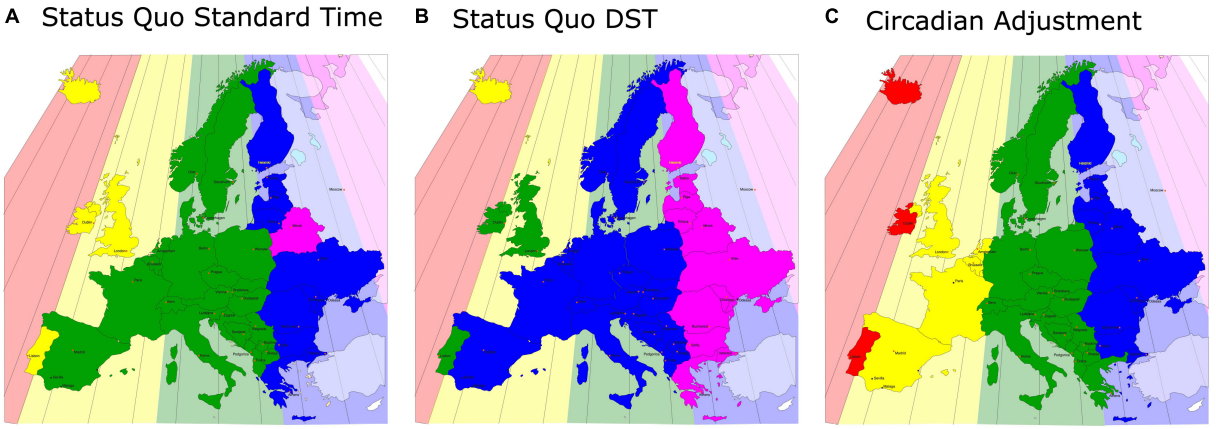


**FIGURE 2 |** A map of Europe equivalent to **Figure 1**: the actual, sun-based time zones are drawn as color-coded backgrounds and the social time zones are shown in the same (stronger) colors in front. Even under Standard Time, the western areas of the social time zones are far away from the respective eastern borders of the sun-based time zones **(A)**, this discrepancy increases by 1 h under DST **(B)** (note that Iceland is on perennial DST). **(C)** A solution to the problem: the political borders of Europe are actually ideal for the correct, chronobiological separations into time zones, so that in no area of Europe the social clock has to be discrepant from the sun clock by more than 30 min.

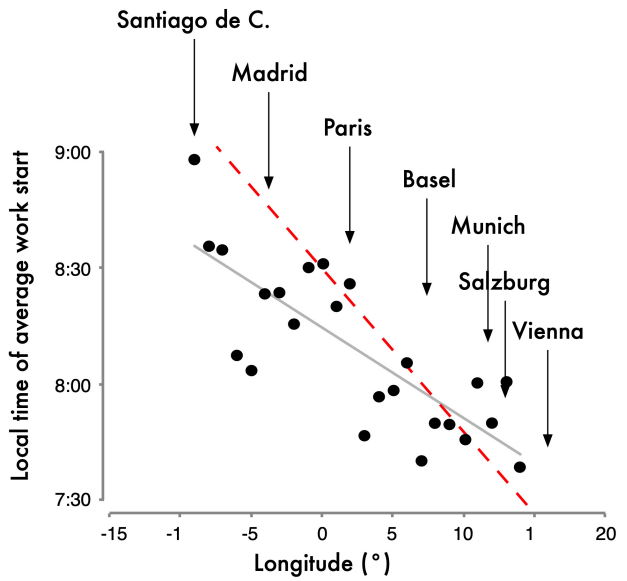


**FIGURE 3 |** Work-start times averaged for longitudinal bins of the Central European Time (CET) Zone. Data were taken from the MCTQ database. For the analysis, participants had to live in the CET zone and their postal code and city name had to match as they were used to derive latitude and longitude. The dashed red line represents the slope parallel to the progression of sunrise (4 min/longitude). The slope of the actual east-west delay (gray line) in work start times is 2.3 min/longitude ($n = 24$; $r^2 = 0.63$; $p < 0.001$). This delay in work-start times despite identical local times is noteworthy since the slope of sleep timing on work-free days is 3.8 min/longitude for rural regions, 2.6 min/longitude for towns with populations between 300,000 and 500,000 and 1.5 min/longitude for the major European cities, perhaps due to the differences in lighting patterns and zeitgeber strength in those environments (Roenneberg et al., 2007b). The geographical location of some major European cities is indicated above the graph. Note that while all cities listed here are currently in the CET zone, some of those cities' longitude is outside the non-political longitude lines for CET and therefore the graph has cities from –15° to +15° instead of –7.5° to +7.5° (see color-coded time zones in **Figure 2**). Data originally published in Roenneberg et al. (2019).

therefore also increase the discrepancy between the *body clock* and the *social clock*, thereby also increasing SJL (see above). SJL is associated with adverse health effects: these include increased likelihood to be a smoker as well as higher caffeine and alcohol consumption (Wittmann et al., 2006); higher incidence of depression (Levandovski et al., 2011) and other mood pathologies such as anxiety disorders and personality disorders (Wittmann et al., 2010; Foster et al., 2013); increased risk of metabolic disorders (Rutters et al., 2014; Parsons et al., 2015), such as obesity (Roenneberg et al., 2012), metabolic syndrome and type II diabetes (Koopman et al., 2017) or increased insulin requirements in adolescent diabetes-type-I patients (Schnurbein et al., 2018); higher rates of cardiovascular problems (Wong et al., 2015) and cognitive performance and academic achievements (Haraszti et al., 2014; Díaz-Morales and Escribano, 2015).

(iii) *Late chronotype.* There is a strong correlation between chronotype and SJL (Wittmann et al., 2006), which is not surprising since two factors come together in generating the modern condition of having a late *body clock* and having to get up earlier than the *body clock* would suggest. Being a late chronotype is associated with reduced health (Partonen, 2015), but it is most likely that most of the associations between chronotype and health act via SJL rather than via chronotype itself (Levandovski et al., 2011; Pilz et al., 2018a). Since DST would delay chronotypes (see above), any association between late chronotypes and reduced health would be an indicator of *chronic* DST effects.

(iv) *Sleep-loss. SJL* and circadian disruption are strongly correlated with a reduction in sleep duration (Foster et al., 2013). Accordingly, the MCTQ database shows a systematic association between SJL and sleep duration (**Figure 4**). The SJL-dependent sleep loss during the workweek (**Figure 4A**) is almost compensated for on work-free days (**Figure 4B**),

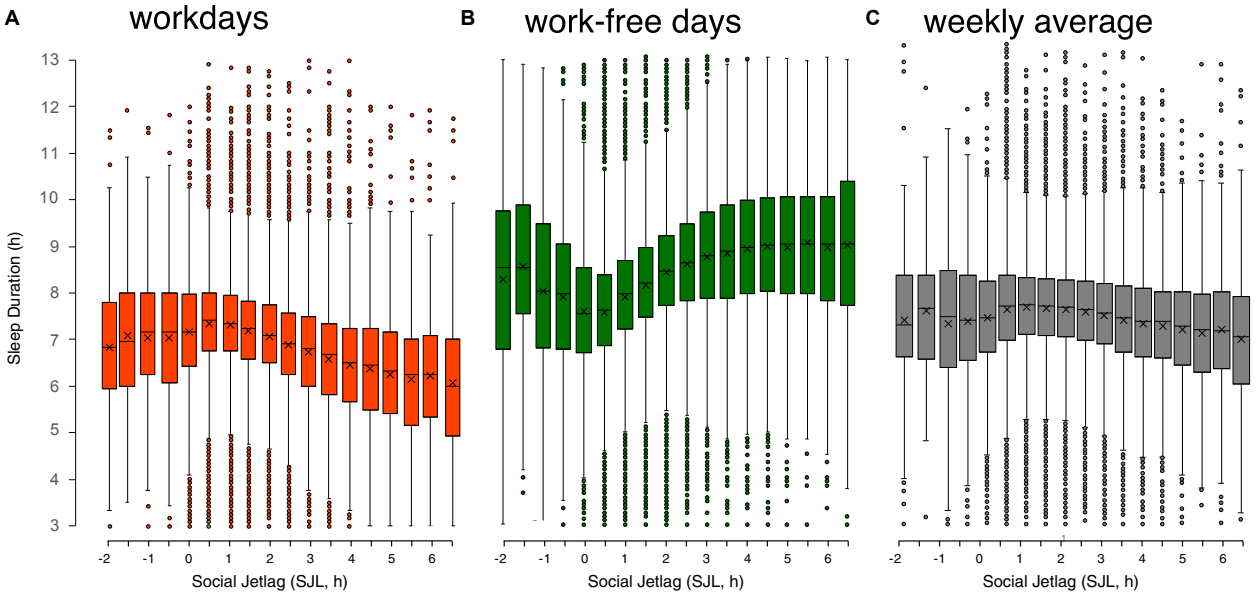


**FIGURE 4 |** Relationship of sleep duration on workdays **(A)**, on work-free days **(B)**, and weekly average sleep duration **(C)** with social jetlag (SJL). Data are taken from the MCTQ database ($n \approx 300{,}000$). Participants with a complete set of questions necessary to compute SJL and with the respective MCTQ variables being within three standard deviations of the mean ($\mu \pm 3\sigma$) were used for the analysis (workdays: $n = 193{,}927$; work-free days: $n = 198{,}096$; weekly average: $n = 193{,}927$). On a weekly average, people who suffer from 3 h of SLJ or more sleep approximately 1 h less per night, adding up to a sleep-loss of 5 h/week. Boxplots are Tukey boxplots with whiskers encompassing all data within 1.5 times the interquartile range; data outside these ranges are depicted as points. ANOVA shows that for free days and workdays significant differences are found on average 3–4 half-hour bins apart while for the weekly average significance is only reached at differences of 7–8 half-hour bins (data originally published in Roenneberg et al., 2019).

so that SJL is characterized by a constant oscillation between under- and over-sleeping. Notably people suffering from less than 30 min of SJL get the longest sleep on workdays and sleep the least on their free days compared to those of other SJL categories. Access to electrical light itself is associated with a decrease in sleep duration (de la Iglesia et al., 2015; Pilz et al., 2018b), which can be explained by a concurrent delay of chronotype (Wright et al., 2013; Pilz et al., 2018b). Of the almost 200,000 people represented in **Figure 4**, only 12% do not suffer from SJL and another 19% suffer from only half an hour of SJL. These two categories are the only ones that get on average more than 7 h of sleep on nights before workdays, all other chronotypes gets less than 7 h of sleep as SJL increases. Notably, sleep deficiency is associated with the same health risks as DST, SJL and being a late chronotype, e.g., with metabolic pathologies (Borel et al., 2013; Reutrakul et al., 2013, 2015), suggesting that the effects have common mechanisms, for which sleep debt could be a good candidate.

## POTENTIAL SOLUTIONS

In summary, the scientific literature strongly argues against the switching between DST and Standard Time and even more so against adopting DST permanently. The latter would exaggerate all the effects described above beyond the simple extension of DST from approximately 8 months/year to 12 months/year (depending on country) since *body clocks* are generally even later during winter than during the long photoperiods of summer (with DST) (Kantermann et al., 2007; Hadlow et al., 2014, 2018; Hashizaki et al., 2018). Perennial DST increases SJL prevalence even more, as described above.

A solution to the problem is shown in **Figure 2C**, which contains a combination of obliterating DST (in favor of permanent Standard Time) and reassigning countries and regions to their actual *sun-clock* based time zones. Under such adjustment, *social (local) clock* time will match *sun clock* time and therefore *body clock* time most closely. Critics of such a solution might argue that this would scatter European social times, but there is no evidence that this would be detrimental. First, we already have three different time zones within Europe (WET/GMT, CET, and EET), and secondly, the United States has four different time zones and several United States states even have multiple time zones with no detriment in commerce, travel, or communications.

If DST should be abandoned, as we suggest as scientists, there are still many people who "like their long evenings." But there is a solution to this problem: DST is simply a work-time arrangement, nothing more than a decision to go to school/work an hour earlier. As such, it is not a decision that should be made by the world, by unions of countries (e.g., the EU), or by individual countries, neither at the federal nor the state level. Work-time arrangements are decisions that a workforce could decide at the company level. Therefore, anyone who wants to

spend more time at home in daylight after work should convince his/her company and co-workers to advance their start time during certain months of the year or even better: introduce flexibility for individual workers where possible to accommodate differences in personal biological and social requirements.

## SUMMARY

Discrepancies and misalignments between *social (local) clock* time, *sun clock* time, and *body clock* time can be caused by political decisions: DST is one example. There are multiple health and safety consequences of these misalignments. Our goal is that this article's facts and reasoning will be used to make clock choices that improve human lives.

## AUTHOR CONTRIBUTIONS

TR wrote the first draft of the manuscript, performed analyses of the MCTQ database, and generated the first version of the figures. EK and EW contributed to the conceptual content of the manuscript and co-wrote the manuscript following the first draft.

## FUNDING

EK was supported by the NIH K24-HL105664, R01-HL128538, and P01-AG009975.

## ACKNOWLEDGMENTS

Parts of this manuscript were presented at the Sapporo Symposium 2018 and published in the Sapporo Conference Book (Roenneberg et al., 2019). Permission was obtained from the editor of the book, Professor Ken-Ichi Honma, to whom we are grateful. We thank Luisa K. Pilz for her help with references and statistics.

## REFERENCES

Barnes, C. M., and Wagner, D. T. (2009). Changing to daylight saving time cuts into sleep and increases workplace injuries. *J. Appl. Psychol.* 94:1305. doi: 10.1037/a0015320

Benloucif, S., Burgess, H. J., Klerman, E. B., Lewy, A. J., Middleton, B., Murphy, P. J., et al. (2008). Measuring melatonin in humans. *J. Clin. Sleep Med.* 4, 66–69.

Bittman, E. L., Kaynard, A. H., Olster, D. H., Robinson, J. E., Yellon, S. M., and Karsch, F. J. (1985). Pineal melatonin mediates photoperiodic control of pulsatile luteinizing hormone secretion in the ewe. *Neuroendocrinology* 40, 409–418. doi: 10.1159/000124106

Borbély, A. A., Daan, S., Wirz-Justice, A., and Deboer, T. (2016). The two-process model of sleep regulation: a reappraisal. *J. Sleep Res.* 25, 131–143. doi: 10.1111/jsr.12371

Borel, A.-L., Pépin, J.-L., Nasse, L., Baguet, J.-P., Netter, S., and Benhamou, P.-Y. (2013). Short sleep duration measured by wrist actimetry is associated with deteriorated glycemic control in type 1 diabetes. *Diabetes Care* 36, 2902–2908. doi: 10.2337/dc12-2038

Borisenkov, M. F. (2011). Latitude of residence and position in time zone are predictors of cancer incidence, cancer mortality, and life expectancy at birth. *Chronobiol. Int.* 28, 155–162. doi: 10.3109/07420528.2010.541312

Borisenkov, M. F., Tserne, T. A., Panev, A. S., Kuznetsova, E. S., Petrova, N. B., Timonin, V. D., et al. (2017). Seven-year survey of sleep timing in Russian children and adolescents: chronic 1-h forward transition of social clock is associated with increased social jetlag and winter pattern of mood seasonality. *Biol. Rhythm Res.* 48, 3–12. doi: 10.1080/09291016.2016.1223778

Buhr, E. D., Yoo, S.-H., and Takahashi, J. S. (2010). Temperature as a universal resetting cue for mammalian circadian oscillators. *Science* 330, 379–385. doi: 10.1126/science.1195262

Cajochen, C., Frey, S., Anders, D., Späti, J., Bues, M., Pross, A., et al. (2011). Evening exposure to a light emitting diodes (LED)-backlit computer screen affects circadian physiology and cognitive performance. *Am. J. Physiol. Heart Circ. Physiol.* 110, 1432–1438. doi: 10.1152/japplphysiol.00165.2011

Carey, R. N., and Sarma, K. M. (2017). Impact of daylight saving time on road traffic collision risk: a systematic review. *BMJ Open* 7:e014319. doi: 10.1136/bmjopen-2016-014319

Chang, A.-M., Aeschbach, D., Duffy, J. F., and Czeisler, C. A. (2015). Evening use of light-emitting eReaders negatively affects sleep, circadian timing, and next-morning alertness. *Proc. Natl. Acad. Sci.* 112, 1232–1237. doi: 10.1073/pnas.1418490112

Chinoy, E. D., Duffy, J. F., and Czeisler, C. A. (2018). Unrestricted evening use of light-emitting tablet computers delays self-selected bedtime and disrupts circadian timing and alertness. *Physiol. Rep.* 6:e13692. doi: 10.14814/phy2.13692

Coren, S. (1996a). Accidental death and the shift to daylight savings time. *Percept. Mot. Skills* 83, 921–922. doi: 10.2466/pms.1996.83.3.921

Coren, S. (1996b). Daylight savings time and traffic accidents. *N. Engl. J. Med.* 334, 924–925. doi: 10.1056/NEJM199604043341416

de la Iglesia, H. O., Fernández-Duque, E., Golombek, D. A., Lanza, N., Duffy, J. F., Czeisler, C. A., et al. (2015). Access to electric light is associated with shorter sleep duration in a traditionally hunter-gatherer community. *J. Biol. Rhythms.* 30, 342–350. doi: 10.1177/0748730415590702

Díaz-Morales, J. F., and Escribano, C. (2015). Social jetlag, academic achievement and cognitive performance: understanding gender/sex differences. *Chronobiol. Int.* 32, 822–831. doi: 10.3109/07420528.2015.1041599

Dominoni, D. M., Helm, B., Lehmann, M., Dowse, H. B., and Partecke, J. (2013). Clocks for the city: circadian differences between forest and city songbirds. *Proc. R. Soc. B Biol. Sci.* 280:20130593. doi: 10.1098/rspb.2013.0593

Dvornyk, V., Vinogradova, O., and Nevo, E. (2003). Origin and evolution of circadian clock genes in prokaryotes. *Proc. Natl. Acad. Sci.* 100, 2495–2500. doi: 10.1073/pnas.0130099100

European Commission (2018). *Public Consultation on EU Summertime Arrangements - Report of Results*. Brussels: European Commission.

Ferguson, S. A., Preusser, D. F., Lund, A. K., Zador, P. L., and Ulmer, R. G. (1995). Daylight saving time and motor vehicle crashes: the reduction in pedestrian and vehicle occupant fatalities. *Am. J. Public Health* 85, 92–95. doi: 10.2105/AJPH.85.1.92

Ferrazzi, E., Romualdi, C., Ocello, M., Frighetto, G., Turco, M., Vigolo, S., et al. (2018). Changes in accident & emergency visits and return visits in relation to the enforcement of daylight saving time and photoperiod. *J. Biol. Rhythms* 33, 555–564. doi: 10.1177/0748730418791097

Fischer, D., Lombardi, D. A., Marucci-Wellman, H., and Roenneberg, T. (2017). Chronotypes in the US–influence of age and sex. *PLoS One* 12:e0178782. doi: 10.1371/journal.pone.0178782

Foster, R. G., Peirson, S. N., Wulff, K., Winnebeck, E., Vetter, C., and Roenneberg, T. (2013). Sleep and circadian rhythm disruption in social jetlag and mental illness. *Prog. Mol. Biol. Transl. Sci.* 119, 325–346. doi: 10.1016/B978-0-12-396971-2.00011-7

Giuntella, O., and Mazzonna, F. (2019). Sunset Time and the Economic Effects of Social Jetlag Evidence from US Time Zone Borders. *J. Health Econ.* 65, 210–226. doi: 10.1016/j.jhealeco.2019.03.007

Goodman, A., Page, A. S., Cooper, A. R., and International Children's Accelerometry Database (Icad) Collaborators (2014). Daylight saving time

as a potential public health intervention: an observational study of evening daylight and objectively-measured physical activity among 23,000 children from 9 countries. *Int. J. Behav. Nutr. Phys. Act.* 11:84. doi: 10.1186/1479-5868-11-84

Gray, T. R., and Jenkins, J. A. (2018). *Congress and the Political Economy of Daylight Saving Time*. Hoboken, NJ: Wiley.

Gu, F., Xu, S., Devesa, S. S., Zhang, F., Klerman, E. B., Graubard, B. I., et al. (2017). Longitude position in a time zone and cancer risk in the United States. *Cancer Epidemiol. Prev. Biomark.* 26, 1306–1311. doi: 10.1158/1055-9965.EPI-16-1029

Hadlow, N., Brown, S., Wardrop, R., Conradie, J., and Henley, D. (2018). Where in the world? Latitude, longitude and season contribute to the complex co-ordinates determining cortisol levels. *Clin. Endocrinol.* 89, 299–307. doi: 10.1111/cen.13754

Hadlow, N. C., Brown, S., Wardrop, R., and Henley, D. (2014). The effects of season, daylight saving and time of sunrise on serum cortisol in a large population. *Chronobiol. Int.* 31, 243–251. doi: 10.3109/07420528.2013.844162

Hafner, M., Stepanek, M., Taylor, J., Troxel, W. M., and Van Stolk, C. (2017). *Why Sleep Matters: The Economic Costs of Insufficient Sleep*. RAND: Santa Monica, CA

Haraszti, R. Á, Ella, K., Gyöngyösi, N., Roenneberg, T., and Káldi, K. (2014). Social jetlag negatively correlates with academic performance in undergraduates. *Chronobiol. Int.* 31, 603–612. doi: 10.3109/07420528.2013.879164

Hashizaki, M., Nakajima, H., Shiga, T., Tsutsumi, M., and Kume, K. (2018). A longitudinal large-scale objective sleep data analysis revealed a seasonal sleep variation in the Japanese population. *Chronobiol. Int.* 35, 933–945. doi: 10.1080/07420528.2018.1443118

Hicks, R. A., Lindseth, K., and Hawkins, J. (1983). Daylight saving-time changes increase traffic accidents. *Percept. Mot. Skills* 56, 64–66. doi: 10.2466/pms.1983.56.1.64

Horne, J. A., and Ostberg, O. (1976). A self-assessment questionnaire to determine morningness-eveningness in human circadian rhythms. *Int. J. Chronobiol.* 4, 97–110.

Huang, A., and Levinson, D. (2010). The effects of daylight saving time on vehicle crashes in Minnesota. *J. Safety Res.* 41, 513–520. doi: 10.1016/j.jsr.2010.10.006

Jagnani, M. (2018). *Poor Sleep: Sunset Time and Human Capital Production*. Available at: https://www.isid.ac.in/~epu/acegd2018/papers/MaulikJagnani.pdf

Janszky, I., and Ljung, R. (2008). Shifts to and from daylight saving time and incidence of myocardial infarction. *N. Engl. J. Med.* 359, 1966–1968. doi: 10.1056/nejmc0807104

Kamstra, M. J., Kramer, L. A., and Levi, M. D. (2000). Losing sleep at the market: the daylight saving anomaly. *Am. Econ. Rev.* 90, 1005–1011. doi: 10.1257/aer.90.4.1005

Kantermann, T., Juda, M., Merrow, M., and Roenneberg, T. (2007). The human circadian clock's seasonal adjustment is disrupted by daylight saving time. *Curr. Biol.* 17, 1996–2000. doi: 10.1016/j.cub.2007.10.025

Kehlmann, D. (2009). *Measuring the World*. New York, NY: Pantheon Books

Klerman, E. B., and Dijk, D.-J. (2005). Interindividual variation in sleep duration and its association with sleep debt in young adults. *Sleep* 28, 1253–1259. doi: 10.1093/sleep/28.10.1253

Knutsson, A. (2003). Health disorders of shift workers. *Occup. Med.* 53, 103–108. doi: 10.1093/occmed/kqg048

Koopman, A. D., Rauh, S. P., van 't Riet, E., Groeneveld, L., Van Der Heijden, A. A., Elders, P. J., et al. (2017). The association between social jetlag, the metabolic syndrome, and type 2 diabetes mellitus in the general population: the new Hoorn study. *J. Biol. Rhythms* 32, 359–368. doi: 10.1177/0748730417713572

Lahti, T., Nysten, E., Haukka, J., Sulander, P., and Partonen, T. (2010). Daylight saving time transitions and road traffic accidents. *J. Environ. Public Health* 2010:657167. doi: 10.1155/2010/657167

Lahti, T. A., Haukka, J., Lönnqvist, J., and Partonen, T. (2008). Daylight saving time transitions and hospital treatments due to accidents or manic episodes. *BMC Public Health* 8:74. doi: 10.1186/1471-2458-8-74

Levandovski, R., Dantas, G., Fernandes, L. C., Caumo, W., Torres, I., Roenneberg, T., et al. (2011). Depression scores associate with chronotype and social jetlag in a rural population. *Chronobiol. Int.* 28, 771–778. doi: 10.3109/07420528.2011.602445

Liu, C., Politch, J. A., Cullerton, E., Go, K., Pang, S., and Kuohung, W. (2017). Impact of daylight savings time on spontaneous pregnancy loss in in vitro fertilization patients. *Chronobiol. Int.* 34, 571–577. doi: 10.1080/07420528.2017.1279173

Lucas, R. J., Peirson, S. N., Berson, D. M., Brown, T. M., Cooper, H. M., Czeisler, C. A., et al. (2014). Measuring and using light in the melanopsin age. *Trends Neurosci.* 37, 1–9. doi: 10.1016/j.tins.2013.10.004

Manfredini, R., Fabbian, F., De Giorgi, A., Zucchi, B., Cappadona, R., Signani, F., et al. (2018). Daylight saving time and myocardial infarction: should we be worried? a review of the evidence. *Eur. Rev. Med. Pharmacol. Sci.* 22, 750–755. doi: 10.26355/eurrev_201802_14306

Monk, T. H., and Aplin, L. C. (1980). Spring and autumn daylight saving time changes: studies of adjustment in sleep timings, mood, and efficiency. *Ergonomics* 23, 167–178. doi: 10.1080/00140138008924730

Monk, T. H., and Folkard, S. (1976). Adjusting to the changes to and from daylight saving time. *Nature* 261:688. doi: 10.1038/261688a0

Olders, H. (2003). Average sunrise time predicts depression prevalence. *J. Psychosom. Res.* 55, 99–105. doi: 10.1016/S0022-3999(02)00479-478

Parsons, M. J., Moffitt, T. E., Gregory, A. M., Goldman-Mellor, S., Nolan, P. M., Poulton, R., et al. (2015). Social jetlag, obesity and metabolic disorder: investigation in a cohort study. *Int. J. Obes.* 39:842. doi: 10.1038/ijo.2014.201

Partonen, T. (2015). Chronotype and health outcomes. *Curr. Sleep Med. Rep.* 1, 205–211. doi: 10.1007/s40675-015-0022-z

Pilz, L. K., Keller, L. K., Lenssen, D., and Roenneberg, T. (2018a). Time to rethink sleep quality: PSQI scores reflect sleep quality on workdays. *Sleep* 41:zsy029. doi: 10.1093/sleep/zsy029

Pilz, L. K., Levandovski, R., Oliveira, M. A. B., Hidalgo, M. P., and Roenneberg, T. (2018b). Sleep and light exposure across different levels of urbanisation in Brazilian communities. *Sci. Rep.* 8:11389. doi: 10.1038/s41598-018-29494-29494

Press Release University of Salzburg (2018). *Permanent Summer Time: Would we Really Become Fatter, More Stupid, and Grumpier?* Available at: http://uni-salzburg.at/index.php?id=41697 (accessed March 9, 2019).

Reutrakul, S., Hood, M. M., Crowley, S. J., Morgan, M. K., Teodori, M., Knutson, K. L., et al. (2013). Chronotype is independently associated with glycemic control in type 2 diabetes. *Diabetes Care* 36, 2523–2529. doi: 10.2337/dc12-2697

Reutrakul, S., Siwasaranond, N., Nimitphong, H., Saetung, S., Chirakalwasan, N., Ongphiphadhanakul, B., et al. (2015). Relationships among sleep timing, sleep duration and glycemic control in Type 2 diabetes in Thailand. *Chronobiol. Int.* 32, 1469–1476. doi: 10.3109/07420528.2015.1105812

Ripley, A. (1974). *Senate Votes Return to Standard Time For Four Months and Sends Bill to Ford. N. Y. Times*. Available at: https://www.nytimes.com/1974/10/01/archives/senate-votes-return-to-standard-time-for-four-months-and-sends-bill.html (accessed April 1, 2019).

Roenneberg, T. (2004). The decline in human seasonality. *J. Biol. Rhythms* 19, 193–195. doi: 10.1177/0748730404264863

Roenneberg, T., Allebrandt, K. V., Merrow, M., and Vetter, C. (2012). Social jetlag and obesity. *Curr. Biol.* 22, 939–943. doi: 10.1016/j.cub.2012.03.038

Roenneberg, T., Daan, S., and Merrow, M. (2003a). The art of entrainment. *J. Biol. Rhythms* 18, 183–194. doi: 10.1177/0748730403018003001

Roenneberg, T., Wirz-Justice, A., and Merrow, M. (2003b). Life between clocks: daily temporal patterns of human chronotypes. *J. Biol. Rhythms* 18, 80–90. doi: 10.1177/0748730402239679

Roenneberg, T., Kantermann, T., Juda, M., Vetter, C., and Allebrandt, K. V. (2013). Light and the human circadian clock. *Handb. Exp. Pharmacol.* 217, 311–331. doi: 10.1007/978-3-642-25950-0_13

Roenneberg, T., Kuehnle, T., Juda, M., Kantermann, T., Allebrandt, K., Gordijn, M., et al. (2007a). Epidemiology of the human circadian clock. *Sleep Med. Rev.* 11, 429–438.

Roenneberg, T., Kumar, C. J., and Merrow, M. (2007b). The human circadian clock entrains to sun time. *Curr. Biol.* 17, R44–R45. doi: 10.1016/j.cub.2006.12.011

Roenneberg, T., Winnebeck, E. C., and Klerman, E. B. (2019). "Time Wars," in *Proceedings of the 2018 Sapporo Conference on Biological Rhythms Sapporo Symposia*, (Sapporo: Hokkaido University Press).

Rutters, F., Lemmens, S. G., Adam, T. C., Bremmer, M. A., Elders, P. J., Nijpels, G., et al. (2014). Is social jetlag associated with an adverse endocrine, behavioral, and cardiovascular risk profile? *J. Biol. Rhythms* 29, 377–383. doi: 10.1177/0748730414550199

Saini, C., Brown, S. A., and Dibner, C. (2015). Human peripheral clocks: applications for studying circadian phenotypes in physiology and pathophysiology. *Front. Neurol.* 6:95. doi: 10.3389/fneur.2015.00095

Samson, D. R., Crittenden, A. N., Mabulla, I. A., Mabulla, A. Z., and Nunn, C. L. (2017a). Chronotype variation drives night-time sentinel-like behaviour in hunter–gatherers. *Proc. R. Soc. B Biol. Sci.* 284:20170967. doi: 10.1098/rspb.2017.0967

Samson, D. R., Crittenden, A. N., Mabulla, I. A., Mabulla, A. Z., and Nunn, C. L. (2017b). Hadza sleep biology: evidence for flexible sleep-wake patterns in hunter-gatherers. *Am. J. Phys. Anthropol.* 162, 573–582. doi: 10.1002/ajpa.23160

Schneider, A.-M., and Randler, C. (2009). Daytime sleepiness during transition into daylight saving time in adolescents: are owls higher at risk? *Sleep Med.* 10, 1047–1050. doi: 10.1016/j.sleep.2008.08.009

Schnurbein, J., von Boettcher, C., Brandt, S., Karges, B., Dunstheimer, D., Galler, A., et al. (2018). Sleep and glycemic control in adolescents with type 1 diabetes. *Pediatr. Diabetes* 19, 143–149. doi: 10.1111/pedi.12538

Scott, A. J. (2000). Shift work and health. *Prim. Care* 27, 1057–1079.

Sipilä, J. O. T., Ruuskanen, J. O., Rautava, P., and Kytö, V. (2016). Changes in ischemic stroke occurrence following daylight saving time transitions. *Sleep Med.* 2, 20–24. doi: 10.1016/j.sleep.2016.10.009

Stothard, E. R., McHill, A. W., Depner, C. M., Birks, B. R., Moehlman, T. M., Ritchie, H. K., et al. (2017). Circadian entrainment to the natural light-dark cycle across seasons and the weekend. *Curr. Biol.* 27, 508–513. doi: 10.1016/j.cub.2016.12.041

Uk Time Zone History (2019). *Time Zone History of the United Kingdom*. Available at: https://www.timeanddate.com/time/uk/time-zone-background.html (accessed April 1, 2019).

VoPham, T., Weaver, M. D., Vetter, C., Hart, J. E., Tamimi, R. M., Laden, F., et al. (2018). Circadian misalignment and hepatocellular carcinoma incidence in the United States. *Cancer Epidemiol. Prev. Biomark.* 27, 719–727. doi: 10.1158/1055-9965.EPI-17-1052

Wehr, T. A., Aeschbach, D., and Duncan, W. C. (2001). Evidence for a biological dawn and dusk in the human circadian timing system. *J. Physiol.* 535, 937–951. doi: 10.1111/j.1469-7793.2001.t01-1-00937.x

White, T. M., Terman, M., Musa, G. C., and Avery, D. H. (2006). The incidence of winter depression varies within time zone. *Chronobiol. Int.* 23, 743–745.

Williams, G. E. (2000). Geological constraints on the Precambrian history of Earth's rotation and the Moon's orbit. *Rev. Geophys.* 38, 37–59. doi: 10.1029/1999RG900016

Wirz-Justice, A., and Benedetti, F. (2019). Perspectives in affective disorders: clocks and sleep. *Eur. J. Neurosci.* doi: 10.1111/ejn.14362 [Epub ahead of print].

Wittmann, M., Dinich, J., Merrow, M., and Roenneberg, T. (2006). Social jetlag: misalignment of biological and social time. *Chronobiol. Int.* 23, 497–509. doi: 10.1080/07420520500545979

Wittmann, M., Paulus, M., and Roenneberg, T. (2010). Decreased psychological well-being in late 'chronotypes' is mediated by smoking and alcohol consumption. *Subst. Use Misuse* 45, 15–30. doi: 10.3109/10826080903498952

Wong, P. M., Hasler, B. P., Kamarck, T. W., Muldoon, M. F., and Manuck, S. B. (2015). Social jetlag, chronotype, and cardiometabolic risk. *J. Clin. Endocrinol. Metab.* 100, 4612–4620. doi: 10.1210/jc.2015-2923

Wright, K. P. Jr., McHill, A. W., Birks, B. R., Griffin, B. R., Rusterholz, T., and Chinoy, E. D. (2013). Entrainment of the human circadian clock to the natural light-dark cycle. *Curr. Biol.* 23, 1554–1558. doi: 10.1016/j.cub.2013.06.039

Yetish, G., Kaplan, H., Gurven, M., Wood, B., Pontzer, H., Manger, P. R., et al. (2015). Natural sleep and its seasonal variations in three pre-industrial societies. *Curr. Biol.* 25, 2862–2868. doi: 10.1016/j.cub.2015.09.046

**Conflict of Interest Statement:** The authors declare that the research was conducted in the absence of any commercial or financial relationships that could be construed as a potential conflict of interest.

frontiers in Physiology

CORRECTION
published: 12 September 2019
doi: 10.3389/fphys.2019.01177

# Corrigendum: Daylight Saving Time and Artificial Time Zones – A Battle Between Biological and Social Times

*Till Roenneberg*[1]*, *Eva C. Winnebeck*[1] and *Elizabeth B. Klerman*[2]

[1] Institute of Medical Psychology, Ludwig Maximilian University of Munich, Munich, Germany, [2] Division of Sleep and Circadian Disorders, Brigham and Women's Hospital, Harvard Medical School, Boston, MA, United States

OPEN ACCESS

**Edited and reviewed by:**
Sara Montagnese,
University of Padova, Italy

***Correspondence:**
Till Roenneberg
roenneberg@lmu.de

**Specialty section:**
This article was submitted to Chronobiology, a section of the journal Frontiers in Physiology

**Received:** 26 August 2019
**Accepted:** 30 August 2019
**Published:** 12 September 2019

**Citation:**
Roenneberg T, Winnebeck EC and Klerman EB (2019) Corrigendum: Daylight Saving Time and Artificial Time Zones – A Battle Between Biological and Social Times. Front. Physiol. 10:1177. doi: 10.3389/fphys.2019.01177

**Keywords: circadian, social jetlag, circadian misalignment, time zones, entrainment (light)**

## A Corrigendum on

**Daylight Saving Time and Artificial Time Zones – A Battle Between Biological and Social Times**
*by Roenneberg, T., Winnebeck, E. C., and Klerman, E. B. (2019). Front. Physiol. 10:944. doi: 10.3389/fphys.2019.00944*

In the original article, there was a mistake in **Figure 2B** as published. In the map, the area of Germany was duplicated and appeared south-west of Norway. The corrected **Figure 2** appears below.

The authors apologize for this error and state that this does not change the scientific conclusions of the article in any way. The original article has been updated.

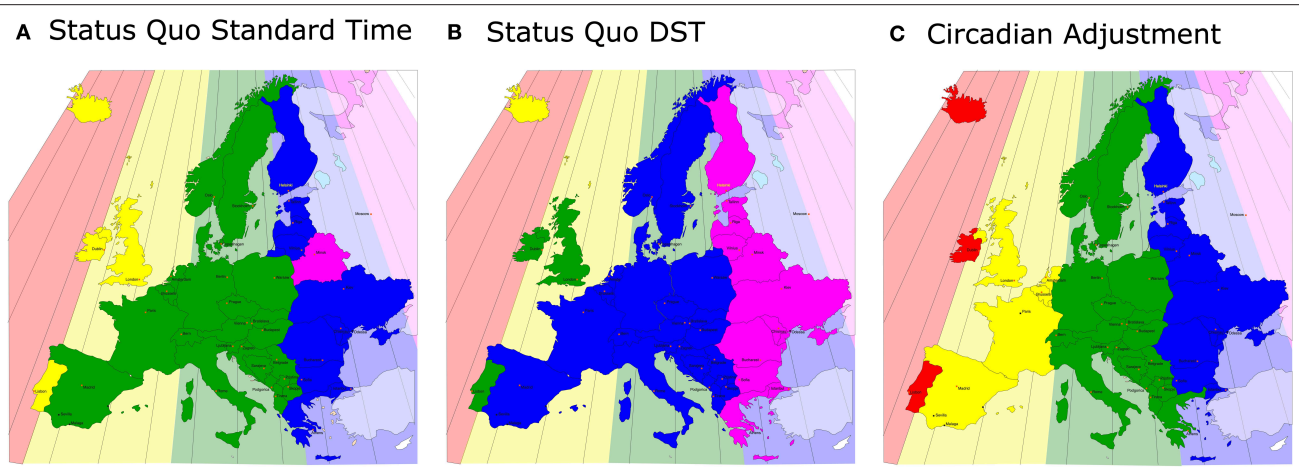


**FIGURE 2 |** A map of Europe equivalent to Figure 1: the actual, sun-based time zones are drawn as color-coded backgrounds and the social time zones are shown in the same (stronger) colors in front. Even under Standard Time, the western areas of the social time zones are far away from the respective eastern borders of the sun-based time zones **(A)**, this discrepancy increases by 1 h under DST **(B)** (note that Iceland is on perennial DST). **(C)** A solution to the problem: the political borders of Europe are actually ideal for the correct, chronobiological separations into time zones, so that in no area of Europe the social clock has to be discrepant from the sun clock by more than 30 min.

frontiers in Physiology

BRIEF RESEARCH REPORT
published: 22 November 2019
doi: 10.3389/fphys.2019.01377

# Long-Term Effects of Altered Photoperiod During Pregnancy on Liver Gene Expression of the Progeny

*Pamela Carmona[1,2], Bárbara Pérez[1], Carlos Trujillo[1,3], Gabriel Espinosa[1], Fernando Miranda[1], Natalia Mendez[4], Claudia Torres-Farfan[4], Hans G. Richter[4], Karina Vergara[4], Priscilla Brebi[2,5] and José Sarmiento[1]**

*[1] Laboratorio de Cronoinmunología, Instituto de Fisiología, Facultad de Medicina, Universidad Austral de Chile, Valdivia, Chile, [2] Programa de Doctorado en Ciencias Médicas, Universidad de La Frontera, Temuco, Chile, [3] Programa de Doctorado en Ciencias Veterinarias, Universidad Austral de Chile, Valdivia, Chile, [4] Laboratorio de Cronobiología del Desarrollo, Instituto de Anatomía, Histología y Patología, Facultad de Medicina, Universidad Austral de Chile, Valdivia, Chile, [5] Laboratorio de Patología Molecular, Departamento de Patología, Facultad de Medicina, Universidad de La Frontera, Temuco, Chile*

OPEN ACCESS

**Edited by:**
*Rodolfo Costa, University of Padua, Italy*

**Reviewed by:**
*Urs Albrecht, Université de Fribourg, Switzerland*
*Erik D. Herzog, Washington University in St. Louis, United States*

***Correspondence:**
*José Sarmiento*
*jsarmien@uach.cl*

**Specialty section:**
*This article was submitted to Chronobiology, a section of the journal Frontiers in Physiology*

**Received:** *11 August 2019*
**Accepted:** *18 October 2019*
**Published:** *22 November 2019*

**Citation:**
*Carmona P, Pérez B, Trujillo C, Espinosa G, Miranda F, Mendez N, Torres-Farfan C, Richter HG, Vergara K, Brebi P and Sarmiento J (2019) Long-Term Effects of Altered Photoperiod During Pregnancy on Liver Gene Expression of the Progeny. Front. Physiol. 10:1377. doi: 10.3389/fphys.2019.01377*

Experimental and epidemiological studies have revealed a relationship between an adverse intrauterine environment and chronic non-communicable disease (NCD) like cardiovascular disease (CVD) in adulthood. An important risk factor for CVD is the deregulation of the fibrinolytic system particularly high levels of expression of plasminogen activator inhibitor 1 (*Pai-1*). Chronic exposure to altered photoperiod disrupts the circadian organization of physiology in the pregnant female, known as gestational chronodisruption, and cause long-term effects on the adult offspring's circadian physiology. The *Pai-1* expression is regulated by the molecular components of the circadian system, termed clock genes. The present study aimed to evaluate the long-term effects of chronic photoperiod shifts (CPS) during pregnancy on the expression of the clock genes and the fibrinolytic system in the liver of adult male offspring. Our results using an animal model demonstrated statistically significant differences at the transcriptional level in males gestated under CPS. At 90 days of postnatal age, the liver transcript levels of the clock gene *Bmal1* were downregulated, whereas *Rorα*, *Rorγ*, *Nfil3,* and *Pai-1* were upregulated. Our data indicate that CPS during pregnancy affects gene expression in the liver of male adult progeny, showing that alteration of the photoperiod in the mother's environment leads to persistent effects in the offspring. In conclusion, these results reveal for the first time the long-term effects of gestational chronodisruption on the transcriptional activity of one well-established risk factor associated with CVD in the adult male offspring.

**Keywords: cardiovascular disease, fibrinolytic system, *Pai-1*, clock genes, gestational chronodisruption, DOHaD**

**Abbreviations:** CCG, clock-controlled gene; CPS, chronic photoperiod shifts; CVD, cardiovascular disease; E18, embryonic day 18; LD, light dark; NCD, non-communicable disease; *Pai-1*, plasminogen activator inhibitor-1; *Plg*, plasminogen; P1, postnatal day 1; P60, postnatal day 60; P90, postnatal day 90; P120, postnatal day 120; ROR, retinoid-related orphan receptor; RORE, ROR-response elements; tPA, tissue Plasminogen Activator; uPA, urokinase Plasminogen Activator; ZT, zeitgeber time.

## INTRODUCTION

The environment during early life influences the risk of developing pathophysiological processes later; the field recognized as the developmental origins of health and disease (DOHaD) (Calkins et al., 2011; Capra et al., 2013; Hanson and Gluckman, 2014). In particular shows an association with NCDs (Fowden et al., 2006; Marsh et al., 2011) as CVD (Thompson and Trask, 2016).

In modern society, exposure to environmental light at night (e.g., chronic shift work, work at night), disarranging the internal biological clock; thus producing a significant disturbance of the circadian organization of physiology known as chronodisruption (Erren and Reiter, 2009). Circadian rhythms are intrinsic biological oscillations with a 24-h period driven by the circadian timing system, coordinating physiology and behavior with the daily light/dark cycle (Mazzoccoli et al., 2012; Partch et al., 2014; Tarquini and Mazzoccoli, 2017). This system is organized by the central clock, located in the suprachiasmatic nucleus; which is entrained by the light/dark cycle as a dominant signal, in addition to several peripheral clocks located throughout the body. At the cell level, circadian rhythmicity relies on clock gene expression in central and accessory interlocking transcription/translation feedback loops (TTFL) (Mohawk et al., 2013; Curtis et al., 2014; Takahashi, 2016). In turn, these core clock genes promote the expression of downstream genes (CCGs) (Albrecht, 2012; Liu and Chu, 2013). Significant changes in the expression of clock genes can affect physiological processes controlled by the biological clock and have been associated with the development of NCDs (Plano et al., 2017; Touitou et al., 2017).

The misalignment of the maternal circadian system (gestational chronodisruption) impacts fetal health (Serón-Ferré et al., 2012, 2013). This field is of great interest because of the potential long-term effects on the adult offspring's health and disease status (Amaral et al., 2014; Varcoe et al., 2017; Richter et al., 2018). The available evidence has demonstrated different consequences of chronodisruption on maternal physiology (Gatford et al., 2019). In animal model, the maternal exposure to CPS disrupted the biological clocks in the pregnant female, altering physiological parameters throughout gestation such as the circadian profile of plasma hormones, changes in the liver metabolic gene expression and alterations in the clock gene expression profile (Varcoe et al., 2013; Mendez et al., 2016). Meanwhile, in the adult offspring gestational chronodisruption induced effects such as hyperleptinemia, hyperinsulinemia, impaired glucose tolerance (Varcoe et al., 2011); alterations in the plasma circadian profile of melatonin and corticosterone (Mendez et al., 2016); as well as alteration of adrenal endocrine messengers. In fact, there is strong evidence suggesting that the adrenal gland loses the ability to respond to ACTH (Mendez et al., 2016; Salazar et al., 2018). Given that the endocrine adrenal outputs play a key role in the development and entrainment of the fetal clock in the suprachiasmatic nucleus (Čečmanová et al., 2019), coordinating metabolic responses and acting as time-giving signals to other peripheral circadian oscillators such as the liver (Pezük et al., 2012); long-term alterations of adrenal function can lead to multiple pathophysiological processes.

The liver is a well-described peripheral clock and as such, its physiology is controlled by circadian rhythms, the clock regulates the transcription of CCGs that participate in a wide array of the physiological process in the liver (Reinke and Asher, 2016; Tahara and Shibata, 2016; Zwighaft et al., 2016) and the evidence supports that synchronized liver clockwork machinery develops gradually during ontogenesis (Sumová et al., 2008). On the other hand, the liver is the major site of *Pai-1* synthesis, being regulated transcriptionally by endocrine signals of the adrenal gland, which in turn strongly responds to light input (Dimova and Kietzmann, 2008; Aoshima et al., 2014). Also, *Pai-1* is a CCG (Haus, 2007) and its expression is upregulated through binding of the CLOCK: BMAL heterodimer to E-box sites of the *Pai-1* gene promoter region (Maemura et al., 2000; Schoenhard et al., 2003; Ohkura et al., 2006). Also, the transcription of *Pai-1* is promoted by RORα and repressed by REV-ERBα acting on RORE sites (Wang et al., 2006), all of them important members of the clock molecular machinery. Of note, epidemiological studies identify PAI-1 as a risk factor for CVD (Tofler et al., 2016; Jung et al., 2018).

Our hypothesis is that gestational chronodisruption promotes changes in the adult offspring, specifically, alterations of the regulation of molecular machinery of the liver clock genes; which in turn regulate the transcriptional pattern of the *Pai-1* in the liver. To test our hypothesis, we used a rat model of gestational chronodisruption. Our specific aims were to investigate the impact of prenatal CPS in the liver of adult male progeny on (1) clock gene transcription patterns; and (2) the fibrinolytic system, particularly in the *Pai-1* transcriptional levels.

## MATERIALS AND METHODS

### Animals

Animal handling and care followed the Guide for the Care and Use of Laboratory Animals of the Institute for Laboratory Animal Research of the National Research Council. The protocols were approved by the Bioethics Commission of the Universidad Austral de Chile (CBA number 267/2016).

The animals were maintained in a control (standard) photoperiod [12 h light, 12 h dark cycle; lights on at 7:00 AM (ZT0), lights off at 7:00 PM (ZT12)]; ∼400 lux at the head level, temperature (18–20°C), humidity (∼48%), food and water were available *ad libitum* (Mendez et al., 2016; Salazar et al., 2018). Sprague Dawley rats (obtained from Charles River Laboratories International Inc.) were mated and raised in our animal facility. Timed-pregnant females were used in the study, and the day in which spermatozoa were observed in the smear of the vaginal contents was considered embryonic day 0 (E0). The pregnant females were separated by weight pairing and allocated to the following two photoperiods: light/dark (LD; control photoperiod) and CPS, using the same protocol reported by Mendez et al. (2016). Briefly, pregnant females were exposed to lighting

schedule manipulation every 3–4 days, reversing the photoperiod completely, during 18 days of pregnancy (**Figure 1**). At 18 days of gestation, the mothers returned to a control 24-h photoperiod (12:12, lights on at ZT0) and continued in this photoperiod thereafter.

## Effects of Gestational Chronodisruption on Daily Rhythms and mRNA Expression in Adult Offspring

After birth, both dams and pups from each pregnancy condition (LD; $n$ = 12 and CPS; $n$ = 6 mothers) were kept under control photoperiod and litters were weighed at postnatal age 1 day (P1) and homogenized to 10 individuals (five males and females), in order to avoid variations in weight gain. Pups were weaned at 21 days old, with the males being raised in the control photoperiod (LD) to be studied at P90 (LD and CPS, $n$ = 30 each group).

Body weight was measured from 30 days old, every 7 days. Males from each pregnancy condition were euthanized at P90 every 4 h for six samplings over 20 h, in LD and CPS ($n$ = 5/each time point), starting at ZT1 and ending at ZT21. To avoid litter effects, each clock time point contained animals from different mothers; thus, no siblings were used at the same time point. Briefly, male rats were deeply anesthetized (isoflurane 3.5%, Baxter Laboratories), a blood sample was collected from the

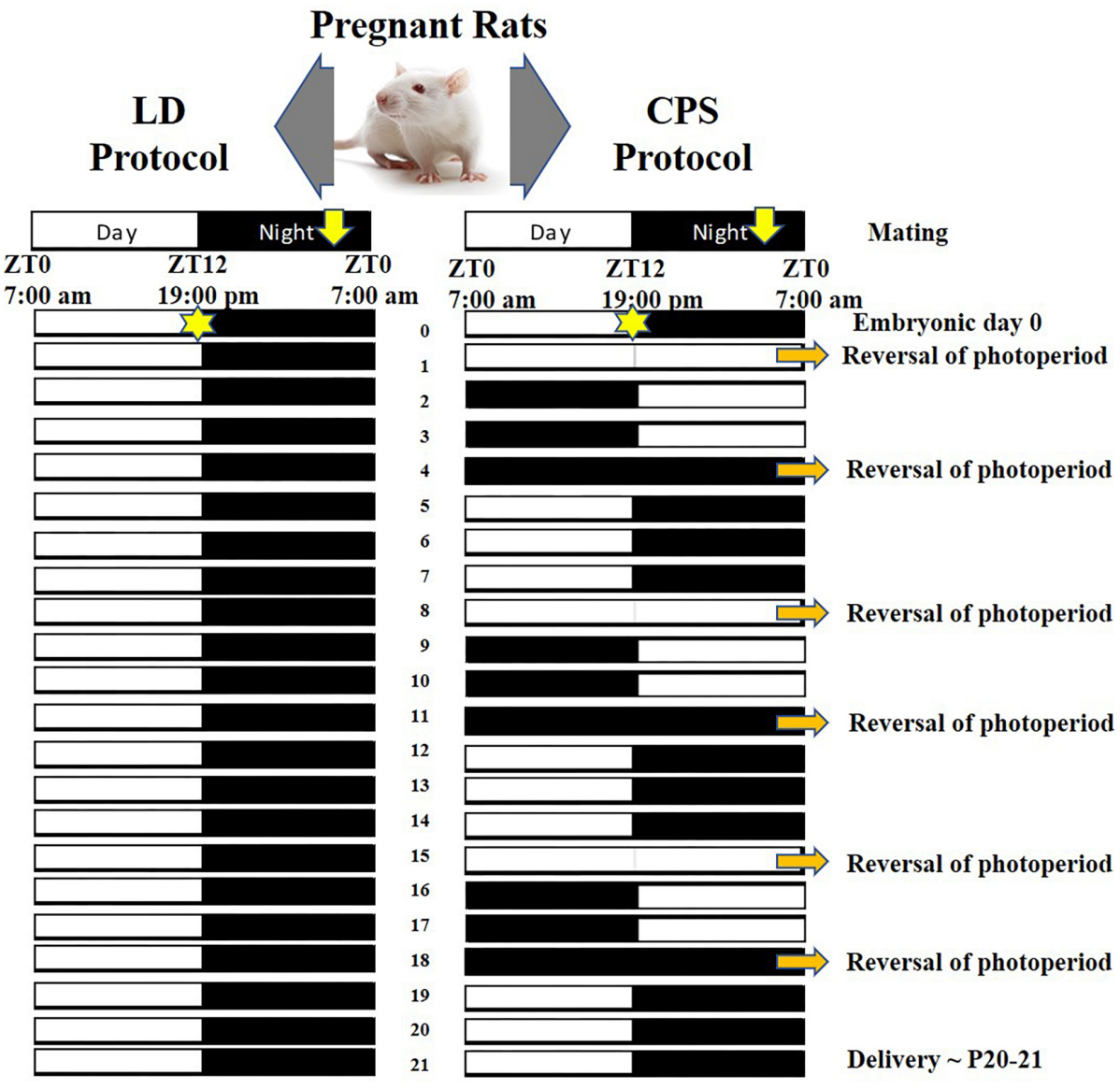


**FIGURE 1 |** Light dark (LD) and CPS protocol scheme during pregnancy. **(Left)** LD control or standard protocol; 12 h light, 12 h dark cycle [lights on at 7:00 AM (ZT0), lights off at 7:00 PM (ZT12)]. **(Right)** CPS protocol; lighting schedule manipulation every 3–4 days, some days of constant light or constant darkness are required to reversing the photoperiod completely (orange narrow) (Mendez et al., 2016).

vena cava, and then an overdose of T61 (0.5 ml/kg body weight; Merck Animal Health, Intervet Canada Corp., Kirkland, QC, Canada) was delivered at the same site. Organs were collected, weighed and stored in RNA stabilization solution (RNAlater$^{TM}$ Invitrogen) at 4°C for 24 h and subsequently at −20°C in our tissue bank.

## RNA Extraction and Quantitative Real-Time PCR (RT-PCR) Analysis of the Liver

Relative quantification by RT-PCR was used to evaluate the mRNA expression of clock genes and fibrinolytic system genes at P90. Total RNA was extracted using the SV Total RNA Isolation System (Promega) according to the manufacturer's instructions. The amount of 2.0 μg of total RNA was reverse transcribed using random primers (Promega) and MLT-V reverse transcriptase (Promega). RT-PCR was performed using primers described in **Supplementary Table 1** and KAPA SYBR FAST quantitative PCR master mix (Kapa Biosystems, Inc.). Quantitative PCR was carried out in a Rotor-Gene Q real-time platform (QIAGEN). Serial dilutions of cDNA were amplified by real-time PCR using specific primers for target and reference gene and determining template dilution for the sample's measurements. A melting curve analysis was performed on each sample after the final cycle to ensure that a single product was obtained. Relative amounts of all mRNAs were calculated by the comparative ΔΔ cycle threshold method using the equation $2^{-\Delta\Delta Ct}$ to linearize the data and then perform the statistical analysis (Livak and Schmittgen, 2001) and normalized to the corresponding 18S-rRNA housekeeping level. For the analysis of daily rhythms we follow the Guidelines for Genome-Scale Analysis of Biological Rhythms (Hughes et al., 2017) and three independent methods were used; single cosinor (Refinetti et al., 2007), JTK_Cycle (Hughes et al., 2010), and RAIN's longitudinal mode (Thaben and Westermark, 2014).

## Statistical Analysis

Statistical analyses were performed using the IBM SPSS software 20.0. The normality of data distribution was determined by the Shapiro Wilk test, and homogeneity of variances was analyzed by Levene's test. The body weight was analyzed by a two-way ANOVA test for repeated measures in one of the factors, with the Bonferroni adjustment and data were expressed as mean ± SEM. Transcript levels between the two groups were analyzed by the Mann–Whitney *U* test and Student's *t*-test.

# RESULTS

## Impact of Gestational CPS on Liver Clock Genes Expression in Adult Male Offspring

The body weight data showed that gestational CPS in both, newborn male (P1) and adult male (P90) offspring was statistically greater than in LD progeny (P1: 7.1 ± 0.09 g CPS vs. 6.78 ± 0.07 g LD, unpaired *t*-test $p = 0.01$; P90: 499.2 ± 5.9 g CPS vs. 476.2 ± 7.9 g LD, ANOVA two way test for repeated measures with Bonferroni adjustment $p = 0.032$). We found no differences in the weight of female offspring at P1, size of the litters, and weight of the liver, lung, thymus, and spleen at P90 between LD and CPS (**Supplementary Table 2** and **Supplementary Figure 1**). Next, we evaluated the effects of gestational CPS on the liver clock genes expression at the transcript level in the male offspring at P90. Our results showed daily rhythm expression of *Bmal1* in the offspring from both conditions (**Figure 2A**, left and **Supplementary Tables 3–5**), but with significantly reduced mRNA expression in the progeny gestated under CPS conditions (**Figure 2A**, right). Interestingly we found that the daily peak of *Clock* and *Nfil3* gene at transcript level was changed by 4 h (ZT 3.7, 4.0, and 1 to 0.4, 0.0, 21 for Cosinor, JKT_Cycle and RAN, respectively) between CPS and LD gestated adult progeny (**Supplementary Tables 3–5**). *Bmal1* and *Clock* are an important positive component of the central loop and promotes the expression of other clock genes. For this reason, we determined the transcript level of other genes of the central loop of the molecular clock (*Clock*, *Per1*, *Per2*, *Per3*, *Cry1,* and *Cry2*). The analysis of results showed that the daily peak of expression in the control condition (LD) of all these genes was in agreement with the reported ZT in other studies on the adult rat (Sládek et al., 2007; **Figure 2B**, black dots and **Supplementary Tables 3–5**). More importantly, the genes positively regulated by *Bmal1* of the central loop evaluated here showed a similar daily rhythm of expression in both progenies with no remarkable effect on the daily rhythm pattern (**Figure 2B** and **Supplementary Tables 3–5**) or total expression (data not shown) at the mRNA level in LD and CPS male offspring.

Interlocked with the central loop there is an additional well-established secondary or accessory loop that involves REV-ERB and RORs transcription factors which influence negatively and positively, respectively on *Bmal1* transcription by binding to its promoter site (RORE site), and also regulate the expression of the Nuclear Factor Interleukin 3 gene (Nfil3). Remarkable differences in the daily expression were found in two clockwork components of the accessory loop. The *Rorα* and *Rorγ* components of this loop were significantly increased at the mRNA level in the CPS male offspring (**Figures 3A,B**). Our results showed that the transcriptional level of *Nfil3* was increased in males gestated under CPS conditions (**Figure 3C**), with a clear acrophase in the active phase (dark phase) of the daily expression (**Figure 3C**, red dots and **Supplementary Tables 3–5**). Interestingly, *Rorα* displayed a pattern of daily rhythm only in adult males gestated in CPS with an acrophase at active phase (**Figure 3A**, red dots and **Supplementary Tables 3–5**). Differences at individuals time points but not in the daily total expression were found in the main repressor component of the accessory loop *Rev-Erbα* between CPS and LD male progeny (**Figure 3D**, right and left, respectively).

## Impact of Gestational CPS on the Expression of the Fibrinolytic System in the Adult Offspring

Alterations of fibrinolytic activity mediated by deregulation in the expression of its components have been associated with a

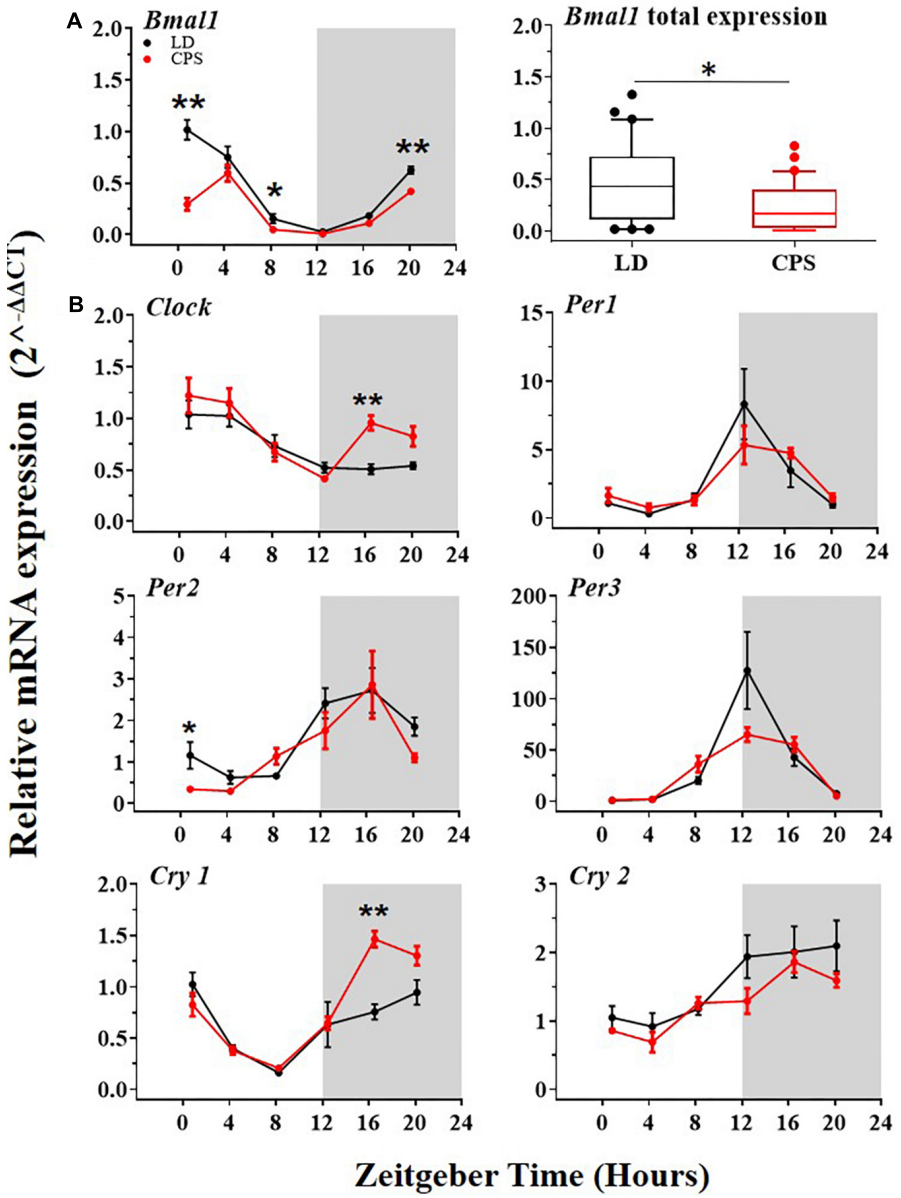


**FIGURE 2 |** The transcription level of clock genes of the central loop in the liver from 90-day-old male rats by RT-PCR. [**A**(left),**B**] Detection of daily rhythm. Black symbols represent males gestated under control conditions (LD, black dots), and red symbols indicate males gestated in CPS (CPS, red dots). Males from each pregnancy condition (LD: $n = 12$ and CPS: $n = 6$ mothers) in LD and CPS offspring ($n = 5$/each time point). Time is expressed as zeitgeber time (ZT), with ZT0 as time lighting onset and ZT12 as lighting end; the gray bar indicates lights off. The RAIN's longitudinal mode, JTK_Cycle and the single cosinor method were used to determine daily rhythm ($p < 0.05$), solid black and red lines represent the detection of a 24-h daily rhythm for the three methods. (**A**,left) Data for *Bmal1* are shown. $^*p < 0.05$ indicate differences between LD and CPS for time point (Mann–Whitney *U* test). (**A**,right) Daily total expression. Data for *Bmal1*, minimum, first quartile, median, third quartile, and maximum were for LD offspring: *Bmal1*: 0.02, 0.11, 0.44, 0.73, and 1.33; and for CPS offspring: 0.01, 0.03, 0.17, 0.40, and 0.83. $^*p < 0.05$. Different from LD (Mann–Whitney *U* test). **(B)** Data for other clock genes are shown $^*p < 0.05$, $^{**}p < 0.01$ Different from LD for time point (Mann–Whitney *U* test).

risk factor for CVD (Mavri et al., 2004; Oishi, 2009). Also, in the liver, the expression of important components of the fibrinolytic system is controlled by the circadian system. Our results showed that males gestated in CPS displayed significant differences in the mRNA expression level in important components of the fibrinolytic system relative to the LD group. More specifically, the main inhibitor of this system, *Pai-1*, was increased (**Figure 4A**, right); in contrast, the precursor of plasmin, *Plg* and *tPA*, were reduced (**Figures 4B,C**, right). On the other hand, *uPA* did not show significant differences between the two progenies (**Figure 4D**, right). Regarding daily oscillations of mRNA components of the fibrinolytic system evaluated here, we only

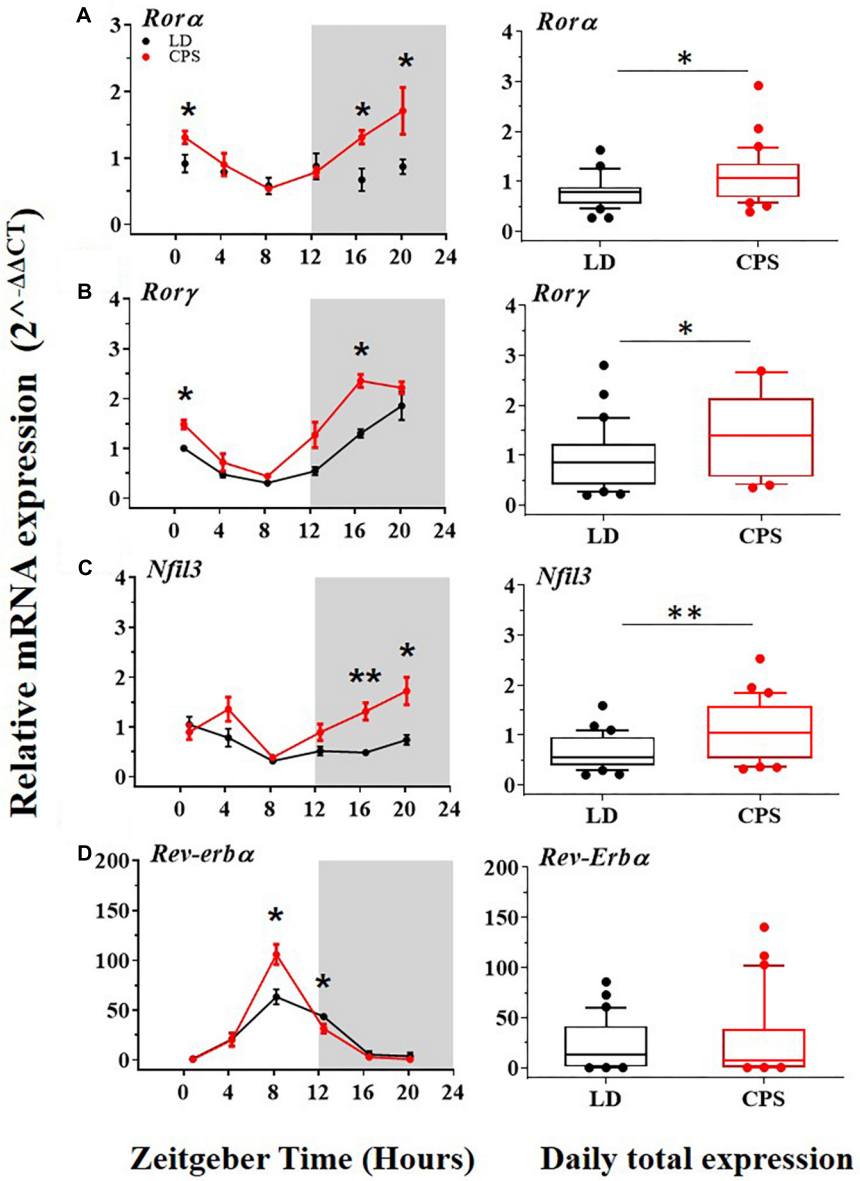


**FIGURE 3 |** The transcription level of clock genes of the accessory loop in the liver from 90-day-old male rats by RT-PCR. (**A–D**,left) Detection of daily rhythm. Black symbols represent males gestated under control conditions (LD, black dots), and red symbols indicate males gestated in CPS (CPS, red dots). Males from each pregnancy condition (LD: $n = 12$ and CPS: $n = 6$ mothers) in LD and CPS offspring ($n = 5$/each time point). Time is expressed as zeitgeber time (ZT), with ZT0 as time lighting onset and ZT12 as lighting end; the gray bar indicates lights off. The RAIN's longitudinal mode, JTK_Cycle and the single cosinor method were used to determine daily rhythm ($p < 0.05$), solid black and red lines represent the detection of a 24-h daily rhythm for the three methods. *$p < 0.05$, **$p < 0.01$. Different from LD for that time point (Mann–Whitney *U* test). (**A–D**,right) Daily total expression. Data and median with interquartile range are shown, in LD and CPS ($n = 30$) offspring. *$p < 0.05$, **$p < 0.01$. Different from LD (Mann–Whitney *U* test). Minimum, first quartile, median, third quartile, and maximum were for LD offspring: *Rorα*:0.27, 0.55, 0.78, 0.86, and 1.63; *Rorγ*: 0.2, 0.41, 0.86, 1.23, and 2.80; *Nfil3*: 0.2, 0.38, 0.55, 0.96, and 1.59; and for CPS offspring: *Rorα*: 0.39, 0.68, 1.07, 1.44, and 2.92; *Rorγ*: 0.35, 0.58, 1.42, 2.15, and 5.6; *Nfil3*: 0.32, 0.53, 1.07, 1.64, and 2.53.

detected a rhythm in tPA but only by RAIN method in CPS but not in LD adult male progeny (**Figures 4A–D** left, and **Supplementary Tables 3–5**).

At the protein level, the results obtained for daily plasma concentration of PAI-1 did not show significant differences between CPS and LD male offspring (**Supplementary Figure 2** and **Supplementary Table 6**). However, daily rhythms were found for PAI-1 plasma protein concentration in both CPS and LD progeny; displaying a daily peak expression of the protein in the active phase (dark) of the circadian cycle (Ohkura et al., 2006). Notably, at P90 of development the amplitude of the oscillation of PAI-1 plasma concentration was increased in

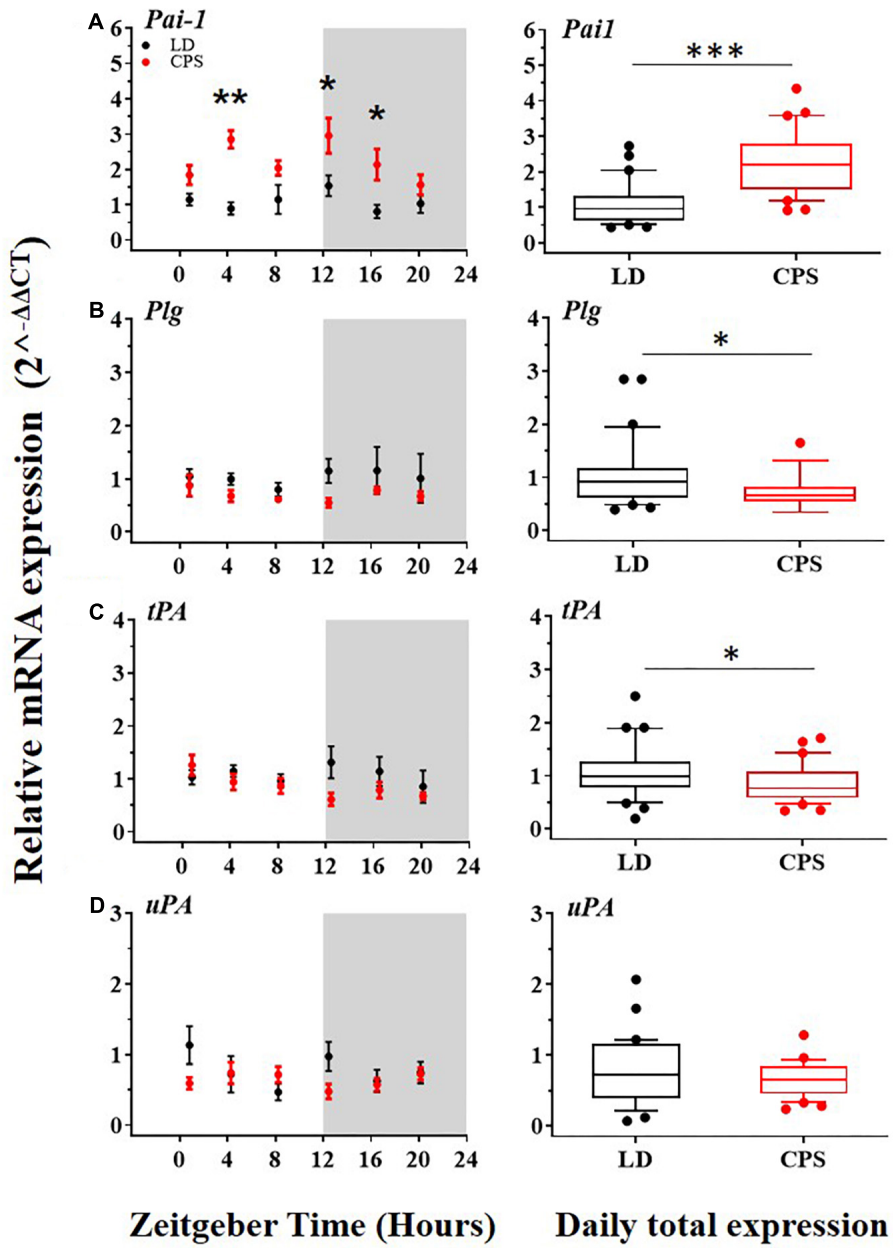


**FIGURE 4 |** The transcription level of *Pai-1*, *Plg*, *tPA,* and *uPA* in the liver from 90-day-old male rats by RT-PCR. (**A–D**,left) Detection of daily rhythm. Black symbols represent males gestated under control conditions (LD, black dots) and red symbols indicate males gestated in CPS (CPS, red dots). Males from each pregnancy condition (LD: $n = 12$ and CPS: $n = 6$ mothers), in LD and CPS offspring ($n = 5$/each time point). Time is expressed as zeitgeber time (ZT), with ZT0 as time lighting onset and ZT12 as lighting end; the gray bar indicates lights off. The RAIN's longitudinal mode, JTK_Cycle and the single cosinor method were used to determine daily rhythm ($p < 0.05$), solid black and red lines represent the detection of a 24-h daily rhythm for the three methods. (**A–D**,right) Daily total expression. Data and median with interquartile range are shown in LD and CPS ($n = 30$) offspring. $^*p < 0.05$, $^{**}p < 0.01$, $^{***}p < 0.001$. Different from LD (Mann–Whitney *U* test). Minimum, first quartile, median, third quartile, and maximum for LD offspring: *Pai-1*: 0.44, 0.62, 0.96, 1.33, and 2.73; *Plg*: 0.39, 0.61, 0.92, 1.15, and 2.85; *tPA*: 0.19, 0.78, 0.99, 1.27, and 2.5 and for CPS offspring: *Pai-1*: 0.92, 1.5, 2.27, 3.01, and 7.76; *Plg*: 0.34, 0.55, 0.66, 0.81, and 1.65; *tPA*: 0.34, 0.58, 0.76, 1.09, and 1.7.

adult males which had been gestated under CPS (A = 198.8 (LD) and 387.9 (CPS); AMP = 96.0 (LD) and 206.0 (CPS) determined by Cosinor and JTK_Cycle, respectively) relative to LD adult offspring (**Supplementary Table 6**). Finally, we found a circadian rhythm in the *ex vivo* coagulation time in both CPS and LD progeny (**Supplementary Figure 3** and **Supplementary Tables 7–9**). Remarkably, at the postnatal age of 180 days, in CPS gestated male the time required to *ex vivo* coagulation was greater than LD. This difference showed seems to be age-dependent because it was not observed at P60 or P120

(**Supplementary Figures 3A,B**). These results point to a putative mayor propensity to a coagulation/fibrinolytic system imbalance in CPS than LD during the aging process.

## DISCUSSION

Modern lifestyles are strongly correlated with misalignment of biological clocks. In this context, circadian disruption act as a sustained environmental factor that leads to conflicts between endogenous biologic clock cycles and the environment (Bass and Lazar, 2016). In the present study, gene expression patterns in the peripheral liver clock and fibrinolytic system were assessed to determine the long-term effects of gestational chronic photoperiod shifting (mimicking repeated night shift work schedules in pregnant women) on the adult offspring.

Hormonal disturbances have also been linked to altered photoperiods. Impaired secretion of corticosterone, aldosterone, and the loss of response to ACTH of the adrenal gland have been observed in progeny gestated under CPS (Mendez et al., 2016; Salazar et al., 2018). Adrenal function is directly regulated by the photoperiod as it is strictly controlled by the master clock residing in the suprachiasmatic nucleus (Aoshima et al., 2014; Plano et al., 2017). Moreover, the adrenal gland is an important oscillator from fetal to postnatal period of life (Torres-Farfan et al., 2011; Roa et al., 2017; Salazar et al., 2018) that synchronizes the rhythmic signaling of glucocorticoids and catecholamines to peripheral clocks such as the liver (Kalsbeek et al., 2012; Pezük et al., 2012). In fact, a significant desynchronization is observed in the liver of adult rats subjected to adrenalectomy (Pezük et al., 2012), strongly suggesting that the adrenal peripheral oscillator plays a crucial role in synchronizing the circadian rhythm of the liver. Previous findings in adult rats gestated under CPS indicate significant desynchronization of daily rhythms of plasma corticosterone, whereas the daily pattern of plasma ACTH was similar in both CPS and control offspring; however, corticosterone response to ACTH was lost in CPS adrenals (Mendez et al., 2016; Salazar et al., 2018). These lines of evidence could be associated with the alteration of the hepatic circadian clock. In the liver, our results demonstrated that transcript levels of *Bmal1* and the phase of the daily peak expression of *Clock* and *Nfil3* were significantly affected in adult males gestated in CPS. Interestingly, gestational CPS disrupted daily rhythms in the liver of these clock-genes even after 3 months of exposure to LD photoperiod during the postnatal developing (P90). These results reveal a long-term effect on the expression of the clock genes that changes the phenotype displayed at the adult stage under LD photoperiod in a male gestated in CPS protocol. Importantly, *Bmal1* plays a key role in the regulation of the hemostatic function of the liver and also in the progression of the prothrombotic state in aging (Hemmeryckx et al., 2011, 2019).

Alterations of the molecular clock at the accessory loop (RORE site) in the male adult progeny were also evidenced. Specifically, transcript levels of the clock genes *Rorα* and *Rorγ* (*Rorα/γ*) were increased in adult CPS males. The expression of *Rorα/γ* clock genes has been described to be positively controlled by the BMAL/CLOCK heterodimer. However, as it was described before, the transcript levels of *Bmal1* were downregulated in adult males gestated under CPS relative to LD conditions. That can be explained by the fact that posttranslational modifications of the BMAL/CLOCK heterodimer have been shown play a key role in terms to modify its activity independently of mRNA level regulation (Hirayama et al., 2007; Bellet and Sassone-Corsi, 2010; Preußner and Heyd, 2016). Additionally, it has been demonstrated that *Rorα/γ* expression is controlled by other circadian signals via cAMP response elements (CREs) (O'Neill et al., 2008) that could increase its role under the effects of gestational CPS. In order to determine if increased transcript levels of *Rorα/γ* may have functional consequences, we evaluated transcript levels of *Nfil3* in the liver, because its expression is principally regulated by *Rorγ* (Ueda et al., 2005; Takeda et al., 2012). The transcription level of *Nfil3* was significantly increased in adult males gestated in CPS. Also, the phase (ZT) of the daily peak expression of *Nfil3* was significantly affected (3.5 h) in males gestated in CPS (**Supplementary Tables 3–5**). This finding emphasizes that the effects on the accessory loop of the molecular clock could deregulate CCGs and therefore alter physiological functions. Moreover, endocrine signal as insulin is also important in the regulation of the expression of *Nfil3* (Keniry et al., 2014) and as previously mentioned, hyperinsulinemia has been reported in adult offspring gestated in CPS (Varcoe et al., 2011).

A reduced fibrinolytic activity due to an increase in the expression of PAI-1 is a characteristic risk factor for CVD (Mavri et al., 2004; Oishi, 2009). Liver physiology is heavily involved in the regulation of fibrinolytic activity since many of its components, like plasminogen (Cesarman-Maus and Hajjar, 2005; Leebeek and Rijken, 2015) and PAI-1 (Oishi, 2009; Declerck and Gils, 2013) are mainly synthesized by this organ. In adult mice, it has been reported that chronic alteration of the photoperiod was associated with the deregulation of the *Pai-1* expression in the liver (Oishi and Ohkura, 2013). On the other hand, previous evidence indicates that clock genes regulate the expression of PAI-1 (Schoenhard et al., 2003; Ohkura et al., 2006; Wang et al., 2006). For instance, a mouse model deficient in *Bmal1* (*Bmal1*$^{-/-}$) displayed elevated plasma levels of PAI-1, which were associated with a prothrombotic phenotype (Hemmeryckx et al., 2011; Somanath et al., 2011). Regarding gestational chronodisruption, our results showed increased levels of *Pai-1* in the liver of male adult offspring gestated under CPS. This observation is relevant because we previously showed a significant increase in blood pressure in CPS males at P90 (Mendez et al., 2016). Both, increased levels of PAI-1 associated with clock genes deregulation here reported and high pressure described previously are recognized like a CVD risk factors. Some factors that induce *Pai-1* gene expression are insulin, glucocorticoids (Irigoyen et al., 1999; Mavri et al., 2004; Dimova and Kietzmann, 2008). Interestingly, factors as hyperinsulinemia and alteration of corticosterone circadian rhythm also described in this animal model (Varcoe et al., 2011; Mendez et al., 2016) have been shown to induce greater expression of *Pai-1* in the liver. On the other hand, our data showed a decreased expression of *Bmal1* clock gene in the males gestated in CPS. Previous evidence supports the idea that reduced expression of *Bmal1* in the liver results in increased expression levels of *Pai-1*. In particular,

the upregulation of PAI-1 is associated with an increase in thrombosis propensity during the aging process (Hemmeryckx et al., 2011, 2019; Somanath et al., 2011). In addition, REV-ERBα is a negative regulator of *Pai-1* (Wang et al., 2006) expression by a mechanism involving its competition with RORα, a positive regulator that our results showed that is increased at transcript level and also rhythmic with a phase (ZT) of the daily peak expression in the active phase (dark) in CPS adult progeny. We did not observe differences in *Rev-Erbα* daily total expression between adult males gestated under CPS and LD conditions, suggesting an inclination to induce *Pai-1* expression by RORα rather than repression by REV-ERBα.

The appearance of a marked daily oscillation at the transcript level of the clock gene *Rorα* in adult CPS but not in LD offspring was another interesting finding. The induction of rhythmic expression of genes that are not oscillatory could be mediated by epigenetic mechanisms, which are involved in the regulation of the transcriptional machinery and reveal that expression of genes that are not rhythmic could be induced (Masri et al., 2014). The induction of the rhythmic expression pattern in *Rorα* in CPS adult males suggests that epigenetic mechanisms might play a role in the long-term effects observed.

At the protein level, results obtained for daily plasma concentration of PAI-1 did not show significant differences between CPS and LD male offspring. However, daily rhythms were found for PAI-1 plasma protein; displaying a daily peak expression of the protein in the active phase (dark) of the daily cycle that are in agreement with data previously reported in rodents for LD condition (Ohkura et al., 2006). Notably, at P90 of development, the amplitude of the oscillation of plasma concentration in the active phase was increased in adult males which had been gestated under CPS relative to LD offspring (**Supplementary Table 6**).

It has been described that older humans are more susceptible to thrombosis under septic conditions (Balleisen et al., 1985; Aillaud et al., 1986). In addition, murine models have been demonstrated that the aging process increases the endotoxin-induced thrombosis by a mechanism that involves increased expression of PAI-1 protein in the plasma and at mRNA level in the liver. This tendency is linked to an enhanced inflammatory response in aged mice (Yamamoto et al., 2002). Connected with this previous literature we found a circadian rhythm in the *ex vivo* coagulation time that was increased at postnatal age of 180 days in CPS gestated male in a process that is age-dependent because this difference was not observed at P60 or P120.

## DATA AVAILABILITY STATEMENT

The datasets generated for this study are available on request to the corresponding author.

## ETHICS STATEMENT

The animal study was reviewed and approved by Bioethics Commission of the Universidad Austral de Chile (CBA number 267/2016).

## AUTHOR CONTRIBUTIONS

PC and JS contributed to the conception, design, and drafting of the work. PC wrote the first draft of the manuscript. PC, BP, CT, NM, GE, and KV worked on animal handling and acquisition of data. PC, JS, and FM analyzed and interpreted the data. CT-F, HR, and PB critically reviewed the manuscript for important intellectual content. All authors contributed to the manuscript revision, and read and approved the submitted version.

## FUNDING

This work was supported by Grant N°1150789 from the Fondo Nacional de Desarrollo Científico y Tecnológico (FONDECYT), Chile, and ANILLO ACT-1116. PC was supported by Fellowship N°21171387 from the Comisión Nacional de Investigación Científica y Tecnológica (CONICYT), Chile.

## SUPPLEMENTARY MATERIAL

The Supplementary Material for this article can be found online at: https://www.frontiersin.org/articles/10.3389/fphys.2019.01377/full#supplementary-material

## REFERENCES

Aillaud, M. F., Pignol, F., Alessi, M. C., Harle, J. R., Escande, M., Mongin, M., et al. (1986). Increase in plasma concentration of plasminogen activator inhibitor, fibrinogen, von Willebrand factor, factor VIII:C and in erythrocyte sedimentation rate with age. *Thromb. Haemost.* 55, 330–332. doi: 10.1055/s-0038-1661557

Albrecht, U. (2012). Timing to perfection: the biology of central and peripheral circadian clocks. *Neuron* 74, 246–260. doi: 10.1016/j.neuron.2012.04.006

Amaral, F. G., Castrucci, A. M., Cipolla-Neto, J., Poletini, M. O., Mendez, N., Richter, H. G., et al. (2014). Environmental control of biological rhythms: effects on development, fertility and metabolism. *J. Neuroendocrinol.* 26, 603–612. doi: 10.1111/jne.12144

Aoshima, Y., Sakakibara, H., Suzuki, T., Yamazaki, S., and Shimoi, K. (2014). Nocturnal light exposure alters hepatic Pai-1 expression by stimulating the adrenal pathway in C3H mice. *Exp. Anim.* 63, 331–338. doi: 10.1538/expanim.63.331

Balleisen, L., Assmann, G., Bailey, J., Epping, P.-H., Schulte, H., and van de Loo, J. (1985). Epidemiological study on factor VII, factor VIII and fibrinogen in an industrial population–II. Baseline data on the relation to blood pressure, blood glucose, uric acid, and lipid fractions. *Thromb. Haemost.* 54, 721–723. doi: 10.1055/s-0038-1660106

Bass, J., and Lazar, M. A. (2016). Transformed more than 14 years later with posi- tional cloning of core clock genes and recognition. *Science* 80:354. doi: 10.1126/science.aah4965

Bellet, M. M., and Sassone-Corsi, P. (2010). Mammalian circadian clock and metabolism - the epigenetic link. *J. Cell Sci.* 123, 3837–3848. doi: 10.1242/jcs.051649

Calkins, K., Devaskar, S. U., and Angeles, L. (2011). Fetal origins of adult disease. *Curr. Probl. Pediatr. Adolesc. Health Care* 41, 158–176. doi: 10.1016/j.cppeds.2011.01.001.Fetal

Capra, L., Tezza, G., Mazzei, F., and Boner, A. L. (2013). The origins of health and disease: the influence of maternal diseases and lifestyle during gestation. *Ital. J. Pediatr.* 39:7. doi: 10.1186/1824-7288-39-7

Čečmanová, V., Houdek, P., Šuchmanová, K., Sládek, M., and Sumová, A. (2019). Development and entrainment of the fetal clock in the suprachiasmatic nuclei: the role of glucocorticoids. *J. Biol. Rhythms* 34, 307–322. doi: 10.1177/0748730419835360

Cesarman-Maus, G., and Hajjar, K. A. (2005). Molecular mechanisms of fibrinolysis. *Br. J. Haematol.* 129, 307–321. doi: 10.1111/j.1365-2141.2005.05444.x

Curtis, A. M., Bellet, M. M., Sassone-Corsi, P., and O'Neill, L. A. J. (2014). Circadian clock proteins and immunity. *Immunity* 40, 178–186. doi: 10.1016/j.immuni.2014.02.002

Declerck, P. J., and Gils, A. (2013). Three decades of research on plasminogen activator inhibitor-1: a multifaceted serpin. *Semin. Thromb. Hemost.* 39, 356–364. doi: 10.1055/s-0033-1334487

Dimova, E. Y., and Kietzmann, T. (2008). Metabolic, hormonal and environmental regulation of plasminogen activator inhibitor-1 (PAI-1) expression: lessons from the liver. *Thromb. Haemost.* 100, 992–1006. doi: 10.1160/TH08-07-0490

Oishi, K., and Ohkura, N. (2013). Chronic circadian clock disruption induces expression of the cardiovascular risk factor plasminogen activator inhibitor-1 in mice. *Blood Coagul. Fibrinolysis* 24, 106–108. doi: 10.1097/MBC.0b013e32835bfdf3

Erren, T. C., and Reiter, R. J. (2009). Defining chronodisruption. *J. Pineal Res.* 46, 245–247. doi: 10.1111/j.1600-079X.2009.00665.x

Fowden, A. L., Giussani, D. A., and Forhead, A. J. (2006). Intrauterine programming of physiological systems: causes and consequences. *Physiology* 21, 29–37. doi: 10.1152/physiol.00050.2005

Gatford, K. L., Kennaway, D. J., Liu, H., Kleemann, D. O., Kuchel, T. R., and Varcoe, T. J. (2019). Simulated shift work disrupts maternal circadian rhythms and metabolism, and increases gestation length in sheep. *J. Physiol.* 579, 1889–1904. doi: 10.1113/JP277186

Hanson, M. A., and Gluckman, P. D. (2014). Early developmental conditioning of later health and disease: physiology or pathophysiology? *Physiol. Rev.* 94, 1027–1076. doi: 10.1152/physrev.00029.2013

Haus, E. (2007). Chronobiology of hemostasis and inferences for the chronotherapy of coagulation disorders and thrombosis prevention. *Adv. Drug Deliv. Rev.* 59, 966–984. doi: 10.1016/j.addr.2006.11.002

Hemmeryckx, B., Frederix, L., and Lijnen, H. R. (2019). Deficiency of bmal1 disrupts the diurnal rhythm of haemostasis. *Exp. Gerontol.* 118, 1–8. doi: 10.1016/J.EXGER.2018.12.017

Hemmeryckx, B., Van Hove, C. E., Fransen, P., Emmerechts, J., Kauskot, A., Bult, H., et al. (2011). Progression of the prothrombotic state in aging bmal1-deficient mice. *Arterioscler. Thromb. Vasc. Biol.* 31, 2552–2559. doi: 10.1161/ATVBAHA.111.229062

Hirayama, J., Sahar, S., Grimaldi, B., Tamaru, T., Takamatsu, K., Nakahata, Y., et al. (2007). CLOCK-mediated acetylation of BMAL1 controls circadian function. *Nature* 450, 1086–1090. doi: 10.1038/nature06394

Hughes, M. E., Abruzzi, K. C., Allada, R., Anafi, R., Arpat, A. B., Asher, G., et al. (2017). Guidelines for genome-scale analysis of biological rhythms. *J. Biol. Rhythms* 32, 380–393. doi: 10.1177/0748730417728663

Hughes, M. E., Hogenesch, J. B., and Kornacker, K. (2010). JTK_CYCLE: an efficient non-parametric algorithm for detecting rhythmic components in genome-scale datasets. *J. Biol. Rhythms* 25:372. doi: 10.1177/0748730410379711

Irigoyen, J. P., Munoz-Canoves, P., Montero, L., Koziczak, M., and Nagamine, Y. (1999). The plasminogen activator system:biology and regulation. *Cell. Mol. Life Sci.* 56, 104–132.

Jung, R. G., Simard, T., Labinaz, A., Ramirez, F. D., Di Santo, P., Motazedian, P., et al. (2018). Role of plasminogen activator inhibitor-1 in coronary pathophysiology. *Thromb. Res.* 164, 54–62. doi: 10.1016/j.thromres.2018.02.135

Kalsbeek, A., van der Spek, R., Lei, J., Endert, E., Buijs, R. M., and Fliers, E. (2012). Circadian rhythms in the hypothalamo–pituitary–adrenal (HPA) axis. *Mol. Cell. Endocrinol.* 349, 20–29. doi: 10.1016/J.MCE.2011.06.042

Keniry, M., Dearth, R. K., Persans, M., and Parsons, R. (2014). New frontiers for the NFIL3 bZIP transcription factor in cancer. *Metabol. Beyond. Discover.* 2:e15. doi: 10.15190/d.2014.7

Leebeek, F. W. G., and Rijken, D. C. (2015). The fibrinolytic status in liver diseases. *Semin. Thromb. Hemost.* 41, 474–480. doi: 10.1055/s-0035-1550437

Liu, Z., and Chu, G. (2013). Chronobiology in mammalian health. *Mol. Biol. Rep.* 40, 2491–2501. doi: 10.1007/s11033-012-2330-4

Livak, K. J., and Schmittgen, T. D. (2001). Analysis of relative gene expression data using real-time quantitative PCR and. *Methods* 25, 402–408. doi: 10.1006/meth.2001.1262

Maemura, K., de la Monte, S. M., Chin, M. T., Layne, M. D., Hsieh, C. M., Yet, S. F., et al. (2000). CLIF, a novel cycle-like factor, regulates the circadian oscillation of plasminogen activator inhibitor-1 gene expression. *J. Biol. Chem.* 275, 36847–36851. doi: 10.1074/jbc.C000629200

Marsh, L. M., Pfefferle, P. I., Pinkenburg, O., and Renz, H. (2011). Maternal signals for progeny prevention against allergy and asthma. *Cell. Mol. Life Sci.* 68, 1851–1862. doi: 10.1007/s00018-011-0644-3

Masri, S., Rigor, P., Cervantes, M., Ceglia, N., Sebastian, C., Xiao, C., et al. (2014). Partitioning circadian transcription by SIRT6 leads to segregated control of cellular metabolism. *Cell* 158, 659–672. doi: 10.1016/j.cell.2014.06.050

Mavri, A., Alessi, M. C., and Juhan-Vague, I. (2004). Hypofibrinolysis in the insulin resistance syndrome: implication in cardiovascular diseases. *J. Intern. Med.* 255, 448–456. doi: 10.1046/j.1365-2796.2003.01288.x

Mazzoccoli, G., Pazienza, V., and Vinciguerra, M. (2012). Clock genes and clock-controlled genes in the regulation of metabolic rhythms. *Chronobiol. Int.* 29, 227–251. doi: 10.3109/07420528.2012.658127

Mendez, N., Halabi, D., Spichiger, C., Salazar, E. R., Vergara, K., Alonso-Vasquez, P., et al. (2016). Gestational chronodisruption impairs circadian physiology in rat male offspring, increasing the risk of chronic disease. *Endocrinology* 157, 4654–4668. doi: 10.1210/en.2016-1282

Mohawk, J. A., Green, C. B., and Takahashi, J. S. (2013). Central and peripheral circadian clocks in mammal. *Annu. Rev. Neurosci.* 35, 445–462. doi: 10.1146/annurev-neuro-060909-153128.CENTRAL

Ohkura, N., Oishi, K., Fukushima, N., Kasamatsu, M., Atsumi, G. I., Ishida, N., et al. (2006). Circadian clock molecules CLOCK and CRYs modulate fibrinolytic activity by regulating the PAI-1 gene expression. *J. Thromb. Haemost.* 4, 2478–2485. doi: 10.1111/j.1538-7836.2006.02210.x

Oishi, K. (2009). Plasminogen activator inhibitor-1 and the circadian clock in metabolic disorders. *Clin. Exp. Hypertens.* 31, 208–219. doi: 10.1080/10641960902822468

O'Neill, J. S., Maywood, E. S., Chesham, J. E., Takahashi, J. S., and Hastings, M. H. (2008). cAMP-dependent signaling as a core component of the mammalian circadian pacemaker. *Science* 320, 949–953. doi: 10.1126/science.1152506

Partch, C. L., Green, C. B., and Takahashi, J. S. (2014). Molecular architecture of the mammalian circadian clock. *Trends Cell Biol.* 24, 90–99. doi: 10.1016/j.tcb.2013.07.002

Pezük, P., Mohawk, J. A., Wang, L. A., and Menaker, M. (2012). Glucocorticoids as entraining signals for peripheral circadian oscillators. *Endocrinology* 153, 4775–4783. doi: 10.1210/en.2012-1486

Plano, S. A., Casiraghi, L. P., Moro, P. G., Paladino, N., Golombek, D. A., and Chiesa, J. J. (2017). Circadian and metabolic effects of light: implications in weight homeostasis and health. *Front. Neurol.* 8:1–21. doi: 10.3389/fneur.2017.00558

Preußner, M., and Heyd, F. (2016). Post-transcriptional control of the mammalian circadian clock: implications for health and disease. *Pflugers Arch. Eur. J. Physiol.* 468, 983–991. doi: 10.1007/s00424-016-1820-y

Refinetti, R., Cornélissen, G., and Halberg, F. (2007). Procedures for numerical analysis of circadian rhythms. *Biol. Rhythm Res.* 38, 275–325. doi: 10.1080/09291010600903692

Reinke, H., and Asher, G. (2016). Circadian clock control of liver metabolic functions. *Gastroenterology* 150, 574–580. doi: 10.1053/j.gastro.2015.11.043

Richter, H. G., Mendez, N., Abarzua-Catalan, L., Valenzuela, G. J., Seron-Ferre, M., and Torres-Farfan, C. (2018). Developmental programming of capuchin monkey adrenal dysfunction by gestational chronodisruption. *Biomed. Res. Int.* 2018:11. doi: 10.1155/2018/9183053

Roa, S. L. R., Martinez, E. Z., Martins, C. S., Antonini, S. R., de Castro, M., and Moreira, A. C. (2017). Postnatal ontogeny of the circadian expression of the

adrenal clock genes and corticosterone rhythm in male rats. *Endocrinology* 158, 1339–1346. doi: 10.1210/en.2016-1782

Salazar, E. R., Richter, H. G., Spichiger, C., Mendez, N., Halabi, D., Vergara, K., et al. (2018). Gestational chronodisruption leads to persistent changes in the rat fetal and adult adrenal clock and function. *J. Physiol.* 596, 5839–5857. doi: 10.1113/JP276083

Schoenhard, J. A., Smith, L. H., Painter, C. A., Eren, M., Johnson, C. H., and Vaughan, D. E. (2003). Regulation of the PAI-1 promoter by circadian clock components: differential activation by BMAL1 and BMAL2. *J. Mol. Cell. Cardiol.* 35, 473–481. doi: 10.1016/S0022-2828(03)00051-8

Serón-Ferré, M., Forcelledo, M. L., Torres-Farfan, C., Valenzuela, F. J., Rojas, A., Vergara, M., et al. (2013). Impact of chronodisruption during primate pregnancy on the maternal and newborn temperature rhythms. *PLoS One* 8:e57710. doi: 10.1371/journal.pone.0057710

Serón-Ferré, M., Mendez, N., Abarzua-Catalan, L., Vilches, N., Valenzuela, F. J., Reynolds, H. E., et al. (2012). Circadian rhythms in the fetus. *Mol. Cell. Endocrinol.* 349, 68–75. doi: 10.1016/J.MCE.2011.07.039

Sládek, M., Jindráková, Z., Bendová, Z., and Sumová, A. (2007). Postnatal ontogenesis of the circadian clock within the rat liver. *Am. J. Physiol. Regul. Integr. Comp. Physiol.* 292, R1224–R1229. doi: 10.1152/ajpregu.00184.2006

Somanath, P. R., Podrez, E. A., Chen, J., Ma, Y., Marchant, K., Antoch, M., et al. (2011). Deficiency in core circadian protein bmal1 is associated with a prothrombotic and vascular phenotype. *J. Cell. Physiol.* 226, 132–140. doi: 10.1002/jcp.22314

Sumová, A., Bendová, Z., Sládek, M., El-Hennamy, R., Matejů, K., Polidarová, L., et al. (2008). Circadian molecular clocks tick along ontogenesis. *Physiol. Res.* 57, S139–S148.

Tahara, Y., and Shibata, S. (2016). Circadian rhythms of liver physiology and disease: experimental and clinical evidence. *Nat. Rev. Gastroenterol. Hepatol.* 13, 217–226. doi: 10.1038/nrgastro.2016.8

Takahashi, J. S. (2016). "Molecular architecture of the circadian clock in mammals," in *A Time for Metabolism and Hormones*, eds P. Sassone and Y. Corsi Christen (Berlin: Springer), 13–24. doi: 10.1007/978-3-319-27069-2_2

Takeda, Y., Jothi, R., Birault, V., and Jetten, A. M. (2012). RORc directly regulates the circadian expression of clock genes and downstream targets in vivo. *Nucleic Acids Res.* 40, 8519–8535. doi: 10.1093/nar/gks630

Tarquini, R., and Mazzoccoli, G. (2017). Clock genes, metabolism, and cardiovascular risk. *Heart Fail. Clin.* 13, 645–655. doi: 10.1016/J.HFC.2017.05.001

Thaben, P. F., and Westermark, P. O. (2014). Detecting rhythms in time series with RAIN. *J. Biol. Rhythms* 29, 391–400. doi: 10.1177/0748730414553029

Thompson, M. D., and Trask, A. J. (2016). Developmental origins of cardiovascular dysfunction: doomed from birth? *Circ J.* 80, 818–820. doi: 10.1253/circj.CJ-16-0207

Tofler, G. H., Massaro, J., O'Donnell, C. J., Wilson, P. W. F., Vasan, R. S., Sutherland, P. A., et al. (2016). Plasminogen activator inhibitor and the risk of cardiovascular disease: the framingham heart study. *Thromb. Res.* 140, 30–35. doi: 10.1016/j.thromres.2016.02.002

Torres-Farfan, C., Mendez, N., Abarzua-Catalan, L., Vilches, N., Valenzuela, G. J., and Seron-Ferre, M. (2011). A circadian clock entrained by melatonin is ticking in the rat fetal adrenal. *Endocrinology* 152, 1891–1900. doi: 10.1210/en.2010-1260

Touitou, Y., Reinberg, A., and Touitou, D. (2017). Association between light at night, melatonin secretion, sleep deprivation, and the internal clock: health impacts and mechanisms of circadian disruption. *Life Sci.* 173, 94–106. doi: 10.1016/j.lfs.2017.02.008

Ueda, H. R., Hayashi, S., Chen, W., Sano, M., Machida, M., Shigeyoshi, Y., et al. (2005). System-level identification of transcriptional circuits underlying mammalian circadian clocks. *Nat. Genet.* 37, 187–192. doi: 10.1038/ng1504

Varcoe, T. J., Boden, M. J., Voultsios, A., Salkeld, M. D., Rattanatray, L., and Kennaway, D. J. (2013). Characterisation of the maternal response to chronic phase shifts during gestation in the rat: implications for fetal metabolic programming. *PLoS One* 8:e53800. doi: 10.1371/journal.pone.0053800

Varcoe, T. J., Gatford, K. L., and Kennaway, D. J. (2017). Maternal circadian rhythms and the programming of adult health and disease. *Am. J. Physiol. Regul. Integr. Comp. Physiol* 314, R231–R241. doi: 10.1152/ajpregu.00248.2017

Varcoe, T. J., Wight, N., Voultsios, A., Salkeld, M. D., and Kennaway, D. J. (2011). Chronic phase shifts of the photoperiod throughout pregnancy programs glucose intolerance and insulin resistance in the rat. *PLoS One* 6, 1–10. doi: 10.1371/journal.pone.0018504

Wang, J., Yin, L., and Lazar, M. A. (2006). The orphan nuclear receptor Rev-erbα regulates circadian expression of plasminogen activator inhibitor type. *J. Biol. Chem.* 281, 33842–33848. doi: 10.1074/jbc.M607873200

Yamamoto, K., Shimokawa, T., Yi, H., Isobe, K.-i., Kojima, T., Loskutoff, D. J., et al. (2002). Aging accelerates endotoxin-induced thrombosis: increased responses of plasminogen activator inhibitor-1 and lipopolysaccharide signaling with aging. *Am. J. Pathol.* 161, 1805–1814. doi: 10.1016/s0002-9440(10)64457-4

Zwighaft, Z., Reinke, H., and Asher, G. (2016). The liver in the eyes of a chronobiologist. *J. Biol. Rhythms* 31, 115–124. doi: 10.1177/0748730416633552

**Conflict of Interest:** The authors declare that the research was conducted in the absence of any commercial or financial relationships that could be construed as a potential conflict of interest.

frontiers in Physiology

ORIGINAL RESEARCH
published: 28 January 2020
doi: 10.3389/fphys.2020.00005

# Effect of Morning Light Glasses and Night Short-Wavelength Filter Glasses on Sleep-Wake Rhythmicity in Medical Inpatients

*Chiara Formentin, Stefano Carraro, Matteo Turco, Lisa Zarantonello, Paolo Angeli and Sara Montagnese**

*Department of Medicine, University of Padua, Padua, Italy*

Sleep and circadian rhythm disorders are common amongst medical inpatients. They are caused by a mixture of factors, including noise, loss of habitual daily routines, and abnormal exposure to light, which tends to be insufficient in the day and too high at night. The aim of the present study was to test the efficacy of morning light therapy plus night short-wavelength filter glasses on sleep quality/timing, and sleepiness/mood over the daytime hours, in a group of well-characterized medical inpatients. Thirty-three inpatients were enrolled and randomized (2:1) to either treatment ($n$ = 22; 13 males, 48.3 ± 13.3 years) or standard of care ($n$ = 11; 8 males, 56.9 ± 12.9 years). On admission, all underwent a baseline assessment of sleep quality/timing and diurnal preference. During hospitalization they underwent monitoring of sleep quality/timing (sleep diaries and actigraphy), plus hourly assessment of sleepiness/mood during the daytime hours on one, standard day of hospitalization. Patients in the treatment arm were administered bright light through glasses immediately after awakening, and wore short-wavelength filter glasses in the evening hours. Treated and untreated patients were comparable in terms of demographics, disease severity/comorbidity, diurnal preference and pre-admission sleep quality/timing. During hospitalization, sleep diaries documented a trend for a lower number of night awakenings in treated compared to untreated patients (1.6 ± 0.8 vs. 2.4 ± 1.3, $p$ = 0.057). Actigraphy documented significantly earlier day mode in treated compared to untreated patients (06:39 ± 00:35 vs. 07:44 ± 00:40, $p$ = 0.008). Sleepiness during a standard day of hospitalization, recorded between 09:30 and 21:30, showed physiological variation in treated compared to untreated patients, who exhibited a more blunted profile. The level of sleepiness reported by treated patients was lower over the 09:30–14:30 interval, i.e., soon after light administration (interaction effect: $F$ = 2.661; $p$ = 0.026). Mood levels were generally higher in treated patients, with statistically significant differences over the 09:30–14:30 time interval, i.e., soon after light administration (treatment: $F$ = 5.692, $p$ = 0.026). In conclusion, treatment with morning bright light and short-wavelength filter glasses in the evening, which was well tolerated, showed positive results in terms of sleepiness/mood over the morning hours and a trend for decreased night awakenings.

**Keywords: light therapy, glasses, entrainment, sleep-wake rhythm, filter**

OPEN ACCESS

***Edited by:***
*Charalambos P. Kyriacou, University of Leicester, United Kingdom*

***Reviewed by:***
*Etienne Challet, Centre National de la Recherche Scientifique (CNRS), France*
*Phyllis Zee, Northwestern University, United States*

***Correspondence:**
*Sara Montagnese*
*sara.montagnese@unipd.it*

***Specialty section:***
*This article was submitted to Chronobiology, a section of the journal Frontiers in Physiology*

***Received:*** *17 October 2019*
***Accepted:*** *08 January 2020*
***Published:*** *28 January 2020*

***Citation:***
*Formentin C, Carraro S, Turco M, Zarantonello L, Angeli P and Montagnese S (2020) Effect of Morning Light Glasses and Night Short-Wavelength Filter Glasses on Sleep-Wake Rhythmicity in Medical Inpatients. Front. Physiol. 11:5. doi: 10.3389/fphys.2020.00005*

## INTRODUCTION

Sleep-wake disturbances are common in hospitalized patients (Tranmer et al., 2003; Humphries, 2008; Missildine et al., 2010). Insomnia derives from both intrinsic, endogenous factors (i.e., physical illness and pain, psychological stress) and unfavorable, exogenous environmental stimuli. Loss of habitual daily routines, fixed schedules, therapeutic and diagnostic procedures are some of the main reasons for sleep interruptions and poor sleep quality (Freedman et al., 2001; van Kamp and Davies, 2008; Kamdar et al., 2012). Patients are removed from their familiar setting and placed in a new environment, which may result in disorientation for time and space, especially in elderly patients, and altered circadian rhythmicity.

Hospital life is very disruptive also in terms of wake quality, as patients spend a significant amount of time in bed, and are rarely capable and/or provided with adequate mobilization. In turn, spending too much time in bed and being inactive during the day can lead to so-called learnt insomnia, and to the prescription of sleep-inducing medication (Spielman et al., 2005).

Abnormal exposure to light, which tends to be too low in the day and too high at night (Friese, 2008; Bano et al., 2014; Bernhofer et al., 2014) may also contribute to sleep-wake disturbance of circadian origin, as light is the main environmental cue (*Zeitgeber*) for synchronizing the circadian clock to the environment. In health-care facilities, low light exposure levels and a reduced difference between day and night environmental lighting conditions may alter rhythmicity, and thus contribute to the impairment in sleep quality (Meyer et al., 1994; Kamdar et al., 2012).

Based on the above observations, the aim of the present study was to test the efficacy of morning light therapy, in combination with night short-wavelength filter glasses, on sleep quality/timing and the time course of sleepiness/mood in a group of well-characterized medical inpatients. The duration of treatment was that of hospitalization.

## PATIENTS AND METHODS

On admission, all patients enrolled in the study underwent an assessment of their pre-hospitalization sleep quality/timing, and were then randomized to either the treatment or the control group, by random numbers generated from a computer. They were asked to complete a sleep diary every morning and to wear a Jawbone actiwatch for the whole duration of their hospitalization. In addition, they were asked to choose a single day for hourly completion of the Karolinska Sleepiness Scale (KSS; *vide infra*) and a 1–10 Visual Analogue Scale (VAS) of mood, from get up time to bedtime. Patients in the treatment arm were also asked to wear light glasses in the morning (*vide infra*) and short-wavelength filter glasses from 18:00 h (*vide infra*). Except for sources of environmental disturbance due to hospital routines, patients were free to go to bed/try to sleep and wake/get up at their chosen times. Spontaneous night awakenings were unlikely to result in lights on, while awakenings related to admissions/hospital routines were likely to result in lights on. Patients in the treatment arm were instructed to wear their short-wavelength filter glasses in the latter instance.

### Patients

Forty-five patients admitted into the medical ward Clinica Medica V of Padua University Hospital between February 2016 and July 2018 were screened. Ten were unwilling to take part in the study and two were subsequently excluded for poor compliance with the study protocol. Thus the final population included 33 inpatients (51 $\pm$ 14 years) randomized (2:1) to either treatment ($n$ = 22; 48 $\pm$ 15 years) or standard of care ($n$ = 11; 58 $\pm$ 5 years).

The majority of patients were hospitalized for liver/biliary/pancreatic diseases (42%), this being due to the fact that the unit also serves as a tertiary referral hepatology center. Other diagnoses on admission were cardiovascular diseases (34%), infections (including pneumonia, urinary tract infection and erysipelas; 12%), and gastrointestinal bleeding or acute anemia (12%).

The Charlson Comorbidity Index was used for purposes of assessment of disease severity/comorbidity. This ranges from 0 to 37, and a weight is assigned to each of 19 medical conditions, based on the corresponding relative risk of death within 12 months (Charlson et al., 1987).

Exclusion criteria were: age >80 years, severe cognitive impairment, inability to adhere to the protocol/comply with the tasks, lack of informed consent, diagnosed sleep–wake disorders (i.e., obstructive sleep apnoea, restless legs syndrome etc.), shift work or intercontinental travel over the preceding 6 months.

Over the inpatient stay, data were collected daily on the administration of sleep-inducing (benzodiazepines or benzodiazepine-like) and other psychoactive drugs (antidepressants, neuroleptics, and opioid analgesics), with the idea that patients could benefit from light-dark treatment in terms of insomnia/sleep problems, thus limiting the need for pharmacological intervention.

The study protocol was approved by the local Ethics Committee and the study conducted according to the Declaration of Helsinki (Hong Kong Amendment) and Good Clinical Practice (European) guidelines. All participants provided written informed consent.

### Sleep-Wake Assessment

On the first day of hospitalization, all participants underwent an assessment of their baseline, pre-hospitalization sleep quality and timing, based on the following questionnaires/scales:

- The Pittsburgh Sleep Quality Index (PSQI), which evaluates subjective sleep quality over the preceding month, and differentiates "good" from "poor" sleepers. Responses to the 24 questions of this self-administered questionnaire are used to generate seven components, each of which is scored from 0 to 3 (0 = best). The PSQI total score is the sum of all domains (range 0–21), and a total score >5 characterizes "poor sleepers" (Buysse et al., 1989; Curcio et al., 2013). Component 4, which allows obtainment of average get up

and bedtime data, was used for purposes of assessment of pre-hospitalization sleep timing.

- The Horne–Östberg (HÖ) questionnaire, which defines diurnal preference as definitely morning (score 70–86), moderately morning (59–69), intermediate (42–58), moderately evening (31–41), and definitely evening (16–30) based on 19 self-administered questions (Horne and Ostberg, 1976).
- The KSS, a self-rated subjective sleepiness scale (range 1: "very alert" – 9: "very sleepy, fighting sleep, difficulty staying awake") (Akerstedt and Gillberg, 1990), which patients were asked to complete hourly (from wake up to sleep onset time) on a standard day of hospitalization, except from hospitalization day 1. This is because the first day of hospitalization often follows a sleepless night, a prolonged stay in the Accident and Emergency area and a generally disrupted routine.
- A VAS of mood (range 1: worst to 10: best); this was also completed hourly (from wake up to sleep onset time) on a standard day of hospitalization, except from hospitalization day 1.

During the whole period of hospitalization, patients were asked to:

- Complete a sleep diary daily, recording bedtime, sleep onset, time taken to fall asleep, wake up time, get up time, and the number and duration of any night awakenings and/or daytime naps. Night awakenings were intended as either spontaneous arousals or sleep interruptions due to environmental factors. Sleep-onset latency was calculated as the difference between bedtime and sleep onset time (in minutes); time spent in bed as the difference between bedtime and get up time (in hours); length of sleep as the difference between sleep onset and wake up time (in hours). Patients were asked to complete their sleep diaries early in the morning, immediately after waking up, in order to limit recall bias, as they could not generally take notes during the night. Each diary page also included a VAS for the assessment of sleep quality during the previous night (range 1: worst to 10: best) (Lockley et al., 1999; Carney et al., 2012);
- Wear a Jawbone$^{TM}$ UP24 (Jawbone, San Francisco, CA, United States), i.e., a bracelet type wrist-worn device which records movement by use of an accelerometer. The simple assumption underlying the technique is wake = movement, sleep = lack of movement (Cellini et al., 2013). Data were then downloaded and analyzed by the pertinent application UP by Jawbone$^{TM}$. The following indices were obtained: time spent in bed, total sleep (i.e., total duration of all epochs of sleep during period of time in bed), sleep latency [(i.e., the difference between "night mode," *vide infra*, and the first epoch qualified as sleep (Cook et al., 2018)], number of awakenings, day mode [i.e., time in the morning, after wake up time, when the patient pressed a button on the actiwatch band to switch from "sleep mode" to "active mode"; this function is a so-called "event marker," a strategy to enhance the quality of information obtained from actigraphy (Martin and Hakim, 2011)], night mode (i.e., time at night, after bedtime, when the patient pressed the same button to switch from "active mode" to "sleep mode").

## Light-Dark Treatment Schedule

Patients in the treatment arm were provided with light glasses (**Figure 1A**) and short-wavelength filter glasses (**Figure 1B**). They were instructed to wear their light glasses for 30 min in the morning, after waking up (i.e., while having breakfast, immediately after their personal hygiene, etc.) and to wear their short-wavelength filter glasses from 18:00 h until sleep onset time, plus at any time overnight when the light in their room was on. Exact timings were patient-driven and both types of glasses were managed individually by the patients (i.e., not distributed and/or operated by staff at any given time).

## Equipment

- Luminette® light glasses (Langevin et al., 2014) (Lucimed, Villers-le-Bouillet, Belgium; **Figure 1A**), which can be worn over prescription glasses, are equipped with eight Light Emitting Diodes (LEDs) distributed on the upper part of the two lenses (four on each side), outside the patient's visual field. The


**FIGURE 1 |** Luminette light glasses [Lucimed, Villers-le-Bouillet, Belgium; **(A)**] with light emitting diodes (approximately 2000 lux; blue-enriched 400–750 nm) and short-wavelength filter glasses [MelaMedic, Viborg, Denmark; **(B)**], which filter light in the blue range of the spectrum, i.e., the one our visual circadian timing system is most sensitive to.

LEDs reflect light (2000 lux; blue-enriched 400–750 nm) toward the eye via a diffractive lens, thus focusing light toward the lower part of the retina, regardless of the position of the head. This also allows for uniform illumination and for dazzling avoidance (Bragard and Coucke, 2013).

- Short-wavelength filter glasses (MelaMedic, Viborg, Denmark; **Figure 1B**), which can be worn over prescription glasses, filter light in the blue range of the spectrum, i.e., the one our visual circadian timing system is most sensitive to (Foster, 2005). Thus they limit exposure to awakening light signals at times when the natural environment is dark but the artificial one inside the hospital is well lit or the patients use mobile phones, tablets, reading devices which emit relatively strong and blue-enriched light (Gringras et al., 2015).

Illuminance levels at night, as measured in a previous study performed by our research group in the same medical ward, were 12 ± 24 lux between 23:30 and 00:30 (Bano et al., 2014). Information on the variability of both day and night lighting conditions, plus noise levels is also provided in the same study (Bano et al., 2014).

## Statistical Analyses

Data are presented as mean ± SD or median and range, as appropriate. The distribution of variables was tested for normality using the Shapiro–Wilk's *W*-test. Differences between normally and non-normally distributed variables were evaluated by the Student *t* or Mann Whitney *U* test, respectively. Categorical variables were compared by the Pearson's $\chi^2$ or Fisher's exact test, as appropriate. The time-course of subjective sleepiness/mood was analyzed by repeated measures ANOVA, by treatment group. After analyzing the whole period 09:30–21:30, analysis was performed also on the 09:30–14:30 interval (*post hoc*, unplanned). Analyses were also repeated after missing data had been imputed by the k-nearest neighbor method. Correlations between sleep diaries and actigraphic variables were tested by the Pearson *r*.

# RESULTS

## Baseline

Treated and untreated patients were comparable in terms of demographic characteristics (**Table 1**). Seven patients slept in single rooms (five treated and two untreated), four in double rooms (two treated and two untreated), 22 in quadruple rooms (15 treated and 7 untreated). Nineteen patients (13 treated and 6 untreated) were qualified as sleeping near (distance < 1 m) and 14 (9 treated and 5 untreated) as sleeping far (distance > 3 m) from the room window. The average length of hospitalization was 4 (range 3–12) days. No significant differences were observed between treated and untreated patients in terms of distribution in single/double/quadruple rooms, position in relation to the window or average length of hospitalization [4 (range 3–12) vs. 3 (range 3–12) days, n.s.; **Table 1**]. The Charlson Comorbidity Index was also comparable in the two groups [1 (range 0–6) vs. 2 (range 0–5), n.s.; **Table 1**].

Diurnal preference and pre-admission sleep quality were comparable in treated and untreated patients (HÖ: 56.8 ± 6.7 vs. 56.1 ± 9.5, n.s.; PSQI: 6.0 ± 3.1 vs. 5.9 ± 3.7, n.s.). Pre-admission sleep timing, as summarized in component 4 of the PSQI, was also comparable (get up time: 06:43 ± 01:11 vs. 07:01 ± 00:48, n.s.; bedtime 23:14 ± 00:44 vs. 23:26 ± 01:22, n.s.).

## Inpatient Stay

Daily sleep diaries were regularly obtained for the whole length of hospitalization for all patients. By contrast, due to poor compliance (i.e., several patients did not wear the Jawbone regularly) and technical issues (depleted battery), only an average 3-day actigraphy recordings (first 3 days of hospitalization) per patient were obtained and analyzable. Actigraphic data were available for 18 patients for day 4, 13 patients for day 5, 10 patients for day 6, and 6–2 patients for days 7–12. There were no significant differences between compliant (actigraphy for the full length of hospitalization) and non-compliant (actigraphy for no more than 3 days) patients in terms of age, Charlson Comorbidity Index, PSQI, HÖ and length of hospitalization.

Diaries documented a trend for a lower number of night awakenings in treated compared to untreated patients (1.65 ± 0.82 vs. 2.42 ± 1.26, $p = 0.057$; **Table 2**). All other

**TABLE 1 |** Patients' features, by treatment group.

| Features | | Total (*n* = 33) | Treated (*n* = 22) | Untreated (*n* = 11) | *p* | t/*U*/$\chi$/*OR* |
|---|---|---|---|---|---|---|
| Demographics | Age (years; mean ± SD) | 51.1 ± 13.6 | 48.3 ± 13.3 | 56.9 ± 12.9 | 0.086 | −1.774 |
| | Gender (% males) | 64 | 59 | 73 | 0.355 | *0.542* |
| | Charlson Comorbidity Index (median; range) | 2 (0–6) | 1 (0–6) | 2 (0–5) | 0.158 | *83.5* |
| Hospitalization | Room type (single/double/quadruple, n) | 7/4/22 | 5/2/15 | 2/2/7 | 0.743 | 0.594 |
| | Bed position (near/far from the window, n) | 19/14 | 13/9 | 6/5 | 0.547 | *0.831* |
| | Length of hospitalization (days; median; range) | 4 (3–12) | 4 (3–12) | 3 (3–12) | 0.909 | *117.5* |
| Diurnal preference and | HÖ (mean ± SD) | 56.6 ± 7.4 | 56.8 ± 6.7 | 56.1 ± 9.5 | 0.841 | 0.203 |
| Night sleep quality | PSQI (mean ± SD) | 6.0 ± 3.2 | 6.0 ± 3.1 | 5.9 ± 3.7 | 0.931 | 0.088 |

*HÖ, Horne–Östberg morningness–eveningness questionnaire; PSQI, Pittsburgh Sleep Quality Index.*

**TABLE 2 |** Sleep-wake timing based on daily diaries (entire hospitalization period).

| | Treated, mean/*median* (n) | Untreated, mean/*median* (n) | *p* | t/*U* value |
|---|---|---|---|---|
| Bedtime (hh:mm ± hh:min) | 22:23 ± 00:43 (21) | 22:16 ± 01:05 (9) | 0.740 | 0.335 |
| Time try to sleep (hh:mm ± hh:min) | 23:01 ± 00:32 (21) | 22:52 ± 00:58 (10) | 0.623 | 0.497 |
| Sleep onset (hh:mm ± hh:min) | 23:22 ± 00:36 (21) | 23:11 ± 00:59 (10) | 0.552 | 0.601 |
| Wake up time (hh:mm ± hh:min) | 06:31 ± 00:44 (21) | 06:20 ± 00:28 (9) | 0.707 | 0.379 |
| Get up time (hh:mm ± hh:min) | 07:02 ± 00:45 (21) | 07:01 ± 00:33 (8) | 0.680 | −0.417 |
| Daytime naps (n) | 0.25 (0–2.57) (21) | 0.67 (0–1.08) (10) | 0.272 | *78.5* |
| Night awakenings (n) | 1.65 ± 0.82* (21) | 2.42 ± 1.26* (10) | 0.057 | −1.978 |
| Sleep onset latency (min) | *22* (3–45) (21) | 15 (6–52) (10) | 0.597 | *92* |
| Length of sleep (h) | 7.17 ± 0.77 (21) | 6.87 ± 1.47 (10) | 0.489 | 0.700 |
| Time spent in bed (h) | 8.5 (7.12–10.03) (21) | 8.54 (5.37–10.44) (8) | 0.733 | *76.5* |
| Sleep quality (1–10) | 5.78 ± 1.62 (20) | 6.27 ± 1.57 (10) | 0.574 | −0.569 |

*$p < 0.05$.

diary parameters were comparable in the two groups (**Table 2**). Actigraphy documented significantly earlier day mode switch time in treated compared to untreated patients (06:39 ± 00:35 vs. 07:44 ± 00:40, $p = 0.008$; **Table 3**). All other Jawbone parameters were comparable in the two groups (**Table 3**).

Comparing get up time before (Component 4 of PSQI) and during hospitalization (get up time on sleep diaries and day mode on actigraphy), by treatment group, no significant changes were observed over time.

Significant correlations were observed between a number of parallel diary- and actigraphy-derived parameters (i.e., number of awakenings, $r = 0.96$; $p < 0.001$; get up times/day mode, $r = 0.53$; $p = 0.029$).

The overall (waking hours) and the morning time-course of sleepiness are shown in **Figures 2A** and **B**, respectively, by treatment group. Over the waking hours (**Figure 2A**), the effect of time was significant ($F = 1.932$, $p = 0.034$), while that of treatment was not ($F = 0.481$, $p = 0.499$), and there was no interaction ($F = 1.164$, $p = 0.313$). By contrast, the levels of sleepiness reported by treated patients were significantly lower over the 09:30–14:30 interval, i.e., immediately after the course of light treatment (interaction effect: $F = 2.661$; $p = 0.026$) (**Figure 2B**). Overall, treated patients exhibited a considerably more physiological time-course of subjective sleepiness, which decreased during the morning, peaked in the early afternoon and then started increasing again in the early evening (Eriksen et al., 2005; Ekstedt et al., 2009; Turco et al., 2015).

**TABLE 3 |** Actigraphic indices averaged over the first three days of hospitalization.

| | Treated (n) | Untreated (n) | *p* | *t* value |
|---|---|---|---|---|
| Total sleep (h) | 6.57 ± 1.43 (13) | 6.58 ± 0.93 (6) | 0.970 | −0.038 |
| Sleep latency (h) | 2.77 ± 0.48 (12) | 1.93 ± 0.98 (6) | 0.257 | 1.176 |
| Time spent in bed (h) | 9.20 ± 1.13 (12) | 8.52 ± 0.97 (6) | 0.253 | 1.185 |
| Awakenings (n) | 1.75 ± 0.85 (21) | 2.37 ± 1.29 (10) | 0.120 | −1.601 |
| Day mode (hh:mm ± min) | 06:39 ± 00:35* (11) | 07:44 ± 00:40* (5) | 0.008 | −3.084 |
| Night mode (hh:mm ± min) | 20:48 ± 02.38 (14) | 21:58 ± 00:28 (5) | 0.352 | −0.958 |

*$p < 0.05$.

The overall (waking hours) and the morning time-course of mood are shown in **Figures 3A** and **B**, respectively, by treatment group. Mood levels were generally higher in treated patients. Over the waking hours (**Figure 3A**), no significant effects were observed. By contrast, over the morning hours, i.e., immediately after the course of light treatment (**Figure 3B**), time was not significant ($F = 1.773$, $p = 0.124$) while treatment was ($F = 5.692$, $p = 0.026$), with no interaction ($F = 0.698$, $p = 0.626$).

Results did not change when the time course of sleepiness and mood (over part of the day) was re-analyzed after missing data had been imputed by the k-nearest neighbor method.

Finally, sleep-inducing drugs were prescribed to three patients in the treatment group and four in the control group. Two of these patients, one per group, were already on sleep-inducing medication prior to hospitalization. When sleep-inducing medication use was expressed as a% (nights on sleep-inducing medication/total inpatient nights), no significant differences in the use of sleep-inducing drugs were observed between treated and untreated patients (10 ± 28 vs. 29 ± 46%, $p = 0.152$).

## DISCUSSION

In hospitalized patients, the combination of disease, modified light, food and activity cues, together with sleeping within a noisy, unusual environment, results in altered circadian rhythmicity, poor sleep quality and increased number of night awakenings. Among the environmental/exogenous factors that influence sleep-wake rhythmicity, inefficient photic resetting of the circadian timing system plays a powerful role within the "arrhythmic" hospital environment, and seems to be a promising field for intervention (Bano et al., 2014). In the present study, we used a combination of short-wavelength filter glasses plus a 30-min course of light administration in a group of well-characterized medical inpatients, with the aim of guaranteeing darkness at night and providing higher amounts of strong, blue-enriched light in the early morning, as an entrainment cue. Treated patients showed a trend for a lower number of night awakenings on sleep diaries and earlier wake up time/day mode on actigraphy records compared to their untreated counterparts.

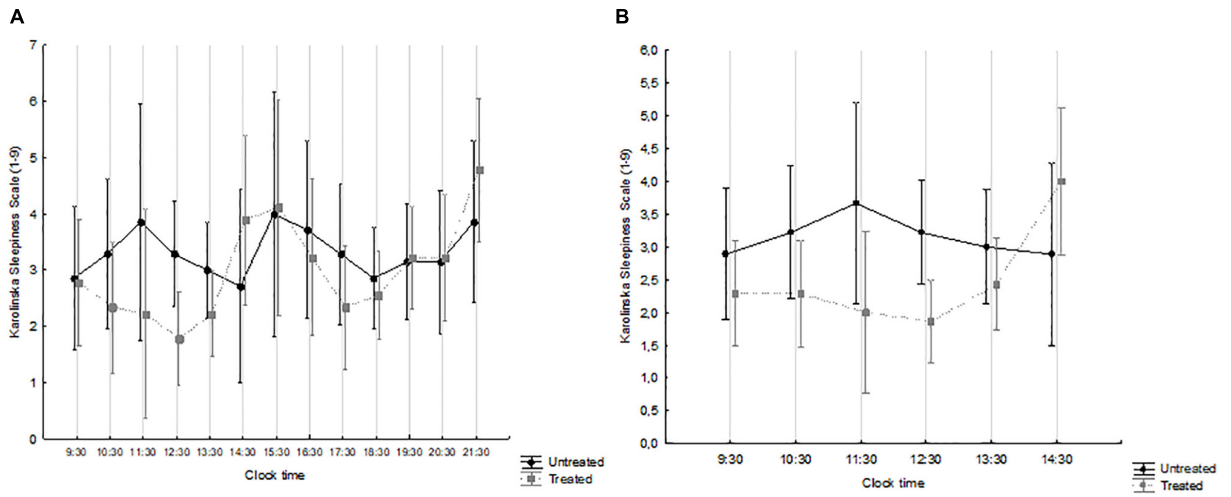


**FIGURE 2 |** Karolinska Sleepiness Scale (KSS) scores, from 09:30 to 21:30 **(A)** and from 09:30 to 14:30 **(B)** in patients treated with Luminette® light glasses plus short-wavelength filter glasses (gray squares and broken line) and untreated patients (black circles and full line). **(A)** Time: $F = 1.932$, $p = 0.034$; treatment: $F = 0.481$, $p = 0.499$; interaction time × treatment: $F = 1.164$, $p = 0.313$. treated $n = 9$; untreated $n = 7$. **(B)** Time: $F = 1.210$, $p = 0.310$; treatment: $F = 2.342$, $p = 0.141$; interaction time × treatment: $F = 2.661$, $p = 0.026$. treated $n = 14$; untreated $n = 9$.

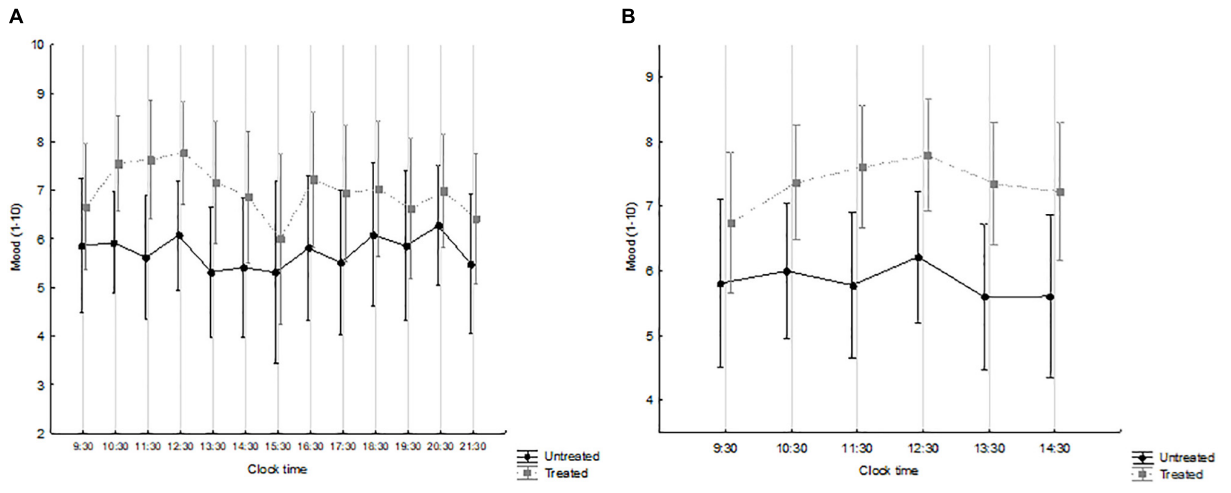


**FIGURE 3 |** Mood (1–10 visual-analogue scale), from 09:30 to 21:30 **(A)** and from 09:30 to 14:30 **(B)** in patients treated with Luminette light glasses plus short-wavelength filter glasses (gray squares and broken line) and untreated patients (black circles and full line). **(A)** Time: $F = 1.583$, $p = 0.100$; treatment: $F = 2.887$, $p = 0.110$; interaction time × treatment: $F = 0.719$, $p = 0.732$. treated $n = 9$; untreated $n = 7$. **(B)** Time: $F = 1.773$, $p = 0.124$; treatment: $F = 5.692$, $p = 0.026$; interaction time × treatment: $F = 0.698$, $p = 0.626$. treated $n = 14$; untreated $n = 9$.

While compliance with actigraphy was limited and a number of technical problems were encountered, correlations were detected between parallel diary and actigraphic parameters. Moreover, in treated patients, the time course of subjective sleepiness over the waking hours was closer to the physiological one (Eriksen et al., 2005; Ekstedt et al., 2009; Turco et al., 2015), and mood was also better. This is in line with a significant amount of literature on the positive effects of light on mood (Wirz-Justice et al., 2005), which have been rarely, however, tested in inpatients. Finally, while statistical significance was not reached, sleep-inducing medication was more commonly prescribed in untreated compared to treated patients. This observation, together with the earlier day mode switch and better mood observed in treated patients, is extremely interesting from a clinical stand point, as a more efficient performance over the early waking hours may have positive domino effects, making medical inpatients more amenable and more responsive to other entrainment cues, such as food intake and physical activity (i.e., if the patient is found to be sleepy in the early morning rounds, he/she is much more likely to skip breakfast and/or a physiotherapy session).

Over recent years, evidence has emerged that abnormalities in circadian regulation (misalignment), altered sleep-wake cycles and poor sleep quality have serious medical consequences,

including an increased incidence of diabetes, obesity, metabolic syndrome (Spiegel et al., 2009), cardio-vascular accidents (Zhong et al., 2005; Haupt et al., 2008; Sauvet et al., 2010; Vetter et al., 2016), and even certain types of cancer (Masri and Sassone-Corsi, 2018; Walasa et al., 2018). It is therefore possible to hypothesize that misalignment, and especially hospitalization-related misalignment, may have a further, negative impact in patients who already have these conditions, making countermeasures akin to those used in this study clinically relevant. Larger, most likely multicenter studies are needed to address this issue.

Overall, compliance with both types of "glasses" was good: only two patients did not regularly use them and were subsequently excluded for poor adherence with the protocol. In general, both types of glasses were well tolerated and seemed comfortable to wear, also on top of prescription glasses. While wearing them, patients were free to perform their usual activities (for example have breakfast, read or walk within their room or the ward communal areas), without significant constraints. This is an advantage over other light-emitting devices we used in previous studies, such as fixed room lighting (De Rui et al., 2015) or light boxes (Turco et al., 2018), which force patients to remain substantially still or at least within one room for the duration of the treatment session. Eye masks and earplugs, which have been shown to be cost-effective in other studies (Le Guen et al., 2014; Hu et al., 2015; Demoule et al., 2017; Bani Younis et al., 2019) often result in discomfort and disorientation from lack of environmental cues, especially in elderly inpatients (Inouye et al., 2014; Marcantonio, 2017).

Poorer compliance and frequent technical problems were encountered with the Jawbone. Several patients did not wear it regularly, often because they forgot to put it back on after removing it to bathe or shower, and several devices stopped working earlier than expected because of battery depletion. We therefore had a less satisfactory experience with this type of device compared to standard actigraphs we used in the past (Montagnese et al., 2009), which are more expensive but evidently also more reliable.

The study was originally designed as a pilot and ecological one, based on relatively inexpensive equipment for patient-directed use, with a considerably less rigid protocol compared to those generally used in chronobiology/chronotherapy studies. These choices, together with a number of problems encountered while the study was being performed, also resulted in significant limitations, including the small sample size (with consequent, limited room for subgrouping and adjustment for variables such as age), the relatively brief duration of the inpatient stay, and thus of the course of treatment. On the other hand, the obtained data also represent an indirect measure of feasibility of chronotherapy in the acute medical setting.

As for most pilot studies, power analysis was not performed *a priori*. Based on the sleepiness results (between effect), the required number of patients in each arm for a future, adequately powered study would be 50.

The limited amount of data available for actigraphic recordings, that forced us to analyze only the first 3 days of hospitalization, may be responsible for some of the discrepancy between sleep diaries and actigraphy findings. It should also be highlighted how not all diary- and actigraphy-derived parameters were strictly comparable, for example wake up time on diaries being only a proxy for the subjective day mode parameter on actigraphy.

Previous studies of light therapy have been conducted over long periods of time, and often set in long-term healthcare facilities such as nursing homes (Van Someren et al., 1999). By contrast, in the medical ward setting patients are usually admitted from the Accident and Emergency, hospitalized for a few days and then discharged as soon as health conditions improve. In addition, the length of hospitalization of the patients included in this study was approximately 4 days, which is shorter than the average for our ward (approximately 9 days). This difference might be due to selection bias on recruitment, as only patients who were sufficiently fit to provide consent and to comply with the protocol were included.

In this study, no objective biomarkers (i.e., 6-sulphatoxy-melatonin) of circadian amplitude or phase were measured. This choice was based on previous experience of significant logistic and analyses difficulties with long, timed urine collections for 6-sulphatoxy-melatonin measurement within the medical/intensive care environments (Gögenur et al., 2007; De Rui et al., 2015). Post-discharge information, i.e., length of convalescence and sleep-wake rhythmicity at home, was not acquired on this occasion and may be of interest for future, similar studies. A final limitation is the lack of a placebo arm, which always represents a significant problem in light treatment trials.

## CONCLUSION

In conclusion, a brief course of treatment with morning bright light and short-wavelength filter glasses overnight, which was well tolerated, showed positive results in terms of wakefulness/mood over the morning hours and a trend for decreased night awakenings in a small group of medical inpatients. These results are promising, and suggest considerable potential for chronotherapy, intended as a rhythm protecting/rhythm enhancing tool (Abbott et al., 2018), within arrhythmic environments such as hospitals.

## DATA AVAILABILITY STATEMENT

The datasets generated for this study are available on request to the corresponding author.

## ETHICS STATEMENT

The studies involving human participants were reviewed and approved by the Ethics Committee, Padua University Hospital (Padua, Italy). The patients/participants provided their written informed consent to participate in this study.

## AUTHOR CONTRIBUTIONS

CF and SC recruited the patients, analyzed the data, and drafted the manuscript. MT and LZ contributed to the patients' recruitment and analyzed the data. PA revised the manuscript for important intellectual content. SM conceived and designed the study, analyzed the data, and reviewed the manuscript.

## REFERENCES


Abbott, S. M., Malkani, R. G., and Zee, P. C. (2018). Circadian disruption and human health: a bidirectional relationship. *Eur. J. Neurosci.* [Epub ahead of print].

Akerstedt, T., and Gillberg, M. (1990). Subjective and objective sleepiness in the active individual. *Int. J. Neurosci.* 52, 29–37. doi: 10.3109/00207459008994241

Bani Younis, M. K., Hayajneh, F. A., and Alduraidi, H. (2019). Effectiveness of using eye mask and earplugs on sleep length and quality among intensive care patients: a quasi-experimental study. *Int. J. Nurs. Pract.* 25:e12740. doi: 10.1111/ijn.12740

Bano, M., Chiaromanni, F., Corrias, M., Turco, M., De Rui, M., Amodio, P., et al. (2014). The influence of environmental factors on sleep quality in hospitalized medical patients. *Front. Neurol.* 5:267. doi: 10.3389/fneur.2014.00267

Bernhofer, E. I., Higgins, P. A., Daly, B. J., Burant, C. J., and Hornick, T. R. (2014). Hospital lighting and its association with sleep, mood and pain in medical inpatients. *J. Adv. Nurs.* 70, 1164–1173. doi: 10.1111/jan.12282

Bragard, I., and Coucke, P. A. (2013). Impact of the use of Luminette® on well-being at work in a radiotherapy department. *Cancer Radiother.* 17, 731–735. doi: 10.1016/j.canrad.2013.05.014

Buysse, D. J., Reynolds, C. F., Monk, T. H., Berman, S. R., and Kupfer, D. J. (1989). The Pittsburgh sleep quality index: a new instrument for psychiatric practice and research. *Psychiatry Res.* 28, 193–213. doi: 10.1016/0165-1781(89)90047-4

Carney, C. E., Buysse, D. J., Ancoli-Israel, S., Edinger, J. D., Krystal, A. D., Lichstein, K. L., et al. (2012). The consensus sleep diary: standardizing prospective sleep self-monitoring. *Sleep* 35, 287–302. doi: 10.5665/sleep.1642

Cellini, N., Buman, M. P., McDevitt, E. A., Ricker, A. A., and Mednick, S. C. (2013). Direct comparison of two actigraphy devices with polysomnographically recorded naps in healthy young adults. *Chronobiol. Int.* 30, 691–698. doi: 10.3109/07420528.2013.782312

Charlson, M. E., Pompei, P., Ales, K. L., and MacKenzie, C. R. (1987). A new method of classifying prognostic comorbidity in longitudinal studies: development and validation. *J. Chronic Dis.* 40, 373–383. doi: 10.1016/0021-9681(87)90171-8

Cook, J. D., Prairie, M. L., and Plante, D. T. (2018). Ability of the multisensory jawbone UP3 to quantify and classify sleep in patients with suspected central disorders of hypersomnolence: a comparison against polysomnography and actigraphy. *J. Clin. Sleep Med.* 15, 841–848. doi: 10.5664/jcsm.7120

Curcio, G., Tempesta, D., Scarlata, S., Marzano, C., Moroni, F., Rossini, P. M., et al. (2013). Validity of the Italian version of the Pittsburgh sleep quality index (PSQI). *Neurol. Sci.* 34, 511–519. doi: 10.1007/s10072-012-1085-y

De Rui, M., Middleton, B., Sticca, A., Gatta, A., Amodio, P., Skene, D. J., et al. (2015). Sleep and circadian rhythms in hospitalized patients with decompensated cirrhosis: effect of light therapy. *Neurochem. Res.* 40, 284–292. doi: 10.1007/s11064-014-1414-z

Demoule, A., Carreira, S., Lavault, S., Pallanca, O., Morawiec, E., Mayaux, J., et al. (2017). Impact of earplugs and eye mask on sleep in critically ill patients: a prospective randomized study. *Crit. Care* 21:284. doi: 10.1186/s13054-017-1865-0

Ekstedt, M., Söderström, M., and Akerstedt, T. (2009). Sleep physiology in recovery from burnout. *Biol. Psychol.* 82, 267–273. doi: 10.1016/j.biopsycho.2009.08.006

Eriksen, C. A., Akerstedt, T., Kecklund, G., and Akerstedt, A. (2005). Comment on short-term variation in subjective sleepiness. *Percept. Mot. Skills* 101, 943–948. doi: 10.2466/pms.101.3.943-948

Foster, R. G. (2005). Neurobiology: bright blue times. *Nature* 433, 698–699. doi: 10.1038/433698a

Freedman, N. S., Gazendam, J., Levan, L., Pack, A. I., and Schwab, R. J. (2001). Abnormal sleep/wake cycles and the effect of environmental noise on sleep disruption in the intensive care unit. *Am. J. Respir. Crit. Care Med.* 163, 451–457. doi: 10.1164/ajrccm.163.2.9912128

Friese, R. S. (2008). Sleep and recovery from critical illness and injury: a review of theory, current practice, and future directions. *Crit. Care Med.* 36, 697–705. doi: 10.1097/CCM.0B013E3181643F29

Gögenur, I., Middleton, B., Burgdorf, S., Rasmussen, L. S., Skene, D. J., and Rosenberg, J. (2007). Impact of sleep and circadian disturbances in urinary 6-sulphatoxymelatonin levels, on cognitive function after major surgery. *J. Pineal Res.* 43, 179–184. doi: 10.1111/j.1600-079x.2007.00460.x

Gringras, P., Middleton, B., Skene, D. J., and Revell, V. L. (2015). Bigger. *Front. Public Health* 3:233. doi: 10.3389/fpubh.2015.00233

Haupt, C. M., Alte, D., Dörr, M., Robinson, D. M., Felix, S. B., John, U., et al. (2008). The relation of exposure to shift work with atherosclerosis and myocardial infarction in a general population. *Atherosclerosis* 201, 205–211. doi: 10.1016/j.atherosclerosis.2007.12.059

Horne, J. A., and Ostberg, O. (1976). A self-assessment questionnaire to determine morrningness-eveningness in human circadian rhythms. *Int. J. Chronobiol.* 4, 97–110.

Hu, R. F., Jiang, X. Y., Chen, J., Zeng, Z., Chen, X. Y., Li, Y., et al. (2015). Non-pharmacological interventions for sleep promotion in the intensive care unit. *Cochrane Database Syst. Rev.* 10:CD008808. doi: 10.1002/14651858.CD008808.pub2

Humphries, J. D. (2008). Sleep disruption in hospitalized adults. *Medsurg Nurs.* 17, 391–395.

Inouye, S. K., Westendorp, R. G., and Saczynski, J. S. (2014). Delirium in elderly people. *Lancet* 383, 911–922. doi: 10.1016/S0140-6736(13)60688-1

Kamdar, B. B., Needham, D. M., and Collop, N. A. (2012). Sleep deprivation in critical illness: its role in physical and psychological recovery. *J. Intensive Care Med.* 27, 97–111. doi: 10.1177/0885066610394322

Langevin, R. H., Laurent, A., and Sauvé, Y. (2014). Preliminary assessment on the effectiveness of the Luminette® in adolescents with a delayed sleep phase syndrome (DSPS): randomized single blind placebo-controlled study. *Med. Sommeil* 11, 91–97. doi: 10.1016/j.msom.2014.03.003

Le Guen, M., Nicolas-Robin, A., Lebard, C., Arnulf, I., and Langeron, O. (2014). Earplugs and eye masks vs routine care prevent sleep impairment in post-anaesthesia care unit: a randomized study. *Br. J. Anaesth.* 112, 89–95. doi: 10.1093/bja/aet304

Lockley, S. W., Skene, D. J., and Arendt, J. (1999). Comparison between subjective and actigraphic measurement of sleep and sleep rhythms. *J. Sleep Res.* 8, 175–183. doi: 10.1046/j.1365-2869.1999.00155.x

Marcantonio, E. R. (2017). Delirium in hospitalized older adults. *N. Engl. J. Med.* 377, 1456–1466. doi: 10.1056/NEJMcp1605501

Martin, J. L., and Hakim, A. D. (2011). Wrist actigraphy. *Chest* 139, 1514–1527. doi: 10.1378/chest.10-1872

Masri, S., and Sassone-Corsi, P. (2018). The emerging link between cancer, metabolism, and circadian rhythms. *Nat. Med.* 24, 1795–1803. doi: 10.1038/s41591-018-0271-8

Meyer, T. J., Eveloff, S. E., Bauer, M. S., Schwartz, W. A., Hill, N. S., and Millman, R. P. (1994). Adverse environmental conditions in the respiratory and medical ICU settings. *Chest* 105, 1211–1216. doi: 10.1378/chest.105.4.1211

Missildine, K., Bergstrom, N., Meininger, J., Richards, K., and Foreman, M. D. (2010). Sleep in hospitalized elders: a pilot study. *Geriatr. Nurs.* 31, 263–271. doi: 10.1016/j.gerinurse.2010.02.013

Montagnese, S., Middleton, B., Mani, A. R., Skene, D. J., and Morgan, M. Y. (2009). Sleep and circadian abnormalities in patients with cirrhosis: features of delayed sleep phase syndrome? *Metab. Brain Dis.* 24, 427–439. doi: 10.1007/s11011-009-9146-5

Sauvet, F., Leftheriotis, G., Gomez-Merino, D., Langrume, C., Drogou, C., Van Beers, P., et al. (2010). Effect of acute sleep deprivation on vascular function in healthy subjects. *J. Appl. Physiol.* 108, 68–75. doi: 10.1152/japplphysiol.00851.2009

Spiegel, K., Tasali, E., Leproult, R., and Van Cauter, E. (2009). Effects of poor and short sleep on glucose metabolism and obesity risk. *Nat. Rev. Endocrinol.* 5, 253–261. doi: 10.1038/nrendo.2009.23

Spielman, A. J., Yang, C. M., and Glovinsky, P. B. (eds) (2005). "Assessment techniques for insomnia," in Principles and Practice of Sleep Medicine (Philadelphia, PA: Elsevier), 1403–1416. doi: 10.1016/b0-72-160797-7/50126-9

Tranmer, J. E., Minard, J., Fox, L. A., and Rebelo, L. (2003). The sleep experience of medical and surgical patients. *Clin. Nurs. Res.* 12, 159–173. doi: 10.1177/1054773803012002004

Turco, M., Cazzagon, N., Franceschet, I., Formentin, C., Frighetto, G., Giordani, F., et al. (2018). Morning bright light treatment for sleep-wake disturbances in primary biliary cholangitis: a pilot study. *Front. Physiol.* 9:1530. doi: 10.3389/fphys.2018.01530

Turco, M., Corrias, M., Chiaromanni, F., Bano, M., Salamanca, M., Caccin, L., et al. (2015). The self-morningness/eveningness (Self-ME): an extremely concise and totally subjective assessment of diurnal preference. *Chronobiol. Int.* 32, 1192–1200. doi: 10.3109/07420528.2015.1078807

van Kamp, I., and Davies, H. (2008). "Environmental noise and mental health: five year review and future directions," in *Proceedings of the 9th International Congress on Noise as a Public Health Problem* (Foxwoods, CT: Mashantucket).

Van Someren, E. J., Swaab, D. F., Colenda, C. C., Cohen, W., McCall, W. V., and Rosenquist, P. B. (1999). Bright light therapy: improved sensitivity to its effects on rest-activity rhythms in Alzheimer patients by application of nonparametric methods. *Chronobiol. Int.* 16, 505–518. doi: 10.3109/07420529908998724

Vetter, C., Devore, E. E., Wegrzyn, L. R., Massa, J., Speizer, F. E., Kawachi, I., et al. (2016). Association between rotating night shift work and risk of coronary heart disease among women. *JAMA* 315, 1726–1734. doi: 10.1001/jama.2016.4454

Walasa, W. M., Carey, R. N., Si, S., Fritschi, L., Heyworth, J. S., Fernandez, et al. (2018). Association between shiftwork and the risk of colorectal cancer in females: a population-based case-control study. *Occup. Environ. Med.* 75, 344–350. doi: 10.1136/oemed-2017-104657

Wirz-Justice, A., Benedetti, F., Berger, M., Lam, R. W., Martiny, K., Terman, M., et al. (2005). Chronotherapeutics (light and wake therapy) in affective disorders. *Psychol. Med.* 35, 939–944.

Zhong, X., Hilton, H. J., Gates, G. J., Jelic, S., Stern, Y., Bartels, M. N., et al. (2005). Increased sympathetic and decreased parasympathetic cardiovascular modulation in normal humans with acute sleep deprivation. *J. Appl. Physiol.* 98, 2024–2032. doi: 10.1152/japplphysiol.00620.2004

**Conflict of Interest:** The authors declare that the research was conducted in the absence of any commercial or financial relationships that could be construed as a potential conflict of interest.

frontiers in Physiology

ORIGINAL RESEARCH
published: 06 March 2020
doi: 10.3389/fphys.2020.00145

# Disrupted Glutamate Signaling in *Drosophila* Generates Locomotor Rhythms in Constant Light

*Renata Van De Maas de Azevedo[1], Celia Hansen[1], Ko-Fan Chen[2†], Ezio Rosato[1] and Charalambos P. Kyriacou[1]**

[1] Department of Genetics and Genome Biology, University of Leicester, Leicester, United Kingdom, [2] School of Biological and Chemical Sciences, Queen Mary University of London, London, United Kingdom

OPEN ACCESS

**Edited by:**
*Elzbieta M. Pyza, Jagiellonian University, Poland*

**Reviewed by:**
*Justin Blau, New York University, United States*
*Patrick Emery, University of Massachusetts Medical School, United States*

***Correspondence:**
*Charalambos P. Kyriacou*
*cpk@leicester.ac.uk*

**†Present address:**
*Ko-Fan Chen, Department of Clinical and Experimental Epilepsy, UCL Queen Square Institute of Neurology, London, United Kingdom*

**Specialty section:**
*This article was submitted to Chronobiology, a section of the journal Frontiers in Physiology*

**Received:** *12 November 2019*
**Accepted:** *11 February 2020*
**Published:** *06 March 2020*

**Citation:**
*Azevedo RVDM, Hansen C, Chen K-F, Rosato E and Kyriacou CP (2020) Disrupted Glutamate Signaling in Drosophila Generates Locomotor Rhythms in Constant Light. Front. Physiol. 11:145. doi: 10.3389/fphys.2020.00145*

We have used the Cambridge Protein Trap resource (CPTI) to screen for flies whose locomotor rhythms are rhythmic in constant light (LL) as a means of identifying circadian photoreception genes. From the screen of ∼150 CPTI lines, we obtained seven hits, two of which targeted the glutamate pathway, *Got1 (Glutamate oxaloacetate transaminase 1)* and *Gs2 (Glutamine synthetase 2).* We focused on these by employing available mutants and observed that variants of these genes also showed high levels of LL rhythmicity compared with controls. It was also clear that the genetic background was important with a strong interaction observed with the common and naturally occurring *timeless (tim)* polymorphisms, *ls-tim* and *s-tim.* The less circadian photosensitive *ls-tim* allele generated high levels of LL rhythmicity in combination with *Got1* or *Gs2,* even though *ls-tim* and *s-tim* alleles do not, by themselves, generate the LL phenotype. The use of dsRNAi for both genes as well as for *Gad (Glutamic acid decarboxylase)* and the metabotropic glutamate receptor DmGluRA driven by clock gene promoters also revealed high levels of LL rhythmicity compared to controls. It is clear that the glutamate pathway is heavily implicated in circadian photoreception. TIM levels in *Got1* and *Gs2* mutants cycled and were more abundant than in controls under LL. *Got1* but not *Gs2* mutants showed diminished phase shifts to 10 min light pulses. Neurogenetic dissection of the LL rhythmic phenotype using the *gal4/gal80 UAS* bipartite system suggested that the more dorsal CRY-negative clock neurons, DNs and LNds were responsible for the LL phenotype. Immunocytochemistry using the CPTI YFP tagged insertions for the two genes revealed that the DN1s but not the DN2 and DN3s expressed Got1 and Gs2, but expression was also observed in the lateral neurons, the LNds and s-LNvs. Expression of both genes was also found in neuroglia. However, downregulation of glial *Gs2* and *Got1* using *repo-gal4* did not generate high levels of LL rhythmicity, so it is unlikely that this phenotype is mediated by glial expression. Our results suggest a model whereby the DN1s and possibly CRY-negative LNds use glutamate signaling to supress the pacemaker s-LNvs in LL.

**Keywords: *Drosophila*, circadian, LL rhythmicity, screen, glutamate, locomotor, dorsal neurons**

## INTRODUCTION

The molecular basis of the *Drosophila* circadian clock has been dissected predominantly by the use of mutant screens (Axelrod et al., 2015). This forward genetics approach has identified a number of cardinal clock genes that generate interconnected feedback loops, in which two transcription factors, CLOCK (CLK) and CYCLE (CYC), play centre stage by dimerizing and activating transcription of *period (per)* and *timeless (tim)* during the subjective day (Hardin and Panda, 2013). PER and TIM begin to accumulate, but a series of posttranslational modification by kinases and phosphatases followed by degradation, delays the accumulation of PER until the late subjective night (Top et al., 2018). Then, PER-TIM enter the nucleus of clock cells and inhibit CLK/CYC, thereby negatively regulating their own *(per* and *tim)* genes. During the next subjective day, PER and TIM are degraded which releases CLK/CYC to return to the *per/tim* promoters and re-activate transcription. CLK also intersects with two other loops defined by PDP1ε/VRI and CWO which stabilize the oscillating system (Hardin and Panda, 2013).

While the clock is self-sustaining in constant conditions, it nevertheless responds to environmental stimuli, particularly light. Under a light-dark cycle, at dawn, CRYPTOCHROME (CRY), a blue light photoreceptor is activated and this leads first to the degradation of TIM (and CRY), followed by PER, and the transcription-translational cycle starts again as CLK/CYC return to the *per/tim* promoters (Stanewsky et al., 1998; Ceriani et al., 1999). The light input pathway to the clock depends not only on the photoreceptor CRY but also on the rhodopsins and the visual system (Kistenpfennig et al., 2017; Leung and Montell, 2017; Li et al., 2018; Ogueta et al., 2018). In addition, a number of other factors, both cell autonomous and non-autonomous including Jetlag, Ramshackle, Quasimodo and cell-to-cell communication are important in the degradation of TIM/CRY after light exposure (Koh et al., 2006; Peschel et al., 2006, 2009; Tang et al., 2010; Chen et al., 2011; Ozturk et al., 2013).

Neurogenetic studies of the fly clock over the past 15 years have identified a set of 150 circadian neurons in the brain divided into seven major groupings, of which the PDF-positive small ventral lateral neurons (s-LNvs) have been described as representing the pacemaker (Top and Young, 2018). However, several laboratories, including ours, have demonstrated that manipulation of any one group of clock neurons has implications for the functioning of the others, highlighting the importance of their network organization (Dissel et al., 2014; Yao and Shafer, 2014; Yao et al., 2016; Chatterjee et al., 2018; Lamba et al., 2018; Delventhal et al., 2019; Schlichting et al., 2019). We have suggested that such organization is of paramount importance in defining the properties of the clock as we have shown that the period of the clock is an emergent property of the network and not a property of any single neuron or group (Dissel et al., 2014). This suggests that other circadian properties, among which, entrainment, might result from network interactions rather than by cell-autonomous properties of clock neurons (Lamba et al., 2018).

Under constant light (LL), wild-type flies become behaviorally arrhythmic but $cry^b$ and $cry^0$ mutants maintain rhythmic locomotor cycles (Emery et al., 2000; Dolezelova et al., 2007). These results suggest that CRY plays a role not only as the dedicated circadian photoreceptor under these conditions, but also as the light gateway into the pacemaker(s) that determine rhythmic behavior, with the mutation apparently blocking all light input including that from the rhodopsins. However, light-dark cycles can still entrain *cry* mutants via the rhodopsins (reviewed in Senthilan et al., 2019). Alternatively, we could argue that such a far-reaching effect of the mutants might derive from CRY regulating the cross-talk among neurons. This hypothesis stems from the finding that light-activated CRY can directly affect neuronal firing (Fogle et al., 2011, 2015; Baik et al., 2017) and has become even more compelling after observing that the PDF-expressing neurons (including the so-called "pacemaker" neurons) are not a hub for circadian light responses. In fact retinal and sub-retinal (Hofbauer-Buchner eyelets) photoreceptors connect to and excite the majority of clock neurons via interneurons (Li et al., 2018).

A strategy to further investigate light entrainment would be to search for mutants that are rhythmic in LL (Dubruille et al., 2009). We have therefore performed such an analysis using the Cambridge Protein Trap Insertion (CPTI) lines in which a pigP (piggyback P-element) that includes YFP and affinity tags (for pulldowns and mass spectrometry) have been inserted between the coding sequences of nearly 400 genes using splice acceptor/donor site targeting (Lowe et al., 2014). The YFP motif generates an additional internal domain within the targeted protein, so it may be that some of these fusion proteins are misfolded and generate a mutant phenotype. With this in mind we screened ∼150 of these lines and report a number which show rhythmicity in LL. Further analysis of two of these lines reveals that the gene traps are located within components of the glutamate signaling pathway. We embark on a series of studies focusing on these two genes as well as other members of the pathway in order to elucidate the role of glutamate signaling in light-dependent behavioral rhythmicity.

## MATERIALS AND METHODS

### Fly Stocks

All fly lines were maintained at 25°C under a light-dark cycle (LD12:12). Candidate genes were downregulated using dsRNAi crossed initially to the *tim-gal4* driver and incorporating *UAS-dicer2* into the crossing scheme to enhance the downregulation. Most of the *UAS-RNAi* lines were obtained from VDRC and available mutants for the genes of interest were obtained from the Bloomington stock centre.

### Locomotor Screening

The CPTI lines (Cambridge Protein Trap Insertions) were screened by placing 2–3 day old male flies in Trikinetics activity monitors at 25°C for 2–3 days in LD12:12 before releasing them under LL (39 $\mu W/cm^2$) for a further 7–10 days. Locomotor activity was collected in 30 min time bins and rhythmicity was analyzed by autocorrelation and spectral analysis using the

CLEAN algorithm. Rhythmic individuals required both analyses to be statistically significant (see Vanin et al., 2012).

## Phase Responses

Flies were maintained in Trikinetics monitors at 25°C in LD12:12 for 3 days. During the third night a 10 min light pulse (39 $\mu W/cm^2$) was administered 3 h (ZT15) or 9 h (ZT21) after lights off (ZT12). The flies were kept in DD after the light pulses and locomotor behavior recorded for several days. A control group of flies of the same genotype did not receive the light pulse. Cross-correlation was used to assess the degree of phase shift by taking the locomotor data from 48 h after the light pulses i.e., the third day, and comparing each individual fly's experimental profile against the average of the control data. This was done by shifting by one bin at a time (lag) the two sets of data against each other and calculating a correlation coefficient for each lag. The number of 30 min bins shifted that produced the maximum correlation provided the experimental phase shift, which could be either a delay or an advance. ANOVA was used to compare the phase shifts of different genotypes.

## Western Blots

Fly heads were collected in LL at CT1, 7, 13 and 19. Western blots were performed as described previously (Sandrelli et al., 2007). α-TIM antibody (gift of Francois Rouyer, Gif, Paris) raised in rat was used at a concentration of 1:2000 with α-rat as secondary (1:10,000). α-Tubulin (1:40000) was used with α-mouse (1:6000, all Sigma-Aldrich). Image J software was used to quantify the TIM bands relative to the corresponding Tubulin.

## Polymorphisms

Naturally occurring polymorphisms were studied by PCR. The *ls-tim/s-tim* variants were genotyped using a PCR strategy published previously (Tauber et al., 2007). We also examined polymorphisms in the *jetlag (jet)* gene by amplifying a 282 bp fragment of *jet* that may harbor two variants, $jet^C$ and $jet^R$, that both cause LL rhythmicity in the *ls-tim* genetic background (Koh et al., 2006; Peschel et al., 2006). Both variants generate an amino acid substitution (phenylalanine to isoleucine, F209I, and serine to leucine S220L). The primers used were *jet 5′-CGCGTACTCAAGCTGTCC* and *jet 3′-CACGCCATAGTCGGAGAT* at an annealing temperature of 64°C and PCR generated fragments were directly sequenced.

## Immunofluorescence

This was performed for the following genotypes: *Got1-YFP/qsm-gal4*$^{104280}$*; dsRed/+*, *Gs2-YFP/qsm-gal4*$^{104280}$*; dsRed/+, Got1-YFP/myr-RFP; repo-gal4/+, Gs2-YFP/myr-RFP; repo-gal4/+*. Prior to collection at the indicated ZT22, flies from different strains were entrained for at least 2 days to LD12:12 conditions. Light intensity was ∼2500 lux. Flies with indicated genotypes were fixed in 4% paraformaldehyde/PBS (3 mM NaH2PO4, 7 mM Na2HPO4, 154 mM NaCl) for 2 h at room temperature. After fixation, the samples were washed 3× by PBS and the fly brains were dissected under a microscope. The dissected brains were collected in PBS 0.1% Triton X-100 and transferred to 4% paraformaldehyde/PBS for 30 min for post dissection fixation. Fly brains were then washed 3× in PBS 0.1% Triton X-100 and blocking with 10% goat serum in 1% PBS-T was applied for 2 h before staining with guinea pig anti-PDP-1ε (1:5000, Benito et al., 2007) in 0.3% PBS-T at 4°C for 48 hr. After washing 3× with 0.1% PBS-T, the samples were incubated at 4°C overnight with anti-guinea pig antibody conjugated with fluorophore, Alexa Fluor 647 nm (Molecular Probes) diluted 1:300 in 0.3% PBS-T. Brains were washed 4× in 0.1% PBS-T and water before being mounted in Vectashield. Samples were stored at 4°C until examination under a LSM-510 META confocal microscope (Zeiss, Germany) or a Leica SP5 confocal microscope.

# RESULTS

## Gene Traps Reveal 7 Putative Loci in the Circadian Light Input Pathway

Of 147 YFP lines screened, 7 showed rhythmicity under LL at levels between 50 and 94%. **Figure 1** shows the average locomotor histograms for the 7 lines plus a control line and examples of individual spectral analyses of locomotor records. **Table 1** provides the statistical analyses of these data. Each CPT line was also tested in constant darkness (DD) and all were rhythmic although the line *CPTI00051* in which the insertion lies in the *Rab11* locus also showed a significantly longer free-running period in DD (26.0 ± 0.3 h). **Table 1** shows the identity of the genes trapped in each of these lines and the free-running period in LL. We then obtained the available *UAS-RNAi* lines or any mutants that existed for these seven loci. **Table 2** shows that RNAi driven by *timgal4* for *Got1 (Glutamate oxaloacetate transaminase 1)* and *Gs2 (Glutamine synthetase 2)* and the available mutant males *w/Y; P(GT1)Got1/P(GT1)Got1 and wP(GT1)Gs2/Y,* confirmed the LL rhythmic phenotype observed in $Got1^{YFP}$ and $Gs2^{YFP}$ (**Supplementary Figure S1**). In the other lines either the mutants could not confirm the phenotype, or the RNAi revealed high levels of LL rhythmicity, but so did their corresponding *UAS-RNAi* parental controls, suggesting leakage and/or a background effect (**Supplementary Table S1**). One interesting exception was *Glycogenin (CPTI-000902)* which gave extremely high levels of LL rhythmicity for both the gene trap and the RNAi (95%) although the *UAS-RNAi* control line also generated 56% LL rhythmicity. Several of the VDRC *UAS-RNAi* lines also gave high levels of rhythmicity in LL suggesting that they carry additional genetic variant(s) within the circadian light input pathway (although not those for *Gs2* nor *Got1,* **Tables 1**, **2**).

## Genetic Background Interacts With *Got1* and *Gs2* Mutations to Generate LL Rhythmicity

As both *Got1* and *Gs2* are involved in glutamate metabolism, we focused on these genes for the rest of the study. Mutations in both genes involved the *w;P(GT1)* element. To test whether

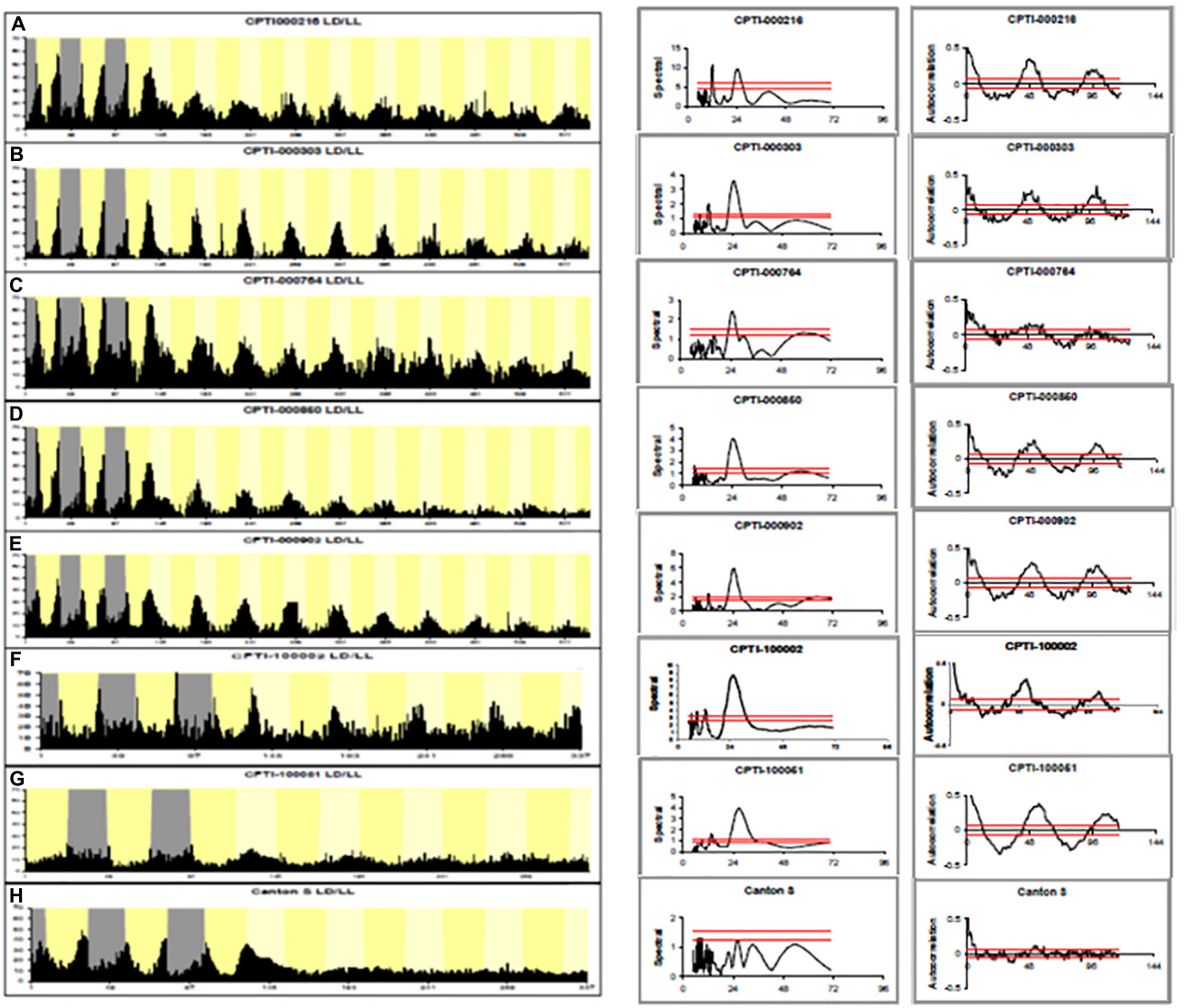


**FIGURE 1 |** Locomotor activity rhythms in LL of CPTI genotypes. Left-hand panels. **(A–E)** 3 days LD, 10 days LL. **(F,H)** 3 days LD, 5 days LL. **(G)** 2 days LD, 5 days LL Gray: dark. Dark yellow: subjective day. Histograms are shown for each CPTI genotype that showed rhythmicity in LL as well as Canton-S controls. Each graph represents the average activity collected in 30 min time bins of all the flies per genotype so arrhythmic flies are included (see **Table 1** for results and N's). **(A)** CPTI-000216. **(B)** CPTI-000303. **(C)** CPTI-000764. **(D)** CPTI-000850. **(E)** CPTI-000902. **(F)** CPTI-100002 **(G)** CPTI-100051. **(H)** Canton S. All the fly lines were rhythmic, except Canton S **(H)**. Middle panels: Spectral analyses using CLEAN of individual activity records. The red horizontal line represent the 99% (top) and 95% (lower) confidence limits based on 1000 random permutations of the data. Right-hand panel: corresponding activity record but analyzed with autocorrelation. 95% confidence limits represented as tapered red horizontal lines.

the *w;P(GT1)* background was sensitized for LL rhythms, we examined another three *w;P(GT1)* insertions in *Tom7, AdhAdhr*, and *prtp*. All three *w;P(GT1)* lines gave low levels of rhythmicity in LL, 22, 20, and 16% respectively (**Table 2**). Consequently the genetic background that provided the *w;P(GT1)* screen was not of itself responsible for the high levels of LL rhythmicity in *Got1* and *Gs2*.

We also crossed the *Got1 w;P(GT1)* mutant females to $w^{1118}$ (white-eyed) mutant males and then assessed the LL rhythmicity in the F2 generation where we could distinguish by eye color the mutant homozygotes, heterozygotes and the white-eyed wild-type. We observed 61% LL rhythmicity in the mutant homozygotes, 44% in heterozygotes (mean periods were 28–29 h) and considerably less LL rhythmicity in the wild-type (**Table 2**). When we performed a similar cross to the sex-linked *Gs2 (wPGT1)* mutant we observed 63% LL rhythmicity in hemizygous mutant males and 31% rhythmicity in the wild-type white-eyed F2 males (**Table 2**). The LL rhythmicity of both *Gs2* and *Got1* mutants after randomizing the genetic background in this way was ∼20% less than the ∼80% we observed with the original YFP gene traps (**Table 1**), suggesting further polymorphisms that were enhancing or reducing the LL effects.

**TABLE 1 |** Results of initial LL screen.

| \CPTI line | Trapped gene | % LL rhythms (N) | Period (sem) | *tim-gal4* RNAi *VDRC* | % (N) rhythmic | Period (sem) | Mutants | % LL rhythms (N) | Period (sem) |
|---|---|---|---|---|---|---|---|---|---|
| 000216 | *lk6 kinase* | 74 (31) | 24.7 (0.2) | *30389* | 31.8 (22) | | *lk61* | 12.5 (8) | – |
| | | | | *32885* | 28.6 (14) | | *lk62* | 18.8 (16) | – |
| | | | | *UAS-30389* | *nd* | | | | |
| 000303 | *Got1* | 90 (20) | 25.0 (0.15) | *108247* | 88.8 (18) | 27.6 (0.7) | *P{GT1}Got1* | 84.6 (22) | 29.8 (0.8) |
| | | | | *108247** | 89.6 (29) | 26.9 (0.5) | *P{wHy}Got1*** | 0 (13) | – |
| | | | | *UAS-108247* | 33.4 (9) | – | | | |
| | | | | *8340-R2* | 62.5 (8) | 26.5 (0.8) | | | |
| | | | | *8340-R2** | 41 (22) | – | | | |
| | | | | *8340-R1* | 26 (27) | – | | | |
| | | | | *8340-R1** | 43 (22) | | | | |
| | | | | *UAS-8340R-2* | 8.0 (13) | – | | | |
| | | | | *UAS-8340R-1* | 9.1 (11) | – | | | |
| 000764 | *kat80 (katanin80)* | 66.6 (21) | 24.5 (0.3) | *24175* | 58.3 | 28.2 (0.6) | *P{SUPor-P}kat80* | 21.6 (26) | – |
| | | | | *UAS-24175* | 55 (11) | 28.8 (1.9) | *P{EP}kat80* | 0 (15) | – |
| 000850 | *Pbl (pebble)* | 69.2 (26 | 25.5 (0.4) | *35349* | 14.3 (7) | – | $pbl^3$/+ | 50 (15) | 25.5 (0.9) |
| | | | | *35350* | 78.5 (28) | 26.4 (0.3) | *pbl5/+* | 12.5 (16) | – |
| | | | | *UAS-3530* | 73 | 26.2 (0.5) | | | |
| 000902 | *Glycogenin* | 94.7 (19) | 24.7 (0.1) | *35452* | 93.7 (6) | 28.9 (0.8) | | | |
| | | | | *UAS-3530* | 56.3 (55) | 28.8 (0.6) | | | |
| 100002 | *Gs2* | 50 (18) | 25.1 (0.2) | *32929* | 81.3 (16) | 25.4 (0.5) | *P{GT1}Gs2* | 80 (25) | 28.6 (0.6) |
| | | | | *3929** | 80.6 (31) | 26.0 (0.3) | | | |
| | | | | *UAS-32929* | 15 (53) | – | | | |
| 100051 | *Rab11* | 69 (9) | 26.3 (0.8) | *22198* | *nd* | *nd* | *P{wHy}Rab11* | 31 (16) | – |

**including UAS-dicer2 **P(wHy)Got1 was also poorly rhythmic in DD (35%).*

## *timeless* but Not *jetlag* Polymorphisms Interact With *Got1* and *Gs2* Mutations to Generate Enhanced Levels of LL Rhythmicity

The best known polymorphism in the light input pathway involves the naturally occurring *s-tim/ls-tim* variant, in which the *ls-tim* allele reduces circadian photosensitivity (Sandrelli et al., 2007; Tauber et al., 2007). We therefore addressed the *tim* status of the w;*P(GT1)* lines and $w^{1118}$ using PCR. The original $Gs2^{YFP}$ and $Got1^{YFP}$ alleles whose results are shown in **Table 1** are in the *ls-tim* background, whereas $w^{1118}$ carries *s-tim*. Consequently, the decrease in levels of LL rhythmicity in the F2 crosses with $w^{1118}$ could be due, in part, to the segregating *ls-tim/s-tim* variant (**Table 2**). We repeated the crosses of each mutant to $w^{1118}$ and inspected the *ls-tim/s-tim* status of each fly after it had also been investigated for LL locomotor rhythmicity. **Table 3** reveals that for both genes, LL rhythmicity is associated with either *ls-tim* homo- or heterozygosity. Almost all the *ls-tim* homozygotes and half the heterozygotes are LL rhythmic. For *Gs2,* 5 homozygous *s-tim* individuals were arrhythmic in LL. Unfortunately we did not obtain any *s-tim* homozygotes for *Got1*. Based on these results it was necessary to verify the *tim* status of the three "control" *w;P(GT1)* induced mutants *Tom7, AdhAdhr, and prtp* which did not show LL rhythmicity. Their *tim* genotyping by PCR revealed that they were all *ls-tim* homozygous (**Table 2**). Consequently the *ls-tim* polymorphism does not by itself cause high levels of LL rhythmicity, supporting previous studies (Sandrelli et al., 2007), yet it does enhance the LL rhythmicity of the *Gs2* and *Got1* *w;P(GT1)* variants.

The behavior of w;*P(GT1)* mutants for *Gs2* and *Got1* resembles that of *Veela* flies which carry the *jetlag* variant $jet^c$, and are rhythmic in LL only in the presence of the less light-sensitive LS-TIM isoform (Peschel et al., 2006). We therefore investigated the *Gs2, Got1* and $w^{1118}$ mutants for the presence of $jet^c$ or the rare allele, $jet^r$. PCR of a 282 *jet* bp fragment that includes both variant sites followed by sequencing did not reveal any polymorphism (data not shown).

**TABLE 2 |** Effects of mutations or *timgal4*-driven downregulation on LL rhythmicity.

| Genotype (id) | % LL rhythms | N | *tim* alleles |
|---|---|---|---|
| ***A. Mutants on w$^{1118}$ background (F2)*** | | | |
| *w$^{1118}$/Y; P{GT1}Got1/ P{GT1}Got1* | 61 | 32 | *ls-tim,s-tim, ls/s-tim* |
| *w$^{1118}$/Y; P{GT1}Got1/+* | 44 | 31 | *ls-tim,s-tim, ls/s-tim* |
| *w$^{1118}$/Y* | 26 | 31 | *ls-tim,s-tim, ls/s-tim* |
| *wP{GT1}Gs2/Y* | 63 | 31 | *ls-tim,s-tim, ls/s-tim* |
| *w$^{1118}$/Y* | 31 | 29 | *ls-tim,s-tim, ls/s-tim* |
| *wP{GT1}Gs2/Y* | 21.8 | 32 | *s-tim* |
| *w/Y; P{GT1}Got1* | 20 | 32 | *s-tim* |
| ***B. RNAi*** | | | |
| *w/Y; tim-gal4/+; Gs2RNAi/+ (32929)* | 81.3 | 16 | *ls-tim,s-tim, ls/s-tim* |
| *UAS 32929* | 15 | 53 | *ls-tim, s-tim. ls/s-tim* |
| *w/Y; tim-gal4/+* | 4 | 51 | *s-tim* |
| *w/Y; tim-gal4/Got1RNAi (UAS VDRC 108247)* | 72.2 | 18 | *ls/s-tim* |
| *w/Y; tim-gal4/+; Got1RNAi/+ (8340R-2)* | 37.5 | 8 | *s-tim* |
| *w/Y; tim-gal4/Got1RNAi (8340R-1)* | 26 | 27 | *s-tim* |
| *UAS VDRC 108247* | 33.4 | 9 | *ls-tim* |
| *UAS 8340R-1* | 9 | 11 | *s-tim* |
| *UAS 8340R-2* | 8 | 13 | *s-tim* |
| ***C. P(GT1) insertion controls*** | | | |
| *w1118/Y; P{GT1}Tom7BG02496 (12698)* | *21.9* | 32 | *ls-tim* |
| *w1118/Y; P{GT1}AdhAdhrBG01049 (12535)* | *20* | 30 | *ls-tim* |
| *w1118/Y; P{GT1}prtpBG00450 (12488)* | *16.2* | 31 | *ls-tim* |

*The tim allelic background for each group is also shown.*

**TABLE 3 |** Segregation analysis in F2 generation for *Gs2* and *Got1* mutants crossed to *w$^{1118}$*.

| | N | $n^R$ | $n^{AR}$ |
|---|---|---|---|
| ***wP{GT1}Gs2/Y*** | | | |
| *ls-tim/ls/tim* | 9 | 9 | 0 |
| *ls-tim/s-tim* | 16 | 10 | 6 |
| *s-tim/s-tim* | 5 | 0 | 5 |
| ***w:P{GT1}Got1/P{GT1}Got1*** | | | |
| *ls-tim/ls/tim* | 14 | 12 | 2 |
| *ls-tim/s-tim* | 17 | 7 | 10 |
| *s-tim/s-tim* | 0 | 0 | 0 |

*$n^R$, $n^{AR}$ represents the numbers rhythmic or arrhythmic in LL respectively. N is total number for each tim genotype.*

We then genotyped the other lines for *Got1* and *Gs2* as well as the parental RNAi lines for the *tim* and *jet* variants. **Table 2** shows that the flies that were downregulated for *Gs2* with *timGal4 (s-tim)* would segregate both *tim* alleles as *UAS 32929* was polymorphic, yet they gave >80% LL rhythmicity. The downregulated lines for *Got1* were heterozygous *s-tim/ls-tim* or *s-tim* homozygous (**Table 2**). Clearly having at least one copy of *ls-tim* enhances LL rhythmicity, but UAS control flies that are *ls-tim* homozygotes do not give high levels of LL rhythmicity (see line *108247*) so the very high levels we observe with *Gs2* and *Got1* variants represent these alleles interacting with *tim.* None of these lines were polymorphic for the *jet* alleles.

We also placed the *Gs2* and *Got1* alleles on the *s-tim* background by crossing to *w$^{1118}$* and generating *s-tim* homozygous lines for *Gs2* and *Got1* from the F2 generation using PCR. We observed that on this genetic background, only 20 and 21% respectively of the males were rhythmic in LL, further underscoring the interaction of these two genes with the *ls-tim* polymorphism (**Table 2**).

## Under LL Conditions *Got1* and *Gs2* Mutants Show High Amplitude TIM Cycling and More Abundant TIM Than Wild-Type

Western blots were performed from fly heads for the *w;P(GT1)Got1* and *wP(GT1)Gs2* mutants and compared to Canton-S. Levels of TIM were compared with tubulin under free running LL conditions for four time points, CT1, 7, 13, and 19. Two replicate blots were performed and both gave almost identical results (**Figure 2**). Levels of TIM compared to tubulin cycled with a 3–5 fold peak-to-trough amplitude for both *Got1* and *Gs2* mutants, with a clear peak at CT19 whereas in wild-type

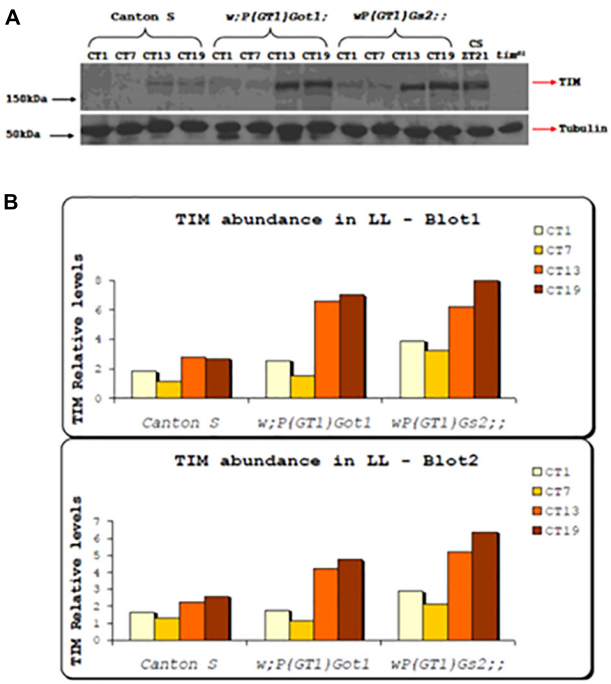


**FIGURE 2 |** TIM expression in *Got1* and *Gs2* mutants. **(A)** Western blot from head extract of *w;P(GT)Got1, wP(GT1)Gs2* and Canton-S flies collected in LL. Canton-S collected in LD cycles and *tim$^{01}$* mutants were used as positive and negative controls respectively. Genotypes and time points for collection (CT) are indicated above the blot. **(B)** Quantitative analysis using Image J of two replicate blots.

the relative amplitude was blunted to 1.5–2 fold with a peak at either CT13 or CT19. Furthermore TIM was approximately 2–4 times as abundant in the mutants compared to wild-type under LL and very similar to wild-type flies maintained in LD cycles (**Figure 2**). These results reinforce the view that under LL the two mutants block the normal light-induced degradation of TIM (Myers et al., 1996) but nevertheless maintain high amplitude TIM cycling.

## *Got1* Mutants Reduce Circadian Locomotor Responses to Brief Light Pulses

We also examined the effects of 10 min light pulses on the phase of the locomotor cycle in the two *w;PGT1 Got1* and *Gs2* mutants and compared them to the *w;P(GT1)AdhAdhr* mutant as a control. We observed that light pulses at ZT15 (3 h after lights off in a LD12:12 cycle) delayed the clock by 3 to 3.5 h for *Gs2* and *AdhAdhr,* whereas the phase delay for *Got1* was significantly reduced to 2 h (**Figure 3**). Similarly, the light pulse at ZT21 late at night caused an advance of 1.2–1.4 h for *Gs2* and *AdhAdhr,* whereas this was again significantly reduced to 0.6 h for *Got1*. All these lines are in the less light-sensitive *ls-tim* background (Sandrelli et al., 2007); nevertheless, the smaller phase shifts under these conditions appear to be specific to *Got1*.

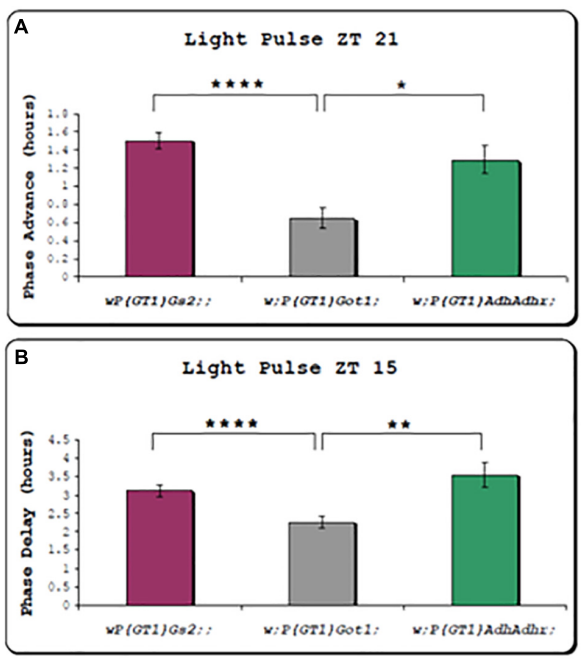


**FIGURE 3 |** Circadian phase responses of locomotor rhythms to brief light pulses for *Got1* and *Gs2* mutants. All three mutants are on the *ls-tim* background. Two replicate experiments were performed for the Got1 and Gs2 lines, and one for the control line. At ZT21 *Got1 n* = 58, *Gs2 n* = 60, *Adh n* = 23. At ZT15 *Got1 n* = 63, *Gs2 n* = 61, *Adh n* = 11. **(A)** Phase advances (± sem) to a light pulse at ZT21 **(B)** Phase delays to a light pulse at ZT15 $^{*}p < 0.05$ $^{**}p < 0.01$ $^{****}p < 0.0001$.

## Anatomical Dissection of Clock Neurons Mediating LL Locomotor Rhythmicity

We attempted to define the relevant clock neurons that were mediating the LL rhythmicity of *Got1* and Gs2 mutants. We therefore used the *UAS-RNAi* constructs to downregulate each gene's expression in different clock neuronal clusters. Knockdown in the peptidergic neurons including the l-LNvs but excluding other clock neurons using the *c929-Gal4* driver resulted in arrhythmicity in LL, thus excluding glutamate from within the l-LNvs from maintaining rhythms in LL (**Table 4**). Similarly the great majority of flies were arrhythmic in LL when the *mai79-gal4* driver was used, which drives expression in the s-LNvs and the three CRY-positive LNds and possibly one

**TABLE 4 |** Anatomical dissection of glutamate-mediated LL rhythmicity and *tim* background genotype.

| ***Genotype (VDRC)*** | **% LL rhythms** | **N** | ***tim* alleles** |
|---|---|---|---|
| ***A. Got1, Gs2*** | | | |
| *w/Y; c929-gal4/ Got1 RNAi (108247)* | 12.5 | 32 | *ls/s-tim* |
| *w/Y; c929-gal4/+; Gs2 RNAi/+ (32929)* | 18.7 | 32 | *ls/s-tim, ls-tim, s-tim* |
| *w/Y; mai79-gal4/Got1 RNAi* | 30 | 30 | *ls/s-tim* |
| *w/Y; mai79-gal4/+; Gs2 RNAi/+* | 18.8 | 32 | *ls/s-tim, ls-tim, s-tim* |
| *yw/Y; timGal4/Got1 RNAi; cry-gal80/+* | 62.5 | 20 | *ls/s-tim* |
| *yw/Y; timGal4/+; cry-gal80/Gs2 RNAi* | 53 | 32 | *ls/s-tim, ls-tim, s-tim* |
| *yw/Y; timGal4 Pdf-gal80/Got 1 RNAi; Pdf-gal80/+* | 73.3 | 30 | *ls/s-tim, ls-tim, s-tim* |
| *yw/Y; timGal4 Pdf-gal80/+;Pdf-gal80/Gs2 RNAi* | 96 | 30 | *ls/s-tim, ls-tim, s-tim* |
| *w/Y; c929-Gal4/+* | 0 | 31 | *s-tim* |
| *yw/Y; tim-gal4/+;cry-gal80/+* | 28 | 32 | *ls/s-tim, ls-tim, s-tim* |
| *yw/Y; tim-gal4 Pdf-gal80/+; Pdf-gal80/+* | 41 | 32 | *ls/s-tim, ls-tim, s-tim* |
| *w/Y mai79-gal4/+* | 15.7 | 19 | *s-tim* |
| ***B. glutamate receptor, GAD*** | | | |
| *w/Y;tim-gal4/+; DmGluRA RNAi/+ (1793)* | 52 | 31 | *ls/s-tim* |
| *w/Y;tim-gal4/+; DmGluRA RNAi/+ (1794)* | 65.6 | 32 | *ls/s-tim* |
| *w/Y;tim-gal4/+; DmGluRA RNAi/+ (103736)* | 64.5 | 31 | *ls/s-tim* |
| *w/Y;tim-gal4/+; Gad1 RNAi/+ (32344)* | 56.3 | 32 | *ls/s-tim, ls-tim, s-tim* |
| *UAS DmGluRA RNAi/+ (1793)* | 26.7 | 30 | *ls-tim* |
| *UAS DmGluRA RNAi/+ (1794)* | 25 | 32 | *ls-tim* |
| *UAS DmGluRA RNAi/+ (103736)* | 15.6 | 32 | *ls-tim* |
| *UAS Gad1 RNAi/+ (32344)* | 31.3 | 30 | *ls/s-tim, ls-tim, s-tim* |
| *w/Y; tim-gal4* | 4 | 51 | *s-tim* |
| ***C. repo-gal4*** | | | |
| *Got1 RNAi/+; repo-gal4/+;* | 27 | 26 | *s-tim ?* |
| *yw/Y; timGal4/Got1 RNAi;* | 68 | 25 | *s-tim* |
| *Gs2RNAi/repo-gal4:* | 29 | 21 | *ls-tim,s-tim, ls/s-tim* |
| *yw/Y; timGal4 /+;+ /Gs2 RNAi* | 66 | 31 | *ls-tim,s-tim, ls/s-tim* |

of the two DN1a neurons (Grima et al., 2004). When we combined *tim-gal4* with *cry-gal80* and targeted expression to the DN1p, DN2, and DN3, and three LNd CRY-negative cells in the dorsal region, *Got1* downregulation generated 62.5% rhythmicity in LL and 53% for *Gs2*. We also combined *tim-gal4* with *Pdf-gal80* and restricted downregulation to all the LNds and DNs. In these cases a much higher level of 73% of flies were rhythmic in LL for *Got1* and a remarkable 90% were rhythmic for *Gs2*. This was in spite of the flies segregating the s-*tim* variant. The parental controls for these crosses were considerably less rhythmic in LL than in the experimental flies (**Table 4**). **Figure 4** illustrates the correlation between LL rhythmicity and anatomical expression for the two downregulated genes. It is clear that the DNs play a major role, particularly those that are CRY-negative but with another significant component arising from the CRY-negative and possibly CRY-positive LNds.

We extended our analysis to include downregulation of the metabotropic glutamate receptor DmGluRA. We used three different VDRC RNAi lines and crossed them to *tim-gal4*. All three lines gave >50% rhythmicity in LL with ∼24 h periods (**Table 4**). We did not, however, observe any lengthening of period in these knockdowns in DD (**Supplementary Table S2**) as reported by Hamasaka et al. (2007), even though we used three independent *UAS-RNAi* lines. Glutamate serves as the precursor for the synthesis of the inhibitory GABA neurotransmitter and this reaction is catalyzed by glutamate decarboxylase (GAD). We downregulated *Gad* using *tim-gal4* and observed a high level of LL rhythmicity. The parental controls for all these manipulations were considerably less rhythmic under LL (**Table 4**). We genotyped the *UAS-RNAi* lines, *DmGluRA* and *Gad* for *tim* and *jet* polymorphisms. All *UAS-DmGluRA* lines were homozygous *ls-tim*, whereas *UAS-Gad* RNAi lines were polymorphic and showed all three *tim* genotypes. All lines were monomorphic

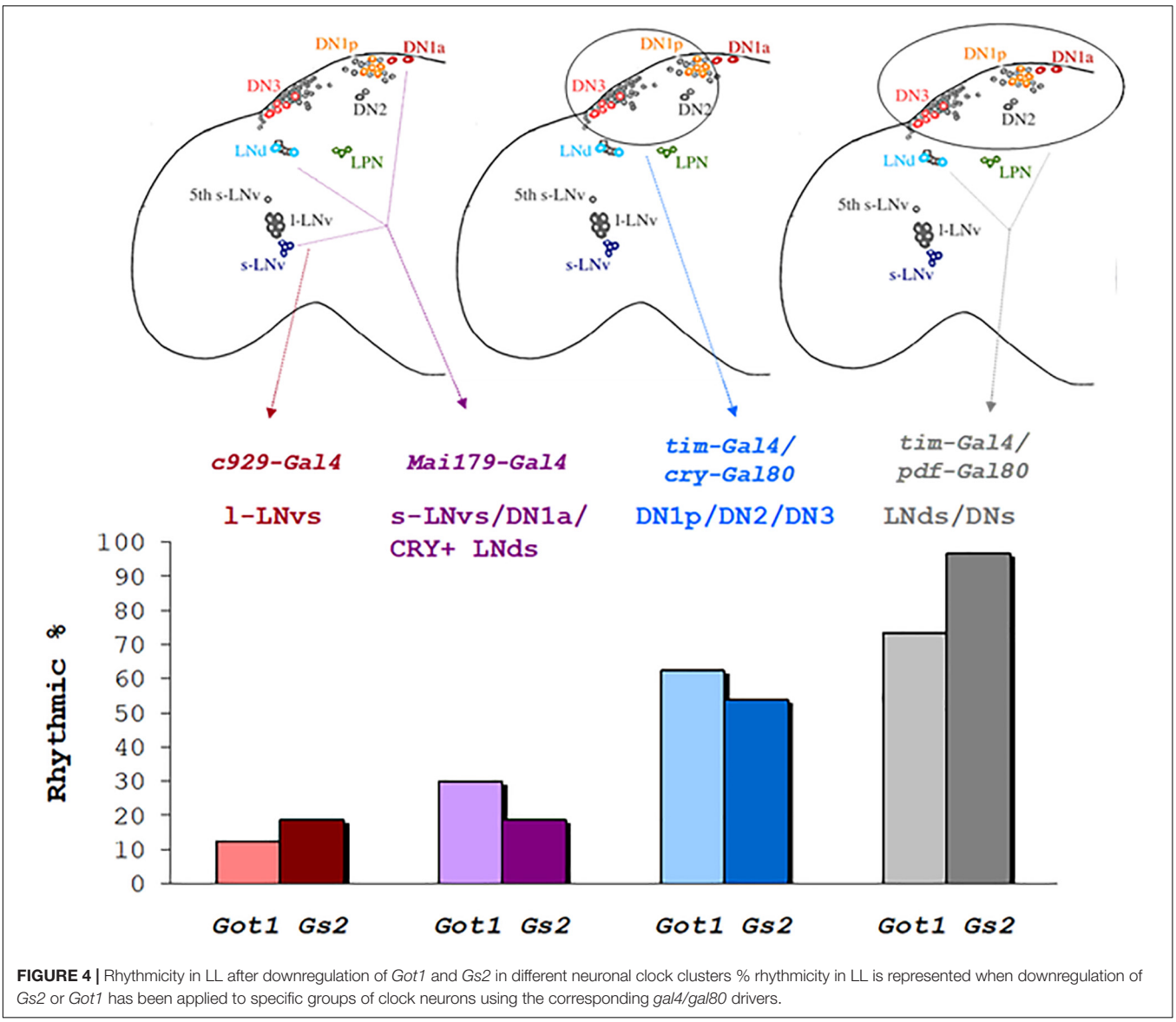


**FIGURE 4 |** Rhythmicity in LL after downregulation of *Got1* and *Gs2* in different neuronal clock clusters % rhythmicity in LL is represented when downregulation of *Gs2* or *Got1* has been applied to specific groups of clock neurons using the corresponding *gal4/gal80* drivers.

for wild-type *jet*. The *w:tim-Gal-4* line they were crossed to was homozygous *s-tim*. Therefore the experimental flies with *UAS-DmGluRA* were heterozygous (*ls/s-tim*) whereas those with *UAS-Gad* were either heterozygous or homozygous for both *tim* alleles (**Table 4**).

## Spatial Distribution of Got1 and Gs2 Positive Cells Among Clock Neurons

To investigate the spatial distribution of Got1 and Gs2 in the fly brain, we examined the endogenous YFP signal in the gene-trap $Got1^{YFP}/+$ and $Gs2^{YFP}/+$ flies. Overall the Got1 and Gs2 derived YFP expression patterns are ubiquitous in various areas between neuropils and in the brain cortex (e.g., around medulla, lobula, and mushroom body, **Figure 5**). This result is consistent with the earlier high throughput study including both YFP trap lines (Knowles-Barley et al., 2010). We did not detected any gross spatial differences of expression between Got1-YFP and Gs2-YFP. Notably the expression patterns for Got1-YFP and Gs2-YFP appeared to include glial cells. To confirm this observation, we examined overlaps between YFP and the glial reporter *repo-gal4* (Awasaki et al., 2008) by driving myr-RFP (membrane tethered RFP by myristoylation signal fusion, from Henry Chang). Consistently, we found Got1 and Gs2 positive cells overlapping with glial cells in brain cortex and between neuropils (**Figures 6A–C**).

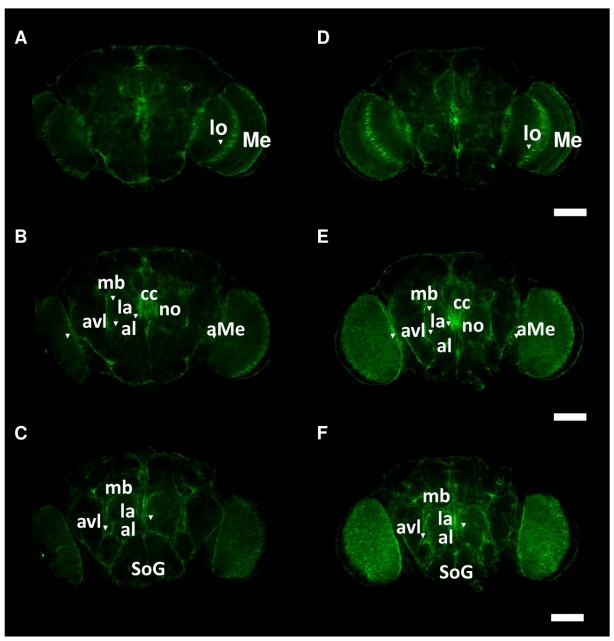


**FIGURE 5 |** Spatial patterns of Got1-YFP and Gs2-YFP expression in the fly brain. Frontal views of anterior **(A,D)**, intermediate **(B,E)** and posterior parts **(C,F)** of brains are shown for Got1-YFP **(A–C)** and Gs2-YFP **(D–F)**. Inverted triangles mark the strong expression foci of YFP signals around following anatomical structures: aMe: accessory medulla, al: antennal lobe, avl: anterior ventral lateral protocerebrum, cc: central complex, la: lateral accessory lobe, lo: lobula, mb: mushroom body, Me: medulla, SoG: suboesophagus ganglion. Scale bars: 75 μm. magnification: 10×. Nine Gs2-YFP and 11 Got1-YFP brains were investigated. The intensity of expression between Gs2-YFP and Got1-YFP were not investigated.

To explore the relationship among YFP positive cells and clock neurons, we applied an antibody against PDP1ε as a nuclear marker for clock neurons (Benito et al., 2007). Both YFP signals were detected peripherally to the cell bodies of the PDP1ε positive neuron, as well as in cells near clock neurons (**Figures 7**, **8**). Within clock neurons, we detected clear cytoplasmic YFP signals in LNvs, LNds, and DN1s (**Figures 7**, **8**). Although the behavioral data suggested that CRY-negative dorsal clock neurons including half of DN1s, DN2s and most DN3s may be responsible for the LL phenotype, we did not detect clear cytoplasmic YFP signals in DN2s and DN3s under higher magnification (**Figures 7**, **8**). We did observe YFP signal surrounding quasimodo (qsm +) expressing DN2s and DN3s ("×" in **Figure 9** and (Chen et al., 2011). Pericellular YFP signals regularly overlapped with *repo>myrRFP* (asterisks in **Figures 7**, **8**), suggesting these signals could be derived from glial cell processes which were previously identified to surround neurons (Awasaki et al., 2008; Ng et al., 2011). Taken together with the behavioral results, these data imply that the LL rhythms observed in $Got1^{YFP}$ and $Gs2^{YFP}$ flies may be derived from abnormal glutamate metabolism in CRY-negative DN1s, the LNds and/or glial cells.

Finally, in order to investigate glial contributions to the LL phenotype we downregulated *Got1* and *Gs2* in glia using *repo-Gal4* with *timgal4* driven RNAi as controls. We observed that entrainment in LD cycles was normal, but most of the *repo-gal4* flies for both *Gs2* and *Got1* knockdown became arrhythmic almost immediately in LL, whereas flies carrying *tim-gal4* crossed to the same *UAS RNAi* constructs were considerably more rhythmic in LL (**Table 4**). We conclude that the LL rhythmic phenotype is predominantly caused by neuronal rather than glial glutamate signaling.

# DISCUSSION

The protein trap screen was original intended to generate lines in which the normal spatial expression of a gene could be determined with YFP and followed up by proteomic analyses using the incorporated tags. We decided to use it as a mutational screen reasoning that the addition of the YFP domain within a protein may alter its conformation and generate behavioral phenotypes. While this was initially an article of faith, it seems to have been supported by the identification of several loci that may contribute to the processing of light input into the circadian clock. We notice that all genes we identified are functional in the nervous system but are not implicated in protein degradation. One of these, the kinase encoding *lk6,* was also identified in an overexpression screen for LL rhythmicity using *EP* elements (Dubruille et al., 2009). Heterozygous *lk6/+* individuals did not give high levels of LL rhythmicity and knockdown using *tim-gal4* gave a moderate ∼30% rhythmicity (**Supplementary Table S1**). It may be that the YFP insertion cassette led to a more stable Lk6 product which would imitate an overexpression phenotype. However, the two most interesting genes were,

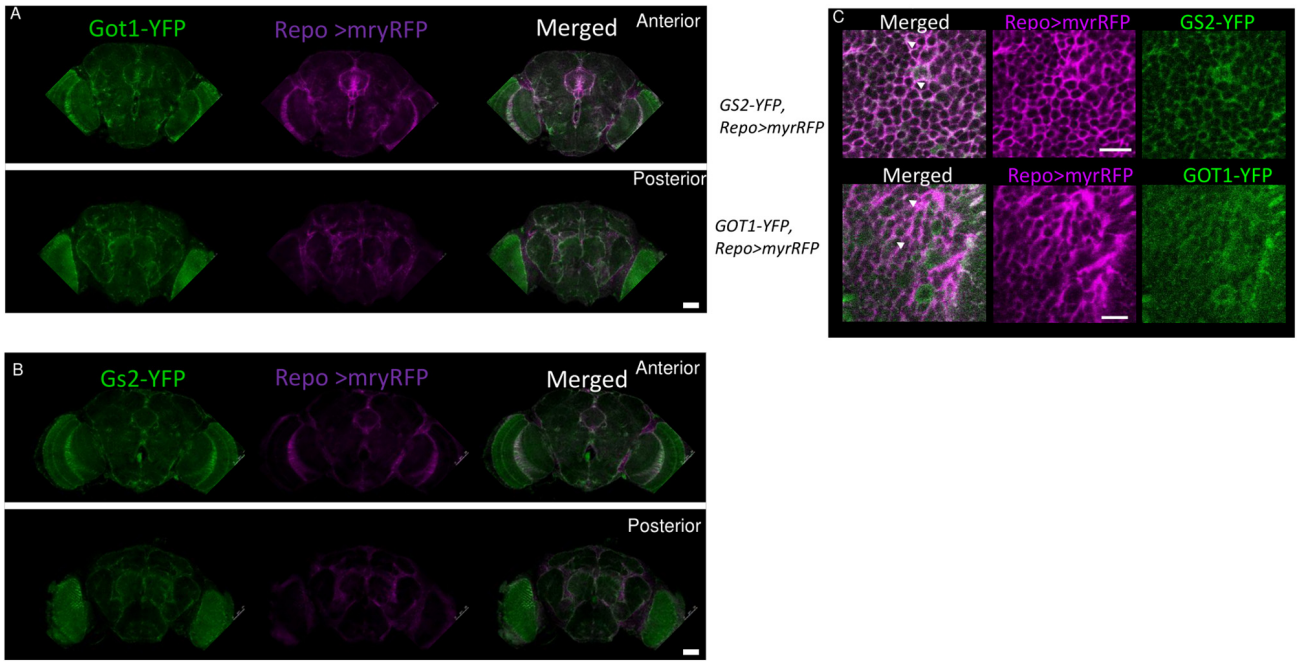


**FIGURE 6 |** Got1-YFP and Gs2-YFP expression in glial cells in the fly brain. Frontal views of anterior and posterior parts the fly brains are shown for Got1-YFP **(A)** and Gs2-YFP **(B)**. *repo*>myrRFP marks the cell membranes of glial cells (magenta), which overlap with both Got1-YFP and Gs2-YFP signal (green) in optic lobes and inter-neuropils (white areas in merged section). Scale bars: 50 μm. Magnification: 10×. Nine Gs2-YFP and seven1 Got1-YFP brains were investigated. **(C)** Detailed overlaps between GS2-YFP and GOT1-YFP (green) and repo-gal4 driven myrRFP (magenta). An example image at inter-neuropil regions are shown. Similar patterns are detected between YFP and RFP signals. White areas and arrowheads indicate examples of overlaps between the YFP and RFP signals at glial membranes. Scale bars: 10 μm. Magnification: 40×.

*Got1* and *Gs2,* because they implicated glutamatergic signaling (**Figure 10**). The initial gene trap results for these two genes were supported with independently generated mutants in these genes as well as dsRNAi knockdown. The only mutation that did not give a similar phenotype was *P(wHy)Got1,* but this variant also showed a very low proportion of weakly rhythmic individuals in DD.

*tim* and *jet* polymorphisms can dramatically alter circadian photo-responsiveness (Koh et al., 2006; Peschel et al., 2006; Sandrelli et al., 2007; Tauber et al., 2007) with the $jet^C$ variant interacting with *ls-tim* to generate LL rhythmicity at high levels (Peschel et al., 2006, 2009). We studied polymorphisms at both loci and it was clear that the *ls-tim* allele interacted with *P{GT1} Got1* and *Gs2* variants to enhance LL rhythmicity. However, by itself *ls-tim* was not sufficient for high levels of LL rhythmicity because several *P{GT1}* mutants homozygous for *ls-tim* were arrhythmic in LL (see also Sandrelli et al., 2007). Nevertheless, our results underline how important it is to identify these common *tim* genetic variants in the genetic background of any LL screen or indeed in any analysis of circadian photo-responsiveness.

In spite of the compelling LL phenotypes with both *Got1* and *Gs2* mutants, when the circadian clock was probed with brief 10 min light pulses, only the *Got1* mutant showed a compromised phase response in both advance and delay zones, suggesting that it is less sensitive to light than *Gs2* mutants under these conditions. This difference was not reflected under the more stringent environment of LL as the levels of rhythmicity for both mutants when on the same *tim* genetic background were very similar (**Tables 1**, **2**), as was the enhanced stability/levels of TIM in the two mutants under LL (**Figure 2**). The latter result from the western blots of fly heads is intriguing because the level of TIM cycling in the mutants in LL was similar to that of wild-type in DD. This in turn suggests that the eyes of the mutants are still cycling for TIM in LL, implying that the TIM status of the dorsal clock neurons (see below) is driving the same TIM pattern in the eye. Alternatively, glutamate signaling has been reported in the eye (Kolodziejczyk et al., 2008; Richter et al., 2018) and this would also be expected to be compromised in the mutants. How this might disrupt the normal TIM cycle damping in the eye under LL is open for speculation.

In *Drosophila*, neurotransmission by glutamate is mediated by ionotropic receptors that form cation/anion channels (Dingledine et al., 1999; Anwyl, 2009; McCarthy et al., 2011) and metabotropic G-protein coupled receptors (Bogdanik et al., 2004). Previous work has implicated glutamate and its metabotropic receptor, DmGluRA, in the *Drosophila* clock circuitry (Hamasaka et al., 2007). Transgenic flies with altered expression of DmGluRA in the LNvs showed altered locomotor activity under LD and DD with a modest lengthening of the free-running (DD) period by 0.3 to 0.6 h observed with *Pdf,*

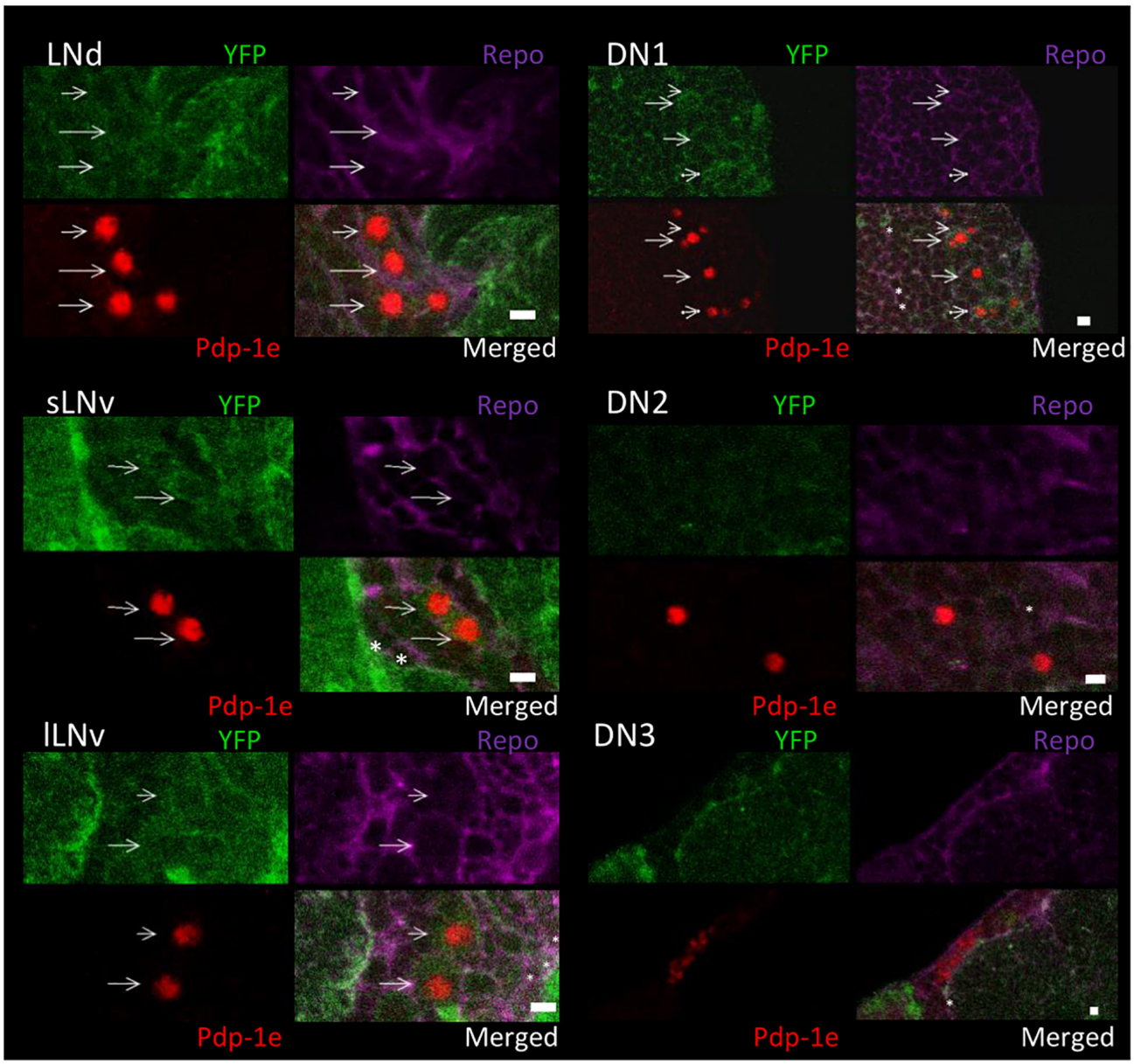


**FIGURE 7 |** Got1-YFP expression in clock neurons in the fly brain. Four panels of each clock neuronal group are shown, Pdp-1ε (red) indicates clock neuron nucleus. Repo >myrRFP marks the cell membranes of glial cells (magenta). Individual cell containing both cytosolic Got1-YFP signal (green) and Pdp-1ε nuclear staining are detected in LNs and DN1s and are indicated by arrows. Asterisks indicate the example of overlaps between glial cells and YFP signals. Scale bars: 4 μm. Magnification: 40×. Five brains were investigated. Single optical slides are shown with dorsal on the top position.

*cry* and *timgal4* drivers. In LD cycles a strong increase in the activity after lights-off was also noticed (Hamasaka et al., 2007). However, knockdown of the receptor did not affect DD rhythms in our study using three independent *UAS-RNAi* constructs. Similarly, Collins et al. (2012) observed that reducing presynaptic glutamate levels by overexpressing Gad1 with the *timgal4; Pdfgal80* or *timgal4; crygal80* drivers had little effect on the locomotor period in DD but had an effect on the robustness of the cycle, with the former showing reduced power compared to the latter (Collins et al., 2012). This implied that the non-sLNv CRY + expressing neurons (including the DNs and LNds) were releasing glutamate and contributing to robust rhythmicity in DD.

Knockdown of the receptor *DmGluRA* using *timgal4* in our experiments led to high levels of LL rhythmicity compared to controls, further revealing the association between glutamate and circadian photo-responsiveness. Furthermore, knockdown of *Glutamate decarboxylase (Gad)* using *timgal4* also generated LL rhythmicity. The distribution of GABA, the major inhibitory neurotransmitter produced in *Drosophila* neurons, has been

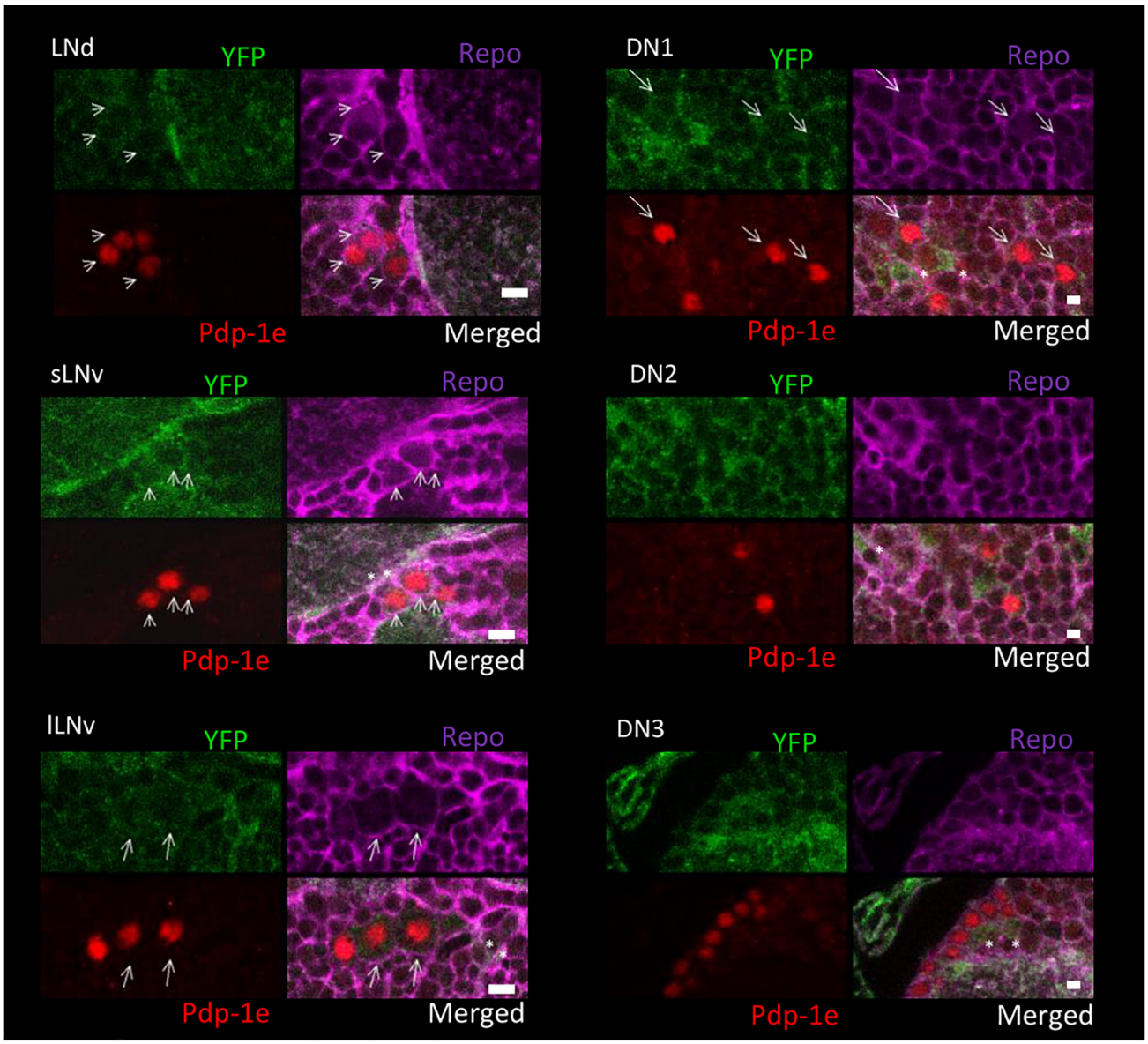


**FIGURE 8 |** Gs2-YFP expression in clock neurons in the fly brain. Four panels of each clock neuronal group are shown, Pdp-1ε (red) indicates clock neuron nucleus. *Repo* >myrRFP marks the cell membranes of glial cells (magenta). Individual cell containing both cytosolic Gs2-YFP signal (green) and Pdp-1ε nuclear staining are detected in LNs and DN1s and are indicated by arrows. Asterisks indicate the example of overlaps between glial cells and YFP signals. Scale bars: 4 μm. Magnification: 40×. Four brains were investigated. Single optical slides are shown with dorsal on the left-top position.

previously mapped to different areas of the brain (Kuppers et al., 2003). Although clock neurons do not appear to express GABA (Dahdal et al., 2010) application of GABA antisera and the use of flies expressing GFP driven by the *Gad1* promoter revealed that s-LNvs receive GABAergic inputs and utilize GABA as a slow inhibitory neurotransmitter (Hamasaka et al., 2005). DN1s and DN3s are glutamatergic, since these cells were immunolabeled for vesicular glutamate transporter (DvGluT) (Hamasaka et al., 2007). Additionally, antiserum against DmGluRA labeled the LNvs dendrites, indicating that the glutamate signal from the DNs modulates the behavior of the LNvs (Hamasaka et al., 2007). Indeed, axons from DN3s may communicate with the LNvs (Veleri et al., 2003) whereas axons from DN1s may contact the s-LNvs (Guo et al., 2016). Our neurogenetic dissection suggests that the normal arrhythmic response to LL is mediated by glutamate signaling from the DNs to the s-LNvs. The fact that *Gad1* RNAi driven by *tim-gal4* also leads to enhanced LL rhythmicity (**Table 4**) suggests that other GABA producing neurons [*timgal4* is broadly expressed beyond just the canonical clock neurons (Kaneko and Hall, 2000)] are nevertheless communicating with them and are important for normal photoresponsiveness.

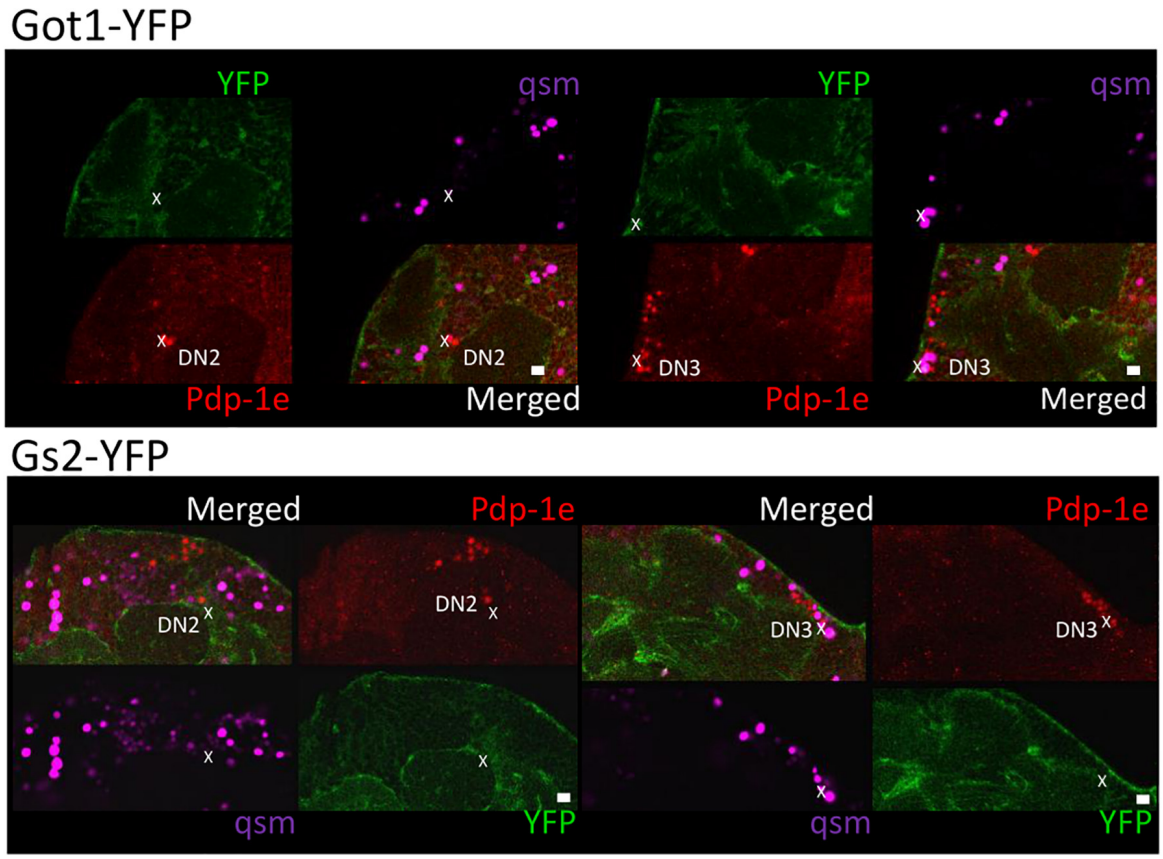


**FIGURE 9 |** Gs2-YFP and Got1-YFP surround qsm + DNs in the fly brain. Four panels of each brain area close to DN2 and DN3 are shown for Got1-YFP **(upper panel)** and Gs2-YFP **(lower panel)**. Pdp-1ε (red) indicates clock neuron nuclei. *qsm*$^{104}$*-gal4* >dsRED marks qsm + dorsal cells (qsm, magenta). Individual cell containing both dsRED and Pdp-1ε nuclear staining are qsm + DN2-3s and are indicated by "x." YFP signal surround qsm + DN2-3s but no clear overlaps could be detected. Scale bars: 10 μm. Magnification: 40×. Four brains were investigated. Single optical slides are shown with dorsal on the left-top position.

Previous studies have also implicated the role of the DN1s, LNds, and DN3s in mediating LL behavioral rhythmicity using various neurogenetic manipulations (Murad et al., 2007; Picot et al., 2007; Stoleru et al., 2007). In particular, Murad et al. (2007) showed how *per* overexpression in clock neurons driven by *timgal4* (but not *crygal4 or Pdfgal4*) led to LL rhythmicity with the additional key observation that molecular rhythms were observed only in a subset of DN1s (Murad et al., 2007). In spite of considerable speculation in this study, the mechanism by which DN1s could escape the influence of the molecularly arrhythmic sLNvs under LL was not clear. Our study would also suggest that in *Got1*$^{YFP}$ and *Gs2*$^{YFP}$ and the other mutants we have used, the DN1s would be similarly liberated from the influence of the sLNvs in LL, which are likely to be molecularly arrhythmic. How compromised inhibitory glutamate signaling from DNs to the sLNvs might generate the LL TIM rhythms that we observe is difficult to explain. Nevertheless, our results are consistent with the DN1s generating the LL rhythmicity because it is maintained in *timgal4;crygal80* and *timgal4;Pdfgal80* driven flies (**Figure 4**). Furthermore the relatively low levels of LL rhythmicity we observed with *maigal4* driving *Got1* and *Gs2* RNAi, largely excludes the three strongly CRY-positive LNds, as well as those in the LNv cluster (also from the use of *timgal4;Pdfgal80).* The DN1a neurons may communicate through their connection with the s-LNv fibers in the dorsal brain and accessory medulla (Shafer et al., 2006; Helfrich-Forster et al., 2007).

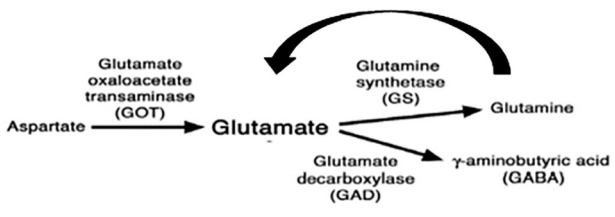


**FIGURE 10 |** Enzymes involved in glutamate metabolism (modified from Featherstone et al., 2002).

While these other studies have been performed without identification of the *tim* background, which is very likely to have modulated their results, a consensus appears to be growing that glutamate signaling from DNs to s-LNvs may provide the network mechanism that lies at the root of the arrhythmia observed in LL. However, further proof will require the use of

more refined genetic and molecular tools that identify inter-neuronal contacts as well as revealing the activities and the direction of flow of information among the clock neurons themselves as well as with associated GABA pathways.

## DATA AVAILABILITY STATEMENT

All datasets generated for this study are included in the article/**Supplementary Material**.

## AUTHOR CONTRIBUTIONS

CK and ER designed and supervised the study. RA and CH performed the experiments. K-FC performed the ICC. CK wrote the first draft. All authors contributed to the final manuscript. CK and ER obtained funding for the work.

## FUNDING

RA thanks Programma Alban and EC grant EUCLOCK (6th Framework 018741) to CK for support. CK and ER acknowledge BBSRC grants (BB/C006941/1 and BB/H018093/1).

## ACKNOWLEDGMENTS

We thank Daniel St Johnston for including us in the CPTI screening program.

## SUPPLEMENTARY MATERIAL

The Supplementary Material for this article can be found online at: https://www.frontiersin.org/articles/10.3389/fphys.2020.00145/full#supplementary-material

## REFERENCES

Anwyl, R. (2009). Metabotropic glutamate receptor-dependent long-term potentiation. *Neuropharmacology* 56, 735–740. doi: 10.1016/j.neuropharm.2009.01.002

Awasaki, T., Lai, S. L., Ito, K., and Lee, T. (2008). Organization and postembryonic development of glial cells in the adult central brain of *Drosophila*. *J. Neurosci.* 28, 13742–13753. doi: 10.1523/JNEUROSCI.4844-08.2008

Axelrod, S., Saez, L., and Young, M. W. (2015). Studying circadian rhythm and sleep using genetic screens in *Drosophila*. *Methods Enzymol.* 551, 3–27. doi: 10.1016/bs.mie.2014.10.026

Baik, L. S., Fogle, K. J., Roberts, L., Galschiodt, A. M., Chevez, J. A., Recinos, Y., et al. (2017). CRYPTOCHROME mediates behavioral executive choice in response to UV light. *Proc. Natl. Acad. Sci. U.S.A.* 114, 776–781. doi: 10.1073/pnas.1607989114

Benito, J., Zheng, H., and Hardin, P. E. (2007). PDP1epsilon functions downstream of the circadian oscillator to mediate behavioral rhythms. *J. Neurosci.* 27, 2539–2547. doi: 10.1523/JNEUROSCI.4870-06.2007

Bogdanik, L., Mohrmann, R., Ramaekers, A., Bockaert, J., Grau, Y., Broadie, K., et al. (2004). The *Drosophila* metabotropic glutamate receptor DmGluRA regulates activity-dependent synaptic facilitation and fine synaptic morphology. *J. Neurosci.* 24, 9105–9116. doi: 10.1523/jneurosci.2724-04.2004

Ceriani, M. F., Darlington, T. K., Staknis, D., Mas, P., Petti, A. A., Weitz, C. J., et al. (1999). Light-dependent sequestration of timeless by cryptochrome. *Science* 285, 553–556. doi: 10.1126/science.285.5427.553

Chatterjee, A., Lamaze, A., De, J., Mena, W., Chelot, E., Martin, B., et al. (2018). Reconfiguration of a multi-oscillator network by light in the *Drosophila* circadian clock. *Curr. Biol.* 28, 2007.e4–2017.e4.

Chen, K. F., Peschel, N., Zavodska, R., Sehadova, H., and Stanewsky, R. (2011). QUASIMODO, a Novel GPI-anchored zona pellucida protein involved in light input to the *Drosophila* circadian clock. *Curr. Biol.* 21, 719–729. doi: 10.1016/j.cub.2011.03.049

Collins, B., Kane, E. A., Reeves, D. C., Akabas, M. H., and Blau, J. (2012). Balance of activity between LN(v)s and glutamatergic dorsal clock neurons promotes robust circadian rhythms in *Drosophila*. *Neuron* 74, 706–718. doi: 10.1016/j.neuron.2012.02.034

Dahdal, D., Reeves, D. C., Ruben, M., Akabas, M. H., and Blau, J. (2010). *Drosophila pacemaker neurons require g protein signaling and GABAergic inputs to generate twenty-four hour behavioral rhythms*. *Neuron* 68, 964–977. doi: 10.1016/j.neuron.2010.11.017

Delventhal, R., O'Connor, R. M., Pantalia, M. M., Ulgherait, M., Kim, H. X., Basturk, M. K., et al. (2019). Dissection of central clock function in *Drosophila* through cell-specific CRISPR-mediated clock gene disruption. *eLife* 8:48308.

Dingledine, R., Borges, K., Bowie, D., and Traynelis, S. F. (1999). The glutamate receptor ion channels. *Pharmacol. Rev.* 51, 7–61.

Dissel, S., Hansen, C. N., Ozkaya, O., Hemsley, M., Kyriacou, C. P., and Rosato, E. (2014). The logic of circadian organization in *Drosophila*. *Curr. Biol.* 24, 2257–2266. doi: 10.1016/j.cub.2014.08.023

Dolezelova, E., Dolezel, D., and Hall, J. C. (2007). Rhythm defects caused by newly engineered null mutations in *Drosophila*'s cryptochrome gene. *Genetics* 177, 329–345. doi: 10.1534/genetics.107.076513

Dubruille, R., Murad, A., Rosbash, M., and Emery, P. (2009). A constant light-genetic screen identifies KISMET as a regulator of circadian photoresponses. *PLoS Genet.* 5:e1000787. doi: 10.1371/journal.pgen.1000787

Emery, P., Stanewsky, R., Hall, J. C., and Rosbash, M. A. (2000). unique circadian-rhythm photoreceptor. *Nature* 404, 456–457. doi: 10.1038/35006558

Featherstone, D. E., Rushton, E., and Broadie, K. (2002). Developmental regulation of glutamate receptor field size by nonvesicular glutamate release. *Nat. Neurosci.* 5, 141–146. doi: 10.1038/nn789

Fogle, K. J., Baik, L. S., Houl, J. H., Tran, T. T., Roberts, L., Dahm, N. A., et al. (2015). CRYPTOCHROME-mediated phototransduction by modulation of the potassium ion channel beta-subunit redox sensor. *Proc. Natl. Acad. Sci. U.S.A.* 112, 2245–2250. doi: 10.1073/pnas.1416586112

Fogle, K. J., Parson, K. G., Dahm, N. A., and Holmes, T. C. (2011). CRYPTOCHROME is a blue-light sensor that regulates neuronal firing rate. *Science* 331, 1409–1413. doi: 10.1126/science.1199702

Grima, B., Chelot, E., Xia, R., and Rouyer, F. (2004). Morning and evening peaks of activity rely on different clock neurons of the *Drosophila* brain. *Nature* 431, 869–873. doi: 10.1038/nature02935

Guo, F., Yu, J., Jung, H. J., Abruzzi, K. C., Luo, W., Griffith, L. C., et al. (2016). Circadian neuron feedback controls the *Drosophila* sleep–activity profile. *Nature* 536, 292–297. doi: 10.1038/nature19097

Hamasaka, Y., Rieger, D., Parmentier, M. L., Grau, Y., Helfrich-Forster, C., and Nassel, D. R. (2007). Glutamate and its metabotropic receptor in *Drosophila* clock neuron circuits. *J. Comp. Neurol.* 505, 32–45. doi: 10.1002/cne.21471

Hamasaka, Y., Wegener, C., and Nassel, D. R. (2005). GABA modulates *Drosophila* circadian clock neurons via GABAB receptors and decreases in calcium. *J. Neurobiol.* 65, 225–240. doi: 10.1002/neu.20184

Hardin, P. E., and Panda, S. (2013). Circadian timekeeping and output mechanisms in animals. *Curr. Opin. Neurobiol.* 23, 724–731. doi: 10.1016/j.conb.2013.02.018

Helfrich-Forster, C., Shafer, O. T., Wulbeck, C., Grieshaber, E., Rieger, D., and Taghert, P. (2007). Development and morphology of the clock-gene-expressing lateral neurons of *Drosophila* melanogaster. *J. Comp. Neurol.* 500, 47–70. doi: 10.1002/cne.21146

Kaneko, M., and Hall, J. C. (2000). Neuroanatomy of cells expressing clock genes in *Drosophila*: transgenic manipulation of the period and timeless genes to mark the perikarya of circadian pacemaker neurons and their projections. *J. Comp. Neurol.* 422, 66–94. doi: 10.1002/(sici)1096-9861(20000619)422:1<66::aid-cne5>3.0.co;2-2

Kistenpfennig, C., Grebler, R., Ogueta, M., Hermann-Luibl, C., Schlichting, M., Stanewsky, R., et al. (2017). A new rhodopsin influences light-dependent daily activity patterns of fruit flies. *J. Biol. Rhythms* 32, 406–422. doi: 10.1177/0748730417721826

Knowles-Barley, S., Longair, M., and Armstrong, J. D. (2010). BrainTrap: a database of 3D protein expression patterns in the *Drosophila* brain. *Database* 2010:baq005. doi: 10.1093/database/baq005

Koh, K., Zheng, X., and Sehgal, A. (2006). JETLAG resets the *Drosophila* circadian clock by promoting light-induced degradation of TIMELESS. *Science* 312, 1809–1812. doi: 10.1126/science.1124951

Kolodziejczyk, A., Sun, X., Meinertzhagen, I. A., and Nassel, D. R. (2008). Glutamate, GABA and acetylcholine signaling components in the lamina of the *Drosophila* visual system. *PLoS One* 3:e2110. doi: 10.1371/journal.pone.0002110

Kuppers, B., Sanchez-Soriano, N., Letzkus, J., Technau, G. M., and Prokop, A. (2003). In developing *Drosophila* neurones the production of gamma-amino butyric acid is tightly regulated downstream of glutamate decarboxylase translation and can be influenced by calcium. *J. Neurochem.* 84, 939–951. doi: 10.1046/j.1471-4159.2003.01554.x

Lamba, P., Foley, L. E., and Emery, P. (2018). Neural network interactions modulate CRY-dependent photoresponses in *Drosophila*. *J. Neurosci.* 38, 6161–6171. doi: 10.1523/jneurosci.2259-17.2018

Leung, N. Y., and Montell, C. (2017). Unconventional roles of opsins. *Annu. Rev. Cell Dev. Biol.* 33, 241–264. doi: 10.1146/annurev-cellbio-100616-060432

Li, M. T., Cao, L. H., Xiao, N., Tang, M., Deng, B., Yang, T., et al. (2018). Hub-organized parallel circuits of central circadian pacemaker neurons for visual photoentrainment in *Drosophila*. *Nat. Commun.* 9:4247. doi: 10.1038/s41467-018-06506-5

Lowe, N., Rees, J. S., Roote, J., Ryder, E., Armean, I. M., Johnson, G., et al. (2014). Analysis of the expression patterns, subcellular localisations and interaction partners of *Drosophila* proteins using a pigP protein trap library. *Development* 141, 3994–4005. doi: 10.1242/dev.111054

McCarthy, E. V., Wu, Y., Decarvalho, T., Brandt, C., Cao, G., and Nitabach, M. N. (2011). Synchronized bilateral synaptic inputs to *Drosophila melanogaster* neuropeptidergic rest/arousal neurons. *J. Neurosci.* 31, 8181–8193. doi: 10.1523/JNEUROSCI.2017-10.2011

Murad, A., Emery-Le, M., and Emery, P. (2007). A subset of dorsal neurons modulates circadian behavior and light responses in *Drosophila*. *Neuron* 53, 689–701. doi: 10.1016/j.neuron.2007.01.034

Myers, M. P., Wager-Smith, K., Rothenfluh-Hilfiker, A., and Young, M. W. (1996). Light-induced degradation of TIMELESS and entrainment of the *Drosophila* circadian clock. *Science* 271, 1736–1740. doi: 10.1126/science.271.5256.1736

Ng, F. S., Tangredi, M. M., and Jackson, F. R. (2011). Glial cells physiologically modulate clock neurons and circadian behavior in a calcium-dependent manner. *Curr. Biol.* 21, 625–634. doi: 10.1016/j.cub.2011.03.027

Ogueta, M., Hardie, R. C., and Stanewsky, R. (2018). Non-canonical phototransduction mediates synchronization of the *Drosophila melanogaster* circadian clock and retinal light responses. *Curr. Biol.* 28, 1725.e3–1735.e3.

Ozturk, N., VanVickle-Chavez, S. J., Akileswaran, L., Van Gelder, R. N., and Sancar, A. (2013). Ramshackle (Brwd3) promotes light-induced ubiquitylation of *Drosophila* cryptochrome by DDB1-CUL4-ROC1 E3 ligase complex. *Proc. Natl. Acad. Sci. U.S.A.* 110, 4980–4985. doi: 10.1073/pnas.1303234110

Peschel, N., Chen, K. F., Szabo, G., and Stanewsky, R. (2009). Light-dependent interactions between the *Drosophila* circadian clock factors cryptochrome, jetlag, and timeless. *Curr. Biol.* 19, 241–247. doi: 10.1016/j.cub.2008.12.042

Peschel, N., Veleri, S., and Stanewsky, R. (2006). Veela defines a molecular link between Cryptochrome and Timeless in the light-input pathway to *Drosophila*'s circadian clock. *Proc. Natl. Acad. Sci. U.S.A.* 103, 17313–17318. doi: 10.1073/pnas.0606675103

Picot, M., Cusumano, P., Klarsfeld, A., Ueda, R., and Rouyer, F. (2007). Light activates output from evening neurons and inhibits output from morning neurons in the *Drosophila* circadian clock. *PLoS Biol.* 5:e315. doi: 10.1371/journal.pbio.0050315

Richter, F. G., Fendl, S., Haag, J., Drews, M. S., and Borst, A. (2018). Glutamate signaling in the fly visual system. *Science* 7, 85–95. doi: 10.1016/j.isci.2018.08.019

Sandrelli, F., Tauber, E., Pegoraro, M., Mazzotta, G., Cisotto, P., Landskron, J., et al. (2007). A molecular basis for natural selection at the timeless locus in *Drosophila melanogaster*. *Science* 316, 1898–1900. doi: 10.1126/science.1138426

Schlichting, M., Diaz, M. M., Xin, J., and Rosbash, M. (2019). Neuron-specific knockouts indicate the importance of network communication to *Drosophila* rhythmicity. *eLife* 8:48301.

Senthilan, P. R., Grebler, R., Reinhard, N., Rieger, D., and Helfrich-Forster, C. (2019). Role of rhodopsins as circadian photoreceptors in the *Drosophila melanogaster*. *Biology* 8:E6.

Shafer, O. T., Helfrich-Forster, C., Renn, S. C., and Taghert, P. H. (2006). Reevaluation of *Drosophila melanogaster*'s neuronal circadian pacemakers reveals new neuronal classes. *J. Comp. Neurol.* 498, 180–193. doi: 10.1002/cne.21021

Stanewsky, R., Kaneko, M., Emery, P., Beretta, B., Wager-Smith, K., Kay, S. A., et al. (1998). The cryb mutation identifies cryptochrome as a circadian photoreceptor in *Drosophila*. *Cell* 95, 681–692. doi: 10.1016/s0092-8674(00)81638-4

Stoleru, D., Nawathean, P., Fernandez Mde, L., Menet, J. S., Ceriani, M. F., and Rosbash, M. (2007). The *Drosophila* circadian network is a seasonal timer. *Cell* 129, 207–219. doi: 10.1016/j.cell.2007.02.038

Tang, C. H., Hinteregger, E., Shang, Y., and Rosbash, M. (2010). Light-mediated TIM degradation within *Drosophila* pacemaker neurons (s-LNvs) is neither necessary nor sufficient for delay zone phase shifts. *Neuron* 66, 378–385. doi: 10.1016/j.neuron.2010.04.015

Tauber, E., Zordan, M., Sandrelli, F., Pegoraro, M., Osterwalder, N., Breda, C., et al. (2007). Natural selection favors a newly derived timeless allele in *Drosophila melanogaster*. *Science* 316, 1895–1898. doi: 10.1126/science.1138412

Top, D., O'Neil, J. L., Merz, G. E., Dusad, K., Crane, B. R., and Young, M. W. (2018). CK1/Doubletime activity delays transcription activation in the circadian clock. *eLife* 7:32679.

Top, D., and Young, M. W. (2018). Coordination between differentially regulated circadian clocks generates rhythmic behavior. *Cold Spring Harb. Perspect. Biol.* 10:a033589. doi: 10.1101/cshperspect.a033589

Vanin, S., Bhutani, S., Montelli, S., Menegazzi, P., Green, E. W., Pegoraro, M., et al. (2012). Unexpected features of *Drosophila* circadian behavioural rhythms under natural conditions. *Nature* 484, 371–375. doi: 10.1038/nature10991

Veleri, S., Brandes, C., Helfrich-Forster, C., Hall, J. C., and Stanewsky, R. (2003). A self-sustaining, light-entrainable circadian oscillator in the *Drosophila* brain. *Curr. Biol.* 13, 1758–1767. doi: 10.1016/j.cub.2003.09.030

Yao, Z., Bennett, A. J., Clem, J. L., and Shafer, O. T. (2016). The *Drosophila* clock neuron network features diverse coupling modes and requires network-wide coherence for robust circadian rhythms. *Cell Rep.* 17, 2873–2881. doi: 10.1016/j.celrep.2016.11.053

Yao, Z., and Shafer, O. T. (2014). The *Drosophila* circadian clock is a variably coupled network of multiple peptidergic units. *Science* 343, 1516–1520. doi: 10.1126/science.1251285

**Conflict of Interest:** The authors declare that the research was conducted in the absence of any commercial or financial relationships that could be construed as a potential conflict of interest.

frontiers in Physiology

ORIGINAL RESEARCH
published: 26 March 2020
doi: 10.3389/fphys.2020.00229

# A Functional Clock Within the Main Morning and Evening Neurons of *D. melanogaster* Is Not Sufficient for Wild-Type Locomotor Activity Under Changing Day Length

*Pamela Menegazzi†, Katharina Beer†, Verena Grebler, Matthias Schlichting‡, Frank K. Schubert and Charlotte Helfrich-Förster**

*Neurobiology and Genetics, Theodor-Boveri Institute, Biocenter, University of Würzburg, Würzburg, Germany*

OPEN ACCESS

**Edited by:**
*Rodolfo Costa, University of Padova, Italy*

**Reviewed by:**
*Patrick Emery, University of Massachusetts Medical School, United States*
*Joanna C. Chiu, University of California, Davis, United States*
*Emi Nagoshi, Université de Genève, Switzerland*

***Correspondence:**
*Charlotte Helfrich-Förster charlotte.foerster@biozentrum.uni-wuerzburg.de*

*†These authors have contributed equally to this work*

***‡Present address:***
*Matthias Schlichting, Howard Hughes Medical Institute, Brandeis University, Waltham, MA, United States*

**Specialty section:**
*This article was submitted to Chronobiology, a section of the journal Frontiers in Physiology*

**Received:** *20 December 2019*
**Accepted:** *27 February 2020*
**Published:** *26 March 2020*

**Citation:**
*Menegazzi P, Beer K, Grebler V, Schlichting M, Schubert FK and Helfrich-Förster C (2020) A Functional Clock Within the Main Morning and Evening Neurons of D. melanogaster Is Not Sufficient for Wild-Type Locomotor Activity Under Changing Day Length. Front. Physiol. 11:229. doi: 10.3389/fphys.2020.00229*

A major challenge for all organisms that live in temperate and subpolar regions is to adapt physiology and activity to different photoperiods. A long-standing model assumes that there are morning (M) and evening (E) oscillators with different photoreceptive properties that couple to dawn and dusk, respectively, and by this way adjust activity to the different photoperiods. In the fruit fly *Drosophila melanogaster*, M and E oscillators have been localized to specific circadian clock neurons in the brain. Here, we investigate under different photoperiods the activity pattern of flies expressing the clock protein PERIOD (PER) only in subsets of M and E oscillators. We found that all fly lines that expressed PER only in subsets of the clock neurons had difficulties to track the morning and evening in a wild-type manner. The lack of the E oscillators advanced M activity under short days, whereas the lack of the M oscillators delayed E activity under the same conditions. In addition, we found that flies expressing PER only in subsets of clock neurons showed higher activity levels at certain times of day or night, suggesting that M and E clock neurons might inhibit activity at specific moments throughout the 24 h. Altogether, we show that the proper interaction between all clock cells is important for adapting the flies' activity to different photoperiods and discuss our findings in the light of the current literature.

**Keywords: entrainment (light), two-oscillator model, photoperiod alterations, *drosophila melanogaster* meigen, clock neurons**

## INTRODUCTION

Endogenous clocks that tick with an ∼24 h period control circadian rhythms. They entrain to the 24 h cycles of the earth via external Zeitgebers, the strongest of which is light. Since activity must occur at the most favorable time of the day, the rest–activity rhythm is one of the most tightly clock-controlled behaviors. In natural conditions, many animal species display bimodal rest–activity profiles with pronounced morning (M) and evening (E) activity bouts, and little activity during the middle of the day or night (Aschoff, 1966; Saunders, 2002; Dunlap et al., 2004). In long summer days, M activity occurs earlier and E activity later, helping the animals to avoid the midday heat

by being active mainly in the morning and evening. Such an adaptation is especially important for small insects such as fruit flies that are in danger of desiccation (Hamblen-Coyle et al., 1992; Majercak et al., 1999; Bywalez et al., 2012). This behavior occurs also in the laboratory under light–dark (LD) cycles but constant temperatures showing that light is the major cue that drives these changes (Rieger et al., 2003, 2007, 2012; Shafer et al., 2004; Menegazzi et al., 2017; Schlichting et al., 2019b).

The long-standing two-oscillator model of Pittendrigh and Daan (1976), originally developed for mammals, explains the described seasonal adaptations by assuming an M oscillator that shortens its period and an E oscillator that lengthens its period when exposed to light for an extended time. The cellular basis of the two oscillators has been described first in the fruit fly: M and E oscillators are located in distinct groups of circadian clock neurons – the so-called M and E neurons (Grima et al., 2004; Stoleru et al., 2004; Rieger et al., 2006).

The *Drosophila* brain clock consists of ∼150 neurons that express the PERIOD (PER) protein and are divided into different clusters of lateral and dorsal neurons (LN and DN) (**Figure 1**). All clock neurons form an interconnected neuronal network that has been partially morphologically and functionally dissected (Rieger et al., 2006; Shafer et al., 2006; Helfrich-Förster et al., 2007; Yao and Shafer, 2014; Schubert et al., 2018).

As defined in original work, the M neurons consist of a ventral group of the lateral clock neurons – the four PDF-positive small ventral lateral neurons (s-$LN_v$) – whereas the E cells are composed of the dorsal group of the LNs, the $LN_d$ (Grima et al., 2004; Stoleru et al., 2004). Later work showed that the so-called 5th s-$LN_v$ also behaves as an E oscillator, whereas only three of the six $LN_d$ lengthen their period in response to light and thus work as bonafide E oscillators (Rieger et al., 2006). These three E-$LN_d$ are most likely identical with the three cryptochrome (CRY)-expressing $LN_d$ cells (Picot et al., 2007). Work that is more recent showed that the three CRY-positive E-$LN_d$ can be further divided into two short neuropeptide F (s-NPF)-expressing neurons and one ion transporter peptide (ITP)-expressing cell (**Figure 1**; Johard et al., 2009). Most interestingly, ITP is also present in the 5th s-$LN_v$, and this cell turned out to be morphologically very similar to the ITP-positive E-$LN_d$ cell and not with the PDF-positive M s-$LN_v$ cells, suggesting that the 5th s-$LN_v$ belongs to the E-$LN_d$ neurons (Schubert et al., 2018). Even functionally, the two ITP-positive E neurons are closely related (Yao and Shafer, 2014). Therefore, to avoid confusion with the $LN_v$ M neurons, we proposed to refer to the 5th s-$LN_v$ simply as 5th LN (see **Figure 1**). As depicted in **Figure 1**, Yao and Shafer (2014) classified the E cells into three groups, E1, E2, and E3. E1 corresponds to the s-NPF-positive E-LN, E2 corresponds to the ITP-expressing E-LN, and E3 corresponds to the CRY-negative E-LN (**Figure 1**). Depending on the environmental conditions, the three groups of E-LN appear to behave differently (Rieger et al., 2009; Yoshii et al., 2012; Yao and Shafer, 2014). There are also indications that the ∼15 $DN_{1p}$ dorsal neurons consist of M and E oscillators. Half of them express CRY and the simplest view is that the CRY-negative $DN_{1p}$ are E neurons while the CRY-positive $DN_{1p}$ are M neurons (Murad et al., 2007; Zhang Y. et al., 2010; Yoshii et al., 2012). In the following, we call these neurons E-DN and M-DN, respectively (**Figure 1**).

Consistent with the two-oscillator model, *Drosophila*'s M and E neurons respond differently to light, with M cells shortening their period and some E cells lengthening their period when the flies are exposed to constant light conditions (Rieger et al., 2006; Yoshii et al., 2012). The M neurons advance their phase under dim constant light and light moonlight cycles, whereas the E neurons delay their phase, thereby lengthening the time between M and E activity peaks (Bachleitner et al., 2007).

To understand the contribution of the different clock neurons to rhythmic behavior, a UAS-*period* transgene was generated in order to rescue *per* expression with the help of specific *gal4-drivers* in subsets of M or E neurons of $per^0$ mutant flies (Grima et al., 2004). As expected, these flies show differences in the appearance of M and E activity bouts when recorded under LD cycles with 12 h of light and 12 h of darkness (LD 12:12) (Grima et al., 2004; Picot et al., 2007; Zhang L. et al., 2010; Zhang Y. et al., 2010). Nevertheless, so far, the activity of these flies has not been recorded under different photoperiods. If the original Pittendrigh-Daan two-oscillator model is valid, and M and E oscillators control M and E activity in an autonomous manner, the morning activity of flies with functional M oscillators should track lights-on even in the absence of the E oscillators. Vice versa, the evening activity of flies with functional E oscillators should track lights-off even in the absence of the M oscillators. Here, we tested this hypothesis and found that the situation is more complex. Our results are in line with the findings of several other groups that manipulated the molecular clocks in M and E oscillators in different ways (Picot et al., 2007; Stoleru et al., 2007; Zhang L. et al., 2010; Zhang Y. et al., 2010; Guo et al., 2014, 2016, 2018; Chatterjee et al., 2018; Schlichting et al., 2019b). In the end, we show that the original M and E oscillator model is too simple to explain all findings.

# MATERIALS AND METHODS

## Fly Strains

To restrict PER expression to specific M or E clock neurons, we started from arrhythmic $per^0$ mutants and rescued PER with the help of the UAS-Gal4 system in subsets of the clock neurons as done previously (Grima et al., 2004; Picot et al., 2007; Zhang L. et al., 2010; Zhang Y. et al., 2010). The neurons to which PER is finally restricted are shown in **Figure 1**. In the following, we will describe the employed lines and the crosses that yielded the experimental and control animals.

*Pdf-gal4/ +* flies, *Mai179-gal4/ +* flies, *tim-gal4/ +* flies, *Clk4.1 M-gal4* flies, $per^0$; *uas-per16*, and *Pdf-gal80* were described previously (Renn et al., 1999; Kaneko and Hall, 2000; Siegmund and Korge, 2001; Grima et al., 2004; Stoleru et al., 2004; Zhang L. et al., 2010).

In order to get flies with PER only in the M-LN cells, we crossed female $per^0$;*uas-per16* to male *Pdf-gal4/ +* flies and selected the male offspring to obtain $per^0$;*Pdf-gal4/ +*;*uas-per16/ +* flies. To get flies with PER in the majority of the LN

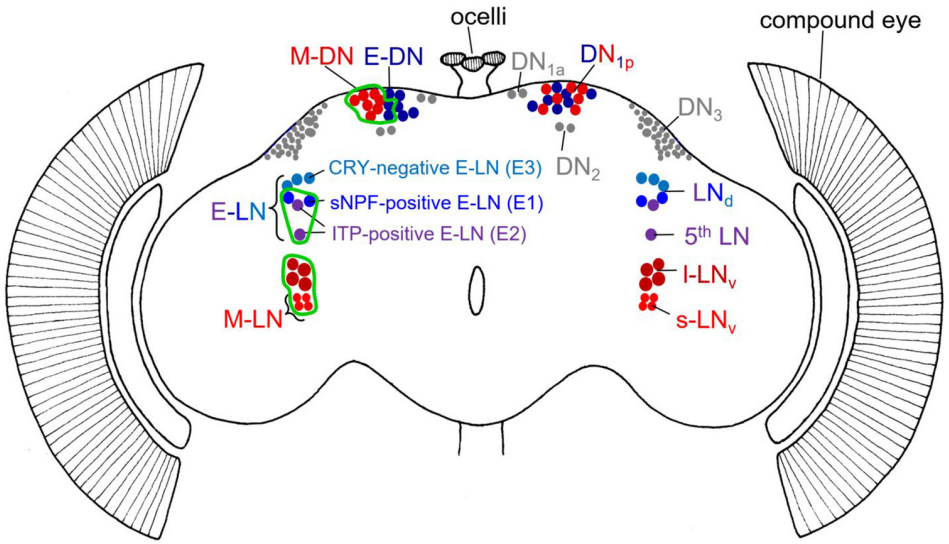


**FIGURE 1 |** Schematic representation of the different clock neurons in the *Drosophila* brain. The right brain hemisphere depicts the traditional division in different clock neurons including their classification in morning (M) and evening (E) neurons in reddish and bluish colors, respectively. Clock neurons that cannot be unequivocally assigned as M or E neurons are shown in gray. Note that the $DN_{1p}$ consist of a mixture of M and E neurons. The left-brain hemisphere depicts the M and E neurons in more detail and indicates in which specific neurons we rescued PER in *per*$^0$ mutants (green edging). Due to limited gal4-drivers, we were not always able to restrict PER to only M or E neurons. For example, our M-DN driver (*Clk4.1M-gal4*) included also ~2 $DN_{1p}$ that belong to the E-DN. Note that we clustered M- and E-DN in the left brain hemisphere to indicate the expression of the *Clk4.1M-gal4* driver line. In the case of the M-LN, only the s-$LN_v$ are bonafide M-oscillators, but by using the *Pdf-gal4* driver, we rescued PER also in the l-$LN_v$. In the case of E-LN, we rescued PER in the sNPF-positive (E1) and ITP-positive (E2) neurons (using the *PDF-gal80 Mai179-gal4* driver). The Cryptochrome (CRY)-negative neurons (E3) are not included.

(M- and E-LN flies), we crossed female *per*$^0$;*uas-per16* to male *Mai179-gal4/ +* flies and obtained male *per*$^0$;*Mai179-gal4/ +*;*uas-per16/ +* flies. We also generated a stable per$^0$;*Mai179-gal4*;*uas-per16* that was crossed to the *Pdf-gal80* strain to obtain w *per*$^0$;*Mai179-gal4/Pdf-gal80;uas-per16/ +* males that express PER only in the E-LN. These flies express PER in the sNPF-positive and ITP-positive E-LN (E1 and E2 cells) (Yao and Shafer, 2014; Schubert et al., 2018). Male flies that express PER in 8–10 $DN_{1p}$ cells were obtained by crossing male *Clk4.1 M-gal4* flies with female *per*$^0$;*uas-per16* flies. The genotype of these flies is *per*$^0$;*Clk4.1 M-gal4/uas-per16*. These flies express PER in all CRY-positive $DN_{1p}$ cells, which are regarded as M cells (Yoshii et al., 2012). Therefore, for simplicity, we call these flies M-DN flies, in spite of the fact that they express PER additionally also in some CRY-negative neurons (Chatterjee et al., 2018). *Clk4.1 M-gal4* males were also crossed to per$^0$;*Mai179-gal4*;*uas-per16* females to obtain per$^0$;*Mai179-gal4/ +*; *Clk4.1 M-gal4/uas-per16* that express PER in the M-LN, E-LN, and M-DN. As positive control flies, we used *per*$^0$;*tim-gal4/ + ;uas-per16/ +* males that express PER in all clock neurons. As negative controls, we used flies that do not express PER, i.e., *per*$^0$;*Mai179-gal4/+; + / +*, *per*$^0$;*tim-gal4/ +; + / +*, and *per*$^0$;*+;uas-per16/ +*.

## Behavioral Experiments and Analysis

All flies were raised on cornmeal/agar medium supplemented with yeast at 20°C in LD12:12. At the age of 1–3 days, individual male flies were transferred into the recording chambers. Locomotor activity was recorded for 3 days under a LD12:12 cycle with the same phase as during rearing and a light intensity of 100 lux. Subsequently, the duration of the photoperiod was either increased to 14 h or reduced to 10 h for half of the animals, respectively (see **Figure 2B**). After 6 days of recording, the photoperiod was further increased (to 16 h) or reduced (to 8 h). This was repeated after further 6 days of recording, so that photoperiod was finally 18 or 6 h, respectively. Thus, the flies' activity was recorded under the following LDs: (1) 12:12, 14:10, 16:8, 18:6, or (2) 12:12, 10:14, 8:16, 6:18. Throughout the whole recording period, data were collected every minute (i.e., in 1 min bins).

The raw data were displayed as actograms using the program actogramJ (Schmid et al., 2011). Flies that did not survive the first two light regimes were excluded from the analysis. From the others, average actograms and average activity profiles were calculated as described previously (Schlichting and Helfrich-Förster, 2015). For calculating average activity profiles, first, an average day was calculated for each fly including the second to the last day under each condition. The average days of individual flies were then used to calculate the average activity profiles for each fly group. We normalized the average activity profiles so that the maximal activity was 1. To reveal the phase of the beginning and maximum of morning (M) and evening (E) activity bouts, respectively, the raw data were smoothed with a moving average filter of 51 (i.e., each recorded bin is plotted as the average activity levels of 51 bins in total: the bin of interest plus 25 bins that precede and the 25 follow the bin of interest). This degree of smoothing made the activity profile more compact. The relevant times of M and E bouts could then be determined by manually selecting the starts and

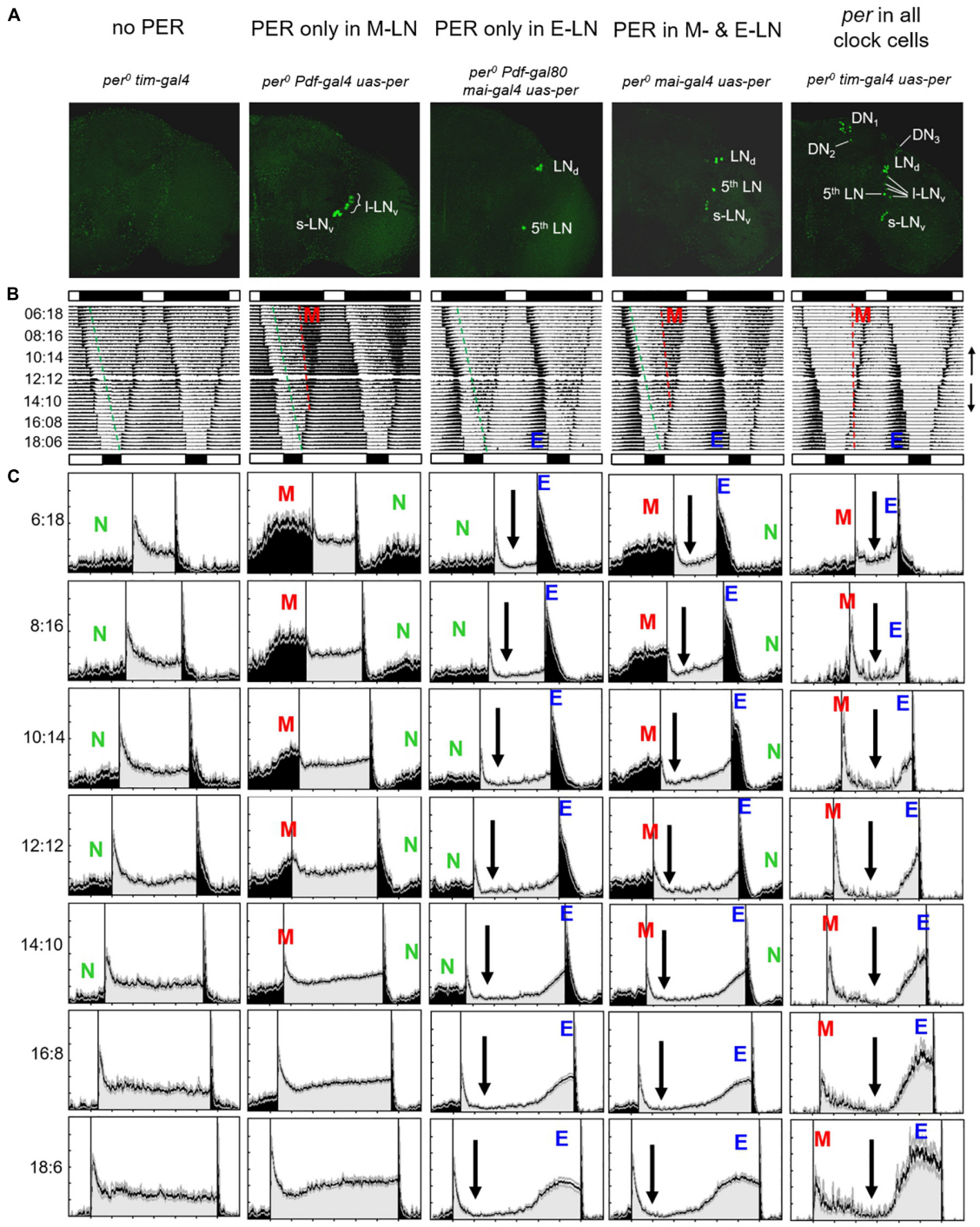


**FIGURE 2 |** Average actograms and activity profiles of 25–30 flies, respectively, of the following lines: (1) *per*$^{0}$ *tim-gal4* mutant controls (no PER), (2) flies with PER only in the eight PDF-positive lateral neurons (PER only in M-LN), (3) flies with PER only in the ITP-positive and sNPF-positive lateral neurons (per only in E-LN), (4) flies with PER in most lateral neurons (*per* in M- and E-LNs) and flies with PER in all clock neurons. **(A)** Representative anti-PER staining for the right brain hemisphere of each genotype, respectively. **(B)** Double plots of average actograms of all fly strains. The flies were entrained to subsequent LD cycles in which day length was either stepwise reduced (LD 12:12, 10:14, 8:16, and 6:18) or in which day length was stepwise increased (LD 12:12, 14:10, 16:8, and 6:18). Black and white bars above and below each actogram indicate the LD cycle of the shortest and longest photoperiod, respectively. To see the overall entrainment pattern, the average actograms of the short days and long days were combined in one composite actogram for each genotype, in which the short-day actogram (upper part of the composed actograms) was vertically flipped (see small arrows on the right margin indicating the directional flow of the actograms). These actograms give a rough comparison of the behavior of the different genotypes. Morning (M) and evening (E) activity bouts are visible in flies with PER in all clock cells as well as in M- and

*(Continued)*

**FIGURE 2 |** Continued
E-LN-oscillator flies (see red and blue letters). Only an M activity bout is present in flies with PER only in the M-LN, and only an E activity bout is present in flies with PER only in the E-LN. Such activity bouts are absent in flies without PER. Under short days, $per^0$ mutants show a considerably amount of nocturnal activity that starts a few hours after lights-off. The onset of this nocturnal activity is visible in all fly strains except the ones with per in all clock neurons and is marked by stippled green lines. The onset of M activity, which is only visible in flies with functional M oscillators and occurs clearly before lights-on, is marked by red stippled lines. **(C)** Average activity profiles for each strain under all photoperiods (the LD cycles are indicated at the left margin; activity during the light phase of the relevant LD cycle is shown in gray and activity during the dark phase is shown in black). The activity profiles are normalized in such a way that the highest activity was set to a value of 1. Colored letters mark nocturnal (N), morning (M), and evening (E) activity, respectively. Black arrows indicate reductions in activity level during the day.

maxima with the mouse pointer. Mean phases with respect to midnight were calculated for each genotype under each photoperiod. The phase relationship between M and E peak ($Y_{M,E}$) was determined for each fly and averaged for the different genotypes and photoperiods. In addition, we calculated the absolute average activity (beam crosses/10 min) for each fly during the entire 24 h day (= overall activity level), during the light phase (= diurnal activity), and during the dark phase (= nocturnal activity).

## Statistics

Activity levels and $\Psi_{M,E}$ were tested for significant influence of photoperiod and genotype (different strains) using two-way analysis of variance (ANOVA) after testing the data for normal distribution with the Kolmogorov–Smirnov test (Systat 13 Version 13.00.05; SPSS, Chicago, IL). A Bonferroni *post hoc* test was applied for pairwise comparisons. Values were regarded as significantly different at $p < 0.05$ and as highly significantly different at $p < 0.001$. When data were non-normally distributed, *p*-values were adjusted through multiplication by 10, according to Glaser (1978).

# RESULTS

## General Activity Patterns

### $per^0$ Controls

All flies that lacked PER completely exhibited the same behavior, which is shown for "$per^0$ *tim-gal4*" controls ($per^0$;*tim-gal4/ +;uas-per16/ +*) in **Figures 2B,C** (1st column) and for "$per^0$ *uas-per*" controls ($per^0$*; +;uas-per16/ +*) in **Figure 3** (1st column). Under all tested photoperiods, the flies responded with high activity to lights-on and lights-off (the so-called lights-on and lights-off peaks), but they exhibited neither morning nor evening activity bouts and were more active during the day than during the night. After the lights-on peak, their diurnal activity level remained rather constant, whereas their nocturnal activity level dropped temporarily after the lights-off peak. This activity drop was more pronounced and lasted for the entire night under long photoperiods (light phase > 14 h), probably because the flies had been active throughout the entire long light phase and therefore physically exhausted (see average actograms in **Figure 2B**). The green stippled line in the average actogram (**Figure 2B**, 1st column) indicates the increase of nocturnal activity (as determined by visual inspection) after the initial drop. The latter is also visible in the average activity profiles and is marked by a green "N" in **Figures 2**, **3**. The increase in nocturnal activity was slightly larger in $per^0$ *uas-per* controls than in $per^0$ *tim-gal4* controls (compare first columns in **Figure 2** with that of **Figure 3**). Nevertheless, the absolute amount of nocturnal activity was the same in both $per^0$ control strains (see later). In summary, the daily changes in activity of the $per^0$ controls can be explained as responses to the external LD cycles and to their internal sleep need.

### $per^0$ Mutants With PER Rescued in All Clock Cells and Wild-Type Controls

The activity pattern of $per^0$ mutants, in which PER was rescued under control of the *timeless* promotor in all clock cells ("$per^0$ *tim-gal4 uas-per*" = $per^0$;*tim-gal4/ +;uas-per16/ +*), was indistinguishable from that of wild-type flies (compare last row of **Figure 2** with that of **Figure 3**). Both strains showed the typical activity pattern with M activity bouts around lights-on and E activity around lights-off under short and medium photoperiods. Only under long photoperiods (light phase > 16 h) did E activity peaks occur before lights-off. Between M and E activity, the flies held a siesta, which was longer under long photoperiods (arrows in **Figures 2**, **3**). The activity pattern of $per^0$ *tim-gal4 uas-per* (**Figure 2C**, last column) showed strong similarity to that of wild-type flies (**Figure 3**, last column). This suggests that the expression pattern of PER plays a more critical role in shaping locomotor activity than PER expression levels, which might differ between the transgenic $per^0$ *tim-gal4 uas-per* line and wild types.

### Flies With PER Only in the M-LN

In contrast to $per^0$ controls, the flies with PER in the M-LN ("$per^0$ *Pdf-gal4 uas-per*" = $per^0$;*Pdf-gal4/ +;uas-per16/ +*) exhibited a pronounced M activity bout that occurred before lights-on under short photoperiods (**Figure 2**, 2nd column). Under LD12:12, M activity was still visible; it started before lights-on and reached peak levels around lights-on. However, under long photoperiods, morning activity and the lights-on peak were barely distinguishable. Under LD16:08, the "lights-on peak" of M-LN flies lasted still longer than that of $per^0$ controls, but under LD18:06, the activity pattern of M-LN flies and $per^0$ controls was very similar. Most importantly, M-LN flies showed no siesta and no E activity bout. Their diurnal activity level remained constantly high throughout the light phase without any activity increase in anticipation of lights-off (**Figure 2**, 2nd column). As already observed in $per^0$ controls, lights-off provoked a lights-off peak after which nocturnal activity dropped almost to zero (see average actogram in **Figure 2B**, 2nd column). This activity drop lasted for about 2–3 h and then the nocturnal activity level visibly increased (green line in the average actogram and green "N" in the activity profiles). The M activity bout then constituted

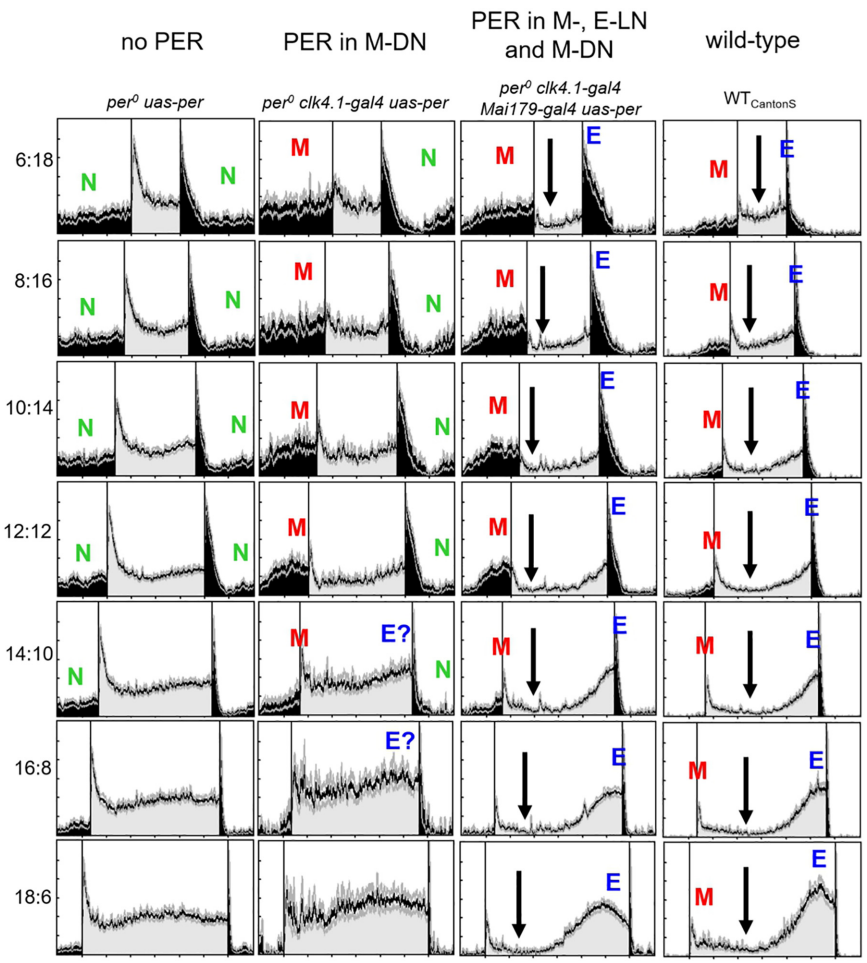


**FIGURE 3 |** Normalized average activity profiles of 25–30 flies, respectively, of the following lines: (1) $per^0$ mutant controls (no *per*), (2) flies with *per* only in ~8 CRY-positive dorsal posterior neurons (*per* in $DN_{1p}$), (3) flies with *per* in most lateral neurons and in the $DN_{1p}$ (*per* in M- and E-LNs and $DN_{1p}$), and (4) wild-type flies ($WT_{CantonS}$). Labeling as in **Figure 1C**.

a second strong increase in nocturnal activity (red stippled line in the average actogram and red "M" in the activity profiles).

## Flies With PER Only in the E-LN

Flies with PER in the E-LN ("$per^0$ *Pdf-gal80 mai-gal4 uas-per*" = $per^0$*;Mai179-gal4/Pdf-gal80;uas-per16/ +*) exhibited no morning activity bout. Their nocturnal activity was very similar to that of the $per^0$ controls (see stippled green line in the average actogram and the "N" in the activity profiles shown in **Figure 2**, 3rd column). However, the E-LN flies exhibited a less pronounced lights-on peak as compared to $per^0$ mutants and their diurnal activity level after the lights-on peak dropped to very low levels (arrows in **Figure 2B**, 3rd column). Under short photoperiods, activity increased only after lights-off and manifested itself as a long and pronounced lights-off peak. Under long photoperiods, however, the E-LN flies showed a pronounced evening bout of activity that seemed to occur at about the same phase as it did in control flies with PER rescued in all clock cells (**Figure 2B**, 3rd column).

## Flies With PER in the M- and E-LN

The activity pattern of flies with PER in M- and E-LN can be regarded as a mixture of that of flies with only M-LN or only E-LN (**Figure 2**, 4th column). The flies exhibited M and E activity bouts with a very similar phase to the flies with only one of the two LN oscillators. Most importantly, under short photoperiods, the phases of the two were not wild type like, but occurred earlier and later, respectively. After lights-on, the diurnal activity level dropped and remained low until the increase of evening activity (arrows in **Figure 2B**, 4th column).

## Flies With PER Only in the M-DN

The activity pattern of flies with PER only in the M-DN was in principle similar to that of the M-LN flies. However, M activity was lower and the M activity bout was less defined (**Figure 3**, 2nd column), suggesting that the M-LN are needed for a pronounced M activity bout. Furthermore, the flies showed signs of E activity (marked as "E?" in **Figure 3**), suggesting that the CRY-positive

$DN_{1p}$ cells that express PER in this line may also include some E oscillators.

### Flies With PER in the M-, E-LN, and M-DN

The activity pattern of flies with PER in M-LN and M-DN plus E-LN was very similar to that of flies with PER in M-LN and E-LN, suggesting that PER in the M-DN does only marginally contribute to the appearance and phase of M and E activity (**Figure 3B**, 3rd column). Nevertheless, nocturnal activity (green "N" in **Figure 2**) appeared considerably lower in flies that had PER additionally in the M-DN. Diurnal activity dropped after M activity and remained low until the increase in E activity (arrows in **Figure 3**).

## Phases of M and E Activity Bouts and Phase Relationship Between the Two

Since the precise phases of M and E activity bouts are hard to see in the average activity profiles, we determined the onset of M and E activity and their relevant peak phases for each fly and calculated the means for each fly strain (**Figure 4**). These plots show that only flies that expressed PER in all clock cells showed a wild-type phase of M and E activity. Flies with PER only present in the M-LN, in the M-LN and E-LN, or in the M-LN, E-LN, and M-DN had a very early onset of M activity as well as an early activity peak. E activity started the latest in flies with PER only in the E-LN, significantly earlier in flies with PER in the M-LN and E-LN or in the M-LN, E-LN, and M-DN, and the earliest in wild-type flies followed by flies with PER in all clock cells (**Figure 4A**). Interestingly, the slope of activity onset in dependence of photoperiod was different for the flies that expressed PER only in the subset of the clock neurons and those that expressed it in all cells. In flies with PER in all clock cells, E activity onset became later with increasing photoperiod, while in those that had per only in subsets of clock cells, this was only the case until a photoperiod of 12 h. With longer photoperiods (14, 16, 18 h), the phases of E onsets were advancing again, finally becoming earlier than the phase of E onset in wild-type flies (**Figure 4A**). In respect of M and E activity peaks, the difference between flies that express PER in all cells and flies that do so only in a subset of clock neurons was less dramatic, but otherwise similar: The M activity peak was significantly earlier in the flies with PER in a subset of clock neurons until a photoperiod of 16 h (**Figure 4B**). At longer photoperiods, we could not distinguish the M peak from the lights-on peak, and therefore, we could not determine its phase. The E activity peak occurred after lights-off in the flies that expressed PER only in subsets of the clock neurons, while it was around lights-off in wild-type flies. As observed for the onset of E activity, at long photoperiods, the E peak became earlier in flies with PER only in subsets of the clock neurons than that of wild-type flies (**Figure 4B**).

As observed in earlier studies (Rieger et al., 2012), the distance (phase relationship $Y_{ME}$) between M and E peaks was small in wild-type flies under short photoperiods and lengthened considerably with increasing photoperiod (**Figure 4C**). The same was true for flies with PER in all clock cells. The other two strains, in which we could calculate $Y_{ME}$ (flies with PER in M- and E-LN and flies with PER in M-, E-LN, and M-DN) had a significantly larger $Y_{ME}$ at short photoperiods and $Y_{ME}$ lengthened less dramatically with increasing photoperiod (**Figure 4C**). $Y_{ME}$ was always longer in the flies that expressed PER only in the M- and E-LN than in those that possessed PER additionally in the M-LN. In summary, this indicates that $Y_{ME}$ is the shorter the more clock cells express PER.

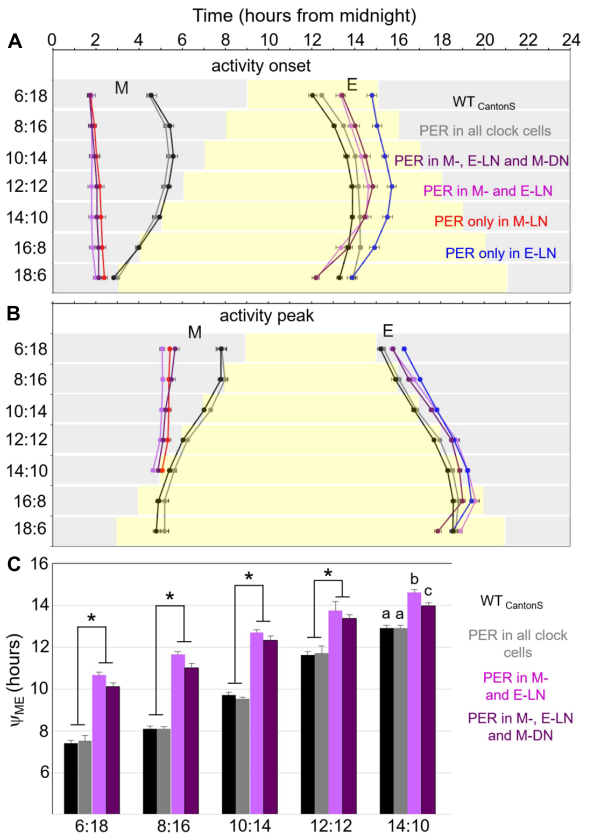


**FIGURE 4 |** Timing of morning and evening activity in most of the strains shown in **Figures 1**, **2** under the different photoperiods. We were not able to reliably determine the phases of M activity in flies with PER only in the M-DN. Therefore, these flies are not included here. **(A)** Timing of onset of morning and evening activity, respectively. **(B)** Timing of morning and evening activity peaks. **(C)** Distances between morning and evening activity peaks ($Y_{ME}$) until a photoperiod of 14 h. Error bars show standard errors of the mean. A two-way ANOVA revealed a clear dependence of $Y_{ME}$ on photoperiod [$F_{(5, 604)} = 486.579$; $p < 0.001$] and on the strain [$F_{(3, 604)} = 173.384$; $p < 0.001$], as well as a significant interaction between both [$F_{(15, 604)} = 7.204$; $p < 0.001$], which indicates that the response to photoperiod is significantly different in the different strains. A *post hoc* analysis showed that $Y_{ME}$ is significantly shorter in the wild-type strain ($WT_{CantonS}$) and flies with PER rescued in all clock cells as compared to flies in which PER was only rescued in specific subgroups ($p < 0.001$, asterisks). At all photoperiods, there is a tendency that $Y_{ME}$ is shorter in the flies, in which PER is rescued in the M-DN in addition to the M- and E-LN as compared to only in the M- and E-LN. However, this difference turned out to be only significant ($p = 0.018$) under the longest day (14:10) as indicated by different letters.

## Nocturnal Activity Bouts

One striking result of our study is the high nocturnal activity of most strains that express PER only in subsets of the clock cells

under short photoperiods. To visualize nocturnal activity in more detail, we plotted the same normalized activity profiles shown in **Figures 2**, **3** once again, but this time with the night centered and only for the short photoperiods (**Figure 5**). While wild-type flies and flies with PER in all clock cells exhibited only minimal nocturnal activity, the nocturnal activity of all other strains was clearly higher. First, this indicates that a fully functional clock with PER present in all clock cells inhibits nocturnal activity (two large arrows in **Figure 5**, 3rd and 4th columns, respectively). In $per^0$ controls, nocturnal activity (N) occurred at moderate constant levels throughout the night (**Figure 5A**, 1st column). This was comparable in flies with PER only in the E-LN (**Figure 5A**, 4th column), but here, N activity was lower and appeared already inhibited directly after E activity, as soon as the days get longer (>8 h, black arrows). In the other strains, activity was clearly inhibited directly after E activity (black arrows in **Figure 5**) or, in the case of flies with PER only in the M-LN (**Figure 5A**, 3rd column), directly after the lights-off peak, and this happened already under short photoperiods. After this drop, activity increased in two steps that can be best seen in flies with PER only in the M-LN or in the M- and E-LN (indicated as green "N" and red "M" in **Figure 5A**, 3rd column, and **Figure 5B**, 1st column, respectively). We interpret the second increase in activity as early M peak. In flies, in which PER is only present in the M-DN (**Figure 5A**, 2nd column), the second step in nocturnal activity increase is barely visible, suggesting that the M-DN activate the M peak only slightly so that it is hard to distinguish from the N peak. Nevertheless, when compared to $per^0$ (**Figure 5A**, 1st column) controls, nocturnal activity is clearly enhanced when PER is present in the M-DN (**Figure 5A**, 2nd column). In flies expressing PER only in M-LN, E-LN, and M-DN (**Figure 5B**, 2nd column), the nocturnal activity is strongly suppressed, suggesting an inhibitory effect of the E-LN. Together, these findings indicate that some clock neurons inhibit nocturnal activity at certain times during the night while others promote it at other times of the night.

## Absolute Diurnal and Nocturnal Activity Levels

So far, we have considered the relative activity of the flies throughout day and night on the normalized activity profiles. In order to see the effects of PER in the different clock neurons on real activity levels, we calculated the absolute average values of overall, diurnal, and nocturnal activity (in beam crosses per 10 min) at the different photoperiods (**Figure 6**). We found that, in most fly strains, the overall activity level was maximal at equinox (LD12:12) (**Figure 6A**). Nevertheless, the activity level was very different in the different strains. The highest overall activity level was found in flies that expressed PER only in the M-LN, while the lowest activity was present in wild-type flies. Arrhythmic $per^0$ mutants showed intermediate activity levels and the activity of flies with PER rescued in different clock neurons clustered around that of the $per^0$ mutants, sometimes below, sometimes above it (**Figure 6A**). These activity differences are consistent with the hypothesis that certain clock neurons promote activity (e.g., the M-LN), while other clock neurons rather inhibit activity (e.g., the E-LN and M-DN).

To get more insight into strain-dependent and photoperiod-dependent effects on diurnal and nocturnal activity, we calculated diurnal and nocturnal activity of the different strains at all photoperiods (**Figures 6B,C**). With few exceptions, diurnal activity was higher during the day than during the night. Deviations from this general pattern were found in flies that possessed PER in the M- and E-LN only or additionally in the M-DN. At short photoperiods, these flies were clearly more active during the night than during the day. Flies with PER only in the E-LN were also more active during the night than during the day but only under LD12:12 and 14:10.

As already found for overall activity, the highest diurnal and nocturnal activity levels of most strains occurred during equinox (LD12:12), respectively (compare **Figures 6B,C**). Diurnal activity decreased in most strains when the days became shorter or longer (**Figure 6B**), while nocturnal activity dropped only moderately under short days but prominently under long days (**Figure 6C**). Again, some strains differed from this pattern. For example, diurnal activity of flies with PER only in the E-LN or in the M- and E-LN remained high even under long days. Diurnal activity of flies with PER only in M-DN remained almost the same under all photoperiods (with a slight increase under very short days) and diurnal activity of flies with PER in the M-, E-LN, and M-DN steadily increased with photoperiod. Nocturnal activity of the latter flies remained constantly high under short photoperiods (until LD10:14) and then steadily decreased.

In sum, our analysis of the activity profiles and activity levels revealed that activity promotion and activity inhibition appear to happen in a time-dependent and photoperiod-dependent manner (see also **Figures 2**, **3**, **5**).

# DISCUSSION

Since the discovery that specific clock neurons control M and E activity of *D. melanogaster*, many studies tested the properties of M and E oscillators in detail. In the following, we will discuss these studies in the light of our findings.

Most studies manipulated either the light sensitivity or the oscillation speed in the M and E clock neurons and tested the consequences on entrainment or free-running behavior of the flies (Stoleru et al., 2005, 2007; Murad et al., 2007; Picot et al., 2007; Zhang L. et al., 2010; Zhang Y. et al., 2010). They found that M and E oscillators do not only differ in their responsiveness to light as originally proposed by Pittendrigh and Daan (1976), but that they have in addition different capabilities to control rhythmicity under darkness and light.

Stoleru et al. (2007) expressed the kinase Shaggy in either the M cells or the E cells, which speeds up the clock in the relevant neurons, and recorded the flies' activity under short and long photoperiods. They found that the M neurons controlled the phase of M and E activity phase under short days (both became early), while the E cells had no influence on the phase of M activity under these conditions. However, under long days, the situation was the other way around. Now, the E cells determined

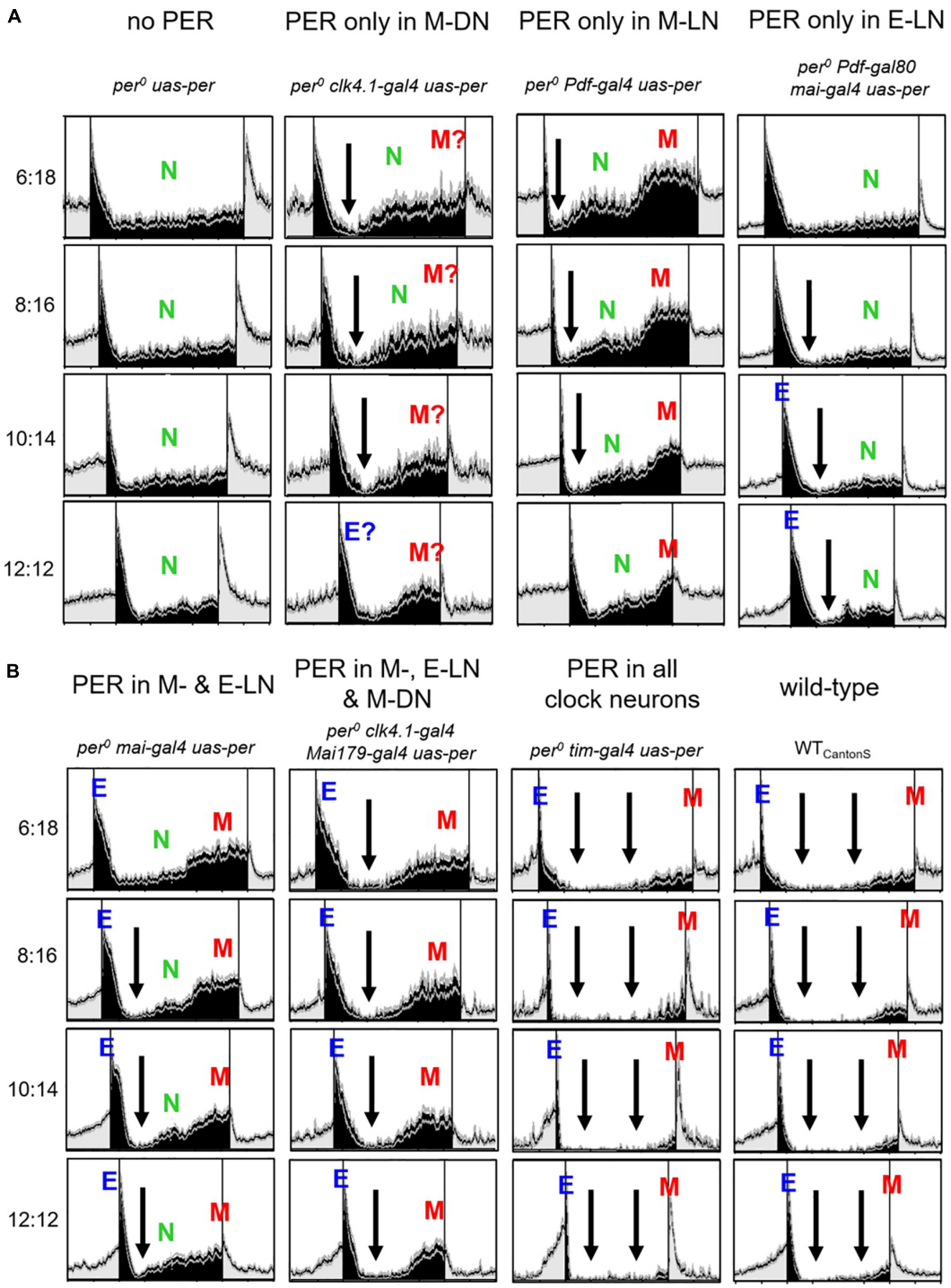


**FIGURE 5 |** Nocturnal activity bouts of the different strains at short photoperiods (photoperiods between 6 and 12 h). The same normalized activity profiles shown in **Figures 1**, **2** are plotted in a way that the night is centered. In **(A)** are shown *per*$^0$ *uas-per*; *per*$^0$ *clk4.1-gal4 uas-per*; *per*$^0$ *clk4.1-gal4 uas-per*; *per*$^0$ *Pdf-gal4 uas-per*; and *per*$^0$ *Pdf-gal80 mai-gal4 uas-per*; whereas in **(B)**, *per*$^0$ *mai-gal4 uas-per*; *per*$^0$ *clk4.1-gal4 mai-gal4 uas-per*; *per*$^0$ *tim-gal4 uas-per*; and $WT_{CantonS}$ are shown. Black arrows indicate times at which nocturnal activity is reduced. Otherwise, the labeling is similar to **Figures 1**, **2**. Flies with PER in the M-DN show a lower M activity than flies with PER in the M-LN. Therefore, in these flies, it is more difficult to distinguish M activity from general nocturnal (N) activity and we added a question mark to the M peak. In flies with PER in M-, E-LN, and M-DN, N activity appeared absent and only the early M peak was visible, whereas in wild-type flies, N and M activity appeared largely suppressed. The latter is indicated by two black arrowheads.

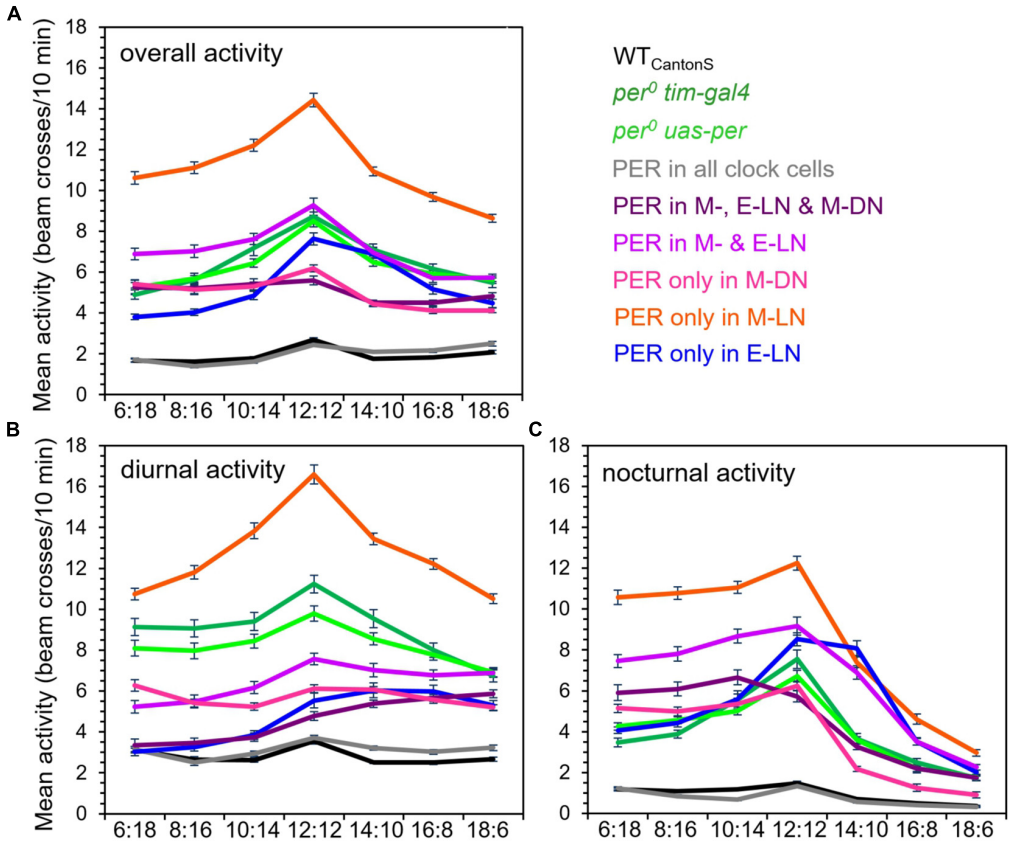


**FIGURE 6 |** Absolute overall **(A)**, diurnal **(B)**, and nocturnal **(C)** activity levels in the different fly strains at all photoperiods (± SD). The activity values for the different strains are shown in different colors [color codes are given right to **(A)**]. A two-way ANOVA revealed a clear dependence of overall activity, on photoperiod [$F_{(7, 2,209)} = 42.997$; $p < 0.001$] and on strain [$F_{(8, 2,209)} = 150.759$; $p < 0.001$], as well as a significant interaction between both [$F_{(56, 2,209)} = 3.677$; $p < 0.001$]. Furthermore, two-way ANOVA revealed a clear dependence of diurnal and nocturnal activity on photoperiod [for diurnal activity, $F_{(7, 2,209)} = 14.046$; $p < 0.001$; for nocturnal activity, $F_{(7, 2,209)} = 180.902$; $p < 0.001$] and on the strain [for diurnal activity, $F_{(8, 1,109)} = 125.203$; $p < 0.001$; for nocturnal activity, $F_{(8, 2,209)} = 107.405$; $p < 0.001$], as well as a significant interaction between both [for diurnal activity, $F_{(56, 2,209)} = 3.957$; $p < 0.001$; for nocturnal activity, $F_{(56, 2,209)} = 9.585$; $p < 0.001$]. Together, this indicates that the responses of diurnal and nocturnal activity to photoperiod are significantly different in the different strains. No differences in overall, diurnal, and nocturnal activity levels were found between the *per*$^0$ and wild-type controls, respectively. For more detailed explanations, see text.

the phase of M and E activity, while the M neurons did not influence the phase of E activity. Stoleru et al. (2007) concluded that the M cells dominate on long nights and the E cells dominate on long days. Although the definition of E cells was not very accurate in this study (all clock cells except those of the M-LN were regarded as E cells), this result is very interesting. It fits our observation that flies with PER only in the M-LN drive a strong M activity bout in darkness under short days, but that this diminishes under long days. Vice versa, in flies with PER only in the E-LN, E activity is best visible in the light phase of long days. The differential dominance of M and E oscillators may even be reflected in the amplitudes of M and E peaks in wild-type flies under short and long photoperiods (Rieger et al., 2003) and in the flies with PER rescued in all cells shown in **Figure 1**. Under short days (LD 8:16 and 10:14), their M peak was higher than their E peak, whereas the opposite was true under long days (LD 16:8 and 18:6).

Other studies used the same definition of M and E neurons as we did in the present study, but they did not record activity under different photoperiods, but instead varied light intensity at equinox (LD 12:12) or recorded the flies under constant darkness (DD) or constant light (LL) (Picot et al., 2007; Rieger et al., 2009; Zhang Y. et al., 2010; Chatterjee et al., 2018). These studies found that functional M-LN neurons alone can control rhythmic behavior in constant darkness (DD), while functional M-DN or E-LN neurons alone cannot. Vice versa, the E-LN neurons alone can control rhythmicity in constant light (LL), but the M-LN or the M-DN alone cannot. Thus, the M neurons (especially the M-LN) appear to be dominant under DD, while the E neurons appear dominant under LL (reviewed in Yoshii et al., 2012), which fits the studies of Stoleru et al. (2007) and our observations. Picot et al. (2007) suggested the existence of a light-dependent switch between M and E oscillators that requires the visual system and helps the animal to adapt to seasonal changes in day length, but unfortunately, they have not recorded the flies under different photoperiods to test their hypothesis.

Finally, Chatterjee et al. (2018) found that M-LN are master oscillators that signal to the M-DN and both together control M

activity. In other words, a functional clock is necessary in the M-LN and M-DN to control M activity in a wild-type manner. Indeed, we found here that flies that possessed PER in the M-LN and M-DN (in addition to the E-LN) had a more defined M activity under short days (they lacked the nocturnal activity peak "N"; see **Figure 5**). In addition, they had a more wild-type-like $Y_{M,E}$ (**Figure 4C**) as compared to flies that possessed PER only in the M- and E-LN.

Chatterjee et al. (2018) also found that the E-LN and E-DN control E activity in parallel at low light intensities (∼50 lux), but that at higher light intensities (∼1,000 lux), the activity of the E-DN is blocked and solely the E-LN controls E activity. Thus, there is a light-dependent switch in the neuronal network controlling E activity. Most importantly, the *Clk4.1M* driver that we used to manipulate the M-DN drives also in some E-DN (Zhang Y. et al., 2010; Chatterjee et al., 2018; **Figure 1**) and the light intensity of 100 lux that we have used to record the flies probably allows the E-DN to contribute to E activity. This may explain why we have seen signs of E activity in our flies with PER in the M-LN, especially under long photoperiods (**Figure 3**), but most of the E activity in our recordings appears to stem from the E-LN.

Nevertheless, the situation is even more complex, because the E neurons are not independent of the M-LN (= s-$LN_v$), or better to say from PDF stemming from the s-$LN_v$ and the l-$LN_v$ (Stoleru et al., 2005; Shafer and Taghert, 2009; Yoshii et al., 2009; Guo et al., 2014; Seluzicki et al., 2014; Yao and Shafer, 2014; Liang et al., 2016, 2017; Schlichting et al., 2016; Menegazzi et al., 2017; Chatterjee et al., 2018). In brief, the E neurons express the PDF receptor and respond to PDF, secreted from either the s-$LN_v$ or the l-$LN_v$ neurons, with a delay of their rhythm in neuronal activity (visualized by cellular $Ca^{2+}$ levels). Subsequently, this leads to a delay in E activity. Such a delay is especially important under long photoperiods in order to keep E activity close to dusk. Two studies show that under long photoperiods, PDF comes predominantly from the l-$LN_v$ neurons (Menegazzi et al., 2017; Schlichting et al., 2019b), while it appears to originate mainly from the s-$LN_v$ cells under short photoperiods and equinox (Guo et al., 2014). Once more, this indicates that there is a light-mediated circuit switching in the *Drosophila* neuronal clock network, when light conditions change. The neuronal activity of the l-$LN_v$ is highly dependent on light (Cao and Nitabach, 2008; Shang et al., 2008; Sheeba et al., 2008), which fits their dominant role as E activity-delaying mediators under long photoperiods.

Finally, yet importantly, there is also evidence that the M-DN cells feedback on the E-LN (Guo et al., 2016, 2018) and M-LN (Hamasaka et al., 2007) and block their activity via glutamate signaling. This leads to a block in M and E activity during midday, provoking the flies' siesta. Most interestingly, high light prolongs the siesta even under equinox conditions (Rieger et al., 2007), and this is provoked by a special high light intensity pathway that signals to the M-LN and then via PDF to the M-DN that in turn blocks the activity of M-LN and E-LN (Schlichting et al., 2019a). These studies have been performed only under equinox conditions; nevertheless, it is well imaginable that the described pathways are also valid under long photoperiods in which a blocking of M and E oscillators during midday is especially important to prolong the siesta and delay E activity.

In the present study, we found that wild-type flies exhibited very little activity during midday and the night, while the activity level of $per^0$ mutants was significantly higher throughout the entire 24 h day; in particular, no siesta was visible during midday. Although we cannot exclude the idea that the genetic background of the strains used might play a role, our results indicate that a main function of the circadian clock is to inhibit activity at less favorable times of the day. This nicely coincides with the findings of Menegazzi et al. (2012) and Schlichting et al. (2015), who tested the function of PER under more natural-like conditions and found that PER was especially needed to prevent activity of the flies during midday and the night. The same may be true for mammals. Chipmunks [in which the clock in the suprachiasmatic

**TABLE 1 |** Contribution of different clock neuron clusters in shaping the wild-type locomotor activity profile of *D. melanogaster*.

| Genotype | $PER^+$ cells | Function/Phenotype short days | Function/Phenotype long days |
|---|---|---|---|
| *$per^0$ pdf-gal4 uas-per* | M-LN | Promote M activity | |
| *$per^0$ pdf-gal80 mai-gal4 uas-per* | E-LN | Promote E activity | Promote E activity |
| | | Inhibit day activity | Inhibit day activity |
| *$per^0$ mai-gal4 uas-per* | M-LN, E-LN | Promote M activity | Promote E activity |
| | | Promote E activity | Inhibit day activity |
| | | Inhibit day activity | Partially inhibit E activity |
| *$per^0$ clk4.1-gal4 uas-per* | M-DN | Promote M activity | Might promote E activity |
| *$per^0$ mai-gal4 clk4.1-gal4 uas-per* | M-LN, E-LN, M-DN | Promote M activity | Promote E activity |
| | | Promote E activity | Inhibit day activity |
| | | Inhibit day activity | |
| | | Inhibit N activity | |
| $per^0$ tim-gal4 uas-per | All clock cells | M and E activity that track lights-on and -off | |
| | | (reduced time difference between M and E) | |
| | | Strong inhibition of day activity | |
| | | (i.e., pronounced siesta) | |
| | | Strong inhibition of night activity | |

nuclei (SCN) was lesioned] that were released into the wild spent significantly more time outside their burrow during the night and consequently had a higher predation risk as compared to control animals (DeCoursey et al., 2000).

Here, we show that a functional circadian clock restricted to the main neuronal clusters composing the M and E oscillators (M-LN, M-DN, and E-LN) is not sufficient to inhibit activity in a wild-type-like manner. We also show that the different clock neurons do not all inhibit activity, and if they do so, they inhibit it at different times of the day. For example, the M-LN did not inhibit activity at all, but instead strongly provoked it. This is especially true for nocturnal activity under short photoperiods, conditions under which the M-LN induce a prominent nocturnal M activity bout (**Figures 5**, **6**). However, also diurnal activity of the M-LN was rather high. No siesta occurred, and this was valid under all photoperiods. In contrast to the M-LN, the M-DN clearly inhibited activity, especially diurnal activity (**Figure 6**), which is in concordance with their siesta-inducing role. The absolute level of nocturnal activity was similar to that of $per^0$ mutants, but as discussed above, the M-DN nonetheless suppressed nocturnal activity (N) after the lights-off peak (or the weak "E?" peak) (**Figure 5**). The highest activity inhibition during the day is caused by the E-LN, or by the E-LN in combination with the M-DN (as discussed above, the M-LN that also contain PER in the latter combination do not contribute at all to the inhibition of diurnal activity).

After having said this, the impression arises that nothing is left of the original Pittendrigh and Daan (1976) model, which explained the increasing $Y_{M,E}$ by an acceleration of the M oscillators and slowing down of the E oscillators by light with increasing photoperiod. All appears explainable by provoking and inhibiting activity via different clock neurons at specific times of the day. However, this is only true at first glance. We found that the action of the different clock neurons on activity clearly depended on the photoperiod. Furthermore, $Y_{M,E}$ also depended significantly on photoperiod and increased with increasing day length, even in the flies that expressed PER only in subsets of the clock neurons (**Figure 4C**). Thus, light has most likely different effects on the oscillation speed of M and E neurons. Indeed, flies with PER only in the M-LN, M-DN, and E-LN and that additionally lacked CRY showed an internal desynchronization into two components that free-run with short and long periods, respectively – a behavior that was similar to that of $cry^0$ mutants with fully functional clock (Yoshii et al., 2012). Thus, in principle, the M oscillators appear to speed up and the E oscillators appear to slow down upon light, as predicted by Pittendrigh and Daan (1976). However, in addition to the oscillation speed, the dominance of *Drosophila's* M and E oscillators changes with increasing light. This makes it hard to observe the velocity changes in M and E cells of flies that possess all sets of photoreceptors, including CRY. Furthermore, not all clock neurons behave as M and E oscillators (e.g., the l-$LN_v$), and of several clock neurons, we still do not know the exact function (see **Figure 1**). Most likely, there are more than just M and E neurons and the so-called M and E neurons can adjust their function depending on the environmental conditions.

In summary, there is growing evidence that the circadian clock of *Drosophila* is composed of a plastic network of oscillators that rearrange themselves depending on the environmental demands. This explains why the original M and E oscillator model of Pittendrigh and Daan (1976) is too simple to describe the situation in *Drosophila*. Here, we show that PER expression within different subsets of clock neurons is not sufficient to adapt the behavior of the flies to different photoperiods in a wild-type manner (see **Table 1**). Perhaps PER is not only necessary in all clock neurons, but additionally in all glial cells for a wild-type behavior. Glial cells are still largely neglected in circadian studies, although several studies show that they play active roles in the clock (Zerr et al., 1990; Ewer et al., 1992; Ng et al., 2011; Jackson et al., 2015, 2019; Brancaccio et al., 2019). Future studies are warranted to test this important issue.

## DATA AVAILABILITY STATEMENT

The raw data supporting the conclusions of this article will be made available by the authors, without undue reservation, to any qualified researcher.

## AUTHOR CONTRIBUTIONS

PM, KB, VG, and MS performed the experiments. PM, KB, and CH-F conceived the study and planned the experiments. CH-F wrote the manuscript with contributions from PM, KB, and FS. All authors analyzed the experiments.

## FUNDING

This study was supported by the German Research Foundation (DFG) in projects A1 and A2 of the Collaborative Research Center (SFB1047) and by individual grants to CH-F (FO 207/15-1) and PM (ME 4866/1-1).

## ACKNOWLEDGMENTS

We thank Francois Rouyer and Patrick Emery for providing fly strains, Ralf Stanewsky for donating the PER antibody, Christiane Hermann-Luibl and Taishi Yoshii for advice and practical assistance, and Dirk Rieger for carrying out preliminary studies.

## REFERENCES

Aschoff, J. (1966). Circadian activity pattern with two peaks. *Ecology* 47, 657–662. doi: 10.2307/1933949

Bachleitner, W., Kempinger, L., Wülbeck, C., Rieger, D., and Helfrich-Förster, C. (2007). Moonlight shifts the endogenous clock of *Drosophila melanogaster*. *Proc. Natl. Acad. Sci. U.S.A.* 104, 3538–3543. doi: 10.1073/pnas.0606870104

Brancaccio, M., Edwards, M. D., Patton, A. P., Smyllie, N. J., Chesham, J. E., Maywood, E. S., et al. (2019). Cell-autonomous clock of astrocytes drives circadian behavior in mammals. *Science* 363, 187–192. doi: 10.1126/science.aat4104

Bywalez, W., Menegazzi, P., Rieger, D., Schmid, B., Helfrich-Förster, C., and Yoshii, T. (2012). The dual-oscillator system of *Drosophila melanogaster* under natural-like temperature cycles. *Chronobiol. Int.* 29, 395–407. doi: 10.3109/07420528.2012.668505

Cao, G., and Nitabach, M. N. (2008). Circadian control of membrane excitability in *Drosophila melanogaster* lateral nentral clock neurons. *J. Neurosci.* 28, 6493–6501. doi: 10.1523/JNEUROSCI.1503-08.2008

Chatterjee, A., Lamaze, A., De, J., Mena, W., Chélot, E., Martin, B., et al. (2018). Reconfiguration of a multi-oscillator network by light in the *Drosophila* circadian clock. *Curr. Biol.* 28, 2007.e4–2017.e4. doi: 10.1016/j.cub.2018.04.064

DeCoursey, P. J., Walker, J. K., and Smith, S. A. (2000). A circadian pacemaker in free-living chipmunks: essential for survival? *J. Comp. Physiol. A* 186, 169–180. doi: 10.1007/s003590050017

Dunlap, J. C., Loros, J. J., and DeCoursey, P. J. (2004). *Chronobiology: Biological Timekeeping*. Sunderland, MA: Sinauer Associates.

Ewer, J., Frisch, B., Hamblen-Coyle, M., Rosbash, M., and Hall, J. (1992). Expression of the period clock gene within different cell types in the brain of *Drosophila* adults and mosaic analysis of these cells' influence on circadian behavioral rhythms. *J. Neurosci.* 12, 3321–3349. doi: 10.1523/JNEUROSCI.12-09-03321.1992

Glaser, W. R. (1978). *Varianzanalyse*. Stuttgart: Gustav Fischer.

Grima, B., Chélot, E., Xia, R., and Rouyer, F. (2004). Morning and evening peaks of activity rely on different clock neurons of the *Drosophila* brain. *Nature* 431, 869–873. doi: 10.1038/nature02935

Guo, F., Cerullo, I., Chen, X., and Rosbash, M. (2014). PDF neuron firing phase-shifts key circadian activity neurons in *Drosophila*. *eLife* 3:e02780. doi: 10.7554/eLife.02780

Guo, F., Yu, J., Jung, H. J., Abruzzi, K. C., Luo, W., Griffith, L. C., et al. (2016). Circadian neuron feedback controls the *Drosophila* sleep–activity profile. *Nature* 536, 292–297. doi: 10.1038/nature19097

Guo, X., Wang, Y., Sinakevitch, I., Lei, H., and Smith, B. H. (2018). Comparison of RNAi knockdown effect of tyramine receptor 1 induced by dsRNA and siRNA in brains of the honey bee, *Apis mellifera*. *J. Insect Physiol.* 111, 47–52. doi: 10.1016/j.jinsphys.2018.10.005

Hamasaka, Y., Rieger, D., Parmentier, M.-L., Grau, Y., Helfrich-Förster, C., and Nässel, D. R. (2007). Glutamate and its metabotropic receptor in *Drosophila* clock neuron circuits. *J. Comp. Neurol.* 505, 32–45. doi: 10.1002/cne.21471

Hamblen-Coyle, M. J., Wheeler, D. A., Rutila, J. E., Rosbash, M., and Hall, J. C. (1992). Behavior of period-altered circadian rhythm mutants of *Drosophila* in light?: dark cycles (Diptera: Drosophilidae). *J. Insect Behav.* 5, 417–446. doi: 10.1007/BF01058189

Helfrich-Förster, C., Shafer, O. T., Wülbeck, C., Grieshaber, E., Rieger, D., and Taghert, P. (2007). Development and morphology of the clock-gene-expressing lateral neurons of *Drosophila melanogaster*. *J. Comp. Neurol.* 500, 47–70. doi: 10.1002/cne.21146

Jackson, F. R., Ng, F. S., Sengupta, S., You, S., and Huang, Y. (2015). Glial cell regulation of rhythmic behavior. *Methods Enzmol.* 552, 45–73. doi: 10.1016/bs.mie.2014.10.016

Jackson, F. R., You, S., and Crowe, L. B. (2019). Regulation of rhythmic behaviors by astrocytes. *Wiley Interdiscip. Rev. Dev. Biol.* doi: 10.1002/wdev.372 [Epub a head of print].

Johard, H. A. D., Yoishii, T., Dircksen, H., Cusumano, P., Rouyer, F., Helfrich-Förster, C., et al. (2009). Peptidergic clock neurons in *Drosophila*?: Ion transport peptide and short neuropeptide F in subsets of dorsal and ventral lateral neurons. *J. Comp. Neurol.* 516, 59–73. doi: 10.1002/cne.22099

Kaneko, M., and Hall, J. C. (2000). Neuroanatomy of cells expressing clock genes in *Drosophila*: transgenic manipulation of the period and timeless genes to mark the perikarya of circadian pacemaker neurons and their projections. *J. Comp. Neurol.* 422, 66–94. doi: 10.1002/(sici)1096-9861(20000619)422:1<66::aid-cne5>3.0.co;2-2

Liang, X., Holy, T. E., and Taghert, P. H. (2016). Synchronous *Drosophila* circadian pacemakers display nonsynchronous Ca2+ rhythms *in vivo*. *Science* 351, 976–981. doi: 10.1126/science.aad3997

Liang, X., Holy, T. E., and Taghert, P. H. (2017). A series of suppressive signals within the *Drosophila* circadian neural circuit generates sequential daily outputs. *Neuron* 94, 1173.e4–1189.e4. doi: 10.1016/j.neuron.2017.05.007

Majercak, J., Sidote, D., Hardin, P. E., and Edery, I. (1999). How a circadian clock adapts to seasonal decreases in temperature and day length. *Neuron* 24, 219–230. doi: 10.1016/S0896-6273(00)80834-X

Menegazzi, P., Dalla Benetta, E., Beauchamp, M., Schlichting, M., Steffan-Dewenter, I., and Helfrich-Förster, C. (2017). Adaptation of circadian neuronal network to photoperiod in high-latitude European Drosophilids. *Curr. Biol.* 27, 833–839. doi: 10.1016/j.cub.2017.01.036

Menegazzi, P., Yoshii, T., and Helfrich-Forster, C. (2012). Laboratory versus nature: the two sides of the *Drosophila* circadian clock. *J. Biol. Rhythms* 27, 433–442. doi: 10.1177/0748730412463181

Murad, A., Emery-Le, M., and Emery, P. (2007). A subset of dorsal neurons modulates circadian behavior and light responses in *Drosophila*. *Neuron* 53, 689–701. doi: 10.1016/j.neuron.2007.01.034

Ng, F. S., Tangredi, M. M., and Jackson, F. R. (2011). Glial cells physiologically modulate clock neurons and circadian behavior in a calcium-dependent manner. *Curr. Biol.* 21, 625–634. doi: 10.1016/j.cub.2011.03.027

Picot, M., Cusumano, P., Klarsfeld, A., Ueda, R., and Rouyer, F. (2007). Light activates output from evening neurons and inhibits output from morning neurons in the *Drosophila* circadian clock. *PLoS Biol.* 5:e315. doi: 10.1371/journal.pbio.0050315

Pittendrigh, C. S., and Daan, S. (1976). A functional analysis of circadian pacemakers in nocturnal rodents. *J. Comp. Physiol. A* 106, 333–355. doi: 10.1007/bf01417860

Renn, S. C. P., Park, J. H., Rosbash, M., Hall, J. C., and Taghert, P. H. (1999). A pdf neuropeptide gene mutation and ablation of PDF neurons aach cause severe abnormalities of behavioral circadian rhythms in *Drosophila*. *Cell* 99, 791–802. doi: 10.1016/s0092-8674(00)81676-1

Rieger, D., Fraunholz, C., Popp, J., Bichler, D., Dittmann, R., and Helfrich-Förster, C. (2007). The fruit fly *Drosophila melanogaster* favors dim light and times its activity peaks to early dawn and late dusk. *J. Biol. Rhythms* 22, 387–399. doi: 10.1177/0748730407306198

Rieger, D., Peschel, N., Dusik, V., Glotz, S., and Helfrich-Förster, C. (2012). The ability to entrain to long photoperiods differs between 3 *Drosophila melanogaster* wild-type strains and is modified by twilight simulation. *J. Biol. Rhythms* 27, 37–47. doi: 10.1177/0748730411420246

Rieger, D., Shafer, O. T., Tomioka, K., and Helfrich-Förster, C. (2006). Functional analysis of circadian pacemaker neurons in *Drosophila melanogaster*. *J. Neurosci.* 26, 2531–2543. doi: 10.1523/JNEUROSCI.1234-05.2006

Rieger, D., Stanewsky, R., and Helfrich-Förster, C. (2003). Cryptochrome, compound eyes, hofbauer-buchner eyelets, and ocelli play different roles in the entrainment and masking pathway of the locomotor activity rhythm in the fruit fly *Drosophila melanogaster*. *J. Biol. Rhythms* 18, 377–391. doi: 10.1177/0748730403256997

Rieger, D., Wülbeck, C., Rouyer, F., and Helfrich-Förster, C. (2009). Period gene expression in four neurons is sufficient for rhythmic activity of *Drosophila melanogaster* under dim light conditions. *J. Biol. Rhythms* 24, 271–282. doi: 10.1177/0748730409338508

Saunders, D. S. (2002). *Insect Clocks*. Amsterdam: Elsevier.

Schlichting, M., and Helfrich-Förster, C. (2015). Photic entrainment in *Drosophila* assessed by locomotor activity recordings. *Methods Enzymol.* 552, 105–123. doi: 10.1016/bs.mie.2014.10.017

Schlichting, M., Menegazzi, P., and Helfrich-Förster, C. (2015). Normal vision can compensate for the loss of the circadian clock. *Proc. R. Soc. B* 282:20151846. doi: 10.1098/rspb.2015.1846

Schlichting, M., Menegazzi, P., Lelito, K. R., Yao, Z., Buhl, E., Dalla Benetta, E., et al. (2016). A neural network underlying circadian entrainment and photoperiodic adjustment of sleep and activity in *Drosophila*. *J. Neurosci.* 36, 9084–9096. doi: 10.1523/JNEUROSCI.0992-16.2016

Schlichting, M., Menegazzi, P., Rosbash, M., and Helfrich-Förster, C. (2019a). A distinct visual pathway mediates high light intensity adaptation of the circadian clock in *Drosophila*. *J. Neurosci.* 39, 1621–1630. doi: 10.1523/JNEUROSCI.1497-18.2018

Schlichting, M., Weidner, P., Diaz, M., Menegazzi, P., Dalla Benetta, E., Helfrich-Förster, C., et al. (2019b). Light-mediated circuit switching in the *Drosophila* neuronal clock network. *Curr. Biol.* 29, 3266.e3–3276.e3. doi: 10.1016/j.cub.2019.08.033

Schmid, B., Helfrich-Forster, C., and Yoshii, T. (2011). A new ImageJ plug-in "ActogramJ" for chronobiological analyses. *J. Biol. Rhythms* 26, 464–467. doi: 10.1177/0748730411414264

Schubert, F. K., Hagedorn, N., Yoshii, T., Helfrich-Förster, C., and Rieger, D. (2018). Neuroanatomical details of the lateral neurons of *Drosophila melanogaster* support their functional role in the circadian system. *J. Comp. Neurol.* 526, 1209–1231. doi: 10.1002/cne.24406

Seluzicki, A., Flourakis, M., Kula-Eversole, E., Zhang, L., Kilman, V., and Allada, R. (2014). Dual PDF signaling pathways reset clocks via TIMELESS and acutely excite target neurons to control circadian behavior. *PLoS Biol.* 12:e1001810. doi: 10.1371/journal.pbio.1001810

Shafer, O., Levine, J., Truman, J., and Hall, J. (2004). Flies by night: effects of changing day length on *Drosophila*'s circadian clock. *Curr. Biol.* 14, 424–432. doi: 10.1016/S0960-9822(04)00131-9

Shafer, O. T., Helfrich-Förster, C., Renn, S. C. P., and Taghert, P. H. (2006). Reevaluation of *Drosophila melanogaster's* neuronal circadian pacemakers reveals new neuronal classes. *J. Comp. Neurol.* 498, 180–193. doi: 10.1002/cne.21021

Shafer, O. T., and Taghert, P. H. (2009). RNA-interference knockdown of *Drosophila* pigment dispersing factor in neuronal subsets: the anatomical basis of a neuropeptide's circadian functions. *PLoS One* 4:e8298. doi: 10.1371/journal.pone.0008298

Shang, Y., Griffith, L. C., and Rosbash, M. (2008). Light-arousal and circadian photoreception circuits intersect at the large PDF cells of the *Drosophila* brain. *Proc. Natl. Acad. Sci. U.S.A.* 105, 19587–19594. doi: 10.1073/pnas.0809577105

Sheeba, V., Gu, H., Sharma, V. K., O'Dowd, D. K., and Holmes, T. C. (2008). Circadian- and light-dependent regulation of resting membrane potential and spontaneous action potential firing of *Drosophila* circadian pacemaker neurons. *J. Neurophysiol.* 99, 976–988. doi: 10.1152/jn.00930.2007

Siegmund, T., and Korge, G. (2001). Innervation of the ring gland of *Drosophila melanogaster*. *J. Comp. Neurol.* 431, 481–491. doi: 10.1002/1096-9861(20010319)431:4<481::aid-cne1084>3.0.co;2-7

Stoleru, D., Nawathean, P., de la Paz Fernández, M., Menet, J. S., Ceriani, M. F., and Rosbash, M. (2007). The *Drosophila* circadian network is a seasonal timer. *Cell* 129, 207–219. doi: 10.1016/j.cell.2007.02.038

Stoleru, D., Peng, Y., Agosto, J., and Rosbash, M. (2004). Coupled oscillators control morning and evening locomotor behaviour of *Drosophila*. *Nature* 431, 862–868. doi: 10.1038/nature02926

Stoleru, D., Peng, Y., Nawathean, P., and Rosbash, M. (2005). A resetting signal between *Drosophila* pacemakers synchronizes morning and evening activity. *Nature* 438, 238–242. doi: 10.1038/nature04192

Yao, Z., and Shafer, O. T. (2014). The *Drosophila* circadian clock is a variably coupled network of multiple peptidergic units. *Science* 343, 1516–1520. doi: 10.1126/science.1251285

Yoshii, T., Rieger, D., and Helfrich-Forster, C. (2012). Two clocks in the brain: an update of the morning and evening oscillator model in *Drosophila*. *Prog. Brain Res.* 199, 59–82. doi: 10.1016/B978-0-444-59427-3.00027-7

Yoshii, T., Wülbeck, C., Sehadova, H., Veleri, S., Bichler, D., Stanewsky, R., et al. (2009). The neuropeptide pigment-dispersing factor adjusts period and phase of *Drosophila*'s clock. *J. Neurosci.* 29, 2597–2610. doi: 10.1523/JNEUROSCI.5439-08.2009

Zerr, D. M., Hall, J. C., Rosbash, M., and Siwicki, K. K. (1990). Circadian fluctuations of period protein immunoreactivity in the CNS and the visual system of *Drosophila*. *J. Neurosci.* 10, 2749–2762. doi: 10.1523/jneurosci.10-08-02749.1990

Zhang, L., Chung, B. Y., Lear, B. C., Kilman, V. L., Liu, Y., Mahesh, G., et al. (2010). DN1p circadian neurons coordinate acute light and PDF inputs to produce robust daily behavior in *Drosophila*. *Curr. Biol.* 20, 591–599. doi: 10.1016/j.cub.2010.02.056

Zhang, Y., Liu, Y., Bilodeau-Wentworth, D., Hardin, P. E., and Emery, P. (2010). Light and temperature control the contribution of specific DN1 neurons to *Drosophila* circadian behavior. *Curr. Biol.* 20, 600–605. doi: 10.1016/j.cub.2010.02.044

**Conflict of Interest:** The authors declare that the research was conducted in the absence of any commercial or financial relationships that could be construed as a potential conflict of interest.

frontiers in Physiology

ORIGINAL RESEARCH
published: 31 March 2020
doi: 10.3389/fphys.2020.00268

# Regulation of Rest, Rather Than Activity, Underlies Day-Night Activity Differences in Mice

*Bharath Ananthasubramaniam*[1]* *and Johanna H. Meijer*[2]

[1] *Institute for Theoretical Biology, Charité – Universitätsmedizin Berlin, Berlin, Germany,* [2] *Leiden University Medical Center, Leiden University, Leiden, Netherlands*

The suprachiasmatic nucleus (SCN), which serves as the central pacemaker in mammals, regulates the 24-h rhythm in behavioral activity. However, it is currently unclear whether and how bouts of activity and rest are regulated within the 24-h cycle (i.e., over ultradian time scales). Therefore, we used passive infrared sensors to measure temporal behavior in mice housed under either a light–dark (LD) cycle or continuous darkness (DD). We found that a probabilistic Markov model captures the ultradian changes in the behavioral state over a 24-h cycle. In this model, the animal's behavioral state in the next time interval is determined solely by the animal's current behavioral state and by the "toss" of a proverbial "biased coin." We found that the bias of this "coin" is regulated by light input and by the phase of the clock. Moreover, the bias of this "coin" for an animal is related to the average length of rest and activity bouts in that animal. In LD conditions, the average length of rest bouts was greater during the day compared to during the night, whereas the average length of activity bouts was greater during the night compared to during the day. Importantly, we also found that day-night changes in the rest bout lengths were significantly greater than day-night changes in the activity bout lengths. Finally, in DD conditions, the activity and rest bouts also differed between subjective night and subjective day, albeit to a lesser extent compared to LD conditions. The ultradian regulation represented by the model does not result in ultradian rhythms, although some weak ultradian rhythms are present in the data. The persistent differences in bout length over the circadian cycle following loss of the external LD cycle indicate that the central pacemaker plays a role in regulating rest and activity bouts on an ultradian time scale.

**Keywords: spontaneous behavior, probabilistic model, light cycles, circadian clock, activity duration**

OPEN ACCESS

***Edited by:***
*Rodolfo Costa,*
*University of Padua, Italy*

***Reviewed by:***
*Charalambos P. Kyriacou,*
*University of Leicester,*
*United Kingdom*
*Marco Brancaccio,*
*Imperial College London,*
*United Kingdom*

***Correspondence:**
*Bharath Ananthasubramaniam*
*bharath.ananth@charite.de*

***Specialty section:***
*This article was submitted to Chronobiology, a section of the journal Frontiers in Physiology*

***Received:*** *08 November 2019*
***Accepted:*** *09 March 2020*
***Published:*** *31 March 2020*

***Citation:***
*Ananthasubramaniam B and Meijer JH (2020) Regulation of Rest, Rather Than Activity, Underlies Day-Night Activity Differences in Mice. Front. Physiol. 11:268. doi: 10.3389/fphys.2020.00268*

## INTRODUCTION

In most organisms, the circadian clock facilitates adaptation to the natural periodic light cycle. This clock regulates a wide range of physiological processes, including behavior (Herzog, 2007). Therefore, behavior has been used to determine the state of the clock *in vivo* since the early days of the field of chronobiology (Pittendrigh, 1960; Pittendrigh and Daan, 1976). In mammals, the

circadian clock is located in the suprachiasmatic nucleus (SCN) at the base of the hypothalamus (Ralph et al., 1990). The neurons in the SCN have near 24-h oscillations in both protein expression and neuronal firing (Nakamura et al., 2002; Quintero et al., 2003; Schaap et al., 2003; Yamaguchi et al., 2003; Hastings et al., 2018).

Recording the frequency of action potential firing in the SCN of freely moving animals has allowed researchers to measure the degree of correspondence between SCN firing and behavioral activity (Houben et al., 2009, 2014). These studies showed that the onset and offset of behavioral activity are regulated probabilistically by differences in firing between high levels of firing activity during the day and low levels during the night (Houben et al., 2009). Moreover, the 24-h rhythmic waveform of SCN firing is correlated with the distribution of behavioral activity within the active phase (Houben et al., 2009, 2014). Does the circadian clock then also regulate temporal behavior within the circadian cycle (i.e., over ultradian time scales)? If so, how is temporal behavior organized and by what law, if any, can the alteration of activity and rest at the ultradian time scale be described?

Suprachiasmatic nucleus lesions resulted in the loss of ultradian rhythms in rats (Wollnik and Turek, 1989), almost no disruption of ultradian rhythms in voles (Gerkema et al., 1990) and low power or unstable ultradian rhythms in mice (Schwartz and Zimmerman, 1991) and hamsters (Rusak, 1977). Furthermore, genetic manipulation of the molecular clocks in the entire mouse (including the SCN) still retained arrhythmic ultradian bouts of behavior (Vitaterna et al., 1994; Horst et al., 1999). Moreover, scale-invariant patterns of behavior are disrupted by SCN lesions at time scales from 4 h to 24 h, but not at time scales below 4 h (Hu et al., 2007). In summary, whether – and to what extent – the SCN regulates temporal behavior over ultradian time scales is largely unknown. In our study, we use "ultradian" to indicate a scale much smaller than 24 h, but do not imply rhythmicity.

As a first step in addressing this question, we examined whether bouts of activity and rest (i.e., prolonged stretches of activity and rest, respectively) are regulated at ultradian time scales in mice. We present a simple probabilistic model of the transitions between behavioral states fit to behavioral data collected under a light–dark (LD) cycle or continuous darkness (DD). Our model shows how bouts of rest and activity are regulated on a scale of seconds to minutes. This time scale is far below the scale that has been explored and detected by detrended fluctuation analysis (Hu et al., 2007). In addition, the model shows that changes in the duration of rest bouts, rather than changes in the duration of activity bouts, determine the differences in activity between day and night.

# MATERIALS AND METHODS

## Ethics Statement

All animal experiments were performed in accordance with Dutch law and were approved by the Animal Ethics Committee at the Leiden University Medical Center (Leiden, Netherlands).

## Animals

Wild-type C57BL6 mice were purchased from Harlan (Harlan, Horst, Netherlands). All mice were between 12 and 24 weeks of age.

## Behavioral Data

Each animal's behavioral activity was recorded using passive IR (PIR) motion detection sensors (Hygrosens Instruments) mounted under the lid of the cage and connected to a ClockLab data collection system (Actimetrics Software), which recorded sensor activity in 10-sec bins.

Mice were housed under either continuous darkness (DD) or an LD cycle with a 22-, 24-, or 26-h period with equal duration of light and dark (also termed T-cycles); for example, a 22-h T-cycle consisted of 11 h of light and 11 h of darkness. Only recordings of mice with at least four circadian cycles in DD or four cycles in an LD cycle were included in our analysis; the lengths of the activity recordings are presented in **Supplementary Figure 1**. Furthermore, all mice housed under an LD cycle were entrained to the external *Zeitgeber*. In this study, a total of 16 mice were housed under DD conditions, and 32 mice were housed under a 22-h ($N$ = 8 mice), 24-h ($N$ = 16 mice), or a 26-h ($N$ = 8 mice) T-cycle.

The data consist of the start time of the 10 s bin, with lights "on" or "off" marked as "L" and "D," respectively (**Figure 1**); in addition, behavioral activity was counted in 10-s intervals. For this study, activity counts were converted to either "A" (active; activity counts $>$ 0) or "R" (rest; activity counts = 0); thus, we studied the duration of activity and rest, not the intensity of activity.

## Description of the Probabilistic Model

The probabilistic model describes the transitions in the animal's behavioral state between "rest" and "activity" (**Figure 1A**). The animal's behavioral state in the next 10-sec bin $S_{n+1}$ is determined solely by the behavioral state in the current 10-sec bin ($S_n$) and the probability of transition; such a property defines a Markov model. The transition probability from rest to activity is defined as α, and the transition probability from activity to rest is defined as β. Probabilities were allowed to change between day and night under LD conditions and between subjective day and subjective night under DD conditions. Under an LD cycle, both the central clock and the external LD cycle contribute to the behavioral state; in contrast, under DD, the effect of the external LD cycle is absent.

For mice in LD, α and β were fit separately for day and night using the following equations:

$$\alpha(X) = P(S_{n+1} = \text{“}A\text{”} | S_n = \text{“}R\text{”}, L_n = \text{“}X\text{”}) = \frac{\#(S_{n+1} = \text{“}A\text{”} | S_n = \text{“}R\text{”}, L_n = \text{“}X\text{”})}{\#(S_n = \text{“}R\text{”}, L_n = \text{“}X\text{”})}, X = \{L, D\}$$

and

$$\beta(X) = P(S_{n+1} = \text{“}R\text{”} | S_n = \text{“}A\text{”}, L_n = \text{“}X\text{”}) = \frac{\#(S_{n+1} = \text{“}R\text{”} | S_n = \text{“}A\text{”}, L_n = \text{“}X\text{”})}{\#(S_n = \text{“}A\text{”}, L_n = \text{“}X\text{”})}, X = \{L, D\}$$

where $L_n$ represents the lighting condition during state $S_n$ and #(.) is the number of occurrences of the condition within the parenthesis. Thus, the data obtained from each animal in LD yields four probabilities, two for the day phase and two for night phase.

For mice housed in DD, cosine curves were fit to the raw behavioral activity counts in order to identify the subjective day and subjective night phases. α and β were computed for the subjective day and subjective night using the equations shown above, producing a similar set of four probabilities.

We define bouts of activity and rest to be one or more adjacent bins of activity and rest, respectively (**Figure 1B**). Bouts of activity and rest (**Figure 1C**) are easier to interpret and identify in the data compared to the probability parameters. The Markov model leads to a geometric distribution of the bout durations, and the mean bout durations are conveniently dependent only upon α and β. The mean activity bouts and rest bouts (expressed in min) are $1/6\beta$ and $1/6\alpha$. In addition, the average activity during a phase of the clock is defined using the following formula: $\alpha/\alpha + \beta$.

## Statistical Analysis

The average activity of the mice was analyzed using the analysis of variance (aov) function in R (version 3.5.1). The duration of bouts estimated using the model were first transformed in order to ensure uniform variance across groups; because each animal contributed multiple estimates, they were then analyzed using linear mixed models with the lmer function in the R package ("lme4" version 1.1-21).

# RESULTS

## Model Fits Are Robust and Consistent With the Assumptions

First, we determined the ability of our model to produce reasonable parameter estimates that are consistent with the model's assumptions.

The estimates of transition probability obtained from the behavioral data were stable over the course of acquisition. The estimates of α and β obtained from the first half of each acquisition were highly correlated with the estimates obtained from the second half (**Supplementary Figure 2A**, α: $r(96) = 0.85$, $p < 0.001$; β: $r(96) = 0.69$, $p < 0.001$). Thus, the data can be considered stationary for the purposes of this model.

The data also support the Markov assumption made in the probabilistic model, which can be paraphrased as the "the future is independent of the past, given the present." Estimates derived from the data regarding dependence (via mutual information) between the next state ($S_{n+1}$) and the previous state ($S_{n-1}$), given the current state ($S_n$), were all close to

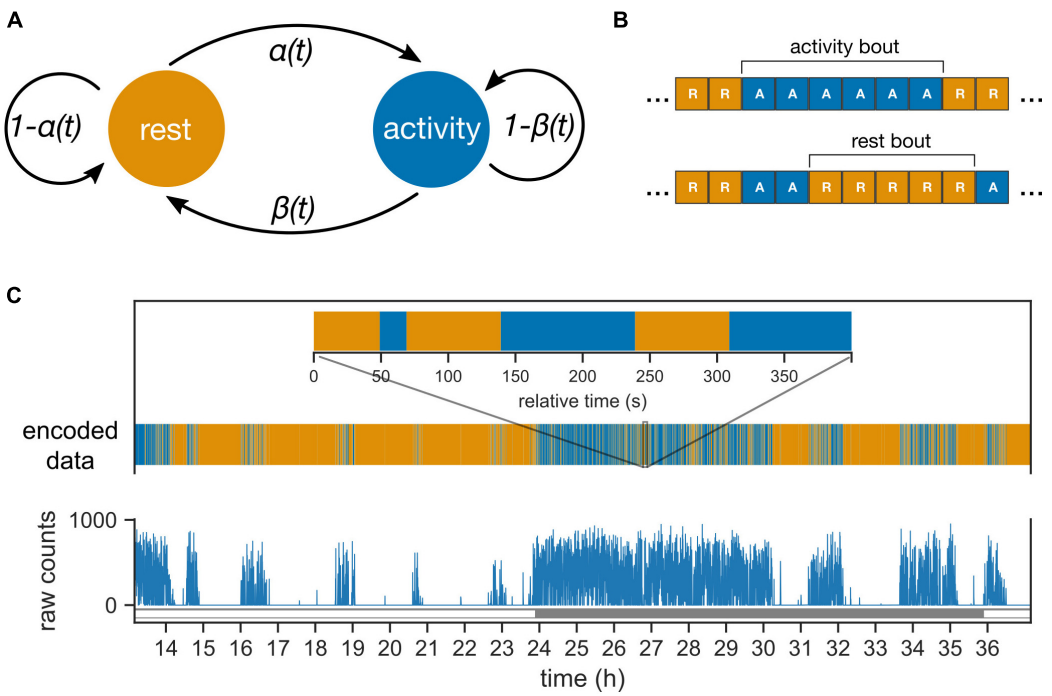


**FIGURE 1 |** Probabilistic model of mouse behavior. **(A)** The transitions between the two behavioral states "rest" and "activity" are controlled by the two probability parameters, α and β. The parameters can vary between day and night (or subjective day and night in constant darkness). **(B)** The behavioral activity data is encoded into sequences of "activity" (behavioral activity > 0) and "rest" (behavioral activity = 0) bins. The encoded sequences are inputs to the model in panel **(A)**. One or more contiguous occurrences of "activity" and "rest" bins are termed activity and rest bouts, respectively. **(C)** The behavioral activity of an animal is recorded as raw counts in 10 s bins (shown here for a mouse under 24 h light–dark cycles). The corresponding encoded sequence is shown with the same color-coding as in panel **(B)** for rest and activity. Inset zooms into a 400 s interval during the night (active phase).

zero (**Supplementary Figure 2B**), indicating near independence. In summary, our model provides a consistent representation of the data and produces robust estimates of the average duration of activity and rest bouts.

## Activity and Rest in Mice Are Not Restricted to Night and Day, Respectively

Next, we examined the distribution of activity during the day and night under 22-, 24-, and 26-h T-cycles (i.e., LD cycles consisting of 11 h light/11 h dark, 12 h light/12 h dark, and 13 h light/13 h dark, respectively).

We defined *average activity* as the average fraction of time an animal was active in an interval; the interval is the length of the day for the average activity during the day. The average activity across day and night (the interval here is the T-cycle period) was similar between the 22-h and the 24-h T-cycles, but was significantly higher in the 26-h T-cycle compared to the 24-h T-cycle (**Supplementary Figure 3**, $F(2, 29) = 4.95$, $p = 0.01$, Tukey *post hoc* test). The mice were more active at night than during the day, consistent with their nocturnal nature (**Figure 2A**). The mice spent about ∼30% of the night and about ∼10% of the day being active. Thus, the mice were active for a minority of the time not only in their rest phase (day), but also in their active phase (night). Moreover, in the rest phase, the mice were not inactive, but rather active for 10% of the time.

The night to day change in average activity was similar among the three T-cycles. Specifically, the average activity during the day was one-third of the levels during the night for all three T-cycles (**Figure 2A**). The fold reduction of 0.38, 0.35, and 0.40 for the 22-, 24-, and 26-h T-cycles had 95% confidence intervals (CI) of [0.31, 0.45], [0.31, 0.40], and [0.33, 0.47], respectively. Despite the higher average activity under the 26-h T-cycle, the night to day change in the 26-h T-cycle was indistinguishable from the night to day change in the other two T-cycles.

## Activity and Rest Bouts Are Inversely Regulated During the Day and Night

Next, we examined whether the average duration of the activity and rest bouts were different between the day (i.e., the resting phase) and the night (i.e., the active phase) for the three different T-cycles.

We observed higher activity during the night than during the day (**Figure 2A**). This could result from three different scenarios: (i) rest bouts are longer during the day than during the night, but activity bouts are unchanged between day and night (ii) activity bouts are longer during the night than during the day, but rest bouts are unchanged between day and night (iii) rest bouts are shortened and activity bouts are lengthened from day to night. In this section, we identify the scenario that is most consistent with the data.

According to our analysis, on average, the rest bouts were longer during the day compared to during the night under all three T-cycles (**Figure 2B**). Average bouts of rest during the day were 2.75-fold longer during the night (CI: [2.44, 3.09]) with no significant differences across the three T-cycles; fold-change for the 22-h and the 26-h T-cycles relative to the 24-h T-cycle had CIs of [0.94, 1.27] and [0.78, 1.05].

On the other hand, the activity bouts on average were shorter during the day compared to during the night under all three T-cycles (**Figure 2C**). Average activity bouts were 0.74-fold shorter during the day compared to during the night with only 26-h T-cycle having a slightly larger decrease in the activity bout length; fold-change for 22-h and 26-h T-cycles relative to 24-h T-cycle had CIs of [0.96, 1.29] and [1.05, 1.41].

Thus, both rest and activity bouts are indeed regulated reciprocally between day and night.

## Day-Night Changes in Rest Bouts Dominate Day-Night Changes in Activity Bouts

This section compares the relative durations of rest and activity bouts during the day and during the night.

We observed that the average rest bout was always longer than the average activity bout (**Figures 2B,C**, $\text{ratio}_{\text{rest/activity}} = 2.53$, CI: [2.25, 2.86]). This agrees with mice having more rest than activity (average activity $< 0.5$) during both day and night (**Figure 2A**). The average rest bout was about twice as long as the average activity bout in the night ($\text{ratio}_{\text{rest/activity}} = 2.28$, CI: [2.08, 2.49], **Figure 2D**). The ratio increased to about eight-fold in the day ($\text{ratio}_{\text{rest/activity}} = 8.06$, CI: [7.37, 8.81]) and was significantly greater under the 24-h T-cycle (ratio = 1.17, CI: [1.05, 1.31]).

It appears therefore that the average rest bout is always longer than the average activity bout and the absolute day-night change in the rest bouts is also greater than the absolute day-night change in the activity bouts (**Figures 2B–D**). We therefore hypothesize that the day-night changes in rest bouts dominate the day-night changes in activity bouts. Quantifying the day-night change in the number of bouts can help test this hypothesis.

Given that "rest" is defined as the lack of activity, bouts of rest and bouts of activity always alternate (**Figures 1B,C**); therefore, the number of rest and activity bouts in any given time interval is equal (or differs by no more than one). As a result, we only report the total number of bouts in an interval. If rest bouts were to dominate the day-night change, then the number of bouts would be expected to be higher during the night than during the day (rest bouts are shorter during the night). If, on the other hand, the activity bouts dominate, then the number of bouts would be expected to be lower during the night than during the day. Since the total number of bouts during the night was higher than during the day (**Supplementary Figure 4A**), we conclude that rest bouts rather than activity bouts dominate the day-night change in activity.

## Mice in DD Are Less Active Than in LD Due to Reduced Activity During the Subjective Night

In LD cycles, both light and the central pacemaker influence behavioral activity, while DD conditions allow us to study behavior without the influence of light. This section compares

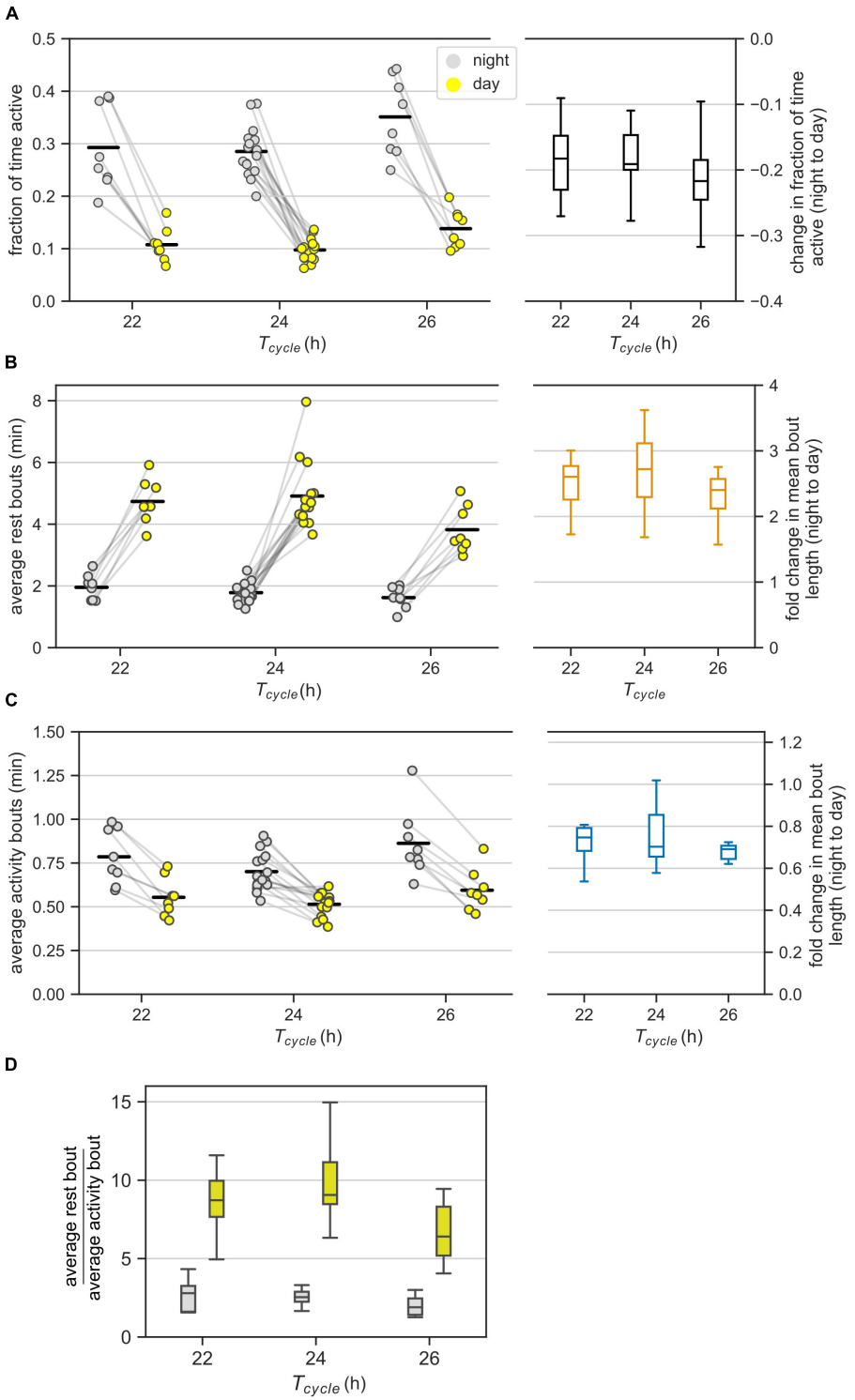


**FIGURE 2 |** Ultradian behavior under LD cycles: **(A)** Average activity of mice in the day and night under different LD cycles. Average activity is the fraction of bins with activity during an interval of day or night. Each animal contributed two points (one each for the day and the night) that are connected. The changes in the average activity from night to day for different T-cycles are shown in the boxplot. **(B,C)** The average bout lengths for rest **(B)** and activity **(C)** estimated by the model in the day and the night under different T-cycles. The pair of points (one each for day and night) contributed by each animal is connected. The fold-change in mean bout length from night to day is provided as boxplots on the right. **(D)** The relative lengths of mean rest and mean activity bouts in the night and day for different T-cycles. The same data in panels **(B)** and **(C)** are visualized differently in panel **(D)**. Color-coding is maintained throughout the figure. Horizontal black bars in the scatter plots represent mean of the values in that column.

ultradian behavior in DD with LD in order to distinguish between the effect of the circadian system and light.

In DD, mice had lower average activity overall, particularly during the subjective night. Mice in DD were about 20% less active than mice in LD (**Supplementary Figure 3**, $F(1, 46) = 11.68$, $p = 0.0013$, $\text{ratio}_{DD/LD} = 0.79$); we pooled data from all three T-cycles in **Figure 2** into the LD group. In DD, mice were active for about 20% of the time during the subjective night and about 12% of the time during the subjective day. Thus, a difference in activity between night and day also existed in DD (**Figure 3A**, $\text{ratio}_{light/dark} = 0.61$, CI: [0.54, 0.69])), but was considerably smaller than in LD ($\text{ratio}_{DD/LD} = 0.59$, CI: [0.51, 0.68]). Interestingly, this difference resulted only from reduced activity during the subjective night in DD ($\text{ratio}_{DD/LD}$ during the subjective day = 1.13, CI: [0.97, 1.31]; $\text{ratio}_{DD/LD}$ during the subjective night = 0.66, CI: [0.57, 0.77]).

## Day-Night Changes in Bout Lengths Persisted in DD, but Were Moderated

This section continues the comparison between DD and LD cycles with a focus on the model-based estimates of mean bout lengths.

Mean rest bout and mean activity bout lengths changed inversely between subjective day and subjective night also in DD (**Figures 3B,C**). The mean length of the rest bouts increased 1.5-fold from the subjective night to the subjective day (**Figure 3B** and **Table 1**), whereas the mean length of the activity bouts decreased by 20% from the subjective night to the subjective day (**Figure 3C** and **Table 1**).

This day-night change in the mean length of the rest bouts in DD was smaller in comparison to the corresponding change in LD (**Figure 3B**, $\text{ratio}_{DD/LD} = 0.59$, CI: [0.50, 0.69]). However, the day-night change in the mean length of the activity bouts was statistically indistinguishable between LD and DD conditions (**Figure 3C**, $\text{ratio}_{DD/LD} = 1.16$, CI: [0.99, 1.36]). Thus, day-night changes in the rest bout lengths, but not in the activity bout lengths, were moderated in DD.

The mean rest bouts were longer than the mean activity bouts during both the subjective day and the subjective night in DD (**Figure 3D**). The day-night changes in the rest bout lengths and the activity bout lengths result in different ratios of mean rest bout and mean activity bout lengths between subjective day and subjective night. The ratio of rest bout lengths to activity bout lengths during the night was significantly greater under DD than under a LD cycle (**Figure 3D** and **Table 1**). However, the ratio of rest bout lengths to activity bout lengths during the day was similar in DD and LD (**Table 1**). As a result, the ratio of rest bout lengths to activity bout lengths varied less in DD than in LD.

Day-night changes in the rest bouts rather than in the activity bouts predominantly contributed to the day-night changes in activity. The number of total bouts was higher during the subjective night compared to the subjective day, which coincides with the shorter rest bouts during the subjective night (**Figure 3B**). However, the day-night difference in the total number of bouts was smaller in DD than in LD (**Supplementary Figure 4B**).

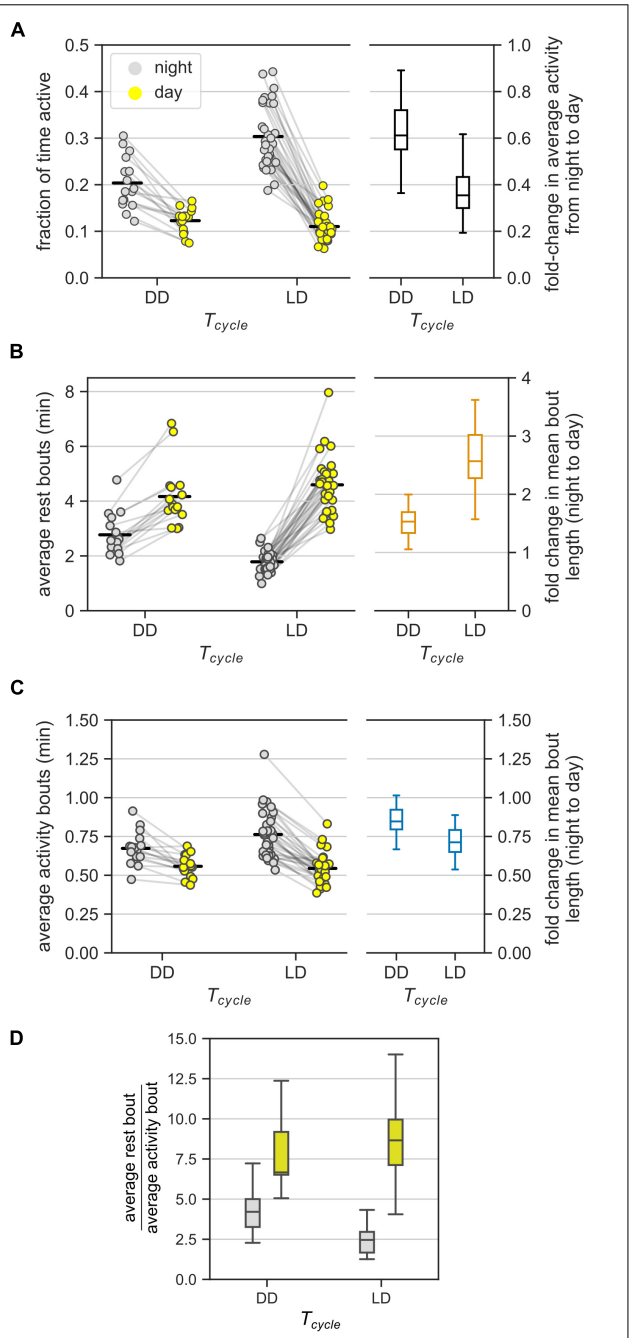


**FIGURE 3 |** Ultradian behavior under constant darkness (DD). **(A)** Average activity of mice (measured as the fraction of active bins) during the day and during the night under DD and LD cycles. In DD, day and night refer to *subjective* day and *subjective* night, respectively. The LD group consists of data from the three T-cycles. Each animal contributed two points, one each to the day and the night groups – pairing is denoted by gray lines. Fold-change in the average activity between night and day is presented as a boxplot. **(B,C)** The model-based estimates of the mean rest **(B)** and mean activity **(C)** bout lengths in the (subjective) night and (subjective) day in DD and LD. Data points from the same mice are connected by gray lines. The bout length averaged over all individuals is marked with black bars. Boxplots show the fold-change in bout lengths from night to day. **(D)** The relative lengths of the mean rest and mean activity bouts in the (subjective) day and (subjective) night in DD and LD [a different representation of data in panels **(B)** and **(C)**].

**TABLE 1 |** Mean and 95% confidence intervals (CI) for the average bout lengths under DD and LD cycles.

| | DD | | | LD | | |
|---|---|---|---|---|---|---|
| | **Subjective night** | **Subjective day** | $\frac{\text{subj.day}}{\text{subj.night}}$ | **Night** | **Day** | $\frac{\textit{day}}{\textit{night}}$ |
| Activity bout | 0.67 min [0.60, 0.73] | 0.55 min [0.50, 0.61] | 0.83 [0.73, 0.95] | 0.75 min [0.70, 0.80] | 0.54 min [0.50, 0.57] | 0.71 [0.65, 0.79] |
| Rest bout | 2.68 min [2.44, 2.95] | 4.05 min [3.68, 4.45] | 1.51 [1.32, 1.72] | 1.75 min [1.64, 1.87] | 4.50 min [4.21, 4.81] | 2.57 [2.35, 2.82] |
| $\frac{\text{rest}}{\text{activity}}$ | 4.03 [3.54, 4.60] | 7.32 [6.43, 8.33] | 1.81 [1.51, 2.18] | 2.34 [2.13, 2.56] | 8.39 [7.65, 9.19] | 3.59 [3.15, 4.08] |

*The relative values of the bouts lengths are included as ratios (including their respective CIs).*

## Model Underestimates the Number of Very Short and Very Long Rest Bouts

The probabilistic model fitting ensures that the mean bout lengths in the behavioral data and the model are identical (fitting probability parameters is tantamount to fitting the means). In this section, the observed distribution of the rest and activity bout lengths is contrasted against the distribution predicted by the model.

The model-derived rest bout length distribution deviates from the observed distribution. Under the probabilistic model (**Figure 1A**), bout lengths follow a geometric distribution with a mean given by the model parameters. The model predicts fewer extremely short and extremely long rest bouts than those observed in the data (**Figure 4**). Nevertheless, the activity bout distribution in the data closely matched the predicted distribution. This predicted rest bout distribution consistently differed from the data across the three T-cycles and constant darkness.

## Ultradian Rhythms in Behavior Are Absent Under This Model

The utility of a model is its ability to make predictions. We found ultradian regulation in bout lengths. Can the ultradian regulation (represented by the model) also result in ultradian *rhythms*? In the probabilistic model, (i) rest and activity bouts alternate, (ii) the duration of rest and activity bouts are independent of the preceding bout (Markov property) in both light and dark, and (iii) bouts have random durations. If there is a rhythmic pattern of bouts, then the repeating sequence of bouts must be of approximately constant length (the period). Here, the duration of a sequence of bouts is also random (as each bout has a random length) and has a variance that grows with the length of the sequence. Thus, ultradian rhythms cannot occur under this simple model.

To confirm this expectation, we first simulated behavioral data using our fitted models and produced an artificial dataset with the same composition of animals at each T-cycle and the same length of behavioral recording. We then applied the $\chi^2$-periodogram (Sokolove and Bushell, 1978) to this artificial data to check for ultradian rhythms in the range 1 min-2 h. As expected, we did not observe any rhythms in this time scale at the 0.05 level (**Figure 5A**).

We applied the same analysis next to the original encoded behavioral data (**Figure 5B**). Although none of the animals showed any ultradian rhythms on the order of the average bout length (time scale of minutes), many animals showed noisy weak ultradian rhythms in the range 1.5–3 h. However, the mice showed circadian rhythmicities, with a few mice also showing weak harmonic frequencies (**Supplementary Figure 5**). The model prediction was thus partially confirmed.

# DISCUSSION

The central pacemaker in mammals contributes to daily rhythmic patterns of behavioral activity. This paper set out to test whether behavioral activity is also regulated within the 24 h circadian cycle. Using data on spontaneous behavioral activity of mice under LD and DD, we quantified activity in terms of rest and activity bouts in the day and in the night using a probabilistic model. We observed day-night differences in the average bouts lengths of rest and activity under LD that persisted also under DD. The probabilistic model was able to exploit the structure in the behavioral activity to accurately capture the distribution of bouts (with the exception of extremely short and extremely long rest bouts). The model is evidence that (a) behavioral activity is indeed regulated at the level of bouts and (b) these bouts are under the control of both light input and the circadian system.

The main analytical contribution of this work is the probabilistic model of mouse behavior. A probabilistic, as opposed to a deterministic, model is necessary, since there is clearly large intra-individual (across the length of the recordings) and inter-individual variability even in isogenic mice kept under identical conditions. A simpler model would have a single probability parameter defining the switch between rest and activity and vice-versa (i.e., $\alpha = \beta$). But, the stark difference in activity between the day and night makes this simpler model inadequate. The model we propose is thus the simplest (non-trivial) model of mouse behavior in the ultradian timescale. Such Markov models are well established in many fields including genomics (Pardoux, 2010) and sleep research (Kemp and Kamphuisen, 1986; Stephenson et al., 2013).

The model has several benefits over traditional spectral analysis methods, such as MESA, Lomb-Scargle and Enright periodograms, to study behavior at different time scales. Spectral analysis only identifies statistically significant patterns in the behavioral data. However, the model is a mechanistic description, albeit abstracted and simplified, of the biological mechanism driving spontaneous behavior. In that sense, the model is generative, i.e., the model can simulate the behavioral activity

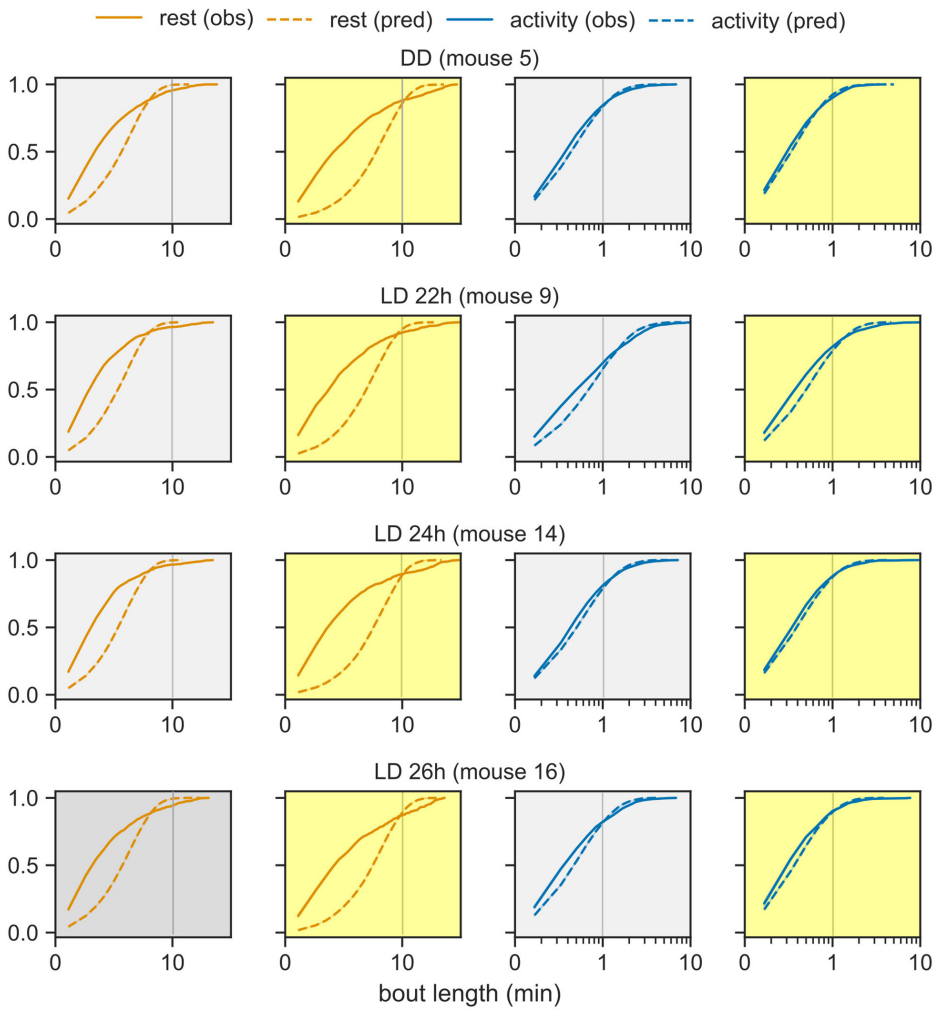


**FIGURE 4 |** Distribution of bout lengths of activity and rest. The observed distribution of bout lengths (solid lines) is compared against the distribution predicted by the model (dashed lines). The rest and activity bouts in the day and in the night are plotted in separate panels for one representative animal from each group: LD cycles of 22-, 24-, and 26- h and DD. The x-axis is plotted in logarithmic scale in order to see the very short and very long bouts in one graph. The color-coding from earlier figures is maintained.

of a mouse. We used simulation to predict the lack of ultradian rhythms under our probabilistic model. Enright periodogram analysis of behavior did not find ultradian rhythms at the time scale of the bouts. But, noisy weak ultradian rhythms in 1.5–3 h time scale were identified in many mice. This is likely the consequence of unaccounted features in the model, such as very short and very long rest bouts.

Conveniently, the model directly relates to behavior of mice at the level of bouts. Early studies qualitatively described the organization of behavior in small mammals into characteristic bouts (Kavanau and Rischer, 1968; Davis and Menaker, 1980). Penev et al. (1997) studied temporal patterns of behavior in hamsters and showed increased fragmentation with age. Farajnia et al. (2012) showed similar fragmentation in aged mice. Ultradian periodicity of behavior in mammals also manifests as rhythmic consolidated bouts of activity. Ultradian rhythms are observed under natural conditions in the common vole (Gerkema and van der Leest, 1991) and mice (del Pozo et al., 1978; Poon et al., 1997; Dowse et al., 2010), and after surgical or genetic manipulation of the clock in rats and mice (Vitaterna et al., 1994; Horst et al., 1999; Blum et al., 2014).

Mice were inactive for a majority of the day and the night, but with significant activity even during the day. Nevertheless, the mice showed more activity in the night versus the day. Spontaneous behavior (measured using passive IR sensors) is not as clearly segregated into an active phase and a rest phase as is wheel-running activity (Schwartz and Zimmerman, 1990). The mean rest bouts were shortened and the mean activity bouts lengthened in the night relative to the day in the 22-, 24-, and 26-h T-cycles. The different T-cycles affect clock function under the entrained conditions studied here. Since the day-night differences in bout lengths were unaltered across T-cycles, we conclude that light regulates the length of rest and activity bouts independent of the central clock. To fully support the latter conclusion, we may

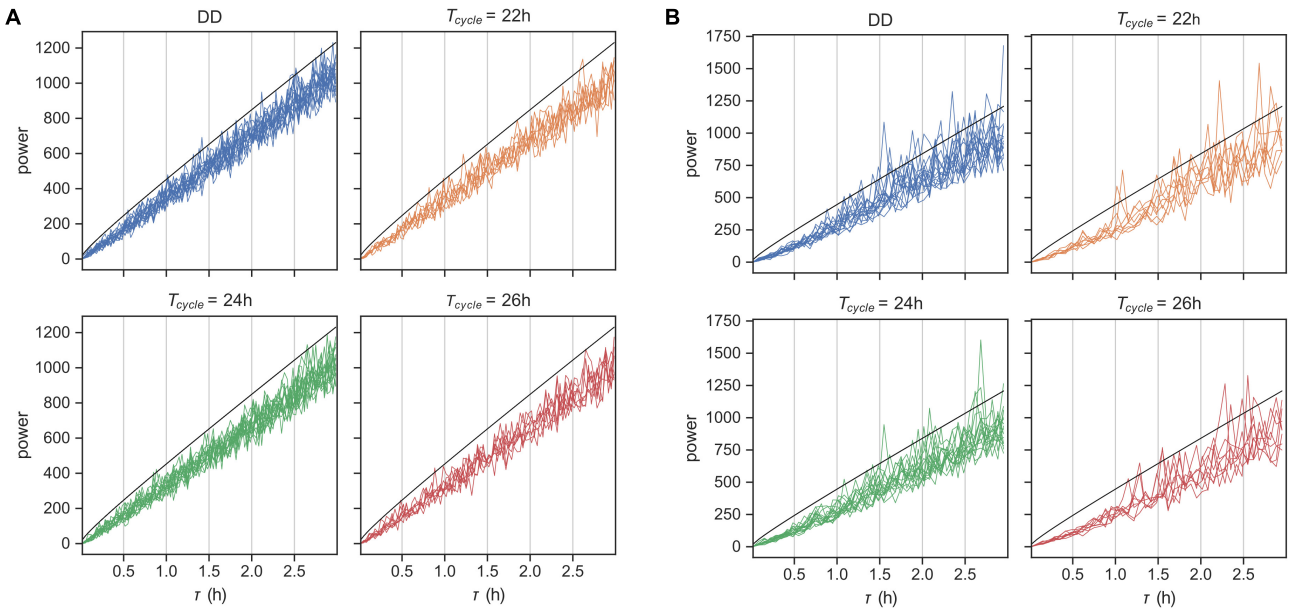


**FIGURE 5 |** Rhythms in behavior at ultradian time scales. $\chi^2$-periodogram analysis of behavioral data simulated using the probabilistic model in **Figure 1** in panel **(A)** and for the original encoded data in panel **(B)**. Simulated data matched the original data in number of replicates and length of data record. The periodograms are grouped according to the *Zeitgeber* input. The black line is the significance threshold for rhythmicity at the tested period with Bonferroni-adjusted $p$-value $< 0.05$.

study ultradian behavioral regulation in animals under short and long photoperiod, as an additional modifier of clock function.

We observed that, on average, rest bouts were always longer than activity bouts. Moreover, the day-night changes in mean rest bout lengths were about two-fold larger than the changes in mean activity bout lengths in LD. Taken together, the day-night changes in rest bouts (in minutes) is significantly larger than day-night changes in activity bouts. Therefore, we conclude that regulation of rest bouts predominantly underlies the differences between the active and rest phases. If this were true, we would expect higher number of bouts (rest and activity) in the night compared to the day. This is indeed the case. Thus, the LD environment regulates rest bouts rather than activity bouts over the 24 h cycle.

Under a LD cycle, both light and the central clock affect behavioral activity. To determine the effects of the central clock on behavior, animals are routinely exposed to constant darkness in the absence of all potential time cues. In DD, mice continued to show the same qualitative changes in mean bout lengths between subjective day and subjective night. The persistence of bout regulation in DD between subjective day and night suggests that the central clock also regulates bout length.

The day-night difference in activity and rest bout duration was larger in LD cycles than in DD. Given the enhanced difference between the day and night under LD cycles, we conclude that environmental light cycles reinforce the SCN effect on bout regulation. In other words, exposure to LD cycles increases the "amplitude" of circadian regulation of bouts. Interestingly, the amplitude of the circadian rhythm is also increased under LD as compared to DD conditions. This is the case both at the level of behavioral activity and also at the level of SCN electrical discharge rate (Coomans et al., 2013). It is possible therefore, that even the influence of light on ultradian behavior involves the SCN. At least, and given our results obtained from DD conditions, we suggest that the SCN is a node in the central regulation of ultradian behavioral activity, and is a regulator of the duration of ultradian bouts. Thus, in the absence of the SCN, ultradian bouts will still be present, but the day-night difference in their duration will be completely lost. This interpretation is in line with the ongoing presence of ultradian behavioral rhythmicity in transgenic clockless animals (Vitaterna et al., 1994; Horst et al., 1999; Blum et al., 2014), as well as in voles with SCN lesions (Gerkema et al., 1990).

Surprising, the Markov model predicted well the behavior at the next 10 s bin based on the current bin and a coin toss. We also confirmed explicitly the validity of the Markov assumption for our behavioral data. The rest and activity states in the Markov model have positive (auto-enforcing) feedback loops (**Figure 1**). When the strength of this positive feedback is large ($>0.5$, which is the case for all fits in this study), then the Markov model shows inertia, i.e., a tendency to remain at the state it is in. Occasionally, behavior breaks out of this state and switches to the alternative state. We found that this principle applies well to the ultradian regulation of rest and activity. The parameters describing the duration in a state are apparently under the control of environmental light and the central clock. The model is analogous to the proposed "flip-flop" switch between sleep and wakefulness, where various neuronal inputs regulate the balance between the two states (Saper et al., 2001). It is very likely that other brain areas are also involved in the underlying circuitry, and for instance, there is good evidence for the role of dopamine (Blum et al., 2014).

The Markov property is manifested as a geometric distribution of bout lengths, where short bouts are more common than long bouts. While the model predicted the distribution of activity bouts accurately, it underestimated both the number of very short and very long rest bouts. Nevertheless, our model is elegant in its simplicity in that it captures most features of murine behavior with some exceptions. In fact, there are multiple reports showing that especially rest bouts do not follow an exponential distribution. The first quantitative analysis of bouts (Penev et al., 1997) already proposed that rest bouts were of two types: short bouts within an activity bout or long bouts between activity bouts. More generally, rest bout lengths appear to follow a power-law (heavy-tailed) distribution in mice, humans and fruit flies (Nakamura et al., 2008; Cascallares et al., 2018) that breakdown under certain pathologies. The rest bout distribution in this study did not show power-law characteristics (not shown). The deviation of the rest bout distribution might be due to the presence of different types of rest bouts, such as a "pause" in activity explaining the very short bouts, and the existence of other processes regulating rest bouts, such as homeostatic sleep drive.

Our conclusions must be viewed in the context of our analysis methodology. The model treats behavior within the dark and light phases as homogeneous, which is not often the case (Houben et al., 2014). The simplified data capture the duration of activity, but ignore the intensity of activity. Thus, there could be differences in intensity of activity across LD cycles or between DD and LD, which our analysis overlooked. All these limitations provide interesting avenues for further study. Finally, the behavioral activity was collected in 10 s bins and although bout lengths were of the order of minutes, the effect of bin size on the results cannot be excluded.

## DATA AVAILABILITY STATEMENT

Requests to access the datasets from this study should be directed to JM, j.h.meijer@lumc.nl.

## ETHICS STATEMENT

The animal study was reviewed and approved by the Animal Ethics Committee at the Leiden University Medical Center (Leiden, Netherlands).

## AUTHOR CONTRIBUTIONS

BA conceived and designed the study, performed the analysis, and wrote the manuscript. JM acquired the data and critically revised the manuscript. Both authors interpreted the data, contributed to the manuscript revision, and read and approved the submitted version.

## FUNDING

BA acknowledges support from the BMBF grant 01GQ1503 and Deutsche Forschungsgemeinschaft (DFG) grant HE2168/11-1 (SPP 2041). JM acknowledges support from the Swiss VELUX Foundation (project 1131), Dutch Research Council (NWO) grant ALW.OP.389, and European Research Council grant 854513 ERC-2018-ADG. We acknowledge support from the German Research Foundation (DFG) and the Open Access Publication Fund of Charité – Universitätsmedizin Berlin.

## ACKNOWLEDGMENTS

The authors thank Hanspeter Herzel and Achim Kramer for useful discussions and Jos H. T. Rohling for compiling data from prior studies.

## SUPPLEMENTARY MATERIAL

The Supplementary Material for this article can be found online at: https://www.frontiersin.org/articles/10.3389/fphys.2020.00268/full#supplementary-material

## REFERENCES

Blum, I. D., Zhu, L., Moquin, L., Kokoeva, M. V., Gratton, A., Giros, B., et al. (2014). A highly tunable dopaminergic oscillator generates ultradian rhythms of behavioral arousal. *eLife* 3:e05105. doi: 10.7554/eLife.05105

Cascallares, G., Riva, S., Franco, D. L., Risau-Gusman, S., and Gleiser, P. M. (2018). Role of the circadian clock in the statistics of locomotor activity in *Drosophila*. *PLoS One* 13:e0202505. doi: 10.1371/journal.pone.0202505

Coomans, C. P., van den Berg, S. A. A., Houben, T., van Klinken, J.-B., van den Berg, R., Pronk, A. C. M., et al. (2013). Detrimental effects of constant light exposure and high-fat diet on circadian energy metabolism and insulin sensitivity. *FASEB J.* 27, 1721–1732. doi: 10.1096/fj.12-210898

Davis, F. C., and Menaker, M. (1980). Hamsters through time's window: temporal structure of hamster locomotor rhythmicity. *Am. J. Physiol. Regul. Integr. Comp. Physiol.* 239, R149–R155. doi: 10.1152/ajpregu.1980.239.1.R149

del Pozo, F., DeFeudis, F. V., and Jimenez, J. M. (1978). Motilities of isolated and aggregated mice; A difference in ultradian rhythmicity. *Experientia* 34, 1302–1304. doi: 10.1007/BF01981433

Dowse, H., Umemori, J., and Koide, T. (2010). Ultradian components in the locomotor activity rhythms of the genetically normal mouse, *Mus musculus*. *J. Exp. Biol.* 213, 1788–1795. doi: 10.1242/jeb.038877

Farajnia, S., Michel, S., Deboer, T., vanderLeest, H. T., Houben, T., Rohling, J. H. T., et al. (2012). Evidence for neuronal desynchrony in the aged suprachiasmatic nucleus clock. *J. Neurosci.* 32, 5891–5899. doi: 10.1523/JNEUROSCI.0469-12.2012

Gerkema, M. P., Groos, G. A., and Daan, S. (1990). Differential elimination of circadian and ultradian rhythmicity by hypothalamic lesions in the common vole, *Microtus arvalis*. *J. Biol. Rhythms* 5, 81–95. doi: 10.1177/074873049000500201

Gerkema, M. P., and van der Leest, F. (1991). Ongoing ultradian activity rhythms in the common vole. *Microtus arvalis*, during deprivations of food, water and rest. *J. Comp. Physiol. A* 168, 591–597. doi: 10.1007/BF00215081

Hastings, M. H., Maywood, E. S., and Brancaccio, M. (2018). Generation of circadian rhythms in the suprachiasmatic nucleus. *Nat. Rev. Neurosci.* 19, 453–469. doi: 10.1038/s41583-018-0026-z

Herzog, E. D. (2007). Neurons and networks in daily rhythms. *Nat. Rev. Neurosci.* 8, 790–802. doi: 10.1038/nrn2215

Houben, T., Coomans, C. P., and Meijer, J. H. (2014). Regulation of circadian and acute activity levels by the murine suprachiasmatic nuclei. *PLoS One* 9:e110172. doi: 10.1371/journal.pone.0110172

Houben, T., Deboer, T., van Oosterhout, F., and Meijer, J. H. (2009). Correlation with behavioral activity and rest implies circadian regulation by SCN neuronal activity levels. *J. Biol. Rhythms* 24, 477–487. doi: 10.1177/0748730409349895

Hu, K., Scheer, F. A., Ivanov, P. Ch, Buijs, R. M., and Shea, S. A. (2007). The suprachiasmatic nucleus functions beyond circadian rhythm generation. *Neuroscience* 149, 508–517. doi: 10.1016/j.neuroscience.2007.03.058

Kavanau, J. L., and Rischer, C. E. (1968). Program clocks in smail mammals. *Science* 161, 1256–1259. doi: 10.1126/science.161.3847.1256

Kemp, B., and Kamphuisen, H. A. (1986). Simulation of human hypnograms using a Markov chain model. *Sleep* 9, 405–414. doi: 10.1093/sleep/9.3.405

Nakamura, T., Takumi, T., Takano, A., Aoyagi, N., Yoshiuchi, K., Struzik, Z. R., et al. (2008). Of mice and men – universality and breakdown of behavioral organization. *PLoS One* 3:e2050. doi: 10.1371/journal.pone.0002050

Nakamura, W., Honma, S., Shirakawa, T., and Honma, K. (2002). Clock mutation lengthens the circadian period without damping rhythms in individual SCN neurons. *Nat. Neurosci.* 5, 399–400. doi: 10.1038/nn843

Pardoux, E. (2010). *Markov Processes and Applications: Algorithms, Networks, Genome and Finance*. Hoboken, NJ: Wiley.

Penev, P. D., Zee, P. C., and Turek, F. W. (1997). Quantitative analysis of the age-related fragmentation of hamster 24-h activity rhythms. *Am. J. Physiol. Regul. Integr. Comp. Physiol.* 273, R2132–R2137. doi: 10.1152/ajpregu.1997.273.6.R2132

Pittendrigh, C. S. (1960). Circadian rhythms and the circadian organization of living systems. *Cold. Spring Harb. Symp. Quant. Biol.* 25, 159–184. doi: 10.1101/SQB.1960.025.01.015

Pittendrigh, C. S., and Daan, S. (1976). A functional analysis of circadian pacemakers in nocturnal rodents. *J. Comp. Physiol.* 106, 291–331. doi: 10.1007/BF01417859

Poon, A. M. S., Wu, B. M., Poon, P. W. F., Cheung, E. P. W., Chan, F. H. Y., and Lam, F. K. (1997). Effect of cage size on ultradian locomotor rhythms of laboratory mice. *Physiol. Behav.* 62, 1253–1258. doi: 10.1016/s0031-9384(97)00305-3

Quintero, J. E., Kuhlman, S. J., and McMahon, D. G. (2003). The biological clock nucleus: a multiphasic oscillator network regulated by light. *J. Neurosci.* 23, 8070–8076. doi: 10.1523/JNEUROSCI.23-22-08070.2003

Ralph, M., Foster, R., Davis, F., and Menaker, M. (1990). Transplanted suprachiasmatic nucleus determines circadian period. *Science* 247, 975–978. doi: 10.1126/science.2305266

Rusak, B. (1977). The role of the suprachiasmatic nuclei in the generation of circadian rhythms in the golden hamster, *Mesocricetus auratus*. *J. Comp. Physiol.* 118, 145–164. doi: 10.1007/BF00611819

Saper, C. B., Chou, T. C., and Scammell, T. E. (2001). The sleep switch: hypothalamic control of sleep and wakefulness. *Trends Neurosci.* 24, 726–731. doi: 10.1016/s0166-2236(00)02002-6

Schaap, J., Albus, H., vanderLeest, H. T., Eilers, P. H. C., Detari, L., and Meijer, J. H. (2003). Heterogeneity of rhythmic suprachiasmatic nucleus neurons: implications for circadian waveform and photoperiodic encoding. *Proc. Natl. Acad. Sci. U.S.A.* 100, 15994–15999. doi: 10.1073/pnas.2436298100

Schwartz, W., and Zimmerman, P. (1990). Circadian timekeeping in BALB/c and C57BL/6 inbred mouse strains. *J. Neurosci.* 10, 3685–3694. doi: 10.1523/JNEUROSCI.10-11-03685.1990

Schwartz, W. J., and Zimmerman, P. (1991). Lesions of the suprachiasmatic nucleus disrupt circadian locomotor rhythms in the mouse. *Physiol. Behav.* 49, 1283–1287. doi: 10.1016/0031-9384(91)90364-T

Sokolove, P. G., and Bushell, W. N. (1978). The chi square periodogram: its utility for analysis of circadian rhythms. *J. Theor. Biol.* 72, 131–160. doi: 10.1016/0022-5193(78)90022-X

Stephenson, R., Famina, S., Caron, A. M., and Lim, J. (2013). Statistical properties of sleep-wake behavior in the rat and their relation to circadian and ultradian phases. *Sleep* 36, 1377–1390. doi: 10.5665/sleep.2970

Horst, G. T. J. van der, Muijtjens, M., Kobayashi, K., Takano, R., Kanno, S., Takao, M., et al. (1999). Mammalian Cry1 and Cry2 are essential for maintenance of circadian rhythms. *Nature* 398, 627–630. doi: 10.1038/19323

Vitaterna, M., King, D., Chang, A., Kornhauser, J., Lowrey, P., McDonald, J., et al. (1994). Mutagenesis and mapping of a mouse gene, clock, essential for circadian behavior. *Science* 264, 719–725. doi: 10.1126/science.8171325

Wollnik, F., and Turek, F. W. (1989). SCN lesions abolish ultradian and circadian components of activity rhythms in LEW/Ztm rats. *Am. J. Physiol. Regul. Integr. Comp. Physiol.* 256, R1027–R1039. doi: 10.1152/ajpregu.1989.256.5.R1027

Yamaguchi, S., Isejima, H., Matsuo, T., Okura, R., Yagita, K., Kobayashi, M., et al. (2003). Synchronization of cellular clocks in the suprachiasmatic nucleus. *Science* 302, 1408–1412. doi: 10.1126/science.1089287

**Conflict of Interest:** The authors declare that the research was conducted in the absence of any commercial or financial relationships that could be construed as a potential conflict of interest.

frontiers in Physiology

ORIGINAL RESEARCH
published: 02 April 2020
doi: 10.3389/fphys.2020.00272

# Clocks in the Wild: Entrainment to Natural Light

*Christoph Schmal*[1]*, *Hanspeter Herzel*[2] and *Jihwan Myung*[3,4,5,6]*

[1] Department of Biology, Faculty of Life Sciences, Institute for Theoretical Biology, Humboldt Universität zu Berlin, Berlin, Germany, [2] Department Basic Sciences, Institute for Theoretical Biology, Charité – Universitätsmedizin Berlin, Berlin, Germany, [3] Graduate Institute of Mind, Brain, and Consciousness, Taipei Medical University, Taipei, Taiwan, [4] Brain and Consciousness Research Centre, Taipei Medical University-Shuang Ho Hospital, Ministry of Health and Welfare, New Taipei City, Taiwan, [5] Graduate Institute of Medical Sciences, Taipei Medical University, Taipei, Taiwan, [6] Computational Neuroscience Unit, Okinawa Institute of Science and Technology Graduate University, Okinawa, Japan

Entrainment denotes a process of coordinating the internal circadian clock to external rhythmic time-cues (Zeitgeber), mainly light. It is facilitated by stronger Zeitgeber signals and smaller period differences between the internal clock and the external Zeitgeber. The phase of entrainment $\psi$ is a result of this process on the side of the circadian clock. On Earth, the period of the day-night cycle is fixed to 24 h, while the periods of circadian clocks distribute widely due to natural variation within and between species. The strength and duration of light depend locally on season and geographic latitude. Therefore, entrainment characteristics of a circadian clock vary under a local light environment and distribute along geoecological settings. Using conceptual models of circadian clocks, we investigate how local conditions of natural light shape global patterning of entrainment through seasons. This clock-side entrainment paradigm enables us to predict systematic changes in the global distribution of chronotypes.

**Keywords: circadian clock, entrainment, photoperiodism, seasonality, chronotype, Arnold onion**

OPEN ACCESS

***Edited by:***
*Rodolfo Costa,*
*University of Padova, Italy*

***Reviewed by:***
*Andrew J. K. Phillips,*
*Monash University, Australia*
*Henrik Oster,*
*University of Lübeck, Germany*

***Correspondence:**
*Christoph Schmal*
*christoph.schmal@hu-berlin.de*
*Jihwan Myung*
*jihwan@tmu.edu.tw*

***Specialty section:***
*This article was submitted to Chronobiology, a section of the journal Frontiers in Physiology*

***Received:*** *21 December 2019*
***Accepted:*** *09 March 2020*
***Published:*** *02 April 2020*

***Citation:***
*Schmal C, Herzel H and Myung J (2020) Clocks in the Wild: Entrainment to Natural Light. Front. Physiol. 11:272. doi: 10.3389/fphys.2020.00272*

## 1. INTRODUCTION

Many organisms on Earth are subject to a precise 24 h light-dark rhythm. To predict the cycle, most organisms including humans maintain their own timekeeping system, the circadian clock running at a close-to-24 h period without external time cues. An organism's internal clock synchronizes to the daily cycles of the external environment through light as a time-giving cue, called Zeitgeber. The proper coordination of intrinsic rhythms with environmental cycles upon entrainment contributes to a better evolutionary fitness and health (Ouyang et al., 1998; Dodd et al., 2005; Chen et al., 2010). Elucidating entrainment under realistic conditions of intrinsic (clock properties) and extrinsic (light) factors can provide chronobiological insights into geoecological dynamics. Natural light conditions on Earth vary by latitude and seasons. Given the individual variability of circadian periods, either due to natural variation within the same species or due to differences between species, it is likely that entrainment produces a global patterning of circadian phases that are rich in diversity. We address this question by combining mathematical core clock models with geophysical data on seasonal and latitudinal light intensities.

### 1.1. Mathematical Clock Models

At the organismal level, circadian clocks exhibit properties of endogenous limit cycle oscillators, i.e., their rhythms have a well-defined period as well as amplitude under constant conditions and are robust against perturbations. In the mammalian core clock, tissue-level coupling leads to a precise pacemaker (Herzog et al., 2004), even though cellular rhythms of its constituent single

neurons are relatively imprecise and partially arrhythmic (Hirata et al., 2019). Perturbations of these organismic rhythms, by light pulses, pharmacological treatments or jet-lag usually decay at relatively fast time scales of a few days (Spoelstra et al., 2004; Kiessling et al., 2010; Ono et al., 2017). Under particular circumstances, external perturbations under constant conditions can even stop the clock (singularity behavior) (Winfree, 1970; Engelmann et al., 1978).

Conceptual models make predictions on the dynamical behavior of circadian clocks based on heuristic principles (e.g., the notion of limit cycle behavior) without considering the detailed molecular machinery that leads to circadian rhythm generation at the cellular level. Such conceptual modeling has a long tradition in chronobiology and helped to understand the response of clock dynamics to external perturbations (Engelmann et al., 1978; Peterson, 1980), entrainment schedules (Wever, 1964), or synchronization processes (Kronauer et al., 1982; Liu et al., 1997), to name a few.

In contrast to this, contextual or detailed biochemical models aim to decipher the molecular regulatory machinery (i.e., the interaction of genes, mRNAs, proteins, post-translational modifications, etc.) that leads to rhythm generation within a biological context, specific to different tissues (Pett et al., 2018) or different organisms such as cyanobacteria, plants, fungi, flies, and mammals (Goldbeter, 1995; Hong et al., 2006; Locke et al., 2006; Kim and Forger, 2012; Woller et al., 2016).

## 1.2. Photoperiodic Entrainment of Circadian Clocks

Unidirectional synchronization of an endogenously oscillating system like the circadian clock to an external periodic forcing signal (Zeitgeber) is termed entrainment. Upon entrainment, a circadian clock with an internal free-running period $\tau$ is forced onto the external Zeitgeber period $T$ (period locking). By this means, a stable phase of entrainment $\psi$ emerges as the internal rhythm aligns with the external rhythm (phase locking). The range of entrainment denotes the set of periods that are able to entrain to a Zeitgbeber at a given strength. It usually gets wider (or narrower) with increasing (or decreasing) Zeitgeber strength. The entrainment region within the parameter plane spanned by the period detuning $\tau - T$ and Zeitgeber strength $Z$ adopts a tongue like geometry, called *Arnold tongue* (Arnold, 1987).

Entrainment ranges, phases of entrainment $\psi$ and entrained amplitudes vary systematically not only with respect to Zeitgeber but also with intrinsic clock properties (Aschoff, 1960). Entrainment protocols have therefore been extensively used to compare circadian clocks in different tissues (Abraham et al., 2010), in different genetic background (clock mutants) within the same species (Rémi et al., 2010; Erzberger et al., 2013), or to compare circadian systems of different species (Aschoff and Pohl, 1978).

We recently extended the concept of Arnold tongues to account for seasonality (Schmal et al., 2015). If we consider a circadian system entrained by Zeitgbeber signals of varying period $T$ and photoperiod $\varkappa$ (**Figure 1A**), the region of entrainment adopts an onion shaped geometry (**Figure 1B**), called *Arnold onion*. Here, the photoperiod $\varkappa$ has been defined as the fraction (in percent) of illumination time (daylength) over the period $T$ of the Zeitgeber cycle. While the entrainment range is largest during equinoctial Zeitgeber cycles ($\varkappa = 50\%$) it tapers toward the free-running periods under constant darkness ($\varkappa = 0\%$) and constant light ($\varkappa = 100\%$) for increasingly extreme photoperiods. Since the free running periods are generally not the same under constant light and constant darkness as predicted by Aschoff's rule (Aschoff, 1960), the Arnold onion appears to be tilted (compare **Figure 1B**).

A similar but conceptually different situation occurs if we consider entrainment of organisms with various circadian free-running periods $\tau$ to Zeitgeber signals of fixed period $T$ but varying $\varkappa$ (**Figure 1C**). Diverse circadian periods exist due to natural variation within a population of the same species or traceable clock gene mutations (Konopka and Benzer, 1971). The entrainment range in the free-running period $\tau$ and photoperiod $\varkappa$ parameter plane adopts an onion shaped geometry similar to the above described case while being tilted in the opposite direction, compare **Figures 1B,D**.

Here, we extend our analysis to the Earth's natural light conditions from photoperiodic entrainment as originally described in Schmal et al. (2015), where we investigated entrainment to square wave Zeitgeber signals, corresponding to typical laboratory conditions. Using a conceptual model of the circadian clock in combination with a simple celestial mechanics-based approximation of local light signals, we illustrate circadian entrainment under ecologically relevant conditions. This reveals a global map of how organisms entrain under different seasons and at different latitudes. It also proposes a possibility that the distribution of chronotypes, a quantitative proxy of the phase of entrainment, can change throughout the year and at different positions on the Earth.

# 2. RESULTS

## 2.1. The Poincaré Oscillator: A Conceptual Model for Limit Cycle Behavior

Circadian clocks share several properties of limit cycle oscillators at the tissue or organismal level. They cause rhythms of gene expression and physiological processes that are stable in period and amplitude, robust against (small) external perturbations. In order not to restrict ourself to a specific biological context (i.e., a particular organism or cell type) we omit detailed biochemical reactions and exploit a generic amplitude-phase model, whose dynamics is determined by

$$\frac{\mathrm{d}r}{\mathrm{d}t} = \lambda\, r(A - r) \tag{1}$$

$$\frac{\mathrm{d}\varphi}{\mathrm{d}t} = \frac{2\,\pi}{\tau} \tag{2}$$

in radial coordinates. Equations (1, 2) describe a Poincaré oscillator (Glass and Mackey, 1988), which exhibits limit cycle oscillations of explicitly defined steady state amplitude $A$ and free-running period $\tau$. Here, $r(t)$ describes the dynamics of the radial component while $\varphi(t)$ describes the angular component.

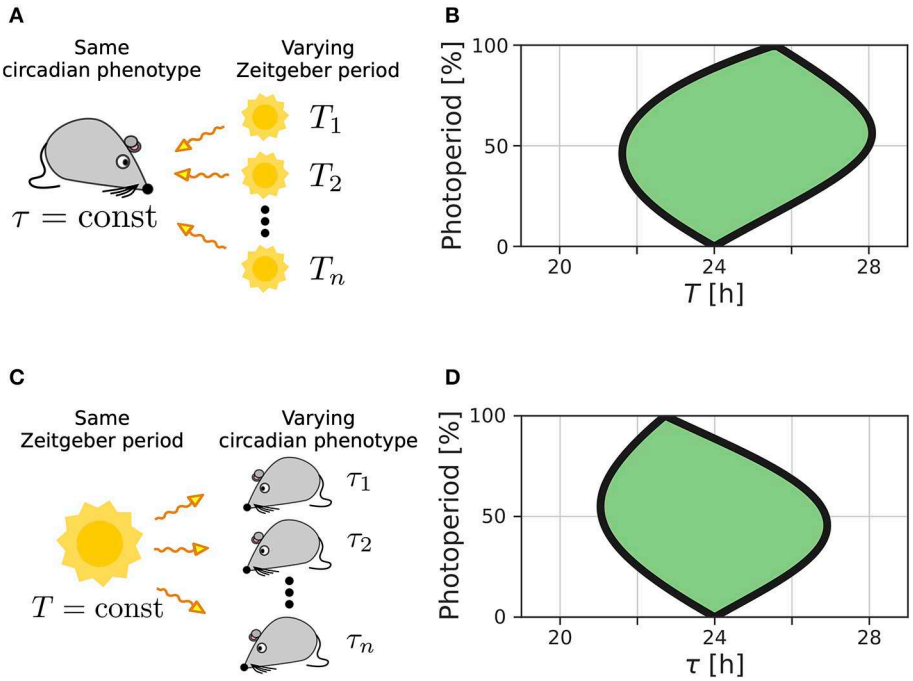


**FIGURE 1 |** Entrainment ranges vary with photoperiod. **(A)** A certain circadian phenotype with free running period $\tau$ is entrained to Zeitgeber cycles of varying $T$. **(B)** Entrainment region (green) of a self-sustained oscillator under entrainment with varying photoperiods $\varkappa$ and Zeitgeber periods $T$. The circadian free-running period under constant darkness ($\varkappa = 0$) has been set to $\tau = 24$ h. **(C)** Different circadian phenotypes with varying free-running period $\tau$, due to variation in a population of organisms or genetic background (e.g., clock mutants), entrained by a Zeitgeber signal with a fixed period $T$. **(D)** For a given Zeitgeber period $T = 24$ h, the entrainment region (green) can be determined for varying free-running periods $\tau$ and different photoperiods $\varkappa$. Simulations underlying panels **(B)** and **(D)** have been done by simulating Equations (4) and (5), applying a square-wave Zeitgeber signal of peak-trough amplitude 0.1 to the $x$-variable and by using oscillator parameters $A = 1$ and $\lambda = 0.5\,\text{h}^{-1}$ as described in Schmal et al. (2015).

Radial-relaxation rate $\lambda$ determines the time-scale of transient dynamics, i.e., the time a Poincaré oscillator needs to return to its steady-state orbit after an amplitude perturbation (e.g., through light pulses) (**Figure 2A**). While parameter dependencies of oscillator properties such as the amplitude or free-running period are usually intertwined in complex molecular models, the Poincaré oscillator (1, 2) conveniently treats these features as independent parameters. Thus, the impact of internal clock parameters on entrainment and synchronization properties can be studied in a straightforward manner as demonstrated in several studies (Abraham et al., 2010; Granada et al., 2013; Gu et al., 2014; Tokuda et al., 2015; Myung et al., 2018; Schmal et al., 2019).

In the following we will represent the circadian clock of an organism by a Poincaré oscillator (1, 2) and study its entrainment under natural light environments, using a simple celestial mechanics derivation.

## 2.2. Approximation of the Perceived Light Intensity on Earth

For a sessile observer at a given position on Earth, the Sun obeys an apparent movement across the celestial sphere. This movement leads to changes in light intensity, predictable from celestial mechanics. While the rotation of the Earth around its own axis leads to daily changes of light intensity, the tilt $\varepsilon$ (obliquity of the ecliptic) of its rotation axis with respect to the plane that is spanned by the Earth's orbit around the Sun (the ecliptic) leads to seasonal variations (**Figure 2B**).

A simple celestial mechanics based model for the light intensity $I$, perceived by an organism at latitude $\phi$ and on a given day $N$ of the solar year, assumes that the declination $\delta$ of the Sun (see **Figure 2B**) varies sinusoidally

$$\delta \approx \varepsilon \sin\left(\frac{2\pi\,(N - 80)}{365.2422}\right) \tag{3}$$

across the year, thus neglecting the elliptical motion of the Earth around the Sun (Khavrus and Shelevytsky, 2012). Here, 365.2422 denotes the mean number of days in a year, i.e., the mean orbital period of the Earth. The ecliptic $\varepsilon$ is subject to fluctuations at timescales that are extremely long (Milanković cycles) compared to any organism's life expectancy such that we consider it constant. It currently takes a value of about $\varepsilon = 23.44°$. In addition to celestial constellations between the Earth and the Sun, scattering and absorption of light within the atmosphere further affects the solar radiation that reaches an observer at the Earth's surface. The extent of absorption, reflection and scattering depends on the path length within the Earth's atmosphere, called the optical air mass (AM), which in turn depends on latitude as well as season (Khavrus and Shelevytsky, 2012).

The orientation of the light-perceiving surface (e.g., the retina or plant leaves) with respect to the direction of the Sun affects the solar irradiance as well. Combining all of these considerations, we can give a closed form expression for the solar irradiance perceived at any position on Earth in dependence on latitude $\phi$, time of year $N$, time of day and the orientation toward the Sun, as given by Equation (11) in section 4.

**Figure 3** illustrates dependencies of the solar irradiance (A), daylength (B), total daily insolation (C) and standard deviation of the daily solar irradiance (D) on geographical latitudes and seasons for sun rays reaching a horizontally oriented surface. While the daylength (see Equation 9) is constantly 12 h throughout the year at the equator as well as at vernal and autumnal equinoxes for all latitudes $\phi$, it adopts the highest variation between different latitudes at summer and winter solstices (**Figure 3B**). The total daily insolation (i.e., the summed irradiance per day) is determined jointly by daylength and irradiance. At summer solstice, for example, the daily insolation adopts similar values at the equator and the arctic pole since a high irradiance is perceived over a shorter daylength near the equator, while a low irradiance is perceived over a long 24 h photoperiod at the arctic pole (**Figure 3C**).

Critical for circadian entrainment is the variation of a Zeitgeber signal, which can be quantified by the standard deviation of the solar irradiance over one day (**Figure 3D**). Its highest values are reached during the equinoxes at the equator and during summer solstice at temperate latitudes, while the lowest variation is found during polar night. These local geographical Zeitgeber variations hint at global variations of the entrainment range.

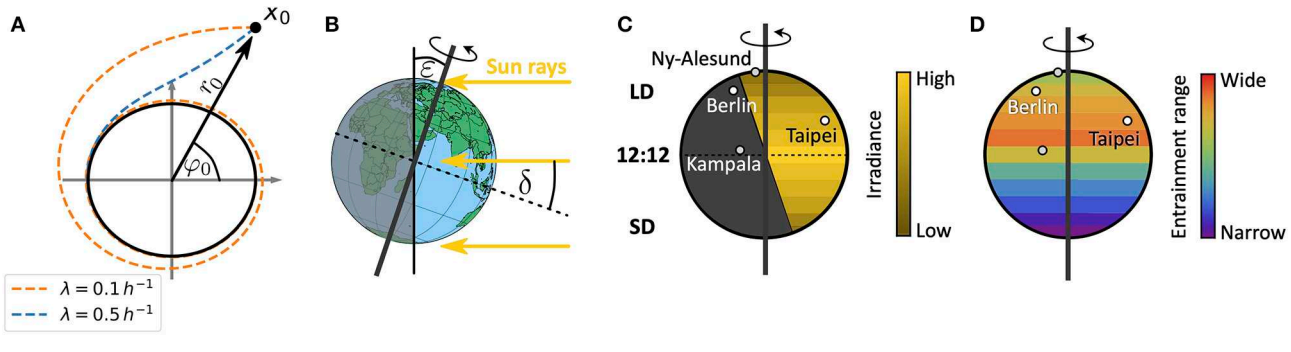


**FIGURE 2 |** Schematics of entrainment range prediction through geophysical considerations. **(A)** Phase plane representation of the conceptual clock model, the Poincaré oscillator. While the black circle denotes the limit cycle of steady state amplitude $A$, dashed lines show transient dynamics for different values of the radial relaxation rate $\lambda$, starting from an initial condition $r_0$ and $\varphi_0$ or $x_0 = (r_0 \cos(\varphi_0), r_0 \sin(\varphi_0))$. Larger values of $\lambda$ lead to shorter transient dynamics after perturbations. **(B)** Illustration of the celestial constellation between the Earth and Sun during summer in the northern hemisphere. Here, $\varepsilon$ denotes the obliquity of the ecliptic while $\delta$ is the declination of Sun. **(C)** Global distribution of daylengths on a summer day in the northern hemisphere, with geographical locations of representative cities used in this study: Kampala (equator), Taipei (sub-tropics), Berlin (temperate), and Ny-Alesund (above arctic circle). Note that the irradiance is lower in the northern extreme despite the longer daylength. LD, long daylength; 12:12, equinox; SD, short daylength. **(D)** Combining a conceptual oscillator model with a celestial mechanics based approximation of the light intensity, we compute entrainment ranges and phases of entrainment $\psi$ under different seasons and latitudes. By this we can study impact of season and latitude on the distribution of chronotypes.

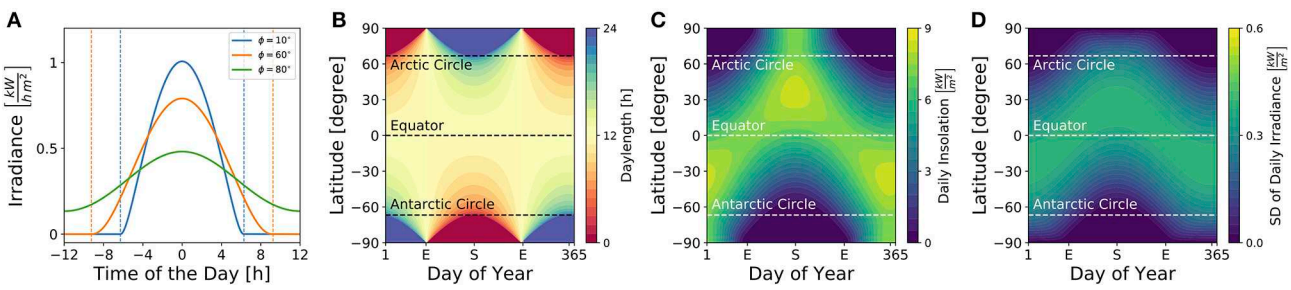


**FIGURE 3 |** Impact of season and latitude on daylength and light intensity. **(A)** Solar irradiance on the Earth's surface for three different latitudes [$\phi = 10°$ (blue), $\phi = 60°$ (orange), $\phi = 80°$ (green)] on day $N = 172$ which corresponds to the 21st of June, i.e., summer solstice in the northern hemisphere. Here, time point zero corresponds to solar noon, i.e., when the Sun reaches the highest point at sky. Dashed lines correspond to sunrise and sunset as given by condition (8). **(B)** Daylength for different latitudes and times of year are depicted as given by Equation (9) in section 4. The daylength corresponds to the distance between sunrise and sunset as exemplified in **(A)** for three different latitudes. **(C)** Daily insolation for different latitudes and times of year. The daily insolation is defined as the daily sum over the solar irradiance as depicted in **(A)** for three exemplary latitudes. Please note that the solar irradiance in **(A)** and solar insolation in **(C)** have been calculated for sun rays reaching a horizontal plane. The direction of the surface (e.g., of plant leaves, the retina, etc.) has an impact on the solar irradiance perceived. **(D)** Standard deviation of the solar irradiance, calculated over a complete day (24 h), for different latitudes and times of year.

## 2.3. Entrainment Ranges Vary Systematically With Season and Latitude

Circadian clock properties vary among different species and even among individuals of the same species as a result of natural (genetic and epigenetic) variation. This eventually translates into variations of entrainment properties such as the phase of entrainment $\psi$, even within the same species that receive the same entrainment cues. Such emergence of different "temporal phenotypes" can be represented as a spread of entrainment phases $\psi$ in a population of individuals of same species. One such representation is commonly known as chronotypes (Pfeffer et al., 2015). In the following we investigate how organisms with different internal clock properties as described by the conceptual oscillator model (1, 2) entrain to natural light signals at different seasons and geographical locations.

**Figure 4** depicts ranges of internal free-running periods $\tau$, for which entrainment upon natural light signals given by Equation (11) can be observed, at different times of the year $N$ and at four different representative latitudes $\phi$, namely in Kampala close to the equator (A), Taipei in the sub-tropics (B), Berlin at a temperate latitude (C), and Ny-Alesund (D) above the arctic circle. Here, we only consider the effect of free-running period $\tau$. Intrinsic clock properties other than $\tau$ are held constant at $A = 6$ and $\lambda = 0.1\ \mathrm{h}^{-1}$ throughout all simulations. Phases of entrainment $\psi$ have been color-coded within the regions of entrainment. Solar noon, the highest position of the Sun at the celestial sphere, is used as a reference point such that $\psi = 0\,\mathrm{h}$ is adopted if the acrophase of the circadian clock oscillations (given by $x(t)$) coincides with solar noon.

Close to the equator, there is little per-day change of daylength, insolation and variation (standard deviation; SD) throughout the year in comparison with higher latitudes (**Figures 3B,D**). Thus, entrainment ranges remain relatively constant throughout the year (**Figure 4A**). Within these small variations, the largest range of entrainment occurs twice a year at vernal and autumnal equinoxes while it becomes the smallest around summer and winter solstices. This is in line with the profiles of solar insolation and SD of daily irradiance, peaking twice per year close to the equator (**Figures 3C,D**).

At higher latitudes, this half-year period in insolation and SD of daily irradiance is absent, leading to entrainment ranges that are maximal during summer solstice and minimal at winter solstice (**Figures 4B,C**). The seasonal effect is stronger as the latitude $\phi$ is higher. At high latitudes, organisms with a circadian clock whose free running period $\tau$ substantially deviates from 24 h might be able to well entrain only during summer but could fail to entrain during winter season, as described for European hamsters (*Cricetus cricetus*) kept under natural lighting conditions (Monecke and Wollnik, 2005).

At latitudes above the arctic circles, the Sun never rises during polar night and never sets during midnight sun (**Figure 3B**). Since our approximation of light intensity ignores diffraction effects by the atmosphere, organisms are unable to entrain during the polar night (**Figure 4D**). Between the vernal and autumnal equinoxes, entrainment is generally possible even during a 24 h midsummer day, that is because the solar altitude above the horizon still exhibits diurnal variations. In line with these results, reindeers (*Rangifer tarandus*) in Spitzbergen do not show diurnal rhythmicity during winter but some residual diurnal activity throughout the summer season (Arnold et al., 2018). Other species such as Svalbard ptarmigans (*Lagopus mutus hyperboreus*) show behavioral arrhyhtmicity during polar night and midnight sun (Williams et al., 2015).

So far, we studied the range of entrainment throughout the year at four different exemplary latitudes (**Figure 4**). In **Figure 5**, we investigate the effect of varying latitudes at three different times of the year. Since the daylength is approximately 12 h at all latitudes (**Figure 3B**) and the dependency of the Zeitgeber intensity (SD of irradiance) on latitude is symmetric for the northern and southern hemispheres, the entrainment region during vernal equinox (and analogously at autumnal equinox) is perfectly symmetric (**Figure 5A**). The largest entrainment range is adopted at the equator ($\phi = 0°$) and tapers toward the polar regions. At summer solstice in the northern hemisphere, an asymmetric entrainment region can be observed (**Figure 5B**). Due to polar night no entrainment is possible above the antarctic circle during this season, but it is possible above the arctic circle. The largest entrainment range is adopted around $\phi \approx 30°$ as the SD of daily irradiance becomes maximal (compare **Figure 3D**). Since summer solstice in the northern hemisphere corresponds to winter solstice on the southern hemisphere and *vice versa*, the entrainment region at winter solstice in the northern hemisphere

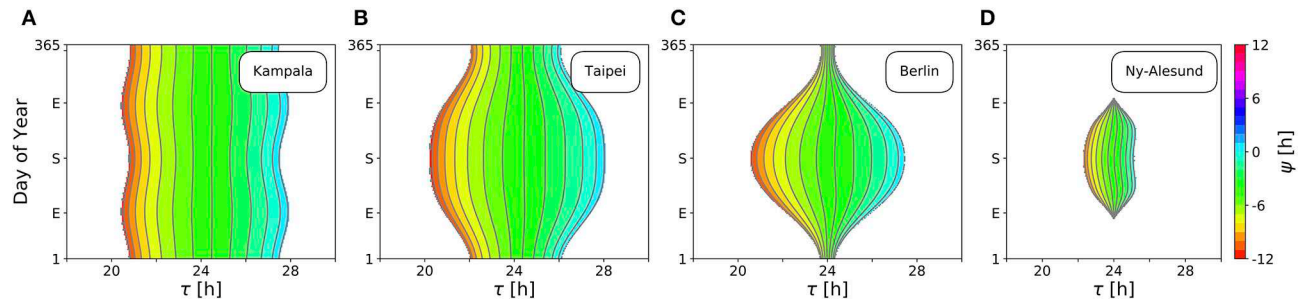


**FIGURE 4 |** Entrainment ranges narrow down at high latitudes. Depicted are the entrainment regions and color-coded phases of entrainment $\psi$ for different times around the year and varying intrinsic free-running periods $\tau$ at four exemplary latitudes $\phi$, namely, $\phi = 0.3°$ **(A)**, $\phi = 25.03°$ **(B)**, $\phi = 52.51°$ **(C)**, $\phi = 78.92°$ **(D)**, corresponding to the latitudes of Kampala, Taipei, Berlin, and Ny-Alesund, respectively. Regions without color-coded phases correspond to parameter combinations of $N$ and $\tau$ where the circadian clock is unable to entrain to the external Zeitgeber cycle. Other intrinsic oscillator properties have been set to $A = 6$ and $\lambda = 0.1\,\mathrm{h}^{-1}$.

is a mirror image of the summer solstice entrainment region (**Figure 5B**) with respect to the equator (**Figure 5C**).

## 2.4. Tracking of Dusk and Dawn Depends on Free-Running Period $\tau$

From an evolutionary point of view, two aspects of circadian entrainment need to be considered. On the one hand, it has to be assured that the circadian program entrains to the environmental Zeitgeber signals at all, which is related to the range of entrainment. Of equal importance, on the other hand, is the existence of a proper phase of entrainment $\psi$, ensuring that physiological processes are executed at most beneficial times around the solar day.

An internal oscillator's activity onset phase can be locked to different phases around the Zeitgeber reference. This is because $\psi$ depends on Zeitgeber properties as well as internal oscillator properties such as the free-running period and amplitude. **Figure 6A** depicts the evolution of $\psi$ throughout the year for three different free running periods $\tau$ (23, 24, and 25 h) at the latitude of Taipei ($\phi = 25.03°$), corresponding to vertical cross-sections through the entrainment regions as depicted in **Figure 4B**. While circadian oscillators with an internal period of 24 h (bold line, **Figure 6A**) appear to be phase locked in parallel to solar noon throughout the year, $\psi$ for clocks with an intrinsic period $\tau$ longer than 24 h (dotted line, **Figure 6A**) occurs earlier during summer days compared to winter and has its earliest value at summer solstice. The opposite is true for circadian clocks with $\tau < 24$ h, where $\psi$ occurs later during summer in comparison to winter days (dashed line, **Figure 6A**). These results quantitatively confirm a similar qualitative description by Pittendrigh (Pittendrigh, 1988). The biological importance can be interpreted within the framework of Aschoff's rule which states that day-active animals typically have a period longer than 24 h while night-active animals have a period shorter than 24 h (Aschoff, 1958). Thus, $\psi$ of day active animals ($\tau > 24$ h) follows the earlier sunrise as photoperiods increase in spring and summer, while night-active animals ($\tau < 24$ h) rather follow a later dusk (onset of night) as photoperiods increase (Pittendrigh, 1988) (compare **Figure 6A**).

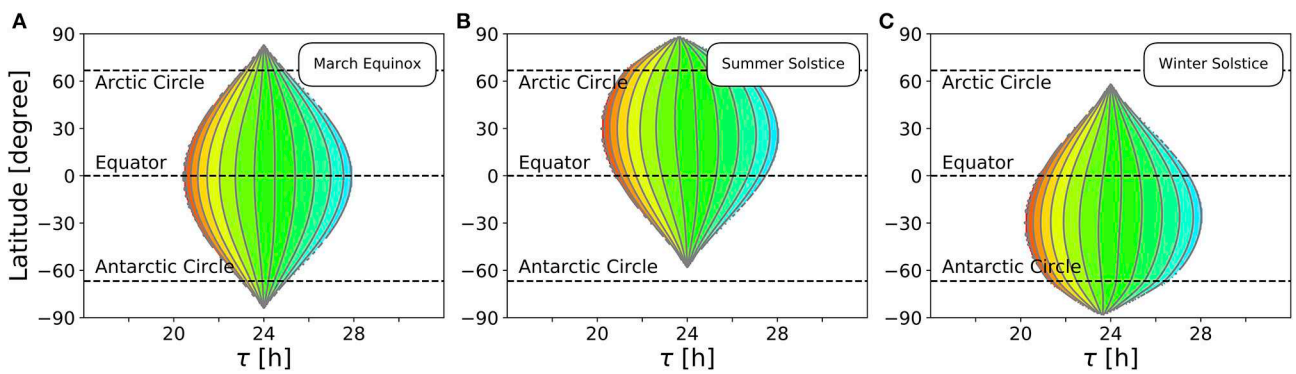


**FIGURE 5 |** Entrainment depends on latitude and time of year. Entrainment regions and color-coded phases of entrainment $\psi$ for different latitudes and internal free-running periods $\tau$ at three different times of the year, namely March equinox **(A)**, summer solstice **(B)** and winter solstice **(C)**. Other internal clock parameters have been set to $A = 6$ and $\lambda = 0.1$ h$^{-1}$. Color coding of $\psi$ is the same as in **Figure 4**.

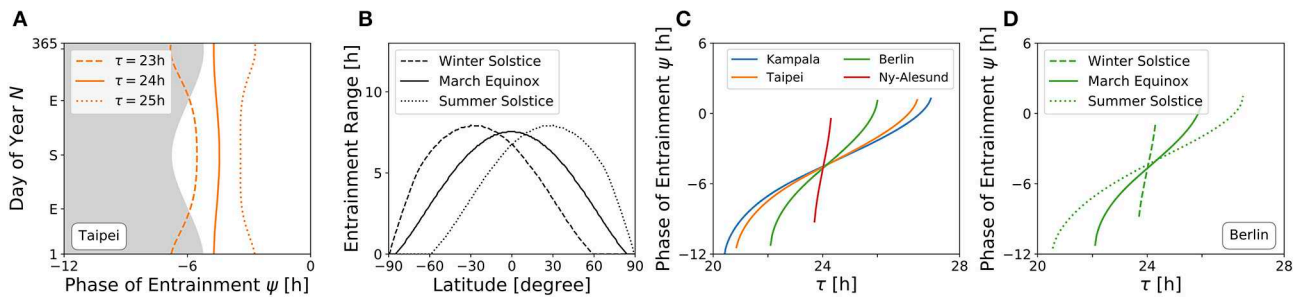


**FIGURE 6 |** High sensitivity of phases during winter and at high latitudes. **(A)** Phase of entrainment $\psi$ at the latitude of Taipei ($\phi = 25.03°$) vs. time of the year ($N$) for three different internal free-running periods $\tau = 23$ h (dashed line), $\tau = 24$ h (bold line), and $\tau = 25$ h (dotted line), respectively. The gray shaded area depicts the duration of darkness. **(B)** Entrainment ranges with respect to variations in $\tau$ as determined by the difference between the upper and lower limits of entrainment in **Figures 5A–C** for different latitudes, respectively. **(C)** Dependency of the phase of entrainment $\psi$ on internal free running period $\tau$ on March equinox for the latitudes of Kampala (blue), Taipei (orange), Berlin (green), and Ny-Alesund (red). **(D)** Dependency of the phase of entrainment $\psi$ on internal free running period $\tau$ at winter solstice (dashed line), March equinox (bold line), and summer solstice (dotted line) at the latitude of Berlin ($\phi = 52.51°$). All simulations have been performed for light perceived by a horizontal plane. Phases of $\psi = \pm 12$ h and $\psi = 0$ h correspond to midnight and solar noon, respectively.

## 2.5. Phases of Entrainment $\psi$ Vary Systematically With Season and Latitude

The range of entrainment depends on Zeitgeber strength and photoperiod. It has been shown that, within the range of period detunings $\tau - T$ that allow for entrainment at a given fixed Zeitgeber strength and photoperiod, the phase of entrainment $\psi$ varies by about 180° (Wever, 1964; Granada et al., 2013; Schmal et al., 2015). This translates to a higher sensitivity of $\psi$ with respect to period detunings $\tau - T$ for small ranges of entrainment.

**Figure 6B** shows the dependency of entrainment ranges on latitude, exemplarily for March equinox as well as for northern hemisphere's summer and winter solstices. It can be seen that the entrainment range gradually decreases as the latitude gets higher. From this, we can infer that on March equinox, $\psi$ has an increased sensitivity to $\tau$ variations as the latitude increases (**Figure 6C**). This corresponds to horizontal cross-sections at March equinox ($N = 79$) in **Figures 4A–D** or to horizontal cross-sections at the latitudes of Kampala (equator), Taipei, Berlin and Ny-Alesund (above arctic circle) in **Figure 5A**, respectively. Likewise, the phase of entrainment $\psi$ has the highest sensitivity to $\tau$ variations ($T = 24$ h) at winter solstice, the lowest sensitivity at summer solstice, and an intermediate sensitivity at March equinox. This is illustrated for the latitude of Berlin ($\psi = 52.51°$) in **Figure 6D**, which corresponds to horizontal cross-sections at the respective times of the year in **Figure 4C**. A similarly strong dependency of the slope of $\psi$ on the Zeitgeber strength has been described for the entrainment of lizards to temperature cycles (Hoffmann, 1969).

The sensitivity of $\psi$ with respect to $\tau$ variations can be used to explain the behavior of chronotypes across different seasons and latitudes as investigated in the following section.

## 2.6. Season and Latitude Affect the Spread of Chronotypes

In our analysis of generic clocks, $\psi$ is referenced to the point of midday. This referencing is arbitrary and is easily translatable to chronotypes. Human chronotype reflects the phase of entrainment, and is commonly referenced to the mid-sleep phase. Variations in the free-running period $\tau$ have been shown to translate into changes of the phase of entrainment $\psi$ (Winfree, 2001; Bordyugov et al., 2015). Genetically modified strains of *Neurospora crassa* with relatively shorter and longer $\tau$, respectively, exhibit early and late values of $\psi$ under light entrainment (Rémi et al., 2010). Likewise, the free-running period of fibroblasts is positively correlated with phase $\psi$ under temperature entrainment (Brown et al., 2008). This has also been seen in weakly coupled *Bmal1* oscillators in the suprachiasmatic nucleus explants cultures (Myung et al., 2012).

Along these lines, it has been hypothesized that small variations of free-running periods $\tau$ within a population of the same species can lead to the emergence of different chronotypes as variations in the phase of entrainment (Phillips et al., 2010; Granada et al., 2013). Chronotypes based on sleep-wake time questionnaires can be a proxy to the phase of entrainment $\psi$, although in higher organisms other factors such as a homeostatic sleep drive interferes with pure circadian effects. "Strong" clocks with a small entrainment range and a large sensitivity of $\psi$ will map a given spread of free-running periods $\tau$ (described by standard deviation $\sigma_\tau$) into a relatively large spread of chronotypes ($\sigma_\psi$) when compared to weak clocks with a large entrainment range and a small sensitivity of $\psi$.

Under a forced desynchronization protocol, it has been shown that human females adopt a distribution of internal free-running periods of mean $\mu_\tau = 24.09$ h and standard deviation $\sigma_\tau = 0.2$ h (Duffy et al., 2011). Taking this data as an illustrative example, we sampled 1,000 periods from a normal distribution with this mean and standard deviation (see **Figure 7A**) and computed the corresponding entrainment phases $\psi$ at different seasons and latitudes. This task corresponds to a convolution of the period distribution with the phase of entrainment profiles as determined in **Figures 4**, **5**, **6C,D**.

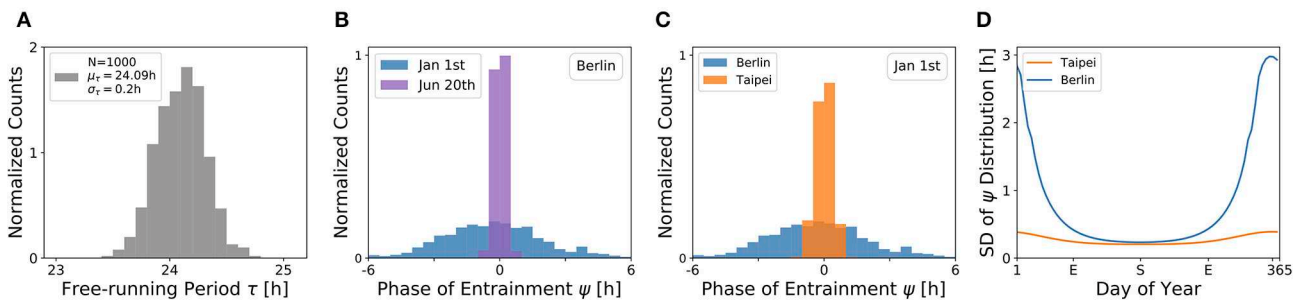


**FIGURE 7 |** The distribution of chronotypes broadens in winter and at higher latitudes. **(A)** Distribution of free-running periods $\tau$ sampled from a normal distribution of mean $\mu_\tau = 24.09$ h and standard deviation $\sigma_\tau = 0.2$ h, following what has been described for female human using a forced desynchronization protocol (Duffy et al., 2011). **(B)** Distribution of entrainment phases $\psi$ (i.e., of chronotypes), that follows from a period distribution as depicted in **(A)** under natural light entrainment in winter (Jan 1st) and summer (Jun 20th) at the latitude of Berlin ($\psi = 52.51°$). Approximately 12% of the (most extreme) sampled periods $\tau$ do not properly entrain under the conditions on Jan 1st. **(C)** Distribution of entrainment phases $\psi$ during winter (Jan 1st) in Berlin (blue) and Taipei (orange). **(D)** Systematic analysis of the standard deviation in the distribution of $\psi$ throughout the year at the latitude in Berlin (blue) and Taipei (orange). In the computations underlying panels **(B–D)**, oscillator parameters others than $\tau$ are held constant to $A = 6$ and $\lambda = 0.1$ h$^{-1}$.

The effect of season on the distribution of chronotypes in our model has been exemplarily calculated for the latitude of Berlin (**Figure 7B**). In summer (Jun 20th), a strong Zeitgeber signal (large SD of irradiance) leads to a wide entrainment range and a small sensitivity of $\psi$ with respect to $\tau$ variations. In other words, the distribution of chronotypes is relatively narrow ($\sigma_\psi$). In winter (Jan 1st), light becomes a relatively weak Zeitgeber, leading to a narrow entrainment range and a high sensitivity of $\psi$. This ultimately leads to a larger spread in chronotypes ($\sigma_\psi$) in winter compared to summer.

If the same population would travel during winter season (Jan 1st) from the latitude of Berlin to latitudes substantially closer to the equator, for example Taipei, the population would find the distribution of chronotypes to become narrower (**Figure 7C**). That is due to the fact that the Zeitgeber is stronger toward the equator in winter (**Figure 3D**), eventually leading to a wider entrainment range and a smaller sensitivity of $\psi$ with respect to $\tau$ variations (see **Figure 5C** in the northern hemisphere).

These theoretical observations imply that the spread in chronotypes ($\sigma_\psi$) varies throughout the year. Examples in **Figure 7D** have been calculated, based on the $\tau$ distribution in **Figure 7A**, the temperate latitude of Berlin and the latitude of Taipei closer to the equator. It can be seen that the seasonal effect is relatively smaller at the latitude of Taipei than in Berlin. At the higher latitude, a standard deviation of $\sigma_\tau = 0.2$ h in free running periods leads to a standard deviation of up to almost $\sigma_\psi = 3$ h in the distribution of $\psi$ during winter solstice.

The combined geographical distributions of entrainment ranges throughout the seasons can be mapped on the globe, using the scheme outlined in **Figure 2**. This visualizes which regions on the globe are easier to entrain to local day-night conditions (**Figure 8**).

## 3. DISCUSSION

The major finding of the present study is the organization of circadian phases in dependence of the geographical and seasonal context and individual clock properties (personal chronotypes). This organization can be assessed by a construct we call *Arnold onion* (Schmal et al., 2015). The clock's ability to entrain to natural light-dark cycles, i.e., the entrainment range, reorganizes across the year, which can be most intuitively visualized for different latitudes on the globe (**Figure 8**). By combining a generic clock model with a geophysical model of local light intensities, we could examine season- and latitude-dependent entrainment properties for circadian systems with different clock properties.

The range of internal periods $\tau$, capable of entraining to daily rhythms of the outside world, remains relatively stable close to the equator but shows strong seasonal variations at high latitudes, having a narrower entrainment range during winter (**Figure 4**). This theoretical prediction is consistent with experimental studies, showing stronger entrainment during summer compared to winter where entrainment might even fail at higher latitudes (Monecke and Wollnik, 2005; Arnold et al., 2018).

For a given circadian phenotype with a well-defined internal period $\tau$ and given amplitude, our model predicts systematic variations of the phase of entrainment $\psi$ across the seasons. Similar to earlier studies (Pittendrigh and Daan, 1976b; Pittendrigh, 1988), dusk tracking is predicted for clocks shorter than a day ($\tau < 24$ h) while dawn tracking occurs for clocks with $\tau > 24$ h (**Figure 6A**). Such seasonal variations in the timing of daily activity have been described for entrainment under natural conditions in several species including birds and rodents (Aschoff and Wever, 1962; Daan and Aschoff, 1975). In some species, other entrainment cues such as social synchronization and temperature can overtake photic entrainment (Robbers et al., 2015; Fuchikawa et al., 2016).

Our theoretical examination predicts that there can be latitudinal and seasonal changes in the global distribution of entrainment phases $\psi$, which can be reflected in chronotype measures. Season and latitude can affect the mean (**Figure 6**) and standard deviation (**Figure 7**) of the chronotype distribution as the average internal free-running periods ($\mu_\tau$) deviate from 24 h. In humans, distributions of the midpoint of sleep on free days (MSF), a common measure of chronotypes, are different between male and female populations and vary also with age (Foster and Roenneberg, 2008). Humans adopt their latest chronotype roughly at the age of 20, and become earlier again with increasing age (Roenneberg et al., 2004). Reliable estimates of population

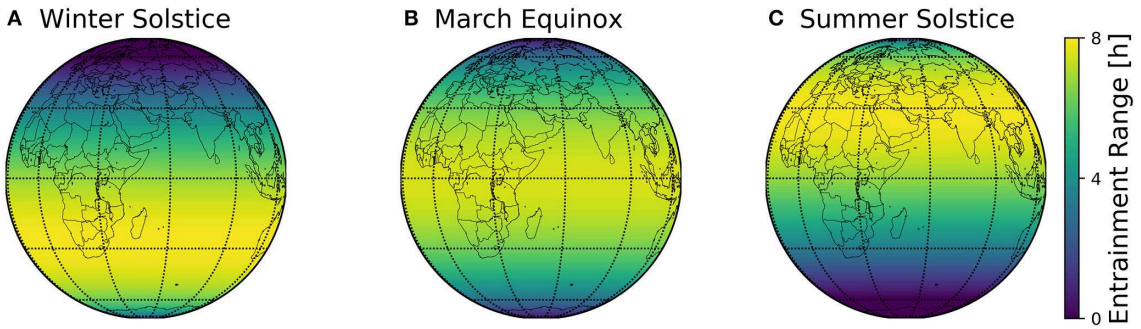


**FIGURE 8 |** Global entrainment patterns across seasons. Entrainment ranges at different latitudes $\phi$ are depicted on a globe map for three different times of the year, namely winter solstice **(A)**, March equinox **(B)**, and summer solstice **(C)**. This representation follows the scheme outlined in **Figure 2**, where the entrainment ranges correspond to those depicted in **Figure 6B**.

variance through seasonal and latitudinal variations are difficult to obtain amidst these internal heterogeneities, in addition to confounding cultural influences amongst studies including societies of different lifestyles (Pilz et al., 2018). We expect that finer details of chronotype diversity can be predicted in defined subpopulations of age and gender when more precise physiological mechanisms of chronotypes are known. It should be noted that our model has been developed to exploit general principles of circadian entrainment and has not been fine-tuned to account for human entrainment characteristics. Human chronotypes are commonly associated with the "preferred sleep-wake schedule," and the sleep-wake cycle is not linearly related to the underlying circadian cycle. Along with the circadian regulation, human sleep patterns are simultaneously affected by homeostatic processes (Phillips et al., 2010; Skeldon et al., 2016). Previous conceptual models of human circadian entrainment more specifically elaborated on light-sensing mechanisms and mimicked human phase-response behavior (Forger et al., 1999; Jewett et al., 1999). It would be interesting to investigate in future studies how these human-specific constraints affect the season and latitude dependent responses of chronotype distributions. However, the occurrence of chronotypes is not exclusive to humans and has been described for other species as well (Pfeffer et al., 2015). Our theoretical predictions could be useful for further studies on the effect of detailed Zeitgeber characteristics upon the distribution of chronotypes or entrainment ranges within a controlled setting, using populations of well-studied model organisms at different geographical locations and seasons.

Parameters other than free-running periods $\tau$ such as the amplitude have been proposed to further affect entrainment characteristics (Lakin-Thomas et al., 1991). Throughout this study we held amplitudes ($A$) and radial relaxation rates ($\lambda$) constant and focused on the impact of $\tau$ on entrainment properties. Analogous to previous studies (Abraham et al., 2010; Bordyugov et al., 2011) we find that decreasing amplitudes and relaxation rates broaden the entrainment range with respect to $\tau$ variations throughout the year (**Figures S1, S2**). Therefore, decreasing amplitudes and relaxation rates will lead to a reduced spread of entrainment phases. A careful interpretation of entrainment characteristics among different circadian phenotypes (organisms, tissues, mutants, etc.) will require inclusion of a thorough analysis of all relevant internal oscillator parameters.

Properties of the circadian clock have been shown to be plastic and diverse within the same species and across an organism's domicile environment and life span. Chronic conditions of external entrainment can alter the intrinsic period of a clock (Pittendrigh, 1960; Pittendrigh and Daan, 1976a). Across several organisms, including mice and human, it has been shown that entrainment at different photoperiods (Ciarleglio et al., 2011; Myung et al., 2015) and different Zeitgeber periods $T$ (Scheer et al., 2007; Azzi et al., 2014, 2017) reversibly or irreversibly changes the free-running period $\tau$, a phenomenon termed aftereffect or imprinting, respectively. Additionally, it has been found that properties of the clock change with increasing age (Pittendrigh and Daan, 1974). Although our conceptual oscillator model does not include light- or age-dependent parameter plasticities, Arnold onions can be used to predict changes of entrainment properties upon plasticities in the circadian clock behavior by highlighting subpopulations of $\tau$. Assuming that plasticities occur either under relatively short (after-effects) or long (aging) time scales in comparison to seasonal changes of light intensity, one can predict plasticity dependent changes of $\psi$ in a latitude and season dependent manner by tracing relevant $\tau$ subpopulations expected from plasticities within an Arnold onion as depicted in **Figures 4**, **5**.

Latitudinal clines of oscillator properties have been observed in various organisms. Plant leaf movements and oviposition or eclosion rhythms in Drosophila show shorter free-running periods in northern compared to southern strains (Mayer, 1966; Hut et al., 2013). The free-running period in tomato decelerates during domestication, most probably to adapt to longer summer days after its transferal from the equator to northern latitudes (Müller et al., 2015). Our conceptual clock model, extended to account for photoperiodic entrainment under natural conditions, can help predict how properties of the internal clock affect the phase of entrainment and thus can help to untangle mechanisms underlying latitudinal clines.

Several approximations have been done with respect to the calculated light intensity that entrains the conceptual clock model. We assumed that a given organism perceives light similar to a horizontal plane. Young sunflowers follow the path of the sun across the celestial sphere during the day, driven by anti-phasic patterns of stem elongation (Vandenbrink et al., 2014; Atamian et al., 2016). By this means, a larger amount of daily insolation can be perceived as compared to a horizontal leaf orientation (Shell et al., 1974; **Figure S3A**). The variation of the light intensity per day, on the other hand, increases with solar tracking (**Figure S3B**) which facilitates the entrainment of the circadian system especially during winter (**Figure S3C**). Active orientation toward the Sun can therefore lead to broader entrainment ranges and a narrowed distribution of chronotypes. Future studies might investigate the impact of orientation toward the light source on entrainment characteristics in more detail.

Light intensity as perceived by an organism on Earth has been calculated as the sum over the whole spectrum of sunlight throughout this study. It is known that some species harbor different wavelength of natural light differentially (Roenneberg and Foster, 1997; Fankhauser and Staiger, 2002). Changes of spectral composition throughout the course of the day have been proposed to serve as an entrainment cue (Walmsley et al., 2015). In modern societies, anthropogenic artificial light interferes with the natural light-dark profiles. Self-selected light during the night has been described to affect the sleep-wake behavior in humans (Skeldon et al., 2017; Pilz et al., 2018). In addition, changing weather and movement between differentially shaded habitats affect the amount of light that a given organism perceives. An extension of our current study could investigate how above described effects on the effective Zeitgeber strength alters our computationally estimated entrainment properties under natural conditions.

The entrainment phase depends on the detuning ($\tau - T$) of the clock and Zeitgeber period, on the ratio of the Zeitgeber strength to clock amplitudes, and on relaxation rates (Wever, 1964;

Granada et al., 2013; Bordyugov et al., 2015; Schmal et al., 2015). These generic dependencies theoretically allow us to predict entrainment properties as a function of season and latitude. It is therefore expected that our modeling approach will provide a framework to analyze empirical data on chronotype distributions under different geographical and ecological contexts.

# 4. MATERIALS AND METHODS

## 4.1. Conceptual Amplitude-Phase Model

Using the identities $x = r\cos(\varphi)$ and $y = r\sin(\varphi)$, we can rewrite Equations (1, 2) of the *main text* as

$$\frac{\mathrm{d}x}{\mathrm{d}t} = \lambda x(A - r) - \tfrac{2\pi}{\tau} y \tag{4}$$

$$\frac{\mathrm{d}y}{\mathrm{d}t} = \lambda y(A - r) + \tfrac{2\pi}{\tau} x \tag{5}$$

in Cartesian coordinates. Similar to previously published studies (Granada et al., 2013; Schmal et al., 2015), we choose that light affects the circadian clock by adding the light intensity $I(t)$ at a given time $t$ to the $x$ direction on the phase plane such that Equation (4) reads as $\frac{dx}{dt} = \lambda x(A - r) - \frac{2\pi}{\tau} y + I(t)$.

## 4.2. Light Intensity on a Cloud-Free Day

Considering a plane of arbitrary orientation with a polar angle $\beta$ and the azimuth angle $\gamma$, the cosine of the angle $\theta$ between the normal of the arbitrarily oriented plane and the direction of the Sun is given by

$$\begin{aligned}\cos(\theta) = &\sin(\delta)\left[\sin(\phi)\cos(\beta) - \cos(\phi)\sin(\beta)\sin(\gamma)\right] \\ &+ \cos(\delta)\left[\cos(\phi)\cos(\beta)\cos(\omega) + \sin(\phi)\sin(\beta)\right. \\ &\left.\cos(\gamma)\cos(\omega) + \sin(\beta)\sin(\gamma)\sin(\omega)\right].\end{aligned} \tag{6}$$

where $\phi$, $\delta$ and $\omega$ are the geographical latitude, declination and hour angle, respectively (Chen, 2011). The hour angle $\omega$ defines the solar time and grows by $2\pi$ between two subsequent crossings of a meridian.

From Equation (6), one can obtain the cosine of the zenith angle $z$, i.e., [the angle between the zenith and the Sun disk], by setting $\beta = 0$, i.e.,

$$\cos(z) = \sin(h) = \cos(\delta)\cos(\omega)\cos(\phi) + \sin(\delta)\sin(\phi), \tag{7}$$

with $h$ being the solar altitude. At sunrise and sunset the sun just touches the horizon ($h = 0$) such that the hour angle $\omega_s$ fulfills the relationship

$$\cos(\omega_s) = -\tan(\delta)\tan(\phi), \tag{8}$$

from which we can obtain the daylength

$$D = 24h\left(1 - \frac{\arccos(\tan(\delta)\tan(\phi))}{\pi}\right) \tag{9}$$

at a given latitude $\phi$ and declination $\delta$ of the Sun (Khavrus and Shelevytsky, 2010; Chen, 2011).

Using a common approximation for the optical air mass (AM) (Kasten and Young, 1989)

$$\mathrm{AM} = \left[\cos(z) + 0.50572(96.07995 - z)^{-1.6364}\right]^{-1} \tag{10}$$

where z is the zenith angle in degrees, we can write the total irradiance $I$ that reaches a plane horizontally-aligned to the Earth's surface as

$$I = \begin{cases} 1.353\frac{kW}{m^2} \times 1.1 \times 0.7^{AM^{0.678}} \times \cos(z) & \text{if} \quad \cos(z) > 0 \\ 0 \quad \text{otherwise} \end{cases} \tag{11}$$

where $1.353\frac{kW}{m^2}$ is the average solar constant and factor 1.1 is for diffuse irradiance (Khavrus and Shelevytsky, 2012).

## 4.3. Numerics

Equations (4, 5) in combination with Equation (11) have been numerically solved using the `SCIentificPYthon` function `odeint` at a step size of $\Delta t = 0.01$ h. Entrainment ranges as well as phases of entrainment have been determined as described earlier (Schmal et al., 2015). The highest position of the Sun at the celestial sphere served as a reference point of the Zeitgeber cycle such that the phase of entrainment $\psi \in [-12h, 12h]$ is defined as the distance between the acrophase of $x(t)$ oscillations and solar noon.

# DATA AVAILABILITY STATEMENT

All datasets generated for this study are included in the article/**Supplementary Material**.

# AUTHOR CONTRIBUTIONS

CS designed the study, performed the analysis, visualized the data and drafted the manuscript. JM designed the study, made a figure, and drafted the manuscript. All authors interpreted the data and wrote the manuscript. All authors read and approved the submitted version.

# FUNDING

CS acknowledges support from the Deutsche Forschungsgemeinschaft (DFG) (SCH3362/2- 1). HH acknowledges support from the Deutsche Forschungsgemeinschaft through grant numbers TRR 186 and SPP 2041. JM acknowledges support from JSPS (16H01652, 16K08538), the Taiwan Ministry of Science and Technology (107-2311-B-038-001-MY2, 107-2410-H-038-004-MY2, 108-2321-B006-023-MY2, 108-2410-H-038-008-MY2), the Higher Education Sprout Project by the Ministry of Education (MOE) in Taiwan, Taipei Medical University (TMU107-AE1-B15), and Taipei Medical University-Shuang Ho Hospital (107TMU-SHH-03).

## ACKNOWLEDGMENTS

We thank Bharath Ananthasubramaniam and Grigory Bordyugov for fruitful discussions.

## SUPPLEMENTARY MATERIAL

The Supplementary Material for this article can be found online at: https://www.frontiersin.org/articles/10.3389/fphys.2020.00272/full#supplementary-material

## REFERENCES

Abraham, U., Granada, A. E., Westermark, P. O., Heine, M., Kramer, A., and Herzel, H. (2010). Coupling governs entrainment range of circadian clocks. *Mol. Syst. Biol.* 6:438. doi: 10.1038/msb.2010.92

Arnold, V. (1987). *Geometrische Methoden in der Theorie der gewöhnlichen Differentialgleichungen*. Basel: Birkhäuser Verlag.

Arnold, W., Ruf, T., Loe, L. E., Irvine, R. J., Ropstad, E., Veiberg, V., et al. (2018). Circadian rhythmicity persists through the polar night and midnight sun in Svalbard reindeer. *Sci. Rep.* 8:14466. doi: 10.1038/s41598-018-32778-4

Aschoff, J. (1958). Tierische Periodik unter dem Einfluß von Zeitgebern. *Z. Tierpsychol.* 15, 1–30. doi: 10.1111/j.1439-0310.1958.tb00552.x

Aschoff, J. (1960). Exogenous and endogenous components in circadian rhythms. *Cold Spring Harb. Symp. Quant. Biol.* 25, 11–28. doi: 10.1101/SQB.1960.025.01.004

Aschoff, J., and Pohl, H. (1978). Phase relations between a circadian rhythm and its zeitgeber within the range of entrainment. *Naturwissenschaften* 65, 80–84. doi: 10.1007/BF00440545

Aschoff, J., and Wever, R. (1962). Beginn und Ende der täglichen Aktivität freilebender Vögel. *J. Ornithol.* 103, 2–27. doi: 10.1007/BF01670845

Atamian, H. S., Creux, N. M., Brown, E. A., Garner, A. G., Blackman, B. K., and Harmer, S. L. (2016). Circadian regulation of sunflower heliotropism, floral orientation, and pollinator visits. *Science* 353, 587–590. doi: 10.1126/science.aaf9793

Azzi, A., Dallmann, R., Casserly, A., Rehrauer, H., Patrignani, A., Maier, B., et al. (2014). Circadian behavior is light-reprogrammed by plastic dna methylation. *Nat. Neurosci.* 17, 377–382. doi: 10.1038/nn.3651

Azzi, A., Evans, J. A., Leise, T., Myung, J., Takumi, T., Davidson, A. J., et al. (2017). Network dynamics mediate circadian clock plasticity. *Neuron* 93, 441–450. doi: 10.1016/j.neuron.2016.12.022

Bordyugov, G., Abraham, U., Granada, A., Rose, P., Imkeller, K., Kramer, A., et al. (2015). Tuning the phase of circadian entrainment. *J. R. Soc. Interface* 12:20150282. doi: 10.1098/rsif.2015.0282

Bordyugov, G., Granada, A. E., and Herzel, H. (2011). How coupling determines the entrainment of circadian clocks. *Eur. Phys. J. B* 82, 227–234. doi: 10.1140/epjb/e2011-20337-1

Brown, S. A., Kunz, D., Dumas, A., Westermark, P. O., Vanselow, K., Tilmann-Wahnschaffe, A., et al. (2008). Molecular insights into human daily behavior. *Proc. Natl. Acad. Sci. U.S.A.* 105, 1602–1607. doi: 10.1073/pnas.0707772105

Chen, C. J. (2011). *Physics of Solar Energy*. Hoboken, NJ: John Wiley and Sons, Inc.

Chen, J.-D., Lin, Y.-C., and Hsiao, S.-T. (2010). Obesity and high blood pressure of 12-hour night shift female clean-room workers. *Chronobiol. Int.* 27, 334–344. doi: 10.3109/07420520903502242

Ciarleglio, C. M., Axley, J. C., Strauss, B. R., Gamble, K. L., and McMahon, D. G. (2011). Perinatal photoperiod imprints the circadian clock. *Nat. Neurosci.* 14, 25–27. doi: 10.1038/nn.2699

Daan, S., and Aschoff, J. (1975). Circadian rhythms of locomotor activity in captive birds and mammals: their variations with season and latitude. *Oecologia* 18, 269–316. doi: 10.1007/BF00345851

Dodd, A. N., Salathia, N., Hall, A., Kévei, E., Tóth, R., Nagy, F., et al. (2005). Plant circadian clocks increase photosynthesis, growth, survival, and competitive advantage. *Science* 309, 630–633. doi: 10.1126/science.1115581

Duffy, J. F., Cain, S. W., Chang, A.-M., Phillips, A. J. K., Münch, M. Y., Gronfier, C., et al. (2011). Sex difference in the near-24-hour intrinsic period of the human circadian timing system. *Proc. Natl. Acad. Sci. U.S.A.* 108, 15602–15608. doi: 10.1073/pnas.1010666108

Engelmann, W., Johnsson, A., Karlsson, H., Kobler, R., and Schimmel, M. (1978). Attenuation of the petal movement rhythm in Kalanchoë with light pulses. *Physiol. Plant.* 43, 68–76. doi: 10.1111/j.1399-3054.1978.tb01569.x

Erzberger, A., Hampp, G., Granada, A., Albrecht, U., and Herzel, H. (2013). Genetic redundancy strengthens the circadian clock leading to a narrow entrainment range. *J. R. Soc. Interface* 10:20130221. doi: 10.1098/rsif.2013.0221

Fankhauser, C., and Staiger, D. (2002). Photoreceptors in *Arabidopsis thaliana*: light perception, signal transduction and entrainment of the endogenous clock. *Planta* 216, 1–16. doi: 10.1007/s00425-002-0831-4

Forger, D. B., Jewett, M. E., and Kronauer, R. E. (1999). A simpler model of the human circadian pacemaker. *J. Biol. Rhythms* 14, 533–538. doi: 10.1177/074873099129000867

Foster, R. G., and Roenneberg, T. (2008). Human responses to the geophysical daily, annual and lunar cycles. *Curr. Biol.* 18, R784–R794. doi: 10.1016/j.cub.2008.07.003

Fuchikawa, T., Eban-Rothschild, A., Nagari, M., Shemesh, Y., and Bloch, G. (2016). Potent social synchronization can override photic entrainment of circadian rhythms. *Nat. Commun.* 7:11662. doi: 10.1038/ncomms11662

Glass, L., and Mackey, M. (1988). *From Clocks to Chaos: The Rhythms of Life*. Princeton, NJ: Princeton University Press.

Goldbeter, A. (1995). A model for circadian oscillations in the *Drosophila* period protein (PER). *Proc. R. Soc. B.* 261, 319–324. doi: 10.1098/rspb.1995.0153

Granada, A. E., Bordyugov, G., Kramer, A., and Herzel, H. (2013). Human chronotypes from a theoretical perspective. *PLoS ONE* 8:e59464. doi: 10.1371/journal.pone.0059464

Gu, C., Ramkisoensing, A., Liu, Z., Meijer, J. H., and Rohling, J. H. (2014). The proportion of light-responsive neurons determines the limit cycle properties of the suprachiasmatic nucleus. *J. Biol. Rhythms* 29, 16–27. doi: 10.1177/0748730413516752

Herzog, E. D., Aton, S. J., Numano, R., Sakaki, Y., and Tei, H. (2004). Temporal precision in the mammalian circadian system: a reliable clock from less reliable neurons. *J. Biol. Rhythms* 19, 35–46. doi: 10.1177/0748730403260776

Hirata, Y., Enoki, R., Kuribayashi-Shigetomi, K., Oda, Y., Honma, S., and Honma, K.-I. (2019). Circadian rhythms in Per1, PER2 and Ca2+ of a solitary SCN neuron cultured on a microisland. *Sci. Rep.* 9:18271. doi: 10.1038/s41598-019-54654-5

Hoffmann, K. (1969). Zum Einfluß der Zeitgeberstärke auf die Phasenlage der synchronisierten circadianen Periodik. *Z. Vergleichende Physiol.* 62, 93–110. doi: 10.1007/BF00298045

Hong, C., Jolma, I., Loros, J., Dunlap, J., and Ruoff, P. (2006). Simulating dark expressions and interactions of frq and wc-1 in the *Neurospora* circadian clock. *Biophys. J.* 94, 1221–1232. doi: 10.1529/biophysj.107.115154

Hut, R. A., Paolucci, S., Dor, R., Kyriacou, C. P., and Daan, S. (2013). Latitudinal clines: an evolutionary view on biological rhythms. *Proc. R. Soc. B* 280:20130433. doi: 10.1098/rspb.2013.0433

Jewett, M. E., Forger, D. B., and Kronauer, R. E. (1999). Revised limit cycle oscillator model of human circadian pacemaker. *J. Biol. Rhythms* 14, 493–500. doi: 10.1177/074873049901400608

Kasten, F., and Young, A. T. (1989). Revised optical air mass tables and approximation formula. *Appl. Opt.* 28, 4735–4738. doi: 10.1364/AO.28.004735

Khavrus, V., and Shelevytsky, I. (2010). Introduction to solar motion geometry on the basis of a simple model. *Phys. Educ.* 45, 641–653. doi: 10.1088/0031-9120/45/6/010

Khavrus, V., and Shelevytsky, I. (2012). Geometry and the physics of seasons. *Phys. Educ.* 47, 680. doi: 10.1088/0031-9120/47/6/680

Kiessling, S., Eichele, G., and Oster, H. (2010). Adrenal glucocorticoids have a key role in circadian resynchronization in a mouse model of jet lag. *J. Clin. Invest.* 120, 2600–2609. doi: 10.1172/JCI41192

Kim, J. K., and Forger, D. B. (2012). A mechanism for robust circadian timekeeping via stoichiometric balance. *Mol. Syst. Biol.* 8:630. doi: 10.1038/msb.2012.62

Konopka, R. J., and Benzer, S. (1971). Clock mutants of *Drosophila melanogaster*. *Proc. Natl. Acad. Sci. U.S.A.* 68, 2112–2116. doi: 10.1073/pnas.68.9.2112

Kronauer, R. E., Czeisler, C. A., Pilato, S. F., Moore-Ede, M. C., and Weitzman, E. D. (1982). Mathematical model of the human circadian system with two interacting oscillators. *Am. J. Physiol.* 242, R3–R17. doi: 10.1152/ajpregu.1982.242.1.R3

Lakin-Thomas, P. L., Brody, S., and Coté, G. G. (1991). Amplitude model for the effects of mutations and temperature on period and phase resetting of the *Neurospora* circadian oscillator. *J. Biol. Rhythms* 6, 281–297. doi: 10.1177/074873049100600401

Liu, C., Weaver, D. R., Strogatz, S. H., and Reppert, S. M. (1997). Cellular construction of a circadian clock: period determination in the suprachiasmatic nuclei. *Cell* 91:855–860. doi: 10.1016/S0092-8674(00)80473-0

Locke, J. C. W., Kozma-Bognar, L., Gould, P. D., Feher, B., Kevei, E., Nagy, F., et al. (2006). Experimental validation of a predicted feedback loop in the multi-oscillator clock of *Arabidopsis thaliana*. *Mol. Syst. Biol.* 2:59. doi: 10.1038/msb4100102

Mayer, W. (1966). Besonderheiten der circadianen Rhythmik bei Pflanzen verschiedener geographischer Breiten. *Planta* 70, 237–256. doi: 10.1007/BF00396490

Monecke, S., and Wollnik, F. (2005). Seasonal variations in circadian rhythms coincide with a phase of sensitivity to short photoperiods in the european hamster. *J. Comp. Physiol. B*. 175, 167–183. doi: 10.1007/s00360-005-0472-6

Müller, N. A., Wijnen, C. L., Srinivasan, A., Ryngajllo, M., Ofner, I., Lin, T., et al. (2015). Domestication selected for deceleration of the circadian clock in cultivated tomato. *Nat. Genet*. 48, 89–93. doi: 10.1038/ng.3447

Myung, J., Hong, S., DeWoskin, D., De Schutter, E., Forger, D. B., and Takumi, T. (2015). Gaba-mediated repulsive coupling between circadian clock neurons in the scn encodes seasonal time. *Proc. Natl. Acad. Sci. U.S.A*. 112, E3920–E3929. doi: 10.1073/pnas.1421200112

Myung, J., Hong, S., Hatanaka, F., Nakajima, Y., De Schutter, E., and Takumi, T. (2012). Period coding of bmal1 oscillators in the suprachiasmatic nucleus. *J. Neurosci*. 32, 8900–8918. doi: 10.1523/JNEUROSCI.5586-11.2012

Myung, J., Schmal, C., Hong, S., Tsukizawa, Y., Rose, P., Zhang, Y., et al. (2018). The choroid plexus is an important circadian clock component. *Nat. Commun*. 9:1062. doi: 10.1038/s41467-018-03507-2

Ono, D., Honma, S., Nakajima, Y., Kuroda, S., Enoki, R., and Honma, K.-I. (2017). Dissociation of Per1 and Bmal1 circadian rhythms in the suprachiasmatic nucleus in parallel with behavioral outputs. *Proc. Natl. Acad. Sci. U.S.A*. 114, E3699–E3708. doi: 10.1073/pnas.1613374114

Ouyang, Y., Andersson, C. R., Kondo, T., Golden, S. S., and Johnson, C. H. (1998). Resonating circadian clocks enhance fitness in cyanobacteria. *Proc. Natl. Acad. Sci. U.S.A*. 95, 8660–8664. doi: 10.1073/pnas.95.15.8660

Peterson, E. L. (1980). A limit cycle interpretation of a mosquito circadian oscillator. *J. Theor. Biol*. 84, 281–310. doi: 10.1016/S0022-5193(80)80008-7

Pett, J. P., Kondoff, M., Bordyugov, G., Kramer, A., and Herzel, H. (2018). Co-existing feedback loops generate tissue-specific circadian rhythms. *Life Sci. Alliance* 1:e201800078. doi: 10.26508/lsa.201800078

Pfeffer, M., Wicht, H., von Gall, C., and Korf, H.-W. (2015). Owls and larks in mice. *Front. Neurol*. 6:101. doi: 10.3389/fneur.2015.00101

Phillips, A. J. K., Chen, P. Y., and Robinson, P. A. (2010). Probing the mechanisms of chronotype using quantitative modeling. *J. Biol. Rhythms* 25, 217–227. doi: 10.1177/0748730410369208

Pilz, L. K., Levandovski, R., Oliveira, M. A. B., Hidalgo, M. P., and Roenneberg, T. (2018). Sleep and light exposure across different levels of urbanisation in brazilian communities. *Sci. Rep*. 8:11389. doi: 10.1038/s41598-018-29494-4

Pittendrigh, C. S. (1960). Circadian rhythms and the circadian organization of living systems. *Cold Spring Harb. Symp. Quant. Biol*. 25, 159–184. doi: 10.1101/SQB.1960.025.01.015

Pittendrigh, C. S. (1988). The photoperiodic phenomena: seasonal modulation of the "day within". *J. Biol. Rythms* 3, 173–188. doi: 10.1177/074873048800300206

Pittendrigh, C. S., and Daan, S. (1974). Circadian oscillations in rodents: a systematic increase of their frequency with age. *Science* 186, 548–550. doi: 10.1126/science.186.4163.548

Pittendrigh, C. S., and Daan, S. (1976a). A functional analysis of circadian pacemakers in nocturnal rodents I: the stability and lability of spontaneous frequency. *J. Comp. Physiol.* 106, 223–252. doi: 10.1007/BF01417856

Pittendrigh, C. S., and Daan, S. (1976b). A functional analysis of circadian pacemakers in nocturnal rodents IV entrainment: pacemaker as clock. *J. Comp. Physiol*. 106, 291–331. doi: 10.1007/BF01417859

Rémi, J., Merrow, M., and Roenneberg, T. (2010). A circadian surface of entrainment: varying t, $\tau$, and photoperiod in *Neurospora crassa*. *J. Biol. Rhythms* 25, 318–328. doi: 10.1177/0748730410379081

Robbers, Y., Koster, E. A., Krijbolder, D. I., Ruijs, A., van Berloo, S., and Meijer, J. H. (2015). Temporal behaviour profiles of *Mus musculus* in nature are affected by population activity. *Physiol. Behav*. 139, 351–360. doi: 10.1016/j.physbeh.2014.11.020

Roenneberg, T., and Foster, R. G. (1997). Twilight times: light and the circadian system. *Photochem. Photobiol*. 66, 549–561. doi: 10.1111/j.1751-1097.1997.tb03188.x

Roenneberg, T., Kuehnle, T., Pramstaller, P. P., Ricken, J., Havel, M., Guth, A., et al. (2004). A marker for the end of adolescence. *Curr. Biol*. 14, R1038–R1039. doi: 10.1016/j.cub.2004.11.039

Scheer, F. A., Wright, K. P. Jr., Kronauer, R. E., and Czeisler, C. A. (2007). Plasticity of the intrinsic period of the human circadian timing system. *PLoS ONE* 2:e721. doi: 10.1371/journal.pone.0000721

Schmal, C., Myung, J., Herzel, H., and Bordyugov, G. (2015). A theoretical study on seasonality. *Front. Neurol*. 6:94. doi: 10.3389/fneur.2015.00094

Schmal, C., Ono, D., Myung, J., Pett, J. P., Honma, S., Honma, K.-I., et al. (2019). Weak coupling between intracellular feedback loops explains dissociation of clock gene dynamics. *PLoS Comput. Biol*. 15:e1007330. doi: 10.1371/journal.pcbi.1007330

Shell, G., Lang, A., and Sale, P. (1974). Quantitative measures of leaf orientation and heliotropic response in sunflower, bean, pepper and cucumber. *Agric. Meteorol*. 13, 25–37. doi: 10.1016/0002-1571(74)90062-4

Skeldon, A. C., Derks, G., and Dijk, D.-J. (2016). Modelling changes in sleep timing and duration across the lifespan: changes in circadian rhythmicity or sleep homeostasis? *Sleep Med. Rev*. 28, 96–107. doi: 10.1016/j.smrv.2015.05.011

Skeldon, A. C., Phillips, A. J., and Dijk, D.-J. (2017). The effects of self-selected light-dark cycles and social constraints on human sleep and circadian timing: a modeling approach. *Sci. Rep*. 7:45158. doi: 10.1038/srep45158

Spoelstra, K., Albrecht, U., van der Horst, G. T. J., Brauer, V., and Daan, S. (2004). Phase responses to light pulses in mice lacking functional per or cry genes. *J. Biol. Rhythms* 19, 518–529. doi: 10.1177/0748730404268122

Tokuda, I. T., Ono, D., Ananthasubramaniam, B., Honma, S., Honma, K.-I., and Herzel, H. (2015). Coupling controls the synchrony of clock cells in development and knockouts. *Biophys. J*. 109, 2159–2170. doi: 10.1016/j.bpj.2015.09.024

Vandenbrink, J. P., Brown, E. A., Harmer, S. L., and Blackman, B. K. (2014). Turning heads: the biology of solar tracking in sunflower. *Plant Sci*. 224, 20–26. doi: 10.1016/j.plantsci.2014.04.006

Walmsley, L., Hanna, L., Mouland, J., Martial, F., West, A., Smedley, A. R., et al. (2015). Colour as a signal for entraining the mammalian circadian clock. *PLoS Biol*. 13:e1002127. doi: 10.1371/journal.pbio.1002127

Wever, R. (1964). Zum Mechanismus der biologischen 24-Stunden-Periodik: III. Mitteilung Anwendung der Modell-Gleichung. *Kybernetik* 2, 127–144. doi: 10.1007/BF00306797

Williams, C. T., Barnes, B. M., and Buck, C. L. (2015). Persistence, entrainment, and function of circadian rhythms in polar vertebrates. *Physiology* 30, 86–96. doi: 10.1152/physiol.00045.2014

Winfree, A. T. (1970). Integrated view of resetting a circadian clock. *J. Theor. Biol*. 28, 327–374. doi: 10.1016/0022-5193(70)90075-5

Winfree, A. T. (2001). *The Geometry of Biological Time, Vol. 12*. New York, NY: Springer Science & Business Media.

Woller, A., Duez, H., Staels, B., and Lefranc, M. (2016). A mathematical model of the liver circadian clock linking feeding and fasting cycles to clock function. *Cell Rep*. 17, 1087–1097. doi: 10.1016/j.celrep.2016.09.060

**Conflict of Interest:** The authors declare that the research was conducted in the absence of any commercial or financial relationships that could be construed as a potential conflict of interest.

frontiers in Physiology

ORIGINAL RESEARCH
published: 02 April 2020
doi: 10.3389/fphys.2020.00242

# Light and Temperature Synchronizes Locomotor Activity in the Linden Bug, *Pyrrhocoris apterus*

*Magdalena Maria Kaniewska[1,2], Hana Vaněčková[1], David Doležel[1,2]* and Joanna Kotwica-Rolinska[1]**

[1] *Institute of Entomology, Biology Centre of Academy of Sciences of the Czech Republic, České Budějovice, Czechia,*
[2] *Faculty of Science, University of South Bohemia, České Budějovice, Czechia*

Circadian clocks are synchronized with the external environment by light and temperature. The effect of these cues on behavior is well-characterized in *Drosophila*, however, little is known about synchronization in non-model insect species. Therefore, we explored entrainment of locomotor activity by light and temperature in the linden bug *Pyrrhocoris apterus* (Heteroptera), an insect species with a strong seasonal response (reproductive diapause), which is triggered by both photoperiod and thermoperiod. Our results show that either light or temperature cycles are strong factors entraining *P. apterus* locomotor activity. *Pyrrhocoris* is able to be partially synchronized by cycles with temperature amplitude as small as 3°C and more than 50% of bugs is synchronized by 5°C steps. If conflicting zeitgebers are provided, light is the stronger signal. Linden bugs lack light-sensitive (*Drosophila*-like) cryptochrome. Notably, a high percentage of bugs is rhythmic even in constant light (LL) at intensity ∼400 lux, a condition which induces 100% arrhythmicity in *Drosophila*. However, the rhythmicity of bugs is still reduced in LL conditions, whereas rhythmicity remains unaffected in constant dark (DD). Interestingly, a similar phenomenon is observed after temperature cycles entrainment. Bugs released to constant thermophase and DD display weak rhythmicity, whereas strong rhythmicity is observed in bugs released to constant cryophase and DD. Our study describes the daily and circadian behavior of the linden bug as a response to photoperiodic and thermoperiodic entraining cues. Although the molecular mechanism of the circadian clock entrainment in the linden bug is virtually unknown, our study contributes to the knowledge of the insect circadian clock features beyond *Drosophila* research.

**Keywords: circadian clock, *Pyrrhocoris apterus*, thermoperiod, photoperiod, synchronization, entrainment, constant light, temperature compensation**

OPEN ACCESS

***Edited by:***
*Charalambos P. Kyriacou, University of Leicester, United Kingdom*

***Reviewed by:***
*Taishi Yoshii, Okayama University, Japan*
*Carla V. Finkielstein, Virginia Tech, United States*
*Eran Tauber, University of Haifa, Israel*

****Correspondence:***
*David Doležel*
*david.dolezel@entu.cas.cz; dolezel@entu.cas.cz*
*Joanna Kotwica-Rolinska*
*askako@entu.cas.cz*

***Specialty section:***
*This article was submitted to Chronobiology, a section of the journal Frontiers in Physiology*

***Received:*** *10 December 2019*
***Accepted:*** *02 March 2020*
***Published:*** *02 April 2020*

***Citation:***
*Kaniewska MM, Vaněčková H, Doležel D and Kotwica-Rolinska J (2020) Light and Temperature Synchronizes Locomotor Activity in the Linden Bug, Pyrrhocoris apterus. Front. Physiol. 11:242. doi: 10.3389/fphys.2020.00242*

## INTRODUCTION

Majority of organisms experience periodic changes in the environment, such as daily alternations of light, dark and temperature. Circadian clocks are time-measuring mechanisms that evolved as an adaptation to prepare for these external changes and thus to anticipate events like sun dawn, the flowering of particular plants, or avoiding predators. Circadian clocks free run under constant conditions, such as constant darkness (DD), with periodicity close to 24 h. This free-running

period (tau, τ) remains almost constant over a physiologically relevant range of temperatures, a phenomenon termed "temperature compensation" (Dunlap et al., 2004). Some clock mutants show impaired temperature compensation, whereas other mutations are temperature-independent (Hamblen et al., 1998; Matsumoto et al., 1999; Rothenfluh et al., 2000; Singh et al., 2019).

Circadian clocks can (and need to) be synchronized with the environment. The strongest cues, the "zeitgebers" (from German Zeit: time, Geber: giver), are light-dark cycles (LD), and temperature cycles (TCs), but circadian clocks can also be synchronized by other cues including food availability and social interaction (Levine et al., 2002; Dunlap et al., 2004; Sharma and Chandrashekaran, 2005; Shaw et al., 2019).

The circadian clock of the fruit fly, *Drosophila melanogaster*, the premiere insect model, is very well understood at the genetic, molecular and anatomical levels. The clock consists of several interlocked transcriptional-translational feedback loops (reviewed in Hardin, 2011; Ozkaya and Rosato, 2012; Tataroglu and Emery, 2015). The light input is mostly mediated by protein CRYPTOCHROME (CRY), a deep brain photoreceptor expressed in clock neurons (Emery et al., 2000). However, flies with mutated or completely removed *cry* gene can be still synchronized by LD, although the synchronization requires more days (Stanewsky et al., 1998; Dolezelova et al., 2007). This second synchronization pathway involves opsins in the compound eyes, ocelli, and the Hofbauer-Buchner eyelet (for review on the light input see Helfrich-Förster, 2019).

In contrast to light entrainment, the mechanism underlying temperature synchronization is less understood. Moreover, temperature affects circadian timekeeping in different ways. While the τ is temperature compensated, the actual daily activity profile and phase are temperature-dependent. Periodic TCs can synchronize the clock, whereas temperature pulses and steps can reset its phase (Sharma and Chandrashekaran, 2005; Tomioka and Yoshii, 2006).

The daily activity profile reflects the life strategy of a specific species used for coping with the environment. Adults of *D. melanogaster* display clear bi-modal locomotor activity with mid-day siesta, although the behavioral pattern is more complex under natural conditions (Menegazzi et al., 2012; Vanin et al., 2012). At simplified regimes in a laboratory with constant temperature and alternation of LD without any ramp of light intensity and color, flies display clear morning and evening activity peaks. At 25°C and LD 12:12 the morning peak corresponds to light-on signal and the evening peak matches light-off. At 18°C, the morning peak is delayed and evening peak advances, whereas at 29°C the morning peak starts already during DD and the evening peak is delayed to DD (Majercak et al., 1999). A similar trend of centering activity to mid-day at low temperatures and spreading activity to morning and evening at high temperatures was reported for the house fly, *Musca domestica*, although the actual molecular mechanism behind the trend differs between *D. melanogaster* and *M. domestica* (Bazalova and Dolezel, 2017).

*Drosophila* behavioral rhythm can be entrained by TCs even in constant light (LL) and requires functional *norpA* and *nocte* genes (Glaser and Stanewsky, 2005). When conflicting TCs and LDs were applied, the light seems to be the dominant signal (Yoshii et al., 2010). However, detailed systematic comparison of conflicting zeitgebers revealed that the light dominates temperature for maximal misalignments, but smaller delays of LD relative to TCs lead to rhythms that predominantly follow the temperature cue. Notably, certain alignments of TCs and LD result in dramatic behavioral disruption during and even after exposure to sensory conflicts (Harper et al., 2016).

Although the circadian clock toolkit is remarkably conserved between the *D. melanogaster* and mammals, certain important differences exist. For instance, mammals lack photosensitive *Drosophila*-like CRY responsible for the light input, instead, two closely related non-photosensitive CRYs work as transcriptional repressors in the feedback loop (Kume et al., 1999). Interestingly, close inspection of insect circadian clocks revealed various combinations of mammalian-like CRY and *Drosophila*-like CRY in different insect species (Yuan et al., 2007; Tomioka and Matsumoto, 2010). In the present study, we explored the effect of the light and temperature cycles on the entrainment of the locomotor activity of the linden bug, *Pyrrhocoris apterus* (Heteroptera), insect species that lacks light-sensitive *Drosophila*-like CRY and instead contains mammalian-like CRY (Bajgar et al., 2013a,b).

The linden bug has been used to elucidate eco-physiological aspects of insect seasonality (Dolezel et al., 2007; Kostal et al., 2008; Ditrich et al., 2018), particularly the photoperiodically induced reproductive diapause (Saunders, 1983, 1987) and the hormonal regulation of this reproductive arrest (Hodkova, 1976; Smykal et al., 2014; Urbanova et al., 2016). The diapause is induced by short photoperiods during the last larval stages resulting in non-reproductive adults. Although *P. apterus* clearly distinguishes between long and short photoperiods at ambient temperature such as 25°C, the photoperiodic response curve is affected by temperature and shifts to longer photoperiods at low temperatures and to short photoperiods at high temperatures, respectively (Numata et al., 1993). Diapausing *P. apterus* females are characterized by reduced locomotor activity, with the activity peak advanced when compared to the activity of reproductive females (Hodkova et al., 2003). Comparable phase advance is observed in the locomotor activity of nymphs (Kotwica-Rolinska et al., 2017). Apart from this basic characterization of locomotor activity in reproductive and diapause animals, no information is available on the role of light and temperature in *P. apterus* circadian entrainment. Therefore, the goal of this study was to provide basic characterization of the linden bug locomotor activity under various thermoperiodic and photoperiodic regimes and to describe the effect of different zeitgebers on the circadian clock entrainment.

# MATERIALS AND METHODS

## Insect Rearing and Locomotor Activity Measurements

The colony of *P. apterus* from the Czech line Oldrichovec (Pivarciova et al., 2016) was maintained in the laboratory

under diapause-preventing conditions (photoperiod LD 18:6 and constant temperature 25°C). Males 3–5 days after adult ecdysis were individually transferred to the LAM (Large Activity Monitors, Trikinetics, Inc., Waltham, MA, United States), supplemented with food and water *ad libitum* and activity was recorded every 5 min during the entire experiments. Unless specified, bugs were entrained for 5 days to a new photo- and thermoregime. Afterward, bugs were released for 12 days into constant conditions (constant temperature with either constant darkness or constant light) to determine their τ. For assessing entrainment ability of *P. apterus* to temperature cycles, males were kept in specific entrainment conditions for 10 days. The actual temperature profile was recorded during the entire experiment by Drosophila Environmental Monitors (Trikinetics, Inc., Waltham, MA, United States). All activity measurements were performed in the Cooled Incubator Sanyo MIR-154 equipped with a built-in electronic timer. Temperature steps between cryophase and thermophase were completed within approximately 20 min and temperature fluctuations during experiments did not exceed ±0.5°C. Light intensity (∼white light, see **Supplementary Figure 1** for the spectrum) in LD and LL experiments was ∼400 lx.

## Locomotor Activity Analysis

Lomb-Scargle periodogram in ActogramJ (Schmid et al., 2011) was used to determine the rhythmicity of bugs and τ in constant conditions, and double-plotted actograms were further inspected by eye (Refinetti et al., 2007; Brown et al., 2019). Three categories were defined: (1) *Strongly rhythmic* males: periodogram peak crossed the significance line and PN value calculated by ActogramJ software was >65. (2) *Weakly rhythmic* males: periodogram peak crossed the significance line and PN values were within 35–65. (3) *Arrhythmic* males: periodogram peak either did not cross the significance line or periodogram peak crossed the significance line but PN value was <35 (Pivarciova et al., 2016).

Daily profile of locomotor activity was analyzed in ActogramJ software (Schmid et al., 2011). The activity of all rhythmic individuals in a particular group was averaged, smoothed (Gaussian smooth 3) and displayed as double-plotted actogram. The activity of the last entrainment day and first 2 days in constant conditions were plotted in 5 min resolution for average from all animals in the experiment without any smoothing. For comparison of the activity phase at 21.5°C, the activity of all measured individuals was averaged to 1-h bins and plotted without any smoothing.

Ability to synchronize locomotor activity to TCs was assessed from 10-day recordings under constant dark and long thermoperiod consisting of 18 h of thermophase and 6 h of cryophase differing by 1, 3, 5, or 7°C (18–19, 18–21, 18–23, 18–25, 24–25, 22–25, and 20–25°C). Periodic locomotor activity was determined by the Chi-square periodogram algorithm in ActogramJ (Schmid et al., 2011). If analyses showed significant rhythm of 24 h (±15 min) and actograms passed visual confirmation, males were considered as "synchronized." The reference locomotor activity under constant dark at 18 or 25°C was analyzed analogously with Chi-square periodogram.

## Statistical Analysis

The differences between τ were tested for statistical significance by *t*-test and Kruskal–Wallis test with Dunn's *post hoc* test using Graphpad7 software (Prism, La Jolla, CA, United States).

# RESULTS

## *Pyrrhocoris apterus* Locomotor Activity Is Synchronized by Light and Temperature Cycles

The first experiments addressed if the locomotor activity of *P. apterus* can be synchronized by light or temperature. Since the Oldrichovec strain has τ longer than 24 h (Pivarciova et al., 2016), simple alignment of activity to 24 h zeitgebers reliably indicates the successful synchronization. Therefore, to simplify the assay, males developing at 25°C and LD 18:6 were transferred to a new regime where ZT0 corresponded to ZT0 during the development.

Data from individual bugs are very noisy. Until now we were not able to reliably determine the precise time of the locomotor activity onset, off-set or acrophase for a single bug, which is usually used for determining the exact phase of activity (Refinetti et al., 2007; Brown et al., 2019). Therefore, the average activity of all bugs was analyzed. Males exposed to LD 18:6 and constant 25°C are active during the majority of the photophase with a small delay of activity onset and anticipation of the light off (**Figure 1A**). The same photoperiod at a lower temperature (18°C) results in a narrower peak with the activity onset comparable to onset at 25°C, but the activity offset was 6 h before light off at 18°C (**Figure 1B**). When released to DD, the first activity cycle is clearly delayed at 18°C (compare **Figures 1A,B**) and the locomotion then continues rhythmically (**Figure 1B**). Locomotor activity is also clearly synchronized by TCs in DD (**Figure 1C**). Notably, the activity onset followed the temperature rise with only minimal delay and this early rise of activity is not observed in DD at a constant temperature. This startling behavior represents most probably a direct response to the temperature rise (masking effect). Although a majority of males were strongly rhythmic in DD, the τ values were quite dispersed after TC entrainment (**Figure 1E**), which resulted in a noisy average activity and thus the offset is visible only for the first two DD cycles. A synergistic combination of the photoperiodic and thermoperiodic entrainment (**Figure 1D**) synchronized locomotion with the onset during the photophase-thermophase comparable to the timing of the onset observed under LD at 25°C (**Figure 1A**). Interestingly, the startling effect to the temperature rise is absent in these conditions. The activity after all entrainment regimes continues rhythmically in DD with average τ longer than 24 h (**Figure 1E** and **Supplementary Table 1**) and shows no significant difference of the τ between bugs synchronized by different entraining protocols ($p > 0.05$ Kruskal–Wallis test). The τ values are quite dispersed in DD

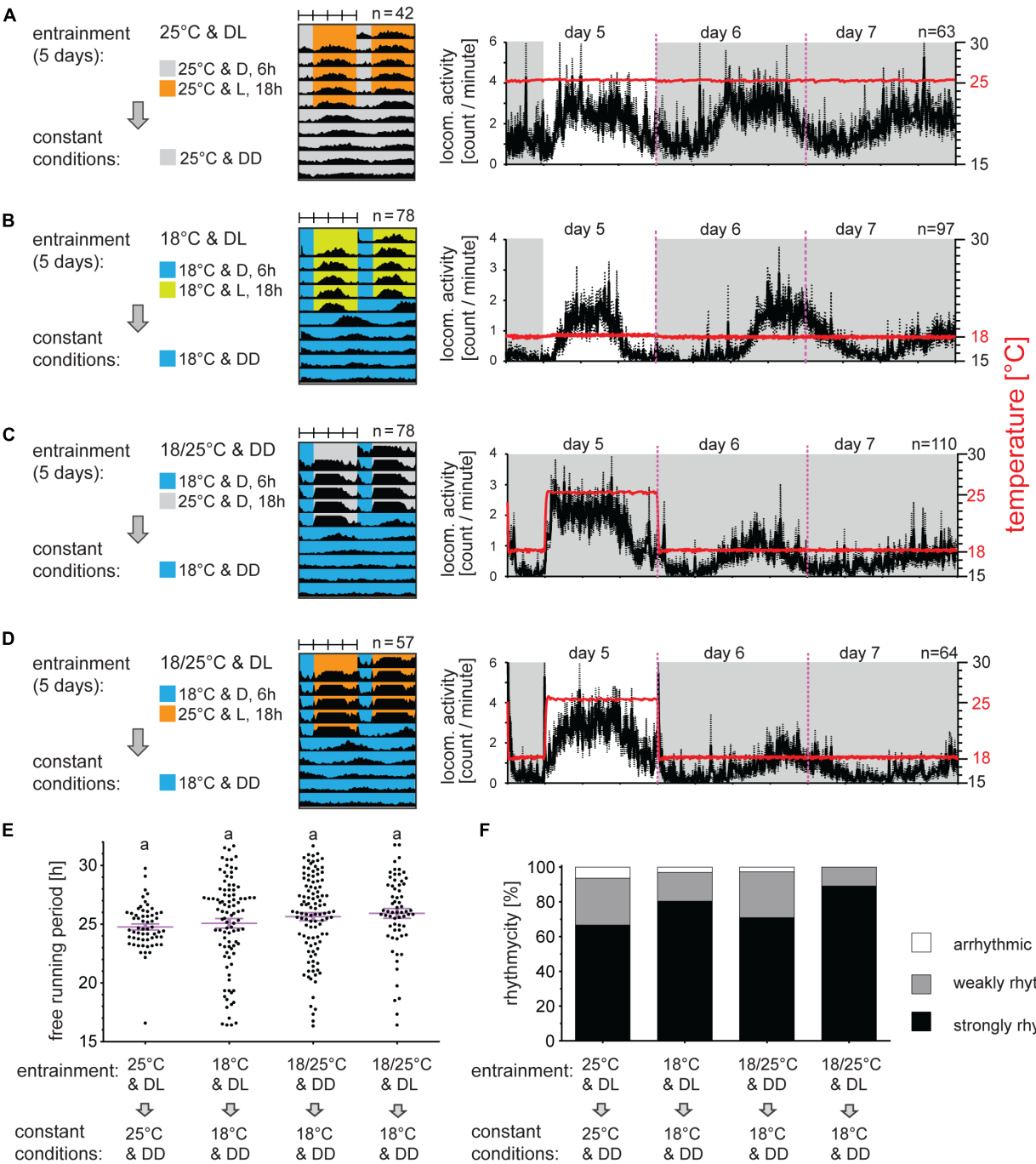


**FIGURE 1 |** Long periods of light and/or temperature synchronize locomotor activity in the linden bug, *Pyrrhocoris apterus*. Adult males raised under long photoperiod D6:L18 at 25°C were entrained for 5 days either by long photoperiods **(A,B)**, long thermoperiods **(C)**, or combination of both light and temperature **(D)** and released to constant dark at either 25°C **(A)** or 18°C **(B–D)**. Double-plotted actograms represent the average activity of all males rhythmic under DD conditions [see panel **(F)** for the rhythmicity]. Detailed activity profile is plotted from all males for day 5–7 [right panels in **(A–D)**]. The actual temperature recorded during the experiment is shown in red (right *y*-axis). The rhythmicity under constant conditions was determined from 10 days and is presented as the free-running period of each individual male (dots) and mean ± SEM shown in magenta **(E)**, there is no difference in the free-running period between groups ($p > 0.05$, Kruskal–Wallis). The same small letters above categories indicate no statistical difference. The percent of arrhythmic, weakly rhythmic and strongly rhythmic males is shown in panel **(F)**.

conditions at 18°C (**Figure 1E**) and extremely short (below 18 h) and long τ (above 30 h) are observed. The correlation analysis between significance level of the Lomb-Scargle periodogram (PN value) and τ (**Supplementary Figure 2**) shows that the shortened τ correlate weakly with the lower PN values (Spearman correlation $p < 0.001$, $r = -0.355$). We cannot rule out

that the extremely short τ could be a result of false-positive signal recognition from noise by the Lomb-Scargle periodogram algorithm (Zielinski et al., 2014). On the other hand, extremely long periods (τ > 30 h) do not show reduced power (PN) values (Spearman correlation $p > 0.05$, $r = 0.0823$) and eye-inspection further confirmed the presence of the long τ. Majority of bugs shows strong rhythmicity in DD and constant temperature after all entrainment regimes, with only a small portion of bugs being arrhythmic (**Figure 1F**). Combination of the photoperiodic and thermoperiodic entrainment produced the highest percentage of strongly rhythmic bugs in DD with no arrhythmic individuals (**Figure 1F**).

## Light Is a Stronger Signal Than Temperature

In the second set of experiments, males were entrained by short (12:12) photoperiodic and/or TCs. Males transferred from

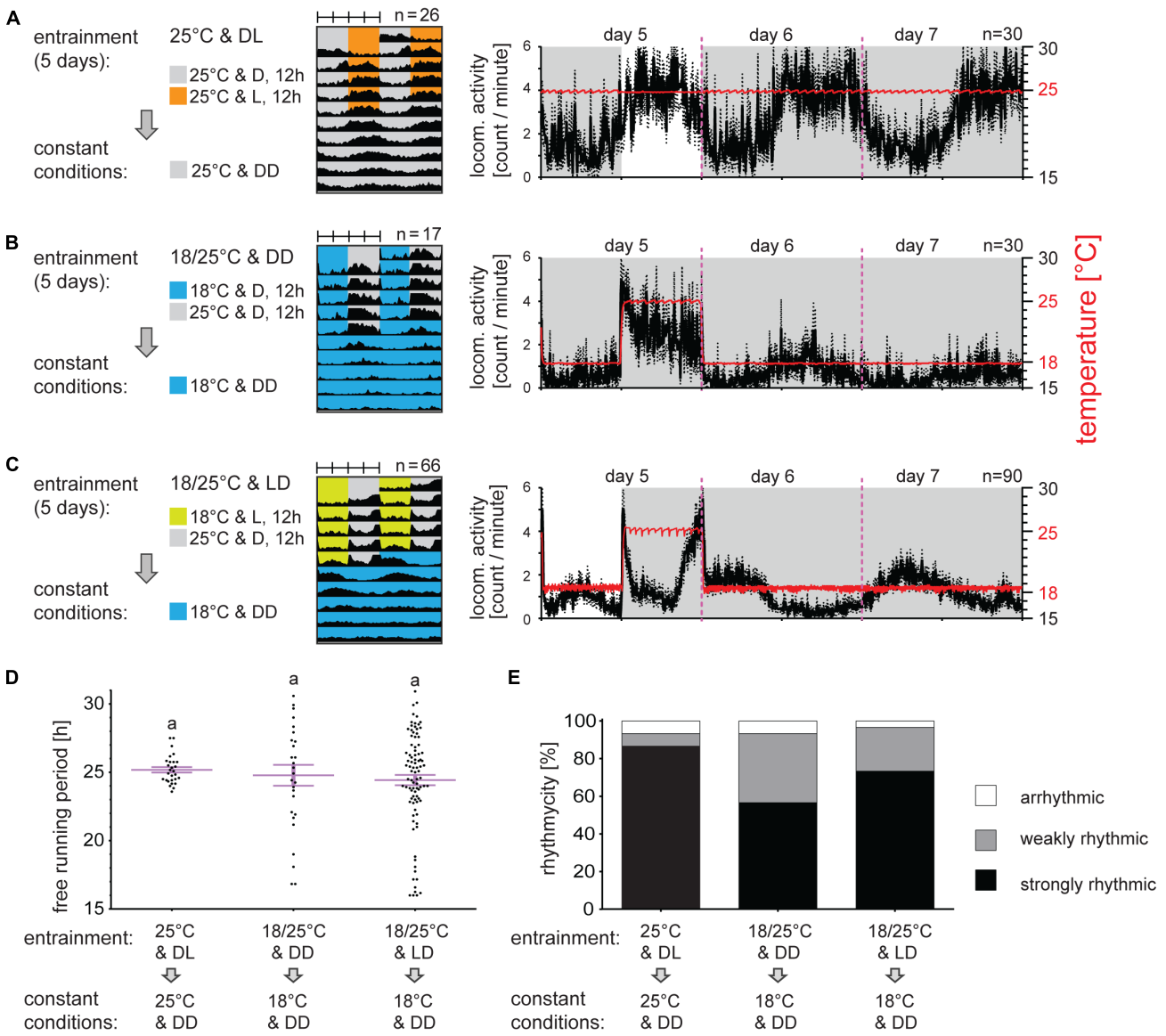


**FIGURE 2 |** Light is a stronger signal than the temperature for locomotor activity synchronization in *P. apterus*. Adult males developing under long photoperiod (D6:L18) were entrained by 5 days of short photoperiod D12:L12 **(A)**, short thermoperiod **(B)** or conflicting cycles of short photoperiod and thermoperiod where the photophase was combined with the cryophase and the thermophase was combined with the scotophase. After 5 day synchronization, males were released to DD at either 25°C **(A)** or 18°C **(B,C)**. Double-plotted actograms represent the average activity of all males rhythmic under DD conditions [see panel **(E)** for the rhythmicity]. Detailed activity profile is plotted from all males for day 5–7 (right panels in **(A–C)**). The actual temperature recorded during the experiment is shown in red (right *y*-axis). The rhythmicity under constant conditions was determined from 10 days and is presented as the free-running period of each individual male (dots) and mean ± SEM shown in magenta **(D)**, there is no difference in the free-running period between groups ($p > 0.05$, Kruskal–Wallis test). The same small letters above categories indicate no statistical difference. The percent of arrhythmic, weakly rhythmic and strongly rhythmic males is shown in panel **(E)**.

LD 18:6 to LD 12:12 and constant 25°C needed approximately two to three cycles for synchronization. The activity in LD 12:12 then covered the entire photophase starting during the scotophase and the activity continued in phase during DD (**Figure 2A**). Under short TC, locomotor activity raised immediately with temperature (**Figure 2B**). Conflicting LD and TC regime (photophase combined with cryophase, and scotophase matching thermophase) resulted in a very mild peak during the photophase/cryophase and clearly bimodal activity during the beginning and end of scotophase/thermophase (**Figure 2C**). Release into constant conditions (DD and 18°C) clearly indicates that the activity phase corresponded to the photophase, thus the activity during the thermophase was clearly a masking effect (compare **Figures 2A–C**). Different cycling condition, even conflicting LD and TC regime did not affect bugs rhythmicity nor the τ of their locomotor activity upon release into DD (**Figures 2D,E**).

## Thermophase Defines the Phase of Activity Under TC

To further characterize thermoperiodic entrainment, males were synchronized by long TC consisting of 18 h at 25°C and 6 h at 18°C. Consistently with TC-induced behavior described in **Figure 1C**, the activity raised immediately with temperature (**Figures 3A,B**). To determine if the phase of activity is influenced by the thermophase or cryophase, males were released to intermediate 21.5°C either from 25°C, or from 18°C (**Figures 3A,B**). Clearly, the activity phase corresponded to previous thermophase (**Figures 3E**) and no phase change is

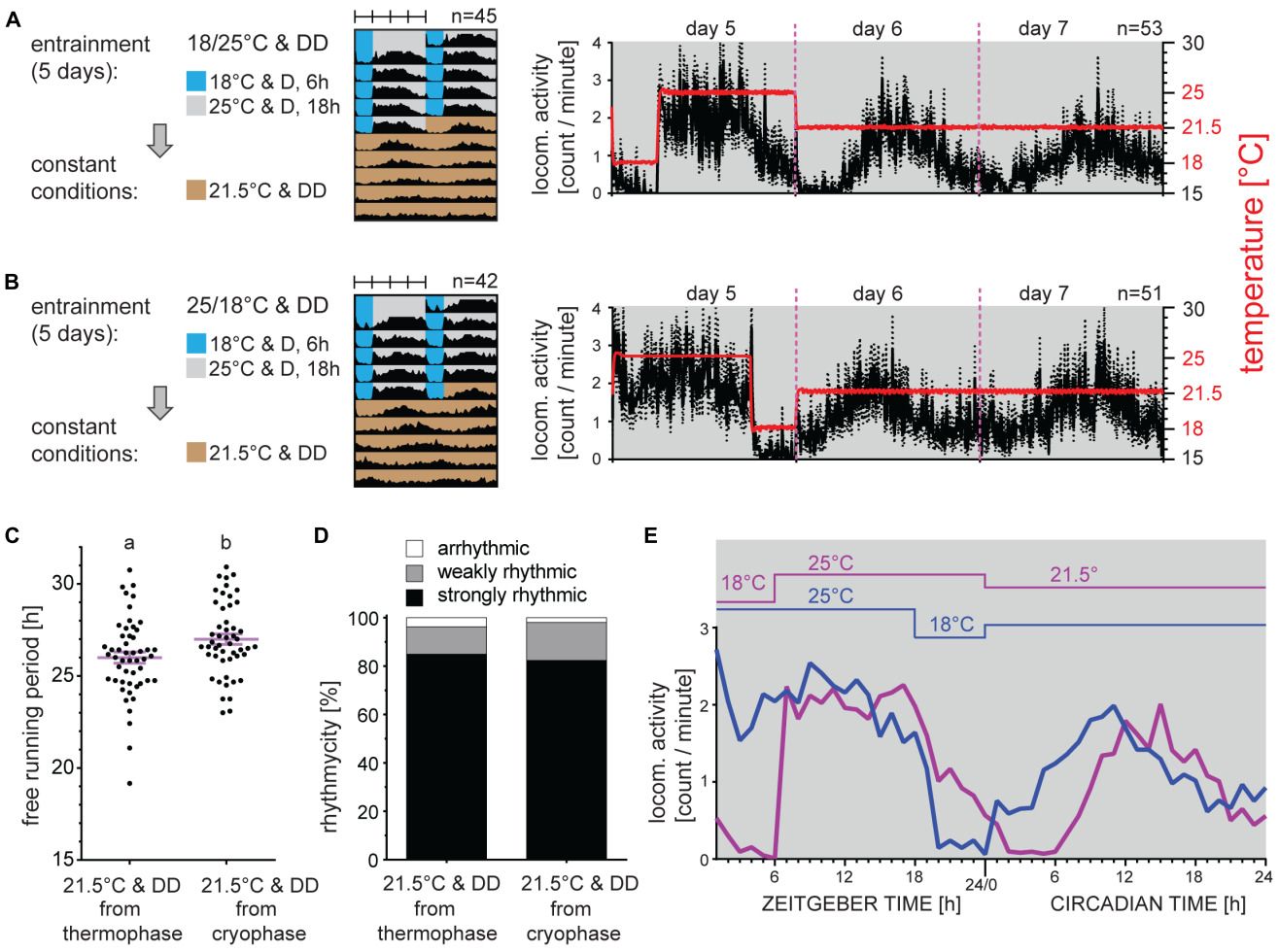


**FIGURE 3 |** Phase of activity is defined by the thermophase. Adult males developing under long photoperiod (D6:L18) were entrained by 5 days of constant dark and long thermoperiod 18:6 with thermophase at 25°C and cryophase at 18°C. Then, males were released to intermediate temperature (21.5°C) either from the thermophase **(A)** or from the cryophase **(B)**. Double-plotted actograms represent the average activity of all males rhythmic under constant conditions (see panel **(D)** for the percent rhythmicity). Detailed activity profile is plotted from all males for day 5–7 [right panels in **(A,B)**]. The actual temperature recorded during the experiment is shown in red (right *y*-axis). Detail activity profiles averaged into 1-h bin are shown for the last day of thermoperiodic entrainment and the first day of constant conditions **(E)**. The rhythmicity under constant conditions was determined from 10 days and is presented as the free-running period of each individual male (dots) and mean ± SEM shown in magenta **(C)**, where different small letter above categories indicate statistical difference $p < 0.05$ (*t*-test). The percent of arrhythmic, weakly rhythmic and strongly rhythmic males is shown in panel **(D)**.

observed in either of tested conditions, when compared to activity during the entrainment. Although the percent rhythmicity in DD was comparable in both groups, a small significant increase in τ was observed for males released from the thermophase (**Figures 3C,D**).

## Synchronization by TC

To determine the sensitivity of *P. apterus* to TC, males were released from LD to TC in the constant dark, where thermophase corresponded to the previous photophase. Since the majority of males have τ that differs from 24 h by more than 15 min (the very left data in **Figures 4A,B**), males with periodic activity within 24 h (±15 min) were considered as "synchronized." Clearly, 1°C range of TC is not sufficient to synchronize locomotion, whereas 3°C synchronized either ∼one quarter (18/21°C) or ∼40% (22/25°C) of males. The percent of synchronized males was higher with a higher difference between thermo- and cryophase, reaching up to ∼80% for the 7°C difference. Thus, temperature cycles of relatively high amplitude were even more potent for synchronizing bugs activity than LD cycles (intensity of light ∼400 lux), which synchronized only ∼60% of males.

## Locomotor Activity Can Be Synchronized by TC in Constant Light

To further test the capacity of TC in synchronization of *P. apterus* activity, males were exposed for 10 days to LL and TC. The activity rose immediately with the temperature during the thermophase and felt down during the cryophase, mimicking temperature cycles (**Figure 5A**). When exposed to LL and constant temperature, males at 25°C were more active than males at 18°C (**Figures 5B,C**). At an individual level, a significant portion of bugs displayed clear rhythm in LL and constant temperature (for the description of this behavior see the next chapter), however, their activity was not synchronized. This eventually resulted in a clearly arrhythmic locomotor activity pattern when the activity of all bugs was averaged (**Figures 5B,C**).

When bugs were kept in LL with TC and then released to constant DD and 18°C, τ of all rhythmic bugs was slightly longer (27.31 h) but not statistically different from bugs entrained by light:dark cycle (25.07 h) and/or TC (25.64 h) (**Figure 5D**). If only strongly rhythmic bugs were compared, τ after combined LL and TC entrainment was significantly different from all other groups (**Supplementary Figure 3**). Bugs released from LL without TCs as a synchronizing agent, showed clear and significant extension of τ (33.45 h if released from LL at 18°C and 35.76 h if released from LL at 25°C) (**Figure 5D**). In all cases, bugs released from LL were only rarely arrhythmic, and the majority of bugs were strongly rhythmic (**Figure 5E**).

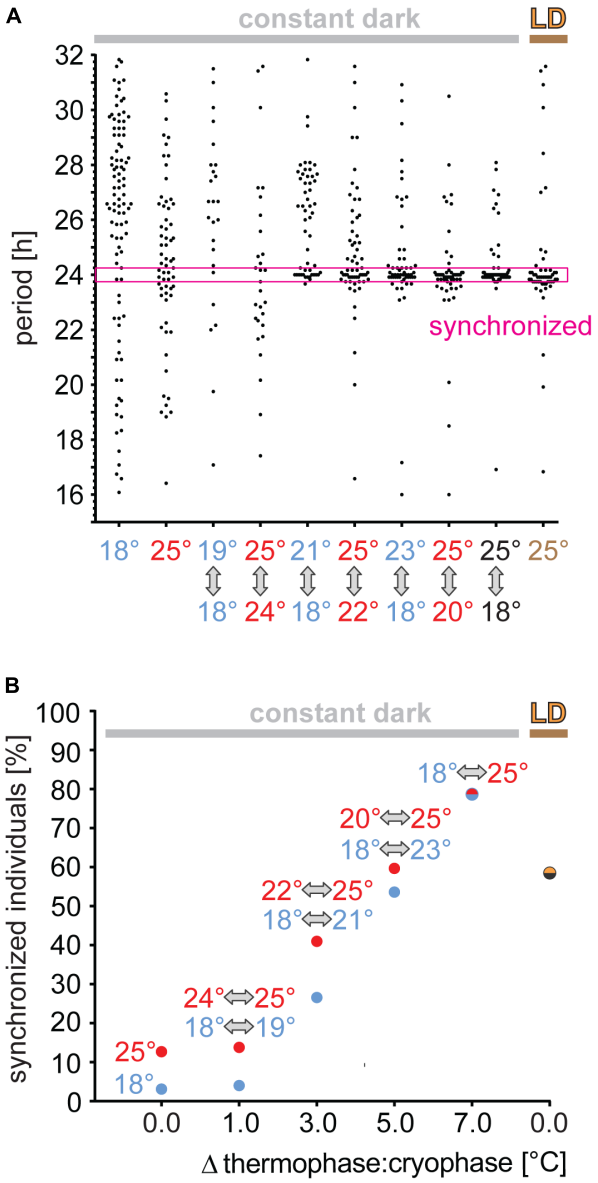


**FIGURE 4 |** Synchronization efficiency to thermoperiodic cycles depends on the temperature range. Adult males developing in long photoperiod (L18:D6) were released to thermoperiodic cycles (thermophase 18 h matched the previous photophase of LD) with 1, 3, 5, or 7°C steps. Periodicity of locomotor activity is determined from 10 days with chi-square algorithm and males with period 24 h (±15 min) are considered as synchronized [magenta window in panel **(A)**]. As a positive control, males synchronized by LD regime at a constant 25°C (brown) are used. As a reference, τ in constant DD at 18°C (blue) or at 25°C (red), respectively, are plotted. The percentage of synchronized males is shown for each temperature steps in panel **(B)**.

## Rhythmicity Is Impaired in Constant Light or Constant Thermophase Conditions

Given the relatively solid rhythmicity observed in LL, we sought to further explore activity resembling day versus night conditions. Males entrained to LD at 25°C and released to DD at 25°C were arrhythmic in 6.35% and weakly rhythmic in 26.98%. Release to LL from the same entrainment regime produces arrhythmicity in 17.86% and weak rhythm in 41.07%.

In the following experiment, males were entrained by TCs and released either to constant cryophase or to constant thermophase. The percent rhythmicity of males at cryophase (2.73% arrhythmic, 26.36% weakly rhythmic) were comparable

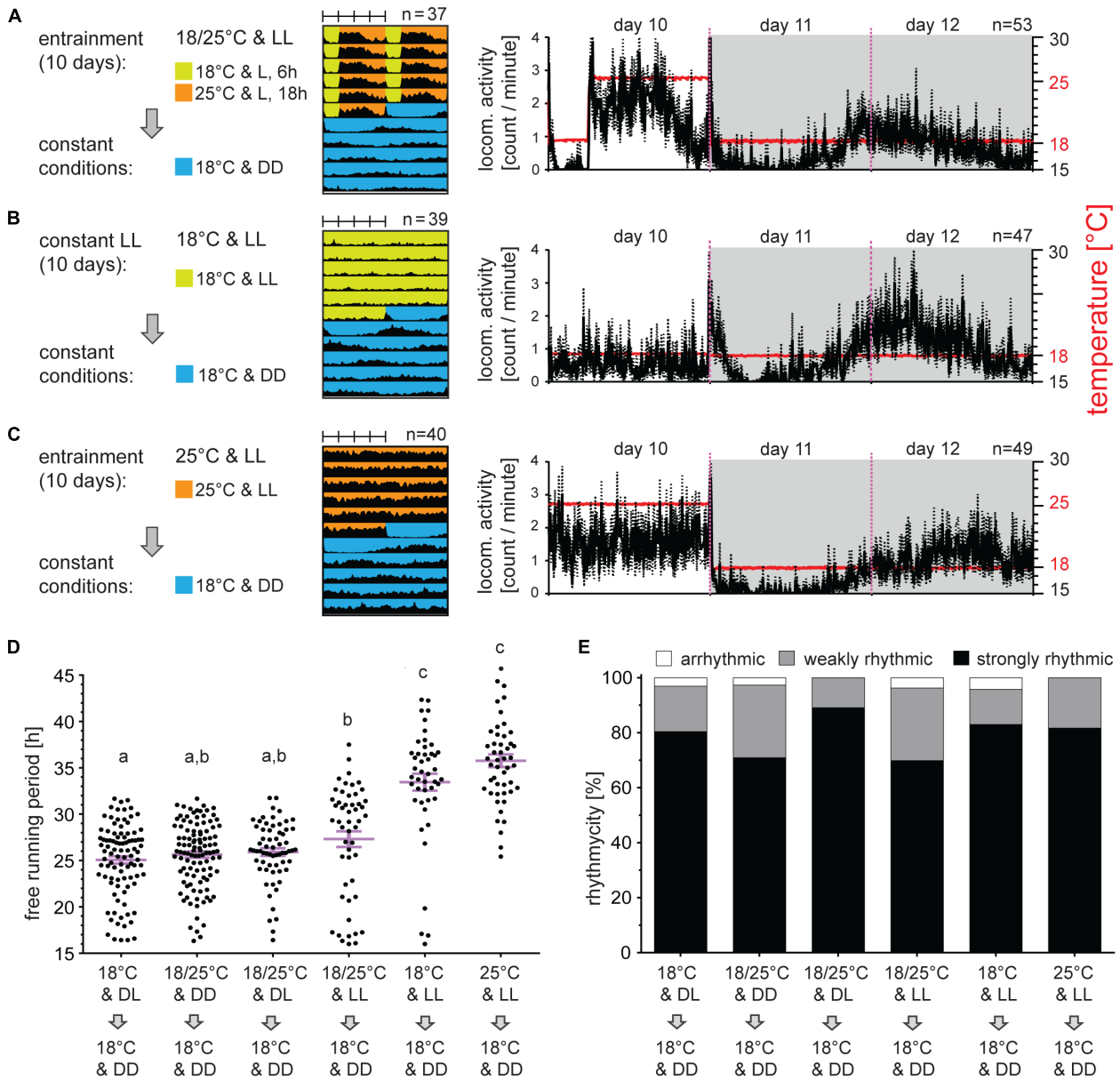


**FIGURE 5 |** Locomotor activity can be synchronized by temperature cycles in constant light. Adult males developed under long photoperiod (D6:L18) and were exposed either to 10 days of constant light and 18°C or 25°C [panels **(B,C)**, respectively] or to constant light and long thermoperiod **(A)**. Afterward, males were released to constant DD at 18°C. Double-plotted actograms represent the average activity of all males rhythmic under DD conditions [see panel **(D)** for the rhythmicity]. Detailed activity profile is plotted from all males for day 10–12 [right panels in **(A–C)**]. The actual temperature recorded during the experiment is shown in red (right *y*-axis). The rhythmicity under constant conditions was determined from 10 days and is presented as the free-running period of each individual male (dots) and mean ± SEM shown in magenta **(D)**, where different small letter above categories indicate statistical difference $p < 0.05$ (Kruskal–Wallis test with Dunn's *post hoc* test). The percent of arrhythmic, weakly rhythmic and strongly rhythmic males is shown in panel **(E)**.

to rhythmicity in DD at 25°C, whereas males released to thermophase showed reduced rhythmicity (26.37% arrhythmic, 31.87% weakly rhythmic), similarly to rhythmicity in LL at 25°C (**Figure 6B** and **Supplementary Table 1**).

The mean τ is significantly longer in constant cryophase than in constant thermopase after thermoperiodic entrainment (25.64 h at 18°C & DD versus 24.31 h at 25°C & DD). Similar, but the non-significant trend is observed in case of photoperiodic entrainment (24.76 h at 25°C and DD versus 24.31 h at 25°C and LL) (**Figure 6A** and **Supplementary Table 1**).

## DISCUSSION

This study explored the role of photoperiod and thermoperiod as zeitgebers in *P. apterus* and clearly indicate that either light

or temperature is sufficient to synchronize their locomotor activity. Under TC conditions, the activity of bugs followed immediately the rise of temperature, resembling masking effect. Similar earlier onset of the activity with temperature cycles when compared to LD cycles was observed also in *Gryllus bimaculatus* (Kannan et al., 2019), honey bees (Moore and Rankin, 1993) and *D. melanogaster* (Boothroyd et al., 2007). *Drosophila* kept in reverse photo- and thermoperiod is active still during the photophase (without any increase in activity during scotophase), however, the evening peak is advanced by ∼5–6 h (Currie et al., 2009). The authors concluded that this effect apparently required interaction between the light- and temperature-dependent entrainment mechanisms because it produced an increase in activity at a time of day when neither light nor temperature elicited this effect on their own. In linden bug, the masking effect was particularly strong in conflicting zeitgebers, when bugs showed bi-modal activity during thermophase. However, when released to a constant temperature, the bi-modal disappeared and the activity peak corresponded and matched the almost negligible peak from the photophase (**Figure 2C**). In nature, these two zeitgebers act synergistically together in order to adjust the temporal activity to environmental conditions. When temperature and light cycles are aligned, linden bugs are showing orchestrated rhythmic activity without any periods of hyperactivity, a situation caused by rapid changes in the ambient temperature in the beginning and the end of the thermophase. Additionally, when both zeitgebers participate synergistically in the entrainment, the stability of the rhythm in constant darkness increases is characterized by an increased % of rhythmic bugs. When LD and TC were applied in maximal misalignment, light dominated temperature. Similarly, the dominance of light over temperature was reported for *Drosophila* (Yoshii et al., 2010) and for the cricket *G. bimaculatus* (Komada et al., 2015; Kannan et al., 2019).

In case of the cricket, this conclusion was obtained from the fact that crickets entrain to the new photoregime much faster (5 cycles) than to the new thermoregime (17 cycles). Here it is important to note that crickets have both type of cryptochromes: the mammalian-like CRY which functions as a transcription repressor, and the *Drosophila*-like CRY that should serve as an efficient light receptor (Tokuoka et al., 2017). It would be very interesting to see if the linden bug, which lacks *Drosophila*-like CRY (Bajgar et al., 2013b), has a lower sensitivity to light. Unfortunately, the relatively low and particularly noisy locomotor activity makes analysis of phase shifts (determining activity on-set, off-set or acrophase) at an individual level virtually impossible. However, the noisy activity records do not prevent reliable determination of the free-running period for individual bugs (Refinetti et al., 2007; Zielinski et al., 2014; Brown et al., 2019). In this context, it is remarkable that ∼40% of males were strongly rhythmic and another ∼40% weakly rhythmic in LL with an intensity of 400 lux (**Figure 6**), whereas even much weaker light intensities cause complete arrhythmicity in *Drosophila* (Saunders, 1997).

When linden bugs were released to DD after LL, the τ was prolonged up to 33.45 h. Similar observations, called after-effect of LL, were observed in mice, cockroaches and chaffinches (Pittendrigh, 1960; Aschoff, 1984). After several weeks in DD animal's τ shortens back to ∼24 h. The duration of our experimental set up in the linden bug did not allow us to determine the expected "return" of τ back to "normal" values observed in DD.

Thermocycles in LL can force linden bugs to align their activity to temperature changes. This involves a masking effect since insects, as ectothermic animals, are very sensitive to temperature. This masking effect was shown for temperature cycling to enforce the rhythmic activity of clock mutant flies in both LL and DD conditions (Yoshii et al., 2002). On the other hand, it was also shown in *Drosophila*, that temperature cycles in LL do not only provoke rhythmic activity but also synchronize molecular machinery of the clock (Glaser and Stanewsky, 2005; Currie et al., 2009). Are temperature cycles in LL conditions entraining the clock in the linden bugs? Different τ between bugs exposed to TC and bugs exposed to constant temperatures suggest that

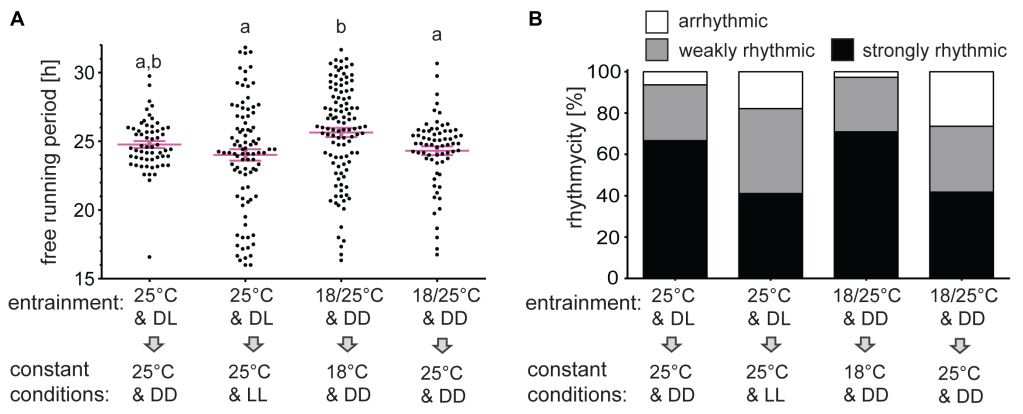


**FIGURE 6 |** Rhythmicity in constant "day" conditions is lower than in constant "night" conditions. Adult males were entrained for 5 days in long photoperiod regime D6:L18 at 25°C and released to DD or LL at 25°C. The second group of males was entrained to long thermoperiod 18°C/25°C in DD and then released to constant cryophase of 18°C or constant thermophase of 25°C. The percent of rhythmic males **(B)** and the free-running period **(A)** differ between groups. The different small letter above categories indicates statistical difference $p < 0.01$ (Kruskal–Wallis test with Dunn's *post hoc* test).

TC did not serve only as a synchronization cue in LL (note that at individual level linden bugs are often rhythmic in LL, but their activity is not synchronized between each other). τ of bugs synchronized by TC in LL is significantly shorter than τ of bugs from LL conditions, however, it still does not reach values observed in bugs synchronized by LD cycles or TC implemented in constant darkness (**Supplementary Table 1**). This observation shows that TC cycles can reduce, but not overcome the after-effect of LL signifying the notion of the stronger impact of the light on *P. apterus* circadian clock.

The rhythmicity of linden bug in different regimes can be approached from a different perspective. Although often rhythmic in LL, the deteriorating effect of the LL on the rhythmicity is clearly observed. The behavior is noisier which is revealed in our quantitative analysis as a higher percentage of weakly rhythmic individuals. The same situation occurs when TCs are used as entraining cues and then bugs are released to the constant thermophase. Because light phase and higher temperature are conditions which bugs are experiencing during the day, we hypothesize that constant "day-like" conditions are in some manner disruptive for the function of the clock. This effect is relatively mild, because rhythmicity of only some portions of animals was affected in this experimental setup. Interestingly, bugs which are still rhythmic in constant thermophase after TC entrainment maintain τ close to 24 h, which shows that the temperature compensation of the clock is not affected. To our knowledge, there is no report in the literature of the constant thermophase to be equivalent to LL conditions. Contrary, two *Drosophila* studies, which had identical experimental set up like ours, showed that releasing flies to constant thermophase after TC entrainment did not affect their rhythmicity (Boothroyd et al., 2007; Currie et al., 2009).

Alternative explanation for observed behavior could be that the high temperature step-up could affect the clock function. Somewhat related observation of the impact of the relative temperature on the functionality of the clock was described in one of *Drosophila* studies. Yoshii et al., 2007 showed that, while single temperature step-down of 10°C can evoke several cycles of behavioral rhythmicity in wild type, $per^S$ and $per^L$ flies kept in LL, the single temperature step-up does not have this potential and all flies lines show arrhythmic behavior (Yoshii et al., 2007).

Difference between linden bug and *Drosophila* was revealed in other sets of experiments. When flies are released from TCs to a constant intermediate temperature, the phase of activity depends, if they were released from thermophase (phase delay) or cryophase (phase advance) (Currie et al., 2009). In the case of *P. apterus* we did not observe any change of the activity phase, and bugs clearly follow phase set up by the thermophase during the entraining conditions. Those results could suggest that for linden bug temperature entrainment works in a slightly different manner than for *Drosophila*, however underpinning mechanism of entrainment still needs to be elucidated.

Different insect species display different sensitivity to temperature cycling amplitude. For example, honeybees are not able to entrain to TCs with an amplitude below 10°C (Moore and Rankin, 1993), whereas *Drosophila* is able to entrain even to temperature oscillations of 1.5–4°C (Wheeler et al., 1993; Currie et al., 2009). Thus the 3–5°C minimal amplitude needed for synchronization of *P. apterus* seems to fit the range observed in insects.

Temperature can effectively synchronize behavior and produce periodic activity patterns even in circadian clock mutants $per^{01}$, $tim^{01}$, and $cyc^{01}$, although the one-peak-profile determined in arrhythmic mutants clearly differs from the bi-modal activity characteristic for rhythmic flies (Currie et al., 2009). Similarly, rhythmic behavior was observed in natural conditions and was further confirmed in a semi-natural laboratory environment (Vanin et al., 2012).

Over the past few years, details of the molecular mechanism of the temperature entrainment of the *Drosophila* circadian clock started to be unveiled (Miyasako et al., 2007; Wolfgang et al., 2013; Maguire and Sehgal, 2015; Roessingh et al., 2019). It is however unknown, if the mechanisms described for *Drosophila* are universal for all insects. Thus, it will be interesting to explore the phenomenon of the temperature entrainment in the other insect models, like *P. apterus*, with circadian clock repertoire slightly different than *Drosophila* (Bajgar et al., 2013a,b) and with recently engineered circadian clock mutants (Kotwica-Rolinska et al., 2019).

## DATA AVAILABILITY STATEMENT

All datasets generated for this study are included in the article/**Supplementary Material**.

## AUTHOR CONTRIBUTIONS

JK-R designed the study with input from DD and MK. MK, JK-R, and HV performed the experiments. MK analyzed the results. DD wrote the manuscript with input from all authors.

## FUNDING

The work was supported by the European Research Council (ERC) under the European Union's Horizon 2020 Program Grant Agreement 726049. MK acknowledges support from the European Union's Horizon 2020 Research and Innovation Program under the Marie Skłodowska-Curie Grant Agreement No. 765937.

## ACKNOWLEDGMENTS

We would like to thank Nirav Takkar for proofreading the manuscript and all members of our laboratory for a warm, friendly and workaholic environment.

## SUPPLEMENTARY MATERIAL

The Supplementary Material for this article can be found online at: https://www.frontiersin.org/articles/10.3389/fphys.2020.00242/full#supplementary-material

## REFERENCES


Aschoff, J. (1984). Circadian timing. *Ann. NY. Acad. Sci.* 423, 442–468. doi: 10.1111/j.1749-6632.1984.tb23452.x

Bajgar, A., Dolezel, D., and Hodkova, M. (2013a). Endocrine regulation of non-circadian behavior of circadian genes in insect gut. *J. Insect Physiol.* 59, 881–886. doi: 10.1016/j.jinsphys.2013.06.004

Bajgar, A., Jindra, M., and Dolezel, D. (2013b). Autonomous regulation of the insect gut by circadian genes acting downstream of juvenile hormone signaling. *Proc. Natl. Acad. Sci. U.S.A.* 110, 4416–4421. doi: 10.1073/pnas.1217060110

Bazalova, O., and Dolezel, D. (2017). Daily activity of the housefly, *Musca domestica*, is influenced by temperature independent of 3' UTR period Gene Splicing. *G3 (Bethesda)* 7, 2637–2649. doi: 10.1534/g3.117.042374

Boothroyd, C. E., Wijnen, H., Naef, F., Saez, L., and Young, M. W. (2007). Integration of light and temperature in the regulation of circadian gene expression in *Drosophila*. *PLoS Genet.* 3:e54. doi: 10.1371/journal.pgen.0030054

Brown, L. A., Fisk, A. S., Pothecary, C. A., and Peirson, S. N. (2019). Telling the time with a broken clock: quantifying circadian disruption in animal models. *Biology (Basel)* 8:18. doi: 10.3390/biology8010018

Currie, J., Goda, T., and Wijnen, H. (2009). Selective entrainment of the *Drosophila* circadian clock to daily gradients in environmental temperature. *BMC Biol.* 7:49. doi: 10.1186/1741-7007-7-49

Ditrich, T., Janda, V., Vaneckova, H., and Dolezel, D. (2018). Climatic variation of supercooling point in the the linden bug *Pyrrhocoris apterus* (Heteroptera: Pyrrhocoridae). *Insects* 9:144. doi: 10.3390/insects9040144

Dolezel, D., Sauman, I., Kost'al, V., and Hodkova, M. (2007). Photoperiodic and food signals control expression pattern of the clock gene, period, in the linden bug, *Pyrrhocoris apterus*. *J. Biol. Rhythms* 22, 335–342. doi: 10.1177/0748730407303624

Dolezelova, E., Dolezel, D., and Hall, J. C. (2007). Rhythm defects caused by newly engineered null mutations in *Drosophila's cryptochrome* gene. *Genetics* 177, 329–345. doi: 10.1534/genetics.107.076513

Dunlap, J. C., Loros, J. J., and DeCoursey, P. J. (2004). *Chronobiology: Biological Timekeeping*. Sunderland, MA: Sinauer Associates.

Emery, P., Stanewsky, R., Helfrich-Forster, C., Emery-Le, M., Hall, J. C., and Rosbash, M. (2000). *Drosophila* CRY is a deep brain circadian photoreceptor. *Neuron* 26, 493–504. doi: 10.1016/s0896-6273(00)81181-2

Glaser, F. T., and Stanewsky, R. (2005). Temperature synchronization of the *Drosophila* circadian clock. *Curr. Biol.* 15, 1352–1363. doi: 10.1016/j.cub.2005.06.056

Hamblen, M. J., White, N. E., Emery, P., Kaiser, K., and Hall, J. C. (1998). Molecular and behavioral analysis of four period mutants in *Drosophila melanogaster* encompassing extreme short, novel long, and unorthodox arrhythmic types. *Genetics* 149, 165–178.

Hardin, P. E. (2011). Molecular genetic analysis of circadian timekeeping in *Drosophila*. *Adv. Genet.* 74, 141–173. doi: 10.1016/B978-0-12-387690-4.00005-2

Harper, R. E., Dayan, P., Albert, J. T., and Stanewsky, R. (2016). Sensory conflict disrupts activity of the *Drosophila* circadian network. *Cell Rep.* 17, 1711–1718. doi: 10.1016/j.celrep.2016.10.029

Helfrich-Förster, C. (2019). Light input pathways to the circadian clock of insects with an emphasis on the fruit fly *Drosophila melanogaster*. *J. Comp. Physiol. A Neuroethol. Sens. Neural Behav. Physiol.* [Epub ahead of print].

Hodkova, M. (1976). Nervous inhibition of corpora allata by photoperoid in *Pyrrhocoris apterus*. *Nature* 263, 521–523. doi: 10.1038/263521a0

Hodkova, M., Syrova, Z., Dolezel, D., and Sauman, I. (2003). *Period* gene expression in relation to seasonality and circadian rhythms in the linden bug, *Pyrrhocoris apterus* (Heteroptera). *Eur. J. Entomol.* 100, 267–273. doi: 10.14411/eje.2003.042

Kannan, N. N., Tomiyama, Y., Nose, M., Tokuoka, A., and Tomioka, K. (2019). Temperature entrainment of circadian locomotor and transcriptional rhythms in the cricket, *Gryllus bimaculatus*. *Zoolog. Sci.* 36, 95–104. doi: 10.2108/zs180148

Komada, S., Kamae, Y., Koyanagi, M., Tatewaki, K., Hassaneen, E., Saifullah, A., et al. (2015). Green-sensitive opsin is the photoreceptor for photic entrainment of an insect circadian clock. *Zoolog. Lett.* 1:11. doi: 10.1186/s40851-015-0011-6

Kostal, V., Tollarova, M., and Dolezel, D. (2008). Dynamism in physiology and gene transcription during reproductive diapause in a heteropteran bug, *Pyrrhocoris apterus*. *J. Insect Physiol.* 54, 77–88. doi: 10.1016/j.jinsphys.2007.08.004

Kotwica-Rolinska, J., Chodakova, L., Chvalova, D., Kristofova, L., Fenclova, I., Provaznik, J., et al. (2019). CRISPR/Cas9 genome editing introduction and optimization in the non-model insect *Pyrrhocoris apterus*. *Front. Physiol.* 10:891. doi: 10.3389/fphys.2019.00891

Kotwica-Rolinska, J., Pivarciova, L., Vaneckova, H., and Dolezel, D. (2017). The role of circadian clock genes in the photoperiodic timer of the linden bug, *Pyrrhocoris apterus*, during the nymphal stage. *Physiol. Entomol.* 42, 266–273. doi: 10.1111/phen.12197

Kume, K., Zylka, M. J., Sriram, S., Shearman, L. P., Weaver, D. R., Jin, X., et al. (1999). mCRY1 and mCRY2 are essential components of the negative limb of the circadian clock feedback loop. *Cell* 98, 193–205. doi: 10.1016/s0092-8674(00)81014-4

Levine, J. D., Funes, P., Dowse, H. B., and Hall, J. C. (2002). Resetting the circadian clock by social experience in *Drosophila melanogaster*. *Science* 298, 2010–2012. doi: 10.1126/science.1076008

Maguire, S. E., and Sehgal, A. (2015). Heating and cooling the *Drosophila melanogaster* clock. *Curr. Opin. Insect Sci.* 7, 71–75. doi: 10.1016/j.cois.2014.12.007

Majercak, J., Sidote, D., Hardin, P. E., and Edery, I. (1999). How a circadian clock adapts to seasonal decreases in temperature and day length. *Neuron* 24, 219–230. doi: 10.1016/s0896-6273(00)80834-x

Matsumoto, A., Tomioka, K., Chiba, Y., and Tanimura, T. (1999). timrit lengthens circadian period in a temperature-dependent manner through suppression of PERIOD protein cycling and nuclear localization. *Mol. Cell. Biol.* 19, 4343–4354. doi: 10.1128/mcb.19.6.4343

Menegazzi, P., Yoshii, T., and Helfrich-Forster, C. (2012). Laboratory versus nature: the two sides of the *Drosophila* circadian clock. *J. Biol. Rhythms* 27, 433–442. doi: 10.1177/0748730412463181

Miyasako, Y., Umezaki, Y., and Tomioka, K. (2007). Separate sets of cerebral clock neurons are responsible for light and temperature entrainment of *Drosophila* circadian locomotor rhythms. *J. Biol. Rhythms* 22, 115–126. doi: 10.1177/0748730407299344

Moore, D., and Rankin, M. N. (1993). Light and temperature entrainment of a locomotor rhythm in honeybees. *Physiol. Entomol.* 18, 271–278. doi: 10.1111/j.1365-3032.1993.tb00599.x

Numata, H., Saulich, A. H., and Volkovich, T. A. (1993). Photoperiodic responses of the linden bug, *Pyrrhocoris apterus*, under conditions of constant-temperature and under thermoperiodic conditions. *Zoolog. Sci.* 10, 521–527.

Ozkaya, O., and Rosato, E. (2012). The circadian clock of the fly: a neurogenetics journey through time. *Adv. Genet.* 77, 79–123. doi: 10.1016/B978-0-12-387687-4.00004-0

Pittendrigh, C. S. (1960). Circadian rhythms and the circadian organization of living systems. *Cold Spring Harb. Symp. Quant. Biol.* 25, 159–184. doi: 10.1101/sqb.1960.025.01.015

Pivarciova, L., Vaneckova, H., Provaznik, J., Wu, B. C., Pivarci, M., Peckova, O., et al. (2016). Unexpected geographic variability of the free running period in the linden bug, *Pyrrhocoris apterus*. *J. Biol. Rhythms* 31, 568–576. doi: 10.1177/0748730416671213

Refinetti, R., Lissen, G. C., and Halberg, F. (2007). Procedures for numerical analysis of circadian rhythms. *Biol. Rhythm Res.* 38, 275–325. doi: 10.1080/09291010600903692

Roessingh, S., Rosing, M., Marunova, M., Ogueta, M., George, R., Lamaze, A., et al. (2019). Temperature synchronization of the *Drosophila* circadian clock protein PERIOD is controlled by the TRPA channel PYREXIA. *Commun. Biol.* 2:246. doi: 10.1038/s42003-019-0497-0

Rothenfluh, A., Abodeely, M., Price, J. L., and Young, M. W. (2000). Isolation and analysis of six timeless alleles that cause short- or long-period circadian rhythms in *Drosophila*. *Genetics* 156, 665–675.

Saunders, D. S. (1983). A diapause induction termination asymmetry in the photoperiodic responses of the linden bug, *Pyrrhocoris apterus* and an effect of near-critical photoperiods on development. *J. Insect Physiol.* 29, 399–405. doi: 10.1016/0022-1910(83)90067-7

Saunders, D. S. (1987). Insect photoperiodism: the linden bug, *Pyrrhocoris apterus*, a species that measures daylength rather than nightlength. *Experientia* 43, 935–937. doi: 10.1007/bf01951677

Saunders, D. S. (1997). Insect circadian rhythms and photoperiodism. *Invert. Neurosci.* 3, 155–164. doi: 10.1007/bf02480370

Schmid, B., Helfrich-Forster, C., and Yoshii, T. (2011). A new imageJ plug-in "ActogramJ" for chronobiological analyses. *J. Biol. Rhythms* 26, 464–467. doi: 10.1177/0748730411414264

Sharma, V. K., and Chandrashekaran, M. K. (2005). Zeitgebers (time cues) for biological clocks. *Curr. Sci.* 89, 1136–1146.

Shaw, B., Fountain, M., and Wijnen, H. (2019). Control of daily locomotor activity patterns in *Drosophila suzukii* by the circadian clock, light, temperature and social interactions. *J. Biol. Rhythms* 734, 463–481. doi: 10.1177/0748730419869085

Singh, S., Giesecke, A., Damulewicz, M., Fexová, S., Mazzotta, G. M., Stanewsky, R., et al. (2019). New *Drosophila* circadian clock mutants affecting temperature compensation induced by targeted mutagenesis of timeless. *Front. Physiol.* 10:1442. doi: 10.3389/fphys.2019.01442

Smykal, V., Bajgar, A., Provaznik, J., Fexova, S., Buricova, M., Takaki, K., et al. (2014). Juvenile hormone signaling during reproduction and development of the linden bug, *Pyrrhocoris apterus*. *Insect Biochem. Mol. Biol.* 45, 69–76. doi: 10.1016/j.ibmb.2013.12.003

Stanewsky, R., Kaneko, M., Emery, P., Beretta, B., Wager-Smith, K., Kay, S. A., et al. (1998). The *cry(b)* mutation identifies cryptochrome as a circadian photoreceptor in *Drosophila*. *Cell* 95, 681–692. doi: 10.1016/S0092-8674(00)81638-4

Tataroglu, O., and Emery, P. (2015). The molecular ticks of the *Drosophila* circadian clock. *Curr. Opin. Insect Sci.* 7, 51–57. doi: 10.1016/j.cois.2015.01.002

Tokuoka, A., Itoh, T. Q., Hori, S., Uryu, O., Danbara, Y., Nose, M., et al. (2017). cryptochrome genes form an oscillatory loop independent of the *per/tim* loop in the circadian clockwork of the cricket *Gryllus bimaculatus*. *Zoolog. Lett.* 3:5. doi: 10.1186/s40851-017-0066-7

Tomioka, K., and Matsumoto, A. (2010). A comparative view of insect circadian clock systems. *Cell. Mol. Life Sci.* 67, 1397–1406. doi: 10.1007/s00018-009-0232-y

Tomioka, K., and Yoshii, T. (2006). Entrainment of *Drosophila* circadian rhythms by temperature cycles. *Sleep Biol. Rhythms* 4, 240–247. doi: 10.1111/j.1479-8425.2006.00227.x

Urbanova, V., Bazalova, O., Vaneckova, H., and Dolezel, D. (2016). Photoperiod regulates growth of male accessory glands through juvenile hormone signaling in the linden bug, *Pyrrhocoris apterus*. *Insect Biochem. Mol. Biol.* 70, 184–190. doi: 10.1016/j.ibmb.2016.01.003

Vanin, S., Bhutani, S., Montelli, S., Menegazzi, P., Green, E. W., Pegoraro, M., et al. (2012). Unexpected features of *Drosophila* circadian behavioural rhythms under natural conditions. *Nature* 484, 371–375. doi: 10.1038/nature10991

Wheeler, D. A., Hamblencoyle, M. J., Dushay, M. S., and Hall, J. C. (1993). Behavior in light dark cycles of *Drosophila* mutants that are arrhythmic, blind, or both. *J. Biol. Rhythms* 8, 67–94. doi: 10.1177/074873049300800106

Wolfgang, W., Simoni, A., Gentile, C., and Stanewsky, R. (2013). The Pyrexia transient receptor potential channel mediates circadian clock synchronization to low temperature cycles in *Drosophila melanogaster*. *Proc. Biol. Sci.* 280:20130959. doi: 10.1098/rspb.2013.0959

Yoshii, T., Fujii, K., and Tomioka, K. (2007). Induction of *Drosophila* behavioral and molecular circadian rhythms by temperature steps in constant light. *J. Biol. Rhythms* 22, 103–114. doi: 10.1177/0748730406298176

Yoshii, T., Hermann, C., and Helfrich-Forster, C. (2010). Cryptochrome-positive and -negative clock neurons in *Drosophila* entrain differentially to light and temperature. *J. Biol. Rhythms* 25, 387–398. doi: 10.1177/0748730410381962

Yoshii, T., Sakamoto, M., and Tomioka, K. (2002). A temperature-dependent timing mechanism is involved in the circadian system that drives locomotor rhythms in the fruit fly *Drosophila melanogaster*. *Zoolog. Sci.* 19, 841–850. doi: 10.2108/zsj.19.841

Yuan, Q., Metterville, D., Briscoe, A. D., and Reppert, S. M. (2007). Insect cryptochromes: gene duplication and loss define diverse ways to construct insect circadian clocks. *Mol. Biol. Evol.* 24, 948–955. doi: 10.1093/molbev/msm011

Zielinski, T., Moore, A. M., Troup, E., Halliday, K. J., and Millar, A. J. (2014). Strengths and limitations of period estimation methods for circadian data. *PLoS One* 9:e96462. doi: 10.1371/journal.pone.0096462

**Conflict of Interest:** The authors declare that the research was conducted in the absence of any commercial or financial relationships that could be construed as a potential conflict of interest.

frontiers in Physiology

ORIGINAL RESEARCH
published: 28 April 2020
doi: 10.3389/fphys.2020.00334

# Conceptual Models of Entrainment, Jet Lag, and Seasonality

*Isao T. Tokuda*[1], *Christoph Schmal*[2], *Bharath Ananthasubramaniam*[3] *and Hanspeter Herzel*[2,3]*

[1] Department of Mechanical Engineering, Ritsumeikan University, Kyoto, Japan, [2] Institute for Theoretical Biology, Humboldt Universität zu Berlin, Berlin, Germany, [3] Institute for Theoretical Biology, Charité—Universitätsmedizin Berlin, Berlin, Germany

Understanding entrainment of circadian rhythms is a central goal of chronobiology. Many factors, such as period, amplitude, *Zeitgeber* strength, and daylength, govern entrainment ranges and phases of entrainment. We have tested whether simple amplitude-phase models can provide insight into the control of entrainment phases. Using global optimization, we derived conceptual models with just three free parameters (period, amplitude, and relaxation rate) that reproduce known phenotypic features of vertebrate clocks: phase response curves (PRCs) with relatively small phase shifts, fast re-entrainment after jet lag, and seasonal variability to track light onset or offset. Since optimization found multiple sets of model parameters, we could study this model ensemble to gain insight into the underlying design principles. We found complex associations between model parameters and entrainment features. *Arnold* onions of representative models visualize strong dependencies of entrainment on periods, relative *Zeitgeber* strength, and photoperiods. Our results support the use of oscillator theory as a framework for understanding the entrainment of circadian clocks.

**Keywords: circadian rhythms, amplitude-phase model, parameter optimization, jet lag, phase response curve, entrainment, seasonality**

OPEN ACCESS

***Edited by:***
*Rodolfo Costa, University of Padova, Italy*

***Reviewed by:***
*Eva C. Winnebeck, Ludwig Maximilian University of Munich, Germany*
*Elizabeth B. Klerman, Harvard Medical School, United States*
*Luísa K. Pilz, Federal University of Rio Grande do Sul, Brazil*

***Correspondence:**
*Hanspeter Herzel*
*h.herzel@biologie.hu-berlin.de*

***Specialty section:***
*This article was submitted to Chronobiology, a section of the journal Frontiers in Physiology*

***Received:*** *18 November 2019*
***Accepted:*** *23 March 2020*
***Published:*** *28 April 2020*

***Citation:***
*Tokuda IT, Schmal C, Ananthasubramaniam B and Herzel H (2020) Conceptual Models of Entrainment, Jet Lag, and Seasonality. Front. Physiol. 11:334. doi: 10.3389/fphys.2020.00334*

## 1. INTRODUCTION

### 1.1. Entrainment and Oscillator Theory

The circadian clock can be regarded as a system of coupled oscillators. Examples include the neuronal network in the SCN (Hastings et al., 2018) and the "orchestra" of body clocks (Dibner et al., 2010). Furthermore, the intrinsic clock is entrained by *Zeitgebers*, such as light, temperature, and feeding. The concept of interacting oscillators (Van der Pol and Van der Mark, 1927; Kuramoto, 1984; Huygens, 1986; Strogatz, 2004) can contribute to the understanding of entrainment (Winfree, 1980). The theory of periodically driven self-sustained oscillators leads to the concept of "*Arnold* tongues" (Glass and Mackey, 1988; Pikovsky et al., 2003; Granada et al., 2009). *Arnold* tongues predict the ranges of periods and *Zeitgeber* strengths in which entrainment occurs (Abraham et al., 2010). The range of *Zeitgeber* periods over which entrainment occurs is called the "range of entrainment" (Aschoff and Pohl, 1978). If seasonal variations are also considered, the entrainment regions are termed "*Arnold* onions" (Schmal et al., 2015). Within these parameter regions, amplitudes and entrainment phases can vary drastically. Amplitude expansion due to external periodic driving is termed "resonance" (Duffing, 1918). Of central importance in chronobiology is the variability of the entrainment phase, since it allows the coordination of the intrinsic clock phase with the environment (Aschoff, 1960). Appropriate periods also provide evolutionary advantages (Ouyang et al., 1998; Dodd et al., 2005).

## 1.2. Phenomenological Amplitude-Phase Models

After the discovery of transcriptional feedback loops (Hardin et al., 1990), many mathematical models have focused on gene-regulatory networks (Forger and Peskin, 2003; Leloup and Goldbeter, 2003; Becker-Weimann et al., 2004). More recent models include many details of the transcriptional-translational feedback loops (Zhou et al., 2015; Bellman et al., 2018). However, most available data on phase response curves (PRCs) (Johnson, 1992), entrainment ranges (Aschoff and Pohl, 1978), and phases of entrainment (Rémi et al., 2010) are based on organismic data. Thus, it seems reasonable to study phenomenological models that are directly based on these empirical features. There is a long tradition of heuristic amplitude-phase models in chronobiology (Klotter, 1960; Wever, 1962; Pavlidis, 1973; Daan and Berde, 1978; Winfree, 1980; Kronauer et al., 1982).

Amplitude-phase models are quite generic and could be applied to any organism. We have adapted the entrainment features, discussed below in detail, to observed data of mammals (Daan and Aschoff, 1975; Reddy et al., 2002; Comas et al., 2006). Here, we have examined the capability of such heuristic amplitude-phase models to reproduce fundamental properties of circadian entrainment. To this end, we combine the traditional amplitude-phase modeling approach with recent oscillator theory and global optimization to identify minimal models that can reproduce essential features of mammalian clocks: PRCs with relatively small phase shifts (Honma et al., 2003), fast re-entrainment after jet lag (Yamazaki et al., 2000), and seasonal variability (Daan and Aschoff, 1975).

## 1.3. Entrainment Features and Model Constraints

Intrinsic periods of various organisms approximate in general the daylength of 24 h (Wyse et al., 2010). For example, *Neurospora* strains exhibit periods between 21 and 27 h (Lakin-Thomas et al., 1991; Merrow et al., 1999; Loros and Dunlap, 2001). Nocturnal rodents typically exhibit periods between 23 and 24 h in constant darkness (Pittendrigh and Daan, 1976a), whereas humans mostly exhibit periods slightly above 24 h (Wever, 1979; Czeisler et al., 1999). *Zeitgeber* signals, such as light, can accelerate or decelerate intrinsic rhythms leading to entrainment. PRCs quantify the amplitude and direction of phase shifts induced by *Zeitgeber* pulses (Wever, 1964; Johnson, 1992). In mammals, the strong coupling of SCN neurons constitutes a strong oscillator (Abraham et al., 2010; Granada et al., 2013), which has PRCs with relatively small phase shifts (Comas et al., 2006). Even bright light pulses of 6.7 h duration can shift the clock by just a few hours (Khalsa et al., 2003). These observations constitute the first constraint on our models. We assume that the maximal phase shifts are just 1 or 2 h.

Small phase shifts due to the *Zeitgeber* can lead to long transients of phase relaxation after jet lag (Kori et al., 2017). In many cases, a surprisingly fast recovery from jet lag is observed (Reddy et al., 2002; Vansteensel et al., 2003). These findings lead to our second model constraint. Along the lines of a previous optimization study (Locke et al., 2008), we request that our models reduce the jet lag-induced phase shift by 50 % within 2 days.

The third constraint refers to the well-known seasonal variability of circadian clocks (Pittendrigh and Daan, 1976b; Hazlerigg and Wagner, 2006; Rémi et al., 2010). It has been reported that phase markers can lock to dusk or dawn for varying daylengths. This implies that the associated phases change by 4 h, if we switch from 16:8 LD conditions to 8:16 LD conditions. Thus, we also optimize our models to exhibit such pronounced phase differences between 16:8 and 8:16 LD cycles.

After having introduced our model and the optimization procedure in the Methods section, we have tested whether or not simple amplitude-phase models can reproduce the three entrainment features discussed above.

# 2. METHODS

## 2.1. Optimization of the Amplitude-Phase Model

As a model of an autonomous circadian clock, we consider the following amplitude-phase oscillator (Glass and Mackey, 1988; Abraham et al., 2010):

$$\frac{dr}{dt} = \lambda r(A - r), \tag{1}$$

$$\frac{d\varphi}{dt} = \omega = \frac{2\pi}{\tau}. \tag{2}$$

The system is described in polar coordinates by radius $r$ and angle $\varphi$ and has a limit cycle with amplitude $A$ and angular frequency $\omega$ (or period $\tau$). Any perturbation away from the limit cycle will relax back with a relaxation rate $\lambda$. This oscillator model can be represented in cartesian $(x, y)$ coordinates as

$$\frac{dx}{dt} = -\lambda x(r - A) - \omega y + Z(t), \tag{3}$$

$$\frac{dy}{dt} = -\lambda y(r - A) + \omega x, \tag{4}$$

where $r = \sqrt{x^2 + y^2}$. The oscillator receives a *Zeitgeber* signal

$$Z(t) = \begin{cases} 1 & \text{if } t \mod T < \varkappa T \\ 0 & \text{otherwise}, \end{cases} \tag{5}$$

where $T$ represents the period of the *Zeitgeber* signal, and $\varkappa$ determines the photoperiod (i.e., fraction of time during $T$ hours when the lights are on). Amplitude-phase models provide the simplest mathematical framework to study limit cycle oscillations, which have been discussed in the context of circadian rhythms (Wever, 1962; Winfree, 1980; Kronauer et al., 1982).

The amplitude-phase model (1), (2) has three unknown parameters $\{A, \omega, \lambda\}$. These parameters were optimized to satisfy the model constraints described in 1.3. The parameter optimization is based on the minimization of a cost function. The cost function takes a set of parameters as arguments, evaluates the model using those parameters, and then returns a "score" indicating the goodness of fit. Scores may only be positive, where

a fit with score closer to zero represents a better fit. The cost function is given by

$$E(A,\omega,\lambda) = \frac{(T_e - 48\text{h})^2}{(24\text{h})^2} + \frac{(\Delta\varphi_{max} - 1\text{h})^2}{(1\text{h})^2} + \frac{(\Delta\psi - 4\text{h})^2}{(4\text{h})^2}, \quad (6)$$

where $T_e$, $\Delta\varphi_{max}$, and $\Delta\psi$ represent half-time to re-entrainment, maximum phase-shift, and seasonal phase variability, respectively. The denominators can be regarded as tolerated ranges. If the values of $T_e$, $\Delta\varphi_{max}$, and $\Delta\psi$ deviate 24, 1, and 4 h from their target values, a score of three results. All parameter sets discussed in this paper had optimized scores below 0.1, i.e., the constrains are well-satisfied. Below we describe in detail how our quantities $T_e$, $\Delta\varphi_{max}$, and $\Delta\psi$ were calculated.

When the circadian oscillator is entrained to the *Zeitgeber* signal, their phase difference $\psi = \Psi - \varphi$ ($\Psi = 2\pi t/T$: phase of the *Zeitgeber*) converges to a stable phase $\psi_e$, which is called the "phase of entrainment." The half-time to re-entrainment $T_e$ denotes the amount of time required for the oscillator to recover from jet lag. As the *Zeitgeber* phase is advanced by $\Delta\Psi$, the phase difference becomes $\psi = \psi_e + \Delta\Psi$. $T_e$ quantifies how long it takes until the advanced phase is reduced to less than half of the original shift due to jet lag (i.e., $|\psi - \psi_e| < 0.5\Delta\Psi$). In our computation, this quantity was averaged over 24 different times during the day, at which 6h-advanced jet lag was applied. Next, the seasonal phase variability, which quantifies variability of the phase of entrainment over photoperiod from long day (16:8 LD) to short day (8:16 LD), is computed as $\Delta\psi = \max_{\varkappa\in[1/3,2/3]}\psi_e - \min_{\varkappa\in[1/3,2/3]}\psi_e$. Finally, the maximum phase-shift is given by $\Delta\varphi_{max} = \max_{\varphi}|PRC(\varphi)|$, where $PRC(\varphi)$ represents PRC of the free-running oscillator, to which a 6 h light pulse is injected at its phase of $\varphi$.

To find optimal parameter values, the cost function was minimized by a particle swarm optimization algorithm (Eberhart and Kennedy, 1995; Trelea, 2003). Search ranges of the parameter values were set to $A\in[0,5]$, $\omega\in[2\pi/30\ \text{rad/h}, 2\pi/18\ \text{rad/h}]$, $\lambda\in[0\text{h}^{-1}, 0.5\text{h}^{-1}]$. Altogether 600 sets of parameter values were obtained. From the estimated parameters, the intrinsic period was obtained as $\tau = 2\pi/\omega$.

## 2.2. Simulations of Jet Lag, Phase Response, and Seasonality

**Figure 1** illustrates our modeling approach. In **Figure 1A**, the amplitude-phase equations (1) and (2) are visualized in the phase plane together with the driving *Zeitgeber* switching between 0 (dark) and 1 (light) for varying photoperiods. Two values of the amplitude relaxation rate λ illustrate how λ affects the decay of perturbations. Starting from an initial condition, a small relaxation rate gives rise to a long transient until its convergence to the limit cycle, while systems with large relaxation rates exhibit only a short transient. **Figure 1B** shows the oscillations in a 3-dimensional phase space. Two coordinates ($x$ and $y$) span the phase plane of the endogenous oscillator. The vertical axis represents the phase of the *Zeitgeber*. The dotted red line marks the periodically driven limit cycle. The jump from 24 to 0 h reflects simply the periodic nature of our daily time.

Interestingly, the relaxation after jet lag can be visualized as a transient convergence to the dotted red limit cycle via the black line after a 6 h phase change due to jet lag (blue arrow). Such a relaxation might be accompanied by amplitude changes (not apparent in the figure) and by steady phase shifts from day to day (note that the jump from 24 to 0 h is shifted day by day). After a few days, the dotted red line is approached, implying a vanishing jet lag. More conventional visualizations of the recovery from jet lag are given in **Figure 2**.

## 2.3. Global Sensitivity Analysis

To study the dependencies of the entrainment features on the model parameters, Sobol's global sensitivity analysis was carried out (Sobol, 1993, 2001; Morio, 2011). The global sensitivity indices computed by Monte Carlo simulations reveal how the input (model parameters) variability influences the variability in the output (entrainment features).

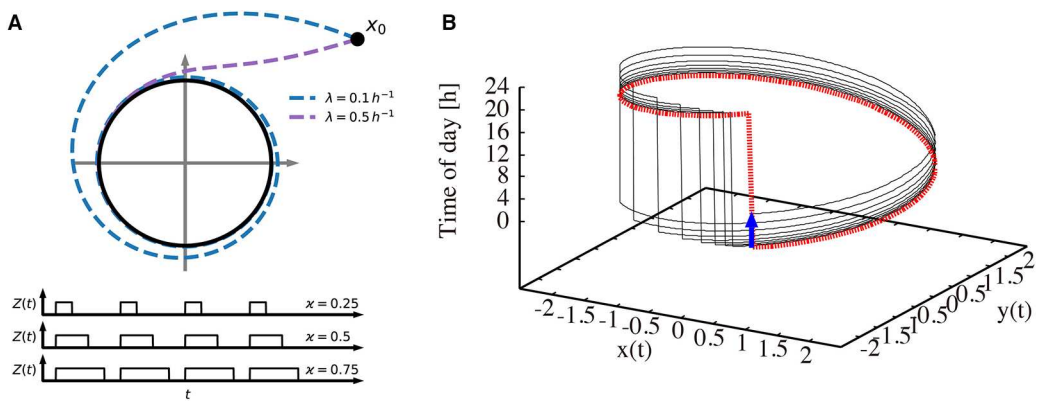


**FIGURE 1 |** Visualization of the amplitude-phase model. **(A)** Schematic illustration of the amplitude-phase oscillator model (top) *Zeitgeber* signals (bottom) of different photoperiods $\varkappa$. Starting from the initial condition $x_0$, a small relaxation rate ($\lambda = 0.1\ \text{h}^{-1}$) gives rise to a long transient until its convergence back to the limit cycle, while transients for large relaxation rates ($\lambda = 0.5\ \text{h}^{-1}$) are short. **(B)** The re-entrainment process of the oscillator after its phase is shifted by a 6 h-advanced jet lag (thin black line). The thick dotted red line represents the trajectory that the system converges to. The thick blue arrow indicates the 6 h jet lag.

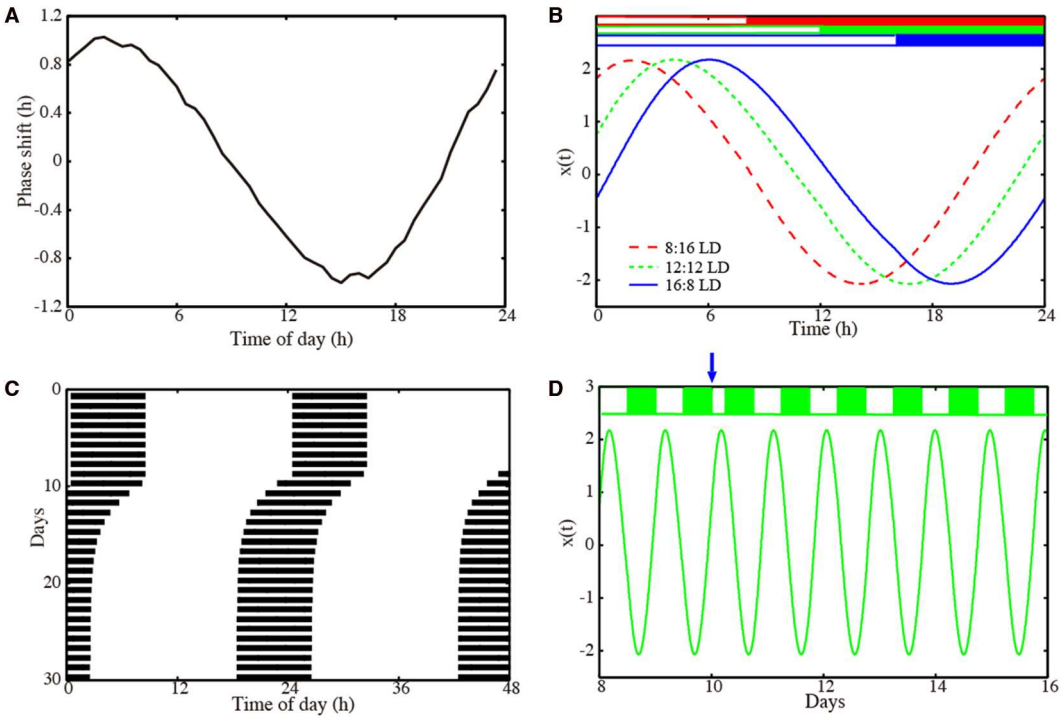


**FIGURE 2 |** Properties of our amplitude-phase model for a representative optimized parameter set. **(A)** Phase response curve with respect to a 6 h light pulse. **(B)** Waveforms $x(t)$ of the oscillator entrained to *Zeitgeber* signals with 8:16 LD (dashed red line), 12:12 LD (dotted green line), and 16:8 LD (solid blue line). **(C)** Actogram of the oscillator, to which a 6 h advancing jet lag was induced on day 10. **(D)** Time-trace $x(t)$ of the oscillators, to which a 6 h advancing jet lag was induced on day 10. Model parameters: $\tau = 23.36$ h, $A = 2.063$, $\lambda = 0.386$ h$^{-1}$ with $\omega = \frac{2\pi}{\tau}$.

We have denoted an entrainment feature (i.e., re-entrainment time $T_e$, maximum shift $\Delta\varphi_{max}$, or seasonal variability $\Delta\psi$) as $Y = \phi(X_1, X_2, X_3)$ using a scalar function $\phi : \mathbb{R}^3 \to \mathbb{R}$. The inputs $\{X_1, X_2, X_3\}$ stand for random variables that represent the model parameters $\{\tau, A, \lambda\}$, respectively. The random variables are assumed to be uniformly distributed. The first-order sensitivity indices $S_i$ for the input $X_i$ $(i = 1, 2, 3)$ are defined as $S_i = Var(E(Y|X_i))/Var(Y)$, where $Var$ and $E$ are variance and expectation, respectively. The second-order sensitivity indices $S_i$ for the inputs $X_i$ and $X_j$ are defined as $S_{ij} = \{Var(E(Y|X_i, X_j)) - Var(E(Y|X_i)) - Var(E(Y|X_j))\}/Var(Y)$. The total sensitivity indices $S_{T_i}$ for the input $X_i$ are finally given by $S_{T_i} = \sum_{k\#i} S_k$, where $\#i$ represents all the sets of indices that contain $i$ (e.g., $S_{T_1} = S_1 + S_{12} + S_{13} + S_{123}$). These indices quantify the influence of the different inputs on the variance of $Y$. In our study, the Sobol indices were estimated with Monte-Carlo methods, where the number of randomly generated samples to estimate the indices was set to $N = 10,000$.

# 3. RESULTS AND DISCUSSIONS

## 3.1. Models Reproduce PRC With Small Phase Shifts, Short Jet Lag, and Seasonality

We performed 200 successful parameter optimizations leading to an ensemble of parameter sets. We analyzed, in this section, the parameters with a PRC having 1 h delay and advance. In **Figures S1, S2**, we also present parameter sets obtained with a modified optimization: in that case, we requested a PRC with a 2 h delay and advance. **Figure 2** shows results for a representative model obtained via optimization. The PRC in **Figure 2A** is almost sinusoidal with maximal delays and advances of 1 h as requested by the optimization. Simulations with different photoperiods are shown in **Figure 2B**. It is evident that there are major phase shifts due to the varying photoperiods. The small-amplitude PRC implies that phase shifts by light are limited. Consequently, long transients after jet lag might be expected. Interestingly, **Figure 2C** visualizes a relatively fast recovery from jet lag. **Figure 2D** illustrates the re-entrainment after a jet lag applied on day 10. Note that no pronounced amplitude changes were observed.

It turns out that simple models with just three free parameters can successfully reproduce phenotypic features. In particular, fast recovery from jet lag for PRCs with quite small phase shifts is surprising. We next exploited the ensembles of parameter sets to understand the underlying principles.

## 3.2. Optimization Produced Highly Clustered Parameter Sets

In this section, we have focused on the 200 parameter sets with the $\pm 1$ h PRCs exemplified in **Figure 2** (see **Figure S1** for $\pm 2$ h PRCs).

The possible search ranges for our parameters were quite large (periods between 18 and 30 h, amplitudes between 0 and 5, and amplitude relaxation rates between 0 and 0.5$h^{-1}$). The histograms from the optimized parameter sets demonstrate that the search leads to quite specific values: periods of around $23.3 \pm 0.1$ h, amplitudes of about $2.1 \pm 0.04$, and large relaxation rates of $0.25 \pm 0.1\ h^{-1}$.

The optimized amplitude can be easily understood from the constraint on PRCs: for a given pulse strength the PRC shrinks monotonically with increasing amplitude (Pittendrigh, 1981; Vitaterna et al., 2006). A large amplitude of about 2.1 can be understood as a result of PRC having small phase shifts ($\pm 1$ h). In contrast, our optimizations with a $\pm 2$ h PRC lead to smaller amplitudes around $\pm 1.2$ (see **Figure S1b**).

Amplitude relaxation rates range between 0.07 and 0.5 $h^{-1}$. A value of 0.07 $h^{-1}$ corresponds to a half-life of amplitude perturbations of about 10 h, while a value of 0.5 $h^{-1}$ corresponds to a half-life of amplitude perturbations of about 1.4 h. Thus, all values in the histogram imply relatively fast amplitude relaxation. In Abraham et al. (2010), we termed limit cycles with fast amplitude relaxation "rigid oscillators." Interestingly, Comas et al. (2007) found that two light pulses separated by 10 h shift phases almost independently. This finding confirms earlier studies of double pulses (Pittendrigh and Daan, 1976b). These observations are consistent with fast amplitude relaxation rates. Jet lag leads to a specific type of transient (compare **Figure 1B**). Thus, it seems reasonable that fast amplitude relaxation helps to achieve short transients after a jet lag.

The most surprising result of our optimization is the narrow range of intrinsic periods. We have argued that specific periods allow appropriate seasonal flexibility (compare **Figure 4**). In short, at specific parts of *Arnold* onions (i.e., the entrainment regions in the $\varkappa$–$T$ parameter plane), the required 4 h phase differences were found to give a reasonable phase shifts between 16:8 LD and 8:16 LD. We emphasize that specific periods (23.36 h in **Figure 2**, 24.64 h in **Figure S2**, 23.48 h in **Figure S6**) were not fitted to specific organisms.

**Figure 3D** illustrates that the optimized parameter values are not independent. For instance, shorter periods are associated with larger amplitude. A possible explanation is that short periods imply larger effective pulse strength (a 6 h pulse is a larger part of a 23 h than a 24 h period) leading to larger amplitude in order to maintain the requested PRC amplitude.

In order to evaluate the robustness of our optimization approach, we generated also 200 parameter sets with PRCs with about a 2 h advance and delay. In these cases, we found intrinsic periods of $24.6 \pm 0.1$ h, amplitudes of $1.18 \pm 0.08$, and relaxation rates of $0.4 \pm 0.1\ h^{-1}$. The relaxation rates and amplitude-period correlations were similar to the results with PRCs of about 1 h advance and delay (compare **Figure 3** and **Figure S1**).

It should be noted that the PRC and the intrinsic period are in a trade-off relationship (**Figures S3l, S4l, S5l**). For a quick recovery from advanced jet lag, a short period ($< 24$ h) is advantageous, since the jet lag-induced phase shift is reduced everyday by the period difference to 24 h. A long period ($> 24$ h), on the other hand, requires a stronger *Zeitgeber* forcing and thus PRC with larger phase shifts, since the phase shift is otherwise increased by the period difference to 24 h. For this reason, $\pm 1$ h PRCs produced short periods, while $\pm 2$ h PRCs leaded to longer periods.

## 3.3. Complex Association Between Model Parameter and Entrainment Features

Our global optimization provided 200 sets of parameters $\{\tau, A, \lambda\}$ that reproduced the entrainment features of PRC with small phase shifts, fast recovery from jet lag, and high seasonal

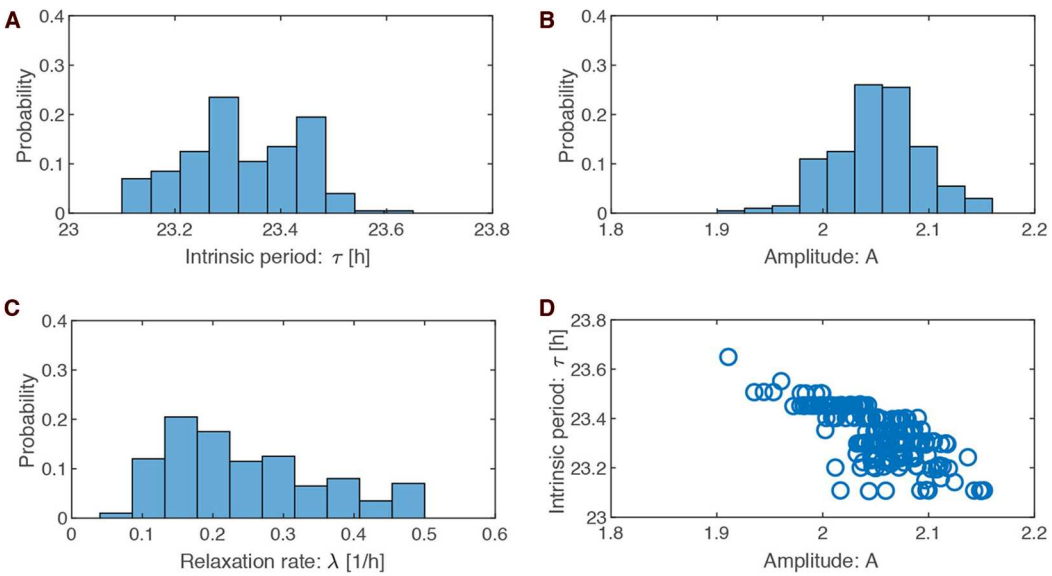


**FIGURE 3 |** Parameter values in the optimized ensemble. **(A–C)** Distributions of the optimized parameter values for intrinsic period $\tau$ ($= 2\pi/\omega$), oscillation amplitude $A$, and relaxation rate $\lambda$, respectively. **(D)** Scatter plots of amplitude $A$ against intrinsic period $\tau$ drawn for the 200 sets of optimized parameters.

variability. **Figures S3, S4** summarize the results for ±1 h PRCs and ±2 h PRCs, respectively. The upper 3 graphs show associations between the model parameters, illustrating that the parameters are not independent. The middle 9 graphs represent associations between the model parameters and the entrainment features (re-entrainment time $T_e$, maximum shift $\Delta\varphi_{max}$, seasonal variability $\Delta\psi$), while the lower 3 graphs display associations between the entrainment features. The resulting patterns are quite complex and depend on specific constraints.

Since the recovery time from jet lag varies strongly even for mice from the same strain (Evans et al., 2015), we also optimized models for 3 day re-entrainment time instead of 2 day. The resulting scatter plots in **Figure S5** reveal interesting changes: the intrinsic periods range from 23.4 h to 24.3 h and there exists a parameter set with a rather low relaxation time of 75 h. Thus, a relaxed jet lag constraint allows other periods and slow amplitude relaxation. Details regarding the parameter set with slow relaxation are provided in **Figure S6**. The recovery from jet lag is now accompanied by a small amplitude change as found in Goodwin models (Ananthasubramaniam et al., 2020) and the *Arnold* onion is less tilted as predicted (Schmal et al., 2015).

In order to quantify the complex associations of the model parameters and the entrainment features, we performed Sobol's global sensitivity analysis (Sobol, 1993, 2001; Morio, 2011). The strongest correlation was found between amplitude ($A$) and PRC size ($\Delta\varphi_{max}$), as expected (**Table 1**). Re-entrainment time ($T_e$) and seasonal variability ($\Delta\psi$) are influenced by all the model parameters ($\tau$, $A$, $\lambda$). Second-order sensitivities reveal that the relaxation rate ($\lambda$) effects re-entrainment time and seasonal variability in synergy with amplitude changes.

**TABLE 1 |** Sobol's global sensitivity analysis, showing dependence of the entrainment features (re-entrainment time: $T_e$, maximum shift: $\Delta\varphi_{max}$, seasonal variability: $\Delta\psi$) on the model parameters (intrinsic period: $\tau$, amplitude: $A$, relaxation rate: $\lambda$).

| | Parameters | Re-entrainment time ($T_e$) | Seasonality ($\Delta\psi$) | PRC size ($\Delta\varphi_{max}$) |
|---|---|---|---|---|
| Total | $\tau$ | 0.627 | 0.535 | 0.022 |
| Sensitivity | $A$ | 0.724 | 0.777 | 0.823 |
| $S_{T_i}$ | $\lambda$ | 0.335 | 0.295 | 0.006 |
| First-order | $\tau$ | 0.228 | 0.088 | 0.145 |
| Sensitivity | $A$ | 0.174 | 0.233 | 0.967 |
| $S_i$ | $\lambda$ | 0.077 | 0.085 | −0.012 |
| Second-order | $\tau$, $A$ | 0.262 | 0.383 | −0.118 |
| Sensitivity | $\tau$, $\lambda$ | −0.029 | 0.049 | 0.044 |
| $S_{ij}$ | $A$, $\lambda$ | 0.122 | 0.146 | 0.023 |

## 3.4. Arnold Onions Provide Insights Into the Optimized Parameters

To systematically investigate the impact of photoperiod ($\varkappa$) and Zeitgeber period ($T$) on entrainment properties, we analyze in **Figure 4** two *Arnold* onions for representative parameter sets with a short period and a ±1 h PRC as well as a large period and a ±2 h PRC. Interestingly, the *Arnold* onions are tilted, i.e., the DD periods (constant darkness at photoperiod $\varkappa = 0$) are smaller than the LL periods (constant light at photoperiod $\varkappa = 1$) as predicted by *Aschoff's rule* for nocturnal animals (Aschoff, 1960). The largest entrainment range is found around a photoperiod of $\varkappa = 0.5$ as predicted by Wever (1964). As expected, a larger PRC implies a wider range of entrainment (compare sizes of the *Arnold* onion in **Figures 4A,B**).

The phase of entrainment is color-coded in **Figure 4**. It is evident that the phases vary strongly with the *Zeitgeber* period $T$. There are theoretical predictions that phases change by about 12 h (Wever, 1964; Granada et al., 2013; Bordyugov et al., 2015) for different *Zeitgeber* periods. Interestingly, the variation

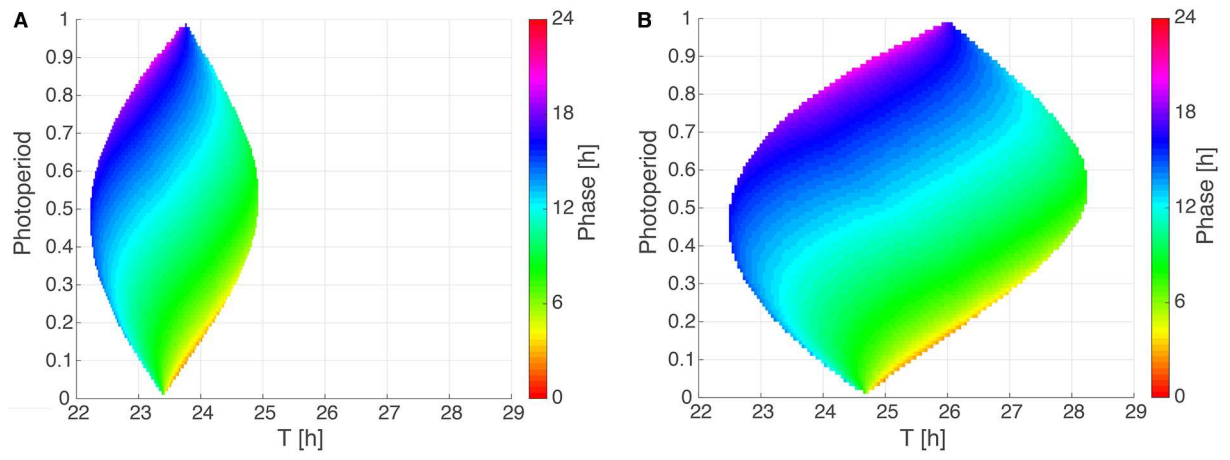


**FIGURE 4 |** *Arnold* onions for the two PRC constraints. **(A,B)** 1:1 entrainment ranges in the $\varkappa$-$T$ parameter plane (*Arnold* onions). Entrainment phases were determined by numerical simulations and have been color-coded within the region of entrainment. Panel **(A)** depicts an *Arnold* onion for an optimized parameter set with a ±1 h PRC, a short-period $\tau = 23.36$ h, $A = 2.063$, and $\lambda = 0.386$ h$^{-1}$. Panel **(B)** shows an *Arnold* onion for an optimized parameter set with a ±2 h PRC, a long–period $\tau = 24.64$ h, $A = 1.144$, $\lambda = 0.50$ h$^{-1}$.

of photoperiods in the vertical direction implies also very pronounced variations of the entrainment phase. Consequently, we could find many parameter sets with about 4 h phase shift between photoperiods of $\varkappa = 1/3$ (8:16 LD) and of $\varkappa = 2/3$ (16:8 LD).

# 4. CONCLUSIONS AND OUTLOOK

## 4.1. Optimized Models Reproduce Phenotypic Features

In most cases, the circadian clock of vertebrates is characterized by a relatively small type 1 PRC, by a narrow entrainment range, by fast recovery from jet lag, and by pronounced seasonal flexibility. We addressed whether or not these phenotypic features can be reproduced by simple amplitude-phase models with just three free parameters: period, amplitude, and relaxation time. To our surprise, we found many parameter sets via global optimization that reproduced the phenotypic features.

The availability of many parameter sets derived from random optimization allows extraction of essential properties of successful models. It turned out that the amplitude $A$ is adjusted to reproduce PRCs with small phase shifts for a given *Zeitgeber* strength $Z$. According to limit cycle theory (Pavlidis, 1969; Peterson, 1980), the strength of a perturbation is governed by the ratio $Z/A$ of *Zeitgeber* strength to amplitude. This implies that large limit cycles exhibit small phase shifts for a fixed *Zeitgeber* strength (Vitaterna et al., 2006).

In all suitable models, we found relatively fast amplitude relaxation rates with half-lives of perturbations below 10 h. This "rigidity" of limit cycles (Abraham et al., 2010) can support fast relaxation to the new phase after jet lag (compare **Figure 1B**). Double pulse experiments (Pittendrigh and Daan, 1976b; Comas et al., 2007) are consistent with fast relaxation rates.

In order to reproduce seasonality, we optimized our model under the constraint that 16:8 and 8:16 LD cycles have entrainment phases that are about 4 h apart from each other. This implies that the phase could follow dusk or dawn (Daan and Aschoff, 1975). In other words, we requested that the entrainment phase depends strongly on the photoperiod. As illustrated in **Figure 4**, such a strong dependency is indeed reproduced by our simple amplitude-phase models. Our optimization procedure selected specific periods that lead to a 4 h phase variation between photoperiods $\varkappa = 1/3$ and $\varkappa = 2/3$. Note that other periods can give large phase differences as well (compare the large vertical phase variations in **Figure 4**).

We have emphasized that our constraints were chosen to represent characteristic mammalian entrainment features: PRC with small phase shifts, relaxation from jet lag within a few days, and pronounced seasonal variability. Moreover, we based our constraints on light-pulse PRCs and considered only 6h-advanced jet lag. The observed increase of period with light intensity (compare **Figure 4**) resembles *Aschoff's rule* for nocturnal mammals.

Consequently, our results do not apply to clocks with type 0 PRCs and immediate phase resetting (Shaw and Brody, 2000; Devlin and Kay, 2001; Buhr et al., 2010). Furthermore, differences between phase advances and delays were not addressed. Other studies (Locke et al., 2005; Lu et al., 2016; Ananthasubramaniam et al., 2020) show that oscillator theory can also help to understand differences between advances and delays.

## 4.2. Relevance of Phenomenological Amplitude-Phase Models

Simplistic models as studied in this paper are quite generally applicable (Ananthasubramaniam et al., 2020). In principle, they could be used to describe single cells, tissue clocks, and organismic data. For single cells, damped stochastic oscillators can represent the observations also surprisingly well (Westermark et al., 2009). Such models have vanishingly small amplitudes and smaller relaxation rates, and they are driven by stochastic terms. Otherwise their complexity is comparable to our models discussed above.

The Poincaré model studied in this paper is particularly simple, since it has just three free parameters. Similar results on PRCs and entrainment have been described by other amplitude-phase models (Kronauer et al., 1982; Klerman et al., 1996; Flôres and Oda, 2020). The simplicity of our models implies that extensions are needed for fitting specific organisms and *Zeitgeber* profiles.

Complex models with multiple gene-regulatory feedback loops (Mirsky et al., 2009; Pokhilko et al., 2010; Relógio et al., 2011; Woller et al., 2016) could be reduced to amplitude-phase models simply by extracting periods, amplitudes, and relaxation rates from simulations. However, in such cases, the amplitudes are not uniquely defined since there are many dynamic variables.

## 4.3. How Can Circadian Amplitudes Be Defined?

This difficulty in defining amplitudes points to a general problem in chronobiology. Most studies focus on periods and entrainment phases. Limit cycle theory emphasizes that amplitudes are essential for understanding PRCs and entrainment. It is, however, not evident which amplitudes properly represent the limit cycle oscillator. Some studies consider gene expression levels (Lakin-Thomas et al., 1991; Wang et al., 2019) or reporter amplitudes (Leise et al., 2012), and other studies quantify activity rhythms (Bode et al., 2011; Erzberger et al., 2013). Since the ratio of *Zeitgeber* strength to amplitude $Z/A$ governs PRCs and entrainment phases, we suggest that amplitudes could be quantified indirectly: the stronger the response to physiological perturbations, the smaller the amplitude. This approach leads to the concept of strong and weak oscillators (Abraham et al., 2010; Granada et al., 2013). Strong oscillators are robust and exhibit small phase shifts and narrow entrainment ranges but large phase variability (Granada et al., 2013). In this sense, wild-type vertebrate clocks represent strong oscillators in contrast to single cell organisms or plants. Indeed, the review of Aschoff and Pohl (1978) demonstrates impressively these properties.

Interestingly, a reduction in relative amplitudes (i.e., amplitudes as a fraction of the mesor) can reduce jet lag drastically, since resetting signals are much more efficient (An et al., 2013; Jagannath et al., 2013; Yamazaki et al., 2013).

## 4.4. Arnold Onions Quantify Entrainment

As shown in **Figure 4**, *Arnold* onions represent entrainment ranges and phases of entrainment in a compact manner. Astonishingly, even quite basic models lead to really complex variations of entrainment phases. As expected, the period mismatch $T$-$\tau$ has a rather strong effect on the entrainment phase. This reflects the well-known feature that short intrinsic periods $\tau$ have earlier entrainment phases ("chronotypes") (Pittendrigh and Daan, 1976b; Merrow et al., 1999; Duffy et al., 2001). These associations are reflected in the horizontal phase variations in the *Arnold* onion. Interestingly, the vertical phase variability is also quite large. This observation demonstrates that also the effective *Zeitgeber* strength $Z/A$ and the photoperiod affect the phase of entrainment strongly. Consequently, the expected correlations between periods and entrainment phase could be masked by varying amplitudes, *Zeitgeber* strength, and photoperiods. In other words, chronotypes are governed by periods only if relative *Zeitgeber* strength and photoperiod are kept constant.

The complexity of entrainment phase regulation indicates that generic properties of coupled oscillators can provide useful insights in chronobiology. In particular, basic amplitude-phase models can help understand the control of jet lag and seasonality.

## DATA AVAILABILITY STATEMENT

All datasets generated for this study are included in the article/**Supplementary Material**.

## AUTHOR CONTRIBUTIONS

HH designed the study. IT performed the model simulations. IT, BA, CS, and HH discussed the results. HH wrote the main text. IT, BA, and CS revised the text.

## ACKNOWLEDGMENTS

The authors thank Serge Daan (†), Achim Kramer, and Adrian Granada for stimulating discussions. IT acknowledges financial support from the Japan Society for the Promotion of Science (JSPS) (KAKENHI Nos. 16K00343, 17H06313, 18H02477, 19H01002, and 20K11875). BA, CS, and HH acknowledge support from the Deutsche Forschungsgemeinschaft (DFG) (SPP 2041, TRR 186-A16, and TRR 186-A17). In addition, CS acknowledges support from the DFG (SCH3362/2-1) and the JSPS (PE17780).

## SUPPLEMENTARY MATERIAL

The Supplementary Material for this article can be found online at: https://www.frontiersin.org/articles/10.3389/fphys.2020.00334/full#supplementary-material

**Figure S1 |** Results of parameter optimization based on cost function $E(A,\omega,\lambda)=\frac{(T_e-48\text{h})^2}{(24\text{h})^2}+\frac{(\Delta\varphi_{max}-2\text{h})^2}{(1\text{h})^2}+\frac{(\Delta\psi-4\text{h})^2}{(4\text{h})^2}$, where ±2 h PRC was requested. **(a–c)** Distributions of the 200 optimized parameter sets for $\tau$ (24.6±0.1 h), $A$ (1.18±0.08), $\lambda$ (0.4±0.1 $\text{h}^{-1}$), respectively. **(d)** Scatter plots of amplitude $A$ against intrinsic period $\tau$ drawn for 200 sets of optimized parameters.

**Figure S2 |** Simulation of the amplitude-phase oscillator model using one of the 200 parameter sets optimized for a ±2 h PRC. **(a)** Phase response curve with respect to a 6 h light pulse. **(b)** Waveforms $x(t)$ of the oscillator entrained to *Zeitgeber* signals with 8:16 LD (dashed red line), 12:12 LD (dotted green line), and 16:8 LD (solid blue line). **(c)** Actogram drawn for the oscillator, to which a 6 h advancing jet lag was induced on day 10. **(d)** Time-trace $x(t)$ of the oscillators, to which a 6h advancing jet lag was induced on the 10th day. Parameter values: $\tau=24.64$ h, $A=1.144$, $\lambda=0.50\ \text{h}^{-1}$.

**Figure S3 |** Scatter plots for 200 data sets optimized for ±1 h PRC with cost function $E(A,\omega,\lambda)=\frac{(T_e-48\text{h})^2}{(24\text{h})^2}+\frac{(\Delta\varphi_{max}-1\text{h})^2}{(1\text{h})^2}+\frac{(\Delta\psi-4\text{h})^2}{(4\text{h})^2}$. **(a)** Amplitude $A$ vs. relaxation rate $\lambda$. **(b)** Amplitude $A$ vs. intrinsic period $\tau$. **(c)** Relaxation rate $\lambda$ vs. intrinsic period $\tau$. **(d)** Amplitude $A$ vs. re-entrainment time $T_e$. **(e)** Amplitude $A$ vs. phase variability $\Delta\psi$. **(f)** Amplitude $A$ vs. maximum PRC $\Delta\varphi_{max}$. **(g)** Relaxation rate $\lambda$ vs. re-entrainment time $T_e$. **(h)** Relaxation rate $\lambda$ vs. phase variability $\Delta\psi$. **(i)** Relaxation rate $\lambda$ vs. maximum PRC $\Delta\varphi_{max}$. **(j)** Intrinsic period $\tau$ vs. re-entrainment time $T_e$. **(k)** Intrinsic period $\tau$ vs. phase variability $\Delta\psi$. **(l)** Intrinsic period $\tau$ vs. maximum PRC $\Delta\varphi_{max}$. **(m)** Re-entrainment time $T_e$ vs. phase variability $\Delta\psi$. **(n)** Re-entrainment time $T_e$ vs. maximum PRC $\Delta\varphi_{max}$. **(o)** Phase variability $\Delta\psi$ vs. maximum PRC $\Delta\varphi_{max}$.

**Figure S4 |** Scatter plots for 200 data sets optimized for ±2 h PRC with cost function $E(A,\omega,\lambda)=\frac{(T_e-48\text{h})^2}{(24\text{h})^2}+\frac{(\Delta\varphi_{max}-2\text{h})^2}{(1\text{h})^2}+\frac{(\Delta\psi-4\text{h})^2}{(4\text{h})^2}$. **(a)** Amplitude $A$ vs. relaxation rate $\lambda$. **(b)** Amplitude $A$ vs. intrinsic period $\tau$. **(c)** Relaxation rate $\lambda$ vs. intrinsic period $\tau$. **(d)** Amplitude $A$ vs. re-entrainment time $T_e$. **(e)** Amplitude $A$ vs. phase variability $\Delta\psi$. **(f)** Amplitude $A$ vs. maximum PRC $\Delta\varphi_{max}$. **(g)** Relaxation rate $\lambda$ vs. re-entrainment time $T_e$. **(h)** Relaxation rate $\lambda$ vs. phase variability $\Delta\psi$. **(i)** Relaxation rate $\lambda$ vs. maximum PRC $\Delta\varphi_{max}$. **(j)** Intrinsic period $\tau$ vs. re-entrainment time $T_e$. **(k)** Intrinsic period $\tau$ vs. phase variability $\Delta\psi$. **(l)** Intrinsic period $\tau$ vs. maximum PRC $\Delta\varphi_{max}$. **(m)** Re-entrainment time $T_e$ vs. phase variability $\Delta\psi$. **(n)** Re-entrainment time $T_e$ vs. maximum PRC $\Delta\varphi_{max}$. **(o)** Phase variability $\Delta\psi$ vs. maximum PRC $\Delta\varphi_{max}$.

**Figure S5 |** Scatter plots for 200 data sets optimized for ±1 h PRC and 3 days re-entrainment time with cost function $E(A,\omega,\lambda)=\frac{(T_e-72\text{h})^2}{(24\text{h})^2}+\frac{(\Delta\varphi_{max}-1\text{h})^2}{(1\text{h})^2}+\frac{(\Delta\psi-4\text{h})^2}{(4\text{h})^2}$. **(a)** Amplitude $A$ vs. relaxation rate $\lambda$. **(b)** Amplitude $A$ vs. intrinsic period $\tau$. **(c)** Relaxation rate $\lambda$ vs. intrinsic period $\tau$. **(d)** Amplitude $A$ vs. re-entrainment time $T_e$. **(e)** Amplitude $A$ vs. phase variability $\Delta\psi$. **(f)** Amplitude $A$ vs. maximum PRC $\Delta\varphi_{max}$. **(g)** Relaxation rate $\lambda$ vs. re-entrainment time $T_e$. **(h)** Relaxation rate $\lambda$ vs. phase variability $\Delta\psi$. **(i)** Relaxation rate $\lambda$ vs. maximum PRC $\Delta\varphi_{max}$. **(j)** Intrinsic period $\tau$ vs. re-entrainment time $T_e$. **(k)** Intrinsic period $\tau$ vs. phase variability $\Delta\psi$. **(l)** Intrinsic period $\tau$ vs. maximum PRC $\Delta\varphi_{max}$. **(m)** Re-entrainment time $T_e$ vs. phase variability $\Delta\psi$. **(n)** Re-entrainment time $T_e$ vs. maximum PRC $\Delta\varphi_{max}$. **(o)** Phase variability $\Delta\psi$ vs. maximum PRC $\Delta\varphi_{max}$.

**Figure S6 |** Entrainment features of the amplitude-phase model for $\tau=23.48$ h, $A=2.458$, $\lambda=0.0134\ \text{h}^{-1}$ with $\omega=0.268$. **(a)** The re-entrainment process of the oscillator after its phase is shifted by a 6 h–advanced jet lag. The red line represents the trajectory that the system converges to. **(b)** Phase response curve with respect to a 6h light pulse. **(c)** Waveforms $x(t)$ of the oscillator entrained to *Zeitgeber* signal with 8:16 LD (purple), 12:12 LD (green), and 16:8 LD (blue). **(d)** Actogram drawn for the oscillator, to which a 6 h-advanced jet lag was induced on day 10. **(e)** Time-trace $x(t)$ of the oscillators, to which a 6 h-advanced jet lag was induced on day 10. **(f)** *Arnold* onion (1:1 entrainment ranges in the $\varkappa$-$T$ parameter plane).

## REFERENCES


Abraham, U., Granada, A. E., Westermark, P. O., Heine, M., Kramer, A., and Herzel, H. (2010). Coupling governs entrainment range of circadian clocks. *Mol. Syst. Biol.* 6:438. doi: 10.1038/msb.2010.92

An, S., Harang, R., Meeker, K., Granados-Fuentes, D., Tsai, C. A., Mazuski, C., et al. (2013). A neuropeptide speeds circadian entrainment by reducing intercellular synchrony. *Proc. Natl. Acad. Sci. U.S.A.* 110, E4355–E4361. doi: 10.1073/pnas.1307088110

Ananthasubramaniam, B., Schmal, C., and Herzel, H. (2020). Amplitude effects allow short jetlags and large seasonal phase shifts in minimal clock models. *J. Mol. Biol.* doi: 10.1016/j.jmb.2020.01.014

Aschoff, J. (1960). "Exogenous and endogenous components in circadian rhythms," in *Cold Spring Harbor Symposia on Quantitative Biology,* ed L. Frisch, Vol. 25 (New York, NY: Cold Spring Harbor Laboratory Press), 11–28. doi: 10.1101/SQB.1960.025.01.004

Aschoff, J., and Pohl, H. (1978). Phase relations between a circadian rhythm and its Zeitgeber within the range of entrainment. *Naturwissenschaften* 65, 80–84. doi: 10.1007/BF00440545

Becker-Weimann, S., Wolf, J., Herzel, H., and Kramer, A. (2004). Modeling feedback loops of the mammalian circadian oscillator. *Biophys. J.* 87, 3023–3034. doi: 10.1529/biophysj.104.040824

Bellman, J., Kim, J. K., Lim, S., and Hong, C. I. (2018). Modeling reveals a key mechanism for light-dependent phase shifts of neurospora circadian rhythms. *Biophys. J.* 115, 1093–1102. doi: 10.1016/j.bpj.2018.07.029

Bode, B., Shahmoradi, A., Rossner, M. J., and Oster, H. (2011). Genetic interaction of per1 and dec1/2 in the regulation of circadian locomotor activity. *J. Biol. Rhythms* 26, 530–540. doi: 10.1177/0748730411419782

Bordyugov, G., Abraham, U., Granada, A., Rose, P., Imkeller, K., Kramer, A., et al. (2015). Tuning the phase of circadian entrainment. *J. R. Soc. Interface* 12:108. doi: 10.1098/rsif.2015.0282

Buhr, E. D., Yoo, S.-H., and Takahashi, J. S. (2010). Temperature as a universal resetting cue for mammalian circadian oscillators. *Science* 330, 379–385. doi: 10.1126/science.1195262

Comas, M., Beersma, D., Spoelstra, K., and Daan, S. (2006). Phase and period responses of the circadian system of mice (*Mus musculus*) to light stimuli of different duration. *J. Biol. Rhythms* 21, 362–372. doi: 10.1177/0748730406292446

Comas, M., Beersma, D., Spoelstra, K., and Daan, S. (2007). Circadian response reduction in light and response restoration in darkness: a "skeleton" light pulse PRC study in mice (*Mus musculus*). *J. Biol. Rhythms* 22, 432–444. doi: 10.1177/0748730407305728

Czeisler, C. A., Duffy, J. F., Shanahan, T. L., Brown, E. N., Mitchell, J. F., Rimmer, D. W., et al. (1999). Stability, precision, and near-24-h period of the human circadian pacemaker. *Science* 284, 2177–2181. doi: 10.1126/science.284.5423.2177

Daan, S., and Aschoff, J. (1975). Circadian rhythms of locomotor activity in captive birds and mammals: their variations with season and latitude. *Oecologia* 18, 269–316. doi: 10.1007/BF00345851

Daan, S., and Berde, C. (1978). Two coupled oscillators: simulations of the circadian pacemaker in mammalian activity rhythms. *J. Theor. Biol.* 70, 297–313. doi: 10.1016/0022-5193(78)90378-8

Devlin, P. F., and Kay, S. A. (2001). Circadian photoperception. *Annu. Rev. Physiol.* 63, 677–694. doi: 10.1146/annurev.physiol.63.1.677

Dibner, C., Schibler, U., and Albrecht, U. (2010). The mammalian circadian timing system: organization and coordination of central and peripheral clocks. *Annu. Rev. Physiol.* 72, 517–549. doi: 10.1146/annurev-physiol-021909-135821

Dodd, A. N., Salathia, N., Hall, A., Kévei, E., Tóth, R., Nagy, F., et al. (2005). Plant circadian clocks increase photosynthesis, growth, survival, and competitive advantage. *Science* 309, 630–633. doi: 10.1126/science.1115581

Duffing, G. (1918). Erzwungene Schwingungen bei veränderlicher Eigenfrequenz und ihre technische Bedeutung. Braunschweig: F. Vieweg & Sohn.

Duffy, J. F., Rimmer, D. W., and Czeisler, C. A. (2001). Association of intrinsic circadian period with morningness-eveningness, usual wake time, and circadian phase. *Behav. Neurosci.* 115, 895–899. doi: 10.1037/0735-7044.115.4.895

Eberhart, R., and Kennedy, J. (1995). "Particle swarm optimization," in *Proceedings of the IEEE International Conference on Neural Networks,* Vol. 4 (Perth, WA: Citeseer), 1942–1948.

Erzberger, A., Hampp, G., Granada, A., Albrecht, U., and Herzel, H. (2013). Genetic redundancy strengthens the circadian clock leading to a narrow entrainment range. *J. R. Soc. Interface* 10:20130221. doi: 10.1098/rsif.2013.0221

Evans, J. A., Leise, T. L., Castanon-Cervantes, O., and Davidson, A. J. (2015). Neural correlates of individual differences in circadian behaviour. *Proc. R. Soc. B Biol. Sci.* 282:20150769. doi: 10.1098/rspb.2015.0769

Flôres, D. E., and Oda, G. A. (2020). Quantitative study of dual circadian oscillator models under different skeleton photoperiods. *J. Biol. Rhythms.* doi: 10.1177/0748730420901939

Forger, D. B., and Peskin, C. S. (2003). A detailed predictive model of the mammalian circadian clock. *Proc. Natl. Acad. Sci. U.S.A.* 100, 14806–14811. doi: 10.1073/pnas.2036281100

Glass, L., and Mackey, M. C. (1988). *From Clocks to Chaos: The Rhythms of Life*. Princeton, NJ: Princeton University Press.

Granada, A. E., Bordyugov, G., Kramer, A., and Herzel, H. (2013). Human chronotypes from a theoretical perspective. *PLoS ONE* 8:e59464. doi: 10.1371/journal.pone.0059464

Granada, A. E., Hennig, R. M., Ronacher, B., Kramer, A., and Herzel, H. (2009). Phase response curves: elucidating the dynamics of coupled oscillators. *Methods Enzymol.* 454, 1–27. doi: 10.1016/S0076-6879(08)03801-9

Hardin, P. E., Hall, J. C., and Rosbash, M. (1990). Feedback of the drosophila period gene product on circadian cycling of its messenger RNA levels. *Nature* 343, 536–540. doi: 10.1038/343536a0

Hastings, M. H., Maywood, E. S., and Brancaccio, M. (2018). Generation of circadian rhythms in the suprachiasmatic nucleus. *Nat. Rev. Neurosci.* 19, 453–469. doi: 10.1038/s41583-018-0026-z

Hazlerigg, D. G., and Wagner, G. C. (2006). Seasonal photoperiodism in vertebrates: from coincidence to amplitude. *Trends Endocrinol. Metab.* 17, 83–91. doi: 10.1016/j.tem.2006.02.004

Honma, K.-i., Hashimoto, S., Nakao, M., and Honma, S. (2003). Period and phase adjustments of human circadian rhythms in the real world. *J. Biol. Rhythms* 18, 261–270. doi: 10.1177/0748730403018003008

Huygens, C. (1986). *Horologium Oscillatorium ("The Pendulum Clock, or Geometrical Demonstrations Concerning the Motion of Pendula as Applied to Clocks" Translated by Richard J. Blackwell)*. Ames, IA: Iowa State University Press.

Jagannath, A., Butler, R., Godinho, S. I., Couch, Y., Brown, L. A., Vasudevan, S. R., et al. (2013). The CRTC1-SIK1 pathway regulates entrainment of the circadian clock. *Cell* 154, 1100–1111. doi: 10.1016/j.cell.2013.08.004

Johnson, C. H. (1992). "Phase response curves: what can they tell us about circadian clocks," in *Circadian Clocks From Cell to Human*, eds T. Hiroshige and K.-I. Honma (Sapporo: Hokkaido University Press), 209–249.

Khalsa, S. B. S., Jewett, M. E., Cajochen, C., and Czeisler, C. A. (2003). A phase response curve to single bright light pulses in human subjects. *J. Physiol.* 549, 945–952. doi: 10.1113/jphysiol.2003.040477

Klerman, E. B., Dijk, D., Kronauer, R. E., and Czeisler, C. A. (1996). Simulations of light effects on the human circadian pacemaker: implications for assessment of intrinsic period. *Am. J. Physiol. Regul. Integr. Comp. Physiol.* 270, R271–R282. doi: 10.1152/ajpregu.1996.270.1.R271

Klotter, K. (1960). "Theoretical analysis of some biological models," in *Cold Spring Harbor Symposia on Quantitative Biology,* ed L. Frisch, Vol. 25 (New York, NY: Cold Spring Harbor Laboratory Press), 189–196. doi: 10.1101/SQB.1960.025.01.017

Kori, H., Yamaguchi, Y., and Okamura, H. (2017). Accelerating recovery from jet lag: prediction from a multi-oscillator model and its experimental confirmation in model animals. *Sci. Rep.* 7:46702. doi: 10.1038/srep46702

Kronauer, R. E., Czeisler, C. A., Pilato, S. F., Moore-Ede, M. C., and Weitzman, E. D. (1982). Mathematical model of the human circadian system with two interacting oscillators. *Am. J. Physiol. Regul. Integr. Comp. Physiol.* 242, R3–R17. doi: 10.1152/ajpregu.1982.242.1.R3

Kuramoto, Y. (1984). *Chemical Oscillations, Waves, and Turbulence*, Berlin: Springer.

Lakin-Thomas, P. L., Brody, S., and Coté, G. G. (1991). Amplitude model for the effects of mutations and temperature on period and phase

resetting of the neurospora circadian oscillator. *J. Biol. Rhythms* 6, 281–297. doi: 10.1177/074873049100600401

Leise, T. L., Wang, C. W., Gitis, P. J., and Welsh, D. K. (2012). Persistent cell-autonomous circadian oscillations in fibroblasts revealed by six-week single-cell imaging of per2:: Luc bioluminescence. *PLoS ONE* 7:e33334. doi: 10.1371/journal.pone.0033334

Leloup, J.-C., and Goldbeter, A. (2003). Toward a detailed computational model for the mammalian circadian clock. *Proc. Natl. Acad. Sci. U.S.A.* 100, 7051–7056. doi: 10.1073/pnas.1132112100

Locke, J. C., Millar, A. J., and Turner, M. S. (2005). Modelling genetic networks with noisy and varied experimental data: the circadian clock in *Arabidopsis thaliana*. *J. Theor. Biol.* 234, 383–393. doi: 10.1016/j.jtbi.2004.11.038

Locke, J. C., Westermark, P. O., Kramer, A., and Herzel, H. (2008). Global parameter search reveals design principles of the mammalian circadian clock. BMC Syst. Biol. 2:22. doi: 10.1186/1752-0509-2-22

Loros, J. J., and Dunlap, J. C. (2001). Genetic and molecular analysis of circadian rhythms in neurospora. *Annu. Rev. Physiol.* 63, 757–794. doi: 10.1146/annurev.physiol.63.1.757

Lu, Z., Klein-Cardena, K., Lee, S., Antonsen, T. M., Girvan, M., and Ott, E. (2016). Resynchronization of circadian oscillators and the east-west asymmetry of jet-lag. *Chaos* 26:094811. doi: 10.1063/1.4954275

Merrow, M., Brunner, M., and Roenneberg, T. (1999). Assignment of circadian function for the neurospora clock gene frequency. *Nature* 399, 584–586. doi: 10.1038/21190

Mirsky, H. P., Liu, A. C., Welsh, D. K., Kay, S. A., and Doyle, F. J. (2009). A model of the cell-autonomous mammalian circadian clock. *Proc. Natl. Acad. Sci. U.S.A.* 106, 11107–11112. doi: 10.1073/pnas.0904837106

Morio, J. (2011). Global and local sensitivity analysis methods for a physical system. *Eur. J. Phys.* 32:1577. doi: 10.1088/0143-0807/32/6/011

Ouyang, Y., Andersson, C. R., Kondo, T., Golden, S. S., and Johnson, C. H. (1998). Resonating circadian clocks enhance fitness in cyanobacteria. *Proc. Natl. Acad. Sci. U.S.A.* 95, 8660–8664. doi: 10.1073/pnas.95.15.8660

Pavlidis, T. (1969). Populations of interacting oscillators and circadian rhythms. *J. Theor. Biol.* 22, 418–436. doi: 10.1016/0022-5193(69)90014-9

Pavlidis, T. (1973). The free-run period of circadian rhythms and phase response curves. *Am. Natural.* 107, 524–530. doi: 10.1086/282855

Peterson, E. L. (1980). A limit cycle interpretation of a mosquito circadian oscillator. *J. Theor. Biol.* 84, 281–310. doi: 10.1016/S0022-5193(80)80008-7

Pikovsky, A., Rosenblum, M., and Kurths, J. (2003). *Synchronization: A Universal Concept in Nonlinear Sciences*, Vol. 12. Cambridge: Cambridge University Press.

Pittendrigh, C. S. (1981). "Circadian systems: entrainment," in *Biological Rhythms* ed J. Aschoff (Boston, MA: Springer), 95–124. doi: 10.1007/978-1-4615-6552-9_7

Pittendrigh, C. S., and Daan, S. (1976a). A functional analysis of circadian pacemakers in nocturnal rodents I. The stability and lability of spontaneous frequency. *J. Comp. Physiol.* 106, 223–252. doi: 10.1007/BF01417856

Pittendrigh, C. S., and Daan, S. (1976b). A functional analysis of circadian pacemakers in nocturnal rodents IV. Entrainment: pacemaker as clock. *J. Comp. Physiol.* 106, 291–331. doi: 10.1007/BF01417859

Pokhilko, A., Hodge, S. K., Stratford, K., Knox, K., Edwards, K. D., Thomson, A. W., et al. (2010). Data assimilation constrains new connections and components in a complex, eukaryotic circadian clock model. *Mol. Syst. Biol.* 6:416. doi: 10.1038/msb.2010.69

Reddy, A., Field, M., Maywood, E., and Hastings, M. (2002). Differential resynchronisation of circadian clock gene expression within the suprachiasmatic nuclei of mice subjected to experimental jet lag. *J. Neurosci.* 22, 7326–7330. doi: 10.1523/JNEUROSCI.22-17-07326.2002

Relógio, A., Westermark, P. O., Wallach, T., Schellenberg, K., Kramer, A., and Herzel, H. (2011). Tuning the mammalian circadian clock: robust synergy of two loops. *PLoS Comput. Biol.* 7:e1002309. doi: 10.1371/journal.pcbi.1002309

Rémi, J., Merrow, M., and Roenneberg, T. (2010). A circadian surface of entrainment: varying T, $\tau$, and photoperiod in *Neurospora crassa*. *J. Biol. Rhythms* 25, 318–328. doi: 10.1177/0748730410379081

Schmal, C., Myung, J., Herzel, H., and Bordyugov, G. (2015). A theoretical study on seasonality. *Front. Neurol.* 6:94. doi: 10.3389/fneur.2015.00094

Shaw, J., and Brody, S. (2000). Circadian rhythms in neurospora: a new measurement, the reset zone. *J. Biol. Rhythms* 15, 225–240. doi: 10.1177/074873040001500304

Sobol, I. M. (1993). Sensitivity estimates for nonlinear mathematical models. *Math. Modell. Comput. Exp.* 1, 407–414.

Sobol, I. M. (2001). Global sensitivity indices for nonlinear mathematical models and their monte carlo estimates. *Math. Comput. Simul.* 55, 271–280. doi: 10.1016/S0378-4754(00)00270-6

Strogatz, S. (2004). *Sync: The Emerging Science of Spontaneous Order*. London: Penguin.

Trelea, I. C. (2003). The particle swarm optimization algorithm: convergence analysis and parameter selection. *Inform. Process. Lett.* 85, 317–325. doi: 10.1016/S0020-0190(02)00447-7

Van der Pol, B., and Van der Mark, J. (1927). Frequency demultiplication. *Nature* 120, 363–364. doi: 10.1038/120363a0

Vansteensel, M. J., Yamazaki, S., Albus, H., Deboer, T., Block, G. D., and Meijer, J. H. (2003). Dissociation between circadian per1 and neuronal and behavioral rhythms following a shifted environmental cycle. *Curr. Biol.* 13, 1538–1542. doi: 10.1016/S0960-9822(03)00560-8

Vitaterna, M. H., Ko, C. H., Chang, A.-M., Buhr, E. D., Fruechte, E. M., Schook, A., et al. (2006). The mouse clock mutation reduces circadian pacemaker amplitude and enhances efficacy of resetting stimuli and phase-response curve amplitude. *Proc. Natl. Acad. Sci. U.S.A.* 103, 9327–9332. doi: 10.1073/pnas.0603601103

Wang, B., Kettenbach, A. N., Zhou, X., Loros, J. J., and Dunlap, J. C. (2019). The phospho-code determining circadian feedback loop closure and output in neurospora. *Mol. Cell* 74, 771–784. doi: 10.1016/j.molcel.2019.03.003

Westermark, P. O., Welsh, D. K., Okamura, H., and Herzel, H. (2009). Quantification of circadian rhythms in single cells. *PLoS Comput. Biol.* 5:e1000580. doi: 10.1371/journal.pcbi.1000580

Wever, R. (1962). Zum mechanismus der biologischen 24-stunden-periodik. *Kybernetik* 1, 139–154. doi: 10.1007/BF00289033

Wever, R. (1964). Zum mechanismus der biologischen 24-stunden-periodik: III. Mitteilung anwendung der modell-gleichung. *Kybernetik* 2, 127–144. doi: 10.1007/BF00306797

Wever, R. A. (1979). *The Circadian System of Man: Results of Experiments Under Temporal Isolation.* New York, NY: Springer–Verlag.

Winfree, A. T. (1980). *The Geometry of Biological Time*. New York, NY; Heidelberg; Berlin: Springer-Verlag. doi: 10.1007/978-3-662-22492-2

Woller, A., Duez, H., Staels, B., and Lefranc, M. (2016). A mathematical model of the liver circadian clock linking feeding and fasting cycles to clock function. *Cell Rep.* 17, 1087–1097. doi: 10.1016/j.celrep.2016.09.060

Wyse, C., Coogan, A., Selman, C., Hazlerigg, D., and Speakman, J. (2010). Association between mammalian lifespan and circadian free-running period: the circadian resonance hypothesis revisited. *Biol. Lett.* 6, 696–698. doi: 10.1098/rsbl.2010.0152

Yamaguchi, Y., Suzuki, T., Mizoro, Y., Kori, H., Okada, K., Chen, Y., et al. (2013). Mice genetically deficient in vasopressin v1a and v1b receptors are resistant to jet lag. *Science* 342, 85–90. doi: 10.1126/science.1238599

Yamazaki, S., Numano, R., Abe, M., Hida, A., Takahashi, R.-I., Ueda, M., et al. (2000). Resetting central and peripheral circadian oscillators in transgenic rats. *Science* 288, 682–685. doi: 10.1126/science.288.5466.682

Zhou, M., Kim, J. K., Eng, G.W. L., Forger, D. B., and Virshup, D. M. (2015). A period2 phosphoswitch regulates and temperature compensates circadian period. *Mol. Cell* 60, 77–88. doi: 10.1016/j.molcel.2015.08.022

**Conflict of Interest:** The authors declare that the research was conducted in the absence of any commercial or financial relationships that could be construed as a potential conflict of interest.

frontiers in Physiology

ORIGINAL RESEARCH
published: 18 June 2020
doi: 10.3389/fphys.2020.00429

# Chemical Perturbation of Chloroplast-Related Processes Affects Circadian Rhythms of Gene Expression in *Arabidopsis*: Salicylic Acid Application Can Entrain the Clock

*Koumis Philippou*[1], *Amanda M. Davis*[1,2], *Seth J. Davis*[1,2,3]* *and Alfredo Sánchez-Villarreal*[1†]

[1] Department of Plant Developmental Biology, Max Planck Institute for Plant Breeding Research, Cologne, Germany, [2] Department of Biology, University of York, York, United Kingdom, [3] Key Laboratory of Plant Stress Biology, School of Life Sciences, Henan University, Kaifeng, China

OPEN ACCESS

**Edited by:**
Charalambos P. Kyriacou,
University of Leicester,
United Kingdom

**Reviewed by:**
Carla V. Finkielstein,
Virginia Tech, United States
Rob McClung,
Dartmouth College, United States
Antony Dodd,
John Innes Centre, United Kingdom

***Correspondence:**
Seth J. Davis
seth.davis@york.ac.uk

**†Present address:**
Alfredo Sánchez-Villarreal,
Colegio de Postgraduados Campus
Campeche, Campeche, Mexico

**Specialty section:**
This article was submitted to
Chronobiology,
a section of the journal
Frontiers in Physiology

**Received:** 26 July 2019
**Accepted:** 08 April 2020
**Published:** 18 June 2020

**Citation:**
Philippou K, Davis AM, Davis SJ
and Sánchez-Villarreal A (2020)
Chemical Perturbation
of Chloroplast-Related Processes
Affects Circadian Rhythms of Gene
Expression in Arabidopsis: Salicylic
Acid Application Can Entrain
the Clock. Front. Physiol. 11:429.
doi: 10.3389/fphys.2020.00429

The plant circadian system reciprocally interacts with metabolic processes. To investigate entrainment features in metabolic–circadian interactions, we used a chemical approach to perturb metabolism and monitored the pace of nuclear-driven circadian oscillations. We found that chemicals that alter chloroplast-related functions modified the circadian rhythms. Both vitamin C and paraquat altered the circadian period in a light-quality-dependent manner, whereas rifampicin lengthened the circadian period under darkness. Salicylic acid (SA) increased oscillatory robustness and shortened the period. The latter was attenuated by sucrose addition and was also gated, taking place during the first 3 h of the subjective day. Furthermore, the effect of SA on period length was dependent on light quality and genotype. Period lengthening or shortening by these chemicals was correlated to their inferred impact on photosynthetic electron transport activity and the redox state of plastoquinone (PQ). Based on these data and on previous publications on circadian effects that alter the redox state of PQ, we propose that the photosynthetic electron transport and the redox state of PQ participate in circadian periodicity. Moreover, coupling between chloroplast-derived signals and nuclear oscillations, as observed in our chemical and genetic assays, produces traits that are predicted by previous models. SA signaling or a related process forms a rhythmic input loop to drive robust nuclear oscillations in the context predicted by the *zeitnehmer* model, which was previously developed for *Neurospora*. We further discuss the possibility that electron transport chains (ETCs) are part of this mechanism.

**Keywords: circadian clock, *Arabidopsis*, luciferase imaging, metabolic inputs, entrainment, stress signaling, salicylic acid, redox**

## INTRODUCTION

Stress events often occur at predictable times of the day given the environmentally rhythmic cycling of light, temperature, and humidity. Within these cycles, light causes the accumulation of reactive oxygen species (ROS) (Pitzschke et al., 2006), while pathogen invasion is often favored at a given time of day (Shin et al., 2012; Korneli et al., 2014; Karapetyan and Dong, 2018; Li et al., 2018; Zhang et al., 2019). These perturbations often elicit various types of oxidative bursts (Karapetyan and Dong, 2018; Zhang et al., 2019). Given the predictable, timed nature of these abiotic and biotic stressors, the plant circadian clock provides timed sensitivity resistance to such agents. This 24-h oscillator serves to prime a plant to be most capable of resisting stress when it is most likely to be encountered (Covington et al., 2008; Sánchez et al., 2011; Fornara et al., 2015; Grundy et al., 2015). Whether these stress agents themselves feedback to tune the oscillator is still much less understood. In *Arabidopsis*, transcriptional/translational oscillations (TTOs) form feedback loops thought to be the central circadian oscillator that drives rhythmic gene expression (Bujdoso and Davis, 2013; Staiger et al., 2013; Anwer et al., 2014; Oakenfull and Davis, 2017; McClung, 2019; Webb et al., 2019). Initially, the core circadian clock was regarded as the feedback mechanism between the two morning-expressed MYB transcription factors CIRCADIAN CLOCK ASSOCIATED 1 (CCA1) and LATE ELONGATED HYPOCOTYL (LHY) and the night-phased TIMING OF CAB EXPRESSION 1 (TOC1), also known as PSEUDO RESPONSE REGULATOR 1 (PRR1) (Alabadí et al., 2001). Respective single mutants display a short-period phenotype, and rhythmicity is arrested in the triple mutant (Ding et al., 2007). Computational approaches that aimed to introduce photoperiodic perception and reconcile accumulated experimental findings led to more complex models that comprised additional TTO loops (Locke et al., 2005, 2006; Bujdoso and Davis, 2013). These models incorporated the post-transcriptional and the post-translational regulation of CCA1, LHY, TOC1, PRR9, PRR7, and GIGANTEA (GI) (Locke et al., 2006; Zeilinger et al., 2006; Pokhilko et al., 2010; Bujdoso and Davis, 2013) and the EVENING COMPLEX (EC) comprised by EARLY FLOWERING 3 (ELF3), ELF4, and LUX ARRHYTHMO (LUX) (Nusinow et al., 2011; Herrero et al., 2012; Pokhilko et al., 2012; Anwer et al., 2014; Ronald and Davis, 2017). Recently, a model with interconnected activation and repression activities within the loops including *BROTHER OF LUX ARRYTHMO* (*BOA*), *REVEILLE8* (*RVE8*), *RVE6*, *RVE4* and *LIGHT-REGULATED WD1* (*LWD1*) and *LWD2* has been proposed (McClung, 2019). This network is in constant cross-talking with plant physiology and the environment (McClung, 2019).

In 1960, Aschoff described a "rule" according to which the period of free-running oscillations changes linearly with alterations in light intensity. Aschoff's Rule is illustrated with fluence response curves (FRCs) (Bunning, 1967). In *Arabidopsis*, photoreceptors have been linked with light input to the clock through genetic studies (Somers et al., 1998; Devlin and Kay, 2000; Somers et al., 2000, 2004; Oakenfull and Davis, 2017). From these studies, it was established that *PHYTOCHROME A* (*PHYA*) is a low-fluence photoreceptor, *PHYB* is the main red light (RL) photoreceptor, and *CRTYPTOCHROME* (*CRY1*) is the blue light (BL) photoreceptor (Somers et al., 1998). In addition to these, a BL-chromoprotein was recognized in the F-box protein ZEITLUPE (ZTL) that displays involvement in light signaling and clock protein stability (Más et al., 2003b; Kim et al., 2007; Fujiwara et al., 2008).

Entrainment to light and light-input to the clock are not identical entities (Oakenfull and Davis, 2017). For example, light input to the clock seen in the induction of *LHY* gene expression (Kim et al., 2003) is not correlated to entrainment to light pulses (Covington et al., 2001). Furthermore, entrainment can also take place in the absence of the major phytochrome and cryptochrome photoreceptors (Yanovsky et al., 2000; Strasser et al., 2010). These findings suggest that, in *Arabidopsis*, photoreceptor signaling alone cannot fully explain entrainment to light nor Aschoff's Rule.

In cyanobacteria, it has been documented that entrainment to light does not require photoreceptors (Rust et al., 2011; Diamond et al., 2017). Light input to the clock and circadian entrainment in cyanobacteria have been connected to the redox status of the photosynthetic electron transport chain (ETC) and the redox state of the plastoquinone (PQ) pool (Mackey et al., 2011). Thus, light input could be an indirect process in supporting the entrainment without photoreceptors through metabolism as seen in *Arabidopsis*.

Metabolic oscillations have been shown to interact with TTOs in several eukaryotes, including mammals (Rutter et al., 2001; Dioum et al., 2002; Kaasik and Lee, 2004; Asher et al., 2008; Nakahata et al., 2008, 2009; O'Neill et al., 2008; Ramsey et al., 2009), plants (Panda et al., 2002; Dodd et al., 2007; James et al., 2008; Dalchau et al., 2011), fungi (Merrow et al., 1999; Yoshida et al., 2011), and protists (Bunning, 1967). In fungi, this type of interaction has been held responsible for compensation against external and metabolic perturbation (Merrow et al., 1999; Roenneberg and Merrow, 1999). Thus, the clock controls the timing of metabolism and, in return, metabolic signals set the clock.

It has been established that there is a reciprocal connection between TTOs and metabolism in higher plants (Müller et al., 2014). In *Arabidopsis*, cytosolic oscillations in cyclic adenosine diphosphate ribose and TTOs reciprocally regulate each other (Dodd et al., 2007), whereas oscillations in sugar solutes drive rhythmic gene expression (Bläsing et al., 2005). Later it was established that sugars derived from photosynthesis entrain the clock (Haydon et al., 2013), allowing for rhythmic plasticity through anabolic dawn in concordance with the photoperiod (Müller et al., 2014; Webb et al., 2019). Furthermore, perturbations in ionic conditions also have effects on clock performance (Perea-García et al., 2015). It is therefore plausible that metabolism is one driving force which is capable of performing circadian entrainment.

Metabolism can be modulated by molecules with different chemical properties. Crosstalk between metabolic networks and nuclear oscillations can be perturbed by the addition of ROS and redox-related molecules (Karapetyan and Dong, 2018). Here through a chemical biology approach, we observed effects

on circadian clock parameters by paraquat, an oxidizing and uncoupling photosynthetic agent, the antioxidant vitamin C (vitC), the inhibitor of photosynthetic electron transport DCMU [3-(3,4-dichlorophenyl)-1,1-dimethylurea], and rifampicin, an inhibitor of organellar DNA-dependent RNA polymerase. Interestingly, all of these chemicals are known to alter chloroplast-driven metabolic processes. We also tested salicylic acid (SA) because it alters cellular redox status in order to trigger the cellular defense response (Mou et al., 2003), and plant innate immunity is in crosstalk with the circadian clock (Zhang et al., 2013; Korneli et al., 2014). Furthermore, even though a previous study reported that SA application did not influence circadian parameters (Hanano et al., 2006), later it was shown that SA application reinforces rhythmicity in *Arabidopsis* (Zhou et al., 2015). Here we confirm the latter effect of SA on circadian clock robustness and also show that, depending on sucrose supplementation, SA accelerates oscillations. Moreover, we show that SA affects entrainment to light–dark cycles and light pulses (parametric and non-parametric entrainment, respectively). Finally, we propose that SA signaling acts in entrainment in the context predicted by the *zeitnehmer* model, previously developed for *Neurospora* (Merrow et al., 1999; Roenneberg and Merrow, 1999), that describes rhythmic input pathways to oscillations that serve a time-keeping function.

# RESULTS

A chemical approach was used to investigate the potential crosstalk between TTOs and metabolism in *Arabidopsis thaliana*. Redox-related chemicals were exogenously applied on seedlings and the effect of the chemicals on circadian promoter activity was monitored with the luciferase system. We tested chemicals affecting the thioredoxin and glutaredoxin systems (chlorodinitrobenzene and buthionine sulfoximine, inhibitors of thioredoxin reductase and glutathione synthesis, respectively), respiration inhibitors (antimycin A, rotenone, and salicylhydroxamic acid, which is an inhibitor of the RESPIRATORY ALTERNATIVE OXIDASE), oxidant agents such as menadione, paraquat (methylviologen), and butylhydroxyperoxide, and antioxidants, such as vitamin C and dithiocarbamate. We also tested the hormone SA, norbornadiene (inhibitor of ethylene perception), diphenyleneiodonium (inhibitor of plasma membrane NADPH oxidases involved in hypersensitive reaction during pathogen recognition), butanedione monoxime (a ROS-inducing inhibitor of cytoplasmic streaming), and photosynthesis inhibitors DCMU [3-(3,4-dichlorophenyl)-1,1-dimethylurea] and DBMIB (2,5-dibromo-3-methyl-6-isopropylbenzoquinone). This approach is similar to the chemical biology strategies previously used to investigate the *Arabidopsis* circadian clock (Toth et al., 2001; Belbin et al., 2019; Uehara et al., 2019).

Several luciferase reporters of promoter activity were examined for their relative amplitude error (RAE) and RAE-normalized period (noPer) in a medium with or without sucrose. The chemicals that altered the noPer of rhythmic markers on a medium that contained sucrose are shown in **Figure 1A** (for *GI:LUC*) and **Supplementary Figure S1**; the statistical analyses are shown in **Supplementary Tables S1–S5**. The hormone SA shortened the circadian period of *GI:LUC* (**Figure 1A**) in the dark (DD). The aforementioned effects of SA in DD were also reproduced with *CCR2:LUC* (**Supplementary Figure S1D**). The antioxidant vitC shortened the circadian period of *GI:LUC* under red light (RL) and in the dark (**Figure 1A**) but had no effect under blue light (BL) (**Supplementary Figure S1A**). Rifampicin, an inhibitor of organellar transcription, lengthened the circadian period of *GI:LUC* in DD (**Figure 1A** and **Supplementary Figure S1B**) and under BL (**Supplementary Figure S1C**). The inhibitor of photosynthetic electron transport DCMU lengthened the circadian period of *GI:LUC* under RL and under BL (**Figure 1A**). However, this effect took place at different concentrations of this chemical depending on the light conditions. **Figure 1B** shows the period-altering effects of the oxidant paraquat on the period using *GI:LUC* or *CCR2:LUC* [also referred to as *GRP7* (Nicaise et al., 2013)] as reporters of promoter activity under monochromatic light. Under RL, paraquat application shortened the period of *GI:LUC*, whereas it lengthened the period of *CCR2:LUC*. However, under BL, paraquat application lengthened the period of circadian oscillations of both *GI:LUC* and *CCR2:LUC*. Furthermore, the effect was more pronounced and statistically significant with the *CCR2:LUC* marker. As with the effect of DCMU, the plants displayed a higher sensitivity under RL than on BL. Conclusively, the addition to the medium of chemicals known to alter chloroplast-driven metabolic processes affected the circadian-clock parameters.

## Salicylic Acid Action on the Clock

Salicylic Acid signaling has been implicated in connecting environmental stress cues to metabolic reactions driven by the plastid (Muhlenbock et al., 2008; Huang et al., 2010). Moreover, SA is involved in photosynthetic homeostatic regulation in the absence of stress (Rivas-San Vicente and Plasencia, 2011). Hence, SA could be a chemical that links chloroplast function to circadian rhythms. As such, we tested the SA perturbation of clock action in greater depth than in our previous effort (Hanano et al., 2006).

Interestingly, a visual inspection revealed that under RL plus BL, the application of SA increased the robustness of oscillations in all promoter activity reporters tested, which included *GI:LUC* (**Figures 1C,E**), *CCA1:LUC* (**Figures 1D,F**), *CCR2:LUC*, and *TOC1:LUC* (**Supplementary Figures S1E,F**, respectively). To test this further statistically, we distinguished between parameters that define circadian robustness, these being rhythmicity and precision. Here we define rhythmicity as the average of RAE values within a population that represents the fit between the theoretical and the experimental curves after a fast Fourier transform (FFT) analysis has been performed. Precision is defined as the standard deviation of period (descriptive or RAE-normalized, see also "Materials and Methods"). A population of plants generates robust oscillations when individual plants are rhythmic (low RAE values AND high rhythmicity), are in phase with each other, and show similar period values (high precision AND low SD-noPer). Moreover, we distinguish between direct and indirect rhythmicity, the first relating to the mean RAE

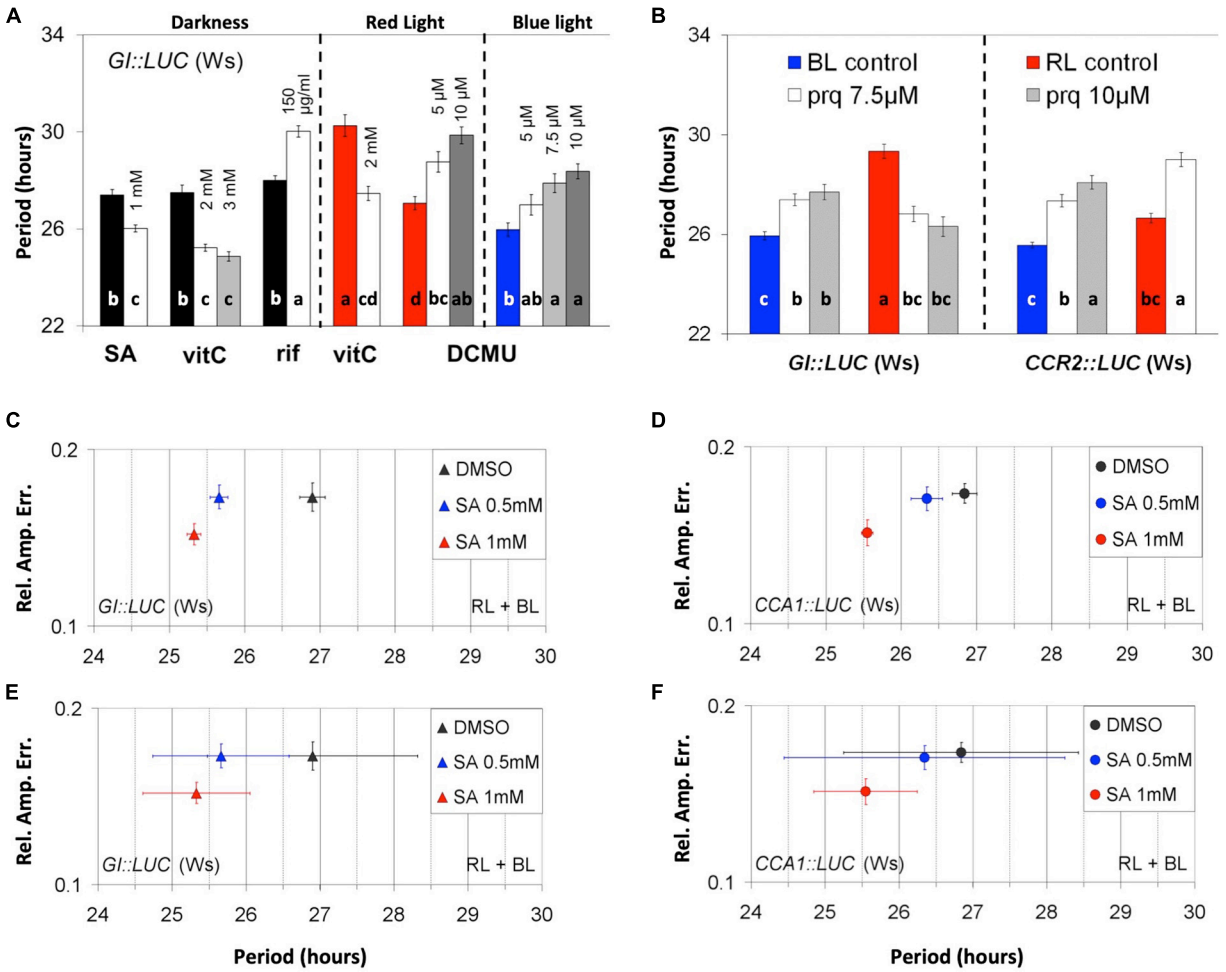


**FIGURE 1 |** Chloroplast-related chemicals alter the parameters of nuclear oscillations. **(A)** Effect of chemicals on the circadian period under darkness (left panel), red light (middle panel) and blue light (right panel). Dark, red, and blue bars represent the respective controls. **(A)** One-way ANOVA was performed for each panel (see "Materials and Methods"). **(B)** Light quality and construct specificity effect of paraquat on period. Red and blue bars indicate respective controls. An independent ANOVA analysis was performed for each marker, *GI:LUC* (left panel) and *CCR2:LUC* (right panel). The output of the statistical analysis is shown in **Supplementary Tables S1–S5**). In **(A)** and **(B)**, different letters (a–d) indicate statistically significant differences between means of period. **(C–F)** Relative amplitude error of plants treated with salicylic acid (SA) using either *GI:LUC* marker **(C,E)** or *CCA1:LUC* marker **(D,F)**. The plants received two dawn events in the presence of SA, one in a white light cabinet and one in a luminometer, and then were released into free running conditions. The results shown are derived from pooled data from several experiments. Error bars represent standard error except in **(E)** and **(F)** where they represent the SD of period.

generated by FFT analysis and the second to the same mean after the plants discarded by the FFT analysis were assigned with an RAE value of 1.

We found that SA application at 1 mM increased the precision and the direct rhythmicity of all reporters tested, whereas SA at 0.5 increased the direct rhythmicity of *TOC1:LUC* and *CCR2:LUC* and increased the precision of *GI:LUC* and *TOC1:LUC* (see **Supplementary Tables S6A,B**) in a reproducible manner. We should note that the changes in direct rhythmicity mentioned above were minor. Under continuous RL plus BL, the application of SA shortened the circadian period of *GI:LUC*, *CCA1:LUC*, *CCR2:LUC*, and *TOC1:LUC*, but this effect was inconsistent between experiments. Nonetheless, when the results from independent experiments were combined, thus increasing the size of the population, the period shortening effect of SA was statistically significant (see **Supplementary Tables S6A,B**) for the markers *GI:LUC* (**Figure 1C**) and *CCA1:LUC* (**Figure 1D**). This result contradicts our previous report, where SA was not found to have a circadian effect (Hanano et al., 2006). Conclusively, during these early experiments conducted in the presence of supplementary sucrose, the application of SA at high doses affected the circadian parameters and this effect was mostly due to changes in oscillatory precision.

We next tested the effect of SA on *PHYB:LUC* expression because phyB is part of SA signaling in defense responses (Genoud et al., 2002). SA application at a concentration of 0.5 mM or more increased the expression under monochromatic RL or BL (**Figures 2A,B**, **Supplementary Tables S7, S8**). Interestingly, the inductive effect of SA on the expression of *PHYB:LUC* required sucrose in the medium (**Figures 2A,B** and

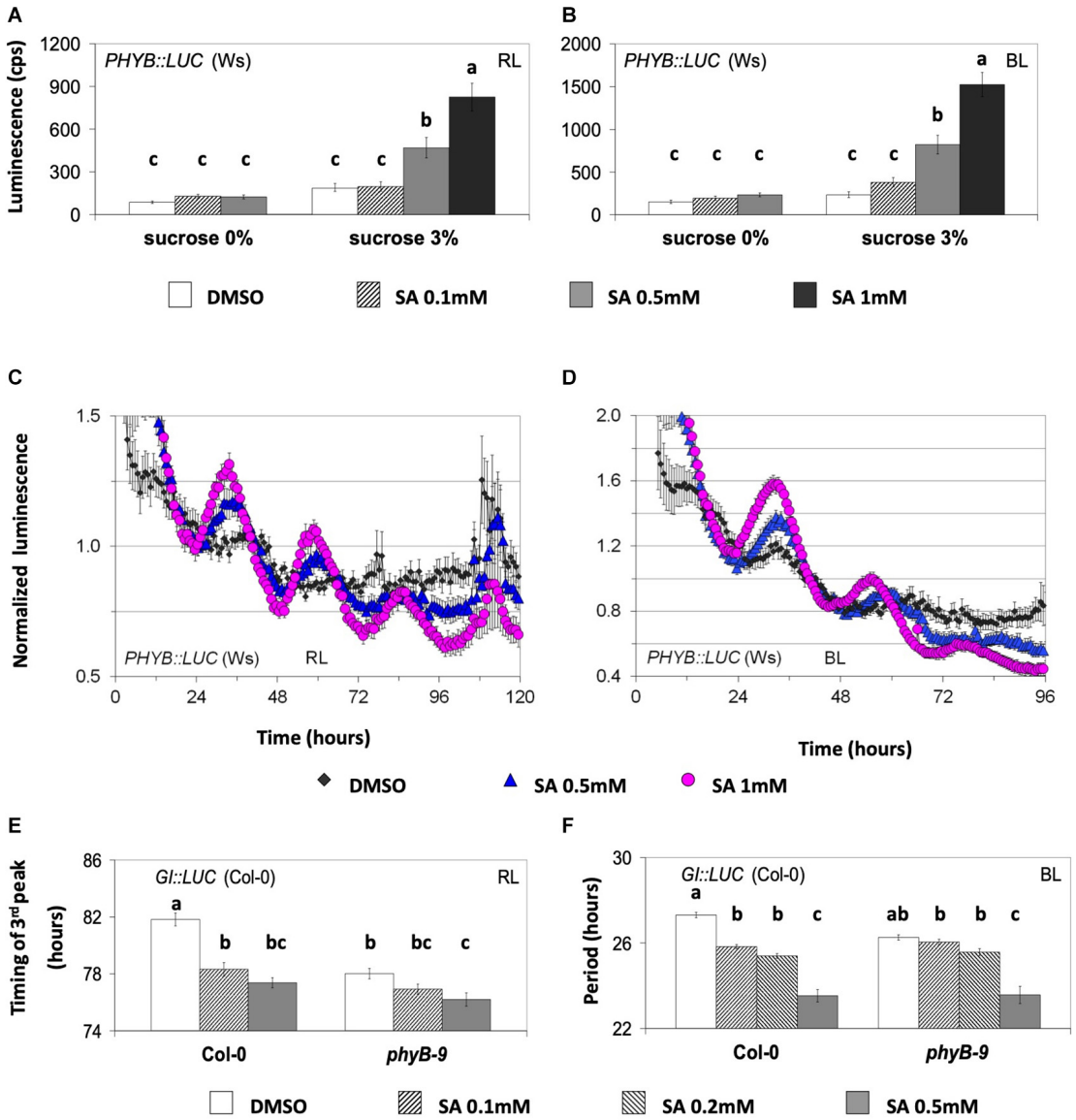


**FIGURE 2 |** The circadian effect of salicylic acid (SA) is dependent on phyB. **(A,B)** The effect of SA on the expression of *PHYB:LUC* under monochromatic red light (RL, left) and blue light (BL, right) is shown. The plants were entrained on medium with sucrose and then placed on medium with or without sucrose at the indicated SA concentrations. SA at 0.5 mM or higher increased the expression of *PHYB:LUC* only in media supplemented with sucrose. A one-way ANOVA was performed for each dataset (see "Materials and Methods" and **Supplementary Tables S7, S8**) considering two factors: sucrose concentration and SA concentration. Different letters (a–c) denote statistically significant differences between treatments. The data shown are pooled from several independent assays. Under RL, the bars represent the luminescence of the acute peak that followed dawn. Under BL, the bars represent the luminescence of the first circadian peak. **(C,D)** The effect of SA on the oscillatory robustness of *PHYB:LUC* under monochromatic RL and BL. The experiments were conducted in the presence of supplementary sucrose 3%. SA increased the robustness of *PHYB:LUC* oscillations (see text for details and **Supplementary Tables S9A,B**). The plants were entrained for one cycle under monochromatic light before being released into free running conditions in the presence of dimethyl sulfoxide (DMSO) or SA, as indicated. **(E,F)** The *phyB* mutant is less sensitive to SA than the wild type. Transgenic plants expressing the *GI:LUC* construct were placed in 96-well microtiter plates containing growth medium without sucrose and either with DMSO or SA. The *phyB-9* mutant was less sensitive than the wild type to SA-mediated phase advance under RL and to SA-mediated period shortening under BL. An ANOVA analysis was performed for each dataset **(E,F)** considering two factors: genotype and SA concentration (see **Supplementary Tables S19, S20**). Different letters (a–c) denote statistically significant differences between treatments. **(F)** FFT analysis did not include the first circadian peak and spanned at least three cycles. The period interval allowed during FFT analysis was between 15 and 40 h. The gene reporters in **(A–D)** are expressed in the Wassilewskija (Ws) and in **(E)** and **(F)** in the Columbia (Col-0) background. Error bars represent standard error.

**Supplementary Tables S6, S7**). Under RL plus BL, the expression of *TOC1:LUC* (**Supplementary Figure S1G**) was increased by SA, while the expression of *GI:LUC* (**Supplementary Figure S1H**) was decreased. Therefore, we reasoned that the SA-mediated induction of *PHYB:LUC* did not depend on luciferase expression alone since SA changed the expression in a reporter-specific

manner. This would exclude the possibility that SA altered the luciferase activity exclusively due to an effect on ATP levels or on the redox state of the cell, although these effects depend on the addition of sucrose to the media.

*PHYB:LUC* was the most responsive marker to SA in terms of oscillatory robustness. Previously, the promoter of *phyB* was shown to be under circadian control (Bognár et al., 1999); however, this oscillation was found to be weak (Toth et al., 2001). We detected that *PHYB:LUC* plants resulted in weak luminescence oscillations that were strengthened in amplitude by SA application in the presence of supplementary sucrose (**Figures 2C,D**). In more detail, under RL, SA application increased the indirect rhythmicity of the marker at 0.5 and 1 mM and increased its precision at 1 mM; under BL, SA application increased the indirect rhythmicity of the rhythmic marker at 0.5 and 1 mM (statistical analysis shown in **Supplementary Tables S9A,B**). SA application thus not only increases *PHYB* expression but also increases rhythm robustness.

We then proceeded to test whether SA acts on rhythmic transcription through light and/or entrainment pathways. For this, we subjected the plants to parametric (light/dark cycles) and non-parametric (light pulses given in the dark) entrainment protocols in the presence and the absence of SA (the experiments were conducted in the presence of supplementary sucrose). In non-parametric entrainment experiments, we tested circadian responses to 1 mM SA in a time-course because sensitivity to the hormones ABA, GA, JA, and auxin has been previously reported to be gated by the biological clock (Covington and Harmer, 2007; Legnaioli et al., 2009; Robertson et al., 2009; Arana et al., 2011; Shin et al., 2012). Plants harboring *GI:LUC* were used in the non-parametric entrainment experiments to pulses of light and SA. We found that the effect of SA on circadian period was gated and restricted to the first 3 h of the day (**Figure 3A** and **Supplementary Table S10**). Similarly, in these experiments, the effect of SA on phase (timing of the first circadian peak) was greater and statistically significant when pulses were applied between ZT0 and ZT3 relative to later pulses (**Figure 3B**).

We next examined the effect of continuous SA application on circadian oscillations under parametric entrainment. Plants harboring *CCR2:LUC* (**Figure 3C** and **Supplementary Figure S2A**) or *GI:LUC* (**Supplementary Figure S2B**) were placed on agar with various SA concentrations and entrained under WL for 1, 2, or 3 days. Luminescence rhythms were thereafter monitored in the dark, starting at the last objective dusk. We observed that after 3 days of entrainment had taken place in 96-well microtiter plates, the FFT process did not successfully assign a theoretical curve to 27.56% of *CCR2:LUC*-expressing plants (from a total of 156) and that this percentage dropped to 10.89% by the application of 0.5 mM SA (102 plants) and even to 0% by the application of SA 1 mM (102 plants). In agreement to this, oscillations that produced an FFT output gradually dampened with every entrainment event, unless SA was applied (**Supplementary Figure 2A**). Similarly, the parametric entrainment of seedlings in 96-well microtiter plates caused the oscillations to be less precise, unless SA was applied (**Supplementary Figure 2A** and **Supplementary Table S11**). Consecutive parametric entrainment events in 96-well microtiter plates also caused the oscillations to be less rhythmic, and this effect was attenuated by SA application (**Figure 3C** and **Supplementary Table S12**). Moreover, the circadian phase of the control plants was delayed by these consecutive entrainment events; but in the presence of SA, the phase was found to be relatively constant or even advanced with each entrainment event (see **Figure 3C** for *CCR2:LUC* and **Supplementary Figure S2B** for *GI:LUC*). Collectively, we found that the entrainment of *Arabidopsis* seedlings in 96-well microtiter plates causes oscillations to dampen and delays the circadian phase, unless SA is applied. In addition to this, a statistical analysis revealed that the effect of SA on the circadian parameters was enhanced by parametric entrainment. This was shown for the combined effects of entrainment and SA application on the indirect rhythmicity of *CCR2:LUC* (**Supplementary Table S13**) and on the phase of *CCR2:LUC* (**Supplementary Table S14**) and of *GI:LUC* (**Supplementary Table S15**). All of these observations were made with as little as 0.2 mM of SA.

In our assays, the highest SA concentration used (1 mM) caused chlorosis of plants. This could be attributed to SA induction of ROS (Chen et al., 2009), which was our reasoning to include SA in the initial ROS-related chemical screen. We observed that *Arabidopsis* plants were more sensitive to SA-mediated chlorosis if SA was applied without sucrose supplementation. We did not record this, but it is reflected in **Figure 4**, where SA of 1 mM is applied only when sucrose is supplemented. We should note that this chlorosis observed with SA at 1 mM could not have hindered the luciferase activity as the later was promoter specific (**Figures 2A,B**, **4D,E** and **Supplementary Figures S1G,H, S4**).

We then proceeded to test if sucrose modifies the effect of SA in circadian assays. We found that, under monochromatic RL and BL, sucrose abolished SA-mediated period shortening of *GI:LUC* (**Figure 4** and **Supplementary Tables S16–S18**) unless this hormone was applied at 0.75–1.0 mM range. Under BL, sucrose prevented the period shortening unless SA was applied with a concentration of 0.75 mM or higher, whereas in media without sucrose, SA at 0.1-mM concentration sufficed to reduce period (**Figure 4A**). A similar result was observed under RL, with SA requiring concentrations of 0.5 mM in media with sucrose to present period shortening (**Figure 4B**) and as little as 0.1 mM in media without sucrose. This result was consistent with our previous publication (Hanano et al., 2006) and explains the previous conclusion that SA does not act on the circadian period as Hanano et al. (2006) performed all experiments in the presence of sucrose. It should be noted that non-ionic osmotic stress (Mannitol) at 200 mM lengthens the circadian period (Litthauer et al., 2018), a concentration much higher than the 3% sucrose (∼90 mM) used in this study.

In order to identify loci that mediate SA signaling in the clock, we performed genetic tests with clock mutants. These were *gi-11*, *toc1-21*, *cca1-11*, and *lhy-21*. The *phyB-9* mutant was also tested in this genetic analysis for the distinct response to SA displayed by *PHYB:LUC* (**Figure 2**) and because the *phyB* mutant is defective in SA signaling during defense responses (Genoud et al., 2002).

*GI:LUC* was used to assess the effect of SA in a phyB context. Under RL, the *phyB-9* (Col-0) mutant was less sensitive to

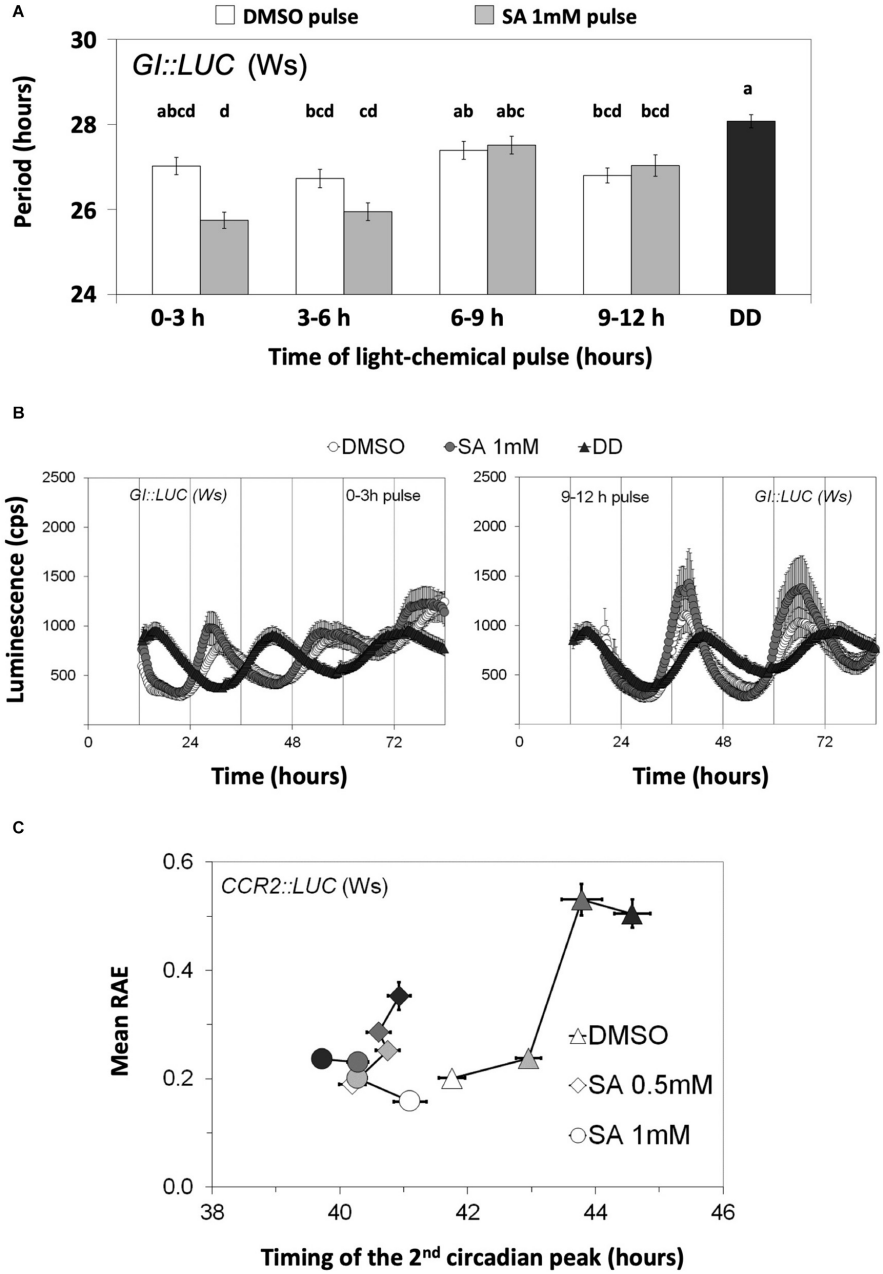


**FIGURE 3 |** Salicylic acid (SA) affects circadian rhythms through entrainment. **(A)** The effect of SA on the circadian period of *GI:LUC* is gated. Plants were grown and entrained for 5 days under white light and then released into continuous darkness at dusk. A subset of plants was retrieved every 3 h between ZT0 and ZT12 and received a light pulse on medium with 3% sucrose and either dimethyl sulfoxide (DMSO) or SA. Combined data from two independent experiments are shown. The effect of SA on circadian period was gated and restricted to the first 3 h of the day. DD corresponds to the DMSO control that did not receive SA nor light pulses. The results from the ANOVA analysis are shown in **Supplementary Table S10**. Different letters (a–d) indicate statistically significant differences between means of period. **(B)** Time-course of luminescence obtained from the first and the last chemical/light pulses depicted in **(A)** are shown. **(C)** The effect of SA on the circadian parameters of *CCR2:LUC* is enhanced by parametric entrainment. Populations that did not receive the additional entrainment events are represented by white symbols; pale gray, dark gray, and black symbols correspond to additional entrainment events: 1, 2, or 3, respectively. The plants received the indicated number of entrainment events on medium with sucrose 3% and SA or DMSO in 96-well microtiter plates. Then, they were placed in an automated scintillation counter in continuous darkness and at a constant temperature of 21°C. On the horizontal axis, the medium with DMSO (SA solvent) is shown; consecutive entrainment events in 96-well microtiter plates (0, 1, 2, or 3 days) delayed phase as measured with the timing of the second circadian peak (0 day vs. 1 day, $\Delta$phase = 1.20 h, $p = 3.0 \times 10^{-5}$; 0 day vs. 2 days, $\Delta$phase = 2.03 h, $p = 4.1 \times 10^{-7}$; 0 day vs. 3 days, $\Delta$phase = 2.82 h, $p = 4.9 \times 10^{-14}$). The phase was not substantially affected by such entrainment if SA at 0.5 mM was applied (0.42 h $<$ $\Delta$phase $<$ 0.74 h). The application of 1 mM SA reversed the effect of entrainment on phase by the third day (0 days vs. 3 days, $\Delta$phase = –1.38 h, $p = 1.5 \times 10^{-6}$). Moreover, the SA-mediated phase advances were enhanced by the preceding parametric entrainment events (**Supplementary Table S13**). On the vertical axis, the SA-mediated increase in indirect rhythmicity is shown to be enhanced by parametric entrainment (**Supplementary Table S14**). Moreover, consecutive entrainment events in 96-well microplates decreased the indirect rhythmicity and this response was attenuated by SA application. Error bars in all graphs represent standard error.

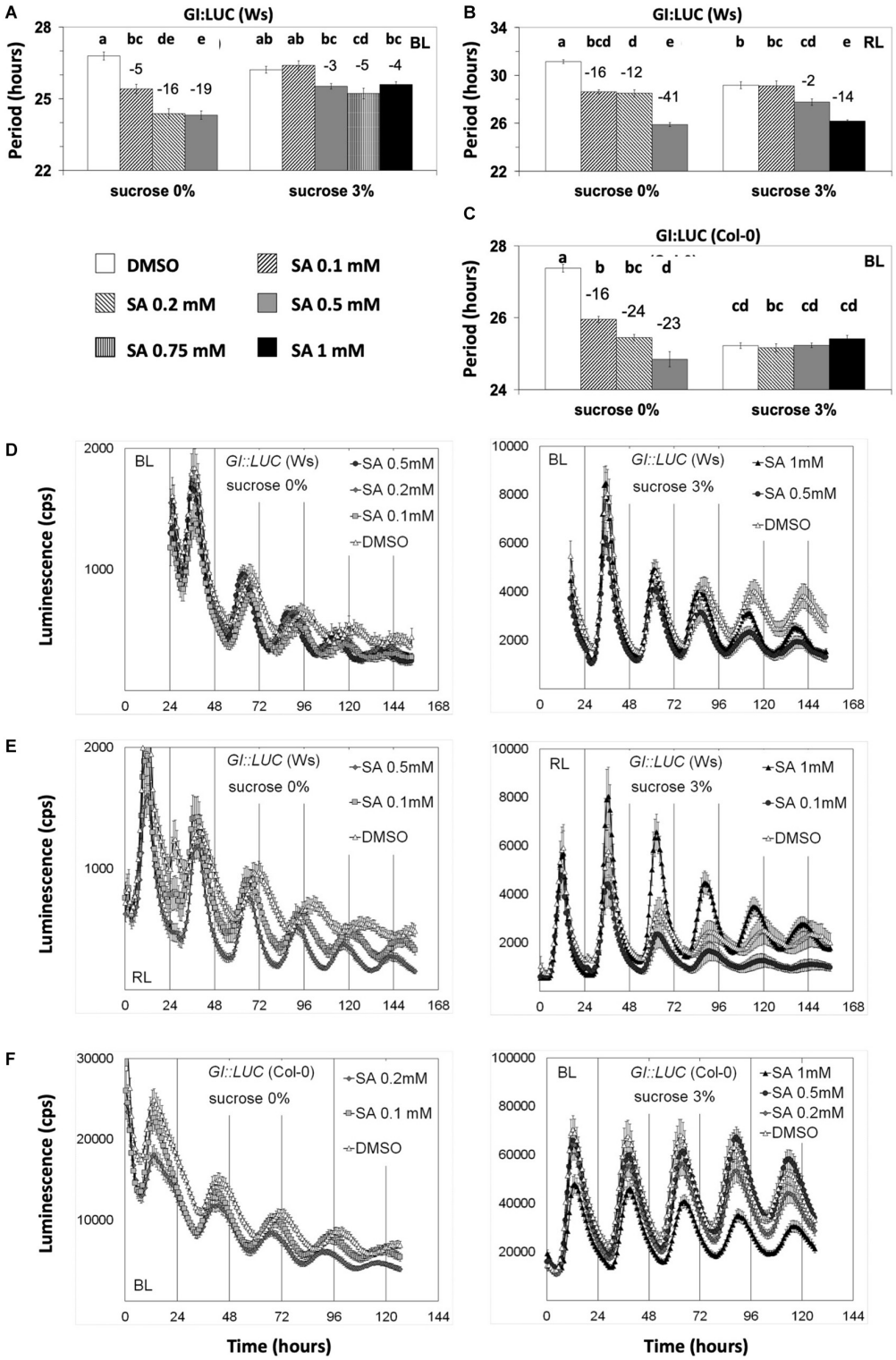


**FIGURE 4 |** Salicylic acid (SA)-induced period shortening is moderated or inhibited by sucrose. Transgenic plants carrying the designated promoter:luciferase transgenes were grown and entrained under white light before being released into free running conditions under monochromatic blue light (BL) or red light on media with SA and sucrose concentrations as indicated. The period shortening effect of SA was inhibited by sucrose unless a higher concentration of SA was applied. Nonetheless, under BL, even SA at 1 mM could not reduce the period of *Gl:LUC*. Reporters in **(A,B,D,E)** and **(F)** are expressed in Wassilewskija, whereas in figures **(C)** and **(F)** in Columbia (Col-0) background. Results from one-way ANOVA statistical analysis for each dataset in **(A–C)** are shown in **Supplementary Tables S16–S18**, respectively. Different letters (a–e) represent statistically significant differences. Error bars in all graphs represent standard error.

SA-mediated phase advance relative to the wild type (**Figure 2E** and **Supplementary Table S19**). Under BL, the phyB mutant similarly was less sensitive to SA-mediated period shortening compared to the wild type (**Figure 2F** and **Supplementary Table S20**). In both cases, the mutant required a concentration of 0.5 mM of SA to have an effect. Oscillations in the *phyB-9* mutant were previously reported to be advanced under white light (Salomé et al., 2002), which we confirm under RL here (**Figure 2E**). Consequently, it cannot be excluded that under RL the early phase phenotype of the *phyB-9* mutant accounts for its decreased sensitivity to SA-mediated phase advance.

We analyzed the effect of SA application on the *toc1-21* mutant under monochromatic RL or BL in the absence of sucrose. *GI:LUC* was used to assess the rhythm. Previously, it was shown that TOC1 is required for oscillations of *CCR2:LUC* and *CAB2:LUC* under monochromatic RL in experiments where sucrose was supplemented (Más et al., 2003a). Here we show that the *GI:LUC* construct exhibits weak oscillations in the *toc1-21* background that were strengthened by SA application (**Figure 5A**). The FFT analysis yielded a free running period for the mutant that was, strikingly, slightly longer than that of the wild type (**Figures 5A,C**). *toc1-21* is known to be a short period mutant (Strayer et al., 2000; Alabadí et al., 2001), and because this phenotype has been reported in the presence of sucrose, we proceeded to test whether the *toc1-21* phenotype under RL is sucrose dependent. **Figure 5B** shows that, under monochromatic RL, the short period phenotype of the *toc1-21* mutant is sucrose dependent (see also **Supplementary Table S21**). The *toc1-21* mutant did not display a short period phenotype in the absence of sucrose, even when the plants were placed on agar with 0.1 mM of SA that restores the oscillations in the mutant (compare the dashed bars in **Figure 5C** and the black curve in **Figure 5A**; the period values are shown in **Supplementary Tables S21, S22**). It is noteworthy that, under red light (**Figure 5C**), the *toc1-21* mutant exhibited a long period phenotype, whereas under BL we recorded a short period phenotype of the *toc1-21* mutant (**Figure 5D** and **Supplementary Table S23**), which was not affected by SA application. Previously, we have shown that the *lhy-21*, *cca1-11*, and *gi-11* mutants also show sucrose-dependent phenotypes (Philippou et al., 2019).

The *toc1-21* mutant was oversensitive to SA under RL. As expected, in the absence of sucrose, the wild-type plants responded to SA with period shortening, while the mutant responded similarly but to a greater extent (**Figures 5A,C** and **Supplementary Tables S21, S22**). The oversensitivity phenotype of *toc1-21* to SA was also seen for the effect of SA on oscillatory robustness, which was mostly due to changes in precision (see how the black dots collide together compared to the more dispersed gray dots in **Figure 5A**, lower panel). Under BL, the *toc1-21* mutant was less sensitive to SA-mediated period shortening than the wild type (**Figure 5D** and **Supplementary Table S23**). This was observed in experiments conducted without sucrose supplementation, either with the *GI:LUC* construct (**Figure 5D** and **Supplementary Table S23**) and at least in one experiment with the *CAB2:LUC* construct (**Supplementary Figure S3**). As such, light quality had a significant impact on the SA-related circadian phenotypes of *toc1-21*, the mutant being oversensitive to SA under RL and less sensitive under BL than the wild type. However, it cannot be excluded that under BL the short period phenotype of *toc1-21* accounts for its reduced sensitivity to SA-mediated period shortening.

It has been suggested that GI acts within light-input pathways (Park et al., 1999; Locke et al., 2006) *via* phyB signaling in particular (Huq et al., 2000). Moreover, phyB is recognized as a mediator of SA signaling during defense responses (Genoud et al., 2002). Thus, we proceeded to examine whether the effect of SA on *PHYB:LUC* expression (observed in **Figures 2A,B**) is modified in the *gi-11* background. We found that the *gi-11* mutant was consistently oversensitive to SA relative to the wild type when analyzing the effect of the hormone on the expression of *PHYB:LUC* either under RL or BL (**Figures 6A,B** and **Supplementary Tables S24, S25**). It is worth noting that this oversensitivity phenotype was observed on the medium that did not contain sucrose.

We next tested the *lhy-21* (**Figure 6C** and **Supplementary Table S26**) and *cca1-11* (**Supplementary Figure S4**) mutants for their responses to SA under BL with *CAB2:LUC*. Luminescence rhythms indicated that, in the presence of supplementary sucrose, *lhy-21* was responsive to SA with period shortening, unlike the wild type. A FFT–non-linear least squares (NLLS) analysis confirmed this in only two out of the four experiments conducted. Consequently, we calculated the timing of the third peak after release into free running conditions and found that *lhy-21* was more sensitive to SA-mediated peak advance than the wild type in every experiment (**Figure 6C** and **Supplementary Figure S4**, **Supplementary Tables S26, S27**). *cca1-11* did not display a detectable SA-related phenotype in terms of period or phase (timing of the third peak of oscillations) (**Supplementary Figure S4**). Thus, here we only detected that the *lhy* mutant displayed a SA-mediated phenotype.

# DISCUSSION

## Chemical Perturbation of Chloroplast Function Is Reflected in Nuclear Oscillations

The pace of the clock is resilient to most chemicals as the application of thousands of compounds of various structures has no action on clock performance (Toth et al., 2012). Interestingly, the chemicals that we examined alter the circadian parameters and are related to chloroplast function (**Figure 1**). Thus, our data support the notion that photosynthesis and ETCs exert an input to nuclear oscillations.

Rifampicin, an inhibitor of organellar transcription, lengthened the circadian period in the dark as well as under continuous light. Previously, Vanden Driessche et al. (1970) and Mergenhagen and Schweiger (1975) reported that rifampicin does not affect the rhythmic oxygen evolution from individual cells of the unicellular algae *Acetabularia*. The antioxidant vitC and the oxidant paraquat altered the circadian period in a light quality- and reporter-specific manner. The importance of vitC in photosynthesis is underlined by its high concentration in

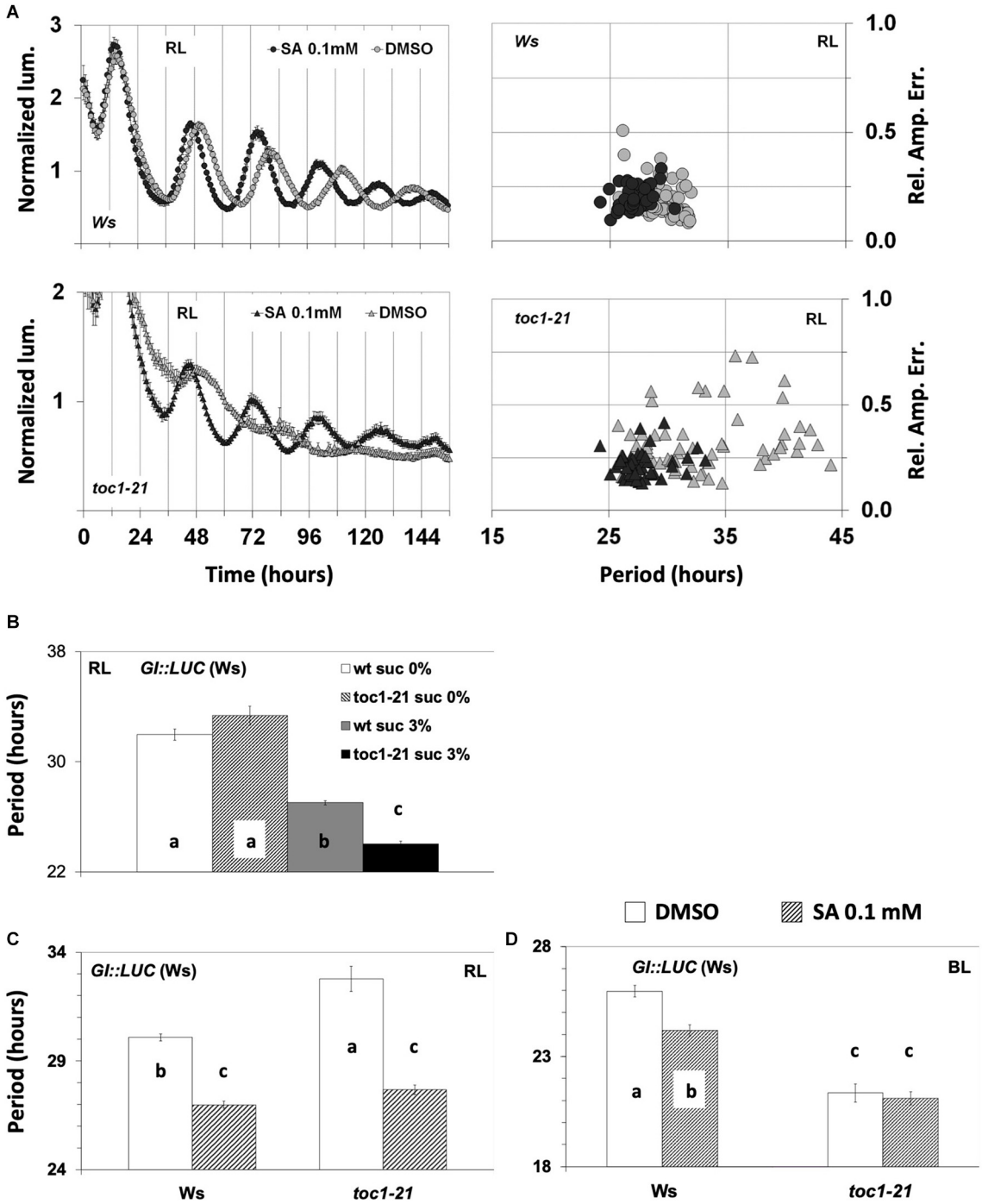


**FIGURE 5 |** Response of circadian clock mutants to salicylic acid (SA) application. **(A)** The *toc1-21* mutant was more sensitive than the wild type to SA under red light (RL). The experiments were conducted in the absence of supplementary sucrose. In the absence of multiple entrainment events, SA did not improve the oscillatory robustness of *Gl:LUC* in the wild type (see also **Figure 3C** and **Supplementary Figure 2A**). Note that *toc1-21* treated with SA displays a more concise population, whereas the non-treated is spread, thus has less precision. **(B)** The short period phenotype of the *toc1-21* mutant under RL is sucrose dependent. In the absence of supplementary sucrose, the *toc1-21* mutant exhibited a period similar to that of the wild type; only in the presence of supplementary sucrose did the mutant display a short-period phenotype. Data were analyzed with one-way ANOVA considering two factors: genotype and sucrose concentration (see **Supplementary Table S21**). **(C)** SA application under RL shortened the circadian period of both the wild type and the *toc1-21* mutant in media without sucrose. Note that without sucrose the mutant period length is longer than that of the wild type. The output of the ANOVA analysis with two factors is shown in **Supplementary Table S22**. **(D)** The *toc1-21* mutant is irresponsive to period shortening by SA application under blue light in media without sucrose. Note that under these conditions the mutant displayed a short period. Results of the data analysis are shown in **Supplementary Table S23**. In **(B–D)** different letters (a–c) denote statistically significant differences between means of period means. Error bars in all graphs represent standard error.

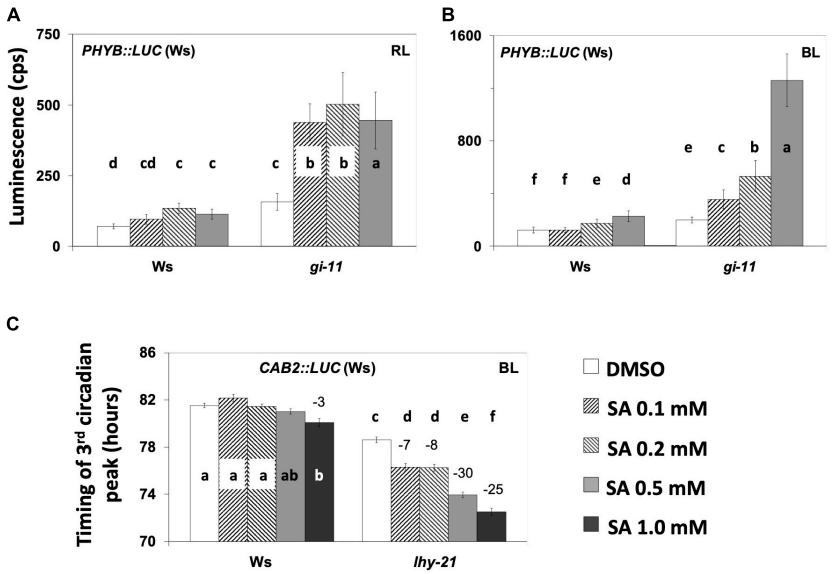


**FIGURE 6 | (A,B)** The *gi-11* mutant has an exacerbated increase in the expression of *PHY:LUC* by salicylic acid (SA) application under red light (RL) **(A)** and blue light (BL) **(B)** on medium without sucrose. SA increased the expression of marker *PHYB:LUC*, although this response was exacerbated in the *gi-11* mutant requiring solely 0.1 mM of SA to produce this effect compared to a higher SA concentration in the wild type. Under RL, bars represent the luminescence of the acute peak that followed dawn; under BL, bars represent the luminescence of the first circadian peak that followed the acute peak of dawn. Statistical analysis are shown in **Supplementary Tables S24, S25**. **(C)** SA application diminishes the expression of *CAB2:LUC* in the *lhy-21* mutant under BL in the presence of supplementary sucrose. Note that under these conditions, the wild type did not respond to SA application even at 1.0 mM, whereas the *lhy-21* mutant was hypersensitive. ANOVA statistical results are shown in **Supplementary Table S26**. Different letters (a–f) denote statistically significant differences between treatments. Error bars in all graphs represent standard error.

chloroplasts (20–300 mM). Its photo-protective activities are manifested in the regulation of the redox state of photosynthetic electron carriers in the direct or the enzymatic detoxification of ROS and in the role of vitC as an enzymatic cofactor during thermal dissipation of excess excitation energy (Smirnoff, 2000). Paraquat is a non-selective contact herbicide that generates ROS by accepting electrons from photosystem I (PSI) and transfers them to molecular oxygen. Interestingly, the *gi* mutant was shown to be resistant to paraquat-induced oxidative stress (Kurepa et al., 1998), whereas the circadian clock-related mutant *time for coffee* (*tic-2*) is overly sensitive to it (Sánchez-Villarreal et al., 2013), although it is not known if this behavior is related to a circadian phenotype (Shin et al., 2013). However, Lai et al. (2012) demonstrated that CCA1 acts as a master regulator of oxidative stress within the circadian clock. DCMU, which lengthened the circadian period in our experiments, is known to shift the PQ poll to its oxidized state as it inhibits the photosynthetic ETC upstream of PQ. The relationship of SA to chloroplasts has been reported in several studies (see the references below). Altogether our data are consistent with the hypothesis that chloroplast energy homeostasis creates a plastid-derived signal that intersects with the nuclear TTO to define a circadian period.

Major effects on entrainment were found to be altered by SA application (**Figure 3** and **Supplementary Figure S2**). This could relate to the nature of the hormone. SA is increased after exposure to high light (Chang et al., 2009) and contributes to acclimation and photosynthetic energy dissipation through photorespiration (Mateo et al., 2004) as well as through the induction of the antioxidant molecule glutathione (Mateo et al., 2006) and likely vitC (Chang et al., 2009). Thus, it makes sense to observe an effect early in the daytime (**Figures 3A,B**) as previously found by Covington et al. (2008).

A role for phyB in red light and blue light input to the clock (in the absence of supplementary sucrose) is supported by the reduced sensitivity of the *phyB-9* mutant to SA (**Figures 2E,F**). It is noteworthy that phyB is required downstream of SA signaling during certain aspects of host-plant defense mechanisms, such as the hypersensitive response that requires functional chloroplasts (Genoud et al., 2002). Our work provides further evidence that a pathway involving SA functions during parametric and non-parametric light entrainment (**Figure 3**). These findings together raise the possibility that the aforementioned pathway involved in defense responses, might also relate to photic entrainment. It is noteworthy that photic entrainment in cyanobacteria does not require photoreceptors. In this case, light input to the clock and circadian entrainment have been connected to the redox state of the photosynthetic ETC and the redox state of the PQ pool (Mackey et al., 2011).

## ETCs Affect Nuclear Oscillations

The role of ETCs in the regulation of a given process has been shown with distinct experimentation. Yabuta et al. (2007) have suggested that vitC levels are under the regulation of photosynthetic ETCs rather than of sugars because DCMU and sucrose both had a negative impact on the accumulation of vitC

after exposure to continuous light. This argument was based on the fact that, similarly to DCMU, photosynthates inhibit photosynthesis (Paul and Foyer, 2001). The involvement of ETCs in the regulation of a given process has also been demonstrated through the controlled manipulation of the redox state of PQ by chemicals and light quality. In more detail, treatment of low light-grown plants with the inhibitors of photosynthetic ETCs DCMU or DBMIB elicits similar effects on the redox status of the PQ pool as light enriched with far red light (FRL, 700 nm) or red light (RL, 680 nm). DCMU and FRL cause the oxidation of PQ, while DBMIB and RL cause the reduction of PQ. An antagonistic effect between these factors is therefore indicative that a process is sensitive to signals derived from PQ (Pfannschmidt et al., 2009). We found that the photosynthesis inhibitor DCMU and SA at low concentrations, which favors photosynthetic electron transport (Rivas-San Vicente and Plasencia, 2011), had opposite effects on circadian period. This would suggest that nuclear oscillations are under the regulation of ETCs. Our observation that the period-shortening effect of SA was inhibited by sucrose (see **Figure 4** and **Supplementary Figure S4**) further supports this notion as photosynthates, including sucrose, inhibit photosynthetic activity (Koch, 1996). Moreover, our results suggest that under BL, DBMIB (**Supplementary Figure S5**) and DCMU (**Figure 1A**) did not perturb the clock synergistically. Consequently, DCMU might lengthen the circadian period through its effect on the redox state of the PQ pool.

## Photosynthetic Electron Transport Activity Might Be Correlated to Circadian Period

Wenden et al. (2011) showed that, under RL, the circadian period is shorter than under FRL. This observation and the results presented in **Figure 1** suggest a correlation between photosynthetic electron transport activity and circadian period. Factors that reduce the PQ pool, such as RL, and those that could exert a protective role during photosynthesis through the regulations of PSII, such as SA and vitC (Karpinski et al., 1999; Smirnoff, 2000), induce period shortening, whereas factors that cause oxidation of the PQ pool such as DCMU, FRL (Muhlenbock et al., 2008), DD, or low light intensity (Oswald et al., 2001), or that inhibit photosynthesis, such as rifampicin (**Figure 1**) and iron deficiency [reviewed in Wilson and Connolly (2013)], all promote period lengthening. This correlation between the expected changes in the redox state of the PQ pool and the observed changes in the circadian period was also seen with the oxidant paraquat under blue light (**Figure 1B**). This is further supported by the aforementioned experiments with DBMIB and DCMU in which these photosynthesis inhibitors did not affect the circadian period similarly (compare **Figure 1A** with **Supplementary Figure S5**).

This and the reported studies together suggest a positive correlation between circadian period length and electron transport downstream of PSII. Based on this correlation, we propose the following: (a) ETCs might be involved in photic entrainment. This is further implied by the fact that the circadian effect of SA, directly connected to entrainment (**Figure 3**), is inhibited by sucrose application (**Figure 4**) that also inhibits photosynthesis (Koch, 1996); (b) ambient light intensity would contribute to circadian period, as predicted by the rule of Aschoff and FRCs, through the observed effect of fluence rate on the redox state of PQ (Oswald et al., 2001). In agreement, James et al. (2008) showed that the root clock, lacking photosynthetic activity, does not obey the rule of Aschoff; (c) oscillations in SA levels (Goodspeed et al., 2012) and in SA time-specific activity (**Figure 3**) and potential oscillations in photosynthetic electron transport would meet certain criteria as predicted by the *zeitnehmer* model (see below).

Mathematical modeling (Roenneberg and Merrow, 1999), confirmed experimentally in *Neurospora* (Merrow et al., 1999), has led to the identification of certain criteria that define *zeitnehmer* loops. Amongst these criteria are (1) rhythmicity *per se* of a biochemical pathway, the *zeitnehmer*, that perceives *zeitgeber* signals for the purpose of entrainment and then (2) through coupling of the *zeitnehmer* loop to a central oscillator provision of rhythm sustainability. The gated effect of SA on circadian timing (**Figure 3A**) implies an oscillatory potential in SA signaling. This is also suggested by the observation that SA levels are circadian-regulated (Goodspeed et al., 2012). Moreover, SA was shown here to be involved in parametric and non-parametric entrainment (**Figure 3** and **Supplementary Figure S2**) as well as in rhythm sustainability (**Figures 2C,D**, **3C**, **5A** and **Supplementary Figure S2**). This strongly supports that SA is directly or indirectly involved in a *zeitnehmer* loop that could entrain nuclear oscillations and provide rhythm sustainability. Coupling between TTOs and SA signaling or a related process is further supported by the SA-related phenotypes of *phyB-9* (**Figure 2**), *toc1-21* (**Figure 5**), *gi-11*, and *lhy-21* (**Figure 6**). Photosynthetic electron transport might be a potential candidate for such an SA-related process, given the correlation between the expected changes in the redox state of the PQ pool and the observed changes in circadian period presented here and in the literature. It is noteworthy that retrograde signaling and ROS produced as a consequence of the normal functioning of photosynthesis and respiration are being considered in the literature as circadian determinants (Dodd et al., 2015; Guadagno et al., 2018; Jones, 2018).

# MATERIALS AND METHODS

## Plant Materials

Rhythmicity was monitored using the promoter:luciferase system (Gould et al., 2006; Hanano et al., 2006; Kevei et al., 2006) in the *A. thaliana* Columbia (Col-0) and Wassilewskija (Ws) genetic backgrounds. Rhythmic promoter:luciferase markers in the Ws wild-type background are described in the literature as follows: *CCR2:LUC*, *CCA1:LUC* (Doyle et al., 2002), *CAB2:LUC* (Hall et al., 2001), *TOC1:LUC* (McWatters et al., 2007), *GI:LUC* (Ding et al., 2007), *PHYB:LUC* (Toth et al., 2001), *cca1-11*, *lhy-21*, and *toc1-21* mutants with the *CAB2:LUC* marker (Ding et al., 2007), and *CAB2:LUC* in the *gi-11* mutant (Gould et al., 2006); *PHYB:LUC* was introduced in the *gi-11* mutant and *GI:LUC* in the *toc1-21* by crossing transgenic plants expressing *GI:LUC*

in the wild-type Col-0 background and in the *phyB-9* mutant (Oh et al., 2004).

## Growth Conditions and Luciferase Imaging

The seeds were surface-sterilized, sown on 1% agar containing Murashige and Skoog basal salt mixture (pH 5.7) (Murashige and Skoog, 1962), and stratified for 3 days. The seedlings were entrained under 12-h light/12-h dark photoperiods under a fluence rate of white light (WL) at 100 μmol $m^{-2}$ $s^{-1}$ and a constant temperature of 22°C. During the second half of the subjective day and before dusk, the 6-day-old seedlings were transferred into 96-well microtiter plates (Perkin Elmer, Jügesheim, Germany) containing agar with chemicals or their respective diluents [dimethyl sulfoxide (DMSO) or water in the case of vitC] as controls with or without sucrose (3% w/v) as indicated. The seedlings were imaged in a luminescence scintillation counter (TopCount NXT, Perkin Elmer) at dusk (Southern and Millar, 2005; Hanano et al., 2006), allowing imaging under low fluence rates of red light (RL) and blue light (BL). The plants received a dark period of 12 h that corresponds to the subjective night and then entered free running conditions under monochromatic RL or BL at a low fluence rate (∼2 μmol $m^{-2}$ $s^{-1}$) provided by LEDs (Boikoglou et al., 2011). In some experiments, an additional entrainment event was applied in the automated scintillation counter before the onset of the free run.

## Data Analysis

The luminescence levels were quantified and graphically depicted using TopTempII and Biological Rhythms Analysis Software System (Southern and Millar, 2005). Period length and RAE were estimated using the FFT–NLLS program (Plautz et al., 1997).

To assess differences in period between and within chemical treatments, genotypes, and/or lighting conditions, we performed a one-way ANOVA with *post hoc* Tukey for multiple testing, using SAS 9.0 with default parameters (*p*-value 0.05). We used a two-factor experimental design for most of the data (**Figures 1A,B**, **2F**, **4A–C**, **5B–D**, **6A–C**) or a completely random design (**Supplementary Tables S3, S10**). Each analyzed dataset results are depicted in the supplementary tables and in **Figure 1A** separated within the figure with dashed lines. Statistically significant differences are shown with different letters in each panel and/or figure. Similarly, to evaluate differences in luminescence and the timing of the third peak (**Figures 2A,B,E**, **6**), we used a one-way ANOVA with Tukey for multiple testing, using SAS 9.0 with default parameters (*p*-value 0.05) using a two-factor experimental design. For simpler datasets, Student's *t*-test was used to compare between two populations using Microsoft Excel (see **Supplementary Tables**).

Period length is either a descriptive (not normalized) or a RAE-normalized period (noPer), in which case the contribution of a given period measurement is negatively correlated to its corresponding RAE value. The *p* values for differences in period (or any other circadian parameter) refer to descriptive data. Therefore, both measures for period are presented, RAE-normalized in graphs and with *p* values after a Student's *t*-test. The precision of a rhythmic population is defined by its inverse relation to the standard deviation (SD) of period (normalized or descriptive). The rhythmicity of a rhythmic population is defined by its inverse relation to the SD of period (normalized or descriptive). We distinguish between direct and indirect rhythmicity, the first relating to the mean RAE generated by FFT analysis and the second to the same mean after the plants discarded by FFT analysis were assigned with a RAE value of 1.

Sinusoidal curves represent luminescence activity or luminescence normalized to luciferase activity. Luminescence was automatically averaged by TopTempII for each plant separately. The normalized luminescence graphs were then generated by TopTempII for each population (**Figures 2C,D**, **5A**).

To quantify the expression of the luminescence of *PHYB:LUC* (Ws), the timing of the first acute peak after dawn (**Figure 2A**) or the first circadian peak (**Figure 2B**) was defined for each oscillating population by a visual inspection of the normalized luminescence graphs generated in TopTempII. The average luminescence at that time point was then used to assess the effect of SA on the expression of the marker.

## Light/Chemical Pulse Experiments

The range of the chemicals tested is illustrated in **Table 1**. For the experiments presented in **Figures 3A,B**, the plants harboring *GI:LUC* construct were entrained for 5 days under 12-h light/12-h dark photoperiod at a constant temperature of 22°C before entering continuous darkness at dusk. This was similar to the carbon and sucrose examinations by Perea-García et al. (2015); Perea-Garcia et al. (2016), and Philippou et al. (2019). Briefly, every 3 h, a subset of plants was retrieved from the basal growth medium (MS) and subjected to non-parametric entrainment with 3-h light pulses (WL) on the growth medium that contained SA at 1 mM or DMSO. The chemical pulse was 15 min shorter than the light pulse for technical reasons. At the end of each light/chemical pulse, the plants were placed in 96-well microtiter plates on basal MS media (without SA or DMSO) and luminescence was monitored in continuous darkness. Four time windows for light–chemical pulses were applied between ZT0 and ZT12 hours (ZT for *zeitgeber* time; ZT0 is objective dawn that marks the beginning of the free run).

**TABLE 1** | Range of concentrations reported in the literature for the chemicals that affected the circadian period in this study.

| Chemical | Active concentration in the present study | Concentration used in the cited reference | References |
|---|---|---|---|
| SA | 0.1–1 mM | 0.25–0.5 mM | Genoud et al. (2002) |
| DCMU | 5–10 μM | 8 μM | Muhlenbock et al. (2008) |
| DBMIB | 5–10 μM | 14 μM | Muhlenbock et al. (2008) |
| VitC | 2–3 mM | 10 mM | Horling et al. (2003) |

*Rifampicin concentrations vary widely in the literature.*

## DATA AVAILABILITY STATEMENT

All datasets generated for this study are included in the article/**Supplementary Material**.

## AUTHOR CONTRIBUTIONS

All authors contributed to the writing of this manuscript. KP, AS-V, and AD contributed to the work. SD oversaw the study.

## FUNDING

Additional funding is acknowledged from the University of York, the University of Henan, the Max Planck Society and their IMPRS program. The data in this manuscript are included in the thesis entitled "Identification and Genetic Analysis of Metabolic–Transcriptional Interactions Within the Circadian System of *Arabidopsis thaliana*" at the University of Cologne (Philippou, 2015) and is available at https://kups.ub.uni-koeln.de/6212/. This research was funded by the BBSRC, grant numbers BBB/M000435/1 and BB/N018540/1, the DFG grant SFB635, and is supported by the 111 Project #D16014.

## ACKNOWLEDGMENTS

We are thankful to Dr. Mónica Ramírez-Mella for her guidance on the SAS 9.0 software. This work is dedicated to the memory of Exakoustodianos Philippou.

## SUPPLEMENTARY MATERIAL

The Supplementary Material for this article can be found online at: https://www.frontiersin.org/articles/10.3389/fphys.2020.00429/full#supplementary-material

**FIGURE S1 |** Effect of different chemicals on circadian rhythm. **(A)** Vitamin C did not alter the circadian period of *Gl:LUC* under blue light (BL). Standard errors were omitted for clarity. **(B,C)** Rifampicin lengthened the circadian period of *Gl:LUC* in the dark **(B)** and under BL **(C)**. **(D)** Salicylic acid (SA) induces a short period of *CCR2:LUC* under BL. **(E,F)** SA increased the oscillatory robustness of *CCR2:LUC* **(E)** and of *TOC1:LUC* **(F)**; horizontal error bars represent the standard deviation (SD) of period and vertical error bars represent the standard error of the relative amplitude error. Note that SA application diminishes the SD. **(G,H)** Effect of SA on luciferase activity under RL plus BL is marker-specific. SA increased the expression of *TOC:LUC* **(G)** and decreased the expression of *Gl:LUC* **(H)**. Consequently, the effect of SA on luciferase activity, being marker-specific, could not be dependent on luciferase activity alone. Experiments were conducted in the presence of supplementary sucrose. Growth and entrainment took place as described in **Figure 1**. Error bars represent standard errors in **(A–D,G,H)**.

**FIGURE S2 |** Salicylic acid (SA) affects the circadian rhythms through entrainment. **(A)** SA increases the oscillatory robustness of *CCR2:LUC* through parametric entrainment. The plants received the indicated number of entrainment events on medium with 3% sucrose and SA or dimethyl sulfoxide (DMSO) in 96-well microtiter plates. Then, the seedlings were placed in a TopCount in continuous darkness and at a constant temperature of 21°C. The panels on the right represent the combined data from three independent experiments that produced similar results to each other. The panels on the left show one of these experiments; the error bars represent standard error and are occasionally smaller than the respective symbols. The *y*-axis in the right panels is negatively correlated to direct rhythmicity and the standard deviation on the *x*-axis is negatively correlated to precision. **(B)** Consecutive entrainment events (0, 1, 2, or 3 days and in one experiment 7 days) in 96-well microplates delayed the phase (timing of the second circadian peak) of *Gl:LUC* expression (0 day vs. 1 day, $\Delta$phase = 1.33 h, $p = 0.01$; 0 day vs. 2 days, $\Delta$phase = 3.49 h, $p = 1.3 \times 10^{-4}$; 0 day vs. 3 days, $\Delta$phase = 4.29 h, $p = 6.0 \times 10^{-13}$; 0 day vs. 7 days, $\Delta$phase = 3.13 h, $p = 8.8 \times 10^{-4}$). Phase, however, did not change after 7 days of entrainment if SA was applied at 0.1 mM ($\Delta$phase = 1.18 h, $p = 0.10$). Application of SA at 0.5 mM reversed the effect of entrainment on phase by the 7th day (0 day vs. 7 days, $\Delta$phase = $-1.84$ h, $p = 3.1 \times 10^{-4}$). Similarly, the application of SA at 1 mM resulted in phase advances (0 d vs. 1 day, $\Delta$phase = $-2.69$ h, $p = 2.9 \times 10^{-5}$; 0 day vs. 2 days, $\Delta$phase = $-1.18$ h, $p = 0.01$; 0 day vs. 3 days, $\Delta$phase = $-0.70$ h, $p > 0.05$). Student's *t*-test for each pair comparison is shown. Statistical analysis showed that the SA-mediated phase advances were enhanced by the preceding parametric entrainment events. Error bars in all graphs represent standard error.

**FIGURE S3 |** Salicylic acid (SA)-related phenotypes of the *toc1-21* mutant. Under blue light, in the absence of supplementary sucrose, the application of SA at 0.1 mM accelerated the oscillations of *CAB2:LUC* in the wild-type ($p = 0.01$) but not in the *toc1-21* mutant ($p = 0.79$). Error bars represent standard error.

**FIGURE S4 | (A,B)** Sucrose moderated the period-shortening effect of salicylic acid (SA) of the wild type harboring the *CAB2:LUC* transgene. **(A,C)** The *cca1-11* mutant did not display any SA-related circadian phenotypes. **(B,D)** The *lhy-21* mutant was slightly more sensitive than the wild type to SA-mediated peak advance [third peak shown with arrow in **(D)**]. Note that **(D)** does not display the first two peaks from *zeitgeber* time 0–48 h as in the other figures. Error bars represent standard error.

**FIGURE S5 |** 2,5-Dibromo-3-methyl-6-isopropylbenzoquinone, unlike 3-(3,4-dichlorophenyl)-1,1-dimethylurea (**Figure 1A**), did not disturb the rhythmic expression of *Gl:LUC* under blue light. The error bars are smaller than the symbols and represent standard error.

## REFERENCES

Alabadí, D., Oyama, T., Yanovsky, M. J., Harmon, F. G., Más, P., and Kay, S. A. (2001). Reciprocal regulation between *TOC1* and *LHY/CCA1* within the *Arabidopsis* circadian clock. *Science* 293, 880–883. doi: 10.1126/science.1061320

Anwer, M. U., Boikoglou, E., Herrero, E., Hallstein, M., Davis, A. M., James, G. V., et al. (2014). Natural variation reveals that intracellular distribution of ELF3 protein is associated with function in the circadian clock. *eLife* 3: e02206.

Arana, M. V., Marín-De La Rosa, N., Maloof, J. N., Blázquez, M. A., and Alabadí, D. (2011). Circadian oscillation of gibberellin signaling in *Arabidopsis*. *Proc. Natl. Acad. Sci. U.S.A.* 108, 9292–9297. doi: 10.1073/pnas.1101050108

Asher, G., Gatfield, D., Stratmann, M., Reinke, H., Dibner, C., Kreppel, F., et al. (2008). SIRT1 regulates circadian clock gene expression through PER2 deacetylation. *Cell* 134, 317–328. doi: 10.1016/j.cell.2008.06.050

Belbin, F. E., Hall, G. J., Jackson, A. B., Schanschieff, F. E., Archibald, G., Formstone, C., et al. (2019). Plant circadian rhythms regulate the effectiveness of a glyphosate-based herbicide. *Nat. Commun.* 10:3704. doi: 10.1038/s41467-019-11709-5

Bläsing, O. E., Gibon, Y., Günther, M., Höhne, M., Morcuende, R., Osuna, D., et al. (2005). Sugars and circadian regulation make major contributions to the global regulation of diurnal gene expression in *Arabidopsis*. *Plant Cell* 17, 3257–3281. doi: 10.1105/tpc.105.035261

Bognár, L. K., Hall, A., Adám, É, Thain, S. C., Nagy, F., and Millar, A. J. (1999). The circadian clock controls the expression pattern of the circadian input

photoreceptor, phytochrome B. *Proc. Natl. Acad. Sci. U.S.A.* 96, 14652–14657. doi: 10.1073/pnas.96.25.14652

Boikoglou, E., Ma, Z., Davis, A. M., von Korff, M., Nagy, F., and Davis, S. J. (2011). Environmental memory from a circadian oscillator: the *Arabidopsis thaliana* clock differentially integrates perception of photic vs. thermal entrainment. *Genetics* 189, 655–664. doi: 10.1534/genetics.111.131417

Bujdoso, N., and Davis, S. J. (2013). Mathematical modeling of an oscillating gene circuit to unravel the circadian clock network of *Arabidopsis thaliana*. *Front. Plant Sci.* 4:3. doi: 10.3389/fpls.2013.00003

Bunning, E. (1967). *The Physiological Clock*. New York, NY: Springer.

Chang, C. C., Ślesak, I., Jordá, L., Sotnikov, A., Melzer, M., Miszalski, Z., et al. (2009). Arabidopsis chloroplastic glutathione peroxidases play a role in cross talk between photooxidative stress and immune responses. *Plant Physiol.* 150, 670–683. doi: 10.1104/pp.109.135566

Chen, Z., Zheng, Z., Huang, J., Lai, Z., and Fan, B. (2009). Biosynthesis of salicylic acid in plants. *Plant Signal. Behav.* 4, 493–496.

Covington, M. F., and Harmer, S. L. (2007). The circadian clock regulates auxin signaling and responses in *Arabidopsis*. *PLoS Biol.* 5:e222. doi: 10.1371/journal.pbio.0050222

Covington, M. F., Maloof, J. N., Straume, M., Kay, S. A., and Harmer, S. L. (2008). Global transcriptome analysis reveals circadian regulation of key pathways in plant growth and development. *Genome Biol.* 9:R130. doi: 10.1186/gb-2008-9-8-r130

Covington, M. F., Panda, S., Liu, X. L., Strayer, C. A., Wagner, D. R., and Kay, S. A. (2001). ELF3 modulates resetting of the circadian clock in Arabidopsis. *Plant Cell* 13, 1305–1316. doi: 10.1105/tpc.13.6.1305

Dalchau, N., Baek, S. J., Briggs, H. M., Robertson, F. C., Dodd, A. N., Gardner, M. J., et al. (2011). The circadian oscillator gene GIGANTEA mediates a long-term response of the *Arabidopsis thaliana* circadian clock to sucrose. *Proc. Natl. Acad. Sci. U.S.A.* 108, 5104–5109. doi: 10.1073/pnas.1015452108

Devlin, P. F., and Kay, S. A. (2000). Cryptochromes are required for phytochrome signaling to the circadian clock but not for rhythmicity. *Plant Cell* 12, 2499–2509. doi: 10.1105/tpc.12.12.2499

Diamond, S., Rubin, B. E., Shultzaberger, R. K., Chen, Y., Barber, C. D., and Golden, S. S. (2017). Redox crisis underlies conditional light-dark lethality in cyanobacterial mutants that lack the circadian regulator, RpaA. *Proc. Natl. Acad. Sci. U.S.A.* 114, E580–E589. doi: 10.1073/pnas.1613078114

Ding, Z., Doyle, M. R., Amasino, R. M., and Davis, S. J. (2007). A complex genetic interaction between *Arabidopsis thaliana* TOC1 and CCA1/LHY in driving the circadian clock and in output regulation. *Genetics* 176, 1501–1510. doi: 10.1534/genetics.107.072769

Dioum, E. M., Rutter, J., Tuckerman, J. R., Gonzalez, G., Gilles-Gonzalez, M.-A., and Mcknight, S. L. (2002). NPAS2: a gas-responsive transcription factor. *Science* 298, 2385–2387. doi: 10.1126/science.1078456

Dodd, A. N., Belbin, F. E., Frank, A., and Webb, A. A. (2015). Interactions between circadian clocks and photosynthesis for the temporal and spatial coordination of metabolism. *Front. Plant Sci.* 6:245. doi: 10.3389/fpls.2015.00245

Dodd, A. N., Gardner, M. J., Hotta, C. T., Hubbard, K. E., Dalchau, N., Love, J., et al. (2007). The *Arabidopsis* circadian clock incorporates a cADPR-based feedback loop. *Science* 318, 1789–1792. doi: 10.1126/science.1146757

Doyle, M. R., Davis, S. J., Bastow, R. M., Mcwatters, H. G., Kozma-Bognár, L., Nagy, F., et al. (2002). The ELF4 gene controls circadian rhythms and flowering time in *Arabidopsis thaliana*. *Nature* 419, 74–77. doi: 10.1038/nature00954

Fornara, F., de Montaigu, A., Sanchez-Villareal, A., Takahashi, Y., Ver Loren van Themaat, E., Huettel, B., et al. (2015). The GI-CDF module of Arabidopsis regulates freezing tolerance and growth as well as flowering. *Plant J.* 81, 695–706. doi: 10.1111/tpj.12759

Fujiwara, S., Wang, L., Han, L., Suh, S.-S., Salomé, P. A., Mcclung, C. R., et al. (2008). Post-translational regulation of the Arabidopsis circadian clock through selective proteolysis and phosphorylation of pseudo-response regulator proteins. *J. Biol. Chem.* 283, 23073–23083. doi: 10.1074/jbc.M803471200

Genoud, T., Buchala, A. J., Chua, N. H., and Metraux, J. P. (2002). Phytochrome signalling modulates the SA-perceptive pathway in *Arabidopsis*. *Plant J.* 31, 87–95. doi: 10.1046/j.1365-313x.2002.01338.x

Goodspeed, D., Chehab, E. W., Min-Venditti, A., Braam, J., and Covington, M. F. (2012). Arabidopsis synchronizes jasmonate-mediated defense with insect circadian behavior. *Proc. Natl. Acad. Sci. U.S.A.* 109, 4674–4677. doi: 10.1073/pnas.1116368109

Gould, P. D., Locke, J. C., Larue, C., Southern, M. M., Davis, S. J., Hanano, S., et al. (2006). The molecular basis of temperature compensation in the *Arabidopsis* circadian clock. *Plant Cell* 18, 1177–1187. doi: 10.1105/tpc.105.039990

Grundy, J., Stoker, C., and Carré, I. A. (2015). Circadian regulation of abiotic stress tolerance in plants. *Front. Plant Sci.* 6:648. doi: 10.3389/fpls.2015.00648

Guadagno, C. R., Ewers, B. E., and Weinig, C. (2018). Circadian rhythms and redox state in plants: till stress do us part. *Front. Plant Sci.* 9:247. doi: 10.3389/fpls.2018.00247

Hall, A., Kozma-Bognar, L., Toth, R., Nagy, F., and Millar, A. J. (2001). Conditional circadian regulation of *PHYTOCHROME A* gene expression. *Plant Physiol.* 127, 1808–1818. doi: 10.1104/pp.010294

Hanano, S., Domagalska, M. A., Nagy, F., and Davis, S. J. (2006). Multiple phytohormones influence distinct parameters of the plant circadian clock. *Genes Cells* 11, 1381–1392. doi: 10.1111/j.1365-2443.2006.01026.x

Haydon, M. J., Mielczarek, O., Robertson, F. C., Hubbard, K. E., and Webb, A. A. (2013). Photosynthetic entrainment of the *Arabidopsis thaliana* circadian clock. *Nature* 502, 689–692. doi: 10.1038/nature12603

Herrero, E., Kolmos, E., Bujdoso, N., Yuan, Y., Wang, M., Berns, M. C., et al. (2012). EARLY FLOWERING4 Recruitment of EARLY FLOWERING3 in the Nucleus Sustains the *Arabidopsis* Circadian Clock. *Plant Cell* 24, 428–443. doi: 10.1105/tpc.111.093807

Horling, F., Lamkemeyer, P., König, J., Finkemeier, I., Kandlbinder, A., Baier, M., et al. (2003). Divergent light-, ascorbate-, and oxidative stress-dependent regulation of expression of the peroxiredoxin gene family in Arabidopsis. *Plant Physiol.* 131, 317–325. doi: 10.1104/pp.010017

Huang, X., Li, Y., Zhang, X., Zuo, J., and Yang, S. (2010). The Arabidopsis LSD1 gene plays an important role in the regulation of low temperature-dependent cell death. *New Phytol.* 187, 301–312. doi: 10.1111/j.1469-8137.2010.03275.x

Huq, E., Tepperman, J. M., and Quail, P. H. (2000). GIGANTEA is a nuclear protein involved in phytochrome signaling in *Arabidopsis*. *Proc. Natl Acad. Sci. U.S.A.* 97, 9789–9794. doi: 10.1073/pnas.170283997

James, A. B., Monreal, J. A., Nimmo, G. A., Kelly, C. L., Herzyk, P., Jenkins, G. I., et al. (2008). The circadian clock in *Arabidopsis* roots is a simplified slave version of the clock in shoots. *Science* 322, 1832–1835. doi: 10.1126/science.1161403

Jones, M. A. (2018). Retrograde signaling as an informant of circadian timing. *New Phytol.* 221, 1749–1753. doi: 10.1111/nph.15525

Kaasik, K., and Lee, C. C. (2004). Reciprocal regulation of haem biosynthesis and the circadian clock in mammals. *Nature* 430, 467–471. doi: 10.1038/nature02724

Karapetyan, S., and Dong, X. (2018). Redox and the circadian clock in plant immunity: a balancing act. *Free Radic. Biol. Med.* 119, 56–61. doi: 10.1016/j.freeradbiomed.2017.12.024

Karpinski, S., Reynolds, H., Karpinska, B., Wingsle, G., Creissen, G., and Mullineaux, P. (1999). Systemic signaling and acclimation in response to excess excitation energy in *Arabidopsis*. *Science* 284, 654–657. doi: 10.1126/science.284.5414.654

Kevei, E., Gyula, P., Hall, A., Kozma-Bognar, L., Kim, W. Y., Eriksson, M. E., et al. (2006). Forward genetic analysis of the circadian clock separates the multiple functions of *ZEITLUPE*. *Plant Physiol.* 140, 933–945. doi: 10.1104/pp.105.074864

Kim, J. Y., Song, H. R., Taylor, B. L., and Carre, I. A. (2003). Light-regulated translation mediates gated induction of the *Arabidopsis* clock protein LHY. *EMBO J.* 22, 935–944. doi: 10.1093/emboj/cdg075

Kim, W. Y., Fujiwara, S., Suh, S. S., Kim, J., Kim, Y., Han, L., et al. (2007). ZEITLUPE is a circadian photoreceptor stabilized by GIGANTEA in blue light. *Nature* 449, 356–360. doi: 10.1038/nature06132

Koch, K. E. (1996). Carbohydrate-modulated gene expression in plants. *Ann. Rev. Plant Physiol. Plant Mol. Biol.* 47, 509–540. doi: 10.1146/annurev.arplant.47.1.509

Korneli, C., Danisman, S., and Staiger, D. (2014). Differential control of pre-invasive and post-invasive antibacterial defense by the Arabidopsis circadian clock. *Plant Cell Physiol.* 55, 1613–1622. doi: 10.1093/pcp/pcu092

Kurepa, J., Smalle, J., Van Montagu, M., and Inze, D. (1998). Oxidative stress tolerance and longevity in *Arabidopsis*: the late-flowering mutant gigantea is tolerant to paraquat. *Plant J.* 14, 759–764. doi: 10.1046/j.1365-313x.1998.00168.x

Lai, A. G., Doherty, C. J., Mueller-Roeber, B., Kay, S. A., Schippers, J. H., and Dijkwel, P. P. (2012). *CIRCADIAN CLOCK-ASSOCIATED 1* regulates ROS

homeostasis and oxidative stress responses. *Proc. Natl. Acad. Sci. U.S.A.* 16, 17129–17134. doi: 10.1073/pnas.1209148109

Legnaioli, T., Cuevas, J., and Mas, P. (2009). TOC1 functions as a molecular switch connecting the circadian clock with plant responses to drought. *EMBO J.* 28, 3745–3757. doi: 10.1038/emboj.2009.297

Li, Z., Bonaldi, K., Uribe, F., and Pruneda-Paz, J. L. (2018). A localized *Pseudomonas syringae* infection triggers systemic clock responses in Arabidopsis. *Curr. Biol.* 28, 630–639.e4. doi: 10.1016/j.cub.2018.01.001

Litthauer, S., Chan, K. X., and Jones, M. A. (2018). 3'-Phosphoadenosine 5'-Phosphate accumulation delays the circadian system. *Plant Phys.* 176, 3120. doi: 10.1104/pp.17.01611

Locke, J. C., Kozma-Bognar, L., Gould, P. D., Feher, B., Kevei, E., Nagy, F., et al. (2006). Experimental validation of a predicted feedback loop in the multi-oscillator clock of *Arabidopsis thaliana*. *Mol. Syst. Biol.* 2:59. doi: 10.1038/msb4100102

Locke, J. C., Southern, M. M., Kozma-Bognar, L., Hibberd, V., Brown, P. E., Turner, M. S., et al. (2005). Extension of a genetic network model by iterative experimentation and mathematical analysis. *Mol. Syst. Biol.* 1:2005.0013.

Mackey, S. R., Golden, S. S., and Ditty, J. L. (2011). The itty-bitty time machine genetics of the cyanobacterial circadian clock. *Adv. Genet.* 74, 13–53. doi: 10.1016/B978-0-12-387690-4.00002-7

Más, P., Alabadí, D., Yanovsky, M. J., Oyama, T., and Kay, S. A. (2003a). Dual role of TOC1 in the control of circadian and photomorphogenic responses in Arabidopsis. *Plant Cell* 15, 223–236. doi: 10.1105/tpc.006734

Más, P., Kim, W. Y., Somers, D. E., and Kay, S. A. (2003b). Targeted degradation of TOC1 by ZTL modulates circadian function in *Arabidopsis thaliana*. *Nature* 426, 567–570. doi: 10.1038/nature02163

Mateo, A., Funck, D., Muhlenbock, P., Kular, B., Mullineaux, P. M., and Karpinski, S. (2006). Controlled levels of salicylic acid are required for optimal photosynthesis and redox homeostasis. *J. Exp. Bot.* 57, 1795–1807. doi: 10.1093/jxb/erj196

Mateo, A., Muhlenbock, P., Rusterucci, C., Chang, C. C., Miszalski, Z., Karpinska, B., et al. (2004). *LESION SIMULATING DISEASE 1* is required for acclimation to conditions that promote excess excitation energy. *Plant Physiol.* 136, 2818–2830. doi: 10.1104/pp.104.043646

McClung, C. R. (2019). The plant circadian oscillator. *Biology* 8:14. doi: 10.3390/biology8010014

McWatters, H. G., Kolmos, E., Hall, A., Doyle, M. R., Amasino, R. M., Gyula, P., et al. (2007). ELF4 is required for oscillatory properties of the circadian clock. *Plant Physiol.* 144, 391–401. doi: 10.1104/pp.107.096206

Mergenhagen, D., and Schweiger, H. G. (1975). The effect of different inhibitors of transcription and translation on the expression and control of circadian rhythm in individual cells of Acetabularia. *Exp. Cell Res.* 94, 321–326. doi: 10.1016/0014-4827(75)90499-1

Merrow, M., Brunner, M., and Roenneberg, T. (1999). Assignment of circadian function for the Neurospora clock gene frequency. *Nature* 399, 584–586. doi: 10.1038/21190

Mou, Z., Fan, W., and Dong, X. (2003). Inducers of plant systemic acquired resistance regulate NPR1 function through redox changes. *Cell* 113, 935–944. doi: 10.1016/s0092-8674(03)00429-x

Muhlenbock, P., Szechynska-Hebda, M., Plaszczyca, M., Baudo, M., Mateo, A., Mullineaux, P. M., et al. (2008). Chloroplast signaling and *LESION SIMULATING DISEASE1* regulate crosstalk between light acclimation and immunity in *Arabidopsis*. *Plant Cell* 20, 2339–2356. doi: 10.1105/tpc.108.059618

Müller, L. M., von Korff, M., and Davis, S. J. (2014). Connections between circadian clocks and carbon metabolism reveal species-specific effects on growth control. *J. Exp. Bot.* 65, 2915–2923. doi: 10.1093/jxb/eru117

Murashige, T., and Skoog, F. J. P. P. (1962). A revised medium for rapid growth and bio assays with tobacco tissue cultures. *Physiol. Plant.* 15, 473–497. doi: 10.1111/j.1399-3054.1962.tb08052.x

Nakahata, Y., Kaluzova, M., Grimaldi, B., Sahar, S., Hirayama, J., Chen, D., et al. (2008). The NAD+-dependent deacetylase SIRT1 modulates CLOCK-mediated chromatin remodeling and circadian control. *Cell* 134, 329–340. doi: 10.1016/j.cell.2008.07.002

Nakahata, Y., Sahar, S., Astarita, G., Kaluzova, M., and Sassone-Corsi, P. (2009). Circadian control of the NAD+ salvage pathway by CLOCK-SIRT1. *Science* 324, 654–657. doi: 10.1126/science.1170803

Nicaise, V., Joe, A., Jeong, B. R., Korneli, C., Boutrot, F., Westedt, I., et al. (2013). *Pseudomonas* HopU1 modulates plant immune receptor levels by blocking the interaction of their mRNAs with GRP7. *EMBO J.* 32, 701–712. doi: 10.1038/emboj.2013.15

Nusinow, D. A., Helfer, A., Hamilton, E. E., King, J. J., Imaizumi, T., Schultz, T. F., et al. (2011). The ELF4-ELF3-LUX complex links the circadian clock to diurnal control of hypocotyl growth. *Nature* 475, 398–402. doi: 10.1038/nature10182

Oakenfull, R. J., and Davis, S. J. (2017). Shining a light on the Arabidopsis circadian clock. *Plant Cell Environ.* 40, 2571–2585. doi: 10.1111/pce.13033

Oh, E., Kim, J., Park, E., Kim, J. I., Kang, C., and Choi, G. (2004). PIL5, a phytochrome-interacting basic helix-loop-helix protein, is a key negative regulator of seed germination in *Arabidopsis thaliana*. *Plant Cell* 16, 3045–3058. doi: 10.1105/tpc.104.025163

O'Neill, J. S., Maywood, E. S., Chesham, J. E., Takahashi, J. S., and Hastings, M. H. (2008). cAMP-dependent signaling as a core component of the mammalian circadian pacemaker. *Science* 320, 949–953. doi: 10.1126/science.1152506

Oswald, O., Martin, T., Dominy, P. J., and Graham, I. A. (2001). Plastid redox state and sugars: interactive regulators of nuclear-encoded photosynthetic gene expression. *Proc. Natl. Acad. Sci. U.S.A.* 98, 2047–2052. doi: 10.1073/pnas.98.4.2047

Panda, S., Poirier, G. G., and Kay, S. A. (2002). tej defines a role for poly(ADP-ribosyl)ation in establishing period length of the *Arabidopsis* circadian oscillator. *Dev. Cell* 3, 51–61. doi: 10.1016/s1534-5807(02)00200-9

Park, D. H., Somers, D. E., Kim, Y. S., Choy, Y. H., Lim, H. K., Soh, M. S., et al. (1999). Control of circadian rhythms and photoperiodic flowering by the *Arabidopsis GIGANTEA* gene. *Science* 285, 1579–1582. doi: 10.1126/science.285.5433.1579

Paul, M. J., and Foyer C. H. (2001). Sink regulation of photosynthesis. *J. Exp. Bot.* 52, 1383–1400.

Perea-García, A., Andrés-Bordería, A., Mayo De Andrés, S., Sanz, A., Davis, A. M., Davis, S. J., et al. (2015). Modulation of copper deficiency responses by diurnal and circadian rhythms in *Arabidopsis thaliana*. *J. Exp. Bot.* 67, 391–403. doi: 10.1093/jxb/erv474

Perea-Garcia, A., Sanz, A., Moreno, J., Andres-Borderia, A., De Andres, S. M., Davis, A. M., et al. (2016). Daily rhythmicity of high affinity copper transport. *Plant Signal. Behav.* 11, e1140291. doi: 10.1080/15592324.2016.1140291

Pfannschmidt, T., Bräutigam, K., Wagner, R., Dietzel, L., Schröter, Y., Steiner, S., et al. (2009). Potential regulation of gene expression in photosynthetic cells by redox and energy state: approaches towards better understanding. *Ann. Bot.* 103, 599–607. doi: 10.1093/aob/mcn081

Philippou, K. (2015). *Identification and Genetic Analysis of Metabolic – Transcriptional Interactions within the Circadian System of Arabidopsis thaliana*. Köln: University of Cologne.

Philippou, K., Ronald, J., Sanchez-Villarreal, A., Davis, A. M., and Davis, S. J. (2019). Physiological and genetic dissection of sucrose inputs to the *Arabidopsis thaliana* circadian system. *Genes* 10:334. doi: 10.3390/genes10050334

Pitzschke, A., Forzani, C., and Hirt, H. (2006). Reactive oxygen species signaling in plants. *Antioxid. Redox Signal.* 8, 1757–1764.

Plautz, J. D., Straume, M., Stanewsky, R., Jamison, C. F., Brandes, C., Dowse, H. B., et al. (1997). Quantitative analysis of Drosophila period gene transcription in living animals. *J. Biol. Rhythms* 12, 204–217.

Pokhilko, A., Fernandez, A. P., Edwards, K. D., Southern, M. M., Halliday, K. J., and Millar, A. J. (2012). The clock gene circuit in *Arabidopsis* includes a repressilator with additional feedback loops. *Mol. Syst. Biol.* 8:574. doi: 10.1038/msb.2012.6

Pokhilko, A., Hodge, S. K., Stratford, K., Knox, K., Edwards, K. D., Thomson, A. W., et al. (2010). Data assimilation constrains new connections and components in a complex, eukaryotic circadian clock model. *Mol. Syst. Biol.* 6:416. doi: 10.1038/msb.2010.69

Ramsey, K. M., Yoshino, J., Brace, C. S., Abrassart, D., Kobayashi, Y., Marcheva, B., et al. (2009). Circadian clock feedback cycle through NAMPT-mediated NAD+ biosynthesis. *Science* 324, 651–654. doi: 10.1126/science.1171641

Rivas-San Vicente, M., and Plasencia, J. (2011). Salicylic acid beyond defence: its role in plant growth and development. *J. Exp. Bot.* 62, 3321–3338. doi: 10.1093/jxb/err031

Robertson, F. C., Skeffington, A. W., Gardner, M. J., and Webb, A. A. (2009). Interactions between circadian and hormonal signalling in plants. *Plant Mol. Biol.* 69, 419–427. doi: 10.1007/s11103-008-9407-4

Roenneberg, T., and Merrow, M. (1999). Circadian systems and metabolism. *J. Biol. Rhythms* 14, 449–459.

Ronald, J., and Davis, S. (2017). Making the clock tick: the transcriptional landscape of the plant circadian clock [version 1; referees: 2 approved]. *F1000 Res.* 6:951. doi: 10.12688/f1000research.11319.1

Rust, M. J., Golden, S. S., and O'shea, E. K. (2011). Light-driven changes in energy metabolism directly entrain the cyanobacterial circadian oscillator. *Science* 331, 220–223. doi: 10.1126/science.1197243

Rutter, J., Reick, M., Wu, L. C., and Mcknight, S. L. (2001). Regulation of clock and NPAS2 DNA binding by the redox state of NAD cofactors. *Science* 293, 510–514.

Salomé, P. A., Michael, T. P., Kearns, E. V., Fett-Neto, A. G., Sharrock, R. A., and McClung, C. R. (2002). The *out of phase 1* mutant defines a role for PHYB in circadian phase control in Arabidopsis. *Plant Physiol.* 129, 1674–1685.

Sánchez, A., Shin, J., and Davis, S. J. (2011). Abiotic stress and the plant circadian clock. *Plant Signal. Behav.* 6, 223–231.

Sánchez-Villarreal, A., Shin, J., Bujdoso, N., Obata, T., Neumann, U., Du, S. X., et al. (2013). *TIME FOR COFFEE* is an essential component in the maintenance of metabolic homeostasis in *Arabidopsis thaliana*. *Plant J.* 76, 188–200.

Shin, J., Du, S., Bujdoso, N., Hu, Y., and Davis, S. J. (2013). Overexpression and loss-of-function at *TIME FOR COFFEE* results in similar phenotypes in diverse growth and physiological responses. *J. Plant Biol.* 56, 152–159.

Shin, J., Heidrich, K., Sanchez-Villarreal, A., Parker, J. E., and Davis, S. J. (2012). TIME FOR COFFEE represses accumulation of the MYC2 transcription factor to provide time-of-day regulation of jasmonate signaling in *Arabidopsis*. *Plant Cell* 24, 2470–2482. doi: 10.1105/tpc.111.095430

Smirnoff, N. (2000). Ascorbate biosynthesis and function in photoprotection. *Philos. Trans. R. Soc. Lond. B Biol. Sci.* 355, 1455–1464.

Somers, D. E., Devlin, P. F., and Kay, S. A. (1998). Phytochromes and cryptochromes in the entrainment of the *Arabidopsis* circadian clock. *Science* 282, 1488–1490.

Somers, D. E., Kim, W. Y., and Geng, R. (2004). The F-box protein ZEITLUPE confers dosage-dependent control on the circadian clock, photomorphogenesis, and flowering time. *Plant Cell* 16, 769–782.

Somers, D. E., Schultz, T. F., Milnamow, M., and Kay, S. A. (2000). *ZEITLUPE* encodes a novel clock-associated PAS protein from *Arabidopsis*. *Cell* 101, 319–329.

Southern, M. M., and Millar, A. J. (2005). Circadian genetics in the model higher plant, *Arabidopsis thaliana*. *Methods Enzymol.* 393, 23–35.

Staiger, D., Shin, J., Johansson, M., and Davis, S. J. (2013). The circadian clock goes genomic. *Genome Biol.* 14:208. doi: 10.1186/gb-2013-14-6-208

Strasser, B., Sanchez-Lamas, M., Yanovsky, M. J., Casal, J. J., and Cerdan, P. D. (2010). *Arabidopsis thaliana* life without phytochromes. *Proc. Natl. Acad. Sci. U.S.A.* 107, 4776–4781. doi: 10.1073/pnas.0910446107

Strayer, C., Oyama, T., Schultz, T. F., Raman, R., Somers, D. E., Más, P., et al. (2000). Cloning of the *Arabidopsis* clock gene *TOC1*, an autoregulatory response regulator homolog. *Science* 289, 768–771.

Toth, R., Gerding-Reimers, C., Deeks, M. J., Menninger, S., Gallegos, R. M., Tonaco, I. A., et al. (2012). Prieurianin/endosidin 1 is an actin-stabilizing small molecule identified from a chemical genetic screen for circadian clock effectors in *Arabidopsis thaliana*. *Plant J.* 71, 338–352. doi: 10.1111/j.1365-313X.2012.04991.x

Toth, R., Kevei, E., Hall, A., Millar, A. J., Nagy, F., and Kozma-Bognar, L. (2001). Circadian clock-regulated expression of phytochrome and cryptochrome genes in Arabidopsis. *Plant Physiol.* 127, 1607–1616.

Uehara, T. N., Mizutani, Y., Kuwata, K., Hirota, T., Sato, A., Mizoi, J., et al. (2019). Casein kinase 1 family regulates PRR5 and TOC1 in the Arabidopsis circadian clock. *Proc. Natl. Acad. Sci. U.S.A.* 116, 11528–11536. doi: 10.1073/pnas.1903357116

Vanden Driessche, T., Bonotto, S., and Brachet, J. (1970). Inability of rifampicin to inhibit circadian rhythmicity in Acetabularia despite inhibition of RNA synthesis. *Biochim. Biophys. Acta* 224, 631–634.

Webb, A. A. R., Seki, M., Satake, A., and Caldana, C. (2019). Continuous dynamic adjustment of the plant circadian oscillator. *Nat. Commun.* 10:550.

Wenden, B., Kozma-Bognar, L., Edwards, K. D., Hall, A. J., Locke, J. C., and Millar, A. J. (2011). Light inputs shape the Arabidopsis circadian system. *Plant J.* 66, 480–491. doi: 10.1111/j.1365-313X.2011.04505.x

Wilson, G. T., and Connolly, E. L. (2013). Running a little late: chloroplast Fe status and the circadian clock. *EMBO J.* 32, 490–492.

Yabuta, Y., Mieda, T., Rapolu, M., Nakamura, A., Motoki, T., Maruta, T., et al. (2007). Light regulation of ascorbate biosynthesis is dependent on the photosynthetic electron transport chain but independent of sugars in *Arabidopsis*. *J. Exp. Bot.* 58, 2661–2671.

Yanovsky, M. J., Mazzella, M. A., and Casal, J. J. (2000). A quadruple photoreceptor mutant still keeps track of time. *Curr. Biol.* 10, 1013–1015.

Yoshida, Y., Iigusa, H., Wang, N., and Hasunuma, K. (2011). Cross-talk between the cellular redox state and the circadian system in Neurospora. *PLoS One* 6:e28227. doi: 10.1371/journal.pone.0028227

Zeilinger, M. N., Farré, E. M., Taylor, S. R., Kay, S. A., and Doyle, FJ 3rd (2006). A novel computational model of the circadian clock in *Arabidopsis* that incorporates PRR7 and PRR9. *Mol. Syst. Biol.* 2:58.

Zhang, C., Gao, M., Seitz, N. C., Angel, W., Hallworth, A., Wiratan, L., et al. (2019). LUX ARRHYTHMO mediates crosstalk between the circadian clock and defense in Arabidopsis. *Nat. Commun.* 10:2543. doi: 10.1038/s41467-019-10485-6

Zhang, C., Xie, Q., Anderson, R. G., Ng, G., Seitz, N. C., Peterson, T., et al. (2013). Crosstalk between the circadian clock and innate immunity in Arabidopsis. *PLoS Pathog.* 9:e1003370. doi: 10.1371/journal.ppat.1003370

Zhou, M., Wang, W., Karapetyan, S., Mwimba, M., Marques, J., Buchler, N. E., et al. (2015). Redox rhythm reinforces the circadian clock to gate immune response. *Nature* 523, 472–476. doi: 10.1038/nature14449

**Conflict of Interest:** The authors declare that the research was conducted in the absence of any commercial or financial relationships that could be construed as a potential conflict of interest.

frontiers in Physiology

ORIGINAL RESEARCH
published: 14 August 2020
doi: 10.3389/fphys.2020.01002

# Zebrafish Circadian Clock Entrainment and the Importance of Broad Spectral Light Sensitivity

*Inga A. Frøland Steindal[1]* and David Whitmore[1,2]*

*[1] Centre for Cell and Molecular Dynamics, Department of Cell and Developmental Biology, University College London, London, United Kingdom, [2] College of Public Health, Medical and Veterinary Sciences, Department of Molecular and Cell Biology, James Cook University, Townsville, QLD, Australia*

One of the key defining features of an endogenous circadian clock is that it can be entrained or set to local time. Though a number of cues can perform this role, light is the predominant environmental signal that acts to entrain circadian pacemakers in most species. For the past 20 years, a great deal of work has been performed on the light input pathway in mammals and the role of intrinsically photosensitive retinal ganglion cells (ipRGCs)/melanopsin in detecting and sending light information to the suprachiasmatic nucleus (SCN). In teleost fishes, reptiles and birds, the biology of light sensitivity is more complicated as cells and tissues can be directly light responsive. Non-visual light signalling was described many years ago in the context of seasonal, photoperiodic responses in birds and lizards. In the case of teleosts, in particular the zebrafish model system, not only do peripheral tissues have a circadian pacemaker, but possess clear, direct light sensitivity. A surprisingly wide number of opsin photopigments have been described within these tissues, which may underpin this fundamental ability to respond to light, though no specific functional link for any given opsin yet exists. In this study, we show that zebrafish cells show wide spectral sensitivities, as well as express a number of opsin photopigments – several of which are under direct clock control. Furthermore, we also show that light outside the visual range, both ultraviolet and infrared light, can induce clock genes in zebrafish cells. These same wavelengths can phase shift the clock, except infrared light, which generates no shift even though genes such as *per2* and *cry1a* are induced.

**Keywords: zebrafish, entrainment, opsin, non-visual photopigment, circadian clock, phase shift, monochromatic light**

OPEN ACCESS

***Edited by:***
*Charalambos P. Kyriacou, University of Leicester, United Kingdom*

***Reviewed by:***
*Cristiano Bertolucci, University of Ferrara, Italy*
*Rachel Ben-Shlomo, University of Haifa, Israel*

****Correspondence:***
*Inga A. Frøland Steindal*
*inga.steindal.12@ucl.ac.uk*

***Specialty section:***
*This article was submitted to Chronobiology, a section of the journal Frontiers in Physiology*

***Received:*** *04 April 2020*
***Accepted:*** *23 July 2020*
***Published:*** *14 August 2020*

***Citation:***
*Steindal IAF and Whitmore D (2020) Zebrafish Circadian Clock Entrainment and the Importance of Broad Spectral Light Sensitivity. Front. Physiol. 11:1002. doi: 10.3389/fphys.2020.01002*

## INTRODUCTION

The most ancient and predictable environmental cue for life on Earth is the onset of sunrise and sunset. In fact, it is hard to imagine any other environmental stimulus that an animal or plant experiences that lacks any biologically significant noise. As a consequence, most life under the Sun, from bacteria to plants to humans have evolved a circadian clock which internally represents this highly predictable change in day and night. A critical aspect of having such a circa 24-hour

pacemaker is that it needs to be entrained or set each day to the environmental light-dark cycle. Natural selection acts on correct phase relationships rather than clock period, such that it is essential both internal and external oscillations are appropriately phase aligned. Consequently, entrainment is an essential and defining feature of the circadian clock and the topic addressed in this study.

Light sensing and entrainment were always thought to be a process associated exclusively with the eyes and the Suprachiasmatic Nucleus (SCN) in mammals, and the pineal gland in non-mammalian vertebrates (Suburo and de Iraldi, 1969; Ibuka and Kawamura, 1975; Elliott, 1976; Underwood and Groos, 1982; Cahill, 1996). It therefore came as a surprise, some 20 years ago, that the process of non-visual photoreception is something that all tissues in the zebrafish are capable of Whitmore et al. (1998). Although the zebrafish pineal has key functions (Ben-Moshe et al., 2014; Livne et al., 2016), teleost clock systems appear to be highly decentralised, with all tissues and the majority of cells possessing a directly light entrainable circadian pacemaker (Whitmore et al., 1998, 2000; Carr and Whitmore, 2005; Tamai et al., 2005; Steindal and Whitmore, 2019).

Peripheral light sensitivity is not exclusive to zebrafish, as most non-mammalian vertebrates such as fish, reptiles and birds show high opsin diversity (Davies et al., 2015). Deep-brain photoreception has been researched in avian seasonal physiology for many years, as has similar hypothalamic responses in reptiles (Benoit, 1935a,b; Underwood and Menaker, 1976; Takahashi and Menaker, 1979; Underwood and Groos, 1982; Wyse and Hazlerigg, 2009). So, perhaps it should not have come as such a surprise when this well-established direct brain light-sensitivity was expanded to include the majority of other tissues. Monotremes and mammals also express non-visual opsins that facilitate a range of biological processes, of which, melanopsin in mammalian clock entrainment is the most explored (Provencio et al., 1998; Halford et al., 2001; Tarttelin et al., 2003).

When peripheral photoreception was discovered in anamniotes, the next obvious question concerns the nature of the photopigment responsible for this peripheral light detection and clock entrainment? Visual photopigments have been studied extensively since the 19th century (Norris, 1895; Arey, 1915). However, a whole century past before science turned its interest to the discovery of the non-visual photopigments, and several candidates appeared through the late 1990s and early 2000s (Okano et al., 1994; Blackshaw and Snyder, 1997; Soni and Foster, 1997; Sun et al., 1997; Provencio et al., 1998). The number of opsins discovered since the early 1990s has increased to include 32 non-visual and 10 visual opsins in zebrafish (Davies et al., 2015), and new opsins, splice variants and isoforms are discovered in new species on a regular basis (Musilova et al., 2019). The non-visual and visual opsins are divided into 8 classes based on photoisomerase activity, molecular function and how they couple and signal though G-proteins. What sets several of the non-visual opsins apart from the visual opsins, is that they are bistable, meaning that instead of bleaching like the visual opsins, the photoproduct can convert between photoproduct and photopigment without releasing the chromophore (Tsukamoto, 2014). Such a process makes sense in the context of a tissue that lacks the more sophisticated pigment-regeneration mechanisms found in the retina.

With such a large diversity of opsins, identifying key candidates in the fish for photoentrainment of the clock, or how these photopigments work synergistically together is now more complicated than ever. Absorption spectra has been performed on many of these zebrafish opsins. Most are monophasic, but seemingly with somewhat broad absorption peaks, with most opsins absorbing in the blue-green, while some absorb up in the red end of the spectrum (Su et al., 2006; Davies et al., 2011, 2015; Koyanagi et al., 2015; Morrow et al., 2016; Sato et al., 2016, 2018; Sugihara et al., 2016; Steindal and Whitmore, 2019). Thus, the zebrafish has the theoretical capacity to detect light ranging from UV to IR and across the visual spectrum. Zebrafish cell lines and other teleost cell lines have been used for years in clock studies, yet we do not actually know what opsins are expressed in these cultures.

This raises the question, do zebrafish show such a diversity in opsins in order to be able to capture all photons of any wavelength, such that the system is simply designed to detect the presence or absence of light, regardless of wavelength? Or does this different opsin expression pattern mean that particular organs have specific wavelength sensitivities and therefore differing responses to the environmental light signal?

In this paper, we demonstrate that the light response goes well beyond the visual wavelengths, with both UV and infrared (IR) light pulses having the ability to induce clock gene expression, but interestingly with IR not able to phase shift the molecular clock, at least in cell lines. Furthermore, we show that zebrafish cell lines, rather like the adult tissues (Davies et al., 2015), display a diversity of expressed opsins, a number of which are under clock-control and as such show robust daily rhythms in expression. Whether this transcriptional rhythm in specific opsins translates into matching protein changes is yet to be determined, but it opens up the possibility of a direct temporal regulation of light sensitivity, as well as the more conventional spatial aspects. In this regard, the clock is likely to be gating the process of its own entrainment by regulating expression of components of the light-input pathway; with a specific pathway acting as a zeitnehmer or "time taker" (McWatters et al., 2000).

# MATERIALS AND METHODS

## Cell Culture

PAC2 and *clockDN* (clock "mutant" cells) cell lines were kept in Leibovitz -15 medium (Gibco) supplemented with 15% FBS (Biowest), 0.05 mg/ml of gentamicin (Gibco) and 1x Penicillin-Streptomycin (Dekens and Whitmore, 2008). Cells were seeded at 50 000 cells/ml and kept at 28°C in a water bath on a 12:12 LD cycle for 3 days before receiving a light-pulsed with different wavelengths (IR 850 nm, red 650 nm, blue 450 nm, UV 350 nm and white 400-700 nm) with an intensity of 200 $\mu W/cm^2$ for 3 h starting light pulse at ZT21 (LED Array Light source, Thorlabs). After a 3-hour light pulse, cells were washed with PBS and homogenised in TRIzol with a cell scraper.

## RNA, cDNA and RT-qPCR

RNA was extracted according to manufacturer's guidelines (TRIzol, Invitrogen) and the RNA pellet re-suspended in 30 μl of RNase free water (Ambion). 2 μg of RNA was reverse transcribed to cDNA using Superscript II Reverse Transcriptase (Invitrogen), random hexamers (Invitrogen) and oligo dT primers (Invitrogen) according to manufacturer's protocol. RT-qPCR was performed on a C1000 Touch$^{TM}$ Thermal Cycler with the CFX96$^{TM}$ Optical Reaction Module (Bio-Rad) using KAPA SYBR FAST qPCR mix (Kapa Biosystems) in technical triplicates with gene specific-primers at a concentration of 500 nM. ΔCt was determined using β-actin as a reference gene and relative expression levels were plotted using the ΔΔCt method. Gene specific primers are listed in **Table 1**.

## Bioluminescent Assays

*Per-1 luciferase* cells, described by Vallone et al. (2004), were plated at 100,000 cell/ml in media (described above) in a white 96-well plate (Greiner) $n$ = 16. Cells settled over night at 28°C, and the following day the media was changed for media supplemented with 0.5 nM beetle luciferin (Promega). Plates were sealed with TopSeal clear adhesive from (Perkin Elmer). Bioluminescence was monitored on a TopCount NXT scintillation counter (Packard Instrument Company), in a temperature-controlled chamber (28°C). Cells were entrained on a 12:12 LD cycle and given a light pulse (as described

**TABLE 1 |** Gene specific primers used for qPCR.

| Accession no. | Current name | Alt. Name | Forward 5′ -> 3′ | Reverse 5′ -> 3′ |
|---|---|---|---|---|
| KT008391 | Exorhodopsin | | GTA CGC TCC GCT ATC CCA TA | ACG TGT GAA AGC CCC TAC TG |
| KT008402 | Valopa | Val | ACT TCC ACG ACC ACA CCT TC | CGG ATG AGT TTG CAG TAG CA |
| KT008403 | Valopb | Va2 | GGC GAG GAT GGT CGT TGT AA | ATG CTG CAT AAG GCG TCC AT |
| KT008404 | parapinopsin-1 | | CTG TGG TCG TTC ATC TGG AA | GGC CAG ATC TCT GCT GTA CC |
| KT008405 | parapinopsin-2 | | GCA GCA CTG TAT ACA ACC CCT | ATA CGT CGT CCT CTG AAG GC |
| KT008406 | parietopsin | | TGT TGG CGT ATG AGC GTT AT | AGC CAT ACC AAC AGC AGA CC |
| KT008407 | TMTla | tmt6 | TGT TAC AGT CGG CTC ATC TGT GCT | ATG TGG TAC TCT CTC CGT CTT GCT |
| KT008408 | TMTlb | tmt9 | TGT TGG TGT GTA TGT TCG GGACGA | AGG AGT TGA TGA AGC CGT ACC ACA |
| KT008409 | TMT2a | tmtlO | TTA GTA AGA AGC GGA GCA GAA CCT | ATC CCA TAG GGA TGC AGT GTT GTT |
| KT008410 | TMT2b | tmtl4 | CGC AGA GGA GAG AGA ACC AC | TTA GTC CCG TTC TGC CAA AG |
| KT008411 | TMT3a | tmt2 | AGG TCG ATG CGA CCA ACT ACA AGA | AAA CAG AGG AGG CAG GGT CCA AAT |
| KT008412 | TMT3b | tmt24 | TGC GTG TGG TAC GGT TTC ATC AAT | ATC ATG GTG CAG TAA CGC TCG TAT |
| KT008413 | encephalopsin (opn3) | panopsin | CCCTAT GCT GTG GTC TCC AT | TAG ATG ACG GGG TTG TAG GC |
| KT008414 | neuropsin (opn5) | OPN5ml | ACA CCA TCT GTC GCT CCA TC | CTG CAA ATT GCC CAG TGT C |
| KT008415 | 0PN6a | novo3b | GTG GTC AAC ATC CCC TGG AG | ACA ACC AGC CGA GTA TGA GC |
| KT008416 | 0PN6b | novo3a | AAT CCA GCC AGG GAG GAG AT | AAG GCG GAC CAC ATG GAA AT |
| KT008417 | 0PN7a | novolx | GTT TAA ACA CTA CCCGCG CC | GCTCTG GCTCCA ATT CAG GT |
| KT008418 | 0PN7b | novola | TGC TAT ATC GTG CCC TG C TG | CGTACC GTC ACC AGG ATG AG |
| KT008419 | 0PN7c | novolb | GTG AAC CTG TCT GTG AGC GA | CTC CCC AAA CAA CCA CCT GT |
| KT008420 | 0PN7d | novoly | CTG CCA CTT GGA ATC ATC CT | GCG ACA CAT GCT GCT GTA CT |
| KT008421 | 0PN8a | novo2b | TGA CTG ACA TTG GCA TGG CT | TGG TTG AAA GCA GAG GCG AT |
| KT008422 | 0PN8b | novo2a | TTC GCT TCA TCG TGT CTT TG | CAG TGG GAA AAT AGC CCA GA |
| KT008423 | 0PN8c | novo2x | TGG GCT TTA TCC TTG CCT GG | AGA TGAAGC CTT CTG GTG CC |
| KT008424 | 0PN9 | OPN5m2 | TCA G GG CTT TG T TTT CGG G A | GCA GCG GTC AAG GGA TAT GA |
| KT008425 | Peropsin (RRH) | | AGT GGT TGC CAT TGA CCG AT | ATG CGG CCA CAA TCA GAA GA |
| KT008426 | RGR1 | | CCT GGC TTT CTA CGC CGC AG | GGA CTT GTT CTC AAT AGC AGG ACT CTC |
| KT008427 | RGR2 | | GAG CAC GTC TAT CAC CAT CAG CT | ACA CCC CAG CCA ATG GCA GG |
| KT008428 | OPN4ml | | CGT CAT CAC CTC TGA GTC CA | GCT GGA TTT GTC CCA ACA GT |
| KT008429 | OPN4m2 | | AGC AAT GCT AGT GGG CAG AA | CGT CTG CTG CAT CCG TTT CA |
| KT008430 | OPN4m3 | | AAG GCC AAT GGT TCG GAT CC | CCA GGT ATG AGC CTG GAA GA |
| KT008431 | OPN4xl | | GCT ACA CCT TGA TGC TCT GC | CTG TTG GAT GAG GGT GGT CT |
| KT008432 | OPN4 × 2 | | CTT TGT GAA GCA GCA GTC CA | TAT GGA GCC CAG GAC AAA AC |
| NM_001077297.2 | Cry 1a | | AGG CTT ACA CAG CAG CAT CA | CTG CAC TGC CTC TGG ACT TT |
| NM 182857.2 | Per2 | | TGG CTC TGG ACA GAA GTG AG | GGA TGT CTC GAG AAG GCA AC |
| NM 198143.1 | L13 | | TCT GGA GGA CTG TAA GAG GTA TGC | AG A CGC ACA ATC TTG AG A GCA G |
| AB042254.1 | 6–4 photolyase | cry5 | TGT GGA TCA TGA GGT TGT CC | TTG ATG GAT GGA CTC GCT TT |
| NM_001030183.1 | Perla | perl | ATC CAG ACC CCA ATA CAA C | GGG AGA CTC TGC TCC TTC T |
| AF057040.1 | Beta a ctin | | CGC AAA TAC TCC GTC TGG AT | TCC CTG GAG AAG AGC TAC GA |

above) at ZT21 after 2 days. Cells were then kept in DD on the TopCount for two more days, at constant temperature, in order measure any phase shift in the gene expression rhythm. Luminescence from the cells was measured in counts per second approximately every hour taking approximately 10 min for a 96-well plate to be read.

### Statistical Analysis

*T*-tests, ANOVAs and post-test were performed with the standard add-in software in Excel. Alpha was set at 0.5. Tukey numbers were calculated using values from a standard Tukey table.

## RESULTS

### Opsin Expression in Cell Culture

As well as having directly light sensitive organs, zebrafish cell lines, typically generated from early stage larvae such as the PAC2 cell line, are also directly light responsive (Whitmore et al., 2000). To examine which opsins are present in the cells, both PAC2 cells, and transformed cells expressing a *clock*-dominant negative construct (*clock*DN cells) were kept on a 12:12 light dark cycle at constant temperature, and cells were harvested at ZT3 and ZT15. Both cell lines express opsins from all classes of non-visual opsins, with a total of 11 out of 32 non-visual opsins expressed at a detectable level ($C_t$ lower than 30) (**Figure 1**). There is no apparent difference between PAC2 and the *clockDN* lines in opsin expression pattern. By comparing the expression pattern at two different times of day, we also observed that half of the opsins show a day-night difference in expression pattern in PAC2, but not *clockDN* cells, which shows that some opsin expression is clock controlled (**Figure 1**). Interestingly, two forms of OPN4 are expressed in these zebrafish cell lines and one, OPN4 × 2, shows a strong day-night difference in expression. This is also the case for exo-rhodopsin, which is typically considered to be a pineal specific photopigment. RGR1, a putative photoisomerase, also shows robust daily changes, and is the most abundant transcript.

### Impact of Light on Clock Genes in Cells

To explore how monochromatic light of selected wavelengths impacts gene expression in zebrafish cell lines, *ClockDN* and *PAC2* cells were entrained, like the organs, on a 12:12 LD cycle at constant temperature and given a monochromatic light pulse for 3-hour at ZT21, when cells are most light responsive (Tamai et al., 2005). Using RT-qPCR, we examined the effect of these light pulses on different, well-established light responsive clock genes, such as *cryptochrome1a* (*cry1a*) and *period2* (*per2*), as well as the light induced DNA repair gene, *6-4 Photolyase* (*6-4 Ph*) (Tamai et al., 2007; Vatine et al., 2009). In *PAC2* cells, white, blue and UV light pulses of the same intensity give very similar induction in all genes explored, whilst red generates a slightly smaller, yet not statistically different induction (**Figures 2A–C**). IR pulses give the smallest induction of the genes explored. In *cry1a* we see a significant 1.6-fold induction, as opposed to ∼4-fold induction by the other wave lengths (**Figure 2A**). For *per2* IR give a ∼5-fold induction as opposed to 20–30-fold by the other wavelengths (**Figure 2B**). Finally, IR gives a 2.6-fold induction as opposed to up to 13-fold induction, by the other wavelengths (**Figure 2C**). IR does indeed induce significant induction of the light sensitive clock and a DNA repair gene. However, compared to the other wavelengths, it is between 2.5 and 6 times less potent, depending on the gene in question.

*ClockDN* cells show a reduced fold induction to all the wavelengths (**Figures 2A–C**). The raw $C_t$ values seen in *clockDN* and PAC2 cells are, however, very similar when given a light-pulse. These clock mutant cells show a higher basal DD expression of the clock and DNA repair genes, and thus the fold induction is subsequently lower (**Supplementary Figure S1**). This is particularly evident when giving an IR light pulse (**Figure 2D**).

### Phase Shift in Cell Culture

To explore how the monochromatic light phase shifts the molecular clock in cell culture, *per1-luciferase* luminescent reporter cells (Vallone et al., 2004) were entrained for 3 days at 28°C and pulsed the same way as the cells described above (**Figure 3A**). *Per1* luminescent traces were then monitored for 2 days post light pulse in DD using the Packard TopCount. UV, blue, red and white light are all capable of causing a phase advance in the cell culture clocks when light is applied at this particular time in the cycle (ZT21) (**Figure 3B**). Interestingly, a 3-hour light exposure of IR light does not give a phase shift regardless of the acute molecular response to this light signal, increasing both *cry1a* and *per2* expression, a result which is worthy of further discussion.

## DISCUSSION

### Cells Show a Diversity in Opsin Expression Patterns

Zebrafish cell cultures have long been used because of their direct light sensitivity. However, the opsin composition of these cells lines has never previously been published. We, therefore, performed RT-qPCR on PAC2 cell lines to explore what opsins are expressed. With RT-qPCR and setting a cut off value at $C_q$ 30 as a measure of "no expression," we can identify the presence of 11 out of 32 non-visual opsins (**Figure 1A**). Interestingly, 6 of these opsins show a clear day-night difference in expression and appear to oscillate. All of these opsins show higher levels of expression during the day time-point compared to night. To explore this further, we therefore also examined expression in the *ClockDN* cell line, lacking a functional circadian clock, to manifest whether this difference is light-driven or clock-dependent. Interestingly, the *ClockDN* cells express the same specific opsins exactly, but they no longer oscillate (**Figure 1B**), which supports the idea that expression of these opsins is directly clock controlled and not directly light-driven. Furthermore, averaging expression of ZT3 and ZT15, there is no significant difference in the amount of transcript produced in the two different cell lines. The opsin expression profile in cells does

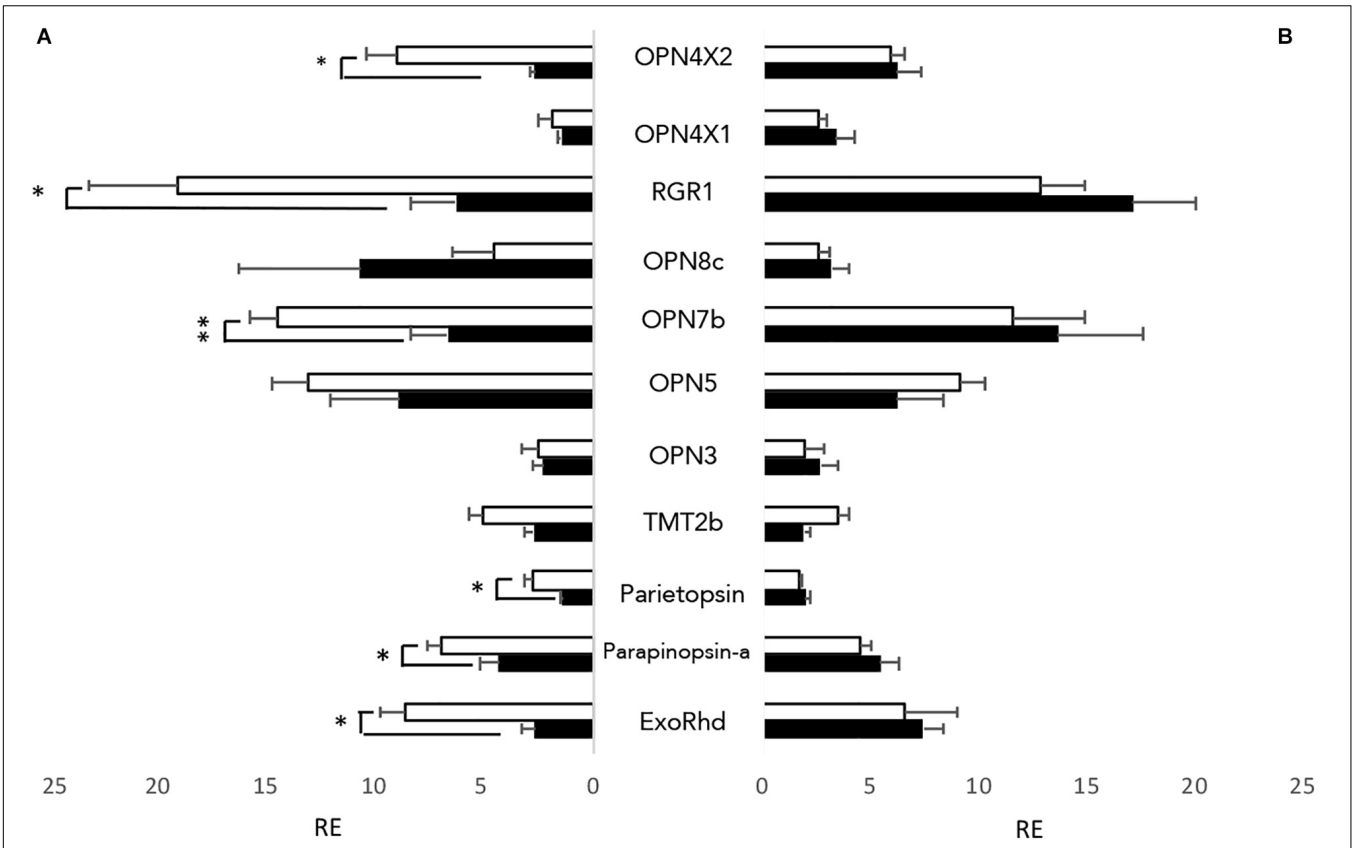


**FIGURE 1 |** Non-visual opsins expressed in zebrafish cell lines. All 32 non-visual opsins were explored by RT-qPCR in entrained zebrafish cell lines at opposite times of day; ZT3 (white) and ZT15 (black). 11 opsins showed detectable expression levels, using a cut-off value of $<C_q$ 30. **(A)** Opsins expressed in PAC2 cell lines. **(B)** Opsins expressed in *clockDN* cell lines. Opsin expression is plotted relative to the lowest detectable opsin, with error bars depicting SEM. An unpaired students *t*-test was used to assess if the opsins expressed show a time of day specific expression pattern. $*p < 0.05$ and $**p < 0.001$ ($n = 4$).

not resemble any particular tissue type that we know of today. However, it is worth noting that the cell line express one opsin from all the opsin families, like most tissue types, and thus possess $G_q$, $G_t$, $G_i$, and $G_o$ coupled opsins, as well as a putative photoisomerase (RGR1). The cell line should, therefore, be able to signal through the same pathways in response to light as any other fish tissue.

## Monochromatic Light (350–650 nm) Are Potent Inducers of Light Responsive Genes in Cell Culture

Expression of the light responsive clock genes in cell culture is rather flat with a broad response to white, blue and UV light. There is a slight but statistically significant drop in the response to red light in the cells, and a marked drop in the response to IR (**Figure 2**).

6–4 photolyase catalyses the photo-reversal of the (6–4) dipyrimidine photoproducts induced in DNA by ultraviolet light (Zhao et al., 1997). A simple prediction might be that UV/blue light should be more efficient at inducing expression of this DNA repair enzyme. However, this does not appear to be the case, with red light and even IR light able to increase transcript levels. Red light photons have lower energy than blue light photons, therefore, the same intensity of blue and red light will have different number of emitted photons. Consequently, one hypothesis is that the opsins simply "count" photons, not the energy of the photons they absorb, meaning that the zebrafish cell simply wants to know whether there is light present or not. To address such issues, these experiments will need to be repeated considering aspects of photon flux over a wider range of light intensities. Of course, it may be biologically essential to activate expression of your DNA repair machinery in the presence of light, regardless of the subtleties of the specific wavelength, and of course the 6–4 photolyase protein itself absorbs light to perform its role in replacing cross-linked nucleotides. It is this aspect of light driven DNA repair that is most likely to be wavelength sensitive.

Comparing cells without a functional clock to "wild type" cells, we also see that the fold induction of genes in response to light is lower, due to a higher basal transcription of these target genes in DD. *ClockDN* cells show a higher basal DD expression of the clock and DNA repair genes, and the fold induction is subsequently lower (**Figures 2A–C**). This is interesting, as it demonstrates the steady state expression levels that these

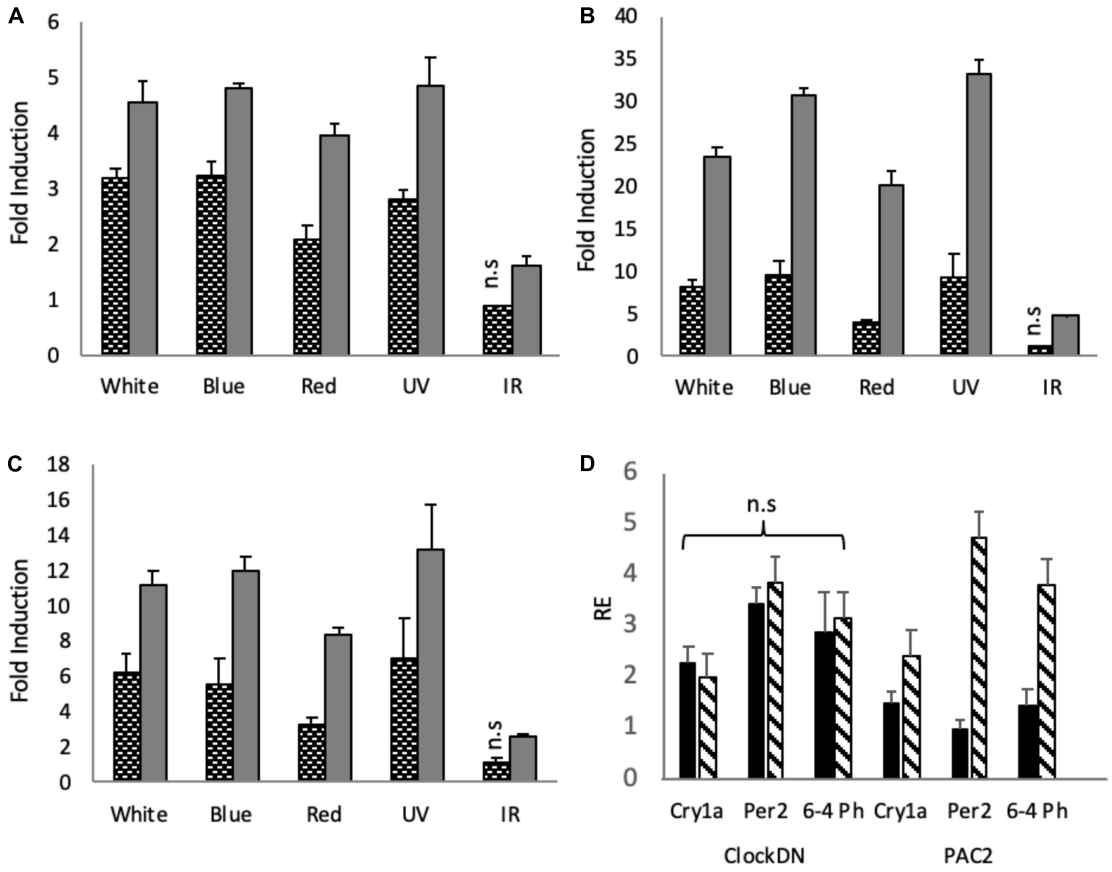


**FIGURE 2 |** Light induction by monochromatic light-pulses in PAC2 and *clockDN* cell lines. Zebrafish cell lines were maintained on a 12:12 light-dark cycle before being given a 3-hour light pulse of varying wavelengths. *B*lack and white bars represent *clockDN* cell line expression, whilst solid grey represent PAC2 cell line expression. **(A)** Light induction of *cry1a*. **(B)** Light induction of *per2*. **(C)** Light induction of 6–4 Photolyase. **(A–C)** is plotted as fold induction relative to dark control. **(D)** Dark controls (black bars) vs. IR monochromatic light pulse (striped bars) plotted relative to lowest expressed gene (PAC2 *per2* DD) in *clockDN* and PAC2 cells. Significance was addressed with an one-way ANOVA ($\alpha = 0.05$) for each light-pulse, cell line and gene, followed by a Bonferroni post-test. All light pulses give a significant increase of $p < 0.05$ unless marked on the graph ($n = 3$).

genes reach in a non-rhythmic mutant background. The absolute expression remains the same (**Supplementary Figure S1**). Interestingly, the high basal level of transcript means that there is no induction of light responsive clock genes in the *clockDN* cells in response to IR.

## UV- Red Light Can Alter Gene Expression and Phase-Shift Cell Lines

The impact of "visible" wavelengths of light (380–740 nm) on the zebrafish clock system has been described in numerous previous studies. However, exploring this phenomenon outside of the visual spectrum are rarely performed in fish. UV light of 350 nm (UVA) has a clear impact on gene expression and can clearly phase shift the circadian clock in cell lines. Perhaps this is not so surprising from what we now know about zebrafish photobiology. After all, 350 nm is only 50 nm below the violet/blue wavelengths that can so robustly impact the clock in an aquatic organism. In future, it would be interesting to try wavelengths at the more extreme end of the UVA range and well away from the visual spectrum. This UV response also fits well with the previously determined absorption spectra for purified opsin proteins, which reveals a wide sensitivity in the UV/blue wavelengths (Davies et al., 2015).

The impact of these monochromatic light pulses was explored using our luminescent reporter cell lines. At the phase (ZT21) and intensity used, each wavelength generated a very similar phase advance in the rhythm, including UV light pulses, but not IR at 850 nm (**Figure 3A**). This similarity in size of phase advance correlates well with the similarity in molecular response, induction of *cry1a* and *per2*, seen in the cell lines (**Figure 2**). Furthermore, using a Tukey post-test, there is statistical difference in the size of phase shift generated by each of these light pulses (except between blue and UV) (**Figure 3B**). Since this difference in shift is so small, it may be due to the sampling frequency (plate counted once an hour) rather than real difference, thus we do not speculate any further.

Compared to previous studies on phase shifting in zebrafish cell lines, in response to white light, the size of the phase shift

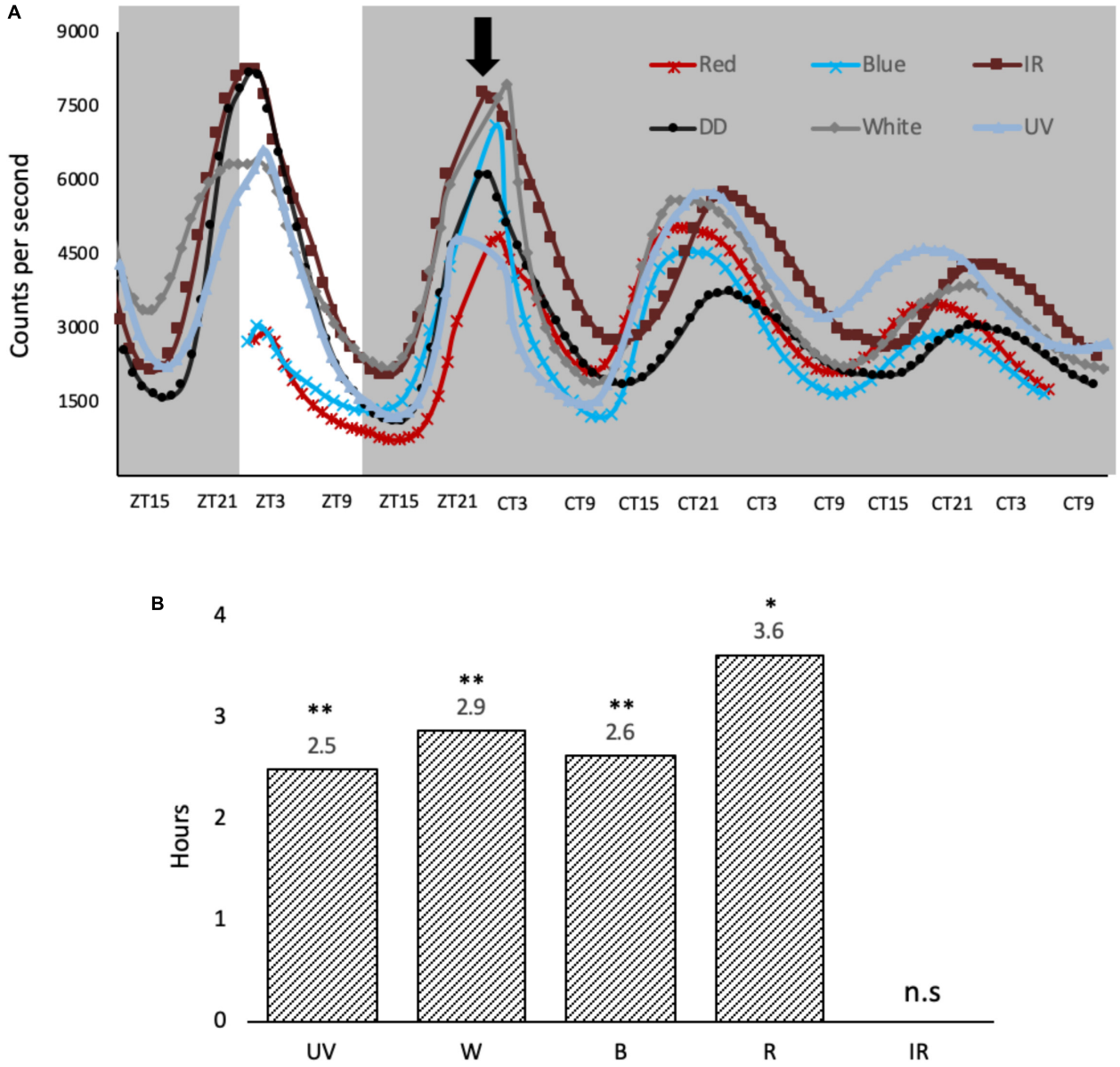


**FIGURE 3 |** Light-induced phase shifts in response to monochromatic light-pulses in *per1-luciferase* zebrafish cells. **(A)** Cells were entrained for 3 days on a 12:12 LD cycle, before they were given a variety of monochromatic light pulses at ZT21, denoted by black arrow. The cells were kept in constant dark over two subsequent days. **(B)** Light pulses cause a phase advance in hours, determined at the half maximum between peak and trough vs. no LP controls. A two-way ANOVA (time, wavelength) was used to determine significant variation between samples. Amplitude and baseline were detrended using BioDare2 (Zielinski et al., 2014), and a Tukey post-test was used to determine significance in phase shift relative to DD control. $*p < 0.01$ and $**p < 0.001$ ($n = 8$).

is relatively small and is actually a phase advance rather than a large phase delay previously reported (Tamai et al., 2007). The reasons for this simply relate to the differences in light intensity used. Early studies applied light at 5000 $\mu W/cm^2$, compared to the 200 $\mu W/cm_2$ used in this study. Consequently, the Type 0 PRC previously reported switches to a more "standard" Type 1 PRC as the lower light intensity, as historically seen in many previous studies. Interestingly the switch in PRC amplitude, therefore, occurs between these two intensities, and strongly suggests that fish under natural conditions, as a diurnal animal, will be "working with" a Type 0 PRC.

The response to infrared light was not expected. As a stimulus, it is generally avoided in clock studies, due to the strong link with temperature effects/artefacts and the ability of temperature pulses to phase shift the circadian clock. It is a stimulus typically one aims to control against in circadian analysis. Yet the response to IR when controlling for temperature, of the zebrafish clock system is very interesting. IR of 850 nm can clearly cause

specific transcriptional changes in zebrafish cells. Obviously, in our experiments we aimed to avoid the thermal heating effect of IR exposure, and none was detected in our cultures. Equally, the IR light pulse did not phase shift the clock, which has been shown to be robustly phase-shifted by temperature pulses (Lahiri et al., 2005). For cells in culture, IR causes a small, yet significant induction of *cry1a* and *per2,* however, there is no subsequent phase shift. As mentioned earlier, IR is up to 6 times less potent in cell lines, and the reduced induction of *cry1a* and *per2* compared the other wavelengths may not be sufficient to cause a downstream phase shift in these studies. Of course, it could also be the fact that *cry1a* and *per2* are not as central to phase shifting the teleost clock as has been previously proposed.

How IR signals to cells in a meaningful way is a fascinating question. It could be through mitochondrial-driven processes or it could be through the "re-purposing" of the mass of opsin in fish to perform other key sensory roles. If fish opsins are acting as "thermal" or IR sensors, as has been proposed in Drosophila, then this opens up a whole new world of interesting (fish) biology.

In this study, we have shown that the spectral sensitivity of zebrafish cell lines extends beyond the classically perceived "visual" wavelengths of light and that supporting this wide spectral sensitivity, these cells express a large number of opsins. Furthermore, the clock itself regulates the temporal expression of these opsins, raising the interesting possibility that the clock itself controls light input to the pacemaker – the zeitnehmer concept that has so eloquently been described for plant clock systems.

## DATA AVAILABILITY STATEMENT

The raw data supporting the conclusions of this article will be made available by the authors, without undue reservation.

## AUTHOR CONTRIBUTIONS

Both authors performed the experiments, analysed the data, wrote the manuscript and contributed to the article and approved the submitted version.

## FUNDING

MRC supported Ph.D. for IAF Steindal and consumables through the MRC DTP programme. Leverhulme Trust grant RPG-2017-299 used for consumables.

## ACKNOWLEDGMENTS

We would like to thank past and present lab members of the Whitmore for discussions and historical input. Especially Kathy Tamai, Lucy Young, and Amanda Carr for their involvement. We would also like to thank the Leverhulme Trust for funding to DW and the MRC-DTP for funding to IAFS.

## SUPPLEMENTARY MATERIAL

The Supplementary Material for this article can be found online at: https://www.frontiersin.org/articles/10.3389/fphys.2020.01002/full#supplementary-material

**FIGURE S1 |** Monochromatic light pulses in PAC2 vs. *clockDN* cell lines. *ClockDN* cell lines (light grey) show increased basal expression of all genes explored in the dark control compared to PAC2 (dark grey). Significance was addressed with a one-way ANOVA ($\alpha = 0.05$) for each light-pulse, cell line and gene, followed by a Bonferroni post-test. All light pulses give a significant increase of $p < 0.05$, except *clockDN* DD vs. IR ($n = 3$).

## REFERENCES

Arey, L. B. (1915). Do movements occur in the visual cells and retinal pigment of man? *Science* 42, 915–916. doi: 10.1126/science.42.1095.915

Ben-Moshe, Z., Alon, S., Mracek, P., Faigenbloom, L., Tovin, A., Vatine, G. D., et al. (2014). The light-induced transcriptome of the zebrafish pineal gland reveals complex regulation of the circadian clockwork by light. *Nucleic Acids Res.* 42, 3750–3767. doi: 10.1093/nar/gkt1359

Benoit, J. (1935a). Le role des yeux dans l'action stimulante de la lumiere sur le developpement testiculaire chez le canard. *C. R. Seances Soc. Biol. Fil.* 118, 669–671.

Benoit, J. (1935b). Stimulation par la lumiere artificielle du developpement testiculaire chez des canards aveugles par section du nerf optique. *C. R. Seances Soc. Biol. Fil.* 118, 133–136.

Blackshaw, S., and Snyder, S. H. (1997). Parapinopsin, a novel catfish opsin localized to the parapineal organ. Defines a new gene family. *J. Neurosci.* 17, 8083–8092. doi: 10.1523/jneurosci.17-21-08083.1997

Cahill, G. M. (1996). Circadian regulation of melatonin production in cultured zebrafish pineal and retina. *Brain Res.* 708, 177–181. doi: 10.1016/0006-8993(95)01365-2

Carr, A.-J. F., and Whitmore, D. (2005). Imaging of single light-responsive clock cells reveals fluctuating free-running periods. *Nat. Cell Biol.* 7, 319–321. doi: 10.1038/ncb1232

Davies, W. I. L., Tamai, T. K., Zheng, L., Fu, J. K., Rihel, J., Foster, R. G., et al. (2015). An extended family of novel vertebrate photopigments is widely expressed and displays a diversity of function. *Genome Res.* 25, 1666–1679. doi: 10.1101/gr.189886.115

Davies, W. I. L., Zheng, L., Hughes, S., Tamai, T. K., Turton, M., Halford, S., et al. (2011). Functional diversity of melanopsins and their global expression in the teleost retina. *Cell Mol. Life Sci.* 68, 4115–4132. doi: 10.1007/s00018-011-0785-4

Dekens, M. P. S., and Whitmore, D. (2008). Autonomous onset of the circadian clock in the zebrafish embryo. *EMBO J.* 27, 2757–2765. doi: 10.1038/emboj.2008.183

Elliott, J. A. (1976). Circadian rhythms and photoperiodic time measurement in mammals. *Fed. Proc.* 35, 2339–2346.

Halford, S., Freedman, M. S., Bellingham, J., Inglis, S. L., Poopalasundaram, S., Soni, B. G., et al. (2001). Characterization of a Novel Human Opsin Gene with Wide Tissue Expression and Identification of Embedded and Flanking Genes on Chromosome 1q43. *Genomics* 72, 203–208. doi: 10.1006/geno.2001.6469

Ibuka, N., and Kawamura, H. (1975). Loss of circadian rhythm in sleep-wakefulness cycle in the rat by suprachiasmatic nucleus lesions. *Brain Res.* 96, 76–81. doi: 10.1016/0006-8993(75)90574-0

Koyanagi, M., Wada, S., Kawano-Yamashita, E., Hara, Y., Kuraku, S., Kosaka, S., et al. (2015). Diversification of non-visual photopigment parapinopsin in spectral sensitivity for diverse pineal functions. *BMC Biol.* 13:73. doi: 10.1186/s12915-015-0174-9

Lahiri, K., Vallone, D., Gondi, S. B., Santoriello, C., Dickmeis, T., and Foulkes, N. S. (2005). Temperature regulates transcription in the zebrafish circadian clock. *PLoS Biol.* 3:e351. doi: 10.1371/journal.pbio.0030351

Livne, Z. B.-M., Alon, S., Vallone, D., Bayleyen, Y., Tovin, A., Shainer, I., et al. (2016). Genetically blocking the zebrafish pineal clock affects circadian behavior. *PLoS Genet.* 12:e1006445. doi: 10.1371/journal.pgen.1006445

McWatters, H., Bastow, R., Hall, A., et al. (2000). The *ELF3* zeitnehmer regulates light signalling to the circadian clock. *Nature* 408, 716–720. doi: 10.1038/35047079

Morrow, J. M., Lazic, S., Fox, M. D., Kuo, C., Schott, R. K., Gutierrez, E., et al. (2016). A second visual rhodopsin gene, rh1-2, is expressed in zebrafish photoreceptors and found in other ray-finned fishes. *J. Exp. Biol.* 220, 294–303. doi: 10.1242/jeb.145953

Musilova, Z., Cortesi, F., Matschiner, M., Davies, W. I. L., Patel, J. S., Stieb, S. M., et al. (2019). Vision using multiple distinct rod opsins in deep-sea fishes. *Science* 364, 588–592. doi: 10.1126/science.aav4632

Norris, W. F. (1895). The Terminal Loops of the Cones and Rods of the human retina, with Photo-micrographs. *T Am. Ophthal. Soc.* 7, 346.2–352.

Okano, T., Yoshizawa, T., and Fukada, Y. (1994). Pinopsin is a chicken pineal photoreceptive molecule. *Nature* 372, 94–97. doi: 10.1038/372094a0

Provencio, I., Jiang, G., Grip, W. J. D., Hayes, W. P., and Rollag, M. D. (1998). Melanopsin: an opsin in melanophores, brain, and eye. *Proc. Natl. Acad. Sci. U.S.A.* 95, 340–345. doi: 10.1073/pnas.95.1.340

Sato, K., Yamashita, T., Haruki, Y., Ohuchi, H., Kinoshita, M., and Shichida, Y. (2016). Two UV-Sensitive Photoreceptor Proteins, Opn5m and Opn5m2 in Ray-Finned Fish with Distinct Molecular Properties and Broad Distribution in the Retina and Brain. *PLoS One* 11:e0155339. doi: 10.1371/journal.pone.0155339

Sato, K., Yamashita, T., Kojima, K., Sakai, K., Matsutani, Y., Yanagawa, M., et al. (2018). Pinopsin evolved as the ancestral dim-light visual opsin in vertebrates. *Commun. Biol.* 1:156. doi: 10.1038/s42003-018-0164-x

Soni, B. G., and Foster, R. G. (1997). A novel and ancient vertebrate opsin. *FEBS Lett.* 406, 279–283. doi: 10.1016/s0014-5793(97)00287-1

Steindal, I. F., and Whitmore, D. (2019). Circadian Clocks in Fish—What Have We Learned so far? *Biology* 8:17. doi: 10.3390/biology8010017

Su, C.-Y., Luo, D.-G., Terakita, A., Shichida, Y., Liao, H.-W., Kazmi, M. A., et al. (2006). Parietal-eye phototransduction components and their potential evolutionary implications. *Science* 311, 1617–1621. doi: 10.1126/science.1123802

Suburo, A. M., and de Iraldi, A. P. (1969). An ultrastructural study of the rat's suprachiasmatic nucleus. *J. Anat.* 105, 439–446.

Sugihara, T., Nagata, T., Mason, B., Koyanagi, M., and Terakita, A. (2016). Absorption Characteristics of Vertebrate Non-Visual Opsin, Opn3. *PLoS One* 11:e0161215. doi: 10.1371/journal.pone.0161215

Sun, H., Gilbert, D. J., Copeland, N. G., Jenkins, N. A., and Nathans, J. (1997). Peropsin, a novel visual pigment-like protein located in the apical microvilli of the retinal pigment epithelium. *Proc. Natl. Acad. Sci. U.S.A.* 94, 9893–9898. doi: 10.1073/pnas.94.18.9893

Takahashi, J. S., and Menaker, M. (1979). Physiology of avian circadian pacemakers. *Fed. Proc.* 38, 2583–2588.

Tamai, T., Carr, A., and Whitmore, D. (2005). Zebrafish circadian clocks: cells that see light. *Biochem Soc Trans* 33(Pt 5), 962–966. doi: 10.1042/bst0330962

Tamai, T. K., Young, L., and Whitmore, D. (2007). Light signaling to the zebrafish circadian clock by Cryptochrome 1a. *Proc. Natl. Acad. Sci. U.S.A.* 104, 14712–14717. doi: 10.1073/pnas.0704588104

Tarttelin, E. E., Bellingham, J., Hankins, M. W., Foster, R. G., and Lucas, R. J. (2003). Neuropsin (Opn5): a novel opsin identified in mammalian neural tissue 1. *FEBS Lett.* 554, 410–416. doi: 10.1016/s0014-5793(03)01212-2

Tsukamoto, H. (2014). *Evolution of Visual and Non-visual Pigments*. Berlin: Springer, 219–239. doi: 10.1007/978-1-4614-4355-1_7

Underwood, H., and Groos, G. (1982). Vertebrate circadian rhythms: retinal and extraretinal photoreception. *Experientia* 38, 1013–1021. doi: 10.1007/bf01955345

Underwood, H., and Menaker, M. (1976). Extraretinal photoreception in lizards. *Photochem. Photobiol.* 23, 227–243. doi: 10.1111/j.1751-1097.1976.tb07247.x

Vallone, D., Gondi, S. B., Whitmore, D., and Foulkes, N. S. (2004). E-box function in a period gene repressed by light. *Proc. Natl. Acad. Sci. U.S.A.* 101, 4106–4111. doi: 10.1073/pnas.0305436101

Vatine, G., Vallone, D., Appelbaum, L., Mracek, P., Ben-Moshe, Z., Lahiri, K., et al. (2009). Light directs zebrafish period2 expression via conserved D and E boxes. *PLoS Biol* 7:e223. doi: 10.1371/journal.pbio.1000223

Whitmore, D., Foulkes, N., and Sassone-Corsi, P. (2000). Light acts directly on organs and cells in culture to set the vertebrate circadian clock. *Nature* 404, 87–91. doi: 10.1038/35003589

Whitmore, D., Foulkes, N. S., Strähle, U., and Sassone-Corsi, P. (1998). Zebrafish Clock rhythmic expression reveals independent peripheral circadian oscillators. *Nat. Neurosci.* 1, 701–707. doi: 10.1038/3703

Wyse, C., and Hazlerigg, D. (2009). Seasonal biology: avian photoreception goes deep. *Curr. Biol.* 19, R685–R687. doi: 10.1016/j.cub.2009.07.036

Zhao, X., Liu, J., Hsu, D. S., Zhao, S., Taylor, J.-S., and Sancar, A. (1997). Reaction Mechanism of (6-4) Photolyase. *J. Biol. Chem.* 272, 32580–32590. doi: 10.1074/jbc.272.51.32580

Zielinski, T., Moore, A. M., Troup, E., Halliday, K. J., and Millar, A. J. (2014). Strengths and limitations of period estimation methods for circadian data. *PLoS One* 9:e96462. doi: 10.1371/journal.pone.0096462

**Conflict of Interest:** The authors declare that the research was conducted in the absence of any commercial or financial relationships that could be construed as a potential conflict of interest.

frontiers in Physiology

REVIEW
published: 04 September 2020
doi: 10.3389/fphys.2020.00997

# Better Sleep at Night: How Light Influences Sleep in *Drosophila*

*Gabriella M. Mazzotta[1]*, Milena Damulewicz[2] and Paola Cusumano[1]**

[1] Department of Biology, University of Padova, Padua, Italy, [2] Department of Cell Biology and Imaging, Jagiellonian University, Kraków, Poland

Sleep-like states have been described in *Drosophila* and the mechanisms and factors that generate and define sleep-wake profiles in this model organism are being thoroughly investigated. Sleep is controlled by both circadian and homeostatic mechanisms, and environmental factors such as light, temperature, and social stimuli are fundamental in shaping and confining sleep episodes into the correct time of the day. Among environmental cues, light seems to have a prominent function in modulating the timing of sleep during the 24 h and, in this review, we will discuss the role of light inputs in modulating the distribution of the fly sleep-wake cycles. This phenomenon is of growing interest in the modern society, where artificial light exposure during the night is a common trait, opening the possibility to study *Drosophila* as a model organism for investigating shift-work disorders.

**Keywords: *Drosophila*, wake-sleep pattern, light, photoreception, neurotransmitters**

OPEN ACCESS

***Edited by:***
*Charalambos P. Kyriacou, University of Leicester, United Kingdom*

***Reviewed by:***
*Ko-Fan Chen, University of Leicester, United Kingdom*
*Stephane Dissel, University of Missouri–Kansas City, United States*

****Correspondence:***
*Gabriella M. Mazzotta*
*gabriella.mazzotta@unipd.it*
*Paola Cusumano*
*paola.cusumano@unipd.it*

***Specialty section:***
*This article was submitted to Chronobiology, a section of the journal Frontiers in Physiology*

***Received:*** *28 May 2020*
***Accepted:*** *22 July 2020*
***Published:*** *04 September 2020*

***Citation:***
*Mazzotta GM, Damulewicz M and Cusumano P (2020) Better Sleep at Night: How Light Influences Sleep in Drosophila. Front. Physiol. 11:997. doi: 10.3389/fphys.2020.00997*

## INTRODUCTION

Life on Earth has been shaped by rhythmic changes of environmental cues and living organisms have evolved endogenous mechanisms to coordinate physiological and behavioural functions. For example, in humans and other diurnal animals, most activities occur during the day, contrary to nocturnal animals, mostly active during the night. Among environmental factors, light plays a major role in adjusting temporal niches of animal behaviour in relation to natural surroundings, in the sense that it acts as an arousal signal for diurnal animals and at the same time promotes sleep in nocturnal ones (Redlin, 2001). *Drosophila* exhibits a very well-established daily activity pattern: under 12 h Light-12 h Dark cycles (LD12:12), flies display distinct morning and evening bouts of activity, separated by a prolonged siesta in the middle of the day. This behavioural output is the result of an orchestrated activity of different clusters of clock cells and signals (Grima et al., 2004; Stoleru et al., 2004; Picot et al., 2007; Cusumano et al., 2009; Zhang et al., 2009; Yao and Shafer, 2014; Chatterjee et al., 2018; Díaz et al., 2019; Schlichting et al., 2019b). In *Drosophila*, the circadian oscillator is located in about 150 neurons that, based on their anatomical location, are classified as: small and large ventral-lateral neurons (s-LNvs and l-LNvs, respectively), dorsal-lateral neurons (LNds), lateral posterior neurons (LPN), and three groups of dorsal neurons (DN1s, DN2s, and DN3s) (Schubert et al., 2018; **Figure 1A**). Among these, the s-LNvs and LNds are specifically involved in the control of morning and evening activity, respectively (Grima et al., 2004; Stoleru et al., 2004). Daily activity has specific pattern with two peaks: just after lights-on and around lights-off (**Figure 1B**). Morning peak is mostly driven by light, as in constant darkness (DD) it is much weaker, while evening peak is under circadian control. In addition, morning and evening anticipation is observed, which means that activity starts to increase around 3 h before the lights-on and lights-off (**Figure 1B**). Moreover, bimodal pattern of activity is observed also in clock mutants, but only in

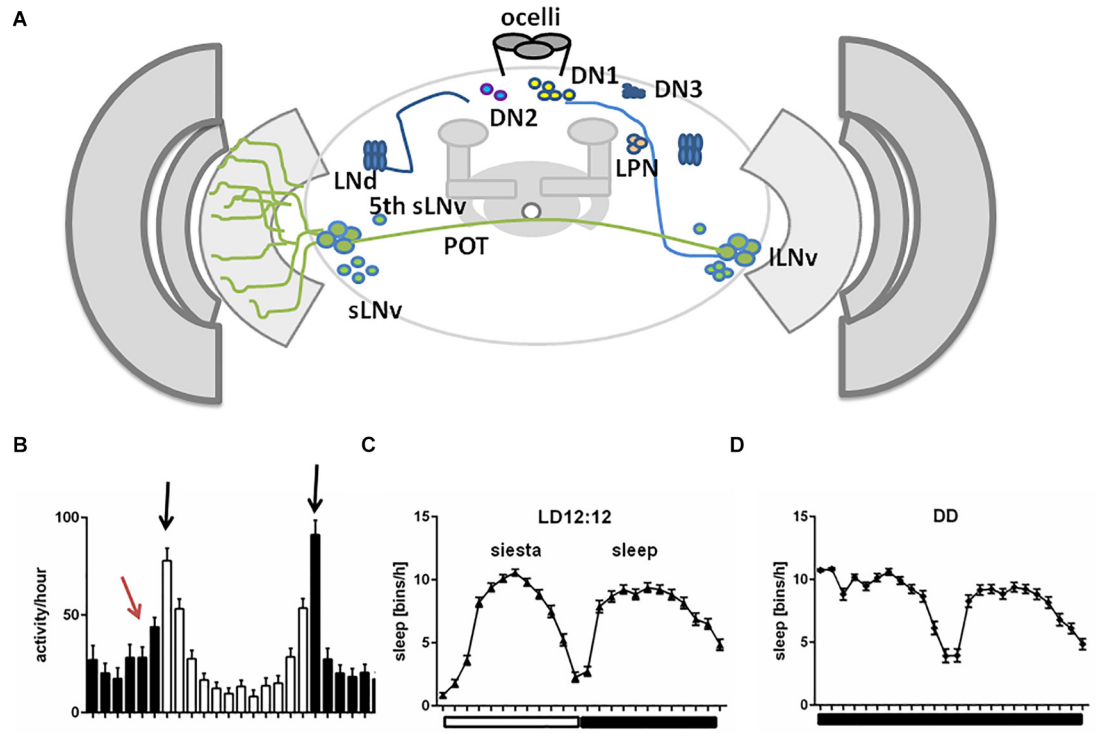


**FIGURE 1 |** A schematized representation of clock network in *Drosophila* brain. **(A)** The main pacemaker cells, lateral ventral neurons, small (s-LNvs) and large (l-LNvs) are located in accessory medulla. l-LNvs send projections, called posterior optic tract (POT), to the contralateral hemisphere and form network of processes in the medulla neuropil, while s-LNvs innervate dorsal brain. Six lateral dorsal neurons (LNds) and three lateral posterior neurons (LPNs) are located above the main pacemakers. In the dorsal brain, three groups of dorsal neurons are located (DN1s, DN2s, DN3). **(B)** Representative activity profile in light:dark (LD12:12) conditions with pointed morning/evening peaks (black arrows) and morning anticipation (red arrow). **(C,D)** Representative sleep pattern observed in LD cycles **(C)**, with siesta during the day and sleep during the night and constant darkness (DD) conditions **(D)**.

light-dark conditions, in constant darkness flies are completely arrhythmic. Clock mutants do not show morning anticipation, as they need light pulse to enhance activity level.

Compelling evidence attests to the influence of light on *Drosophila* rest-activity rhythms (recently reviewed in Helfrich-Förster, 2019). For instance, flies kept in constant darkness are sensitive to brief light pulses: they delay or advance their activity when the light stimulus is delivered in the early or late subjective night, respectively (Stanewsky et al., 1998). Also flies lacking compound eyes, $cli^{eya}$ mutants (Helfrich-Förster et al., 2001), or with impaired photoreceptor signal transduction, due to deficiency in norpA-encoded phospholipase C-β activity (Bloomquist et al., 1988), have a clearly advanced evening activity (Schlichting et al., 2019a) and a similar phenotype has been recently reported in flies with degenerated photoreceptors (Cusumano et al., 2018; Niu et al., 2019; Weigelt et al., 2019).

Here we will review the role of light and light input pathways in shaping the fly sleep-wake pattern. In particular, we will initially describe neurotransmitters that regulate sleep in *Drosophila*. We will then focus on the sleep centers and pathways (visual and not visual) mediating light signal to the brain. Then, we will review the neuronal networks involving circadian pacemaker cells and finally the influence of light (timing and intensity) on sleep architecture.

## SLEEP IN *DROSOPHILA*

As in mammals, sleep in insects is characterized by specific sleep posture and elevated sensory threshold. Although sleep patterns vary between different strains, sleep is always composed of daytime sleep, called "siesta," with the maximum around noon, and nighttime sleep with peak at midnight (**Figures 1C,D**). Daytime sleep is less deep, with shorter single sleep episodes and lower arousal threshold (the level of sensory stimuli required for behavioural response), meaning that flies are more sensitive to awakening factors during the day than during the night (Hendricks et al., 2000; Huber et al., 2004). Wake/rest daily rhythms in *Drosophila* can be recorded by placing individuals in glass tubes and monitoring the movements using infrared beam-based activity monitors (DAMS, Trikinetics) or video recordings. Sleep in flies is defined as at least 5 min of total inactivity (Shaw et al., 2000), meaning that during this time no infrared break is recorded by the system. Recordings of local field potential in the brain suggest that *Drosophila* sleep can be divided to specific phases of different intensities, similar to mammalian sleep (Nitz et al., 2002; van Alphen et al., 2013; Raccuglia et al., 2019). Sleep differs according to sex: males sleep more, with comparable resting time during the day and night, while mated females sleep mostly during the night, and they are more active

during the day (Huber et al., 2004). Sleep in *Drosophila* can be defined by the following parameters: bouts of sleep (number of sleep episodes), sleep bout length, which is useful for analysis of sleep fragmentation, and sleep latency/night offset (time between lights-off and the first sleep bout).

## Neurotransmitters

Sleep is controlled through neurotransmitters, divided into sleep-promoting [serotonin and gamma-aminobutyric acid (GABA)], wake-promoting (dopamine, octopamine, histamine) and those playing a dual role depending on target cells (acetylcholine, glutamate) (**Table 1**; reviewed in Ly et al., 2018). Both sleep-promoting neurotransmitters are released by dorsal pair medial neurons (DPMs) and directly affect mushroom bodies by inhibiting their activity (Haynes et al., 2015). GABA inhibits l-LNvs activity through Rdl receptor (Chung et al., 2009), and the pharmacological administration of GABA-A agonist (Gaboxadol) induces sleep behaviour in flies (Dissel et al., 2015) and humans (Faulhaber et al., 1997), indicating conserved role of GABA receptors in promoting sleep. Among wake-promoting molecules, dopamine and octopamine regulate the activity of sleep centers, central complex (CC), and mushroom bodies (MB) (Friggi-Grelin et al., 2003; Mao and Davis, 2009; Crocker et al., 2010), while histamine links retinal and extra-retinal photoreceptors to clock neurons (Oh et al., 2013). The role of octopamine is not well defined as recent data showed that the effect of octopamine could be sleep-promoting rather than wake-promoting (Deng et al., 2019). Finally, glutamate can promote sleep (Tomita et al., 2015) or wakefulness (Zimmerman et al., 2017) depending on the postsynaptic receptors. A similar effect is described for acetylcholine which promotes wakefulness by exciting l-LNvs when released from extra-retinal photoreceptors, Hofbauer–Buchner eyelets, and L2 neurons (McCarthy et al., 2011; Muraro and Ceriani, 2015; Schlichting et al., 2016), and has a sleep-promoting effect when released from mushroom bodies (Yi et al., 2013).

## Sleep Centers

*Drosophila* sleep centers are located in different brain regions, although the most essential ones reside in the central and dorsal region, as MB and CC, composed of dorsal fan-shaped body (FB), and ellipsoid body (EB) with the ring structure (EB-R2) (Joiner et al., 2006; Pitman et al., 2006; Donlea et al., 2011; Liu et al., 2012, 2016; Guo et al., 2016; **Figures 2A,B**).

Mushroom bodies are composed of neurons called Kenyon cells (Technau, 2007), whose axons form lobes: two vertical (α, α') and three horizontal (β, β', γ). MB contains both wake-promoting and sleep-promoting neurons, located in β'2, γ3/4 and α'1, γ2 region, respectively (Joiner et al., 2006; Sitaraman et al., 2015b; Artiushin and Sehgal, 2017; **Figure 2C**). MB receive inhibiting, wake-promoting signals through serotonin and GABA (Yuan et al., 2006; Haynes et al., 2015). Specific MB compartments send information to mushroom body output neurons (MBONs) *via* glutamate and acetylcholine, that have a wake- or sleep- promoting effect, respectively (Aso et al., 2014; Sitaraman et al., 2015a). MB express additional sleep-promoting factors. Among these, Neurocalcin (NCA) and Noktochor (Nkt) promote nighttime sleep by suppressing nocturnal arousal (Chen et al., 2019; Sengupta et al., 2019).

The CC is involved in the regulation of locomotor activity and visual processing (Liu et al., 2006; Poeck et al., 2008; Triphan et al., 2010; Seelig and Jayaraman, 2013). The upper part of CC contains the FB, with sleep-promoting ExFl2-cells, which receive signals from the protocerebral posterolateral cluster 1 (PPL1) and protocerebral posteromedial 3 (PPM3) (Liu et al., 2016). This dopaminergic pathway inhibits FB activity and suppresses sleep (Liu et al., 2012; Ueno et al., 2012; Kayser et al., 2014; Pimentel et al., 2016; Ni et al., 2019). FB can be also activated by glutamatergic input from the circadian clock, represented by Allatostatin A (AstA)-expressing LPN cells (Ni et al., 2019). Both inputs are integrated in FB to precisely control its activity and ultimately regulate shifts between sleep and wake states. In the final step, active FB releases GABA, which inhibits octopaminergic output arousal neurons (OAA), thus promoting sleep (Ni et al., 2019; **Figure 3**).

Below the FB, EB is located, which is involved in memory formation and startle response to mechanical stimulation. The major neurons composing EB are called ring neurons (R), and they receive synaptic signals from the anterior visual tract, through tubercular bulbar (TuBu) neurons (Omoto et al., 2017). Additional cells, called helicon cells, receive and integrate visual inputs and connect FB and EB: during wakefulness, helicon cells are sensitive to visual inputs and propagate signals to R2 cells, which are important for the regulation of sleep depth. R2 cells activate sleep-promoting ExFl2 neurons, thus increasing sleep need. In turn, during sleep AstA released by FB inhibits helicon cells, which causes decreased responsiveness to visual stimuli (Donlea et al., 2018; **Figure 3**).

# HOW DO LIGHT INPUTS MODULATE SLEEP IN *DROSOPHILA*?

Light signals to *Drosophila* brain are mediated either by visual structures, such as two large compound eyes (retinal photoreceptors) and two Hofbauer–Buchner eyelets (HB eyelets, extraretinal photoreceptors), and non-visual pathways, involving three ocelli and deep brain photoreceptors CRYPTOCHROME (CRY), QUASIMODO (QSM), and Rhodopsin 7 (Rh7) (reviewed in Helfrich-Förster, 2019).

## Compound Eyes

*Drosophila* compound eyes comprise ∼800 units, called ommatidia, organized in regular structures innervating and conveying visual signals to the four distinct neuropil regions of the optic lobe (lamina, medulla, lobula, and lobula plate). Each ommatidium houses 20 cells, eight of which are photoreceptors (R1–R8) designated in processing light inputs as function of position, spectral composition, and axonal projections. The six outer photoreceptors (R1–R6), expressing the broad spectrum rhodopsin (Rh1) (Hardie, 1979; O'Tousa et al., 1985; Zuker et al., 1985), project to the lamina (Braitenberg, 1967; Strausfeld, 1971) and are intended for motion detection and image formation (Heisenberg and Buchner, 1977; Yamaguchi et al., 2008). The

**TABLE 1 |** Neurotransmitters involved in sleep regulation.

| | Expression | Target cells | Receptor | References |
|---|---|---|---|---|
| Wake-promoting | | | | |
| Dopamine | Sleep centers:<br>MB<br>PPL1, PPL3 | Sleep centers:<br>CC, FB<br>l-LNvs<br>MBON | D1-like (DopR1, DopR2)<br>D2-like (DD2R) | Liu et al., 2012<br>Ueno et al., 2012<br>Sitaraman et al., 2015b<br>Friggi-Grelin et al., 2003<br>Mao and Davis, 2009 |
| Octopamine | APL | Visual system:<br>Optic lobes<br>Sleep centers:<br>CC, MB<br>l-LNvs<br>protocerebrum,<br>DILP2-expressed cells | Oamb<br>Octß1R<br>Octß2R<br>Octß3R | Crocker et al., 2010 |
| Histamine | Visual system:<br>Photoreceptors, HB eyelets<br>18 cells in the brain | Visual system:<br>Glial cells in the lamina,<br>R1-8, LMC<br>l-LNvs | HisCl1<br>Ort | Oh et al., 2013<br>Alejevski et al., 2019<br>Pantazis et al., 2008<br>Hamasaka and Nässel, 2006 |
| Sleep-promoting | | | | |
| Serotonin | DPM<br>LBO5HT<br>LMlo | Sleep centers:<br>MB, FB<br>LNvs<br>Visual system:<br>Epithelial glia,<br>Mi, Mt, wide-field neurons<br>in the lamina, wide field<br>cells in the lobula and<br>lobula plate | 5-HT-1a<br>5-HT-2b<br>5-HT1b<br>5-HT-2a<br>5-HT-7 | Yuan et al., 2005, 2006<br>Qian et al., 2017<br>Haynes et al., 2015 |
| GABA | DPM,<br>Visual system:<br>C2, C3, amc, LMC (L1, L2),<br>Mi4, CT1, TmY15 | l-LNvs<br>antennal lobes<br>Sleep centers:<br>MB, CC<br>Visual system:<br>large-field tangential<br>neurons, C2, C3, LMC (L4) | GABAA (Rdl)<br>GABAB (R1, R2, R3) | Chung et al., 2009<br>Haynes et al., 2015 |
| Dual role | | | | |
| Glutamate | Sleep centers:<br>MB<br>Visual system:<br>LMC (L1), Tm (Tm9, Tm20),<br>TmY, Mi (Mi9), Mt, Pm, Dm,<br>Mi, bushy T (T), Tlp, Li,<br>LPTC, LPi,<br>amc | Visual system:<br>large-field tangential cells,<br>Mi9<br>Sleep centers:<br>EB | iGluR (ionotropic), (Nmdar1,<br>Nmdar2, GluRIIA-E,<br>GluRIA, GluRIB)<br>GluClα<br>mGluR (metabotropic) | Tomita et al., 2015<br>Robinson et al., 2016<br>Raghu and Borst, 2011<br>Takemura et al., 2011<br>Liu and Wilson, 2013<br>Mauss et al., 2014, 2015<br>Sinakevitch-Pean et al., 2001 |
| Acetylcholine | Sleep centers:<br>MB<br>Visual system:<br>HB eyelets, LMC (L2, L4),<br>amc, C2, Tm2 | l-LNvs<br>Visual system:<br>LMC (L2, L4), Tm2 | Muscarinic mAChR (A-C)<br>Nicotinic nAChR (α1-7,<br>β1-3) | McCarthy et al., 2011<br>Takemura et al., 2011<br>Buchner et al., 1986<br>Yasuyama and Salvaterra, 1999 |

*MB, mushroom bodies; FB, fan-shaped body; PPL, protocerebral posterior lateral cells; CC, central complex; MBON, mushroom body output neurons; APL, anterior paired lateral neurons; LMC, lamina monopolar cells; R, retina photoreceptors; DPM, dorsal pair medial; LBO5HT, large bilateral optic lobe 5-HTi neurons; LMlo, Lamina MIoinhibitory peptide-expressing cell; LNvs, ventral-lateral neurons; C2, C3, centrifugal cells; Tm, transmedullar cells; Amc, amacrine cells; TmY, transmedullar cells Y; Tlp, translobula plate cells; CT, complex tangential cell; Li, lobula intrinsic; cells; LPi, lobula plate intrinsic cells; Pm, proximal medulla cells; Dm, distal medulla cells; LPTC, lobula plate tangential cells; Mi, medulla intrinsic cells; Mt, medulla tangential cells.*

two inner central photoreceptors (R7–R8) reach and innervate the distant medulla and participate in color, UV, and polarized light detection (Melamed and Trujillo-Cenóz, 1967; Montell, 2012). R7–R8 photoreceptors are clustered in 30% "pale" [R7 expressing UV-sensitive-Rh3 (331 nm) and R8 expressing blue-sensitive-Rh5 (442 nm)] and 70% "yellow" ommatidia [R7 expressing UV-sensitive-Rh4 (355 nm) and R8 expressing green-sensitive-Rh6 (515 nm)] (Fryxell and Meyerowitz, 1987; Montell et al., 1987; Zuker et al., 1987; Feiler et al., 1992; Chou et al., 1996, 1999; Huber et al., 1997; Papatsenko et al., 1997; Salcedo et al., 1999). A seventh Rhodopsin (Rh7) (Adams et al., 2000) is expressed also in the compound eyes (specifically in R8)

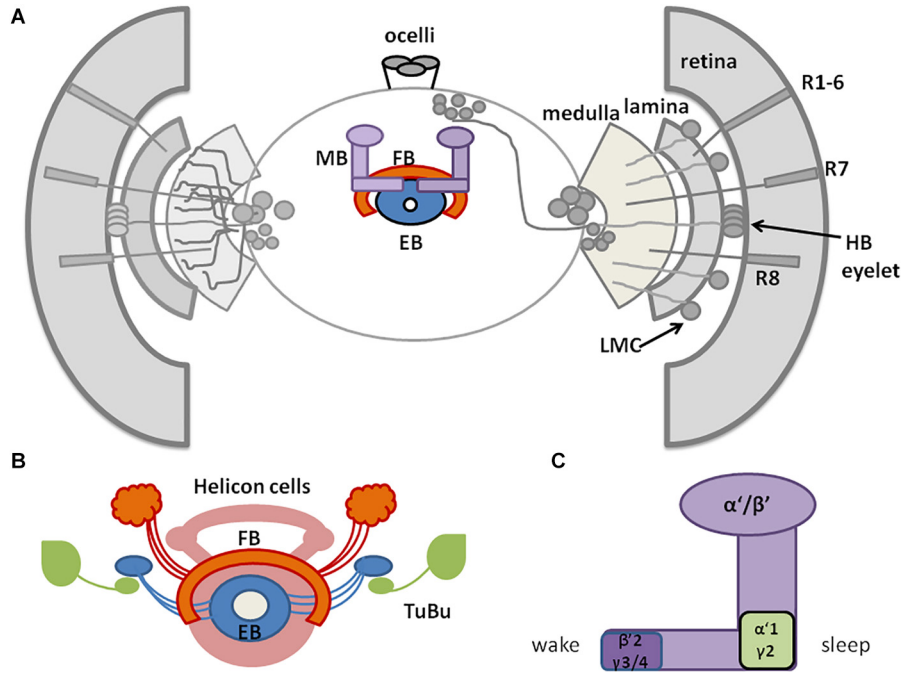


**FIGURE 2 |** A schematic representation of *Drosophila* sleep centers and structures mediating light signals. **(A)** *Drosophila* brain with three photoreceptive structures: visual system (composed of retina and three optic neuropils: lamina, medulla, and lobula), extra-retinal Hofbauer–Buchner (HB) eyelets and ocelli, located on the top of head. Light is received by retinal photoreceptors R1–6, which terminate in the lamina, and R7–8, terminating in the medulla and transmitting through lamina monopolar cells (LMC) to the deep brain. HB eyelets, located between retina and lamina, are sensitive to high intensity light and transmit signal directly to clock neurons (ventral-lateral neurons_LNvs). In the central brain sleep centers are located with mushroom bodies (MB), ellipsoid body (EB), and fan-shaped body (FB). **(B)** Scheme of sleep center, composed of fan-shaped body (FB), mushroom bodies (MB), ellipsoid body (EB), and additional cells: tubercular bulbar neurons (TuBu) and helicon cells. **(C)** Mushroom bodies are composed of vertical (α, α') and horizontal (β, β', γ) lobes. Wake-promoting neurons are located in β'2, γ3/4, while sleep-promoting ones in α'1, γ2 region of MB.

as well as in other brain neurons (including some clock neurons) (Senthilan and Helfrich-Förster, 2016; Grebler et al., 2017; Kistenpfennig et al., 2017; Ni et al., 2017; Senthilan et al., 2019). Its role and expression pattern have been recently discussed (Senthilan et al., 2019).

The visual cascade complex is located in the rhabdomeres of photoreceptor cells: the G-protein (Gq) activates the phospholipase C (PLC), [encoded by *norpA* (Bloomquist et al., 1988; Scott et al., 1995)] which hydrolyzes phosphatidylinositol 4,5-bisphosphate ($PIP_2$) and promotes the opening of the TRP and the TRP-like (TRPL) cation channels (reviewed in Montell, 2012). The triggered calcium current is then balanced by the $Na^{2+}/Ca^{2+}$ exchanger, Calx (Wang et al., 2005).

Each outer photoreceptor cell forms a tetrad synapse with L1 and L2 laminar neurons and L3 or amacrine cell or epithelial glia. Under certain conditions (bright light and impaired synaptic transmission) lamina interneurons feed back to photoreceptor cells, modulating their output (Zheng et al., 2006). In the lamina, projections from R1–6 are organized in synaptic modules called cartridges, in which three epithelial glial cells surround six photoreceptor terminals with invaginating capitate projections (Stuart et al., 2007). On the other hand, inner photoreceptors and lamina neurons form synaptic modules (columns) with medulla interneurons and neurons that convey visual information to the lobula and lobula plate neuropils (Stark and Carlson, 1986; Meinertzhagen and O'Neil, 1991; Perez and Steller, 1996; Rivera-Alba et al., 2011; Millard and Pecot, 2018). Recently, a new class of *Drosophila* interneurons has been discovered: the Allatostatin C (AstC)/crustacean cardioactive peptide receptor (CcapR) expressing neurons, which convey light input from the compound eyes directly to the circadian pacemaker neurons, through the accessory medulla (aMe) (Li et al., 2018). The medulla thus receives and processes both motion and colour information coming from different retinotopic maps (Rister et al., 2007; Gao et al., 2008).

The epithelial glial cells surrounding lamina cartridges express the Mesencephalic Astrocyte-derived Neurotrophic Factor DmMANF, orthologue of mammalian MANF and CDNF (cerebral dopamine neurotrophic factor), involved in supporting the survival of dopaminergic neurons (Lindholm and Saarma, 2010). DmMANF is also involved in the maintenance of dopaminergic neurons, as *DmMANF* null mutants display extremely low levels of dopamine and decreased dopaminergic neurites (Palgi et al., 2009). In the adult fly, DmMANF is also expressed in the retina, specifically in the photoreceptor cell bodies, and in the lamina (lamina cortex and synaptic neuropil) (Stratoulias and Heino, 2015). At structural level, the silencing of *DmMANF* in glial cells induces degeneration of the lamina,

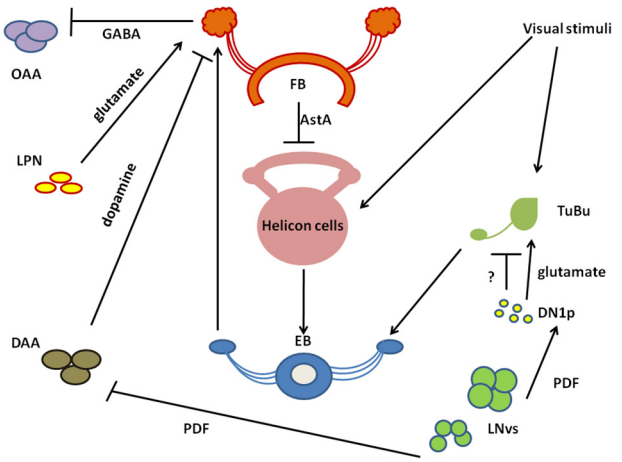


**FIGURE 3 |** A schematized circuit of neurotransmission regulating sleep centers. Light affects clock neurons (ventral-lateral neurons_LNvs) activity, which stimulates pigment dispersing factor (PDF) release. In turn, PDF inhibits dopamine arousal neurons (DAAs), which normally decrease fan-shaped body (FB) activity through dopamine. Lack of dopamine signalling promotes sleep. PDF activates also Dorsal Neurons posterior (DN1sp), which can inhibit tubercular bulbar cells (TuBu), or activate them through glutamate. Visual stimuli affect Tubu and helicon cells activity, both send signals to the ellipsoid body (EB). EB coordinates FB activity and receives feedback signals from FB through helicon cells, which are inhibited by AstA released from FB. In addition, FB obtains signals from lateral posterior neurons (LPNs) through glutamate. FB processes all inputs and sends final sleep-promoting information through inhibiting GABA signalling to output arousal neurons (OAAs).

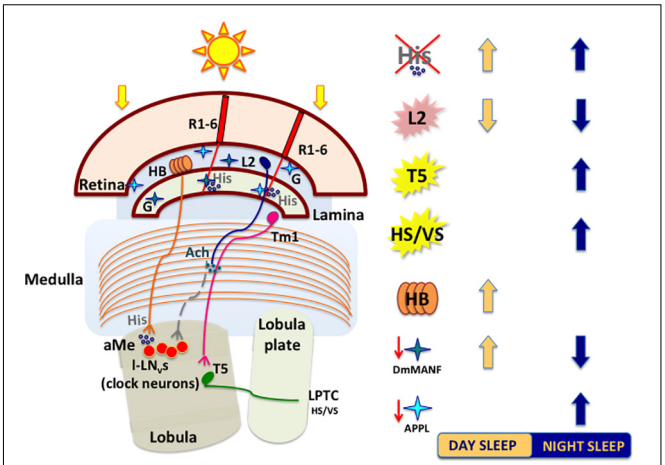


**FIGURE 4 |** A schematized and simplified circuit showing how light perceived by retinal and extra-retinal structures impacts sleep. Light-activated retinal photoreceptors release histamine (His). Mutations affecting the histamine biosynthesis pathway (*hdc* mutants) lead to increase in sleep. R1–R6 photoreceptors convey signals to cholinergic large monopolar laminar cells (L2) that connect indirectly both clock neurons (l-LNvs) and neurons involved in motion pathways (T5). Temperature-Sensing TRP Channel activation in L2 neurons strongly suppresses sleep by releasing ACh that, in turn, promotes the bursting of l-LNvs. T5 cells axons transfer motion information to various types of lobula plate tangential neurons (LPTCs), like HS (horizontal motion) and VS (vertical motion) neurons, to further reach the central brain. Optogenetic activation of motion processing neurons (T5 or HS/VS) increases nighttime sleep. The extraretinal photoreceptors (HB eyelets) release histamine in the accessory Medulla (aMe), preventing l-LNvs from firing and thus increasing siesta during the day. Glia cells in lamina interact with photoreceptors and shape the wake/sleep pattern of flies. Downregulation of *DmMANF* (mesencephalic astrocytes-derived neurotrophic factor) in epithelial glia induces lamina neurodegeneration and leads to increase in daytime sleep. Downregulation of *Appl* (amyloid precursor protein like) in glia cells increases nighttime sleep. Light blue (APPL) and dark blue (DmMANF) stars indicate cortex and epithelial lamina glia, respectively. L2: heat-activated (pink); T5 and HS/VS: optogenetically activated (yellow). G, glia cell; His, histamine; Ach, acetylcholine.

in particular in the lamina epithelial glial cells, which exhibits holes and/or tightly packed membranes and also a decrease of capitate projections in the cartridges (Walkowicz et al., 2017). In glial cells, DmMANF is also involved in controlling the levels of dopamine and other neurotransmitters responsible for *Drosophila* behaviour. In fact, downregulation of *DmMANF* in glia alters the sleep/activity pattern of flies in LD, with decreased activity in the light phase and increased activity in the dark phase of the cycle (Walkowicz et al., 2017). Conversely, these flies display a reduction of nighttime sleep and a slight increase of sleep in the early day (**Figure 4**). The sleep modulating role of DmMANF is supported by the significant upregulation of transcripts involved in the dopamine synthesis pathway observed in hypomorphic *DmMANF* mutant embryos (Palgi et al., 2012).

Glial cells express the Amyloid Precursor Protein-Like (APPL), known for its crucial role in neuronal physiology and cellular biology and its involvement in age-dependent behavioural deficits and neurodegeneration, as consequence of production and deposition of toxic β-amyloid peptides, in both mammals and flies (Carmine-Simmen et al., 2009). In *Drosophila*, this is true also for the glial cells in the subretinal layer of lamina cortex, where the correct cleavage of APPL is fundamental for their survival. Indeed, loss of function mutation or knock-down of the beta-site Amyloid Precursor Cleaving Enzyme (dBACE) in photoreceptor neurons result in glial cell death and progressive lamina degeneration (Bolkan et al., 2012).

The role of APPL in glia is not only related to its neurotoxic effects, as it has been recently shown to be involved in the physiology and regulation of sleep/wake cycles (Farca Luna et al., 2017). The downregulation of *Appl* in cortex and astrocyte-like glia significantly increases nighttime sleep, which exhibits longer sleep-bouts (**Figure 4**) and, conversely, the overexpression of *Appl* in these cells results in reduced sleep amount and increased sleep latency (Farca Luna et al., 2017). This effect on sleep/wake regulation is due to an altered glutamate recycling, as the downregulation of *Appl* increases the expression of genes involved in reuptake and recycling of the neurotransmitter, such as the glutamate transporter *excitatory amino acid transporter 1* (*dEaat1*) and the *glutamine synthetase* (*Gs*) (Farca Luna et al., 2017). Moreover, the downregulation of *Appl* changes also the cellular distribution of Innexin 2 (Inx2), highly expressed in the layers of laminar pseudocartridge and satellite glia, where it plays a fundamental role in modulating the level of carcinine, and therefore histamine, essential for a proper visual synaptic transmission (Chaturvedi et al., 2014).

As previously mentioned, R1–6 photoreceptors are also involved in visual motion, that is the detection of direction-selective signals, fundamental for fly survival. The luminance information from R1–6 is integrated by some large motion-sensitive neurons in the lobula plate, called lobula plate tangential cells (LPTCs), specific for vertical or horizontal motion (VS and HS, respectively) and responding by selective hyperpolarization or depolarization (reviewed in Borst et al., 2020). Each lamina cartridge specifically conveys brightness increments or decrements information to subsets of downstream motion detecting neurons, *via* a specific set of cells in the medulla, called trans-medulla Y (TmY). In particular, L1 pathway conveys luminance increments to specific layers of the lobula (T4 cells-ON channels), while the L2–4 pathway transmits information about brightness decrements to the lobula plate (T5 cells-OFF channels) (Borst et al., 2020). Axon terminals from T4 and T5 neurons then connect to the dendrites of LPTCs (HS and VS) in the lobula plate (Borst et al., 2020), from where the information is further transmitted to the central brain likely through descending neurons (Suver et al., 2016). LPTCs also receive direction information from another source. Indeed, T4 and T5 cells contact and send an inhibitory glutamatergic signal to a group of neurons in the lobula plate, the bi-stratified lobula plate intrinsic (LPi) cells, that convey this signal to the tangential cells expressing glutamatergic $Cl^-$ channel α (reviewed in Borst et al., 2020).

Visual information processed by motion circuits play an important role in sleep regulation. Flies lacking HS and VS neurons ($omb^{H31}$ mutants) display a reduced and fragmented sleep compared to wild-type (wt), while the optogenetic activation of these cells results in an increase of nighttime sleep (Kirszenblat et al., 2019). Moreover, the optogenetic activation of T5 neurons leads to a consolidation of nighttime sleep, with increased bout duration and lower bouts number (Kirszenblat et al., 2019; **Figure 4**).

### Histamine, the Major Neurotransmitter in the Compound Eyes

Histamine is the most important neurotransmitter released by the compound eyes (Hardie, 1987, 1989), and histamine-immunoreactivity has been detected in the optic lobes, in neurons adjacent to LNs and DNs, ocelli, in the eyelets axons, in 18 cell bodies in protocerebrum (HP1–4) and 2 cell bodies in the subesophageal ganglion (Nässel, 1999; Hamasaka and Nässel, 2006; Hong et al., 2006; Oh et al., 2013). The biogenic amine is synthetized in photoreceptors, from L-histidine, by the histidine decarboxylase (Hdc) and flies deficient for this enzyme activity ($hdc^{P218}$) have disrupted photoreceptor synaptic transmission (Burg et al., 1993). Light-depolarization of retinal photoreceptors triggers the fast release of histamine to the downstream lamina monopolar neurons; this, in turn, opens the histamine-gated chloride channels and leads to hyperpolarization (Wang and Montell, 2007; Pantazis et al., 2008). Electroretinograms in postsynaptic lamina neurons record ON and OFF transient peaks as a function of light (Alawi and Pak, 1971; Heisenberg, 1971). The epithelial glia cells surrounding synaptic cartridges work in coordinating photoreceptor-glia communication in the lamina: in fact, in capitate projections histamine is conjugated to β-alanine by Ebony, to form β-alanylhistamine (carcinine) (Stark and Carlson, 1986; Meinertzhagen and O'Neil, 1991; Borycz et al., 2002; Richardt et al., 2002, 2003; Hartwig et al., 2014). Carcinine is then transported back to photoreceptors by the transporter CarT (Stenesen et al., 2015; Xu et al., 2015; Chaturvedi et al., 2016) and cleaved again into histamine and β-alanine by Tan (Borycz et al., 2002; Wagner et al., 2007). Interruption of this cycle results in the loss of visual transmission (Rahman et al., 2012).

In *Drosophila*, histamine gates two chloride channels: the outer rhabdomeres transientless (ort) and histamine-gated chloride channel subunit 1 (HisCl1) (Gengs et al., 2002; Gisselmann et al., 2002; Witte et al., 2002; Zheng et al., 2002). Ort is expressed in lamina (L1–L3 cells), medulla, lobula neuropils, ocellar postsynaptic interneurons, Pars Intercerebralis (PI), FB, cells in the lateral and central brain and thoracic ganglia (Hong et al., 2006; Gao et al., 2008; Pantazis et al., 2008; Lin et al., 2016; Schnaitmann et al., 2018). In lamina interneurons, it plays a key role in transmitting motion detection inputs coming from retina photoreceptors: its overexpression in L1 and L2 can restore the ON and OFF transients in electroretinograms and motion detection responses lost in *ort*-null mutants (Gengs et al., 2002; Rister et al., 2007; Gao et al., 2008; Pantazis et al., 2008). HisCl1 receptor is strongly expressed in lamina epithelial glial cells surrounding cartridges, in neurons in the medulla (Gao et al., 2008; Pantazis et al., 2008), in R7 and R8 photoreceptors (Tan et al., 2015; Schnaitmann et al., 2018; Alejevski et al., 2019; Davis et al., 2020) and many other cell types, including the large LNvs (Hamasaka and Nässel, 2006; Hong et al., 2006).

Histamine released by light-activated photoreceptors likely acts in at least two different pathways directly involved in sleep regulation: the visual (photic) input and the motion detection pathways, distinct signalling dynamics both relying on activation of lamina interneurons L2 (Meinertzhagen and O'Neil, 1991; Meinertzhagen and Sorra, 2001; Shinomiya et al., 2014, 2019; Muraro and Ceriani, 2015; Kirszenblat et al., 2019; Borst et al., 2020; **Figure 4**).

In mammals, histamine is known to play a wake-promoting role (Thakkar, 2011), that seems to be conserved in insect. In *Drosophila*, histamine treatment causes sleep time reduction (Oh et al., 2013), while administration of its receptor antagonist increases sleep (Shaw et al., 2000). Moreover, mutations in the *hdc* gene [$hdc^{P211}$ and $hdc^{P218}$ (Burg et al., 1993)], lead to a significant increase of daytime sleep duration and number of sleep episodes in comparison to wt (Oh et al., 2013; **Figure 4**). Similar data obtained in constant darkness indicate that the observed wake-promoting effect depends on histamine, and it is not connected with defects in photoreception in the eye (Oh et al., 2013). Of the two histamine receptors, only HisCl1 located on the surface of l-LN$_v$s is involved in sleep regulation (Oh et al., 2013).

## Ocelli

Ocelli complex is composed of three ocellar cells, interocellar cuticle and bristles (Haynie and Bryant, 1986). They contain 80–100 photoreceptors expressing the UV-sensitive Rhodopsin2 (Mismer and Rubin, 1987; Feiler et al., 1988; Pollock and Benzer, 1988). The role of ocelli is to adjust sensitivity of the compound

eyes (Hu and Stark, 1980) and to collect information about the horizontal position (Krapp, 2009). They also contribute to entrainment to long and short days (Rieger et al., 2003), *via* a norpA-independent pathway (Saint-Charles et al., 2016). They use histamine as neurotransmitter, and they do not contact directly with clock neuron processes (Hamasaka and Nässel, 2006). A specific role for this structure in sleep has not been reported yet.

## Hofbauer–Buchner Eyelets: Direct Light Signalling to the Pacemaker

Hofbauer–Buchner eyelets originate from the larval visual system, called Bolwig organs (BO), involved in the regulation of many light-dependent behaviours (Busto et al., 1999; Hassan et al., 2000). Larval BO is cholinergic (Yasuyama and Salvaterra, 1999), but it uses norpA-dependent phototransduction pathway, similar to retinal photoreceptors (Busto et al., 1999; Hassan et al., 2000). It is composed of 12 cells: eight of them express Rh6 and 4 of them express Rh5 (Sprecher and Desplan, 2008), and their projections terminate in the area of LNvs (Kaneko et al., 1997). Rh6-expressing cells die during development, and four others switch expression from Rh5 to Rh6 (Sprecher and Desplan, 2008). Adult HB express Rh6 and are sensitive to 480 nm wavelength (Helfrich-Förster et al., 2002), yet there are evidences that they may use an alternative mechanism of phototransduction, norpA-independent, like cascade described by Chang and Ready (2000). Although Rh5 expression in HB could not be detected by immunostaining (Yasuyama and Meinertzhagen, 1999; Malpel et al., 2002), the expression of GFP under the Rh5-Gal4 driver was revealed as a weak signal (Malpel et al., 2002). In the adult, HB act as circadian photoreceptive organs (Hofbauer and Buchner, 1989; Yasuyama and Meinertzhagen, 1999) and contribute to the synchronisation of circadian clock, in terms of entrainment to long and short days (Helfrich-Förster et al., 2001, 2002; Rieger et al., 2003). At the molecular level, they are involved in synchronisation of TIM and PER expression in s-LNvs (Helfrich-Förster et al., 2001), l-LNvs and DN1s (Mealey-Ferrara et al., 2003; Veleri et al., 2007).

Hofbauer–Buchner axons terminate in the accessory medulla and they can directly contact with pigment dispersing factor (PDF)-expressing LNvs in aMe (Helfrich-Förster et al., 2002; Malpel et al., 2002). Eyelets express both histamine and acetylcholine as neurotransmitters (Hofbauer and Buchner, 1989; Pollack and Hofbauer, 1991; Yasuyama and Meinertzhagen, 1999; Damulewicz et al., 2020; **Figures 4**, **5**).

Light signals received by HB eyelets in the morning are transmitted *via* acetylcholine and excite s-LNvs *via* nicotinic receptors (Wegener et al., 2004; McCarthy et al., 2011; Schlichting et al., 2016), causing increased cAMP levels (Lelito and Shafer, 2012) and a wake-promoting effect. At the same time, histamine released from HB inhibits l-LNvs (Schlichting et al., 2016). In the morning l-LNvs are less active, with decreased firing observed. Then they start to accumulate $Ca^{2+}$ that reaches its maximal level around midday (Liang et al., 2016), when they could receive input from other cells, that is, from L2 cells in the medulla (Muraro and Ceriani, 2015). l-LNvs increase firing and release PDF to activate evening cells, ultimately increasing the evening activity.

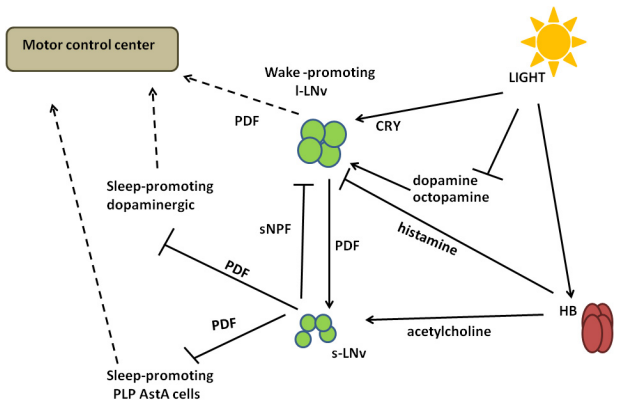


**FIGURE 5 |** A schematized circuit of circadian regulation of sleep. Light signals received by Hofbauer–Buchner eyelets (HB) are transmitted through acetylcholine to small ventral-lateral neurons (s-LNvs) and through histamine to large ventral-lateral neurons (l-LNvs). Activated s-LNvs release pigment dispersing factor (PDF), which inhibits dopaminergic and AstA-expressing sleep-promoting cells. The regulation of l-LNvs activity is more complex, as they express light-sensitive Cryptochrome (CRY) as well as dopamine and octopamine receptors. Light activates CRY, but at the same time it inhibits the response to dopamine and octopamine, decreasing signal inputs to l-LNvs. In addition, l-LNvs receive inhibiting inputs from s-LNvs through short Neuropeptide F (sNPF). Different signalling inputs are processed in l-LNvs and transmitted to the motor control center through PDF.

## Deep Brain Photopigments

Cryptochrome (CRY) is a blue-light-sensitive protein (VanVickle-Chavez and Van Gelder, 2007) playing many different roles, ranging from photoreceptor to magnetoreception and metabolism regulation (for review see Damulewicz and Mazzotta, 2020). It is expressed in a broad range of cells in the brain: in circadian pacemaker neurons (all five s-LNvs, l-LNvs, three of the six LNds, and some of the DN1s), but also in non-clock neurons, glia and visual system (Benito et al., 2008; Yoshii et al., 2008; Damulewicz and Pyza, 2011; Fogle et al., 2011). Its photoreceptive role allows the entrainment of molecular clock to environmental light conditions through conformational changes that expose specific domains and promote binding TIM or PER (Ceriani et al., 1999; Koh et al., 2006; Peschel et al., 2009; Rosato et al., 2001), targeting TIM to ubiquitination and degradation in proteasomes (Peschel et al., 2009). The role of CRY in the visual system is more complex, as it plays a role of circadian transcriptional repressor (Collins et al., 2006), in maintaining the proper localization of phototransduction cascade complex (Mazzotta et al., 2013; Schlichting et al., 2018) and in enhancing photosensitivity during the night (Damulewicz et al., 2017; Mazzotta et al., 2018).

Quasimodo (QSM) is a light-sensitive protein, belonging to the extracellular membrane-anchored Zona pellucida (ZP) domain family. It is expressed in all clock neuronal groups, except for LPNs, however not in every cell within the cluster. Most of the clock cells co-express both, QSM and CRY, but some of

them, like DN2s and DN3s, do not express CRY, suggesting that QSM works in a CRY-independent pathway. In addition, QSM is expressed in non-clock cells, located in close proximity to the pacemaker (Chen et al., 2011). Light exposure increases QSM levels inside the cell, *via* a post-translational mechanism that involves the extracellular ZP domain light-dependent cleavage (Plaza et al., 2010; Buhl et al., 2016). Active QSM was proposed to change membrane conductance following interaction with the $Na^+$, $K^+$, $Cl^-$ co-transporter (NKCC) and the Shaw $K^+$ channel (dKV3.1) (Buhl et al., 2016). QSM regulates electrical excitability also in clock neurons: it modulates l-LNvs daily changes of activity, as its downregulation results in a constitutively more active state, similar to that observed during the day time, while *qsm* overexpression leads to a constitutive less active, night-like state (Buhl et al., 2016). Moreover, QSM is involved in the light-dependent TIM degradation process and it can affect TIM stability in a CRY-independent pathway (Chen et al., 2011).

## Circadian Pacemaker Neurons

Sleep timing and duration are highly influenced by the circadian clock, which promotes the consolidation of sleep during the night in diurnal species, such as *Drosophila* and human, and during the day in nocturnal animals, such as rodents (Kunst et al., 2014; Liu et al., 2014). Indeed, in flies lacking the main clock genes *period* and *timeless*, the sleep episodes are randomly distributed across the 24 h, although the mean rest levels do not differ from wt (Hendricks et al., 2000). Moreover, flies mutants for both *Clock* and *cycle* show a significant decrease in daily consolidated rest in DD conditions, with brief rest and prolonged activity bouts (Shaw et al., 2002; Hendricks, 2003), and $cyc^{01}$ mutants show also an excessive response to sleep deprivation, with a persistent large increase in sleep (Shaw et al., 2002).

### PDF Expressing LNvs

#### *LNvs and serotoninergic signalling: modulation of the circadian light sensitivity*

The serotoninergic pathway regulates many aspects of behaviour, including sleep/wake cycles (Ursin, 2002). In *Drosophila*, it positively controls sleep and negatively modulates circadian photosensitivity: treatment with the serotonin precursor 5-hydroxyl-L-tryptophan (5-HTP) results in significant increase of sleep amount and reduction of the light-induced phase shift, especially in response to high intensity light pulses (Yuan et al., 2005, 2006). This dual role is mediated by two distinct receptors, d5-HT1A and d5-HT1B, sharing high homology with the mammalian counterpart (5-HT1A), that controls many aspects of animal behaviour, including sleep (Boutrel et al., 2002; Yuan et al., 2005).

*d5-HT1A* is highly expressed in the MB, at levels that remain constant during the day (Yuan et al., 2006). d5-HT1A is specifically involved in regulating sleep amount and consolidation, as flies carrying a deleted form of d5-HT1A exhibit a significant reduction and fragmentation in sleep, with nighttime sleep bouts reduced in length but increased in number (Yuan et al., 2006). This behaviour is specifically dependent on d5-HT1A in MB, since it can be completely rescued by overexpression of the receptor in these neurons (Yuan et al., 2006). Treatment with 5-HTP increases sleep in *d5-HT1A* mutant flies, indicating that other unidentified serotonin receptors are also involved in sleep regulation (Yuan et al., 2006).

d5-HT1B is expressed in different brain structures, including LNvs (Yuan et al., 2005). The expression of d5-HT1B in the adult fly brain does not show circadian oscillation, neither as mRNA nor as protein, but its levels are influenced by the clock, as they appear to be upregulated in $tim^{01}$ and downregulated in $cyc^0$ mutants (Yuan et al., 2005).

In clock cells, d5-HT1B is involved in modulating the circadian light sensitivity: flies overexpressing this receptor in the clock neurons exhibit a reduced magnitude of the response to phase shift following light pulse, mirrored by a reduced light-dependent TIM degradation (more evident in s-LNvs compared to l-LNvs). Conversely, the downregulation of d5-HT1B results in an increased phase shift, also toward low light intensities (Yuan et al., 2005).

Serotonin and d5-HT1B effects on circadian light sensitivity are related to the CRY signalling pathway: while the overexpression of d5-HT1B in a wt background induces increased levels of rhythmicity in constant light, the overexpression of d5-HT1B in a *cry* mutant background ($cry^b$) has no effect on the rhythmicity exhibited by $cry^b$ flies (Yuan et al., 2005).

#### *LNvs and Neuronal Structural Remodeling*

Remodeling of neuronal connections is fundamental for the neuronal circuits to detect environmental changes and drive complex behaviour. In *Drosophila*, the circadian behaviour also results from a clock-controlled structural plasticity that contributes to the transmission of information downstream of pacemaker neurons (Fernández et al., 2008).

PDF positive LNvs rhythmically express the miRNA *miR-210* (Chen and Rosbash, 2017), that plays an important role in the phasing of the circadian locomotor activity (Cusumano et al., 2018; Niu et al., 2019). *miR-210* is also involved in the regulation of sleep levels and temporal distribution, and this role is likely correlated to the morphology remodeling of l-LNvs: in fact the *miR-210* overexpression in clock cells results in a significant increase in daytime sleep and a dramatic alteration of l-LNvs morphology and projections (Cusumano et al., 2018).

Small ventral-lateral neurons express dTau, a protein with microtubule-binding properties, homolog to mammalian Tau, known to be involved in the maturation and establishment of synaptic networks regulating complex behaviours (Abruzzi et al., 2017; Tracy and Gan, 2018). dTau plays an important role in shaping behavioural rhythms and sleep patterns: in either LD cycles or DD, *dTau* mutant flies exhibit an increased activity during the day/subjective day, more pronounced in the middle of the day, when wt flies have a "siesta" (Arnes et al., 2019). This altered locomotor phenotype is mirrored by pronounced sleep alterations: *dTau* null flies exhibit a significant alteration of daytime sleep, while nocturnal sleep is not affected: the total daytime sleep is significantly decreased, including the "siesta," the sleep episodes are shorter, that is, sleep is more fragmented, and the sleep latency is significantly longer (Arnes et al., 2019).

At the neuronal level, dTau plays an essential role in modulating the structural plasticity of s-LNvs terminals: in wt flies the dorsal projections of s-LNvs neurons display a rhythmic remodeling, with significantly higher degree of axonal arborisation in the early day (ZT2) compared to early night (ZT14) (Fernández et al., 2008). *dTau* null flies exhibit a significant reduction in the structural morphology of the s-LNv at ZT2 compared to wt, in line with the behavioural defects (increased activity and decreased sleep) displayed in the early day (Arnes et al., 2019). Furthermore, in s-LNvs, dTau shows rhythmic expression at both mRNA and protein levels, with significantly higher levels in the early morning (ZT2) than in the early night (Abruzzi et al., 2017; Arnes et al., 2019). This temporal rhythmic pattern perfectly matches with its role in modulating the structural plasticity of s-LNvs terminals (Arnes et al., 2019).

## Large Ventral-Lateral Neurons: The Heart of the Sleep Circuit

Large ventral-lateral neurons are among the first clock neurons that have been identified (Zerr et al., 1990) and they have a predominant role in detecting light and transferring the photic information to the circadian clock (reviewed in Helfrich-Förster, 2019). By using different signalling pathways l-LNvs integrate light stimuli and produce appropriate behavioural responses (**Figure 5**).

### *l-LNvs are directly activated by light*

Large ventral-lateral neurons display an acute increase in their firing rate in response to light, and this altered electrical activity influences locomotor behaviour, sleep and arousal (Sheeba et al., 2008a). l-LNvs hyperexcited flies exhibit an increase in nocturnal activity compared to controls, mirrored by a disruption in the quantity and quality of nocturnal sleep (Sheeba et al., 2008a). Moreover, the increased nocturnal behaviour of l-LNvs hyperexcited flies is mediated by a PDF-dependent mechanism, as *Pdf* mutants exhibit a nocturnal activity significantly lower compared to wt (Sheeba et al., 2008a). The light-induced firing rate of l-LNvs is dependent on the presence of the circadian photoreceptor CRY, highly expressed in these clock cells (Emery et al., 2000). Indeed, in $cry^{b}$ hypomorphic mutants, the electrophysiological response is attenuated (Sheeba et al., 2008b), while it is completely abolished in *cry*-null flies (Fogle et al., 2011). Conversely, the light-induced firing of l-LNvs is functionally rescued by targeted expression of CRY in the l-LNvs.

Large ventral-lateral neurons are part of the peptidergic arousal pathways in *Drosophila*. The hyperactivation of these cells by overexpression of NaChBacGFP, a bacterial-derived voltage-gated sodium channel (Nitabach et al., 2005), results in a dramatic increase of nighttime activity and, by a genetic manipulation, it has been also shown that the stimulation of l-LNvs is sufficient to promote arousal at night (Shang et al., 2008). Moreover, l-LNvs-mediated arousal is light-dependent: flies in which this subset of clock cells is genetically ablated exhibit an increased sleep in LD, even more evident in LL, a phenotype completely lost when flies are moved to DD (Shang et al., 2008). Another important feature of l-LNvs is that they signal light information to the circadian clock at dawn: indeed, l-LNvs-deficient flies exhibit no phase advance response to light at ZT21 compared to control, while no differences between the two genotypes are observed for light pulse at ZT15 (Shang et al., 2008).

Pigment dispersing factor is specifically involved in increasing flies' activity in the late night: $Pdf^{01}$ mutants, as well as flies with null mutation in the receptor for PDF ($Pdfr^{han5304}$), exhibit an increased sleep during the late night, while flies in which the PDF-expressing neurons are genetically ablated, show a prolonged sleep (Chung et al., 2009). The lack of PDF-mediated signalling is partially compensated by light: in DD, $Pdf^{01}$, $Pdfr^{han5304}$, and PDF-ablated flies exhibit a significant increase in total sleep during the subjective day, which is not visible in LD (Chung et al., 2009; **Figure 5**).

### *Light negatively regulates dopamine and octopamine signalling in l-LNvs*

Large ventral-lateral neurons express high levels of dopamine receptors (DopR, DopR2, and D2R) as well as the two major octopamine GPC receptors, OA2 and OAMB (Kula-Eversole et al., 2010). By GRASP (GFP Reconstitution Across Synaptic Partners) analysis (Feinberg et al., 2008) it has been shown that they form membrane contacts with dopaminergic and octopaminergic neurons (Shang et al., 2011). Both dopamine and octopamine represent arousal signals in l-LNvs (Shafer et al., 2008). The response to dopamine is negatively regulated by light and it is time of day-independent, with no significant difference between day/subjective day *versus* the night/subjective night. However, responses in DD are much stronger during both the subjective day and subjective night, in comparison to those at the same circadian times in LD cycles. The effects of octopamine on l-LNvs are both light and time dependent: the responses from subjective day are similar to those of daytime in LD while during subjective night they are far stronger compared to daytime, nighttime, or subjective day (Shang et al., 2011). The time-sensitivity of l-LNvs response to octopamine is a clock-controlled feature, since in $per^{01}$ mutants the responsiveness during the night is much weaker compared to controls (Shang et al., 2011; **Figure 5**).

Dopamine signalling in l-LNvs also involves the circadian photoreceptor CRY, expressed at high levels in $Clk^{Jrk}$ flies, that display a nocturnal behaviour and a reduction in total sleep (Kim et al., 2002; Lu et al., 2008). This CRY-driven nighttime activity of *Clk* mutants is suppressed when dopamine signalling is blocked either pharmacologically or genetically (Kumar et al., 2012).

### *l-LNvs mediate histamine wake-promoting signals*

Pigment dispersing factor neurons can receive histaminergic wake-activation signals. Loss-of-function mutations in the *HisCl1* and *hdc* genes result in increased sleep duration, especially during the day (Oh et al., 2013). l-LNvs play an important role in mediating these histaminergic wake-promoting signals: the targeted downregulation of *HisCl1* in PDF cells increases both the daytime and nighttime sleep duration, while the targeted overexpression of *HisCl1* with either *tim*-Gal4 or *Pdf*-Gal4 is able to restore the increased sleep duration of *HisCl1* mutant (Oh et al., 2013; **Figure 5**).

### *l-LNvs activity is modulated by potassium channels*

During sleep, neuronal activity undergoes large-scale changes, and different types of potassium channels are required for normal wake–sleep cycles (Cirelli et al., 2005; Bushey et al., 2007; Allebrandt et al., 2013, 2017). In l-LNvs, the Shal/Kv4, voltage-gated $K^+$ channel plays an important role in controlling wake–sleep transition at dusk (Feng et al., 2018). Kv4 acts as sleep-promoter, since flies with a pan-neuronal expression of a dominant-negative form of Kv4 (DNKv4) exhibit a reduced nighttime sleep, as consequence of a decrease in sleep-bout duration. The expression of DNKv4 limited to all PDF positive neurons induces a marked increase in sleep latency and decrease in nighttime sleep, even more evident when the expression is further restricted to l-LNvs (Feng et al., 2018). In l-LNvs, both the frequency of the action potential (AP) currents and the resting membrane potential (RMP) exhibit a strong rhythmicity, with a higher firing rate during daytime and more RMPs significantly depolarized at dawn (ZT1) compared to dusk (ZT13). Both features are dependent on Kv4, since the expression of DNKv4 results in the increase of either the frequency of AP currents or the firing rate during dusk (Feng et al., 2018).

### *l-LNvs and modulation of sleep/wake behaviour at transcriptional level*

Many brain neurons, including PDF-positive LNvs, express apterous (ap), a well-known LIM-homeodomain transcription factor involved in development and neuropeptide expression (Hobert and Westphal, 2000; Shimada et al., 2016). ap levels are particularly high in l-LNvs, where they also exhibit a daily oscillation generated by a light-dependent mechanism. In LD both mRNA and protein show a rhythmic expression with a peak during the night (ZT16 and ZT18, respectively), while this oscillation is lost in DD, at least at protein level (Claridge-Chang et al., 2001; Shimada et al., 2016). This transcription factor is involved in buffering light-driven arousal: specific knock-down of *ap* in these PDF neurons results in promoting arousal (reduction in sleep amount and increase in waking time) under LD conditions, whereas the sleep/wake pattern is not affected in DD (Shimada et al., 2016). *ap* knock-down does not significantly affect PDF, neither its expression nor its release; therefore, other neuropeptides or signalling inputs/synaptic output are involved. ap acts in cooperation with the transcription factor Chip (Chi), to drive the expression of developmental genes (Van Meyel et al., 1999). In PDF neurons, the two transcription factors act as a complex playing a key role in transcriptional modulation of sleep/wake behaviour. In fact, while the knock-down of *ap* only results in a general decrease of sleep, regardless of the time of the day, when both proteins are inactive only the daytime sleep amount is decreased. This indicates that this complex modulates mechanisms that act specifically in regulating sleep/wake at different times of the day (Shimada et al., 2016).

## Small Ventral-Lateral Neurons: A Secondary Role in the Arousal Circuit

### *s-LNvs and PDFR signalling*

The arousal activity of l-LNvs is mediated by PDF and a functional PDFR signalling is required for a proper sleep/wake regulation. In fact, *Pdfr* mutants display an increased sleep, specifically during the day (Parisky et al., 2008; Chung et al., 2009; Potdar and Sheeba, 2018; Sheeba et al., 2008a). The PDFR signalling pathway targets the dopaminergic neurons (i.e., PPM3) and plays a crucial role in regulating daytime wakefulness. The downregulation of *Pdfr* in these neurons results in a significant increase of daytime sleep, with longer sleep bouts, while *Pdfr* overexpression suppresses daytime sleep and delays sleep onset (Potdar and Sheeba, 2018).

PDF and dopaminergic neurons are synaptically connected, specifically in the region of s-LNvs axonal projections (Potdar and Sheeba, 2018). Importantly, this observation confirms not only that dopaminergic neurons are a downstream target of PDFR signalling, but also that s-LNvs contribute to the wake-promoting activity of l-LNvs. The involvement of s-LNvs in the arousal circuit was already suggested: (1) the downregulation of *Pdfr* in s-LNvs results in the increase of total sleep (both daytime and nighttime) (Parisky et al., 2008); and (2) the electrical activity of s-LNvs contributes in modulating the phase of evening activity under long photoperiods (Potdar and Sheeba, 2018).

A PDFR signalling originating from the s-LNvs targets also a group of neurons, posterior lateral protocerebrum (PLP) cells, that express the neuropeptide AstA and are involved in sleep promotion (Chen et al., 2016). The thermogenic activation of AstA-PLP neurons causes a significant decrease in locomotor activity and an increase of sleep, either in LD or DD and LL; conversely, the silencing of AstA cells results in a significant reduction of sleep, especially during the midday siesta time, either in LD or DD (Chen et al., 2016).

PLP cells represent downstream target of PDF signalling; they are post-synaptically connected to s-LNvs and express functional PDF receptors and, furthermore, constitutive activation of PDF signalling in AstA-expressing neurons significantly increases the amount of sleep (Chen et al., 2016; **Figure 5**).

### *s-LNvs and short neuropeptide F (sNPF) signalling*

sNPF is broadly expressed in various brain regions, including MB, PI, and CC neurons (Nässel et al., 2008; Johard et al., 2009), and known to regulate different aspects of fly physiology and behaviour (Kahsai et al., 2010; Nagy et al., 2019). sNPF has an important role in promoting and maintaining normal sleep: flies carrying a hypomorphic mutation in *sNPF* or with a knock-down of *sNPF* in adult brain, exhibit a reduced and fragmented sleep compared to control. Moreover, the silencing of sNPF neurons results in a significant reduction of the sleep levels during the daytime (Shang et al., 2013).

The sleep-promoting activity of sNPF neurons is normally suppressed by $GABA_A$ signalling during the daytime, as the downregulation of the $GABA_A$ receptor *Rdl* in these neurons leads to a significant increase of both daytime and total sleep time and to a lengthening of sleep bouts (Shang et al., 2013). sNPF is also involved in the response to sleep deprivation: the hyperactivation of sNPF neurons during mechanical sleep deprivation causes a partial sleep-like state and induces less sleep rebound or recovery sleep (Shang et al., 2013).

In s-LNvs sNPF acts in promoting normal nighttime sleep. *sNPF* mRNA levels exhibit a robust oscillation in s-LNvs, while in l-LNvs it is barely expressed (Kula-Eversole et al., 2010). Flies with downregulation of *sNPF* in PDF neurons exhibit a decreases in nighttime sleep, while daytime sleep is not affected (Shang et al., 2013). These sNPF sleep-promoting signals from s-LNvs are transmitted to l-LNvs (**Figure 5**); the downregulation of *sNPFR* (sNPF receptor) in l-LNvs, where it is normally expressed at high levels (Kula-Eversole et al., 2010), results in a significant fragmentation of nighttime sleep (Shang et al., 2013).

The sleep-promoting role of sNPF is essentially exerted by an inhibitory effect on arousal neurons activity, as it is the result of a balance between the sNPF and the dopamine (DA) signallings in the l-LNvs: in fact, the co-application of DA and sNPF suppresses the cAMP response in the l-LNvs, strongly elicited by DA alone (Shang et al., 2013).

In this section we have focused on those signalling pathways involving PDF neurons specifically related to both light and sleep. Nevertheless, LNvs participate in many other signalling pathways that act in synchronising their activity and regulating sleep/wake behaviour. Among these, (1) glutamatergic transmission mediated by the metabotropic glutamate receptor DmGluRA is important for inhibiting activity in the dark (Hamasaka et al., 2007); (2) GABAergic signalling in the l-LNvs, mediated by $GABA_A$ receptor Rdl and modulated by the ankyrin repeats domain containing protein WIDE AWAKE (WAKE), plays a role in either the initiation or the maintenance of sleep (Agosto et al., 2008; Parisky et al., 2008; Chung et al., 2009; Liu et al., 2014); and (3) cholinergic inputs to the l-LNvs, mediated by nicotinic acetylcholine receptors (nAChRs) and modulated by glutamate-gated $Cl^-$ channels, ensure a highly synchronized rhythmic membrane activity with a simultaneous occurrence of depolarized and hyperpolarized phases (McCarthy et al., 2011).

## Lateral Posterior Neurons: Connection Between the Clock Network and the Sleep Center

The sleep promoting function of LPNs is modulated by the circadian clock, as the expression of a dominant negative form of *Clock* in these cells reduces the sleep during the daytime (Ni et al., 2019).

The LPN express the neuropeptide AstA and form synaptic connections with the FB; moreover, the inhibition of neurotransmission from the LPNs results in a reduction of sleep (Ni et al., 2019). The excitatory neurotransmitter in LPN that activates FB neurons and promotes sleep is glutamate: in fact, the inhibition of glutamate transport results in a significant reduction of nighttime sleep bouts length and therefore increases sleep fragmentation (Ni et al., 2019).

Fan-shaped body cells are synaptically connected and receive inhibitory input from dopamine arousal (DAA) neurons, as hyperactivation of DAAs antagonizes the effect on sleep promotion observed when LPNs are hyperactivated; moreover, hyperactivation of both LPNs and DAAs significantly fragments sleep (Ni et al., 2019). FB cells promote sleep via GABAergic signalling, as the inhibition of GABA synthesis in these neurons eliminates the sleep promoted by their activation (Ni et al., 2019). FB sleep promoting neurons negatively regulate the activity of OAA neurons: they are closely connected with the FB axon terminals and their neuronal activity is dramatically reduced by the hyperactivation of FB cells (Ni et al., 2019; **Figure 3**).

## Dorsal Neurons: A Major Role in Shaping and Maintaining the Sleep/Wake Pattern

Dorsal neurons (DN1s) are at the same time sleep- and wake-promoting cells, as a result of different signalling pathways that either act on different subsets of neurons or are predominant at different times of day, to promote activity in the morning or sleep at siesta and during the night.

A subgroup of DN1 neurons, the posterior DN1s (DN1ps), express the narrow abdomen (na), involved in light-mediated control of diurnal behaviour (morning activity and lights-on response) (Lear et al., 2005). Under LD cycles, DN1ps promote morning activity and their contribution to circadian behaviour is strongly influenced by light intensity (Zhang et al., 2010). They also express PDF receptor that, in these cells, is necessary for periodicity in DD (Zhang et al., 2010).

### *DN1s and DH31 wake-promoting signalling*

DN1s secrete the neuropeptide diuretic hormone 31 (DH31) and express its receptor DH31-R1, homologous to vertebrate calcitonin gene-related peptide (CGRP) and its receptor (Mertens et al., 2005). DH31/DH31R are involved in sleep regulation: flies with a loss-of-function mutation in *DH31* exhibit a significant increase of sleep, especially during the night, while the pan-neuronal overexpression of *DH31* significantly decreases nighttime sleep (Kunst et al., 2014). More precisely, DH31 acts as negative regulator of sleep maintenance and awakens flies in anticipation of dawn; indeed the increased sleep of *DH31* mutants is more prominent in the second half of the night and immediately before lights-on, and the overexpressing DH31 flies exhibit a decreased sleep and increase of sleep fragmentation, which is more pronounced in the late night (Kunst et al., 2014). These altered sleep features can be completely rescued by restoring expression of DH31 specifically in DN1s, that can also re-establish the anticipation of the lights-on (Kunst et al., 2014). DN1s are a direct target of PDF signalling from s-LNvs, that modulates sleep by controlling the time of DH31 secretion: PDF specifically activates PDFR late at night, and the consequent secretion of DH31 results in a reduced nighttime sleep and an awakening of flies at dawn (Kunst et al., 2014).

### *DN1s and glutamatergic signalling to clock cells*

DN1s neuronal activity is also fundamental in promoting sleep: blocking the synaptic neurotransmission of these cells results in a marked increase of the flies' activity and a decrease of siesta and nighttime total sleep, due to reduced sleep episodes duration (Guo et al., 2016).

DN1s directly contact core pacemaker cells: GRASP assay identifies a functional direct interaction of DN1s presynaptic regions with either dendritic regions of the Evening cells (the CRY-positive LNds and the 5th s-LNv) or dorsal axon regions of Morning cells (the s-LNvs) (Guo et al., 2016). This

neuronal transmission is mediated by glutamatergic signalling, with inhibitory effect. DN1s express the vesicular glutamate transporter, DvGluT, while E cells express the metabotropic glutamate receptor DmGluRA, whose mRNA exhibits cycling levels with a peak in the middle of the day. This support the predominant inhibitory role of DN1s on E cell-derived locomotor activity, which is then confined in the late day-early night (Guo et al., 2016).

***DN1s signals to sleep center***

DN1s can be both wake- and sleep- promoting, according to synaptic types and targets. A CRY-positive subset of DN1s (anterior-projecting DNs, APDNs or a-DN1ps) sends post-synaptic projections also to the anterior region of adult brain, the superior lateral protocerebrum, target of the AstA sleep-promoting signalling from PLPs (Guo et al., 2016), and innervates the anterior optic tubercle (AOTU) (Guo et al., 2018; Lamaze et al., 2018). In particular, they target a small subset of neurons within the AOTU (TuBu), that receive visual inputs from medullo-tubercular neurons and transmit this information to EB-R neurons (Guo et al., 2018; Lamaze et al., 2018). However, DN1ps connect TuBu using both excitatory and inhibitory synapses. They suppress the sleep-promoting activity of TuBu neurons, as their acute inhibition results in an increase of TuBu electrical activity, while thermo-genetic excitation of TuBu neurons profoundly induces sleep throughout both day and night (Lamaze et al., 2018). On the other hand, DN1ps activate TuBu using glutamate, giving sleep-promoting effect (Guo et al., 2018).

Moreover, a CRY-negative subset of DN1s (ventro-contralateral-projecting DN1p neurons, vc-DN1ps) send ventral and contralateral projections to the PI region (Cavanaugh et al., 2014), that represents an activity-promoting output of DN1s, since the activation of these cells promotes wakefulness and inhibits sleep (Guo et al., 2018).

# LIGHT EXPOSURE: TIMING AND INTENSITY

The quality and architecture of sleep is also influenced by the characteristics of the light stimulus, such as the intensity of light and the timing of light exposure (morning/daytime versus evening/nighttime).

## Nocturnal Light Affects Daytime Sleep

Natural pattern of light availability assumes dark nighttime, therefore a different administration of light disrupts the sleep pattern. Sleep analysis of flies exposed to 4 days of discontinuous nocturnal light stimulation (DLS) showed a reduction of sleep episode duration (but not the sleep bouts number) specifically during the day, while it does not affect nighttime sleep. Moreover, during recovery time after light disruption, the quality of nighttime sleep is increased, opposite to daytime sleep. On the molecular level, discontinuous light stimulation disrupts CRY daily oscillation at both mRNA and protein levels, and decreases TIM levels during the night (Liu and Zhao, 2014).

## Light Intensity Impacts on Sleep Timing

In the natural environment, light intensity changes between 0 and 100,000 lux, depending on the time of the day, time of the year, weather, etc. Insects are sensitive to a broad range of light, and they can adjust their behaviour according to light exposure, through an adaptative mechanism that allows avoiding of bright light in the middle of the day, especially during summertime (Lazopulo et al., 2019).

Flies are able to detect low light intensity by using CRY (Vinayak et al., 2013) and the four rhodopsins expressed in photoreceptors cells in the compound eyes (Rh1, Rh3, Rh4, Rh6) (Saint-Charles et al., 2016). In natural conditions, dim light appears during full moon nights and around dawn and dusk. Moonlight causes the phase shift of molecular clock in pacemaker cells, resulting in the advance of morning activity and the delay of the evening one, with the overall flies' activity becoming more nocturnal. Experiments performed with clock mutants have clearly demonstrated that the effect on nighttime activity is light-dependent (Kempinger et al., 2009) and the response to moonlight is mediated by R1–6 and Rh6-expressing R8 photoreceptors (Schlichting et al., 2014), while CRY is not involved (Bachleitner et al., 2007). Moreover, dim light does not affect clock protein expression pattern in peripheral oscillators in the retina (Bachleitner et al., 2007). Periodogram analysis of wt flies under L:ML conditions (Light:MoonLight) reveals that sleep time is also affected: relative level of activity is increased compared with flies reared in light:dark conditions, and activity is continuous during the whole night, with flies sleeping mostly during the day (Schlichting et al., 2014).

The effect of twilight is opposite to moonlight: morning peak of activity is delayed and evening peak is advanced, while nocturnal activity in reduced (Rieger et al., 2007). R7 and R8 photoreceptors are involved in the response to twilight (Schlichting et al., 2014). When flies are exposed to both dim light at dawn/dusk and moonlight, the twilight effect dominates in terms of shifted morning and evening peak of activity and reduced nocturnal locomotor activity. This more composite light exposure has an effect which is more similar to natural conditions: fly activity is not shifted to the nighttime during full moon nights (Schlichting et al., 2014; Vanin et al., 2012).

In the middle of the day, flies are exposed to high intensity light (HI). Response to HI is independent from CRY, ocelli, and compound eyes, and most probably it is mediated by HB eyelets (Schlichting et al., 2016), which communicate with s-LNvs through acetylcholine. The possible mechanism at the basis of activity and sleep regulation mediated by HI assumes that activation of acetylcholine receptor on s-LNvs increases $Ca^{2+}$ level, which, in turn, causes delayed PER degradation during the day. Then, s-LNvs propagate signal through PDF pathway, affecting PER cycling in downstream neurons DN1s, known to be sleep regulators (Guo et al., 2016). Indeed, flies exposed to HI show delayed evening peak of activity and lengthened siesta time (Schlichting et al., 2019a), thus avoiding bright light in the middle of the day during hot summer time.

### Light Influences Temperature-Dependent Regulation of Sleep

Light plays a role in the regulation of temperature-dependent sleep pattern. Nighttime sleep is decreased by high temperature, but this effect is influenced by light presence during the preceding day, as it was shown in experiments performed in DD conditions. The mechanism of this process requires CRY, as $cry^{out}$ mutants do not show decreased nighttime sleep in response to heat (Parisky et al., 2016). This effect seems to be connected with the wake-promoting role of dopamine on nighttime sleep, as it was shown that light increases expression of inhibitory dopamine receptors (Shang et al., 2011). The involvement of light in temperature-dependent sleep control was comprehensively reviewed elsewhere (Lamaze and Stanewsky, 2020).

## CONCLUSION

Understanding the mechanisms underlying the relations between light exposure and sleep disturbances has become a challenge. Modern society no longer relies on the day-night differences in external conditions that have shaped life on Earth: from shift-work schedules to the current widespread use of digital technology until late at night, we are more and more exposed to stimuli that not only are not coordinated with our body's internal time but can also stimulate alertness and extend sleep latency. Taking advantage of the fruit fly *Drosophila melanogaster*, we have tried to address the contribution of the different light signalling pathways involved in promoting, consolidating, or preventing sleep. The picture derived is complex: the architecture of sleep is regulated by an intricate set of structures, neurotransmitters, and networks that integrate environmental signals.

However, as most of the essential sleep features are shared between flies and mammals, the knowledge of how light regulates this complex behaviour in *Drosophila* can be fundamental for future research in humans, addressing how light can promote high wakefulness during the day and good sleep during the night.

## AUTHOR CONTRIBUTIONS

GM, MD, and PC equally contributed to writing the manuscript. All authors contributed to the article and approved the submitted version.

## FUNDING

This work was funded by grants from Department of Biology, University of Padua (Italy) PRID-SEED 2018 to PC and PRID-SEED 2019 to GM, the Polish National Science Centre (Narodowe Centrum Nauki, NCN_Grant UMO-2017/27/B/NZ3/00859), and Polish National Agency for Academic Exchange to MD.

## ACKNOWLEDGMENTS

We thank Sraboni Ghose (Ph.D.) for her comments with regard to this manuscript.

## REFERENCES

Abruzzi, K. C., Zadina, A., Luo, W., Wiyanto, E., Rahman, R., Guo, F., et al. (2017). RNA-seq analysis of Drosophila clock and non-clock neurons reveals neuron-specific cycling and novel candidate neuropeptides. *PLoS Genet.* 13:e1006613. doi: 10.1371/journal.pgen.1006613

Adams, M. D., Celniker, S. E., Holt, R. A., Evans, C. A., Gocayne, J. D., Amanatides, P. G., et al. (2000). The genome sequence of *Drosophila melanogaster*. *Science* 287, 2185–2195. doi: 10.1126/science.287.5461.2185

Agosto, J., Choi, J. C., Parisky, K. M., Stilwell, G., Rosbash, M., and Griffith, L. C. (2008). Modulation of GABAA receptor desensitization uncouples sleep onset and maintenance in Drosophila. *Nat. Neurosci.* 11, 354–359. doi: 10.1038/nn2046

Alawi, A. A., and Pak, W. L. (1971). On-transient of insect electroretinogram: its cellular origin. *Science* 172, 1057–1057. doi: 10.1126/science.172.3987.1055

Alejevski, F., Saint-Charles, A., Michard-Vanhée, C., Martin, B., Galant, S., Vasiliauskas, D., et al. (2019). The HisCl1 histamine receptor acts in photoreceptors to synchronize *Drosophila* behavioural rhythms with light-dark cycles. *Nat. Commun.* 10:252.

Allebrandt, K. V., Amin, N., Müller-Myhsok, B., Esko, T., Teder-Laving, M., Azevedo, R. V. D. M., et al. (2013). A KATP channel gene effect on sleep duration: from genome-wide association studies to function in Drosophila. *Mol. Psychiatry* 18, 122–132. doi: 10.1038/mp.2011.142

Allebrandt, K. V., Teder-Laving, M., Cusumano, P., Frishman, G., Levandovski, R., Ruepp, A., et al. (2017). Identifying pathways modulating sleep duration: from genomics to transcriptomics. *Sci. Rep.* 7:4555.

Arnes, M., Alaniz, M. E., Karam, C. S., Cho, J. D., Lopez, G., Javitch, J. A., et al. (2019). Role of tau protein in remodeling of circadian neuronal circuits and sleep. *Front. Aging Neurosci.* 11:320. doi: 10.3389/fnagi.2019.00320

Artiushin, G., and Sehgal, A. (2017). The Drosophila circuitry of sleep–wake regulation. *Curr. Opin. Neurobiol.* 44, 243–250. doi: 10.1016/j.conb.2017.03.004

Aso, Y., Sitaraman, D., Ichinose, T., Kaun, K. R., Vogt, K., Belliart-Guérin, G., et al. (2014). Mushroom body output neurons encode valence and guide memory-based action selection in Drosophila. *eLife* 3:e04580. doi: 10.7554/eLife.04580

Bachleitner, W., Kempinger, L., Wülbeck, C., Rieger, D., and Helfrich-Förster, C. (2007). Moonlight shifts the endogenous clock of *Drosophila melanogaster*. *Proc. Natl. Acad. Sci. U.S.A.* 104, 3538–3543. doi: 10.1073/pnas.0606870104

Benito, J., Houl, J. H., Roman, G. W., and Hardin, P. E. (2008). The blue-light photoreceptor CRYPTOCHROME is expressed in a subset of circadian oscillator neurons in the Drosophila CNS. *J. Biol. Rhythms* 23, 296–307. doi: 10.1177/0748730408318588

Bloomquist, B. T., Shortridge, R. D., Schneuwly, S., Perdew, M., Montell, C., Steller, H., et al. (1988). Isolation of a putative phospholipase c gene of drosophila, norpA, and its role in phototransduction. *Cell* 54, 723–733. doi: 10.1016/s0092-8674(88)80017-5

Bolkan, B. J., Triphan, T., and Kretzschmar, D. (2012). β-secretase cleavage of the fly amyloid precursor protein is required for glial survival. *J. Neurosci.* 32, 16181–16192. doi: 10.1523/JNEUROSCI.0228-12.2012

Borst, A., Haag, J., and Mauss, A. S. (2020). How fly neurons compute the direction of visual motion. *J. Comp. Physiol. A Neuroethol. Sens. Neural Behav. Physiol.* 206, 109–124. doi: 10.1007/s00359-019-01375-9

Borycz, J., Borycz, J. A., Loubani, M., and Meinertzhagen, I. A. (2002). Tan and ebony genes regulate a novel pathway for transmitter metabolism at fly photoreceptor terminals. *J. Neurosci.* 22, 10549–10557. doi: 10.1523/jneurosci.22-24-10549.2002

Boutrel, B., Monaca, C., Hen, R., Hamon, M., and Adrien, J. (2002). Involvement of 5-HT1A receptors in homeostatic and stress-induced adaptive regulations of paradoxical sleep: studies in 5-HT 1A Knock-Out Mice. *J. Neurosci.* 22, 4686–4692. doi: 10.1523/jneurosci.22-11-04686.2002

Braitenberg, V. (1967). Patterns of projection in the visual system of the fly. I. Retina-lamina projections. *Exp. Brain Res.* 3, 271–298. doi: 10.1007/BF00235589

Buchner, E., Buchner, S., Crawford, G., Mason, W. T., Salvaterra, P. M., and Sattelle, D. B. (1986). Choline acetyltransferase-like immunoreactivity in the brain of *Drosophila melanogaster*. *Cell Tissue Res.* 246, 57–62. doi: 10.1007/BF00218999

Buhl, E., Bradlaugh, A., Ogueta, M., Chen, K. F., Stanewsky, R., and Hodge, J. J. L. (2016). Quasimodo mediates daily and acute light effects on Drosophila clock neuron excitability. *Proc. Natl. Acad. Sci. U.S.A.* 113, 13486–13491. doi: 10.1073/pnas.1606547113

Burg, M. G., Sarthy, P. V., Koliantz, G., and Pak, W. L. (1993). Genetic and molecular identification of a Drosophila histidine decarboxylase gene required in photoreceptor transmitter synthesis. *EMBO J.* 12, 911–919. doi: 10.1002/j.1460-2075.1993.tb05732.x

Bushey, D., Huber, R., Tononi, G., and Cirelli, C. (2007). Drosophila Hyperkinetic mutants have reduced sleep and impaired memory. *J. Neurosci.* 27, 5384–5393. doi: 10.1523/JNEUROSCI.0108-07.2007

Busto, M., Iyengar, B., and Campos, A. R. (1999). Genetic dissection of behaviour: modulation of locomotion by light in the *Drosophila melanogaster* larva requires genetically distinct visual system functions. *J. Neurosci.* 19, 3337–3344. doi: 10.1523/jneurosci.19-09-03337.1999

Carmine-Simmen, K., Proctor, T., Tschäpe, J., Poeck, B., Triphan, T., Strauss, R., et al. (2009). Neurotoxic effects induced by the Drosophila amyloid-β peptide suggest a conserved toxic function. *Neurobiol. Dis.* 33, 274–281. doi: 10.1016/j.nbd.2008.10.014

Cavanaugh, D. J., Geratowski, J. D., Wooltorton, J. R. A., Spaethling, J. M., Hector, C. E., Zheng, X., et al. (2014). Identification of a circadian output circuit for rest: activity rhythms in drosophila. *Cell* 157, 689–701. doi: 10.1016/j.cell.2014.02.024

Ceriani, M. F., Darlington, T. K., Staknis, D., Más, P., Petti, A. A., Weitz, C. J., et al. (1999). Light-dependent sequestration of TIMELESS by CRYPTOCHROME. *Science* 285, 553–556. doi: 10.1126/science.285.5427.553

Chang, H. Y., and Ready, D. F. (2000). Rescue of photoreceptor degeneration in rhodopsin-null Drosophila mutants by activated RAC1. *Science* 290, 1978–1980. doi: 10.1126/science.290.5498.1978

Chatterjee, A., Lamaze, A., De, J., Mena, W., Chélot, E., Martin, B., et al. (2018). Reconfiguration of a multi-oscillator network by light in the Drosophila circadian clock. *Curr. Biol.* 28, 2007–2017.e4. doi: 10.1016/j.cub.2018.04.064

Chaturvedi, R., Luan, Z., Guo, P., and Li, H. S. (2016). Drosophila vision depends on carcinine uptake by an organic cation transporter. *Cell Rep.* 14, 2076–2083. doi: 10.1016/j.celrep.2016.02.009

Chaturvedi, R., Reddig, K., and Li, H. S. (2014). Long-distance mechanism of neurotransmitter recycling mediated by glial network facilitates visual function in Drosophila. *Proc. Natl. Acad. Sci. U.S.A.* 117, 2812–2817. doi: 10.1073/pnas.1323714111

Chen, J., Reiher, W., Hermann-Luibl, C., Sellami, A., Cognigni, P., Kondo, S., et al. (2016). Allatostatin a signalling in drosophila regulates feeding and sleep and is modulated by PDF. *PLoS Genet.* 12:e1006346. doi: 10.1371/journal.pgen.1006346

Chen, K. F., Lowe, S., Lamaze, A., Krätschmer, P., and Jepson, J. (2019). Neurocalcin regulates nighttime sleep and arousal in Drosophila. *eLife* 8:e38114. doi: 10.7554/eLife.38114

Chen, K. F., Peschel, N., Zavodska, R., Sehadova, H., and Stanewsky, R. (2011). QUASIMODO, a novel GPI-anchored Zona Pellucida protein involved in light input to the drosophila circadian clock. *Curr. Biol.* 21, 719–729. doi: 10.1016/j.cub.2011.03.049

Chen, X., and Rosbash, M. (2017). MicroRNA-92a is a circadian modulator of neuronal excitability in Drosophila. *Nat. Commun.* 8:14707. doi: 10.1038/ncomms14707

Chou, W. H., Hall, K. J., Wilson, D. B., Wideman, C. L., Townson, S. M., Chadwell, L. V., et al. (1996). Identification of a novel Drosophila opsin reveals specific patterning of the R7 and R8 photoreceptor cells. *Neuron* 17, 1101–1115. doi: 10.1016/s0896-6273(00)80243-3

Chou, W. H., Huber, A., Bentrop, J., Schulz, S., Schwab, K., Chadwell, L. V., et al. (1999). Patterning of the R7 and R8 photoreceptor cells of Drosophila: evidence for induced and default cell-fate specification. *Development* 126, 607–616.

Chung, B. Y., Kilman, V. L., Keath, J. R., Pitman, J. L., and Allada, R. (2009). The GABAA receptor RDL Acts in Peptidergic PDF neurons to promote sleep in Drosophila. *Curr. Biol.* 19, 386–390. doi: 10.1016/j.cub.2009.01.040

Cirelli, C., Bushey, D., Hill, S., Huber, R., Kreber, R., Ganetzky, B., et al. (2005). Reduced sleep in Drosophila Shaker mutants. *Nature* 434, 1087–1092. doi: 10.1038/nature03486

Claridge-Chang, A., Wijnen, H., Naef, F., Boothroyd, C., Rajewsky, N., and Young, M. W. (2001). Circadian regulation of gene expression systems in the Drosophila head. *Neuron* 32, 657–671. doi: 10.1016/s0896-6273(01)00515-3

Collins, B., Mazzoni, E. O., Stanewsky, R., and Blau, J. (2006). Drosophila CRYPTOCHROME is a circadian transcriptional repressor. *Curr. Biol.* 16, 441–449. doi: 10.1016/j.cub.2006.01.034

Crocker, A., Shahidullah, M., Levitan, I. B., and Sehgal, A. (2010). Identification of a neural circuit that underlies the effects of octopamine on sleep: wake behaviour. *Neuron* 65, 670–681. doi: 10.1016/j.neuron.2010.01.032

Cusumano, P., Biscontin, A., Sandrelli, F., Mazzotta, G. M., Tregnago, C., De Pittà, C., et al. (2018). Modulation of miR-210 alters phasing of circadian locomotor activity and impairs projections of PDF clock neurons in *Drosophila melanogaster*. *PLoS Genet.* 14:e1007500. doi: 10.1371/journal.pgen.1007500

Cusumano, P., Klarsfeld, A., Chélot, E., Picot, M., Richier, B., and Rouyer, F. (2009). PDF-modulated visual inputs and cryptochrome define diurnal behaviour in Drosophila. *Nat. Neurosci.* 12, 1431–1437. doi: 10.1038/nn.2429

Damulewicz, M., and Mazzotta, G. M. (2020). One actor, multiple roles: the performances of cryptochrome in Drosophila. *Front. Physiol.* 11:99. doi: 10.3389/fphys.2020.00099

Damulewicz, M., Ispizua, J. I., Ceriani, M. F., and Pyza, E. M. (2020). Communication among photoreceptors and the central clock affects sleep profile. *Front. Physiol.* 11. doi: 10.3389/fphys.2020.00993

Damulewicz, M., Mazzotta, G. M., Sartori, E., Rosato, E., Costa, R., and Pyza, E. M. (2017). Cryptochrome is a regulator of synaptic plasticity in the visual system of *Drosophila melanogaster*. *Front. Mol. Neurosci.* 10:165. doi: 10.3389/fnmol.2017.00165

Damulewicz, M., and Pyza, E. (2011). The clock input to the first optic neuropil of *Drosophila melanogaster* expressing neuronal circadian plasticity. *PLoS One* 6:e21258. doi: 10.1371/journal.pone.0021258

Davis, F. P., Nern, A., Picard, S., Reiser, M. B., Rubin, G. M., Eddy, S. R., et al. (2020). A genetic, genomic, and computational resource for exploring neural circuit function. *eLife* 9:50901. doi: 10.7554/eLife.50901

Deng, B., Li, Q., Liu, X., Cao, Y., Li, B., Qian, Y., et al. (2019). ). Chemoconnectomics: mapping chemical transmission in Drosophila. *Neuron* 101, 876–893.e4. doi: 10.1016/j.neuron.2019.01.045

Díaz, M. M., Schlichting, M., Abruzzi, K. C., Long, X., and Rosbash, M. (2019). Allatostatin-C/AstC-R2 is a novel pathway to modulate the circadian activity pattern in Drosophila. *Curr. Biol.* 29, 13–22.e3. doi: 10.1016/j.cub.2018.11.005

Dissel, S., Angadi, V., Kirszenblat, L., Suzuki, Y., Donlea, J., Klose, M., et al. (2015). Sleep restores behavioural plasticity to drosophila mutants. *Curr. Biol.* 25, 1270–1281. doi: 10.1016/j.cub.2015.03.027

Donlea, J. M., Pimentel, D., Talbot, C. B., Kempf, A., Omoto, J. J., Hartenstein, V., et al. (2018). Recurrent circuitry for balancing sleep need and sleep. *Neuron* 97, 378–389.e4. doi: 10.1016/j.neuron.2017.12.016

Donlea, J. M., Thimgan, M. S., Suzuki, Y., Gottschalk, L., and Shaw, P. J. (2011). Inducing sleep by remote control facilitates memory consolidation in Drosophila. *Science* 332, 1571–1576. doi: 10.1126/science.1202249

Emery, P., Stanewsky, R., Helfrich-Förster, C., Emery-Le, M., Hall, J. C., and Rosbash, M. (2000). Drosophila CRY is a deep brain circadian photoreceptor. *Neuron* 26, 493–504. doi: 10.1016/s0896-6273(00)81181-2

Farca Luna, A. J., Perier, M., and Seugnet, L. (2017). Amyloid precursor protein in Drosophila glia regulates sleep and genes involved in glutamate recycling. *J. Neurosci.* 37, 4289–4300. doi: 10.1523/JNEUROSCI.2826-16.2017

Faulhaber, J., Steiger, A., and Lancel, M. (1997). The GABA(A) agonist THIP produces slow wave sleep and reduces spindling activity in NREM sleep in humans. *Psychopharmacology* 130, 285–291. doi: 10.1007/s002130050241

Feiler, R., Bjornson, R., Kirschfeld, K., Mismer, D., Rubin, G. M., Smith, D. P., et al. (1992). Ectopic expression of ultraviolet-rhodopsins in the blue photoreceptor cells of Drosophila: visual physiology and photochemistry of transgenic animals. *J. Neurosci.* 12, 3862–3868. doi: 10.1523/jneurosci.12-10-03862.1992

Feiler, R., Harris, W. A., Kirschfeld, K., Wehrhahn, C., and Zuker, C. S. (1988). Targeted misexpression of a Drosophila opsin gene leads

to altered visual function. *Nature* 333, 737–741. doi: 10.1038/333737a0

Feinberg, E. H., VanHoven, M. K., Bendesky, A., Wang, G., Fetter, R. D., Shen, K., et al. (2008). GFP Reconstitution Across Synaptic Partners (GRASP) defines cell contacts and synapses in living nervous systems. *Neuron* 57, 353–363. doi: 10.1016/j.neuron.2007.11.030

Feng, G., Zhang, J., Li, M., Shao, L., Yang, L., Song, Q., et al. (2018). Control of sleep onset by Shal/Kv4 channels in Drosophila circadian neurons. *J. Neurosci.* 38, 9059–9071. doi: 10.1523/JNEUROSCI.0777-18.2018

Fernández, M. P., Berni, J., and Ceriani, M. F. (2008). Circadian remodeling of neuronal circuits involved in rhythmic behaviour. *PLoS Biol.* 6:e69. doi: 10.1371/journal.pbio.0060069

Fogle, K. J., Parson, K. G., Dahm, N. A., Holmes, T. C., Sheeba, V., Parisky, K. M., et al. (2011). CRYPTOCHROME is a blue-light sensor that regulates neuronal firing rate. *Science* 331, 1409–1413. doi: 10.1126/science.1199702

Friggi-Grelin, F., Coulom, H., Meller, M., Gomez, D., Hirsh, J., and Birman, S. (2003). Targeted gene expression in Drosophila dopaminergic cells using regulatory sequences from tyrosine hydroxylase. *J. Neurobiol.* 54, 618–627. doi: 10.1002/neu.10185

Fryxell, K. J., and Meyerowitz, E. M. (1987). An opsin gene that is expressed only in the R7 photoreceptor cell of Drosophila. *EMBO J.* 6, 443–451. doi: 10.1002/j.1460-2075.1987.tb04774.x

Gao, S., Takemura, S.-Y., Ting, C. Y., Huang, S., Lu, Z., Luan, H., et al. (2008). The neural substrate of spectral preference in Drosophila. *Neuron* 60, 328–342. doi: 10.1016/j.neuron.2008.08.010

Gengs, C., Leung, H. T., Skingsley, D. R., Iovchev, M. I., Yin, Z., Semenov, E. P., et al. (2002). The target of Drosophila photoreceptor synaptic transmission is a histamine-gated chloride channel encoded by ort (hclA). *J. Biol. Chem.* 277, 42113–42120. doi: 10.1074/jbc.M207133200

Gisselmann, G., Pusch, H., Hovemann, B. T., and Hatt, H. (2002). Two cDNAS coding for histamine-gated ion channels in *D. melanogaster*. *Nat. Neurosci.* 5, 11–12. doi: 10.1038/nn787

Grebler, R., Kistenpfennig, C., Rieger, D., Bentrop, J., Schneuwly, S., Senthilan, P. R., et al. (2017). Drosophila Rhodopsin 7 can partially replace the structural role of Rhodopsin 1, but not its physiological function. *J. Comp. Physiol. A Neuroethol. Sens. Neural Behav. Physiol.* 203, 649–659. doi: 10.1007/s00359-017-1182-8

Grima, B., Chélot, E., Xia, R., and Rouyer, F. (2004). Morning and evening peaks of activity rely on different clock neurons of the Drosophila brain. *Nature* 431, 869–873. doi: 10.1038/nature02935

Guo, F., Holla, M., Díaz, M. M., and Rosbash, M. (2018). A circadian output circuit controls sleep-wake arousal in Drosophila. *Neuron* 100, 624–635.e4. doi: 10.1016/j.neuron.2018.09.002

Guo, F., Yu, J., Jung, H. J., Abruzzi, K. C., Luo, W., Griffith, L. C., et al. (2016). Circadian neuron feedback controls the Drosophila sleep-activity profile. *Nature* 536, 292–297. doi: 10.1038/nature19097

Hamasaka, Y., and Nässel, D. R. (2006). Mapping of serotonin, dopamine, and histamine in relation to different clock neurons in the brain of Drosophila. *J. Comp. Neurol.* 494, 314–330. doi: 10.1002/cne.20807

Hamasaka, Y., Rieger, D., Parmentier, M. L., Grau, Y., Helfrich-Förster, C., and Nässel, D. R. (2007). Glutamate and its metabotropic receptor in Drosophila clock neuron circuits. *J. Comp. Neurol.* 505, 32–45. doi: 10.1002/cne.21471

Hardie, R. C. (1979). Electrophysiological analysis of fly retina. I: Comparative properties of R1-6 and R 7 and 8. *J. Comp. Physiol. A* 129, 19–33. doi: 10.1007/BF00679908

Hardie, R. C. (1987). Is histamine a neurotransmitter in insect photoreceptors? *J. Comp. Physiol. A* 161, 201–213. doi: 10.1007/BF00615241

Hardie, R. C. (1989). A histamine-activated chloride channel involved in neurotransmission at a photoreceptor synapse. *Nature* 339, 704–706. doi: 10.1038/339704a0

Hartwig, S., Dovengerds, C., Herrmann, C., and Hovemann, B. T. (2014). Drosophila Ebony: a novel type of nonribosomal peptide synthetase related enzyme with unusually fast peptide bond formation kinetics. *FEBS J.* 281, 5147–5158. doi: 10.1111/febs.13054

Hassan, J., Busto, M., Iyengar, B., and Campos, A. R. (2000). Behavioural characterization and genetic analysis of the *Drosophila melanogaster* larval response to light as revealed by a novel individual assay. *Behav. Genet.* 30, 59–69. doi: 10.1023/A:1002090627601

Haynes, P. R., Christmann, B. L., and Griffith, L. C. (2015). A single pair of neurons links sleep to memory consolidation in *Drosophila melanogaster*. *eLife* 7:e03868. doi: 10.7554/eLife.03868

Haynie, J. L., and Bryant, P. J. (1986). Development of the eye-antenna imaginal disc and morphogenesis of the adult head in *Drosophila melanogaster*. *J. Exp. Zool.* 237, 293–308. doi: 10.1002/jez.1402370302

Heisenberg, M. (1971). Separation of receptor and lamina potentials in the electroretinogram of normal and mutant Drosophila. *J. Exp. Biol.* 55, 85–100.

Heisenberg, M., and Buchner, E. (1977). The rôle of retinula cell types in visual behaviour of *Drosophila melanogaster*. *J. Comp. Physiol.* 117, 127–162. doi: 10.1007/BF00612784

Helfrich-Förster, C. (2019). Light input pathways to the circadian clock of insects with an emphasis on the fruit fly *Drosophila melanogaster*. *J. Comp. Physiol. A.* 206, 259–272. doi: 10.1007/s00359-019-01379-5

Helfrich-Förster, C., Edwards, T., Yasuyama, K., Wisotzki, B., Schneuwly, S., Stanewsky, R., et al. (2002). The extraretinal eyelet of Drosophila: development, ultrastructure, and putative circadian function. *J. Neurosci.* 22, 9255–9266. doi: 10.1523/jneurosci.22-21-09255.2002

Helfrich-Förster, C., Winter, C., Hofbauer, A., Hall, J. C., and Stanewsky, R. (2001). The circadian clock of fruit flies is blind after elimination of all known photoreceptors. *Neuron* 30, 249–261. doi: 10.1016/s0896-6273(01)00277-x

Hendricks, J. C. (2003). Invited review: sleeping flies don't lie: the use of *Drosophila melanogaster* to study sleep and circadian rhythms. *J. Appl. Physiol.* 94, 1660–1672. doi: 10.1152/japplphysiol.00904.2002

Hendricks, J. C., Finn, S. M., Panckeri, K. A., Chavkin, J., Williams, J. A., Sehgal, A., et al. (2000). Rest in Drosophila is a sleep-like state. *Neuron* 25, 129–138. doi: 10.1016/s0896-6273(00)80877-6

Hobert, O., and Westphal, H. (2000). Functions of LIM-homeobox genes. *Trends Genet.* 16, 75–83. doi: 10.1016/s0168-9525(99)01883-1

Hofbauer, A., and Buchner, E. (1989). Does Drosophila have seven eyes? *Naturwissenschaften* 76, 335–336. doi: 10.1007/BF00368438

Hong, S. T., Bang, S., Paik, D., Kang, J., Hwang, S., Jeon, K., et al. (2006). Histamine and its receptors modulate temperature-preference behaviours in Drosophila. *J. Neurosci.* 26, 7245–7256. doi: 10.1523/JNEUROSCI.5426-05.2006

Hu, K. G., and Stark, W. S. (1980). The roles of Drosophila ocelli and compound eyes in phototaxis. *J. Comp. Physiol. A* 135, 85–95. doi: 10.1007/BF00660183

Huber, A., Schulz, S., Bentrop, J., Groell, C., Wolfrum, U., and Paulsen, R. (1997). Molecular cloning of Drosophila Rh6 rhodopsin: the visual pigment of a subset of R8 photoreceptor cells. *FEBS Lett.* 406, 6–10. doi: 10.1016/S0014-5793(97)00210-X

Huber, R., Hill, S. L., Holladay, C., Biesiadecki, M., Tononi, G., and Cirelli, C. (2004). Sleep homeostasis in *Drosophila melanogaster*. *Sleep* 27, 628–639. doi: 10.1093/sleep/27.4.628

Johard, H. A. D., Yoishii, T., Dircksen, H., Cusumano, P., Rouyer, F., Helfrich-Förster, C., et al. (2009). Peptidergic clock neurons in Drosophila: ion transport peptide and short neuropeptide F in subsets of dorsal and ventral lateral neurons. *J. Comp. Neurol.* 516, 59–73. doi: 10.1002/cne.22099

Joiner, W. J., Crocker, A., White, B. H., and Sehgal, A. (2006). Sleep in Drosophila is regulated by adult mushroom bodies. *Nature* 441, 757–760. doi: 10.1038/nature04811

Kahsai, L., Martin, J.-R., and Winther, A. M. E. (2010). Neuropeptides in the Drosophila central complex in modulation of locomotor behaviour. *J. Exp. Biol.* 213, 2256–2265. doi: 10.1242/jeb.043190

Kaneko, M., Helfrich-Förster, C., and Hall, J. C. (1997). Spatial and temporal expression of the period and timeless genes in the developing nervous system of drosophila: newly identified pacemaker candidates and novel features of clock gene product cycling. *J. Neurosci.* 17, 6745–6760. doi: 10.1523/jneurosci.17-17-06745.1997

Kayser, M. S., Yue, Z., and Sehgal, A. (2014). A critical period of sleep for development of courtship circuitry and behaviour in Drosophila. *Science* 344, 269–274. doi: 10.1126/science.1250553

Kempinger, L., Dittmann, R., Rieger, D., and Helfrich-Förster, C. (2009). The nocturnal activity of fruit flies exposed to artificial moonlight is partly caused by direct light effects on the activity level that bypass the endogenous clock. *Chronobiol. Int.* 26, 151–166. doi: 10.1080/07420520902747124

Kim, E. Y., Bae, K., Ng, F. S., Glossop, N. R. J., Hardin, P. E., and Edery, I. (2002). Drosophila clock protein is under posttranscriptional control and influences light-induced activity. *Neuron* 34, 69–81. doi: 10.1016/s0896-6273(02)00639-6

Kirszenblat, L., Yaun, R., and Van Swinderen, B. (2019). Visual experience drives sleep need in Drosophila. *Sleep.* 42:zsz102. doi: 10.1093/sleep/zsz102

Kistenpfennig, C., Grebler, R., Ogueta, M., Hermann-Luibl, C., Schlichting, M., Stanewsky, R., et al. (2017). A new Rhodopsin influences light-dependent daily activity patterns of fruit flies. *J. Biol. Rhythms* 32, 406–422. doi: 10.1177/0748730417721826

Koh, K., Zheng, X., and Sehgal, A. (2006). JETLAG resets the Drosophila circadian clock by promoting light-induced degradation of TIMELESS. *Science* 312, 1809–1812. doi: 10.1126/science.1124951

Krapp, H. G. (2009). Ocelli. *Curr. Biol.* 19, R435–R437. doi: 10.1016/j.cub.2009.03.034

Kula-Eversole, E., Nagoshi, E., Shang, Y., Rodriguez, J., Allada, R., and Rosbash, M. (2010). Surprising gene expression patterns within and between PDF-containing circadian neurons in Drosophila. *Proc. Natl. Acad. Sci. U.S.A.* 107, 13497–13502. doi: 10.1073/pnas.1002081107

Kumar, S., Chen, D., and Sehgal, A. (2012). Dopamine acts through Cryptochrome to promote acute arousal in Drosophila. *Genes Dev.* 26, 1224–1234. doi: 10.1101/gad.186338.111

Kunst, M., Hughes, M. E., Raccuglia, D., Felix, M., Li, M., Barnett, G., et al. (2014). Calcitonin gene-related peptide neurons mediate sleep-specific circadian output in Drosophila. *Curr. Biol.* 24, 2652–2664. doi: 10.1016/j.cub.2014.09.077

Lamaze, A., Krätschmer, P., Chen, K. F., Lowe, S., and Jepson, J. E. C. (2018). A wake-promoting circadian output circuit in Drosophila. *Curr. Biol.* 28, 3098–3105.e3. doi: 10.1016/j.cub.2018.07.024

Lamaze, A., and Stanewsky, R. (2020). DN1p or the "Fluffy". Cerberus of Clock Outputs. *Front. Physiol.* 10:1540. doi: 10.3389/fphys.2019.01540

Lazopulo, S., Lazopulo, A., Baker, J. D., and Syed, S. (2019). Daytime colour preference in Drosophila depends on the circadian clock and TRP channels. *Nature* 574, 108–111. doi: 10.1038/s41586-019-1571-y

Lear, B. C., Lin, J. M., Keath, J. R., McGill, J. J., Raman, I. M., and Allada, R. (2005). The ion channel narrow abdomen is critical for neural output of the Drosophila circadian pacemaker. *Neuron* 48, 965–976. doi: 10.1016/j.neuron.2005.10.030

Lelito, K. R., and Shafer, O. T. (2012). Reciprocal cholinergic and GABAergic modulation of the small ventrolateral pacemaker neurons of Drosophila's circadian clock neuron network. *J. Neurophysiol.* 107, 2096–2108. doi: 10.1152/jn.00931.2011

Li, M. T., Cao, L. H., Xiao, N., Tang, M., Deng, B., Yang, T., et al. (2018). Hub-organized parallel circuits of central circadian pacemaker neurons for visual photoentrainment in Drosophila. *Nat. Commun.* 9:4247.

Liang, X., Holy, T. E., and Taghert, P. H. (2016). Synchronous drosophila circadian pacemakers display nonsynchronous Ca2+ rhythms *in vivo*. *Science* 351, 976–981. doi: 10.1126/science.aad3997

Lin, T. Y., Luo, J., Shinomiya, K., Ting, C. Y., Lu, Z., Meinertzhagen, I. A., et al. (2016). Mapping chromatic pathways in the Drosophila visual system. *J. Comp. Neurol.* 524, 213–227. doi: 10.1002/cne.23857

Lindholm, P., and Saarma, M. (2010). Novel CDNF/MANF family of neurotrophic factors. *Dev. Neurobiol.* 70, 360–371. doi: 10.1002/dneu.20760

Liu, G., Seiler, H., Wen, A., Zars, T., Ito, K., Wolf, R., et al. (2006). Distinct memory traces for two visual features in the Drosophila brain. *Nature* 439, 551–556. doi: 10.1038/nature04381

Liu, Q., Liu, S., Kodama, L., Driscoll, M. R., and Wu, M. N. (2012). Two dopaminergic neurons signal to the dorsal fan-shaped body to promote wakefulness in Drosophila. *Curr. Biol.* 22, 2114–2123. doi: 10.1016/j.cub.2012.09.008

Liu, S., Lamaze, A., Liu, Q., Tabuchi, M., Yang, Y., Fowler, M., et al. (2014). WIDE AWAKE mediates the circadian timing of sleep onset. *Neuron* 82, 151–166. doi: 10.1016/j.neuron.2014.01.040

Liu, S., Liu, Q., Tabuchi, M., and Wu, M. N. (2016). Sleep drive is encoded by neural plastic changes in a dedicated circuit. *Cell* 165, 1347–1360. doi: 10.1016/j.cell.2016.04.013

Liu, W. W., and Wilson, R. I. (2013). Glutamate is an inhibitory neurotransmitter in the Drosophila olfactory system. *Proc. Natl. Acad. Sci. U.S.A.* 110, 10294–10299. doi: 10.1073/pnas.1220560110

Liu, Z., and Zhao, Z. (2014). Effects of light interruption on sleep and viability of *Drosophila melanogaster*. *PLoS One* 9:e105678. doi: 10.1371/journal.pone.0105678

Lu, B., Liu, W., Guo, F., and Guo, A. (2008). Circadian modulation of light-induced locomotion responses in *Drosophila melanogaster*. *Genes Brain Behav.* 7, 730–739. doi: 10.1111/j.1601-183X.2008.00411.x

Ly, S., Pack, A. I., and Naidoo, N. (2018). The neurobiological basis of sleep: insights from Drosophila. *Neurosci. Biobehav. Rev.* 87, 67–86. doi: 10.1016/j.neubiorev.2018.01.015

Malpel, S., Klarsfeld, A., and Rouyer, F. (2002). Larval optic nerve and adult extra-retinal photoreceptors sequentially associate with clock neurons during Drosophila brain development. *Development* 129, 1443–1453.

Mao, Z., and Davis, R. L. (2009). Eight different types of dopaminergic neurons innervate the Drosophila mushroom body neuropil: anatomical and physiological heterogeneity. *Front. Neural Circuits* 3:5. doi: 10.3389/neuro.04.005.2009

Mauss, A. S., Meier, M., Serbe, E., and Borst, A. (2014). Optogenetic and pharmacologic dissection of feedforward inhibition in Drosophila motion vision. *J. Neurosci.* 34, 2254–2263. doi: 10.1523/JNEUROSCI.3938-13.2014

Mauss, A. S., Pankova, K., Arenz, A., Nern, A., Rubin, G. M., and Borst, A. (2015). Neural circuit to integrate opposing motions in the visual field. *Cell* 162, 351–362. doi: 10.1016/j.cell.2015.06.035

Mazzotta, G., Rossi, A., Leonardi, E., Mason, M., Bertolucci, C., Caccin, L., et al. (2013). Fly cryptochrome and the visual system. *Proc. Natl. Acad. Sci. U.S.A.* 110, 6163–6168. doi: 10.1073/pnas.1212317110

Mazzotta, G. M., Bellanda, M., Minervini, G., Damulewicz, M., Cusumano, P., Aufiero, S., et al. (2018). Calmodulin enhances cryptochrome binding to INAD in Drosophila photoreceptors. *Front. Mol. Neurosci.* 11:280. doi: 10.3389/fnmol.2018.00280

McCarthy, E. V., Wu, Y., deCarvalho, T., Brandt, C., Cao, G., and Nitabach, M. N. (2011). Synchronized bilateral synaptic inputs to *Drosophila melanogaster* neuropeptidergic rest/arousal neurons. *J. Neurosci.* 31, 8181–8193. doi: 10.1523/JNEUROSCI.2017-10.2011

Mealey-Ferrara, M. L., Montalvo, A. G., and Hall, J. C. (2003). Effects of combining a cryptochrome mutation with other visual-system variants on entrainment of locomotor and adult-emergence rhythms in Drosophila. *J. Neurogenet.* 17, 171–221. doi: 10.1080/neg.17.2-3.171.221

Meinertzhagen, I. A., and O'Neil, S. D. (1991). Synaptic organization of columnar elements in the lamina of the wild type in *Drosophila melanogaster*. *J. Comp. Neurol.* 305, 232–263. doi: 10.1002/cne.903050206

Meinertzhagen, I. A., and Sorra, K. E. (2001). Synaptic organization in the fly's optic lamina: few cells, many synapses and divergent microcircuits. *Prog. Brain Res.* 131, 53–69. doi: 10.1016/S0079-6123(01)31007-5

Melamed, J., and Trujillo-Cenóz, O. (1967). The fine structure of the central cells in the ommatidia of dipterans. *J. Ultrasruct. Res.* 21, 313–334. doi: 10.1016/s0022-5320(67)80098-4

Mertens, I., Vandingenen, A., Johnson, E. C., Shafer, O. T., Li, W., Trigg, J. S., et al. (2005). PDF receptor signalling in Drosophila contributes to both circadian and geotactic behaviours. *Neuron* 48, 213–219. doi: 10.1016/j.neuron.2005.09.009

Millard, S. S., and Pecot, M. Y. (2018). Strategies for assembling columns and layers in the Drosophila visual system. *Neural Dev.* 13:11.

Mismer, D., and Rubin, G. M. (1987). Analysis of the promoter of the ninaE opsin gene in *Drosophila melanogaster*. *Genetics* 116, 565–578.

Montell, C. (2012). Drosophila visual transduction. *Trends Neurosci.* 35, 356–363. doi: 10.1016/j.tins.2012.03.004

Montell, C., Jones, K., Zuker, C., and Rubin, G. (1987). A second opsin gene expressed in the ultraviolet-sensitive R7 photoreceptor cells of *Drosophila melanogaster*. *J. Neurosci.* 7, 1558–1566. doi: 10.1523/jneurosci.07-05-01558.1987

Muraro, N. I., and Ceriani, M. F. (2015). Acetylcholine from visual circuits modulates the activity of arousal neurons in Drosophila. *J. Neurosci.* 35, 16315–16327. doi: 10.1523/JNEUROSCI.1571-15.2015

Nagy, D., Cusumano, P., Andreatta, G., Anduaga, A. M., Hermann-Luibl, C., Reinhard, N., et al. (2019). Peptidergic signalling from clock neurons regulates reproductive dormancy in *drosophila melanogaster*. *PLoS Genet.* 15:e1008158. doi: 10.1371/journal.pgen.1008158

Nässel, D. R. (1999). Histamine in the brain of insects: a review. *Microsc. Res. Tech.* 44, 121–136. doi: 10.1002/(sici)1097-0029(19990115/01)44:2/3<121::aid-jemt6>3.0.co;2-f

Nässel, D. R., Enell, L. E., Santos, J. G., Wegener, C., and Johard, H. A. D. (2008). A large population of diverse neurons in the Drosophila central nervous system expresses short neuropeptide F, suggesting multiple

distributed peptide functions. *BMC Neurosci.* 9:90. doi: 10.1186/1471-2202-9-90

Ni, J. D., Baik, L. S., Holmes, T. C., and Montell, C. (2017). A rhodopsin in the brain functions in circadian photoentrainment in Drosophila. *Nature* 545, 340–344. doi: 10.1038/nature22325

Ni, J. D., Gurav, A. S., Liu, W., Ogunmowo, T. H., Hackbart, H., Elsheikh, A., et al. (2019). Differential regulation of the drosophila sleep homeostat by circadian and arousal inputs. *eLife* 8:e40487. doi: 10.7554/eLife.40487

Nitabach, M. N., Sheeba, V., Vera, D. A., Blau, J., and Holmes, T. C. (2005). Membrane electrical excitability is necessary for the free-running larval Drosophila circadian clock. *J. Neurobiol.* 62, 1–13. doi: 10.1002/neu.20053

Nitz, D. A., Van Swinderen, B., Tononi, G., and Greenspan, R. J. (2002). Electrophysiological correlates of rest and activity in *Drosophila melanogaster*. *Curr. Biol.* 12, 1934–1940. doi: 10.1016/s0960-9822(02)01300-3

Niu, Y., Liu, Z., Nian, X., Xu, X., and Zhang, Y. (2019). miR-210 controls the evening phase of circadian locomotor rhythms through repression of Fasciclin 2. *PLoS Genet.* 15:e1007655. doi: 10.1371/journal.pgen.1007655

Oh, Y., Jang, D., Sonn, J. Y., and Choe, J. (2013). Histamine-HisCl1 receptor axis regulates wake-promoting signals in *Drosophila melanogaster*. *PLoS One* 8:e68269. doi: 10.1371/journal.pone.0068269

Omoto, J. J., Kele??, M. F., Nguyen, B. C. M., Bolanos, C., Lovick, J. K., Frye, M. A., et al. (2017). Visual input to the drosophila central complex by developmentally and functionally distinct neuronal populations. *Curr. Biol.* 27, 1098–1110. doi: 10.1016/j.cub.2017.02.063

O'Tousa, J. E., Baehr, W., Martin, R. L., Hirsh, J., Pak, W. L., and Applebury, M. L. (1985). The Drosophila ninaE gene encodes an opsin. *Cell* 40, 839–850. doi: 10.1016/0092-8674(85)90343-5

Palgi, M., Greco, D., Lindström, R., Auvinen, P., and Heino, T. I. (2012). Gene expression analysis of Drosophilaa Manf mutants reveals perturbations in membrane traffic and major metabolic changes. *BMC Genomics* 13:134. doi: 10.1186/1471-2164-13-134

Palgi, M., Lindström, R., Peränen, J., Piepponen, T. P., Saarma, M., and Heino, T. I. (2009). Evidence that DmMANF is an invertebrate neurotrophic factor supporting dopaminergic neurons. *Proc. Natl. Acad. Sci. U.S.A.* 106, 2429–2434. doi: 10.1073/pnas.0810996106

Pantazis, A., Segaran, A., Liu, C. H., Nikolaev, A., Rister, J., Thum, A. S., et al. (2008). Distinct roles for two histamine receptors (hclA and hclB) at the Drosophila photoreceptor synapse. *J. Neurosci.* 28, 7250–7259. doi: 10.1523/JNEUROSCI.1654-08.2008

Papatsenko, D., Sheng, G., and Desplan, C. (1997). A new rhodopsin in R8 photoreceptors of Drosophila: evidence for coordinate expression with Rh3 in R7 cells. *Development* 124, 1665–1673.

Parisky, K. M., Agosto, J., Pulver, S. R., Shang, Y., Kuklin, E., Hodge, J. J. L., et al. (2008). PDF Cells Are a GABA-responsive wake-promoting component of the Drosophila sleep circuit. *Neuron* 60, 672–682. doi: 10.1016/j.neuron.2008.10.042

Parisky, K. M., Agosto Rivera, J. L., Donelson, N. C., Kotecha, S., and Griffith, L. C. (2016). Reorganization of sleep by temperature in drosophila requires light, the Homeostat, and the circadian clock. *Curr. Biol.* 26, 882–892. doi: 10.1016/j.cub.2016.02.011

Perez, S. E., and Steller, H. (1996). Migration of glial cells into retinal axon target field in *Drosophila melanogaster*. *J. Neurobiol.* 30, 359–373. doi: 10.1002/(sici)1097-4695(199607)30:3<359::aid-neu5>3.0.co;2-3

Peschel, N., Chen, K. F., Szabo, G., and Stanewsky, R. (2009). Light-Dependent Interactions between the Drosophila Circadian Clock Factors Cryptochrome. Jetlag, and Timeless. *Curr. Biol.* 19, 241–247. doi: 10.1016/j.cub.2008.12.042

Picot, M., Cusumano, P., Klarsfeld, A., Ueda, R., and Rouyer, F. (2007). Light activates output from evening neurons and inhibits output from morning neurons in the Drosophila circadian clock. *PLoS Biol.* 5:2513–2521. doi: 10.1371/journal.pbio.0050315

Pimentel, D., Donlea, J. M., Talbot, C. B., Song, S. M., Thurston, A. J. F., and Miesenböck, G. (2016). Operation of a homeostatic sleep switch. *Nature* 536, 333–337. doi: 10.1038/nature19055

Pitman, J. L., McGill, J. J., Keegan, K. P., and Allada, R. (2006). A dynamic role for the mushroom bodies in promoting sleep in Drosophila. *Nature* 441, 753–756. doi: 10.1038/nature04739

Plaza, S., Chanut-Delalande, H., Fernandes, I., Wassarman, P. M., and Payre, F. (2010). From A to Z: apical structures and zona pellucida-domain proteins. *Trends Cell Biol.* 20, 524–532. doi: 10.1016/j.tcb.2010.06.002

Poeck, B., Triphan, T., Neuser, K., and Strauss, R. (2008). Locomotor control by the central complex in Drosophila - An analysis of the tay bridge mutant. *Dev. Neurobiol.* 68, 1046–1058. doi: 10.1002/dneu.20643

Pollack, I., and Hofbauer, A. (1991). Histamine-like immunoreactivity in the visual system and brain of *Drosophila melanogaster*. *Cell Tissue Res.* 266, 391–398. doi: 10.1007/BF00318195

Pollock, J. A., and Benzer, S. (1988). Transcript localization of four opsin genes in the three visual organs of Drosophila. RH2 is ocellus specific. *Nature* 333, 779–782. doi: 10.1038/333779a0

Potdar, S., and Sheeba, V. (2018). Wakefulness is promoted during day time by PDFR signalling to dopaminergic neurons in *Drosophila melanogaster*. *eNeuro* 5:ENEURO.129-18.2018. doi: 10.1523/ENEURO.0129-18.2018

Qian, Y., Cao, Y., Deng, B., Yang, G., Li, J., Xu, R., et al. (2017). Sleep homeostasis regulated by 5HT2b receptor in a small subset of neurons in the dorsal fan-shaped body of drosophila. *eLife* 6:e26519. doi: 10.7554/eLife.26519

Raccuglia, D., Huang, S., Ender, A., Heim, M. M., Laber, D., Suárez-Grimalt, R., et al. (2019). Network-specific synchronization of electrical slow-wave oscillations regulates sleep drive in Drosophila. *Curr. Biol.* 29, 3611–3621.e3. doi: 10.1016/j.cub.2019.08.070

Raghu, S. V., and Borst, A. (2011). Candidate glutamatergic neurons in the visual system of drosophila. *PLoS One* 6:e19472. doi: 10.1371/journal.pone.0019472

Rahman, M., Ham, H., Liu, X., Sugiura, Y., Orth, K., and Krämer, H. (2012). Visual neurotransmission in Drosophila requires expression of Fic in glial capitate projections. *Nat. Neurosci.* 15, 871–875. doi: 10.1038/nn.3102

Redlin, U. (2001). Neural basis and biological function of masking by light in mammals: suppression of melatonin and locomotor activity. *Chronobiol. Int.* 18, 737–758. doi: 10.1081/CBI-100107511

Richardt, A., Kemme, T., Wagner, S., Schwarzer, D., Marahiel, M. A., and Hovemann, B. T. (2003). Ebony, a novel nonribosomal peptide synthetase for β-alanine conjugation with biogenic amines in Drosophila. *J. Biol. Chem.* 278, 41160–41166. doi: 10.1074/jbc.M304303200

Richardt, A., Rybak, J., Störtkuhl, K. F., Meinertzhagen, I. A., and Hovemann, B. T. (2002). Ebony protein in the Drosophila nervous system: optic neuropile expression in glial cells. *J. Comp. Neurol.* 452, 93–102. doi: 10.1002/cne.10360

Rieger, D., Fraunholz, C., Popp, J., Bichler, D., Dittmann, R., and Helfrich-Förster, C. (2007). The fruit fly *Drosophila melanogaster* favors dim light and times its activity peaks to early dawn and late dusk. *J. Biol. Rhythms* 22, 387–399. doi: 10.1177/0748730407306198

Rieger, D., Stanewsky, R., and Helfrich-Förster, C. (2003). Cryptochrome, compound eyes, hofbauer-buchner eyelets, and ocelli play different roles in the entrainment and masking pathway of the locomotor activity rhythm in the fruit fly *Drosophila Melanogaster*. *J. Biol. Rhythms* 18, 377–391. doi: 10.1177/0748730403256997

Rister, J., Pauls, D., Schnell, B., Ting, C. Y., Lee, C. H., Sinakevitch, I., et al. (2007). Dissection of the peripheral motion channel in the visual system of *Drosophila melanogaster*. *Neuron* 56, 155–170. doi: 10.1016/j.neuron.2007.09.014

Rivera-Alba, M., Vitaladevuni, S. N., Mischenko, Y., Lu, Z., Takemura, S. Y., Scheffer, L., et al. (2011). Wiring economy and volume exclusion determine neuronal placement in the Drosophila brain. *Curr. Biol.* 21, 2000–2005. doi: 10.1016/j.cub.2011.10.022

Robinson, J. E., Paluch, J., Dickman, D. K., and Joiner, W. J. (2016). ADAR-mediated RNA editing suppresses sleep by acting as a brake on glutamatergic synaptic plasticity. *Nat. Commun.* 7:10512. doi: 10.1038/ncomms10512

Rosato, E., Codd, V., Mazzotta, G., Piccin, A., Zordan, M., Costa, R., et al. (2001). Light-dependent interaction between Drosophila CRY and the clock protein PER mediated by the carboxy terminus of CRY. *Curr. Biol.* 11, 909–917. doi: 10.1016/S0960-9822(01)00259-7

Saint-Charles, A., Michard-Vanhée, C., Alejevski, F., Chélot, E., Boivin, A., and Rouyer, F. (2016). Four of the six Drosophila rhodopsin-expressing photoreceptors can mediate circadian entrainment in low light. *J. Comp. Neurol.* 524, 2828–2844. doi: 10.1002/cne.23994

Salcedo, E., Huber, A., Henrich, S., Chadwell, L. V., Chou, W. H., Paulsen, R., et al. (1999). Blue- and green-absorbing visual pigments of Drosophila: ectopic expression and physiological characterization of the R8 photoreceptor cell-

specific Rh5 and Rh6 rhodopsins. *J. Neurosci.* 19, 10716–10726. doi: 10.1523/jneurosci.19-24-10716.1999

Schlichting, M., Grebler, R., Peschel, N., Yoshii, T., and Helfrich-Förster, C. (2014). Moonlight detection by drosophila's endogenous clock depends on multiple photopigments in the compound eyes. *J. Biol. Rhythms* 29, 75–86. doi: 10.1177/0748730413520428

Schlichting, M., Menegazzi, P., Lelito, K. R., Yao, Z., Buhl, E., Benetta, E. D., et al. (2016). A neural network underlying circadian entrainment and photoperiodic adjustment of sleep and activity in Drosophila. *J. Neurosci.* 36, 9084–9096. doi: 10.1523/JNEUROSCI.0992-16.2016

Schlichting, M., Menegazzi, P., Rosbash, M., and Helfrich-Förster, C. (2019a). A distinct visual pathway mediates high-intensity light adaptation of the circadian clock in drosophila. *J. Neurosci.* 39, 1621–1630. doi: 10.1523/JNEUROSCI.1497-18.2018

Schlichting, M., Rieger, D., Cusumano, P., Grebler, R., Costa, R., Mazzotta, G. M., et al. (2018). Cryptochrome interacts with actin and enhances eye-mediated light sensitivity of the circadian clock in *Drosophila melanogaster*. *Front. Mol. Neurosci.* 11:238. doi: 10.3389/fnmol.2018.00238

Schlichting, M., Weidner, P., Diaz, M., Menegazzi, P., Dalla Benetta, E., Helfrich-Förster, C., et al. (2019b). Light-mediated circuit switching in the drosophila neuronal clock network. *Current Biology* 29, 3266–3276.e3. doi: 10.1016/j.cub.2019.08.033

Schnaitmann, C., Haikala, V., Abraham, E., Oberhauser, V., Thestrup, T., Griesbeck, O., et al. (2018). Color processing in the early visual system of Drosophila. *Cell* 172, 318–330.e18. doi: 10.1016/j.cell.2017.12.018

Schubert, F. K., Hagedorn, N., Yoshii, T., Helfrich-Förster, C., and Rieger, D. (2018). Neuroanatomical details of the lateral neurons of *Drosophila melanogaster* support their functional role in the circadian system. *J. Comp. Neurol.* 526, 1209–1231. doi: 10.1002/cne.24406

Scott, K., Becker, A., Sun, Y., Hardy, R., and Zuker, C. (1995). Gqα protein function *in vivo*: genetic dissection of its role in photoreceptor cell physiology. *Neuron* 15, 919–927. doi: 10.1016/0896-6273(95)90182-5

Seelig, J. D., and Jayaraman, V. (2013). Feature detection and orientation tuning in the Drosophila central complex. *Nature* 503, 262–266. doi: 10.1038/nature12601

Sengupta, S., Crowe, L. B., You, S., Roberts, M. A., and Jackson, F. R. (2019). A secreted Ig-Domain protein required in both astrocytes and neurons for regulation of Drosophila night sleep. *Curr. Biol.* 25, 2547–2554.e2. doi: 10.1016/j.cub.2019.06.055

Senthilan, P. R., Grebler, R., Reinhard, N., Rieger, D., and Helfrich-Förster, C. (2019). Role of rhodopsins as circadian photoreceptors in the *drosophila melanogaster*. *Biology* 8:6. doi: 10.3390/biology8010006

Senthilan, P. R., and Helfrich-Förster, C. (2016). Rhodopsin 7-The unusual Rhodopsin in Drosophila. *PeerJ* 4:e2427. doi: 10.7717/peerj.2427

Shafer, O. T., Kim, D. J., Dunbar-Yaffe, R., Nikolaev, V. O., Lohse, M. J., and Taghert, P. H. (2008). Widespread receptivity to neuropeptide PDF throughout the neuronal circadian clock network of drosophila revealed by real-time cyclic AMP imaging. *Neuron* 58, 223–237. doi: 10.1016/j.neuron.2008.02.018

Shang, Y., Donelson, N. C., Vecsey, C. G., Guo, F., Rosbash, M., and Griffith, L. C. (2013). Short neuropeptide F is a sleep-promoting inhibitory modulator. *Neuron* 80, 171–183. doi: 10.1016/j.neuron.2013.07.029

Shang, Y., Griffith, L. C., and Rosbash, M. (2008). Light-arousal and circadian photoreception circuits intersect at the large PDF cells of the Drosophila brain. *Proc. Natl. Acad. Sci. U.S.A.* 105, 19587–19594. doi: 10.1073/pnas.0809577105

Shang, Y., Haynes, P., Pírez, N., Harrington, K. I., Guo, F., Pollack, J., et al. (2011). Imaging analysis of clock neurons reveals light buffers the wake-promoting effect of dopamine. *Nat. Neurosci.* 14, 889–895. doi: 10.1038/nn.2860

Shaw, P. J., Cirelli, C., Greenspan, R. J., Tononi, G., Campbell, S. S., Tobler, I., et al. (2000). Correlates of sleep and waking in *Drosophila melanogaster*. *Science* 287, 1834–1837. doi: 10.1126/science.287.5459.1834

Shaw, P. J., Tortoni, G., Greenspan, R. J., and Robinson, D. F. (2002). Stress response genes protect against lethal effects of sleep deprivation in Drosophila. *Nature* 417, 287–291. doi: 10.1038/417287a

Sheeba, V., Fogle, K. J., Kaneko, M., Rashid, S., Chou, Y. T., Sharma, V. K., et al. (2008a). Large ventral lateral neurons modulate arousal and sleep in Drosophila. *Curr. Biol.* 18, 1537–1545. doi: 10.1016/j.cub.2008.08.033

Sheeba, V., Gu, H., Sharma, V. K., O'Dowd, D. K., and Holmes, T. C. (2008b). Circadian- and light-dependent regulation of resting membrane potential and spontaneous action potential firing of Drosophila circadian pacemaker neurons. *J. Neurophysiol.* 99, 976–988. doi: 10.1152/jn.00930.2007

Shimada, N., Inami, S., Sato, S., Kitamoto, T., and Sakai, T. (2016). Modulation of light-driven arousal by LIM-homeodomain transcription factor Apterous in large PDF-positive lateral neurons of the Drosophila brain. *Sci. Rep.* 6:37255. doi: 10.1038/srep37255

Shinomiya, K., Huang, G., Lu, Z., Parag, T., Xu, C. S., Aniceto, R., et al. (2019). Comparisons between the ON- and OFF-edge motion pathways in the Drosophila brain. *eLife* 8:e40025. doi: 10.7554/eLife.40025

Shinomiya, K., Karuppudurai, T., Lin, T. Y., Lu, Z., Lee, C. H., and Meinertzhagen, I. A. (2014). Candidate neural substrates for off-edge motion detection in drosophila. *Curr. Biol.* 24, 1062–1070. doi: 10.1016/j.cub.2014.03.051

Sinakevitch-Pean, I., Geffard, M., and Plotnikova, S. I. (2001). Localization of glutamate in the nervous system of the fly *Drosophila melanogaster*: an immunocytochemical study. *J. Evol. Biochem. Physiol.* 37, 83–88. doi: 10.1023/A:1017574120553

Sitaraman, D., Aso, Y., Jin, X., Chen, N., Felix, M., Rubin, G. M., et al. (2015a). Propagation of homeostatic sleep signals by segregated synaptic microcircuits of the Drosophila mushroom body. *Curr. Biol.* 25, 2915–2927. doi: 10.1016/j.cub.2015.09.017

Sitaraman, D., Aso, Y., Rubin, G. M., and Nitabach, M. N. (2015b). Control of sleep by dopaminergic inputs to the drosophila mushroom body. *Front. Neural Circuits* 9:73. doi: 10.3389/fncir.2015.00073

Sprecher, S. G., and Desplan, C. (2008). Switch of rhodopsin expression in terminally differentiated Drosophila sensory neurons. *Nature* 454, 533–537. doi: 10.1038/nature07062

Stanewsky, R., Kaneko, M., Emery, P., Beretta, B., Wager-Smith, K., Kay, S. A., et al. (1998). The cryb mutation identifies cryptochrome as a circadian photoreceptor in Drosophila. *Cell* 95, 681–692. doi: 10.1016/s0092-8674(00)81638-4

Stark, W. S., and Carlson, S. D. (1986). Ultrastructure of capitate projections in the optic neuropil of Diptera. *Cell Tissue Res.* 246, 481–486. doi: 10.1007/BF00215187

Stenesen, D., Moehlman, A. T., and Krämer, H. (2015). The carcinine transporter CarT is required in Drosophila photoreceptor neurons to sustain histamine recycling. *eLife* 4:e10972. doi: 10.7554/eLife.10972

Stoleru, D., Peng, Y., Agosto, J., and Rosbash, M. (2004). Coupled oscillators control morning and evening locomotor behaviour of Drosophila. *Nature* 431, 862–868. doi: 10.1038/nature02926

Stratoulias, V., and Heino, T. I. (2015). Analysis of the conserved neurotrophic factor MANF in the Drosophila adult brain. *Gene Exp. Patt.* 18, 8–15. doi: 10.1016/j.gep.2015.04.002

Strausfeld, N. J. (1971). The organization of the insect visual system (Light microscopy) - I. Projections and arrangements of neurons in the lamina ganglionaris of Diptera. *Z. Zellforsch. Mikrosk. Anat.* 121, 377–441. doi: 10.1007/BF00337640

Stuart, A. E., Borycz, J., and Meinertzhagen, I. A. (2007). The dynamics of signalling at the histaminergic photoreceptor synapse of arthropods. *Prog. Neurobiol.* 82, 202–207. doi: 10.1016/j.pneurobio.2007.03.006

Suver, M. P., Huda, A., Iwasaki, N., Safarik, S., and Dickinson, M. H. (2016). An array of descending visual interneurons encoding self-motion in Drosophila. *J. Neurosci.* 36, 11768–11780. doi: 10.1523/JNEUROSCI.2277-16.2016

Takemura, S. Y., Karuppudurai, T., Ting, C. Y., Lu, Z., Lee, C. H., and Meinertzhagen, I. A. (2011). Cholinergic circuits integrate neighboring visual signals in a drosophila motion detection pathway. *Curr. Biol.* 21, 2077–2084. doi: 10.1016/j.cub.2011.10.053

Tan, L., Zhang, K. X., Pecot, M. Y., Nagarkar-Jaiswal, S., Lee, P. T., Takemura, S. Y., et al. (2015). Ig superfamily ligand and receptor pairs expressed in synaptic partners in Drosophila. *Cell* 163, 1756–1769. doi: 10.1016/j.cell.2015.11.021

Technau, G. M. (2007). Fiber number in the mushroom bodies of adult *Drosophila melanogaster* depends on age, sex and experience. *J. Neurogenet.* 21, 183–196. doi: 10.1080/01677060701695359

Thakkar, M. M. (2011). Histamine in the regulation of wakefulness. *Sleep Med. Rev.* 15, 65–74. doi: 10.1016/j.smrv.2010.06.004

Tomita, J., Ueno, T., Mitsuyoshi, M., Kume, S., and Kume, K. (2015). The NMDA Receptor promotes sleep in the fruit fly, *Drosophila melanogaster*. *PLoS One* 10:e0128101. doi: 10.1371/journal.pone.0128101

Tracy, T. E., and Gan, L. (2018). Tau-mediated synaptic and neuronal dysfunction in neurodegenerative disease. *Curr. Opin. Neurobiol.* 51, 134–138. doi: 10.1016/j.conb.2018.04.027

Triphan, T., Poeck, B., Neuser, K., and Strauss, R. (2010). Visual targeting of motor actions in climbing Drosophila. *Curr. Biol.* 20, 663–668. doi: 10.1016/j.cub.2010.02.055

Ueno, T., Tomita, J., Tanimoto, H., Endo, K., Ito, K., Kume, S., et al. (2012). Identification of a dopamine pathway that regulates sleep and arousal in Drosophila. *Nat. Neurosci.* 15, 1516–1523. doi: 10.1038/nn.3238

Ursin, R. (2002). Serotonin and sleep. *Sleep Med. Rev.* 6, 55–67. doi: 10.1053/smrv.2001.0174

van Alphen, B., Yap, M. H. W., Kirszenblat, L., Kottler, B., and van Swinderen, B. (2013). A dynamic deep sleep stage in Drosophila. *J. Neurosci.* 33, 6917–6927. doi: 10.1523/JNEUROSCI.0061-13.2013

Van Meyel, D. J., O'Keefe, D. D., Jurata, L. W., Thor, S., Gill, G. N., and Thomas, J. B. (1999). Chip and Apterous physically interact to form a functional complex during Drosophila development. *Mol. Cell* 4, 259–265. doi: 10.1016/s1097-2765(00)80373-1

Vanin, S., Bhutani, S., Montelli, S., Menegazzi, P., Green, E. W., Pegoraro, M., et al. (2012). Unexpected features of Drosophila circadian behavioural rhythms under natural conditions. *Nature* 474, 371–375. doi: 10.1038/nature10991

VanVickle-Chavez, S. J., and Van Gelder, R. N. (2007). Action spectrum of Drosophila cryptochrome. *J. Biol. Chem.* 282, 10561–10566. doi: 10.1074/jbc.M609314200

Veleri, S., Rieger, D., Helfrich-Förster, C., and Stanewsky, R. (2007). Hofbauer-Buchner eyelet affects circadian photosensitivity and coordinates TIM and PER expression in Drosophila clock neurons. *J. Biol. Rhythms* 22, 29–42. doi: 10.1177/0748730406295754

Vinayak, P., Coupar, J., Hughes, S. E., Fozdar, P., Kilby, J., Garren, E., et al. (2013). Exquisite Light Sensitivity of *Drosophila melanogaster* Cryptochrome. *PLoS Genet.* 9:e1003615. doi: 10.1371/journal.pgen.1003615

Wagner, S., Heseding, C., Szlachta, K., True, J. R., Prinz, H., and Hovemann, B. T. (2007). Drosophila photoreceptors express cysteine peptidase Tan. *J. Comp. Neurol.* 500, 601–611. doi: 10.1002/cne.21138

Walkowicz, L., Kijak, E., Krzeptowski, W., Górska-Andrzejak, J., Stratoulias, V., Woznicka, O., et al. (2017). Downregulation of DmMANF in glial cells results in neurodegeneration and affects sleep and lifespan in *Drosophila melanogaster*. *Front. Neurosci.* 11:610. doi: 10.3389/fnins.2017.00610

Wang, T., and Montell, C. (2007). Phototransduction and retinal degeneration in Drosophila. *Pflugers Arch.* 454, 821–847. doi: 10.1007/s00424-007-0251-1

Wang, T., Xu, H., Oberwinkler, J., Gu, Y., Hardie, R. C., and Montell, C. (2005). Light activation, adaptation, and cell survival functions of the Na +/Ca2+ exchanger CalX. *Neuron* 45, 367–378. doi: 10.1016/j.neuron.2004.12.046

Wegener, C., Hamasaka, Y., and Nässel, D. R. (2004). Acetylcholine Increases Intracellular Ca2+ Via Nicotinic Receptors in Cultured PDF-Containing Clock Neurons of Drosophila. *J. Neurophysiol.* 91, 912–923. doi: 10.1152/jn.00678.2003

Weigelt, C. M., Hahn, O., Arlt, K., Gruhn, M., Jahn, A. J., Eßer, J., et al. (2019). Loss of miR-210 leads to progressive retinal degeneration in *Drosophila melanogaster*. *Sci. Alliance* 2:e20180049. doi: 10.26508/lsa.201800149

Witte, I., Kreienkamp, H. J., Gewecke, M., and Roeder, T. (2002). Putative histamine-gated chloride channel subunits of the insect visual system and thoracic ganglion. *J. Neurochem.* 84, 504–514. doi: 10.1046/j.1471-4159.2002.01076.x

Xu, Y., An, F., Borycz, J. A., Borycz, J., Meinertzhagen, I. A., and Wang, T. (2015). Histamine recycling is mediated by CarT, a Carcinine transporter in drosophila photoreceptors. *PLoS Genet.* 11:1005764. doi: 10.1371/journal.pgen.1005764

Yamaguchi, S., Wolf, R., Desplan, C., and Heisenberg, M. (2008). Motion vision is independent of color in Drosophila. *Proc. Natl. Acad. Sci. U.S.A.* 105, 4910–4915. doi: 10.1073/pnas.0711484105

Yao, Z., and Shafer, O. T. (2014). The Drosophila circadian clock is a variably coupled network of multiple peptidergic units. *Science* 343, 1516–1520. doi: 10.1126/science.1251285

Yasuyama, K., and Meinertzhagen, I. A. (1999). Extraretinal photoreceptors at the compound eye's posterior margin in *Drosophila melanogaster*. *J. Comp. Neurol.* 412, 193–202. doi: 10.1002/(sici)1096-9861(19990920)412:2<193::aid-cne1>3.0.co;2-0

Yasuyama, K., and Salvaterra, P. M. (1999). Localization of choline acetyltransferase-expressing neurons in Drosophila nervous system. *Microsc. Res. Tech.* 45, 65–79. doi: 10.1002/(sici)1097-0029(19990415)45:2<65::aid-jemt2>3.0.co;2-0

Yi, W., Zhang, Y., Tian, Y., Guo, J., Li, Y., and Guo, A. (2013). A subset of cholinergic mushroom body neurons requires go signalling to regulate sleep in Drosophila. *Sleep* 36, 1809–1821. doi: 10.5665/sleep.3206

Yoshii, T., Todo, T., Wülbeck, C., Stanewsky, R., and Helfrich-Förster, C. (2008). Cryptochrome is present in the compound eyes and a subset of Drosophila's clock neurons. *J. Comp. Neurol.* 508, 952–966. doi: 10.1002/cne.21702

Yuan, Q., Joiner, W. J., and Sehgal, A. (2006). a sleep-promoting role for the drosophila serotonin receptor 1A. *Curr. Biol.* 16, 1051–1062. doi: 10.1016/j.cub.2006.04.032

Yuan, Q., Lin, F., Zheng, X., and Sehgal, A. (2005). Serotonin modulates circadian entrainment in Drosophila. *Neuron* 47, 115–127. doi: 10.1016/j.neuron.2005.05.027

Zerr, D. M., Hall, J. C., Rosbash, M., and Siwicki, K. K. (1990). Circadian fluctuations of period protein immunoreactivity in the CNS and the visual system of Drosophila. *J. Neurosci.* 10, 2749–2762. doi: 10.1523/jneurosci.10-08-02749.1990

Zhang, L., Lear, B. C., Seluzicki, A., and Allada, R. (2009). The CRYPTOCHROME photoreceptor gates PDF neuropeptide signalling to set circadian network hierarchy in Drosophila. *Curr. Biol.* 19, 2050–2055. doi: 10.1016/j.cub.2009.10.058

Zhang, Y., Liu, Y., Bilodeau-Wentworth, D., Hardin, P. E., and Emery, P. (2010). Light and temperature control the contribution of specific DN1 neurons to Drosophila circadian behaviour. *Curr. Biol.* 20, 600–605. doi: 10.1016/j.cub.2010.02.044

Zheng, L., de Polavieja, G. G., Wolfram, V., Asyali, M. H., Hardie, R. C., and Juusola, M. (2006). Feedback network controls photoreceptor output at the layer of first visual synapses in Drosophila. *J. Gen. Physiol.* 127, 495–510. doi: 10.1085/jgp.200509470

Zheng, Y., Hirschberg, B., Yuan, J., Wang, A. P., Hunt, D. C., Ludmerer, S. W., et al. (2002). Identification of two novel *Drosophila melanogaster* histamine-gated chloride channel subunits expressed in the eye. *J. Biol. Chem.* 277, 2000–2005. doi: 10.1074/jbc.M107635200

Zimmerman, J. E., Chan, M. T., Lenz, O. T., Keenan, B. T., Maislin, G., and Pack, A. I. (2017). Glutamate Is a Wake-Active Neurotransmitter in *Drosophila melanogaster*. *Sleep* 40:zsw046. doi: 10.1093/sleep/zsw046

Zuker, C. S., Cowman, A. F., and Rubin, G. M. (1985). Isolation and structure of a rhodopsin gene from *D. melanogaster*. *Cell* 40, 851–858. doi: 10.1016/0092-8674(85)90344-7

Zuker, C. S., Montell, C., Jones, K., Laverty, T., and Rubin, G. M. (1987). A rhodopsin gene expressed in photoreceptor cell R7 of the Drosophila eye: homologies with other signal-transducing molecules. *J. Neurosci.* 7, 1550–1557. doi: 10.1523/jneurosci.07-05-01550.1987

**Conflict of Interest:** The authors declare that the research was conducted in the absence of any commercial or financial relationships that could be construed as a potential conflict of interest.

frontiers in Physiology

REVIEW
published: 02 February 2021
doi: 10.3389/fphys.2021.622545

# Peripheral Sensory Organs Contribute to Temperature Synchronization of the Circadian Clock in *Drosophila melanogaster*

*Rebekah George and Ralf Stanewsky**

*Institute of Neuro- and Behavioral Biology, Westfälische Wilhelms-Universität Münster, Münster, Germany*

Circadian clocks are cell-autonomous endogenous oscillators, generated and maintained by self-sustained 24-h rhythms of clock gene expression. In the fruit fly *Drosophila melanogaster*, these daily rhythms of gene expression regulate the activity of approximately 150 clock neurons in the fly brain, which are responsible for driving the daily rest/activity cycles of these insects. Despite their endogenous character, circadian clocks communicate with the environment in order to synchronize their self-sustained molecular oscillations and neuronal activity rhythms (internal time) with the daily changes of light and temperature dictated by the Earth's rotation around its axis (external time). Light and temperature changes are reliable time cues (Zeitgeber) used by many organisms to synchronize their circadian clock to the external time. In *Drosophila*, both light and temperature fluctuations robustly synchronize the circadian clock in the absence of the other Zeitgeber. The complex mechanisms for synchronization to the daily light–dark cycles are understood with impressive detail. In contrast, our knowledge about how the daily temperature fluctuations synchronize the fly clock is rather limited. Whereas light synchronization relies on peripheral and clock-cell autonomous photoreceptors, temperature input to the clock appears to rely mainly on sensory cells located in the peripheral nervous system of the fly. Recent studies suggest that sensory structures located in body and head appendages are able to detect temperature fluctuations and to signal this information to the brain clock. This review will summarize these studies and their implications about the mechanisms underlying temperature synchronization.

**Keywords: circadian clock, temperature entrainment, chordotonal organ, antenna, rhodopsin, TRP channels, variant ionotropic glutamate receptors, period and timeless alternative splicing**

OPEN ACCESS

***Edited by:***
*Charalambos P. Kyriacou, University of Leicester, United Kingdom*

***Reviewed by:***
*Taishi Yoshii, Okayama University, Japan*
*Jadwiga Maria Giebultowicz, Oregon State University, United States*

***Correspondence:**
*Ralf Stanewsky*
*stanewsky@uni-muenster.de*

***Specialty section:***
*This article was submitted to Chronobiology, a section of the journal Frontiers in Physiology*

***Received:*** *28 October 2020*
***Accepted:*** *08 January 2021*
***Published:*** *02 February 2021*

***Citation:***
*George R and Stanewsky R (2021) Peripheral Sensory Organs Contribute to Temperature Synchronization of the Circadian Clock in Drosophila melanogaster. Front. Physiol. 12:622545. doi: 10.3389/fphys.2021.622545*

## INTRODUCTION

Ever since Colin Pittendrigh described stable entrainment of *Drosophila pseudobscura* eclosion rhythms to temperature cycles, it was clear that this geophysical rhythm serves as a potent Zeitgeber, at least in poikilothermic animals (Zimmerman et al., 1968). Later studies showed that the adult activity rhythms of *Drosophila melanogaster* can also be synchronized by temperature cycles (Wheeler et al., 1993). Remarkably, the difference between the temperature

"encoding" night and day can be as low 2–3°C, indicating that the fly clock is very sensitive to rhythmic temperature fluctuations (Wheeler et al., 1993; Chen et al., 2015). It was noted early on, that this apparent sensitivity to temperature changes presents some kind of paradox, considering the relative temperature independence of the free-running circadian period, known as temperature compensation (Zimmerman et al., 1968). Although theoretical considerations suggest that temperature entrainment and compensation properties are mechanistically linked (Pavlidis et al., 1968; Zimmerman et al., 1968), an alternative hypothesis is that they are based on largely independent processes. In support of this idea, all genetic variants that are known to affect temperature entrainment properties show normal temperature compensation (Glaser and Stanewsky, 2005; Wolfgang et al., 2013; Lee et al., 2014; Chen et al., 2015, see below).

The fly's central pacemaker consists of 150 clock neurons; all of which express the key clock genes, and are named based on their anatomical distribution in the dorsal and lateral protocerebrum as well as for their relative sizes (reviewed in Hermann-Luibl and Helfrich-Förster (2015)]. Briefly, the lateral neurons consist of four subgroups known as the large and small ventrolateral neurons (l-LNv and s-LNv, respectively), the 5th small ventrolateral neuron (5th s-LNv), the dorsolateral neurons (LNd) and the lateral posterior neurons (LPN). An additional three subgroups of clock neurons are positioned dorsally in the fly brain and are known as the DN1 anterior and posterior (DN1a and DN1p, respectively), DN2 and DN3 clock neurons.

As it is known for entrainment to light:dark (LD) cycles (e.g., Kaneko et al., 2000), all of the 150 clock neurons in the fly brain synchronize to temperature cycles, both in constant darkness (DD) and in constant light (LL) (Yoshii et al., 2005, 2009; Gentile et al., 2013; Chen et al., 2015). For LD entrainment, light input into the clock neurons is mediated both by the visual system and by the blue light photoreceptor Cryptochrome (Cry), which is expressed in about 50% of the central clock neurons (Helfrich-Förster, 2020), showing that both peripheral sensory organs (i.e., the compound eyes) and endogenous clock neuronal light reception (Cry) contribute to entrainment. In principle, the same could apply for temperature entrainment, but it would formally also be possible that (a) temperature perception is exclusively mediated by thermosensors in the PNS, or (b) that the clock neurons are thermosensitive per se, either due to expression of a thermoreceptor, or because aspects of clock gene expression (e.g., mRNA splicing) are directly sensitive to temperature changes. In the following, we summarize what is currently known about temperature synchronization of the circadian clock in *D. melanogaster* with emphasis on the central brain clock, known to drive the activity rhythms of the fly.

## DIRECT EFFECTS OF TEMPERATURE ON *per* AND *tim* SPLICING

Ambient temperature influences gene expression levels of hundreds of genes, including many genes with circadian functions (Boothroyd et al., 2007; Martin Anduaga et al., 2019). In addition, temperature modulates the amplitude and phase of *per* and *tim* expression, including the generation of alternatively spliced mRNAs [reviewed in Shakhmantsir and Sehgal (2019)]. Splicing of a *per* intron in the 3′-UTR (*dmpi8*) is increased at cooler temperatures and associated with higher daytime activity, while reduced *dmpi8* splicing at warm temperatures is correlated with delayed evening activity onset and extended daytime inactivity (siesta) (Majercak et al., 1999). Further studies implicated this *per* splicing event in the behavioral adaptation to hot and long summer days where less splicing leads to an increased siesta and a reduced risk of desiccation. Increased *per* splicing at cooler temperatures, most likely caused by less stringent hybridization of splicing factors with their target RNA, in turn support day activity as it is no longer harmful to the animal (Majercak et al., 1999, 2004; Collins et al., 2004). While these studies focused on potential effects of *per* splicing on *per* mRNA and PER accumulation to explain behavioral adaptation, a more recent study suggests a different molecular mechanism: cold-enhanced *dmpi8* splicing is not only correlated with enhanced *per* transcript levels, but also with increased transcript levels of the *daywake* gene (*dyw*). *dyw* encodes a juvenile hormone binding protein, which suppresses siesta behavior (Yang and Edery, 2019). The 3′ end of *dyw* overlaps with that of *per* and both genes are transcribed in opposite directions. It is therefore possible that the factors binding to the 3′ end of *per* and stabilize *per* mRNA, act *in trans* to stabilize *dyw* RNA. This intriguing mechanism would employ temperature and day-length dependent splicing of a core clock gene, but not its protein gene product (PER), to regulate a different gene (*dyw*) that directly influences siesta-promoting or -suppressing pathways (Yang and Edery, 2019).

The *tim* gene undergoes more complex temperature-dependent alternative splicing, which in contrast to *per* results in the generation of various truncated TIM proteins (Shakhmantsir and Sehgal, 2019). At warm temperatures (25–29°C) *tim* RNA undergoes an alternative splicing event, generating a transcript (named *tim-tiny* or *tim-M*), which retains an intron that introduces a premature stop codon (Shakhmantsir et al., 2018; Martin Anduaga et al., 2019). Rhythmic accumulation of $tim^{tiny}$ during the warm phase of a 30°C:25°C TC in DD and LL correlates with reduced levels of full-length TIM. It appears that translation of $tim^{tiny}$ mRNA is suppressed, resulting in extremely low levels of $TIM^{Tiny}$ protein, while levels of TIM are reduced due to overall *tim* mRNA depletion caused by generation of $tim^{tiny}$ transcripts (Shakhmantsir et al., 2018; Martin Anduaga et al., 2019). This mechanism presumably contributes to low TIM levels normally observed during the day, and to the delay between *tim* RNA and protein (Shakhmantsir et al., 2018). At cooler temperatures (18°C) *tim* RNA undergoes two different alternative splicing events resulting in the accumulation of *tim-cold*, *tim-short*, and cold (*tim-sc*) transcripts, which are translated into the respective truncated TIM proteins (Boothroyd et al., 2007; Martin Anduaga et al., 2019). Interestingly, flies in which generation of the *tim-sc* isoform is prevented ($tim^{sc}$) restrict their behavioral activity to the light phase in LD 25°C, a behavioral pattern that is usually observed at 18°C in wild type flies (Majercak et al., 1999; Martin Anduaga et al., 2019). This shows that the *tim-sc* transcript is not required for behavioral

adaptation to 18°C conditions, which presumably is mediated by increased levels of *tim-cold*. In support of this idea, *tim-cold* levels are strongly increased in $tim^{sc}$ flies (Martin Anduaga et al., 2019) as well as during cold temperatures (<18°C) in natural conditions, suggesting that the TIM-COLD protein plays a role in seasonal adaptation (Montelli et al., 2015). Even lower temperatures (<14°C) in combination with short photoperiods induce diapause or reproductive dormancy in *D. melanogaster* (Saunders and Gilbert, 1990). It has recently been shown that accumulation of the cotranscription factor EYES ABSENT (EYA) is required for an efficient transition to female diapause (Abrieux et al., 2020). Interestingly, TIM-SC is the major Tim isoform under 10°C, and presumably binds to, and stabilizes EYA under these conditions, thereby promoting diapause entry.

Alternative *tim* splicing is directly influenced by the base composition of the respective *tim* introns and their interaction with specific splicing factors (Shakhmantsir et al., 2018; Foley et al., 2019; Martin Anduaga et al., 2019). Down-regulation of the pre mRNA processing factor 4 (PRPR4), part of the tri-SNRP spliceosome, results in accumulation of the *tim-tiny* transcript and increased free-running period length (Shakhmantsir et al., 2018). In contrast, down-regulation of the alternative splicing factor P-element somatic inhibitor (PSI) results in an increase of *tim-cold* and *tim-sc* transcripts, while *tim-tiny* levels are reduced (Foley et al., 2019). These changes of *tim* transcript balance are associated with a shortening of the free-running period, and an altered activity phase during temperature cycles. While PSI does not affect the temperature-sensitivity of the various *tim* splicing events, the circadian function of PSI depends on *tim* splicing. This is because flies in which a *tim* loss-of-function mutant was rescued with a *tim* gene lacking all thermosensitively spliced introns, did not show a period shortening or phase difference after knock down of PSI (Foley et al., 2019).

Collectively, the studies on temperature-dependent *per* and *tim* splicing point to a function in behavioral and physiological (reproductive dormancy) adaptation to different environmental conditions as experienced in temperate climates. There is only limited information about the potential role of alternative splicing in the daily entrainment to temperature cycles. While PSI is required to set the correct activity phase during temperature cycles, it is not required for synchronization to these cycles, suggesting a role in adaptation rather than entrainment. Nevertheless, it is possible that temperature-dependent splicing events of clock gene RNAs within the clock neurons directly contribute to temperature entrainment and it will be of interest to see if mutations that abolish the generation of the various temperature-dependent *per* and *tim* isoforms show defects in temperature entrainment.

## CLOCK NEURONS IN ISOLATED FLY BRAINS ARE LARGELY UNRESPONSIVE TO TEMPERATURE CHANGES

Based on the apparent minor contribution of cell autonomous temperature-dependent clock RNA alternative splicing events to temperature entrainment, it seems plausible that peripheral thermosensors, and/or temperature-sensitive neurons within the brain, signal temperature information to the clock neurons. To distinguish between these possibilities, cultured isolated brains have been exposed to LD and temperature cycles, to study if clock gene expression within the clock neurons can be synchronized to these cycles. LD exposure led to synchronized *period-luciferase* expression in isolated brains, presumably mediated by expression of CRY within subsets of the clock neurons (Sehadova et al., 2009; Roberts et al., 2015). In contrast, exposure of cultured tissues to temperature cycles was able to synchronize *period-luciferase* oscillations in peripheral clock cells, but not in central brain clock neurons (Sehadova et al., 2009). While these results do not exclude the existence of cell autonomous mechanisms operating in a small subset of clock neurons, or that some neurons receive temperature input from a temperature sensor located in the central brain, it seems clear that the majority of clock neurons depends on peripheral input for entrainment to temperature cycles. In support of this, it has been shown that subsets of the DN1p clock neurons can be activated by short cooling steps and inhibited by small heating steps, and that this requires the brain to be part of the intact fly (Yadlapalli et al., 2018). In cultured brains, the clock neurons did not respond to temperature changes, and in the intact fly, the neuronal responses depend on input from peripheral thermosensors located in both the body and the aristae (Yadlapalli et al., 2018).

## SENSORY STRUCTURES LOCATED IN THE FLY BODY: A ROLE FOR THE CHORDOTONAL ORGAN IN TEMPERATURE RESPONSES

What are the peripheral sensory structures involved in circadian thermoreception and which molecules are involved in temperature sensing? A first clue to which structures might be involved came after a forward genetic screen that identified a mutant with defects in temperature entrainment (Glaser and Stanewsky, 2005). $nocte^1$ (for *no circadian temperature entrainment*) was interesting because the mutant abolished *period-luciferase* oscillations during LL and temperature cycles (isolation phenotype), but oscillations were normal in LD and constant temperature (Glaser and Stanewsky, 2005). Similarly, behavioral synchronization to temperature cycles is severely impaired in LL, DD and LD, but $nocte^1$ flies behave normally in LD and constant temperature (Glaser and Stanewsky, 2005; Sehadova et al., 2009; Chen et al., 2018). The *nocte* gene encodes a large (2300 amino acid) glutamine-rich protein of unknown function (Sehadova et al., 2009). $nocte^1$ carries a point mutation that introduces a STOP codon after amino acid 1706 resulting in a truncated protein with severely attenuated function (Sehadova et al., 2009). *nocte* is widely expressed in the fly body and brain, with particularly strong expression in sensory organs of the PNS, including that of the Chordotonal organs (Cho). These are internal stretch receptors found between joints of limbs and within body segments (e.g.: within the femoral joints, base of the wings, halteres, and in the second segment of the auditory

Johnston's organ of the antennae) (Kim et al., 2003; Tuthill and Wilson, 2016). The mechanosensory neurons that make up the chordotonal organs are positioned within scolopidia – the fundamental units of the chordotonal organ. Each scolopidium contains accessory cells like dendritic cap cells and scolopale cells that protect and anchor 1–3 sensory neurons (Tuthill and Wilson, 2016). Most Cho mediate proprioception (Tuthill and Wilson, 2016; Mamiya et al., 2018) but some are also involved in sensing sound, gravity, and wind (Matsuo and Kamikouchi, 2013). More recently it has been shown that rhythmic or monotonous stimulation of Cho neurons, mediates circadian synchronization and vibration-induced sleep, respectively (Simoni et al., 2014; Öztürk-Çolak et al., 2020).

Interestingly, it was shown that RNAi mediated knockdown of *nocte* within the Cho mimicked the *nocte*$^{1}$ behavioral phenotype in LL and temperature cycles (Sehadova et al., 2009). Moreover, both *nocte*$^{1}$ and Cho-specific knockdown reduced the electrical responses of the more dorsally located DN1 neurons (DN1p) to acute temperature changes, and *nocte*$^{1}$ interferes with synchronized PER and TIM expression in most clock neuronal subsets during temperature cycles (Chen et al., 2018; Yadlapalli et al., 2018), strongly implicating Cho as temperature sensors for clock neurons. In support of this, defects in Cho structure were present both in *nocte*$^{1}$ and to a lesser extend in the hypmorphic *nocte*$^{P}$ allele (Sehadova et al., 2009). Moreover, a temperature increase from 20 to 30°C induced movement-independent electrical responses in the leg nerve, which contains afferent projections from Cho neurons to the ventral nerve cord (VNC) (Chen et al., 2015). Finally, excitation of Cho neurons using rhythmic mechanical stimuli resulted in molecular and behavioral synchronization (Simoni et al., 2014). This synchronization was abolished in *nocte*$^{1}$ and in mutations known to interrupt mechanosensing Cho function, strongly indicating a connection between Cho and clock neurons. Existing evidence strongly implicates Cho function in temperature sensing for circadian clock synchronization. While a direct proof of adult Cho neuron temperature-sensitivity is missing, larval Cho are temperature sensitive and double their firing frequency when heated from 15 to 30°C (Liu et al., 2003; Scholz et al., 2017). In addition, the postulated neuronal circuit connecting Cho neurons with clock neurons in the brain remains to be identified.

## POTENTIAL THERMORECEPTORS IN THE CHORDOTONAL ORGAN

While it is very likely that Cho serve thermosensing functions in addition to their dominant role as proprioceptors, it is important to identify the molecular identity of the actual thermosensing molecules. Given the role of *nocte* for structural Cho integrity, it seems unlikely that this gene is important for thermosensing per se. Nevertheless, the NOCTE protein has been used to isolate interacting proteins, one of which belonged to the class of variant ionotropic glutamate receptors, IR25a (Chen et al., 2015). IR25a is expressed within subsets of the Cho neurons, and loss-of-function mutants fail to synchronize to temperature cycles both in LL and DD conditions. They show impaired synchronization of TIM oscillations within most subsets of the clock neurons, but particularly strong defects within the DN1 and DN2 (Chen et al., 2015), suggesting that theses neuronal groups receive temperature input from Cho neurons. Interestingly, entrainment defects of IR25a mutants are only observed in temperature cycles where the difference between night and day is <4°C, irrespective of the absolute temperature. This suggests that IR25a functions as an "amplitude-detector" rather than a thermometer, and that other thermosensors must exist to detect larger day/night temperature differences. That IR25a indeed functions as a temperature sensor in the Cho is supported by the fact that the movement-independent electrical responses to temperature increases in the leg nerve disappear in IR25a mutants. Moreover, ectopic expression of IR25a in the l-LNv clock neurons leads to temperature-dependent increase of neuronal firing, even if the temperature only increases by 2–3°C (Chen et al., 2015). While this is a strong indication that IR25a indeed acts as a thermoreceptor the temperature dependent increase in firing is quite moderate ($Q_{10} > 4$) compared to known thermoreceptors, as for example the thermo TRP channel TRPA1, whose ectopic expression in l-LNv clock neurons resulted in temperature-dependent increase of firing with a $Q_{10} > 12$ (Chen et al., 2015). It is possible that a sensor with weak temperature sensitivity is well suited as a circadian thermoreceptor. In contrast to a receptor that functions in fast avoidance responses to excessive heat or cold, temperature entrainment of the circadian clock requires responses to relatively small temperature changes over a long periods of time (hours) to allow reliable differentiation between night and day. In fact, fast responses to temperature changes, like those mediated by TRPA1, would presumably counteract circadian entrainment, because rapid temperature changes during the day, caused for example by sudden cloud cover or onset of rain, would activate such receptors.

Another potential thermoreceptor expressed in Cho is the TRPA channel PYREXIA (PYX). In contrast to *IR25a* and *nocte*, *pyx* is not expressed in Cho neurons, but in so-called cap cells, which connect the dendritic cilia of the Cho neuron with the cuticle (**Figure 1**; Wolfgang et al., 2013). The same distribution of *pyx* expression is found in Johnston's organ, the prominent Cho in the fly antennae, responsible for fly hearing and gravity sensing (Sun et al., 2009). Loss of *pyx* function results in impaired behavioral synchronization to 16°C:20°C temperature cycles both in LL and DD conditions (Wolfgang et al., 2013), along with altered PER synchronization in subsets of the clock neurons (including DN1 and s-LNv) (Roessingh et al., 2019). Interestingly, synchronization to warmer temperature cycles (e.g., 25°C:29°C) is normal (Wolfgang et al., 2013), indicating that PYX covers the low end of Drosophila's physiological temperature range, and that other receptors are responsible for sensing warmer temperatures. It is surprising that PYX function is required at low temperatures, given that this TRPA channel functions to protect the fly from extreme heat (>40°C) and is activated at these temperatures when expressed heterologously (Lee et al., 2005). Moreover, *pyx* mutants lack morning and evening activity peaks under seminatural LD combined with 25°C:35°C temperature cycles, indicating that this channel operates over a large range of temperatures (Green et al., 2015). While it is

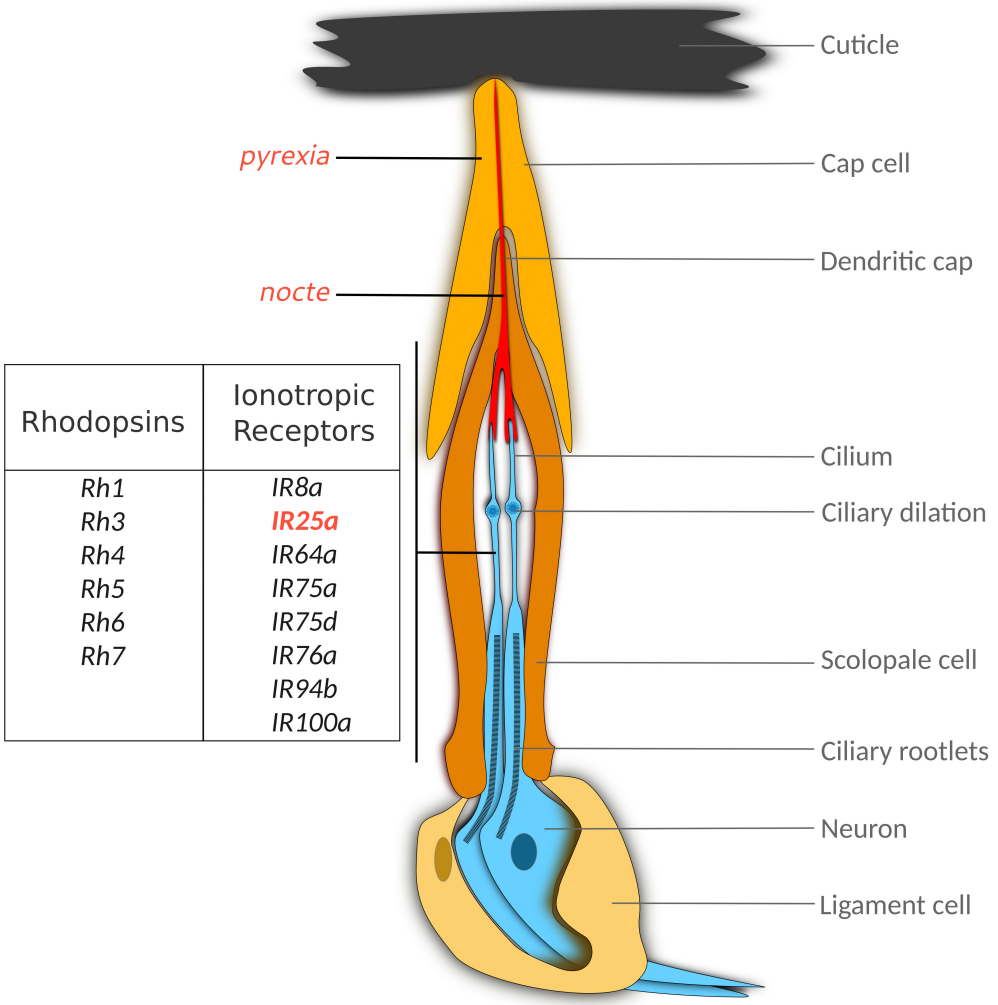


**FIGURE 1 |** Thermoreceptor candidates in the scolopidium, the basic unit of Chordotonal organs. Larval and adult scolopidia consist of three major cell types, (i) the bipoloar Cho neuron(s), (ii) the scolopale cell, which encloses the dendrites and forms an endolymph-filled extracellular space, and (iii), the cap cell, which connects the neuron with the cuticle. While the main function of this unit is the conversion of mechanical vibration to electrical neuronal signals, the genes indicated to the left may contribute to thermal responses described for larval and adult Cho. While *nocte* mutations disrupt the structure of the dendritic cap, it is not clear whether the *pyx, Rh* and *IR* genes fulfill structural or sensory roles (or both). Genes that have been implicated in synchronization to temperature cycles are indicated in red. See text for details.

possible that PYX expression in Cho cap cells contributes to temperature entrainment, recent findings suggest that neuronal *pyx* expression in the fly antennae plays an important role for clock synchronization (see below and Roessingh et al., 2019).

Other molecules potentially contributing to circadian temperature sensing within Cho include the TRPV channel INACTIVE (IAV). Structural integrity of larval Cho is required for choosing the preferred temperature (18°C) over cooler (14°C) temperatures (Kwon et al., 2010). Furthermore, the same study shows that expression of IAV within the larval Cho is required for this response, implicating this TRPV channel in temperature sensing or signaling. The same group showed that most of the Rhodopsin photopigments surprisingly also have temperature sensing capabilities within TRPA1 expressing cells in the larval body wall, the brain, and the VNC (Shen et al., 2011; Sokabe et al., 2016). For example, larvae mutant for the major fly Rhodopsin 1 were not able to choose the ideal temperature (18°C) compared to other comfortable temperatures (19–24°C), and this function could be replaced by substituting Rh1 with any other fly Rhodopsin (Rh2-Rh6), apart from Rh3 (Rh7 had not been identified then), and even by mouse circadian photopigment MELANOPSIN (Shen et al., 2011). Interestingly, two crucial components of the visual transduction cascade, the alpha subunit of the $G_q$ protein and PLC-ß, encoded by the *norpA* gene, are also required for larval temperature discrimination, as well as TRPA1, which is presumably regulated by this cascade (Shen et al., 2011; Sokabe et al., 2016). Recently, it was found that Rh1 and Rh6 are also expressed within larval Cho neurons, where they fulfill proprioceptive functions by supporting the structural integrity of Cho neuron dendrites

(Zanini et al., 2018). It seems therefore possible that Rhodopsins play a role in temperature synchronization, either as structural requirements for Cho integrity (similar to *nocte*), or as actual thermosensors in other cell types (see below).

## THERMORECEPTORS LOCATED IN THE FLY ANTENNAE

The antennae is an important thermosensory organ, housing several sensory structures that help the fly detect temperature changes and confer protection against adverse environmental conditions. In the second antennal segment, cells of the largest stretch-activated Cho of the fly, known as the Johnston's organ (JO) express Rh3, 4, 5 and 6, with Rh5 and Rh6 being important for hearing (Senthilan et al., 2012). Similarly, seven IR genes are expressed in JO (IR8a, 64a, 75a, 75d, 76a, 94b, 100a), and only IR75a has been linked to hearing, while IR64a and IR94b are not required for normal responses to acoustic stimuli (**Figure 1**) (Senthilan et al., 2012). While a role for the Rhodopsins in temperature preference has only been shown in larvae (Shen et al., 2011; Sokabe et al., 2016), it seems possible that a subset of the Cho-expressed Rhodopsin and IR receptors participate in thermal clock resetting (**Figures 1**, **2**). Moreover, the non-neuronal dendritic cap cells of the Cho express *pyrexia* (*pyx*) (**Figure 1**), which may also contribute to temperature entrainment (Sun et al., 2009; Wolfgang et al., 2013; Roessingh et al., 2019).

Thermoreceptors are also found in the sacculus – a multi-chambered invagination in the third segment of the fly antennae (Shanbhag et al., 1995). Ionotropic receptor (IR) expression is found in neurons innervating all three chambers of the sacculus. These receptors belong to the variant ionotropic glutamate receptor family (iGluR) and have been more extensively described for their role in chemo-sensation. Importantly, the neurons expressing the temperature sensitive IR25a and IR93a innervate chambers 1 and 2, while IR21a expression is found near chamber 3 (Benton et al., 2009; Abuin et al., 2011). On the other hand, the IRs functioning in hygrosensation (IR40a and IR68a), surround chambers 1 and 2 (**Figure 2**) (Enjin et al., 2016; Frank et al., 2017). Interestingly, IR25a and IR93a are co-expressed with IR40a here, and are also required for humidity responses (Enjin et al., 2016). The cooling-sensors Brivido 1-3 also function within the cold cells of sacculus chamber 3 (Gallio et al., 2011), as well as in the three cold cells at the base of the aristae – a feather-like extension from the third antennal segment. Flies with impaired function in any of the three *brivido* genes lose their rapid and extremely sensitive responses to cooling steps (Gallio et al., 2011). However, a more recent study indicates that these cold sensors are not required for temperature avoidance behaviors (Budelli et al., 2019).

Instead, expression of three different IRs in the three hot and three cold cells found at the base of the arista is required for mediating thermotactic behavior (Budelli et al., 2019). They first establish that the hot and cold cells do not function as hot and cold sensors, respectively, but can each respond to temperature changes in both the cool and warm range. Electrophysiological recordings show that hot cell responses are slow-adapting in nature, with firing levels correlating with the temperature increase (Q10∼4.4). Conversely, hot cells are inhibited by cooling. On the other hand, cold cells display transient activation in response to cooling and are inhibited by warming. IR25a and IR93a are found in both hot and cold cells, while IR21a expression is confined to the three cold cells. The hot cells also express the gustatory receptor Gr28b (Thorne and Amrein, 2008; Ni et al., 2013), which is necessary for warm responses when the rate of temperature increase is slow (∼1°C per second) (Liu et al., 2015). This warm receptor also plays a role in mediating avoidance of warm temperatures, albeit with less influence than warm avoidance mediated by IR21a expressed in the cold cells (Budelli et al., 2019).

Using transmission electron microscopy for a closer examination, it was shown that the characteristic layers of membrane lamellae of cold cell outer segments, and the "bossy" orthogonal surface substructures (BOSSs) between each layer were absent in IR93a, IR25a and IR21a mutants, with the most dramatic defects seen in the absence of the cold-cell exclusive IR21a (Budelli et al., 2019). These morphological defects likely compromise the efficiency of thermoreception in these cells, and this might explain why the mutants lose their ability to mediate thermotactic behavior. Additionally, ectopically expressing IR21a in hot cells not only allowed for cold-sensing activation in these cells (Ni et al., 2016; Budelli et al., 2019), but it also altered hot cell sensory endings so that they became enveloped by the cold cell's sensory endings, with BOSS structures between each outer segment membrane (Ni et al., 2016; Budelli et al., 2019). Considering these findings, it raises the question as to how exactly these IRs mediate temperature sensation. Are the receptors themselves thermoreceptive, or do they play a more indirect role where they are merely needed for contributing to the morphogenesis of the dendritic endings of sensory neurons? Ectopic expression of IR25a in the l-LNv conferred thermosensitivity to these clock neurons, which are normally imperceptive to temperature input, indicating that at least this IR may directly sense temperature (Chen et al., 2015). Irrespective of whether the IRs in the aristae are directly thermosensitive, it is clear that without the thermosensitive cells in the arista, the normal responses of the dorsal DN1p clock neurons are blunted, and the timing of sleep in Drosophila is altered during temperature cycles (Yadlapalli et al., 2018). Neither the thermosensitive molecules, nor the pathway that is involved to send input to the DN1p have been described.

Confirming if these temperature-sensitive receptors also play a role in entraining circadian rhythms to recurring temperature changes is still an ongoing and challenging effort. Of the potential temperature-sensing molecules in the antennae, only PYX has been shown to contribute to temperature entrainment. As discussed above, *pyx* mutants cannot entrain to temperature cycles in the cooler range (16°C:20°C) (Wolfgang et al., 2013). In addition to non-neuronal cap cell expression described above, *pyx* is also expressed within unidentified neurons of the 2nd and 3rd antennal segment (Sun et al., 2009; Tang et al., 2013; Roessingh and Stanewsky, 2017). Using a transcriptional reporter of intracellular calcium (TRIC) coupled to luciferase

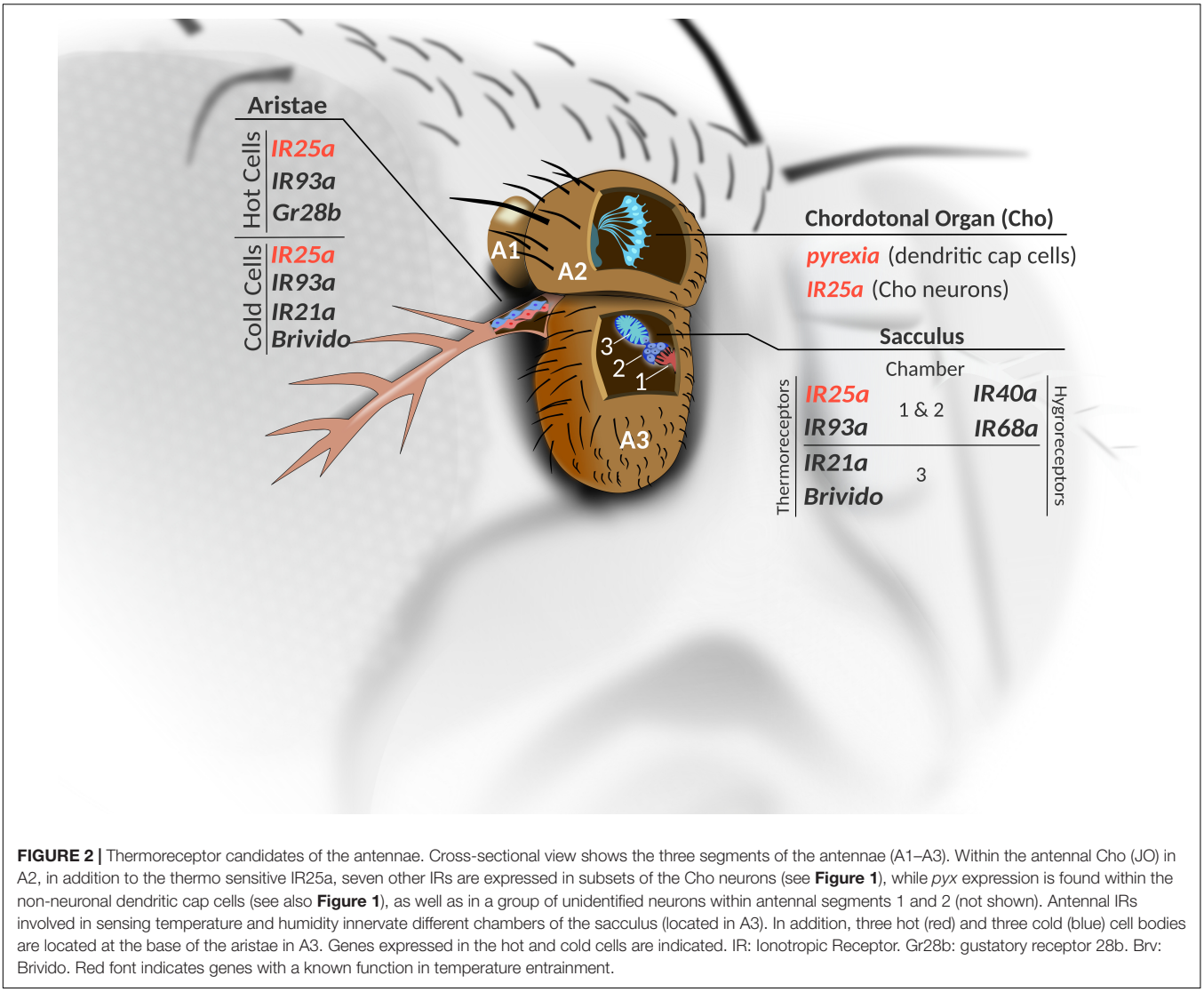


**FIGURE 2 |** Thermoreceptor candidates of the antennae. Cross-sectional view shows the three segments of the antennae (A1–A3). Within the antennal Cho (JO) in A2, in addition to the thermo sensitive IR25a, seven other IRs are expressed in subsets of the Cho neurons (see **Figure 1**), while *pyx* expression is found within the non-neuronal dendritic cap cells (see also **Figure 1**), as well as in a group of unidentified neurons within antennal segments 1 and 2 (not shown). Antennal IRs involved in sensing temperature and humidity innervate different chambers of the sacculus (located in A3). In addition, three hot (red) and three cold (blue) cell bodies are located at the base of the aristae in A3. Genes expressed in the hot and cold cells are indicated. IR: Ionotropic Receptor. Gr28b: gustatory receptor 28b. Brv: Brivido. Red font indicates genes with a known function in temperature entrainment.

for bioluminescence-based reporting, *pyx* mutant cells exhibited higher intracellular calcium levels specifically during temperature cycles, indicating abnormally high neuronal excitation levels (Roessingh et al., 2019). The authors hypothesized that mutant PYX channels result in defective signaling, which consequently affects synchronization of the PDF$^+$ s-LNVs and DN1 clock neuron subgroups. Consistent with this idea, removing these malfunctioning PYX channels by ablating the antennae, improved behavioral synchronization to temperature cycles (Roessingh et al., 2019). The circuit mediating temperature entrainment using input from the pyrexia expressing cells in the antennae has not been described.

The hot and cold cells of the aristae are known to target hot and cold glomeruli situated in the posterior antennal lobe (PAL), respectively (Frank et al., 2015) (**Figure 3**). The cold glomerulus also receives input from the cold cells in the sacculus. On the other hand, the *pyx* expressing neurons of the 2nd antennal segment are suggested to send input to the TRPA1 expressing neurons (AC neurons), and this input ultimately reaches the hot glomerulus of the PAL (Gallio et al., 2011; Tang et al., 2013). Later, it was shown that this region also receives dry and humidity signals sensed by hygrosensitive cells in the antennae (Frank et al., 2015), so that the sensory map of the PAL resembles a "hub" from which dendrites of ascending projection neurons (PNs) can extract and integrate information about temperature and humidity for sending to higher brain centers.

Three primary tracts ascending from PAL PNs take different paths but ultimately target the same higher brain centers like the lateral horn, the calyx of the mushroom body and the posterior lateral protocerebrum (PLP), all of which are important sensory processing centers (Heisenberg, 2003; Frank et al., 2015). It remains a question of interest to identify if any of these pathways carry information about daily temperature cycles from the antennae to entrain the clock neurons.

More recently, the complete circuit of one of the previously described PNs (R60H12, also referred to as thermosensory projection neuron TPN-II), starting from the peripheral temperature sensitive cells of the antennae, all the way to the

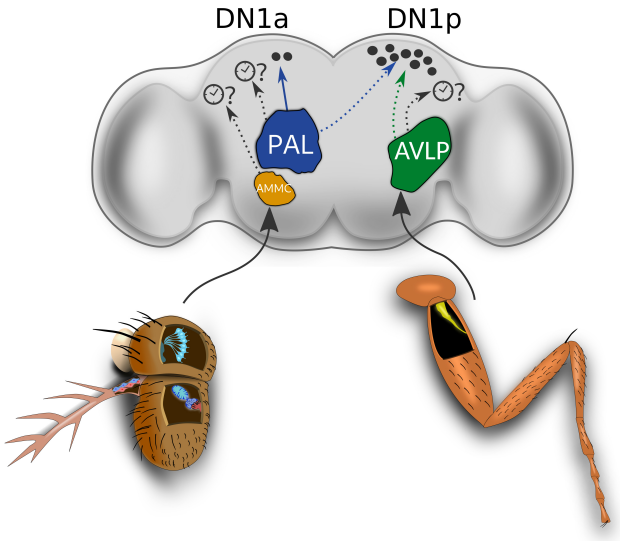


**FIGURE 3 |** Circuits potentially involved in circadian clock resetting by temperature. Temperature input from the thermoreceptive neurons of the sacculus and the aristae terminate in the PAL (shown in blue). From the PAL, a circuit for responses to absolute cold temperatures (below 25°C) to the DN1a clock neurons has been mapped (thermosensory projection neuron shown in the solid blue line). Other predicted thermo circuits from the PAL to the clock neurons are represented as black dotted lines. The antennal ChO neurons are known to target the AMMC (shown in orange), while the leg Cho neurons ascending from the leg neuropil of the VNC (not shown), target the most ventral region of the AVLP (shown in green) (Tsubouchi et al., 2017). Input from the *nocte* expressing Cho neurons in the body (e.g., the leg Cho), as well as from the thermoreceptive cells in the aristae mediate DN1p responses to brief temperature changes via unknown circuits (blue and green dotted lines). Other potential thermosensory circuits arising from the AMMC and the AVLP that could target other central clock neurons are represented as black dotted lines. This could, for example, include a circuit encoding input from the IR25a-expressing neurons within the leg Cho neurons, which mediate behavioral synchronization to shallow temperature cycles. DN1p: Posterior Dorsal Neuron 1. DN1a: Anterior Dorsal Neuron 1. PAL: Posterior Antennal Lobe. AVLP: anterior ventrolateral protocerebrum. AMMC: antennal mechanosensory and motor center.

two more anteriorly positioned DN1 clock neurons, DN1a, has been revealed (Alpert et al., 2020). Live calcium imaging and electrophysiological recordings confirmed that TPN-II is oblivious to heating steps, and only respond in a slow-adapting manner to absolute cold temperatures (below 25°C) with firing rates correlating with the absolute temperature reached. Notably, TPN-II innervates the PAL's cold glomerulus and collects input from three distinct cell types mediating detection of absolute cold temperatures. These include the chamber one cells of the sacculus, the cold cells in the aristae and interestingly – a new IR25a-expressing neuron within the head capsule. This latter thermosensitive neuron bears resemblance to the TRPA-1 anterior cell (AC) neurons, which also sit at the edge of the antennal nerve at the most anterior surface of the brain (Hamada et al., 2008). This finding suggests the existence of other anteriorly positioned neurons (i.e., novel AC neurons) expressing diverse thermoreceptive molecules. Of the three cell types that were shown to elicit slow-adaptive responses to absolute cold temperatures and to cooling steps, only the sacculus neurons exclusively responded to absolute cold temperatures, suggesting that they may be the primary contributors for TPN-II activity.

Importantly, this work showed that input from the cold thermosensors in the antennae was needed for inhibition of DN1a activity to allow normal temporal adaptation of sleep-wake patterns in a cold environment (Alpert et al., 2020). Taking this into consideration, TPN-II holds potential to also be involved in mediating temperature entrainment, since its slow-adapting manner of response to temperature input makes it ideal for resetting behavioral patterns in response to recurring temperature cycles. This work raises many other questions: Would separate TPNs responding to absolute warm be needed for temperature entrainment? Would warm-and cold-excited TPNs target the same clock neurons and if not, how would information about warm and cold signals be integrated by different oscillators to produce synchronization of locomotor activity? What is clear at this point is that much remains to be uncovered about the circuitries that contribute to temperature entrainment.

Despite the potential role for the antennal thermosensors in temperature entrainment, it has been clearly shown that flies can still entrain to temperature cycles without their antennae (Sehadova et al., 2009; Chen et al., 2015; Roessingh et al., 2019), meaning that the antennae and all its thermoreceptors are not required for temperature entrainment. Nevertheless, there are pathways carrying temperature input from the antennae that may actively contribute to temperature entrainment in the fly (Yadlapalli et al., 2018; Roessingh et al., 2019). Identifying the circadian thermoreceptors and mapping out these antennal circuits are still an important part of understanding temperature entrainment in *Drosophila*. Additionally, the dispensability of the antennae supports the existence of alternative thermosensory circuits, including Cho located in the body, and perhaps other thermosensors in the PNS or internal thermoreceptors within the head capsule (e.g., novel AC neurons) that are contributing to temperature entrainment in the absence of the antennae. Finally, one could consider drawing similarities to light entrainment. Both, the photoreceptors in the compound eyes and Cryptochrome in a portion of clock neurons, are known to mediate normal synchronization of the brain clock to light–dark cycles. No obvious light entrainment defects are observed if one of the two systems is impaired (see below and Stanewsky et al., 1998), and this supports the notion that the antenna is still a candidate thermosensory organ for mediating temperature entrainment.

## TRPA1

The involvement of TRPA1 in synchronization to temperature cycles is controversial. While it is clear that TRPA1 mediates an astonishing array of temperature-dependent behaviors during larval development and in adults (e.g., sleep, temperature preference, see above, and (Roessingh and Stanewsky, 2017) for a comprehensive review of TRPA1's role in temperature dependent behaviors), a prominent role in daily temperature entrainment can be excluded. Several TRPA1 isoforms with

different thermal properties exist (Bellemer, 2015). Temperature activation of TRPA1 can occur either directly (between 24 and 36°C depending on the isoform) or indirectly, at temperatures below 24°C, downstream of $G_q$ and PLC-ß signaling (see above and Bellemer, 2015). This complexity is likely responsible for the multitude of TRPA1 functions in regulating temperature-dependent behaviors and at the same time makes it difficult to assign functions to specific TRPA1 isoforms and their underlying activation mechanisms. With regard to temperature entrainment, it seemed possible that TRPA1 expression within thermosensitve "AC" neurons (Hamada et al., 2008) would contribute to temperature entrainment. But although they contact the s-LNv clock neurons, silencing of AC neurons or depleting them of TRPA1 did not prevent synchronization to DD 20°C:25°C or 25°C:29°C temperature cycles (Tang et al., 2017). Different *trpA1* reporter lines reveal varying degrees of *trpA1* expression in subsets of the clock neurons, although antibody staining or other in situ approaches have not confirmed this (Hamada et al., 2008; Lee and Montell, 2013; Yoshii et al., 2015). Nevertheless, analysis of *trpA1* mutants during 18°C:29°C temperature cycles in DD revealed only very subtle effects on behavioral temperature entrainment and PER oscillations within clock neurons (Lee and Montell, 2013). Subsequently, two independent studies concluded that TRPA1 is not required for temperature entrainment in 16°C:25°C, 20°C:29°C, and 21°C:29°C temperature cycles in DD (Roessingh et al., 2015; Das et al., 2016). Interestingly, the same studies revealed a role for TRPA1 in repressing day activity (the "siesta") during 20°C:29°C temperature cycles, which may have contributed to the initial interpretation that TRPA1 mediates temperature entrainment (Lee and Montell, 2013). In summary, while it is well established that TRPA1 regulates multiple temperature dependent behaviors during larval stages and in the adult fly (Roessingh and Stanewsky, 2017), temperature entrainment of the circadian clock appears to be one prominent exception.

## CLOCK NEURONAL TARGETS OF PERIPHERAL TEMPERATURE ENTRAINMENT

Several lines of evidence point to the DN1 group of clock neurons as one important "hub" for receiving temperature input from the periphery. First, DN1p are connected to two distinct sets of thermosensory neurons expressing TRPA1, which regulate the later onset of the siesta at very high temperatures (≥29°C) (Lamaze et al., 2017). Second, the DN1a are connected to a cold sensitive thermosensory circuit originating in the fly aristae (Alpert et al., 2020). The DN1a are inhibited by cold temperature (18°C) and likely contribute to the adaption of behavior to cold conditions (Zhang et al., 2010; Alpert et al., 2020). Interestingly, the sLNvs receive input from the DN1a neurons via CCHamide signaling for proper timing of sleep and activity, indicating that DN1a mediated temperature input could influence other clock neurons (Fujiwara et al., 2018). Third, subsets of the DN1p neurons are activated by brief cold, and inhibited by brief warm temperature changes, most likely related to their function of timing sleep during natural temperature cycles (Chen et al., 2018; Yadlapalli et al., 2018). As discussed above, DN1p temperature responses depend on the presence of intact peripheral thermosensors present in the aristae and Cho organs located in the body (**Figure 3**) (Yadlapalli et al., 2018). It seems therefore logical to assume that peripheral sensory input to the DN1 neurons also mediates synchronization to temperature cycles. Indeed, synchronization of TIM or PER expression in the DN1 was significantly altered in $IR25a^{-}$, $nocte^{1}$, and $pyx^{3}$ mutants (Chen et al., 2015, 2018; Roessingh et al., 2019), strongly supporting a role for this neuronal group in receiving temperature input from multiple peripheral thermosensors. Additionally, impairing DN1p neuronal activity affected temperature entrainment to both rectangular and gradually ramped temperature cycles (Chen et al., 2015; Yadlapalli et al., 2018). Further support for this came from a recent study analyzing the function of the daily plasticity changes of the dorsal s-LNv projections (extend and spread of arborizations), which are observed under constant temperature (LD and DD, Fernández et al., 2008) and, although less pronounced, also under temperature cycles (Fernandez et al., 2020). These projections harbor both pre- and postsynaptic structures, suggesting that apart from the prominent PDF-release dependent output functions, s-LNv dendritic projections in the dorsal brain may also receive signals from other neurons (Yasuyama and Meinertzhagen, 2010). During maximum arborization in the early morning, dorsal PDF-containing s-LNv projections are tightly intermingled with DN1p projections (Fernandez et al., 2020), and direct contacts between both cell types have been reported (Guo et al., 2016). Interestingly, abolishing the daily dorsal spreading of the s-LNv arborizations (and thereby presumably a direct connection between DN1p and s-LNv), resulted in an altered locomotor activity pattern during ramped 20°C:28°C temperature cycles, while behavior under constant temperature (LD and DD) was normal (Fernandez et al., 2020). Subsets of the DN1p release glutamate (Hamasaka et al., 2007; Guo et al., 2016), and mutations in both ionotropic and metabotropic glutamate receptors phenocopied the behavioral pattern of flies with depleted s-LNv arborizations (Fernandez et al., 2020). It therefore seems likely that during temperature cycles, the DN1p inhibit s-LNv activity via glutamate signaling in the early morning. While flies with impaired s-LNv plasticity clearly show altered behavioral patterns during temperature cycles, PER oscillations within their s-LNv were synchronized, albeit with reduced amplitude. Moreover, the behavioral rhythms were still entrained to the temperature cycle, and mainly showed a reduction of the main activity peak normally observed at the end of the warm phase (Fernandez et al., 2020). Therefore, it seems clear that other mechanisms must exist for synchronizing the s-LNv to temperature cycles. For example, it has been shown that the sLNv receive synaptic input from AC neurons, which is important for the regulation of the daily temperature preference rhythm (TPR), although AC neuron silencing did not impair temperature entrainment and various conditions (see above and Tang et al., 2017). Likewise, other clock neurons may receive input from other thermosensors and the DN1 could

also regulate activity of non s-LNv clock neurons, like the LNd (Guo et al., 2016).

## OTHER FACTORS INVOLVED IN TEMPERATURE ENTRAINMENT

To date there are only a few other genes that have been implicated in temperature entrainment of the fly clock. Flies lacking the phospholipase C-ß, (PLC-ß) encoded by the *norpA* gene, were found to block synchronization of *per-luc* expression and behavioral rhythms to temperature cycles in LL (Glaser and Stanewsky, 2005). This gene is also responsible for blocking alternative splicing of *dmpi8* in cold conditions, resulting in a "cold-locked" splicing mode in *norpA* mutants even during warm temperatures and long photoperiods (Collins et al., 2004; Majercak et al., 2004). When tested during temperature cycles in LL, levels of spliced *per* mRNA were higher in the *norpA* mutant flies compared to controls as expected (Glaser and Stanewsky, 2005, 2007). Interestingly, while always higher than in wild type controls, the ratio of spliced to unspliced *per* RNA in *norpA* mutants was not constant during the temperature cycle, but peaked at the end of the cold and beginning of the warm phase (morning), with a clear trough at the transition from warm to cold (evening) (Glaser and Stanewsky, 2005, 2007). Nevertheless, because there were no significant *per* splicing ratio oscillations observed in wild type control flies, it remains questionable if *per* splicing contributes to daily resetting to temperature cycles. While it seems well established that *norpA*-mediated regulation of *per* splicing contributes to seasonal adaptation (Collins et al., 2004; Majercak et al., 2004; Breda et al., 2020), the role of *norpA* in daily temperature entrainment remains elusive, potentially restricted to LL (Chen et al., 2020).

Phosphorylation of the transcription factor CLOCK (CLK) was also found to be important for daily temperature entrainment. Interestingly a mutant *Clock* gene, in which 15 potential serine phosphorylation sites are mutated to alanine, is able to support circadian rhythmicity in LD cycles and DD, while synchronization to temperature cycles is impaired. Both, rhythmicity in constant conditions, after exposure to temperature cycles as well as behavior during such cycles are affected, suggesting that rhythmic temperature signals ultimately influence CLK phosphorylation and thereby the levels and activity of this key circadian transcription factor (Lee et al., 2014).

Finally, in the mouse liver, heat shock factor 1 (HSF1) regulates rhythmic gene expression, including that of *mper2,* during temperature cycles, providing a potential mechanism for temperature entrainment of peripheral clocks in mammals (Saini et al., 2012). Based on these findings, and the observation that components of the HSP/HSP90 are rhythmically expressed in fly heads during temperature cycles (Boothroyd et al., 2007) the potential involvement of *Hsp90* in temperature entrainment was studied (Goda et al., 2014). While there was no clear effect of *Hsp90* mutants on molecular entrainment of *per* and *tim* gene products in whole fly heads, loss of *Hsp90* function surprisingly resulted in faster behavioral resetting to advanced (but not to delayed) temperature cycles (16°C:28°C). While this could point toward a specific role for *Hsp90* in clock neurons, the altered behavioral patterns during temperature resetting more likely reflect the increased behavioral plasticity of *Hsp90* mutants (Hung et al., 2009).

## SYNCHRONIZATION OF PERIPHERAL CLOCKS

There are numerous reports demonstrating that peripheral clocks of the fly can be synchronized to temperature cycles. Most studies used protein or RNA extracts from fly heads, which mainly report clock gene expression in the compound eye photoreceptors, which are considered to contain peripheral clocks. These studies show that clock gene expression can be synchronized to temperature cycles both in LL and DD, both at the RNA and protein level (Stanewsky et al., 1998; Glaser and Stanewsky, 2005; Yoshii et al., 2005; Boothroyd et al., 2007; Martin Anduaga et al., 2019). In addition, whole-fly bioluminescence expression emanating from *period* and *timeless-luciferase* transgenes, which report clock genes expression in abdominal and eye clocks, are robustly synchronized by temperature cycles (Glaser and Stanewsky, 2005; Sehadova et al., 2009; Harper et al., 2017). Interestingly, while CRY is important for light entrainment of peripheral clocks (Ivanchenko et al., 2001), CRY is not required for temperature synchronization of clock gene cycling in the periphery – at least when measured in the context of the intact fly (Stanewsky et al., 1998; Glaser and Stanewsky, 2005; Harper et al., 2017). With regard to actual biological rhythms regulated by peripheral clocks, CRY's role appears ambiguous: While the adult cuticle deposition rhythm can be synchronized to temperature cycles in the absence of CRY (Ito et al., 2011), electroantennogram (EAG) rhythms in the fly antennae, which reflect the daily changes of olfactory sensitivity, cannot (Krishnan et al., 2001). Most likely, this discrepancy is related to an additional, light-independent function of CRY as central clock factor in subsets of the peripheral clocks (Collins et al., 2006).

The experiments described above do not reveal if peripheral clocks can be entrained without a functional connection to the central clock in the fly brain. To address the autonomy of peripheral clock entrainment by temperature cycles, isolated fly tissues (legs, wings, heads, abdomen, proboscis, halteres, and antennae) of *per-luc* and *tim-luc* flies have been exposed to temperature cycles in culture (Krishnan et al., 2001; Glaser and Stanewsky, 2005; Sehadova et al., 2009). These experiments clearly showed that peripheral clocks of all tissues can be synchronized in an at least a tissue autonomous way. While CRY is not required for peripheral clock entrainment by temperature in whole flies (see above), this has not been conclusively addressed in isolated peripheral clocks: Tissues of *per-luc* and *tim-luc* $cry^b$ flies were entrained to temperature cycles, and subsequently measured in constant temperature in DD (Krishnan et al., 2001; Levine et al., 2002). Compared to $cry^+$, the number of rhythmic $cry^b$ tissue samples was significantly reduced, which mostly likely simply reflects the requirement of CRY for

maintaining circadian clock function in peripheral clocks. It remains to be determined if CRY is required for peripheral clock oscillations in isolated tissues during temperature cycles.

It seems likely that cell-autonomous mechanisms mediate peripheral clock entrainment to temperature cycles, perhaps involving some of the temperature-dependent alternative splicing events discussed at the beginning of this article. Nevertheless, all tissues tested so far are located at the surface of the fly; therefore, contribution of sensory thermoreceptors cannot be excluded. It is noteworthy however, that constant light-induced arrhythmic sperm release and transfer in the abdomen of the moth *Spodoptera littoralis* is restored by temperature cycles (Syrova et al., 2003).

## DIFFICULTIES STUDYING TEMPERATURE ENTRAINMENT

From our discussion above, several problems associated with the study of temperature entrainment are obvious. Over a wide range of physiological temperatures, (16–29°C, outside the range of temperatures inducing diapause or heat stress) temperature cycles with a small amplitude (2°C difference between day and night) serve as a potent Zeitgeber for entrainment. It appears that different thermo receptors operate in different temperature intervals (e.g., PYX in the lower range), and that some receptors are able to detect temperature differences over the entire spectrum (e.g., IR25a). It follows, that in order to determine the contribution of a candidate receptor, a multitude of entrainment conditions needs to be tested (e.g., PYX would not have been found if only 20–29°C temperature cycles had been used). Moreover, there is the possibility and likelihood of redundancy as observed in light entrainment. For example, it is difficult to observe entrainment defects of *cry* mutants in standard LD cycles, due to the contribution of the compound eyes (Stanewsky et al., 1998). Only by applying more complex entrainment regimes (e.g., shifts of the LD cycles, light intensity changes) or by combining different mutants (e.g., visual system and *cry*), the contribution of each system is revealed. Therefore, care must be taken before ruling out the contribution of a certain factor or molecular mechanism (for example the alternative splicing mechanisms discussed at the beginning of this article) to temperature entrainment. In addition, a powerful assay for studying light entrainment is not really working for temperature: depending on the time of day, brief light-pulses elicit robust behavioral and molecular phase advances or delays, giving rise to informative phase response curves (PRCs). In contrast, comparable temperature pulses are basically incapable of inducing phase shifts, at least as long as they are within the physiological range (e.g., Busza et al., 2007). While this makes sense from a biological perspective (it would be disadvantageous if sudden weather-inflicted temperature changes would serve as stable resetting cues), it mitigates against a rapid and efficient analysis of potential new temperature entrainment factors.

Finally, constant light (LL) served as a powerful tool for identifying factors acting in the light input pathway (e.g., Emery et al., 2000; Peschel et al., 2006; Dubruille et al., 2009). When it comes to testing if a genetic variation is required for synchronizing the clock to temperature cycles, it makes sense to eliminate the other main *Zeitgeber* (LD cycles) – by keeping the light conditions constant. In DD temperature cycles synchronize behavioral activity peaks to occur in the first half of the thermophase (Gentile et al., 2013). Interestingly, while temperature cycles also robustly synchronize the circadian clock in LL, overriding the effects that normally lead to the constitutive degradation of TIM, (Glaser and Stanewsky, 2005; Yoshii et al., 2005) the behavioral activity peaks occur toward the second half of the thermophase (Gentile et al., 2013). While this (and temperature synchronization in LL) is an interesting and unresolved phenomenon as such, it adds another dimension to the problem of temperature entrainment and even more environmental conditions that need to be scrutinized when genetic variants are tested for their potential contribution. In other words, it is possible that mutants interfere with temperature entrainment in DD but not in LL and vice versa, which is why it is best to test the contribution of candidate genetic variants to temperature entrainment in both DD and LL conditions. While it could be argued that studying temperature entrainment in LL is a somewhat artificial construct, it may actually be a relevant condition experienced by animals (including some fly species) north of the polar circle in summer. While still being exposed to changes in light intensity and quality during the polar summer, temperature cycles may gain importance as more reliable Zeitgeber compared to light (cf., Harper et al., 2016).

## CONCLUSION AND OUTLOOK

It appears that the entrainment mechanisms have evolved to allow for fast behavioral responses to rapidly changing temperature changes to avoid immediately harmful conditions, while still using the relatively small temperature changes between day and night as potent Zeitgeber. Interestingly, and comparable to light-entrainment and direct effects of light on behavior, subsets of the clock neurons are used to integrate both modalities and to coordinate the appropriate behavior. While for temperature this involves the DN1p (see above and Lamaze and Stanewsky, 2019), the l-LNv have been shown to mediate both direct effects of light (e.g., arousal) and entrainment (Rosato and Kyriacou, 2008; Schlichting, 2020). Interestingly, both light and temperature entrainment employ cell-autonomous mechanisms and peripheral sensory organs for proper synchronization. In the case of light, this is accomplished by the compound eyes and CRY expressed in subsets of the clock neurons, as well as by CRY for synchronization of peripheral clocks. For temperature, it appears that the clock neurons mainly rely on peripheral sensory input, while peripheral clocks presumably employ an as yet unidentified cell-autonomous mechanism. From what is known so far, peripheral input to the central clock appears complex, involving various sensory structures and different families of thermos-receptive molecules (IRs and TRP channels). Future work will certainly extend the list of existing players and will shed light on the neuronal circuits

connecting the peripheral sensors with the clock circuit. It will be particularly challenging to disentangle how the clock can distinguish sudden and potentially harmful temperature changes from the regular daily changes of average temperature it needs for clock resetting.

## AUTHOR CONTRIBUTIONS

RG and RS wrote and edited the manuscript. Both authors contributed to the article and approved the submitted version.

## FUNDING

This work was supported by the European Union's Horizon 2020 Research and Innovation Programme under the Marie Skłodowska-Curie grant agreement no. 765937 (CINCHRON).

## ACKNOWLEDGMENTS

We thank Luis Garcia for artwork and Angelique Lamaze and Patrick Emery for comments on the manuscript.

## REFERENCES

Abrieux, A., Xue, Y., Cai, Y., Lewald, K. M., Nguyen, H. N., Zhang, Y., et al. (2020). EYES ABSENT and TIMELESS integrate photoperiodic and temperature cues to regulate seasonal physiology in *Drosophila*. *Proc. Natl. Acad. Sci. U.S.A.* 117, 15293–15304. doi: 10.1073/pnas.2004262117

Abuin, L., Bargeton, B., Ulbrich, M. H., Isacoff, E. Y., Kellenberger, S., and Benton, R. (2011). Functional architecture of olfactory ionotropic glutamate receptors. *Neuron* 69, 44–60. doi: 10.1016/j.neuron.2010.11.042

Alpert, M. H., Frank, D. D., Kaspi, E., Flourakis, M., Zaharieva, E. E., Allada, R., et al. (2020). A circuit encoding absolute cold temperature in *Drosophila*. *Curr. Biol.* 30, 2275–2288.e5. doi: 10.1016/j.cub.2020.04.038

Bellemer, A. (2015). Thermotaxis, circadian rhythms, and TRP channels in *Drosophila*. *Temperature* 2, 227–243. doi: 10.1080/23328940.2015.1004972

Benton, R., Vannice, K. S., Carolina, G.-D., and Vosshall, L. B. (2009). Variant ionotropic glutamate receptors as chemosensory receptors in *Drosophila*. *Cell* 136, 149–162. doi: 10.1016/j.cell.2008.12.001

Boothroyd, C., Wijnen, H., Naef, F., Saez, L., and Young, M. (2007). Integration of light and temperature in the regulation of circadian gene expression in *Drosophila*. *PLoS Genet.* 3:e54. doi: 10.1371/journal.pgen.0030054

Breda, C., Rosato, E., and Kyriacou, C. P. (2020). Norpa signalling and the seasonal circadian locomotor phenotype in *Drosophila*. *Biology* 9:130. doi: 10.3390/biology9060130

Budelli, G., Ni, L., Berciu, C., van Giesen, L., Knecht, Z. A., Chang, E. C., et al. (2019). Ionotropic receptors specify the morphogenesis of phasic sensors controlling rapid thermal preference in *Drosophila*. *Neuron* 101, 738–747.e3. doi: 10.1016/j.neuron.2018.12.022

Busza, A., Murad, A., and Emery, P. (2007). Interactions between circadian neurons control temperature synchronization of *Drosophila* Behavior. *J. Neurosci.* 27, 10722–10733. doi: 10.1523/JNEUROSCI.2479-07.2007

Chen, C., Buhl, E., Xu, M., Croset, V., Rees, J. S., Lilley, K. S., et al. (2015). *Drosophila* Ionotropic Receptor 25a mediates circadian clock resetting by temperature. *Nature* 527, 516–520. doi: 10.1038/nature16148

Chen, C., Xu, M., Anantaprakorn, Y., Rosing, M., and Stanewsky, R. (2018). nocte is required for integrating light and temperature inputs in circadian clock neurons of *Drosophila*. *Curr. Biol.* 28, 1595–1605.e3. doi: 10.1016/j.cub.2018.04.001

Chen, C., Xu, M., Correa, P., and Stanewsky, R. (2020). A temperature-dependent molecular switch to adjust behavior to changing environmental conditions. *Neurosci. bioRxiv [Preprint]* doi: 10.1101/2020.03.27.011361

Collins, B., Mazzoni, E. O., Stanewsky, R., and Blau, J. (2006). *Drosophila* CRYPTOCHROME is a circadian transcriptional repressor. *Curr. Biol.* 16, 441–449. doi: 10.1016/j.cub.2006.01.034

Collins, B., Rosato, E., and Kyriacou, C. (2004). Seasonal behavior in *Drosophila* melanogasterrequires the photoreceptors, the circadian clock, and phospholipase C. *Proc. Natl. Acad. Sci. U.S.A.* 101, 1945–1950. doi: 10.1073/pnas.0308240100

Das, A., Holmes, T., and Sheeba, V. (2016). dTRPA1 in non-circadian neurons modulates temperature-dependent rhythmic activity in *Drosophila* melanogaster. *J. Biol. Rhythms* 31, 272–288. doi: 10.1177/0748730415627037

Dubruille, R., Murad, A., Rosbash, M., and Emery, P. (2009). A constant light-genetic screen identifies KISMET as a regulator of circadian photoresponses. *PLoS Genet.* 5:e1000787. doi: 10.1371/journal.pgen.1000787

Emery, P., Stanewsky, R., Hall, J., and Rosbash, M. (2000). A unique circadian-rhythm photoreceptor. *Nature* 404, 456–457. doi: 10.1038/35006558

Enjin, A., Zaharieva, E. E., Frank, D. D., Mansourian, S., Suh, G. S. B., Gallio, M., et al. (2016). Humidity sensing in *Drosophila*. *Curr. Biol.* 26, 1352–1358. doi: 10.1016/j.cub.2016.03.049

Fernández, M. P., Berni, J., and Ceriani, M. F. (2008). Circadian remodeling of neuronal circuits involved in rhythmic behavior. *PLoS Biol.* 6:e69. doi: 10.1371/journal.pbio.0060069

Fernandez, M. P., Pettibone, H. L., Bogart, J. T., Roell, C. J., Davey, C. E., Pranevicius, A., et al. (2020). Sites of circadian clock neuron plasticity mediate sensory integration and entrainment. *Curr. Biol.* 30, 2225–2237.e5. doi: 10.1016/j.cub.2020.04.025

Foley, L. E., Ling, J., Joshi, R., Evantal, N., Kadener, S., and Emery, P. (2019). *Drosophila* PSI controls circadian period and the phase of circadian behavior under temperature cycle via tim splicing. *eLife* 8:e50063. doi: 10.7554/eLife.50063

Frank, D., Jouandet, G., Kearney, P., Macpherson, L., and Gallio, M. (2015). Temperature representation in the *Drosophila* brain. *Nature* 519, 358–361. doi: 10.1038/nature14284

Frank, D. D., Enjin, A., Jouandet, G. C., Zaharieva, E. E., Para, A., Stensmyr, M. C., et al. (2017). Early integration of temperature and humidity stimuli in the *Drosophila* Brain. *Curr. Biol.* 27, 2381–2388.e4. doi: 10.1016/j.cub.2017.06.077

Fujiwara, Y., Hermann-Luibl, C., Katsura, M., Sekiguchi, M., Ida, T., Helfrich-Förster, C., et al. (2018). The CCHamide1 neuropeptide expressed in the anterior dorsal neuron 1 conveys a circadian signal to the ventral lateral neurons in *Drosophila* melanogaster. *Front. Physiol.* 9:1276. doi: 10.3389/fphys.2018.01276

Gallio, M., Ofstad, T. A., Macpherson, L. J., Wang, J. W., and Zuker, C. S. (2011). The coding of temperature in the *Drosophila* Brain. *Cell* 144, 614–624. doi: 10.1016/j.cell.2011.01.028

Gentile, C., Sehadova, H., Simoni, A., Chen, C., and Stanewsky, R. (2013). Cryptochrome antagonizes synchronization of *Drosophila*'s circadian clock to temperature cycles. *Curr. Biol.* 23, 185–195. doi: 10.1016/j.cub.2012.12.023

Glaser, F., and Stanewsky, R. (2005). Temperature synchronization of the *Drosophila* circadian clock. *Curr. Biol.* 15, 1352–1363. doi: 10.1016/j.cub.2005.06.056

Glaser, F., and Stanewsky, R. (2007). Synchronization of the *Drosophila* circadian clock by temperature cycles. *Cold Spring Harb. Symp. Quant. Biol.* 72, 233–242. doi: 10.1101/sqb.2007.72.046

Goda, T., Sharp, B., and Wijnen, H. (2014). Temperature-dependent resetting of the molecular circadian oscillator in *Drosophila*. *Proc. R. Soc. Lond. B Biol. Sci* 281:20141714. doi: 10.1098/rspb.2014.1714

Green, E. W., Emma, K. O., Hansen, C. N., Bastianello, S., Bhutani, S., Vanin, S., et al. (2015). *Drosophila* circadian rhythms in seminatural environments: Summer afternoon component is not an artifact and requires TrpA1 channels. *Proc. R. Soc. Lond. B Biol. Sci.* 112, 8702–8707. doi: 10.1073/pnas.1506093112

Guo, F., Yu, J., Jung, H., Abruzzi, K., Luo, W., Griffith, L., et al. (2016). Circadian neuron feedback controls the *Drosophila* sleep–activity profile. *Nature* 536, 292–297. doi: 10.1038/nature19097

Hamada, F., Rosenzweig, M., Kang, K., Pulver, S., Ghezzi, A., Jegla, T., et al. (2008). An internal thermal sensor controlling temperature preference in *Drosophila*. *Nature* 454, 217–220. doi: 10.1038/nature07001

Hamasaka, Y., Rieger, D., Parmentier, M., Grau, Y., Charlotte, H.-F., and Nässel, D. (2007). Glutamate and its metabotropic receptor in *Drosophila* clock neuron circuits. *J. Comp. Neurol.* 505, 32–45. doi: 10.1002/cne.21471

Harper, R. E. F., Dayan, P., Albert, J. T., and Stanewsky, R. (2016). Sensory conflict disrupts activity of the *Drosophila* circadian network. *Cell Rep.* 17, 1711–1718. doi: 10.1016/j.celrep.2016.10.029

Harper, R. E. F., Ogueta, M., Dayan, P., Stanewsky, R., and Albert, J. T. (2017). Light dominates peripheral circadian oscillations in *Drosophila melanogaster* during sensory conflict. *J. Biol. Rhythms* 32, 423–432. doi: 10.1177/0748730417724250

Heisenberg, M. (2003). Mushroom body memoir: from maps to models. *Nat. Rev. Neurosci.* 4, 266–275. doi: 10.1038/nrn1074

Helfrich-Förster, C. (2020). Light input pathways to the circadian clock of insects with an emphasis on the fruit fly *Drosophila* melanogaster. *J. Comp. Physiol. A Neuroethol. Sens. Neural. Behav. Physiol.* 206, 259–272. doi: 10.1007/s00359-019-01379-5

Hermann-Luibl, C., and Helfrich-Förster, C. (2015). Clock network in *Drosophila*. *Curr. Opin. Insect Sci.* 7, 65–70. doi: 10.1016/j.cois.2014.11.003

Hung, H.-C., Kay, S., and Weber, F. (2009). HSP90, a capacitor of behavioral variation. *J. Biol. Rhythms* 24, 183–192. doi: 10.1177/0748730409333171

Ito, C., Goto, S. G., Tomioka, K., and Numata, H. (2011). Temperature entrainment of the circadian cuticle deposition rhythm in *Drosophila* melanogaster. *J. Biol. Rhythms* 26, 14–23. doi: 10.1177/0748730410391640

Ivanchenko, M., Stanewsky, R., and Giebultowicz, J. (2001). Circadian photoreception in *Drosophila*: functions of cryptochrome in peripheral and central clocks. *J. Biol. Rhythms* 16, 205–215. doi: 10.1177/074873040101600303

Kaneko, M., Park, J., Cheng, Y., Hardin, P., and Hall, J. (2000). Disruption of synaptic transmission or clock-gene-product oscillations in circadian pacemaker cells of *Drosophila* cause abnormal behavioral rhythms. *J. Neurobiol.* 43, 207–233. doi: 10.1002/(sici)1097-4695(20000605)43:3<207::aid-neu1>3.0.co;2-0

Kim, J., Chung, Y., Park, D., Choi, S., Shin, D., Soh, H., et al. (2003). A TRPV family ion channel required for hearing in *Drosophila*. *Nature* 424, 81–84. doi: 10.1038/nature01733

Krishnan, B., Levine, J. D., Lynch, M. K., Dowse, H. B., Funes, P., Hall, J. C., et al. (2001). A new role for cryptochrome in a *Drosophila* circadian oscillator. *Nature* 411, 313–317. doi: 10.1038/35077094

Kwon, Y., Shen, W. L., Shim, H.-S., and Montell, C. (2010). Fine thermotactic discrimination between the optimal and slightly cooler temperatures via a TRPV channel in chordotonal neurons. *J. Neurosci.* 30, 10465–10471. doi: 10.1523/JNEUROSCI.1631-10.2010

Lamaze, A., Öztürk-Çolak, A., Fischer, R., Peschel, N., Koh, K., and Jepson, J. E. C. (2017). Regulation of sleep plasticity by a thermo-sensitive circuit in *Drosophila*. *Sci. Rep.* 7:40304. doi: 10.1038/srep40304

Lamaze, A., and Stanewsky, R. (2019). DN1p or the "Fluffy" cerberus of clock outputs. *Front. Physiol.* 10:1540. doi: 10.3389/fphys.2019.01540

Lee, E., Jeong, E., Jeong, H., Yildirim, E., Vanselow, J., Ng, F., et al. (2014). Phosphorylation of a central clock transcription factor is required for thermal but not photic entrainment. *PLoS Genet.* 10:e1004545. doi: 10.1371/journal.pgen.1004545

Lee, Y., Lee, Y., Lee, J., Bang, S., Hyun, S., Kang, J., et al. (2005). Pyrexia is a new thermal transient receptor potential channel endowing tolerance to high temperatures in *Drosophila* melanogaster. *Nat. Genet.* 37, 305–310. doi: 10.1038/ng1513

Lee, Y., and Montell, C. (2013). *Drosophila* TRPA1 functions in temperature control of circadian rhythm in pacemaker neurons. *J. Neurosci.* 33, 6716–6725. doi: 10.1523/JNEUROSCI.4237-12.2013

Levine, J. D., Funes, P., Dowse, H. B., and Hall, J. C. (2002). Advanced analysis of a cryptochrome mutation's effects on the robustness and phase of molecular cycles in isolated peripheral tissues of *Drosophila*. *BMC Neurosci.* 3:5. doi: 10.1186/1471-2202-3-5

Liu, L., Yermolaieva, O., Johnson, W., Abboud, F., and Welsh, M. (2003). Identification and function of thermosensory neurons in *Drosophila* larvae. *Nat. Neurosci.* 6, 267–273. doi: 10.1038/nn1009

Liu, W., Mazor, O., and Wilson, R. (2015). Thermosensory processing in the *Drosophila* brain. *Nature* 519, 353–357. doi: 10.1038/nature14170

Majercak, J., Chen, W.-F., and Edery, I. (2004). Splicing of the period gene 3′-terminal intron is regulated by light, circadian clock factors, and phospholipase C. *Mol. Cell. Biol.* 24, 3359–3372. doi: 10.1128/mcb.24.8.3359-3372.2004

Majercak, J., Sidote, D., Hardin, P., and Edery, I. (1999). How a circadian clock adapts to seasonal decreases in temperature and day length. *Neuron* 24, 219–230. doi: 10.1016/S0896-6273(00)80834-X

Mamiya, A., Gurung, P., and Tuthill, J. C. (2018). Neural coding of leg proprioception in *Drosophila*. *Neuron* 100, 636–650.e6. doi: 10.1016/j.neuron.2018.09.009

Martin Anduaga, A., Evantal, N., Patop, I. L., Bartok, O., Weiss, R., and Kadener, S. (2019). Thermosensitive alternative splicing senses and mediates temperature adaptation in *Drosophila*. *eLife* 8:e44642. doi: 10.7554/eLife.44642

Matsuo, E., and Kamikouchi, A. (2013). Neuronal encoding of sound, gravity, and wind in the fruit fly. *J. Comp. Physiol. A Neuroethol. Sens. Neural. Behav. Physiol.* 199, 253–262. doi: 10.1007/s00359-013-0806-x

Montelli, S., Mazzotta, G., Vanin, S., Caccin, L., Corrà, S., De Pittà, C., et al. (2015). period and *timeless* mRNA splicing profiles under natural conditions in *Drosophila melanogaster*. *J. Biol. Rhythms* 30, 217–227. doi: 10.1177/0748730415583575

Ni, L., Bronk, P., Chang, E. C., Lowell, A. M., Flam, J. O., Panzano, V. C., et al. (2013). A gustatory receptor paralogue controls rapid warmth avoidance in *Drosophila*. *Nature* 500, 580–584. doi: 10.1038/nature12390

Ni, L., Klein, M., Svec, K., Budelli, G., Chang, E., Ferrer, A., et al. (2016). The ionotropic receptors IR21a and IR25a mediate cool sensing in *Drosophila*. *eLife* 5:e13254. doi: 10.7554/eLife.13254

Öztürk-Çolak, A., Inami, S., Buchler, J. R., McClanahan, P. D., Cruz, A., Fang-Yen, C., et al. (2020). Sleep induction by mechanosensory stimulation in *Drosophila*. *Cell Rep.* 33:108462. doi: 10.1016/j.celrep.2020.108462

Pavlidis, T., Zimmerman, W. F., and Osborn, J. (1968). A mathematical model for the temperature effects on circadian rhythms. *J. Theor. Biol.* 18, 210–221. doi: 10.1016/0022-5193(68)90162-8

Peschel, N., Veleri, S., and Stanewsky, R. (2006). *Veela* defines a molecular link between Cryptochrome and Timeless in the light-input pathway to *Drosophila*'s circadian clock. *Proc. R. Soc. Lond. B Biol. Sci.* 103, 17313–17318. doi: 10.1073/pnas.0606675103

Roberts, L., Leise, T. L., Noguchi, T., Galschiodt, A. M., Houl, J. H., Welsh, D. K., et al. (2015). Light evokes rapid circadian network oscillator desynchrony followed by gradual phase retuning of synchrony. *Curr. Biol.* 25, 858–867. doi: 10.1016/j.cub.2015.01.056

Roessingh, S., Rosing, M., Marunova, M., Ogueta, M., George, R., Lamaze, A., et al. (2019). Temperature synchronization of the *Drosophila* circadian clock protein PERIOD is controlled by the TRPA channel PYREXIA. *Commun. Biol.* 2:246. doi: 10.1038/s42003-019-0497-0

Roessingh, S., and Stanewsky, R. (2017). The *Drosophila* TRPA1 channel and neuronal circuits controlling rhythmic behaviours and sleep in response to environmental temperature. *Int. J. Mol. Sci.* 18:2028. doi: 10.3390/ijms18102028

Roessingh, S., Wolfgang, W., and Stanewsky, R. (2015). Loss of *Drosophila* melanogaster TRPA1 function affects "siesta" behavior but not synchronization to temperature cycles. *J. Biol. Rhythms* 30, 492–505. doi: 10.1177/0748730415605633

Rosato, E., and Kyriacou, C. (2008). Sleep, arousal, and rhythms in flies. *Proc. Natl. Acad. Sci. U.S.A.* 105, 19567–19568. doi: 10.1073/pnas.0811124106

Saini, C., Morf, J., Stratmann, M., Gos, P., and Schibler, U. (2012). Simulated body temperature rhythms reveal the phase-shifting behavior and plasticity of mammalian circadian oscillators. *Genes Dev.* 26, 567–580. doi: 10.1101/gad.183251.111

Saunders, D. S., and Gilbert, L. I. (1990). Regulation of ovarian diapause in *Drosophila* melanogaster by photoperiod and moderately low temperature. *J. Insect Physiol.* 36, 195–200. doi: 10.1016/0022-1910(90)90122-V

Schlichting, M. (2020). Entrainment of the *Drosophila* clock by the visual system. *Neurosci. Insights* 15, 1–16. doi: 10.1177/2633105520903708

Scholz, N., Guan, C., Nieberler, M., Grotemeyer, A., Maiellaro, I., Gao, S., et al. (2017). Mechano-dependent signaling by Latrophilin/CIRL quenches cAMP in proprioceptive neurons. *eLife* 6:e28360. doi: 10.7554/eLife.28360

Sehadova, H., Glaser, F. T., Gentile, C., Simoni, A., Giesecke, A., Albert, J. T., et al. (2009). Temperature entrainment of *Drosophila*'s circadian clock involves the gene nocte and signaling from peripheral sensory tissues to the brain. *Neuron* 64, 251–266. doi: 10.1016/j.neuron.2009.08.026

Senthilan, P. R., Piepenbrock, D., Ovezmyradov, G., Nadrowski, B., Bechstedt, S., Pauls, S., et al. (2012). *Drosophila* auditory organ genes and genetic hearing defects. *Cell* 150, 1042–1054. doi: 10.1016/j.cell.2012.06.043

Shakhmantsir, I., Nayak, S., Grant, G. R., and Sehgal, A. (2018). Spliceosome factors target timeless (tim) mRNA to control clock protein accumulation and circadian behavior in *Drosophila*. *eLife* 7:e39821. doi: 10.7554/eLife.39821

Shakhmantsir, I., and Sehgal, A. (2019). Splicing the clock to maintain and entrain circadian rhythms. *J. Biol. Rhythms* 34, 584–595. doi: 10.1177/0748730419868136

Shanbhag, S. R., Singh, K., and Singh, R. N. (1995). Fine structure and primary sensory projections of sensilla located in the sacculus of the antenna of *Drosophila* melanogaster. *Cell Tissue Res.* 282, 237–249. doi: 10.1007/BF00319115

Shen, W. L., Kwon, Y., Adegbola, A. A., Luo, J., Chess, A., and Montell, C. (2011). Function of rhodopsin in temperature discrimination in *Drosophila*. *Science* 331, 1333–1336. doi: 10.1126/science.1198904

Simoni, A., Wolfgang, W., Topping, M. P., Kavlie, R. G., Stanewsky, R., and Albert, J. T. (2014). A mechanosensory pathway to the *Drosophila* circadian clock. *Science* 343, 525–528. doi: 10.1126/science.1245710

Sokabe, T., Chen, H.-C., Luo, J., and Montell, C. (2016). A switch in thermal preference in *Drosophila* larvae depends on multiple rhodopsins. *Cell Rep.* 17, 336–344. doi: 10.1016/j.celrep.2016.09.028

Stanewsky, R., Kaneko, M., Emery, P., Beretta, B., Wager-Smith, K., Kay, S., et al. (1998). Thecrybmutation identifiescryptochromeas a circadian photoreceptor inDrosophila. *Cell* 95, 681–692.

Sun, Y., Liu, L., Ben-Shahar, Y., Jacobs, J., Eberl, D., and Welsh, M. (2009). TRPA channels distinguish gravity sensing from hearing in Johnston's organ. *Proc. Natl. Acad. Sci. U.S.A.* 106, 13606–13611. doi: 10.1073/pnas.0906377106

Syrova, Z., Sauman, I., and Giebultowicz, J. M. (2003). Effects of light and temperature on the circadian system controlling sperm release in moth Spodoptera littoralis. *Chronobiol. Int.* 20, 809–821. doi: 10.1081/cbi-120024217

Tang, X., Platt, M. D., Lagnese, C. M., Leslie, J. R., and Hamada, F. N. (2013). Temperature integration at the AC thermosensory neurons in *Drosophila*. *J. Neurosci. Off. J. Soc. Neurosci.* 33, 894–901. doi: 10.1523/JNEUROSCI.1894-12.2013

Tang, X., Roessingh, S., Hayley, S. E., Chu, M. L., Tanaka, N. K., Wolfgang, W., et al. (2017). The role of PDF neurons in setting the preferred temperature before dawn in *Drosophila*. *eLife* 6:e23206. doi: 10.7554/eLife.23206

Thorne, N., and Amrein, H. (2008). Atypical expression of *Drosophila* gustatory receptor genes in sensory and central neurons. *J. Comp. Neurol.* 506, 548–568. doi: 10.1002/cne.21547

Tsubouchi, A., Yano, T., Yokoyama, T. K., Murtin, C., Otsuna, H., and Ito, K. (2017). Topological and modality-specific representation of somatosensory information in the fly brain. *Science* 358, 615–623. doi: 10.1126/science.aan4428

Tuthill, J. C., and Wilson, R. I. (2016). Mechanosensation and adaptive motor control in insects. *Curr. Biol.* 26, R1022–R1038. doi: 10.1016/j.cub.2016.06.070

Wheeler, D., Melanie, H.-C., Dushay, M., and Hall, J. (1993). Behavior in light-dark cycles of *Drosophila* mutants that are arrhythmic, blind, or both. *J. Biol. Rhythms* 8, 67–94. doi: 10.1177/0748730493008 00106

Wolfgang, W., Simoni, A., Gentile, C., and Stanewsky, R. (2013). The Pyrexia transient receptor potential channel mediates circadian clock synchronization to low temperature cycles in *Drosophila* melanogaster. *Proc. Biol. Sci.* 280:20130959. doi: 10.1098/rspb.2013.0959

Yadlapalli, S., Jiang, C., Bahle, A., Reddy, P., Meyhofer, E., and Shafer, O. T. (2018). Circadian clock neurons constantly monitor environmental temperature to set sleep timing. *Nature* 555, 98–102. doi: 10.1038/nature25740

Yang, Y., and Edery, I. (2019). Daywake, an anti-siesta gene linked to a splicing-based thermostat from an adjoining clock gene. *Curr. Biol.* 29, 1728–1734.e4. doi: 10.1016/j.cub.2019.04.039

Yasuyama, K., and Meinertzhagen, I. A. (2010). Synaptic connections of PDF-immunoreactive lateral neurons projecting to the dorsal protocerebrum of *Drosophila* melanogaster. *J. Comp. Neurol.* 518, 292–304. doi: 10.1002/cne.22210

Yoshii, T., Christiane, H.-L., Kistenpfennig, C., Schmid, B., Tomioka, K., and Charlotte, H.-F. (2015). Cryptochrome-dependent and -independent circadian entrainment circuits in *Drosophila*. *J. Neurosci.* 35, 6131–6141. doi: 10.1523/JNEUROSCI.0070-15.2015

Yoshii, T., Heshiki, Y., Ibuki-Ishibashi, T., Matsumoto, A., Tanimura, T., and Tomioka, K. (2005). Temperature cycles drive *Drosophila* circadian oscillation in constant light that otherwise induces behavioural arrhythmicity. *Eur. J. Neurosci.* 22, 1176–1184. doi: 10.1111/j.1460-9568.2005.04295.x

Yoshii, T., Vanin, S., Costa, R., and Charlotte, H.-F. (2009). Synergic entrainment of *Drosophila*'s circadian clock by light and temperature. *J. Biol. Rhythms* 24, 452–464. doi: 10.1177/0748730409348551

Zanini, D., Giraldo, D., Warren, B., Katana, R., Andrés, M., Reddy, S., et al. (2018). Proprioceptive opsin functions in *Drosophila* larval locomotion. *Neuron* 98, 67–74.e4. doi: 10.1016/j.neuron.2018.02.028

Zhang, Y., Liu, Y., Diana, B.-W., Hardin, P. E., and Emery, P. (2010). Light and temperature control the contribution of specific DN1 neurons to *Drosophila* circadian behavior. *Curr. Biol.* 20, 600–605. doi: 10.1016/j.cub.2010.02.044

Zimmerman, W., Pittendrigh, C., and Pavlidis, T. (1968). Temperature compensation of the circadian oscillation in *Drosophila* pseudoobscura and its entrainment by temperature cycles. *J. Insect Physiol.* 14, 669–684. doi: 10.1016/0022-1910(68)90226-6

**Conflict of Interest:** The authors declare that the research was conducted in the absence of any commercial or financial relationships that could be construed as a potential conflict of interest.

frontiers in Physiology

ORIGINAL RESEARCH
published: 08 March 2021
doi: 10.3389/fphys.2021.633866

# Body Temperature and Activity Rhythms Under Different Photoperiods in High Arctic Svalbard ptarmigan (*Lagopus muta hyperborea*)

*Daniel Appenroth[1]*, Andreas Nord[1,2], David G. Hazlerigg[1] and Gabriela C. Wagner[1,3]**

[1]*Arctic Chronobiology and Physiology, Arctic and Marine Biology, UiT The Arctic University of Norway, Tromsø, Norway,* [2]*Section for Evolutionary Ecology, Department of Biology, Lund University, Lund, Sweden,* [3]*Division of Forest and Forest Resources, Norwegian Institute of Bioeconomy Research (NIBIO), Tromsø, Norway*

OPEN ACCESS

***Edited by:***
*Charalambos P. Kyriacou, University of Leicester, United Kingdom*

***Reviewed by:***
*Cory Williams, University of Alaska Fairbanks, United States*
*Gisele Akemi Oda, University of São Paulo, Brazil*

****Correspondence:***
*Gabriela C. Wagner*
*gabriela.wagner@nibio.no;*
*gwa011@uit.no*
*Daniel Appenroth*
*daniel.appenroth@uit.no*

***Specialty section:***
*This article was submitted to Chronobiology, a section of the journal Frontiers in Physiology*

***Received:*** *26 November 2020*
***Accepted:*** *15 February 2021*
***Published:*** *08 March 2021*

***Citation:***
*Appenroth D, Nord A, Hazlerigg DG and Wagner GC (2021) Body Temperature and Activity Rhythms Under Different Photoperiods in High Arctic Svalbard ptarmigan (Lagopus muta hyperborea). Front. Physiol. 12:633866. doi: 10.3389/fphys.2021.633866*

Organisms use circadian rhythms to anticipate and exploit daily environmental oscillations. While circadian rhythms are of clear importance for inhabitants of tropic and temperate latitudes, its role for permanent residents of the polar regions is less well understood. The high Arctic Svalbard ptarmigan shows behavioral rhythmicity in presence of light-dark cycles but is arrhythmic during the polar day and polar night. This has been suggested to be an adaptation to the unique light environment of the Arctic. In this study, we examined regulatory aspects of the circadian control system in the Svalbard ptarmigan by recording core body temperature ($T_b$) alongside locomotor activity in captive birds under different photoperiods. We show that $T_b$ and activity are rhythmic with a 24-h period under short (SP; L:D 6:18) and long photoperiod (LP; L:D 16:8). Under constant light and constant darkness, rhythmicity in $T_b$ attenuates and activity shows signs of ultradian rhythmicity. Birds under SP also showed a rise in $T_b$ preceding the light-on signal and any rise in activity, which proves that the light-on signal can be anticipated, most likely by a circadian system.

**Keywords: Arctic, chronobiology, circadian rhythm, heterothermy, photoperiod, thermoregulation, Svalbard ptarmigan**

## INTRODUCTION

The Earth's rotation around its own axis causes daily oscillations in environmental factors such as light and ambient temperature. Circadian rhythms have evolved to maintain behavioral, physiological, and metabolic synchrony with these ambient cycles, and to anticipate changing conditions within a day. Disruption of this synchrony can consequently affect fitness and survival (DeCoursey et al., 1997, 2000; DeCoursey and Krulas, 1998; Daan et al., 2011; Spoelstra et al., 2016). Biochemical oscillators, so-called circadian clocks, endogenously produce rhythmicity by transcription-translation-feedback loops, in which clock genes are expressed and subsequently inhibited due to the action of their own translated proteins (Hardin et al., 1990; Darlington et al., 1998). In higher vertebrates, circadian rhythmicity is ultimately produced by a single hypothalamic

master clock (the suprachiasmatic nucleus in mammals) or a network of clocks (in the pineal gland, eyes and the hypothalamus of bird and reptiles; Menaker et al., 1997). These master clocks entrain to the environmental cycle primarily through the light-dark signal (Pittendrigh, 1960) and impose rhythmicity onto peripheral tissue, e.g., by circulating hormones such as melatonin produced in the pineal gland (Pevet and Challet, 2011). This ultimately leads to rhythmic physiology and behavior.

At tropical and temperate latitudes, the light-dark progression and other environmental factors, such as ambient temperature, cycle on a 24-h period throughout the year. This is not the case at polar latitudes, which are instead characterized by extended periods of constant light (polar day) and constant darkness (polar night) with short periods of rapidly changing photoperiod in-between. During the polar day and polar night, animals inhabiting these latitudes are either free running, arrhythmic, or entrained to non-photic or photic cues other than photoperiod (Swade and Pittendrigh, 1967; van Oort et al., 2007; Stelzer and Chittka, 2010; Williams et al., 2011; Ashley et al., 2012; Steiger et al., 2013; Arnold et al., 2018; Hüppe et al., 2020; van Beest et al., 2020; Ware et al., 2020). On the Svalbard archipelago, which is among the northernmost landmasses in the Arctic (74°–81°N, **Figure 1B**), the Sun remains ≥6° below the horizon between mid-November and February but is constantly above the horizon between mid-April and mid-September. Despite the high latitude, the climate is relatively mild due to warm ocean currents (average temperature in Longyearbyen in December: −6.0°C; Norwegian-Meterological-Institute, 2020). This is probably why some cold-hardy species can survive there year-round, including the world's most northerly distributed land bird, the Svalbard ptarmigan (*Lagopus muta hyperborea*; **Figure 1A**). Svalbard ptarmigan exhibit rhythmic activity during the short periods of light-dark cycles, but become arrhythmic during the polar day and polar night (Stokkan et al., 1986; Reierth and Stokkan, 1998). Similarly, plasma melatonin rhythms attenuate under such conditions (Reierth et al., 1999). This suggests that either the central circadian clock cannot sustain rhythmicity, or that

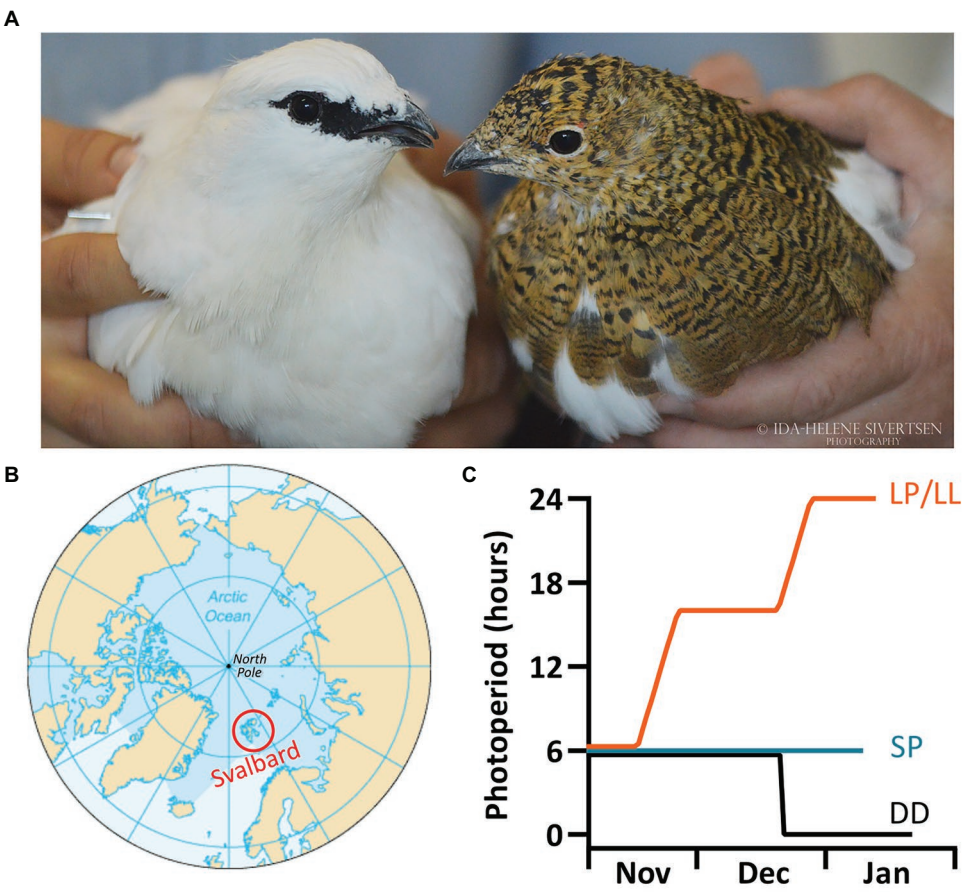


**FIGURE 1 |** Svalbard ptarmigan (*Lagopus muta hyperborea*) and experimental design. **(A)** The picture shows a Svalbard ptarmigan male in white winter plumage and a female in the cryptic brown summer plumage (© Ida-Helene Sivertsen). **(B)** The Svalbard ptarmigan is a subspecies of the rock ptarmigan (*Lagopus muta*) but is geographically isolated to the high Arctic archipelago of Svalbard and Franz Josef Land. **(C)** The experimental birds were bred at the University of Tromsø and were separated into three groups: the short photoperiod (SP) group remained under L:D 6:18. The LP/LL-group was gradually transferred from L:D 6:18 to L:D 16:8 (LP), and subsequently into constant light (LL). The constant darkness (DD) group was directly transferred from L:D 6:18 into DD.

its molecular output is uncoupled from the peripheral tissue responses in constant light and constant darkness (Bloch et al., 2013). The above mentioned studies indicate that adaptation to life in the high Arctic has had profound effects on the circadian system. However, little is known of the physiological parameters that underlie circadian control. For this reason, we explored the implication of Arctic life on the circadian control of core body temperature ($T_b$).

Most endothermic animals display a daily $T_b$ rhythm, which is under circadian control and characterized by lower $T_b$ during the rest phase and higher $T_b$ during the active phase (Menaker, 1959; Aschoff, 1983; Refinetti and Menaker, 1992). The function of the $T_b$ rhythm is still disputed. The decrease in $T_b$ during the rest phase might reduce energy costs by lowering the need for thermogenesis, though in the case of non-torpid and non-hibernating endotherms this reduction in $T_b$ might be too small to have a significant impact on the energy budget (Menaker, 1959; Refinetti and Menaker, 1992). Temperature changes within the physiological range have also been shown to sustain rhythmicity in mammalian liver and lung cultures (Brown et al., 2002; Buhr et al., 2010) and it has been proposed that $T_b$ serves the master clock to synchronize peripheral tissue. In a polar animal, $T_b$ might serve the same purpose, especially since melatonin rhythms are often attenuated under the polar day and polar night (Miché et al., 1991; Reierth et al., 1999; Stokkan et al., 2007). There is evidence of sustained $T_b$-rhythmicity through the polar day in Arctic ground squirrels (*Urocitellus parryii*; Long et al., 2005; Williams et al., 2011), but we are unaware of similar studies in Arctic birds.

In order to characterize the $T_b$ rhythm in a truly Arctic bird and explore its possible circadian control, we implanted abdominal temperature loggers into captive Svalbard ptarmigan and recorded $T_b$ and activity under short photoperiod (SP), long photoperiod (LP), in constant light (LL) and constant darkness (DD; **Figure 1C**). These photoperiodic treatments were chosen to study expression of the $T_b$ and activity rhythm under entrained conditions (SP and LP) as well as under conditions without entrainable cues, i.e., in free running conditions (LL and DD). We also studied if there were differences in the timing of the rise in activity and $T_b$ before the light-on signal when birds were under SP and LP, because this "anticipatory behavior" could indicate the presence of a functional time-keeping system.

# MATERIALS AND METHODS

## Housing

All animals were kept at the University of Tromsø in accordance with the EU directive 201/63/EU and licenses provided by the Nowegian Food Safety authority (Mattilsynet, permit nos. FOTS 8115 for 2015/2016 and FOTS 7971 for 2017/2018). Chicks were hatched from eggs laid by captive females in 2015 and 2017, and were reared either in outdoor cages under natural Tromsø photoperiod (69° 39′ N, 18° 57′ E), or indoors with a photoperiod corresponding to the natural light cycle in Tromsø. When the chicks had reached a body mass of 500 g or more (usually by the end of September in the year of hatching), they were transferred to indoor cages with *ad libitum* access to food (Norgesfor, ref. no. OK2400 070316) and water. Ambient temperature was kept between 3 and 7°C throughout the experiment, which is within the thermo-neutral zone of physically mature Svalbard ptarmigan (Mortensen and Blix, 1986).

Illumination was provided by fluorescent strip lights (Osram L 58W 830 Lumilux, Osram, Munich, Germany), delivering 1,000 lux at floor level. Under constant darkness, illumination was provided by dim red light only (Northlight 36-6557, 15 lm, Clas Ohlson, Insjön, Sweden), which delivered less than 1 lux at floor level.

## Photoperiodic Treatment

All experiments were conducted from 30.09.2015 to 04.02.2016 and from 22.12.2017 to 08.04.2018. Birds hatched in the 2015/2016 season were exposed to three different photoperiodic treatments (**Figure 1C**). Initially, all birds were transferred into a photoperiod of L:D 12:12, which was gradually (1 h/day) decreased to L:D 6:18. The birds were subsequently kept in either L:D 6:18 (SP-group, $n$ = 7) or were gradually (1 h/day) transferred into L:D 16:8 (LP), and then to LL (LP/LL-group, $n$ = 8). Birds from the 2017 cohort were directly transferred from L:D 6:18 to DD (DD-group, $n$ = 3). All birds were kept in their respective final light treatments until the end of the experiment. Photoperiodic treatments and exposure times for each bird can be found online at DataverseNO.[1]

## Core Body Temperature Recording

Core body temperature was measured using iButton temperature loggers (DS1922L, Maxim Integrated, San Jose, CA, United States; accuracy: ±0.5°C, resolution: ±0.0625°C). All iButtons were calibrated in a high precision water bath (model 6025, Hart Scientific, Pleasant Grove, UT, United States), the temperature of which was monitored by a factory-calibrated (Nordtec, Gothenburg, Sweden) Testo 925 thermometer with a type K thermocouple (Testo, PA, United States; birds from the 2015 cohort) or a high precision glass thermometer (birds from the 2017 cohort). Calibration was performed in 5°C increments between 35 and 45°C. This range covered the full range of core $T_b$ shown by Svalbard ptarmigan over the course of the year (Nord and Folkow, 2018).

The calibrated iButtons were implanted into the abdominal cavity under gas anesthesia. Specifically, the birds were anesthetized with a 4% isoflurane air mix (Ref. No.: 9623, KDG Baxter, Deerfield, IL, United States) injected through an anesthetic facemask connected to an Ohmeda vaporizer (Ref. No.: 058294, BOC Health Care, Guildford, United Kingdom) and an isoflurane vaporizer (Vapor 2000, Ref. No.: ARXH-1225, Dräger, Lübeck, Germany). Surgery started as soon as the bird showed muscle relaxation and did not respond to a physical stimulus (pinching of the skin).

The place of incision, i.e., ventrocaudal from the sternum, was located, plucked of feathers and disinfected with 2% iodine

[1]https://doi.org/10.18710/XLDXQ3

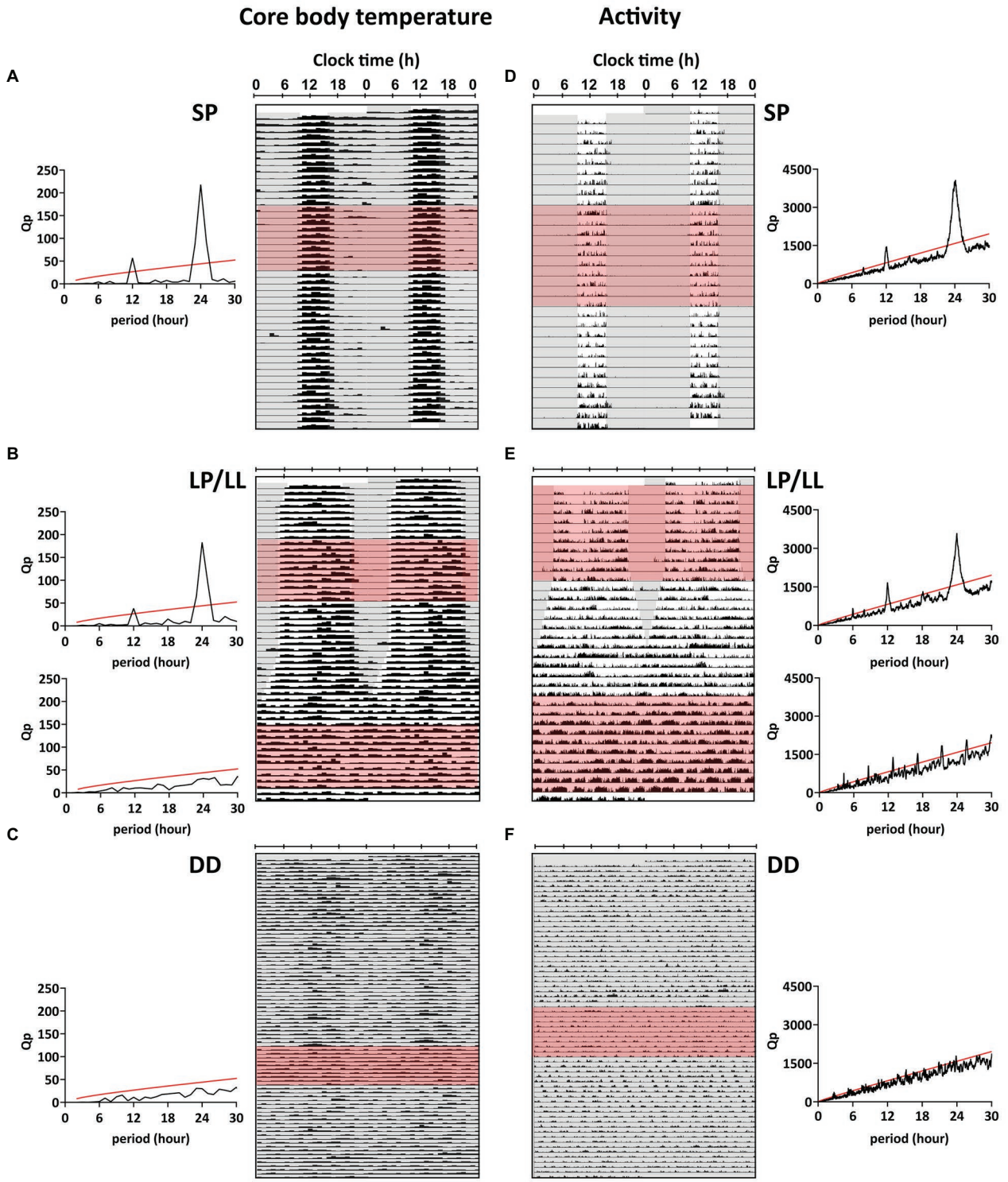


**FIGURE 2 |** Representative double-plotted actograms for body temperature ($T_b$) and activity. **(A-C)** $T_b$ was plotted actogram-like between 40 and 42°C for representative birds from each group (bird IDs **A**: SP3, **B**: LP/LL11, **C**: DD3). **(D–F)** Actograms for normalized activity were plotted between 0 and 1 for representative birds from each group (bird IDs **D**: SP6, **E**: LP/LL15, **F**: DD2). $\chi^2$-periodograms were plotted for 10 consecutive days in each light treatment (red shading in actograms) and are displayed next to the respective recordings. Values above the red line indicate that the cycle period was significant ($p < 0.05$). Additional actograms and periodograms can be found in **Supplementary Figures S1–S3**.

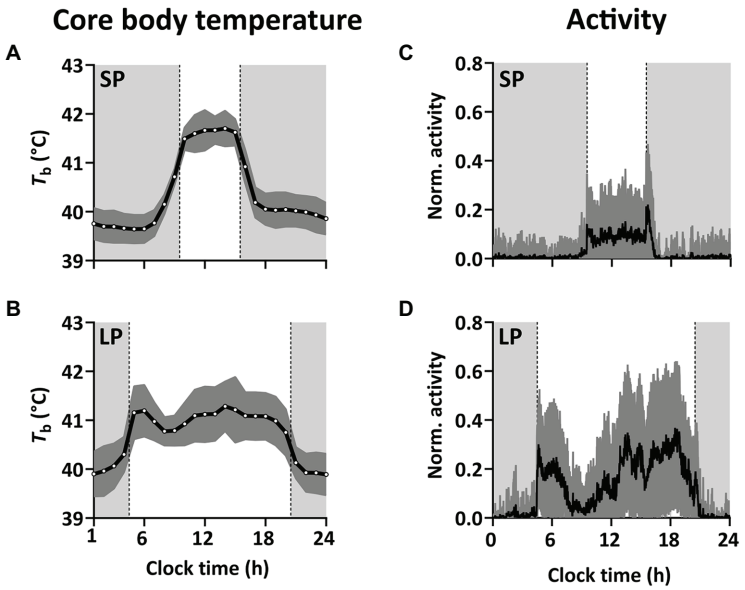


**FIGURE 3 |** Diel variation in $T_b$ and activity in short and long photoperiod. **(A,B)** Mean ± SD $T_b$ over the course of 24 h (01:00 to midnight) in SP (based on 222 × 24-h recordings from five birds) and LP (based on 184 × 24-h recordings from eight birds). $T_b$ was measured every hour throughout the experiment. **(C,D)** Mean normalized activity ± SD over the course of 24 h (midnight to midnight) in SP (61 × 24-h recordings from three birds) and LP (27 × 24-h recordings from three birds). Light gray shadowing in the panels indicate periods of darkness and dark gray indicates SD.

(ref. no.: 332452, Sanivo Pharma AS, Oslo, Norway). The skin and muscle tissue were cut along the *linea alba* and the sterilized (70% EtOH) iButton was then inserted into the abdominal cavity. The muscle tissue was sutured with an absorbable 2-0 Polysorb string (Ref. No.: CL-811, Syneture, Dublin, Ireland) and was disinfected with 2% iodine. The skin was sutured with an absorbable 0 Dexon string (Ref. No.: 7232-61, Syneture, Dublin, Ireland) and again disinfected with 2% iodine. After surgery, the facemask was removed, and the bird was observed until it regained full consciousness. The birds were placed into their home cages as soon as they could stand unaided.

The iButtons recorded hourly $T_b$ for the durations outlined online.[2] Specifically, in the SP-group, the $T_b$ of seven birds was recorded for 48 days (except for bird SP2 which was measured for 30 days). In the LP/LL-group, eight birds were recorded for 23 days under LP and 14 days under LL. In the DD-group, three birds were recorded for 83 days. All recordings were made at the full hour except for two birds in the SP-group, which recorded at half hour. At the end of the experiment, the implanted iButtons were recovered from euthanized birds and the data were downloaded using the Maxim Integrated software OneWireViewer (version 0.3.19.47).

## Activity Recording

Locomotor activity was recorded continuously as movements per minute using passive infrared sensors (HSP 1131, Panasonic, Kadoma, Japan). These were installed on homebuilt circuit boards and mounted on the cage doors. Data were collected for a subset of three birds per photoperiodic group (determined by the number of available recording devices), using an Actimetrics CL200 USB interface coupled to ClockLab data acquisition software Version 2.61 (Actimetrics, Wilmette, IL, United States).

We recorded activity for the experiment during 9 days in three birds in the LP/LL-group under LP, 14 days in three birds in the LP/LL-group under LL, and 66 days in three birds in the DD-group. In the SP-group we measured activity for 12, 18, and 31 days in three birds. Activity was recorded as counts per minute and normalized from 0 to 1 for each individual bird prior to analysis and plotting.

## Data Handling and Analysis

All graphs were plotted with GraphPad Prism 8 (Version 8.3.0, San Diego, CA, United States), except for the actograms, which were plotted using the ImageJ plugin ActogramJ (Schmid et al., 2011).

We plotted actograms for $T_b$ and normalized activity for each bird over the whole experimental period. Actograms illustrate rhythmicity or the lack of it. All actograms were double-plotted to ease inspection. In a double-plotted actogram, one horizontal line represents 2 consecutive days (x-axis). Consecutive days are also plotted from top to bottom (y-axis). Normalized activity is displayed as bars of increasing heights between 0 and 1 on each line. This means that the higher the activity, the higher the bar. Low bars or the absence of

[2]https://doi.org/10.18710/XLDXQ3

bars indicate low activity and rest. Patterns or lack of rhythmicity can be observed by reading the actogram from top to button and by observing how phases of high and low activity relate to each other. We also adapted actograms to display $T_b$ between 40 and 42°C to show $T_b$ rhythmicity. Hence, $T_b$ < 40°C is blank in the actogram, while temperatures > 40°C were plotted as bars of increasing height up to 42°C. Rhythmicity in these actograms was tested by calculating $\chi^2$-periodograms (Sokolove and Bushell, 1978) for 10 consecutive days for each bird in each light treatment. The 10-day period was chosen to coincide with reduced frequency of husbandry practices (see section "Bird Husbandry and the Effect on $T_b$"). The $\chi^2$-periodogram algorithm calculated $Q_p$ indices for each period between 1 and 30 h. $Q_p$ follows a $\chi^2$ distribution, and values corresponding to a value $p < 0.05$ were considered statistically significant.

We also plotted $T_b$ and activity as mean ± SD 24-h profiles for the SP and LP/LL group under LP. For each group, we calculated $T_b$ peak and nadir for each respective light treatment. The peak and nadir means are based on maximum and minimum $T_b$ of each day and each individual bird. We then compared the difference in daily $T_b$ peak and nadir (henceforth "amplitude") between photoperiod groups. For this, we used a mixed effects model fitted with restricted likelihood (lmer function in the lme4 package; Bates et al., 2014) using R version 4.0.0 (R Core Team, 2020) implemented in RStudio (version 1.3.959). Photoperiodic treatment was used as the explanatory variable, and a random intercept for bird ID was included to account for repeated measurements. Group estimates for the amplitude and comparisons between the groups were obtained using the emmeans R package (Lenth et al., 2018). Periods of transition between different photoperiods, and two birds from the SP-group which recorded at half hour, were excluded from this analysis.

Core body temperature and activity were also plotted together for a 5-day period and for three birds for each photoperiod. In the periods selected for this purpose, the birds were acclimatized to their respective photoperiod for at least a week and were undisturbed apart from normal husbandry. In order to analyze effects of photoperiod on dawn anticipation, we calculated mean $T_b$ and activity from the 5-day periods for 5 h before light-on when $T_b$ was at its minimum and for 1 h after light-on. The activity mean was calculated as the mean of the 10 min immediately before each $T_b$ measurement. We defined dawn anticipation as nocturnal rise in $T_b$ or activity that preceded the light-on signal. The 6-h period was analyzed by fitting a segmented linear regression (GraphPad 8) and we considered the break point of the segmented function (i.e., where the two regression segments meet) as the start of anticipatory rise in activity or $T_b$. We plotted the data in Zeitgeber time (ZT), in which ZT 0 corresponds to the light-on signal.

## Bird Husbandry and the Effect on $T_b$

Birds were monitored daily as part of routine husbandry. This might cause stress, which is known to cause increased

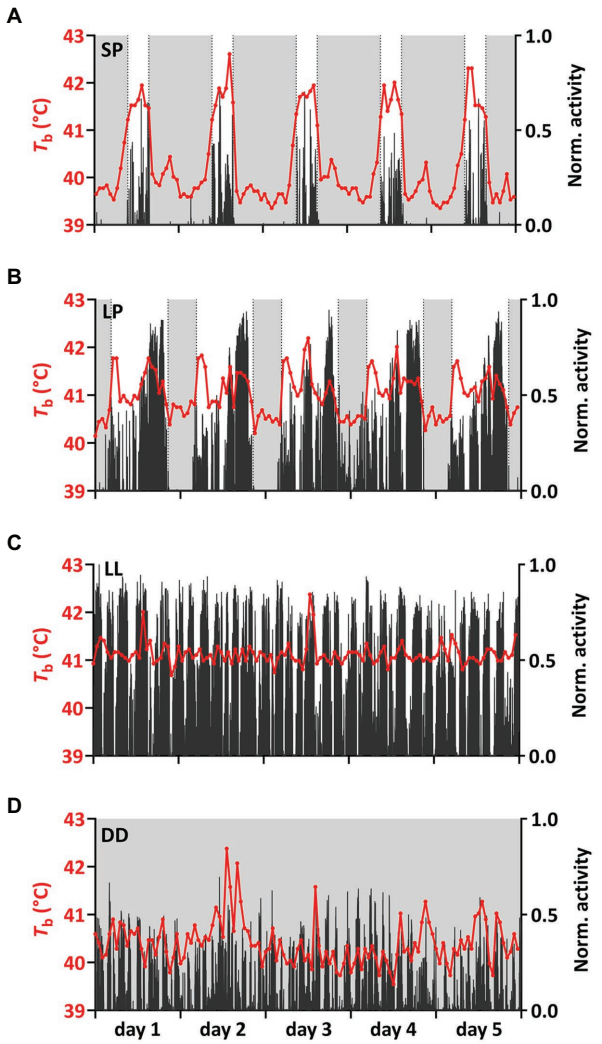


**FIGURE 4 |** Representative time series for $T_b$ and activity. **(A–D)** $T_b$ (red) was plotted together with normalized activity (black) for 5 consecutive days for one representative bird per experimental treatment (bird IDs **A**: SP6, **B,C**: LP/LL13, **D**: DD2). Light gray shadings indicate periods of darkness. Additional time series can be found in **Supplementary Figure S4**.

$T_b$ in birds (Cabanac and Guillemette, 2001; Nord and Folkow, 2019). This might affect rhythmicity analyses, especially in LL and DD. For this reason, we kept records of the timing of husbandry and tested how these visits affected $T_b$. We defined three categories (husbandry, 1 h after husbandry, and no husbandry) and assigned the respective $T_b$ reading to each category for birds under LL and DD. The $T_b$ means for each bird and each category were compared using paired $t$-test (Graphpad 8). In addition, we plotted husbandry in LL and DD in form of actograms and conducted $\chi^2$-periodogram analyses on the rhythm of husbandry and on $T_b$ recording of all birds under LL and DD.

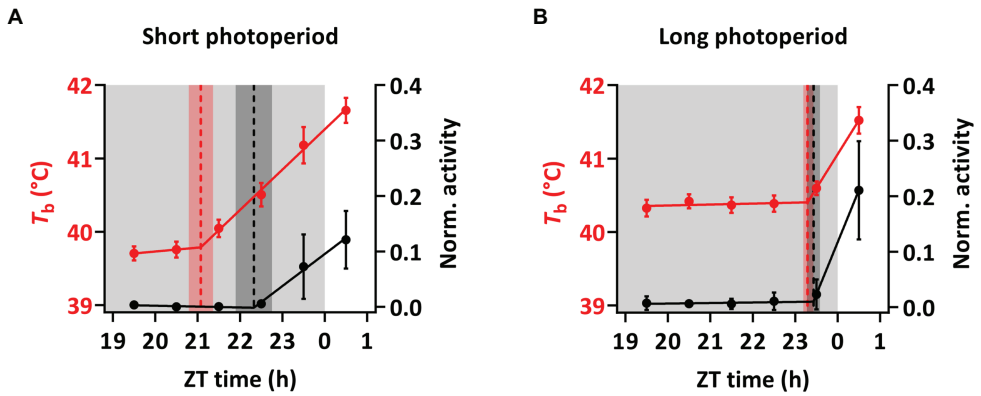


**FIGURE 5 |** Anticipatory rise in $T_b$ based on segmental regression breakpoints. Hourly means of $T_b$ (red) and activity (black) 5 h before and 1 h after the light-on signal, given in Zeitgeber time (ZT). **(A)** $T_b$ in birds under SP was rising 2 h 56 min before the light-on signal while activity rises 1 h 40 min before light-on. **(B)** In birds under LP $T_b$ increased 43 min before light-on, while activity rose 34 min before the light-on signal. The data correspond to the measurement in **Figure 4** and **Supplementary Figure S4** and are displayed as mean ± 95% CI. Dotted lines indicate segmented regression breaking points and the shading shows the corresponding SD. Light gray shadings indicate periods of darkness.

## RESULTS

Svalbard ptarmigan held under SP and LP displayed clear daily rhythms in $T_b$ with a 24-h period ($p < 0.05$ by $\chi^2$-periodogram), while birds under LL and DD showed no significant rhythmicity in $T_b$ for a chosen 10-day period ($p > 0.05$ for all periods by $\chi^2$-periodogram; **Figures 2A–C**). Husbandry caused stress related increase in $T_b$ (**Supplementary Figures S5, S6**) and the 10-day periods (especially under DD) were chosen to coincide with less and randomized husbandry (**Supplementary Figure S6**).

The $T_b$-rhythm under SP and LP is defined by decreased $T_b$ during the dark-phase and increased $T_b$ during the light-phase, which is expressed either as a single peak in SP (**Figures 3A, 4A**) or as a morning and one or several "afternoon peaks" in LP (**Figures 3B, 4B**). Birds under SP and LP displayed $T_b$ amplitudes of 2.52 ± 0.15°C and 2.27 ± 0.12°C, respectively (estimate ± SE by mixed model analysis), while birds under LL and DD showed smaller differences between peak and nadir ($p < 0.001$ by mixed model analysis) with 1.46 ± 0.12°C and 1.30 ± 0.19°C, respectively. The amplitudes between SP vs. LP ($p = 0.532$) and LL vs. DD ($p = 0.891$) did not differ significantly. Results from the mixed model analyzing the amplitude are presented in **Table 1**.

Svalbard ptarmigan under SP and LP displayed clear 24-h rhythmicity in activity ($p < 0.05$ by $\chi^2$-periodogram; **Figures 2D,E**) with high activity in the light-phase and low activity in the dark-phase (**Figures 3C,D**). Similar to $T_b$, birds under LP also displayed two distinct activity peaks during the light phase (**Figure 3D**). Birds under LL and DD showed various significant periods in activity between 1 and 30 h ($p < 0.05$ by $\chi^2$-periodogram; **Figures 2E,F**).

Birds under SP showed a significant nocturnal increase in $T_b$ preceding the light-on signal and the rise in activity (**Figures 4, 5**). Under SP, both activity and $T_b$ increased in the 5-h period immediately preceding the light-on signal. However, $T_b$ rose 3 h before light-on [segmented regression breakpoint: ZT 21:04 ± 00:17 (hh:mm ± SD)] whereas activity increased 1 h 40 m before (breakpoint: ZT 22:20 ± 00:26). In LP, birds showed increased $T_b$ and activity starting around half an hour before light-on (breakpoint for $T_b$: ZT 23:17 ± 00:06; and for activity: ZT 23:26 ± 00:09).

We also observed that SP-birds often expressed a small increase in $T_b$ in the dark-phase around 11 h after the last light-on switch (ZT 11:05 ± 1:00, mean ± SD based on analysis in **Figure 4** and **Supplementary Figure S4**). The nocturnal peak was similar to the expression of the "afternoon peak" in LP-birds that occurred 9 h after the light-on signal (ZT 8:51 ± 1:11).

**TABLE 1 |** Differences in body temperature amplitude (i.e., the difference between the daily core $T_b$ peak and $T_b$ nadir; °C) under different photoperiods.

| | Estimate (SE) | LR | *p* |
|---|---|---|---|
| **Model** | | | |
| Intercept | 1.30 (0.17) | | |
| Treatment | | 61.584 | <0.001 |
| Constant darkness (DD) | 1.30 (0.19) | | |
| Constant light (LL) | 1.46 (0.12) | | |
| Long photoperiod (LP, L:D 16:8) | 2.27 (0.12) | | |
| Short photoperiod (SP, L:D 6:18) | 2.52 (0.15) | | |
| **Contrast** | | | |
| DD vs. LL | −0.16 (0.22) | | 0.891 |
| DD vs. LP | −0.96 (0.22) | | <0.001 |
| DD vs. SP | −1.22 (0.24) | | <0.001 |
| LL vs. LP | −0.81 (0.17) | | <0.001 |
| LL vs. SP | −1.06 (0.19) | | <0.001 |
| LP vs. SP | −0.26 (0.19) | | 0.532 |

Estimates (±SE), likelihood ratios (LR) and *p*-values for the differences between photoperiodic treatments. Data were tested using a linear mixed effects model with bird ID as a random intercept. *p*-values and group estimates were obtained and compared using the emmeans package in R.

## DISCUSSION

In this study, we measured $T_b$ and activity in Svalbard ptarmigan under photoperiods that were representative of those experienced during their annual cycle in the wild. All recorded $T_b$ fell within the reported range of birds (Prinzinger et al., 1991) and were comparable to previous measurements of $T_b$ during subjective daytime in Svalbard ptarmigan (Nord and Folkow, 2018). In SP and LP, birds showed pronounced rhythms in $T_b$ with high temperatures during the light-phase and low temperature during the dark-phase. In LL and DD, the difference between maximal and minimal $T_b$ within a 24-h period was attenuated and our periodogram analysis suggests weakened circadian control over $T_b$ rhythms under these constant photic conditions. Occasionally, birds in LL and DD continued to show transient peaks in $T_b$, which are reminiscent of sustained rhythmicity. However, these peaks coincided with visits for husbandry and we ascribe the observation to consequences of a stress-related increase in $T_b$ (Cabanac and Guillemette, 2001; Nord and Folkow, 2019).

Activity was also rhythmic with a 24-h period in SP and LP, which was not sustained in LL and DD. This is in accordance with previous studies on activity rhythms in Svalbard ptarmigan (Stokkan et al., 1986; Reierth and Stokkan, 1998). Instead of a clear 24-h rhythm, birds under LL and DD showed various significant periods between 1 and 30 h. Especially birds under LL appeared to express ultradian activity rhythms with a period of ca. 4 h (**Figure 2E**) of which subsequent peaks in the periodogram could be subharmonics to the fundamental ultradian period. In the absence of an environmental light-dark cycle, the ultradian rhythm might reflect foraging activity and subsequent rest in Svalbard ptarmigan. At this stage, we can only speculate if this activity pattern is under endogenous control of an ultradian oscillator (Bourguignon and Storch, 2017) or if it is produced by the interplay of hunger and satiety.

Core body temperature rose in anticipation to the light-on signal and, in birds under SP, prior to rises in activity. This suggests, firstly, that, as in most other endothermic animals, $T_b$ is a distinct endogenous feature and not only a consequence of activity (Menaker, 1959; Aschoff, 1983; Refinetti and Menaker, 1992). Secondly, it suggests that the $T_b$-cycle in Svalbard ptarmigan is controlled by a time-measuring system, which accurately anticipates the light-on signal. In nature, this anticipatory rise in $T_b$ might ensure optimal bodily function at the start of the active phase. In mammals, cycles in $T_b$ might be utilized by the central circadian system to impose its rhythm on peripheral tissues (Brown et al., 2002; Buhr et al., 2010). It is possible that Svalbard ptarmigan (and other birds) use $T_b$ in the same manner to ensure synchronized physiology in the short periods of light-dark cycles in-between the long stretches of polar day and polar night. Due to the absence of measurable circadian rhythms in $T_b$ and activity in LL and DD, we propose that the central circadian system of Svalbard ptarmigan either uncouples from its output, or dampens in rhythmicity, when there is no periodic environmental synchronization (Bloch et al., 2013). This might ensure around-the-clock foraging without endogenous restraints during the polar day and polar night. However, we cannot exclude the possibility that under natural conditions Svalbard ptarmigan still express rhythms in $T_b$ during the polar day and polar night due to entrainment to other photic or non-photic cues (Long et al., 2005; Ashley et al., 2012).

We also observed transient increases in $T_b$ in the dark-phase of birds under SP. This could reflect nocturnal digestive activity (Rashotte et al., 1997). Alternatively, this observation might be further support for a circadian drive in $T_b$ under light-dark cycles, in which case the transient nocturnal $T_b$-peak in SP would correspond to the "afternoon peak" seen in LP birds.

Our findings suggest that Svalbard ptarmigan are using a circadian system under SP and LP to control their $T_b$. Under prolonged LL and DD, this circadian control of $T_b$ and activity seems to weaken. They can, therefore, utilize the benefits of a circadian system during times of a rhythmic environment but are able to escape its restrictions in constant photic conditions. Instead of a circadian rhythm, Svalbard ptarmigan show signs of ultradian rhythmicity in activity, especially under LL, but we cannot resolve if this rhythm is endogenous or produced by the interaction of hunger and satiety. Future research should aim to elucidate how Svalbard ptarmigan achieve their duality of circadian organization and how ultradian rhythmicity is controlled.

## DATA AVAILABILITY STATEMENT

The datasets presented in this study can be found in online repositories. The names of the repository/repositories and accession number(s) can be found in the article/**Supplementary Material**.

## ETHICS STATEMENT

The animal study was reviewed and approved by the Norwegian Food Safety Authority (Mattilsynet).

## AUTHOR CONTRIBUTIONS

DA, DH, and GW: conceptualization and project administration. DA: data curation and writing – original draft. DA, AN, and GW: formal analysis, investigation, and visualization. DH and GW: funding acquisition and supervision. DA, AN, DH, and GW: methodology and writing – review and editing. AN, DH, and GW: resources. AN: software. AN and GW: validation. All authors contributed to the article and approved the submitted version.

## FUNDING

DA, DH, and GW were supported by grants from the Tromsø Research Foundation (TFS2016DH) and the Human Frontiers Science Program (RGP0030/2015) to DH. DA and GW received further funding through the Master Program of the University of

Tromsø – The Arctic University. AN was supported by the Swedish Research Council (grant no. 637-2013-7442), the Carl Trygger Foundation for Scientific Research (grant no. CTS14: 347) and the Birgit and Hellmuth Hertz Foundation/the Royal Physiographic Society of Lund (grant no. 2017-39034).

## ACKNOWLEDGMENTS

We would like to thank the animal technicians from the Arctic Chronobiology and Physiology research group. Their dedication and experience are indispensable for past, current, and future research. We would also like to thank Dr. Alexander West for his insightful comments, motivational words, and ongoing support.

## SUPPLEMENTARY MATERIAL

The Supplementary Material for this article can be found online at: https://www.frontiersin.org/articles/10.3389/fphys.2021.633866/full#supplementary-material

## REFERENCES

Arnold, W., Ruf, T., Loe, L. E., Irvine, R. J., Ropstad, E., Veiberg, V., et al. (2018). Circadian rhythmicity persists through the polar night and midnight sun in svalbard reindeer. *Sci. Rep.* 8:14466. doi: 10.1038/s41598-018-32778-4

Aschoff, J. (1983). Circadian control of body temperature. *J. Therm. Biol.* 8, 143–147. doi: 10.1016/0306-4565(83)90094-3

Ashley, N. T., Schwabl, I., Goymann, W., and Buck, C. L. (2012). Keeping time under the midnight sun: behavioral and plasma melatonin profiles of free-living Lapland longspurs (*Calcarius lapponicus*) during the Arctic summer. *J. Exp. Zool. A Ecol. Genet. Physiol.* 319, 10–22. doi: 10.1002/jez.1768

Bates, D., Mächler, M., Bolker, B., and Walker, S. (2014). Fitting linear mixed-effects models using lme4. arXiv [Preprint]. doi: 10.18637/jss.v067.i01.

Bloch, G., Barnes, B. M., Gerkema, M. P., and Helm, B. (2013). Animal activity around the clock with no overt circadian rhythms: patterns, mechanisms and adaptive value. *Proc. Biol. Sci.* 280:20130019. doi: 10.1098/rspb.2013.0019

Bourguignon, C., and Storch, K. -F. (2017). Control of rest: activity by a dopaminergic ultradian oscillator and the circadian clock. *Front. Neurol.* 8:614. doi: 10.3389/fneur.2017.00614

Brown, S. A., Zumbrunn, G., Fleury-Olela, F., Preitner, N., and Schibler, U. (2002). Rhythms of mammalian body temperature can sustain peripheral circadian clocks. *Curr. Biol.* 12, 1574–1583. doi: 10.1016/S0960-9822(02)01145-4

Buhr, E. D., Yoo, S. -H., and Takahashi, J. S. (2010). Temperature as a universal resetting cue for mammalian circadian oscillators. *Science* 330, 379–385. doi: 10.1126/science.1195262

Cabanac, A., and Guillemette, M. (2001). Temperature and heart rate as stress indicators of handled common eider. *Physiol. Behav.* 74, 475–479. doi: 10.1016/S0031-9384(01)00586-8

Daan, S., Spoelstra, K., Albrecht, U., Schmutz, I., Daan, M., Daan, B., et al. (2011). Lab mice in the field: unorthodox daily activity and effects of a dysfunctional circadian clock allele. *J. Biol. Rhythms* 26, 118–129. doi: 10.1177/0748730410397645

Darlington, T. K., Wager-Smith, K., Ceriani, M. F., Staknis, D., Gekakis, N., Steeves, T. D., et al. (1998). Closing the circadian loop: CLOCK-induced transcription of its own inhibitors per and tim. *Science* 280, 1599–1603. doi: 10.1126/science.280.5369.1599

DeCoursey, P. J., and Krulas, J. R. (1998). Behavior of SCN-lesioned chipmunks in natural habitat: a pilot study. *J. Biol. Rhythms* 13, 229–244. doi: 10.1177/074873098129000075

DeCoursey, P. J., Krulas, J. R., Mele, G., and Holley, D. C. (1997). Circadian performance of suprachiasmatic nuclei (SCN)-lesioned antelope ground squirrels in a desert enclosure. *Physiol. Behav.* 62, 1099–1108. doi: 10.1016/S0031-9384(97)00263-1

DeCoursey, P., Walker, J., and Smith, S. (2000). A circadian pacemaker in free-living chipmunks: essential for survival? *J. Comp. Physiol. A.* 186, 169–180. doi: 10.1007/s003590050017

Hardin, P. E., Hall, J. C., and Rosbash, M. (1990). Feedback of the Drosophila period gene product on circadian cycling of its messenger RNA levels. *Nature* 343, 536–540. doi: 10.1038/343536a0

Hüppe, L., Payton, L., Last, K., Wilcockson, D., Ershova, E., and Meyer, B. (2020). Evidence for oscillating circadian clock genes in the copepod *Calanus finmarchicus* during the summer solstice in the high Arctic. *Biol. Lett.* 16:20200257. doi: 10.1098/rsbl.2020.0257

Lenth, R., Singmann, H., and Love, J. (2018). Emmeans: Estimated marginal means, aka least-squares means. R package version, 1.

Long, R. A., Martin, T. J., and Barnes, B. M. (2005). Body temperature and activity patterns in free-living arctic ground squirrels. *J. Mammal.* 86, 314–322. doi: 10.1644/BRG-224.1

Menaker, M. (1959). Endogenous rhythms of body temperature in hibernating bats. *Nature* 184, 1251–1252. doi: 10.1038/1841251a0

Menaker, M., Moreira, L., and Tosini, G. (1997). Evolution of circadian organization in vertebrates. *Braz. J. Med. Biol. Res.* 30, 305–313. doi: 10.1590/S0100-879X1997000300003

Miché, F., Vivien-Roels, B., Pévet, P., Spehner, C., Robin, J., and Le Maho, Y. (1991). Daily pattern of melatonin secretion in an Antarctic bird, the emperor penguin, *Aptenodytes forsteri*: seasonal variations, effect of constant illumination and of administration of isoproterenol or propranolol. *Gen. Comp. Endocrinol.* 84, 249–263. doi: 10.1016/0016-6480(91)90048-B

Mortensen, A., and Blix, A. (1986). Seasonal changes in resting metabolic rate and mass-specific conductance in Svalbard ptarmigan, Norwegian rock ptarmigan and Norwegian willow ptarmigan. *Ornis Scand.* 17, 8–13. doi: 10.2307/3676746

Nord, A., and Folkow, L. P. (2018). Seasonal variation in the thermal responses to changing environmental temperature in the world's northernmost land bird. *J. Exp. Biol.* 221:jeb171124. doi: 10.1242/jeb.171124

Nord, A., and Folkow, L. P. (2019). Ambient temperature effects on stress-induced hyperthermia in Svalbard ptarmigan. *Biol. Open* 8:bio043497. doi: 10.1242/bio.043497

Norwegian-Meterological-Institute (2020). Free meteorological data. Available at: https://www.met.no/ (Accessed November 6, 2020).

Pevet, P., and Challet, E. (2011). Melatonin: both master clock output and internal time-giver in the circadian clocks network. *J. Physiol. Paris* 105, 170–182. doi: 10.1016/j.jphysparis.2011.07.001

Pittendrigh, C. S. (1960). Circadian rhythms and the circadian organization of living systems. *Cold Spring Harb. Symp. Quant. Biol.* 25, 159–184. doi: 10.1101/SQB.1960.025.01.015

Prinzinger, R., Pressmar, A., and Schleucher, E. (1991). Body temperature in birds. *Comp. Biochem. Physiol. A Physiol.* 99, 499–506. doi: 10.1016/0300-9629(91)90122-S

R Core Team (2020). R: A language and environment for statistical computing. R Foundation for Statistical Computing, Vienna, Austria. Available at: https://www.R-project.org

Rashotte, M. E., Phillips, D. L., and Henderson, R. P. (1997). Nocturnal digestion, cloacal excretion, and digestion-related thermogenesis in pigeons (*Columba livia*). *Physiol. Behav.* 61, 83–92. doi: 10.1016/S0031-9384(96)00353-8

Refinetti, R., and Menaker, M. (1992). The circadian rhythm of body temperature. *Physiol. Behav.* 51, 613–637. doi: 10.1016/0031-9384(92)90188-8

Reierth, E., and Stokkan, K. -A. (1998). Activity rhythm in high arctic svalbard ptarmigan (*Lagopus mutus* hyperboreus). *Can. J. Zool.* 76, 2031–2039. doi: 10.1139/z98-173

Reierth, E., Van't Hof, T. J., and Stokkan, K. -A. (1999). Seasonal and daily variations in plasma melatonin in the high-arctic Svalbard ptarmigan (*Lagopus mutus* hyperboreus). *J. Biol. Rhythms* 14, 314–319. doi: 10.1177/074873099129000731

Schmid, B., Helfrich-Förster, C., and Yoshii, T. (2011). A new ImageJ plug-in "ActogramJ" for chronobiological analyses. *J. Biol. Rhythms* 26, 464–467. doi: 10.1177/0748730411414264

Sokolove, P. G., and Bushell, W. N. (1978). The chi square periodogram: its utility for analysis of circadian rhythms. *J. Theor. Biol.* 72, 131–160. doi: 10.1016/0022-5193(78)90022-X

Spoelstra, K., Wikelski, M., Daan, S., Loudon, A. S., and Hau, M. (2016). Natural selection against a circadian clock gene mutation in mice. *Proc. Natl. Acad. Sci. U. S. A.* 113, 686–691. doi: 10.1073/pnas.1516442113

Steiger, S. S., Valcu, M., Spoelstra, K., Helm, B., Wikelski, M., and Kempenaers, B. (2013). When the sun never sets: diverse activity rhythms under continuous daylight in free-living arctic-breeding birds. *Proc. Biol. Sci.* 280:20131016. doi: 10.1098/rspb.2013.1016

Stelzer, R. J., and Chittka, L. (2010). Bumblebee foraging rhythms under the midnight sun measured with radiofrequency identification. *BMC Biol.* 8:93. doi: 10.1186/1741-7007-8-93

Stokkan, K. -A., Mortensen, A., and Blix, A. S. (1986). Food intake, feeding rhythm, and body mass regulation in Svalbard rock ptarmigan. *Am. J. Physiol.* 251, R264–R267. doi: 10.1152/ajpregu.1986.251.2.R264

Stokkan, K. A., Van Oort, B. E., Tyler, N. J., and Loudon, A. S. (2007). Adaptations for life in the Arctic: evidence that melatonin rhythms in reindeer are not driven by a circadian oscillator but remain acutely sensitive to environmental photoperiod. *J. Pineal Res.* 43, 289–293. doi: 10.1111/j.1600-079X.2007.00476.x

Swade, R. H., and Pittendrigh, C. S. (1967). Circadian locomotor rhythms of rodents in the Arctic. *Am. Nat.* 101, 431–466. doi: 10.1086/282510

van Beest, F. M., Beumer, L. T., Chimienti, M., Desforges, J. -P., Huffeldt, N. P., Pedersen, S. H., et al. (2020). Environmental conditions alter behavioural organization and rhythmicity of a large Arctic ruminant across the annual cycle. *R. Soc. Open Sci.* 7:201614. doi: 10.1098/rsos.201614

van Oort, B. E., Tyler, N. J., Gerkema, M. P., Folkow, L., and Stokkan, K. -A. (2007). Where clocks are redundant: weak circadian mechanisms in reindeer living under polar photic conditions. *Naturwissenschaften* 94, 183–194. doi: 10.1007/s00114-006-0174-2

Ware, J. V., Rode, K. D., Robbins, C. T., Leise, T., Weil, C. R., and Jansen, H. T. (2020). The clock keeps ticking: circadian rhythms of free-ranging polar bears. *J. Biol. Rhythms* 35, 180–194. doi: 10.1177/0748730419900877

Williams, C. T., Barnes, B. M., and Buck, C. L. (2011). Daily body temperature rhythms persist under the midnight sun but are absent during hibernation in free-living arctic ground squirrels. *Biol. Lett.* 8, 31–34. doi: 10.1098/rsbl.2011.0435

**Conflict of Interest:** The authors declare that the research was conducted in the absence of any commercial or financial relationships that could be construed as a potential conflict of interest.

# Advantages of publishing in Frontiers

**OPEN ACCESS**
Articles are free to read for greatest visibility and readership

**FAST PUBLICATION**
Around 90 days from submission to decision

**HIGH QUALITY PEER-REVIEW**
Rigorous, collaborative, and constructive peer-review

**TRANSPARENT PEER-REVIEW**
Editors and reviewers acknowledged by name on published articles

**Frontiers**
Avenue du Tribunal-Fédéral 34
1005 Lausanne | Switzerland

**Visit us:** www.frontiersin.org
**Contact us:** frontiersin.org/about/contact

**REPRODUCIBILITY OF RESEARCH**
Support open data and methods to enhance research reproducibility

**DIGITAL PUBLISHING**
Articles designed for optimal readership across devices

**FOLLOW US**
@frontiersin

**IMPACT METRICS**
Advanced article metrics track visibility across digital media

**EXTENSIVE PROMOTION**
Marketing and promotion of impactful research

**LOOP RESEARCH NETWORK**
Our network increases your article's readership